



Common Borders. Common Solutions.

**A Scientific Network
for Earthquake, Landslide & Flood Hazard Prevention**



**Pilot Implementation of Landslide Hazard
Assessment at Regional and Local Scales**

Deliverable No.: D.03.01, Vol. 2

**GA3. Earthquake, Landslide and Flood Hazard Assessment: Implementation
at Regional and Local scales, Activities A.3.1 & A.3.4**

OVERALL RESPONSIBLE for GA3: Democritus University of Thrace (P1)

RESPONSIBLE for A.3.1 & A.3.4: Democritus University of Thrace (P1)

INVOLVED PARTNERS: ALL

Project Details

Programme	Black Sea JOP
Priority and Measure	Priority 2 (Sharing resources and competencies for environmental protection and conservation), Measure 2.1. (Strengthening the joint knowledge and information base needed to address common challenges in the environmental protection of river and maritime systems)
Objective	Development of a Scientific Network
Project Title	A Scientific Network for Earthquake, Landslide and Flood Hazard Prevention
Project Acronym	SciNetNatHaz
Contract No	MIS-ETC 2614
Lead Partner	TEI OF KENTRIKI MAKEDONIA, GREECE
Total Budget	700.000,00 Euro (€)

Time Frame

Start Date – End Date

01/05/2013 – 30/11/2015


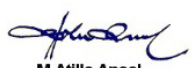

Book Captain:

K. PAPATHEODOROU (TEI of KENTRIKI MAKEDONIA)

**Contributing
Authors:**

N. Klimis, K. Papatheodorou, Em. Psaroudakis, Th. Lazaridis, I. Gkiougkis, El. Petala, S. Skias, I. Markou, K. Ntouros, K. Vosniakos, E. Mouratidis, G. Ntouros, A. Ansal, G. Tönük, O. Ilhan, H. Khanbabazadeh, N. Dobrev, B. Berov, Pl. Ivanov, M. Krastanov, C. Buta, C. Maftei, G. Cracu, Z. Prefac, L. Tofan, O. Bogdevich, A. Sidorenko, N. Fedoronchuk, O. Rubel and N. Andreeva

Document Release Sheet

Book captain:	K. PAPATHEODOROU (TEI CENTRAL MACEDONIA)	Sign  K. Papatheodorou	Date 04.02.2016
Approval	N. KLIMIS (DEMOCRITUS UNIVERSITY OF THRACE - P1)	Sign  N. Klimis	Date 04.02.2016
Approval	K. PAPATHEODOROU (TEI CENTRAL MACEDONIA)	Sign  K. Papatheodorou	Date 11.02.2016
Approval	B. MARGARIS (Partner 2 - EPPO)	 Basil N. Margaris	11.02.2016
Approval	A. ANSAL (IPA - BU-KOERI)	Sign  M. Atilla Ansal	Date 11.02.2016
Approval	V. NENOV (Partner 3 - Burgas Assen Zlatarov University)		11.02.2016
Approval	L. TOFAN (Partner 4 - Ovidius University of Constanta)		11.02.2016
Approval	A. SIDORENKO (Partner 5 - IEN “D.GHITU” Of Academy Of Sciences Of Moldova)		11.02.2016
Approval	K. STEPANOVA (Partner 6 - Ukranian Environmental Academy Of Sciences, Black Sea Branch)		11.02.2016
Approval	K. PAPATHEODOROU	Sign Date 11.02.2016  K. Papatheodorou	
Distribution:	ALL PARTNERS		

RECORD of REVISIONS

Issue/Rev	Date	Page(s)	Description of Change	Release
-	23.10.2015	142	First draft (P1 and LP)	I.01
	24.10.2015	156	Incorporation of P3 contribution	I.02
	25.10.2015	173	Incorporation of P4 contribution	I.03
	29.10.2015	209	Incorporation of IPA contribution	I.04
	06.11.2015	218	Incorporation of P6 contribution	I.05
	09.11.2015	229	Incorporation of P5 contribution	I.06
	10.12.2015	233	Second Draft (P1)	I.07
	28.12.2015	276	Incorporation of Annex A (P1-LP)	I.08
	15.01.2016	407	Appendix (P1)	I.09
	04.02.2016	407	Third Draft with Annexes & Appendix-Distribution	I.10
	11.02.2016	407	Final Version approved by LP	I.11

TABLE OF CONTENTS

1	BACKGROUND OF THE DOCUMENT.....	17
1.1	GENERAL NOTE	17
1.2	SCOPE AND OBJECTIVES.....	17
1.3	RELATED DOCUMENTS	17
1.3.1	<i>Input.....</i>	<i>17</i>
1.3.2	<i>Output.....</i>	<i>18</i>
2	LANDSLIDE HAZARD ASSESSMENT ON A REGIONAL SCALE - PILOT IMPLEMENTATIONS IN GREECE	19
2.1	INTRODUCTION	19
2.2	PROBLEMS IN ASSESSING LANDSLIDE HAZARD - METHODS IMPLEMENTED.....	20
2.3	SCOPE.....	22
2.4	ACTIVITIES	23
2.5	SERRES PILOT IMPLEMENTATION AREA.....	24
2.5.1	<i>Geomorphology</i>	<i>25</i>
2.5.2	<i>Engineering geologic mapping</i>	<i>27</i>
2.5.3	<i>Updating Serres PIA tectonic regime</i>	<i>30</i>
2.6	NYMFAIA PILOT IMPLEMENTATION AREA.....	34
2.6.1	<i>Geomorphology</i>	<i>35</i>
2.6.2	<i>Engineering geologic mapping</i>	<i>36</i>
2.6.3	<i>Updating the Nymfaia PIA tectonic regime</i>	<i>39</i>
3	METHODS USED FOR REGIONAL LANDSLIDE HAZARD ASSESSMENT	42
3.1	MORA & VAHRSON METHOD	42
3.1.1	<i>Data input.....</i>	<i>42</i>
3.2	FEMA METHOD (HAZUS)	47
3.2.1	<i>Landslide susceptibility under static conditions (FEMA)</i>	<i>47</i>
3.2.2	<i>Landslide susceptibility under seismic conditions</i>	<i>50</i>
3.2.3	<i>Landslide hazard under seismic conditions.....</i>	<i>56</i>
3.3	METHOD OF FACTOR OF SAFETY	62
3.3.1	<i>LHA - Infinite slope model under static and seismic conditions</i>	<i>63</i>
3.3.1.1	<i>Data input</i>	<i>64</i>
3.3.1.2	<i>Serres PIA factor of safety of natural slopes.....</i>	<i>67</i>
3.3.2	<i>LHA - Deterministic model under static conditions for circular landslides.....</i>	<i>70</i>
3.4	EVALUATION OF METHODS USED FOR REGIONAL LHA.....	72
3.5	IMPROVEMENT OF REGIONAL LHA PERFORMANCE WITH REMOTE SENSING.....	76

4	LANDSLIDE HAZARD ASSESSMENT ON A LOCAL SCALE - PILOT IMPLEMENTATIONS IN GREECE.....	80
4.1	GEOLOGICAL – GEOTECHNICAL DATA.....	80
4.1.1	PIA Nymfaia: Cut Slope O5.....	81
4.1.2	Nymfaia PIA: Cut Slope O14-O15.....	82
4.1.3	Nymfaia PIA: Cut Slope O16.....	83
4.1.4	Nymfaia PIA: Cut Slope O21.....	84
4.1.5	Nymfaia PIA: Cut Slope O32.....	86
4.1.6	Cut slope on Serres - Promahonas road (Serres PIA)	87
4.2	HYDRAULIC AND SEISMIC DATA AT NYMFAIA PIA	88
4.3	SLOPE STABILITY ANALYSES ON LOCAL SCALE AT NYMFAIA AND SERRES PIAS.....	88
4.3.1	Limit Equilibrium methods.....	89
4.3.2	Modified Bishop Limit Equilibrium method.....	89
4.4	2D ANALYSIS OF CUT SLOPES AT NYMFAIA AND SERRES PIAS.....	90
4.4.1	Cut Slope O5 at Nymfaia PIA	90
4.4.1.1	Typical ground model of the cut slope O5.....	91
4.4.1.2	Slope Stability Analysis Results on the cut slope O5.....	92
4.4.2	Cut Slope O14 - O15 at Nymfaia PIA.....	96
4.4.2.1	Typical ground model of the cut slope O14-O15	97
4.4.2.2	Slope Stability Analysis Results on the cut slope O14-O15.....	97
4.4.3	Cut Slope O16 at Nymfaia PIA	100
4.4.3.1	Typical ground model of the cut slope O16.....	100
4.4.3.2	Slope Stability Analysis Results on cut slope O16	101
4.4.4	Cut Slope O21 at Nymfaia PIA	102
4.4.4.1	Typical ground model of the cut slope O21.....	103
4.4.4.2	Slope Stability Analysis Results on the cut slope O21 (part A & B)	104
4.4.5	Cut Slope O32 at Nymfaia PIA	109
4.4.5.1	Typical ground model of cut slope O32.....	110
4.4.5.2	Slope Stability Analysis Results on the cut slope O32.....	110
4.4.6	Slope along Serres - Promahonas road axis (Serres PIA)	112
4.4.6.1	Typical ground model for a slope in Serres PIA	112
4.4.6.2	Slope Stability Analysis Results on a Slope in Serres PIA	113
4.5	FINITE DIFFERENCE METHOD.....	115
4.5.1	3D Analysis of Cut Slopes O21 and O32 (Nymfaia PIA).....	115
4.5.2	3D Analysis of Cut Slope O21	115
4.5.3	3D Analysis of Cut Slope O32	118
4.5.4	Concluding Remarks	127

4.5.4.1	Comparison of 2D and 3D models	127
4.5.4.2	Comparison of local (2D) and regional LHA models	128
5	LANDSLIDE HAZARD ASSESSMENT ON A REGIONAL SCALE - PILOT IMPLEMENTATIONS IN TURKEY	129
5.1	INTRODUCTION	129
5.2	MONTGOMERY AND DIETRICH METHOD	129
5.2.1	<i>Calculation of terrain related parameters</i>	<i>130</i>
5.2.1.1	Extraction of the DEM using SAGA	130
5.2.1.2	The use of DEM for extraction of slope angle map	131
5.2.1.3	The use of the DEM for extraction of catchment are map	131
5.2.2	<i>Preparation of the rainfall data</i>	<i>131</i>
5.2.3	<i>Compilation of the geotechnical properties of the region</i>	<i>133</i>
5.2.4	<i>Other considerations and advices</i>	<i>133</i>
5.3	MORA AND VAHRSON METHOD	133
5.3.1	<i>Extraction of the DEM using Saga</i>	<i>133</i>
5.3.2	<i>Calculation of the relative relief index</i>	<i>134</i>
5.3.3	<i>Selection of the lithological susceptibility value</i>	<i>134</i>
5.3.4	<i>Selection of the soil natural humidity parameter (S_h)</i>	<i>135</i>
5.4	DETERMINATION OF RELATED HAZARD PARAMETERS	136
5.4.1	<i>The value of influence of seismic intensity (T_s)</i>	<i>136</i>
5.4.2	<i>The value of influence of rainfall precipitation intensity (T_p)</i>	<i>137</i>
5.4.3	<i>Other Considerations and Advice</i>	<i>140</i>
5.5	FEMA METHOD	140
5.6	SIYAHİ AND ANSAL METHOD	141
5.7	MICROZONATION FOR RAINFALL INDUCED LANDSLIDES	144
6	LOCAL MICROZONATION OF TEKİRDAĞ CITY CENTER	145
6.1	GEOLOGY	145
6.2	RESULTS OF THE MICROZONATION OF TEKİRDAĞ FOR RAINFALL INDUCED LANDSLIDE	146
7	LOCAL MICROZONATION OF SAMSUN CITY CENTER	150
7.1	GEOLOGY	150
7.2	RESULTS OF THE MICROZONATION OF SAMSUN FOR RAINFALL INDUCED LANDSLIDE	151
8	REGIONAL MICROZONATION OF TEKİRDAĞ PROVINCE	155
8.1	GEOLOGY	155
8.2	RESULTS OF THE MICROZONATION OF TEKİRDAĞ FOR RAINFALL INDUCED LANDSLIDE	157
9	REGIONAL MICROZONATION OF SAMSUN PROVINCE	162

9.1	GEOLOGY	162
9.2	RESULTS OF THE MICROZONATION OF SAMSUN FOR RAINFALL INDUCED LANDSLIDE	164
10	CONCLUSIONS	169
11	LANDSLIDE HAZARD ASSESSMENT ON A REGIONAL SCALE - PILOT IMPLEMENTATION IN BULGARIAN BLACK SEA COAST	170
11.1	SUSCEPTIBILITY MAPPING.....	177
11.2	PILOT AREA MAP	178
12	LANDSLIDE HAZARD ASSESSMENT ON A REGIONAL SCALE - PILOT IMPLEMENTATIONS IN ROMANIA	181
12.1	DEFINITION OF THE PROBLEM	181
12.2	LOESS DISTRIBUTION	184
12.3	STUDY CASE	188
12.4	FACTOR OF SAFETY METHOD BASED ON INFINITE SLOPE MODEL.....	190
12.5	CONCLUSIONS	195
13	LANDSLIDE HAZARD ASSESSMENT ON A REGIONAL SCALE - PILOT IMPLEMENTATIONS IN MOLDOVA	197
14	LANDSLIDE HAZARD ASSESSMENT ON A REGIONAL SCALE - PILOT IMPLEMENTATIONS IN UKRAINE	207
14.1	LANDSLIDE HAZARD ASSESSMENT OF THE SOUTHERN UKRAINE	207
14.2	SLOPE FACTOR (SR)	208
14.3	GEOLOGY FACTOR (SL)	209
14.4	HUMIDITY FACTOR (SH).....	210
14.5	SEISMIC (EARTHQUAKE) TRIGGERING FACTOR (Ts)	212
14.6	PRECIPITATION TRIGGERING FACTOR (Tp).....	213
15	GENERAL CONCLUSIONS	217
16	REFERENCES	221
17	ADDITIONAL BIBLIOGRAPHY	227
ANNEX A	LANDSLIDE HAZARD MAPS AT REGIONAL SCALE IN GREECE (SERRES AND NYMFAIA PILOT IMPLEMENTATION AREAS)	230
ANNEX B	GEOTECHNICAL PARAMETERS FOR SAMSUN AND TEKIRDAG REGIONS - TURKEY	271
	GEOTECHNICAL PARAMETERS FOR SAMSUN REGION	272
	GEOTECHNICAL PARAMETERS FOR TEKIRDAG REGION	275

LIST OF FIGURES

FIG. 1 A SCHEMATIC REPRESENTATION OF LANDSLIDE DISASTER PREVENTION ACTIONS.....	19
FIG. 9 ORIENTATION OF GEOLOGIC PLANES ON THE GEOLOGIC MAP (LEFT) AND TOBIA SLOPE CLASSES (RIGHT)	33
FIG. 10 TOBIA INDEX CLASSES (MEENTEMEYER ET.AL, 2000)	33
FIG. 11 NYMFAIA PIA (RED DOTTED LINE) ON AN OPEN STREET LANDSCAPE MAP	34
FIG. 12 NYMFAIA PIA MORPHOLOGY: DIGITAL ELEVATION MODEL ON THE LEFT (ELEVATION IN M) AND SLOPE MAP ON THE RIGHT (SLOPE IN DEGREES)	35
FIG. 13 NYMFAIA PIA GEOLOGIC MAP DIGITIZED FROM THE GEOLOGIC MAP OF GREECE 1:50000 (IGE) AND UPDATED USING REMOTE SENSING TECHNIQUES.....	38
FIG. 14 BAND RATIOS (LEFT TO RIGHT): TM4/TM3, TM5/TM3, TM7/TM3, SHOWING LARGE LINEAMENTS (CENTER) WITH WSW-ENE; SW-NE AND NW-SE DIRECTIONS. LANDSAT TM AND ETM+ DATA (NASA) WERE DOWNLOADED FROM HTTP://GLCF.UMD.EDU/DATA/LANDSAT/	39
FIG. 15 LEFT IMAGE: FAULTS DIGITIZED FROM THE GEOLOGIC MAP 1:50.000 (IGME); RIGHT: LINEAMENTS MAPPED USING REMOTE SENSING TECHNOLOGIES AND LANDSAT TM AD ETM+ DATA	40
FIG. 16 UPPER LEFT: EFFECTIVE COHESION (C') BEFORE TAKING INTO CONSIDERATION THE MAPPED LINEAMENTS; UPPER RIGHT: C' WITH THE EFFECT OF LINEAMENTS. BOTTOM: LEFT AND RIGHT THE RESPECTIVE FACTORS OF SAFETY CALCULATED FOR A 5M THICK SLIDING MASS UNDER “WET” CONDITIONS.....	41
FIG. 17 DIGITIZED TOPOGRAPHIC MAP OF SERRES PIA (LEFT) ON A HILLSIDE BACKGROUND. METEOROLOGICAL STATIONS (LABELS CORRESPOND TO THEIR ELEVATION) AND MEAN ANNUAL RAINFALL IN THE AREA (RIGHT)	43
FIG. 18 TS FACTOR (VALUE OF INFLUENCE OF SEISMIC INTENSITY).....	43
FIG. 19 SR FACTOR, RELATIVE RELIEF INDEX.....	44
FIG. 20 H_e LANDSLIDE HAZARD INDICATOR.....	44
FIG. 21 TOPOGRAPHIC MAP WITH ELEVATION POINTS (LEFT) AND SLOPE MAP (RIGHT) OF NYMFAIA PIA.....	45
FIG. 22 NYMFAIA PIA: MORA & VAHRSON METHOD LITHOLOGICAL SUSCEPTIBILITY FACTOR (S_e)	45
FIG. 23 NYMFAIA PIA: MORA & VAHRSON METHOD RELATIVE RELIEF INDEX (S_R)	46
FIG. 24 NYMFAIA PIA: MORA & VAHRSON METHOD LANDSLIDE HAZARD INDEX (H_L)	46
FIG. 25 LANDSLIDE SUSCEPTIBILITY UNDER STATIC CONDITIONS, FEMA METHOD, HAZUS MANUAL. SCALE: I (GREEN) LESS SUSCEPTIBLE; X (RED) MOST SUSCEPTIBLE	47
FIG. 27 LANDSLIDE SUSCEPTIBILITY FOR “WET” CONDITIONS (SERRES PIA)	48
FIG. 26 LANDSLIDE SUSCEPTIBILITY FOR “DRY” CONDITIONS (SERRES PIA).....	48
FIG. 29 LANDSLIDE SUSCEPTIBILITY FOR “WET” CONDITIONS (NYMFAIA PIA)	49
FIG. 28 LANDSLIDE SUSCEPTIBILITY FOR “DRY” CONDITIONS (NYMFAIA PIA)	49
FIG.30 CRITICAL ACCELERATION (A_c) AS A FUNCTION OF SLOPE AND GEOLOGIC GROUP (WILSON AND KEEFER, 1985)	50
FIG.31 CRITICAL ACCELERATION (A_c) FOR “DRY” CONDITIONS (SERRES PIA)	50
FIG. 33 CRITICAL ACCELERATION (A_c) FOR “DRY” CONDITIONS (NYMFAIA PIA).....	51
FIG. 32 CRITICAL ACCELERATION (A_c) FOR “WET” CONDITIONS (SERRES PIA)	51
FIG. 34 CRITICAL ACCELERATION (A_c) FOR “WET” CONDITIONS (NYMFAIA PIA)	52

FIG. 36 SHALLOW LANDSLIDE SUSCEPTIBILITY (A_d/PGA INDEX) UNDER SEISMIC “WET” CONDITIONS (SERRES PIA)	54
FIG. 35 SHALLOW LANDSLIDE SUSCEPTIBILITY (A_d/PGA INDEX) UNDER SEISMIC “DRY” CONDITIONS (SERRES PIA)	54
FIG. 38 SHALLOW LANDSLIDE SUSCEPTIBILITY (A_d/PGA INDEX) UNDER SEISMIC “WET” CONDITIONS (NYMFAIA PIA)	55
FIG. 37 SHALLOW LANDSLIDE SUSCEPTIBILITY (A_d/PGA INDEX) UNDER SEISMIC “DRY” CONDITIONS (NYMFAIA PIA)	55
FIG. 39 INTEGRATION OF ACCELEROGRAMS TO DETERMINE DOWNSLOPE DISPLACEMENTS (GOODMAN AND SEED, 1996).....	56
FIG. 40 RELATIONSHIP BETWEEN EARTHQUAKE MOMENT MAGNITUDE AND NUMBER OF CYCLES (HAZUS 99-SR2 TECHNICAL MANUAL, CHAPTER 4-PESH)	57
FIG. 41 RELATIONSHIP BETWEEN THE DISPLACEMENT FACTOR AND THE RATIO A_d/PGA (MAKDISI AND SEED, 1978)	57
FIG. 42 PERMANENT GROUND DISPLACEMENTS ($E[PGD]$ LOWER LIMIT, CALCULATED FOR “DRY” CONDITIONS ON SERRES PIA.....	58
FIG. 43 PERMANENT GROUND DISPLACEMENTS ($E[PGD]$ UPPER LIMIT, CALCULATED FOR “DRY” CONDITIONS ON SERRES PIA.....	58
FIG. 44 PERMANENT GROUND DISPLACEMENTS ($E[PGD]$ LOWER LIMIT, CALCULATED FOR “WET” CONDITIONS ON SERRES PIA.....	59
FIG. 45 PERMANENT GROUND DISPLACEMENTS ($E[PGD]$ UPPER LIMIT, CALCULATED FOR “WET” CONDITIONS ON SERRES PIA.....	59
FIG. 46 PERMANENT GROUND DISPLACEMENTS ($E[PGD]$ LOWER LIMIT, CALCULATED FOR “DRY” CONDITIONS ON NYMFAIA PIA.....	60
FIG. 47 PERMANENT GROUND DISPLACEMENTS ($E[PGD]$ UPPER LIMIT, CALCULATED FOR “DRY” CONDITIONS ON NYMFAIA PIA.....	60
FIG. 48 PERMANENT GROUND DISPLACEMENTS ($E[PGD]$ LOWER LIMIT, CALCULATED FOR “WET” CONDITIONS ON NYMFAIA PIA	61
FIG. 49 PERMANENT GROUND DISPLACEMENTS ($E[PGD]$ UPPER LIMIT, CALCULATED FOR “WET” CONDITIONS ON NYMFAIA PIA.....	61
FIG. 50 LEFT TO RIGHT: DEM, SLOPE AND ASPECT MAP OF SERRES PIA.....	64
FIG. 51 MECHANICAL PROPERTIES OF ROCKS MASSES CALCULATED USING THE HOEK & BROWN FAILURE CRITERION	65
FIG. 52 SPATIAL DISTRIBUTION OF MECHANICAL PROPERTIES OF ROCKS: C' (kN/m^2), Φ' ($^\circ$), UNIT WEIGHT (kN/m^3)	65
FIG. 53 NORMAL THICKNESS (Z) MAP THE AREA BASED ON THE “Z MODEL” (SAULNIER ET.AL, 1997), THE GEOLOGIC TYPE AND FIELD MEASUREMENTS.....	66
FIG. 54 SATURATION CLASSES (LEFT) AND SATURATION PERCENTAGE (RIGHT) FOR A SLIDING SLAB 5M THICK (SAGA GIS MODULE)	67
FIG. 26 SERRES PIA FACTOR OF SAFETY CALCULATED FOR EARTHQUAKE OF 475YRS RETURN PERIOD AND FOR A 1M NORMAL THICKNESS SLIDING SLAB ($z=1m$)	68
FIG. 55 SERRES PIA FACTOR OF SAFETY CALCULATED FOR PRECIPITATION OF 50YRS RETURN PERIOD AND FOR A FIVE METERS NORMAL THICKNESS SLIDING SLAB ($z=5m$).....	68
FIG. 58 SERRES PIA FACTOR OF SAFETY CALCULATED FOR EARTHQUAKE OF 100YRS RETURN PERIOD AND FOR A VARIABLE NORMAL THICKNESS SLIDING SLAB CALCULATED AS DESCRIBED IN PREVIOUS PARAGRAPHS.....	69
FIG. 57 SERRES PIA FACTOR OF SAFETY CALCULATED FOR PRECIPITATION OF 50YRS RETURN PERIOD AND FOR A VARIABLE NORMAL THICKNESS SLIDING SLAB CALCULATED AS DESCRIBED IN PREVIOUS PARAGRAPHS.....	69

FIG. 59 FACTOR OF SAFETY USING THE DETERMINISTIC MODEL FOR CIRCULAR LANDSLIDES, CALCULATED FOR A 10M HIGH SLOPE	71
FIG. 60 FACTOR OF SAFETY USING THE DETERMINISTIC MODEL FOR CIRCULAR LANDSLIDES, CALCULATED FOR A 20M HIGH SLOPE	71
FIG. 61 FACTOR OF SAFETY USING THE DETERMINISTIC MODEL FOR CIRCULAR LANDSLIDES, CALCULATED FOR A 30M HIGH SLOPE	72
FIG. 62 COMPARISON OF OUTPUTS FROM MORA AND VAHRSON METHOD (LEFT) TO FACTOR OF SAFETY METHOD (RIGHT) BASED ON THE INFINITE SLOPE MODEL IN PIA OF SERRES	74
FIG. 63 COMPARISON OF OUTPUTS FROM MORA AND VAHRSON METHOD (LEFT) TO FACTOR OF SAFETY METHOD (RIGHT) BASED ON THE INFINITE SLOPE MODEL IN PIA OF NYMFAIA	74
FIG. 64 COMPARISON OF OUTPUTS FROM FACTOR OF SAFETY METHOD FOR "WET" CONDITIONS, WITH A THICKNESS OF A SLIDING SLAB OF FIVE METERS (z=5M) ON NATURAL SLOPES IN PIA OF SERRES. THE BLACK CYCLES (RIGHT PART OF THE FIGURE) ARE LOCATIONS OF LANDSLIDES ON NATURAL SLOPES	75
FIG. 65 PREDICTION FROM FACTOR OF SAFETY METHOD FOR "WET" CONDITIONS, WITH A THICKNESS OF A SLIDING SLAB OF FIVE METERS (z=5M) ON NATURAL SLOPES IN PIA OF SERRES (LEFT CORNER) AND LANDSLIDES ON NATURAL SLOPES IN PIA OF SERRES	75
FIG. 66 PREDICTION OF FACTOR OF SAFETY METHOD FOR A RAINFALL OF 50 YEARS, WITH A SLIDING SLAB THICKNESS OF FIVE METERS (z=5M) ON NATURAL SLOPES IN NYMFAIA PIA WITHOUT (LEFT) AND WITH (RIGHT) FRACTURED/WEATHERED ZONES, LOCATED BY REMOTE SENSING TECHNIQUES USED. GRAY COLOR CORRESPONDS TO $F_s > 3$	77
FIG. 67 LOCATIONS ALONG THE VERTICAL ROAD AXIS FROM KOMOTINI - NYMFAIA TO HELLENIC-BULGARIAN, WHERE PREDICTED F_s VALUES HAVE BEEN EVALUATED BY IN-SITU OBSERVATIONS. GREEN COLORED CYCLES DENOTE SUCCESSFUL PREDICTION, WHILST PURPLE COLORED CYCLE REPRESENTS FAILED PREDICTION	78
FIG. 68 LOCATION NO1 ALONG THE VERTICAL ROAD AXIS FROM KOMOTINI - NYMFAIA TO HELLENIC-BULGARIAN, WHERE PREDICTED F_s VALUES ARE EVALUATED BY IN-SITU OBSERVATIONS.....	78
FIG. 69 LOCATION NO 2 ALONG THE VERTICAL ROAD AXIS FROM KOMOTINI - NYMFAIA TO HELLENIC-BULGARIAN, WHERE PREDICTED F_s VALUES ARE EVALUATED BY IN-SITU OBSERVATIONS.....	79
FIG. 70 LOCATION NO 3 ALONG THE VERTICAL ROAD AXIS FROM KOMOTINI - NYMFAIA TO HELLENIC-BULGARIAN, WHERE PREDICTED F_s VALUES ARE EVALUATED BY IN-SITU OBSERVATIONS.....	79
FIG. 71 THE TOTAL NUMBER OF CUT SLOPES (O1 TO O36) ALONG THE VERTICAL ROAD AXIS FROM KOMOTINI - NYMFAIA - HELLENIC/BULGARIAN BORDERS (NYMFAIA PIA)	81
FIG. 72 LOCATION OF THE EXAMINED CUT SLOPE O5	82
FIG. 73A LOCATIONS OF THE EXAMINED CUT SLOPES O14-15 AND O16	84
FIG. 73B LOCATION OF CUT SLOPE O21	86
FIG. 74 LOCATION OF CUT SLOPE O32, CLOSE TO HELLENIC-BULGARIAN BORDERS	87
FIG. 75 PHOTO DURING EXCAVATION OF CUT SLOPE O5	91
FIG. 76 2D ANALYSIS RESULTS (FACTOR OF SAFETY) FROM GSTABL7 WITH STEDWIN SOFTWARE WITHOUT ANY STABILIZATION MEASURES.....	93
FIG. 77 2D ANALYSIS RESULTS FROM GSTABL7 WITH STEDWIN SOFTWARE WITH THE USE OF STABILIZING MEASURES (PASSIVE ANCHORS).....	95
FIG. 78 PHOTO OF THE CUT SLOPE O14-O15 DURING EXCAVATION	96
FIG. 79 2D ANALYSIS RESULTS FROM GSTABL7 WITH STEDWIN SOFTWARE WITHOUT MEASURES	98

FIG. 80 2D ANALYSIS RESULTS FROM GSTABL7 WITH STEDWIN SOFTWARE WITH REINFORCING - STABILIZING MEASURES.....	99
FIG. 81 PHOTO OF O16 CUT SLOPE DURING EXCAVATION	100
FIG. 82 2D ANALYSIS RESULTS FROM GSTABL7 WITH STEDWIN SOFTWARE WITHOUT ANY REINFORCING - STABILIZING MEASURES.....	102
FIG. 83 PHOTO OF CUT SLOPE O21 DURING EXCAVATION (PART A)	103
FIG. 83 2D ANALYSIS RESULTS FROM GSTABL7 WITH STEDWIN SOFTWARE WITHOUT MEASURES (PART A)	106
FIG. 84 2D ANALYSIS RESULTS FROM GSTABL7 WITH STEDWIN SOFTWARE WITHOUT MEASURES (PART B)	107
FIG. 85 2D ANALYSIS RESULTS FROM GSTABL7 WITH STEDWIN SOFTWARE WITH MEASURES (PART A)	108
FIG. 86 PHOTO OF CUT SLOPE O32 DURING CONSTRUCTION	109
FIG. 86 2D ANALYSIS RESULTS FROM GSTABL7 WITH STEDWIN SOFTWARE ON CUT SLOPE O32 WITHOUT ANY MEASURES	111
FIG. 87 PHOTO OF THE SLOPE ANALYZED IN SERRES PIA.....	112
FIG. 88 2D ANALYSIS RESULTS FROM GSTABL7 WITH STEDWIN SOFTWARE FOR A SLOPE AT SERRES PIA.....	114
FIG. 89 GEOMETRY OF THE MODEL PRESENTED IN FLAC 3D PLOT WINDOW TO EVALUATE THE INFLUENCE OF SLOPE CURVATURE	116
FIG. 90 DISPLACEMENT CONTOURS AND SAFETY FACTOR IN FLAC 3D MODEL AT THE FAILURE STATE	117
FIG. 91 GEOMETRY OF THE MODEL PRESENTED IN FLAC 3D PLOT WINDOW TO EVALUATE THE INFLUENCE OF SLOPE CURVATURE	118
FIG. 92 DISPLACEMENT CONTOURS AND SAFETY FACTOR IN FLAC 3D MODEL AT THE FAILURE STATE	120
FIG. 93 CREATING THE FRAME OF THE MODEL	121
FIG. 94 COVERING THE FRAME OF THE MODEL WITH SURFACES.....	121
FIG. 95 THE MODEL IN THE FINAL STAGE	122
FIG. 96 THE CUT SLOPE AS BUILT IN PRESENT.....	122
FIG. 97 KUBRIX GEO VER. 15 (A MESH GENERATOR FOR FLAC 3D SOFTWARE)	123
FIG. 98 GEOMETRY OF THE MODEL PRESENTED IN FLAC 3D PLOT WINDOW.....	124
FIG. 99 DISPLACEMENT CONTOURS IN FLAC 3D MODEL	125
FIG. 100 DISPLACEMENT CONTOURS AND SAFETY FACTOR IN FLAC 3D MODEL AT FAILURE STATE	126
FIG. 101 DISPLACEMENT CONTOURS AND SAFETY FACTOR IN FLAC 3D MODEL AT THE FAILURE STATE	127
FIG. 102 RETURN PERIOD VERSUS DAILY RAINFALL AMOUNT FOR TEKIRDAG REGION BASED ON VEN TE CHOW (1953) METHOD	132
FIG. 103 RETURN PERIOD VERSUS DAILY RAINFALL AMOUNT FOR SAMSUN REGION BASED ON VEN TE CHOW (1953) METHOD	132
FIG. 104 RAINFALL FREQUENCY ANALYSIS WITH RESPECT TO ANNUAL MAXIMA OF RAINFALL DEPTH FOR TEKİRDAĞ REGION (VEN TE CHOW, 1953)	139
FIG. 105 RAINFALL FREQUENCY ANALYSIS WITH RESPECT TO ANNUAL MAXIMA OF RAINFALL DEPTH FOR SAMSUN REGION (VEN TE CHOW, 1953)	139
FIG. 106 A TYPICAL SECTION OF SLOPE AND SHEAR STRENGTH VARIATION WITH DEPTH.....	142
FIG. 107 N1 VS B (SLOPE ANGLE)	143
FIG. 108 FLOW CHART OF THE ANALYSIS.....	144

FIG. 109 TEKIRDAG CITY CENTER GEOLOGY MAP	145
FIG. 110 THE SLOPE MAP OF THE TEKIRDAG CITY CENTER.....	146
FIG. 111 MICROZONATION OF TEKIRDAG CITY CENTER BY MONTGOMERY & DIETRICH (1994).....	147
FIG. 112 MICROZONATION OF TEKIRDAG CITY CENTER BY MORA AND VAHRSON (1994)	147
FIG. 113 MICROZONATION OF TEKIRDAG CITY CENTER BY FEMA METHOD (DRY CONDITION).....	148
FIG. 114 MICROZONATION OF TEKIRDAG CITY CENTER BY FEMA METHOD (WET CONDITION).....	148
FIG. 115 MICROZONATION OF TEKIRDAG CITY CENTER BY SIYAHİ AND ANSAL (1993)	149
FIG. 116 SAMSUN CITY CENTER GEOLOGY MAP.....	150
FIG. 117 THE SLOPE MAP OF SAMSUN CITY CENTER.....	151
FIG. 118 MICROZONATION OF SAMSUN CITY CENTER BY MONTGOMERY AND DIETRICH (1994)	152
FIG. 119 MICROZONATION OF THE SAMSUN CITY CENTER BY MORA AND VAHRSON (1994)	152
FIG. 120 MICROZONATION OF SAMSUN CITY CENTER BY FEMA METHOD (DRY CONDITION)	153
FIG. 121 MICROZONATION OF SAMSUN CITY CENTER BY FEMA METHOD (WET CONDITION)	154
FIG. 122 TEKIRDAG PROVINCE GEOLOGICAL MAP.....	155
FIG. 123 THE SLOPE MAP OF THE TEKIRDAG REGION.....	156
FIG. 124 MICROZONATION OF THE TEKIRDAG REGION BY MONTGOMERY AND DIETRICH (1994)	157
FIG. 125 MICROZONATION OF THE TEKIRDAG REGION BY MORA AND VAHRSON (1994)	158
FIG. 126 MICROZONATION OF TEKIRDAG REGION BY FEMA METHOD (DRY CONDITION).....	159
FIG. 127 MICROZONATION OF TEKIRDAG REGION BY FEMA METHOD (WET CONDITION).....	160
FIG. 128 MICROZONATION OF THE TEKIRDAG REGION BY SIYAHİ AND ANSAL (1993)	161
FIG. 129 SAMSUN PROVINCE GEOLOGICAL MAP	162
FIG. 130 THE SLOPE MAP OF THE SAMSUN REGION	163
FIG. 131 MICROZONATION OF SAMSUN REGION BY MONTGOMERY AND DIETRICH (1994)	165
FIG. 132 MICROZONATION OF SAMSUN REGION BY MORA AND VAHRSON (1994).....	165
FIG. 133 MICROZONATION OF SAMSUN REGION BY FEMA METHOD (DRY CONDITION)	166
FIG. 134 MICROZONATION OF SAMSUN REGION BY FEMA METHOD (WET CONDITION)	167
FIG. 135 MICROZONATION OF THE SAMSUN REGION BY SIYAHİ AND ANSAL (1993)	168
FIG. 136 MAP OF BLACK SEA COAST ACCORDING TO SLOPE FACTOR S_R	171
FIG. 137 MAP OF BLACK SEA COAST ACCORDING TO LITHOLOGICAL FACTOR S_L	172
FIG. 138 MAP OF BLACK SEA COAST ACCORDING TO MOISTURE (HUMIDITY) FACTOR S_H	173
FIG. 139 MAP OF BLACK SEA COAST ACCORDING TO PRECIPITATION TRIGGERING FACTOR T_p	174
FIG. 140 MAP OF BLACK SEA COAST ACCORDING TO SEISMICITY TRIGGERING FACTOR T_s	175
FIG. 141 MAP OF BLACK SEA COAST ACCORDING TO EROSION/ABRASION TRIGGERING FACTOR T_E	176
FIG.142 LANDSLIDE SUSCEPTIBILITY MAP OF THE BULGARIAN BLACK SEA COAST ACCORDING TO THE METHOD OF MORA AND VAHRSON (1993).....	179

FIG. 143 LANDSLIDE SUSCEPTIBILITY MAP OF TSAREVO AREA AND BULGARIAN BLACK SEA COAST, ACCORDING TO THE METHOD OF MORA AND VAHRSON (1993)	180
FIG. 144 FLOW CHART OF METHODS FOR LANDSLIDE SUSCEPTIBILITY EVALUATION	182
FIG. 145 LOESS DISTRIBUTION IN EUROPE. LOESS DISTRIBUTION IS RELATED TO THE FORMER EXTENT OF ICE SHEETS AND THE DISTRIBUTION OF MAJOR RIVER SYSTEMS (SMALLEY ET AL., 2009)	184
FIG. 146 LOCATION OF THE MOST IMPORTANT LOESS - PALAEO SOIL SECTIONS IN THE ROMANIAN PLAIN AND DOBROGEA (ROMANIA)	185
FIG. 147 GRAIN-SIZE TYPES OF LOESS DEPOSITS REPRESENTING THE PARENTAL SOURCE OF THE MODERN SOIL IN DOBROGEA. FROM CONEA (1970b)	186
FIG. 148 THE DOBROGEA REGION	189
FIG. 149 TECTONIC UNITS	190
FIG. 150 METHODOLOGY TO LHA MAP UNDER ARCGIS	191
FIG. 151 DEM AND SLOPE MAP FOR THE INVESTIGATED AREA	192
FIG. 152 F_5 MAP FOR 1M (LEFT) AND 5M (RIGHT) THICKNESS OF THE FAILURE SLAB UNDER SATURATED CONDITION	194
FIG. 153 FS MAP FOR 10M (LEFT) AND 50M (RIGHT) THICKNESS OF THE FAILURE SLAB UNDER SATURATED CONDITION	195
FIG. 154 PILOT AREA FOR LANDSLIDE HAZARD EVALUATION (DURLESTI VILLAGE)	198
FIG. 155 DEM FOR PILOT STUDIED AREA	199
FIG. 156 PERCENTAGE DISTRIBUTION OF SLOPE ANGLES (GRAD)	199
FIG. 157 GEOLOGICAL MAP OF STUDIED AREA (PILOT AREA IS INDICATED BY QUADRAT)	201
FIG. 158 THE DEM IN THE COMPARISON WITH GEOLOGICAL LAYERS	201
FIG. 159 ANNUAL PRECIPITATION DISTRIBUTION IN CENTRAL MOLDOVA (STATE HYDRO METEOROLOGICAL SERVICES OF MOLDOVA)	202
FIG. 160 THE MAP OF SEISMIC ZONING OF REPUBLIC OF MOLDOVA	204
FIG. 161 THE MAP OF SLOPE FACTOR OF SOUTHERN UKRAINE	209
FIG. 162 THE MAP OF GEOLOGY FACTOR OF SOUTHERN UKRAINE	210
FIG. 163 THE MAP OF SEISMIC TRIGGERING FACTOR OF SOUTHERN UKRAINE	213
FIG. 164 THE MAP OF PRECIPITATION TRIGGERING FACTOR OF SOUTHERN UKRAINE	214
FIG. 165 THE RESULTANT MAP OF LANDSLIDE HAZARD OF SOUTHERN UKRAINE	215

LIST OF TABLES

Table 1 Soil amplification factors according to geologic formations and spectral acceleration Hazus 99-SR2 Technical Manual, Chapter 4-PESH).....	53
Table 2 Corrected Relative Relief	134
Table 1 Classification of the lithological influence according to the general conditions, representative for Central America.	135
Table 2 The classes of average monthly precipitation.	136
Table 3 Weighting for annual precipitation.	136
Table 4 The influence of seismic intensity (Modified Mercalli Scale) as a triggering factor for landslide generation	137
Table 5 The influence of rainfall precipitation intensity as a triggering factor for landslides.....	138
Table 6 The influence of rainfall precipitation intensity as a triggering factor for landslides.....	138
Table 7 Landslide susceptibility classification according to the FEMA method – HazUS99-SR2, Technical Manual, Chapter 4-PESH, 1999)	141
Table 9 Slope factor scores (Mora and Vahrson, 1994).....	171
Table 10 Lithology factor criteria, classification and scores.....	172
Table 11 Classification of landslide hazard H.....	177
Table 12 Classification of landslide hazard H.....	177
Table 13 Geotechnical parameters of loess.....	188
Table 14 Geotechnical parameters for the principal lithological groups.....	193
Table 15 Slope factor classification.....	198
Table 16 Slope factor classification.....	208
Table 17 Geology factor classification.....	209
Table 18 Average monthly rainfall values classification	211
Table 19 Moisture factor (Sh) from accumulated AMP values	211
Table 20 Seismic Intensity factor	212
Table 21 Precipitation factor (Tp) originating from the classification of maximum daily precipitations over a return period of 100yrs. An auxiliary classification based on the average yearly maximum values per day is given in column 2.....	214
Table 22 Classification of the Landslide Hazard HI parametric values.	215
Table 23 Geotechnical parameters for Samsun Region	272
Table 24 Geotechnical parameters for Samsun Region (Cont’ d).....	273
Table 25 Geotechnical parameters for Samsun Region (Cont’ d).....	274
Table 26 Geotechnical parameters for Tekirdag Region.....	275

1 Background of the document

1.1 General Note

Pilot implementation on regional and on local scale actions, fall into the GA.3 “Pilot Implementation on Regional and on Local Scales”; started for all types of hazards on March 2014 and ended at the end of October 2015 (instead the end of August) in order to have time to evaluate the outputs and complete the respective reports.

Responsible for the Landslide Hazard Implementation activities was partner P1 (Democritus University of Thrace). All partners, to the exception of P2 (as foreseen in the GAF) have contributed.

1.2 Scope and Objectives

Pilot implementation for LHA were scheduled and implemented by all partners in their respective Pilot Implementation Areas (PIA), in order to evaluate the outputs of the selected methods and their adaptability to specific conditions. Evaluation is based on comparison of their outputs to actual facts and on assessing their dissemination potential in order to promote their use by the project’s stakeholders (administration staff members, scientific community, engineers, geologists, planners etc.).

An additional target is the development of flood hazard maps which can be used by the State Regional and Local Administration to support strategic planning for flood disaster prevention.

1.3 Related Documents

1.3.1 Input

List of former deliverables acting as inputs to this document

Document ID	Descriptor
--------------------	-------------------

1.3.2 Output

List of other deliverables for which this document is an input.

Document ID	Descriptor
-------------	------------

2 LANDSLIDE HAZARD ASSESSMENT ON A REGIONAL SCALE - PILOT IMPLEMENTATIONS IN GREECE

2.1 Introduction

Landslide Hazard Assessment on a regional scale can provide useful information which when combined with a preliminary risk assessment can support decision regarding strategic planning for disaster prevention. Landslide Hazard maps can be used to assess the potential risks, prioritize areas in terms of the necessity to apply preventive measures and plan local investigations (slope stability analyses) which require a more detailed planning for funding and implementation. Such a strategic planning can provide the State Regional and local administration with the tool to effectively plan Landslide disaster mitigation measures in both their financial and technical aspects.

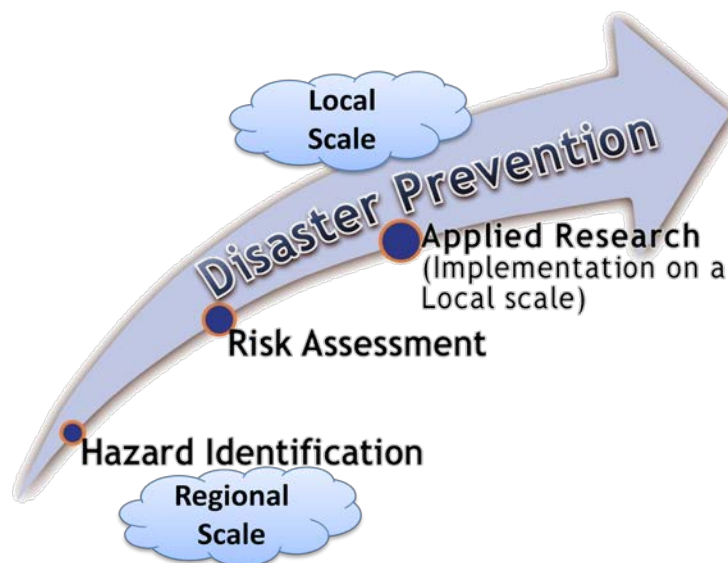


Fig. 1 A schematic representation of Landslide Disaster Prevention actions

The accuracy in locating areas of a high landslide Hazard and the reliability of detecting them are of high importance since this information will be the basis for effective planning.

Numerous methods exist for assessing Landslide Hazard on regional scales each with its own advantages and disadvantages. The multitude of methods used results into non comparable outputs, a fact which especially in cross-border areas forms a block for cross-border cooperation. One of the basic targets of the SciNetNatHaz-Prevention project is the harmonization of methods for Landslide

Hazard Assessment (LHA) taking into consideration the existing status in countries around the Black Sea: lack of accessible landslide inventories, lack of data and meta-data, restricted budgets available for research and investigation.

Within this context, project partners have decided to suggest feasible LHA methods, in order to develop a harmonized basis of communication for this specific issue across the Black Sea area countries.

Three different methodological approaches for LHA have been selected; all of them scientifically recognized and used internationally. Implementation of these methods is feasible under the current circumstances as these were described above so, their adaptability to specific conditions, their reliability and accuracy in mapping areas of a high landslide hazard needs to be once more verified, by pilot implementations in the BSB JOP 2007-13 programme eligible area.

Pilot implementation for LHA were therefore scheduled and implemented by all partners in order to verify the outputs of the selected methods, to assess their adaptability to specific conditions and to evaluate them by comparing their outputs to actual facts; usually landslides recorded in the field as landslide inventories are not accessible for most of the participant countries.

Pilot implementation on regional scale actions fall into the GA.3 “Pilot Implementation on Regional and on Local Scales”; started for all types of hazards on March 2014 and ended at the end of August 2015.

2.2 Problems in Assessing Landslide Hazard - Methods Implemented

As already concluded in previous project documents (D.01.02), the main problems in designing preventive measures to reduce risk from Landslides include:

- Landslide inventories are lacking. Even if such inventories exist, they are inaccessible.
- Usable data are lacking. Even if data (i.e. recordings of past landslides, geotechnical parameters of geologic formations, etc) are found, they are not usable since there are no metadata, so the evaluation of their accuracy and reliability is impossible compromising their potential use.
- Systematic Landslide Hazard on Regional and on Local scales in order to locate the problems and define prevention measure design parameters, have only been sparsely implemented.

- An additional problem especially in cross-border areas where there is a need for cooperation, is the use of various methods by scientists making comparison of outputs impossible and cooperation to find common solutions to common problems, very difficult.

In order to tackle the problems indicated, the SciNetNatHaz proposal and related actions as defined by the project partners, include:

- The selection of widely accepted and used, scientifically sound methods to assess LH on regional scales. The finally selected methods should be applicable in the wider Black Sea area, considering the existing restrictions and problems.
- Adapting the LHA methods to regional conditions in respect to the pilot implementation areas (PIA).
- Evaluation of the selected methods in terms of their “applicability”, adaptability, ease of use and reliability and accuracy of results with pilot implementations in selected areas within the projects eligible area.
- To produce metadata according to the INSPIRE directive and to provide free access to data and outputs produced to the scientific and the technical communities.

After an extensive review of available LHA methods used worldwide (D.01.02), the project partners concluded (D.01.02) to testing the following:

- A. The method proposed by Mora & Vahrson (1994): Macrozonation Method for Landslide Hazard determination. Bulletin of the Association of Engineering Geologists, Vol. XXXI No.1, 1994, pp.49-58.
- B. The method proposed and used for LHA by the Federal Emergency Management Agency of the USA widely known as HazUS (<http://www.fema.gov/hazus>) and
- C. The LHA based on the calculation of Factor of Safety (Fs) using the Infinite Slope Model (ISM) for planar and the Deterministic Method for circular landslides.

The data requirements for applying those LHA methods include:

- A. LHA on a Regional Scale
 - Digitized Topographic Maps and elevation points (scale 1:50.000, contour interval 20m)
 - Digitized Geologic Maps (faults and dip and dip direction of geologic planes was also digitized)
 - Rainfall data (30 years time series, when available)

- Ground Motion: Peak Ground Acceleration for 100, 200, 475 and 1000 years mean return period)
- The Geological Strength Index – GSI (Marinos & Hoek, 1995; Marinos et al., 2005)
- All raster files were created with 15x15m pixel size.

B. LHA on a Local Scale

- Topographic Maps of a 1:500 scale (contour interval 1m for plan view maps) and cross-sections at a 1:200 scale
- Detailed geologic map of the specific location
- Engineering properties of geologic formations

All the above parameters were harmonized and incorporated into a Geographic Information System (GIS) developed for each Pilot Implementation Area (PIA). The Coordinate Reference System used to produce the outputs for each of the PIAs fits the National GRS of the respective country since these outputs have been presented in the Open Seminars that took place on October 2015 , with the scope of transferring competencies to State Authorities and building the capacity of the respective public bodies, to prevent landslide disasters.

In PIAs within the Hellenic territory, the Hellenic Geodetic Reference System 1987 (HGRS 87 or GGRS 87) was used in order for the produced maps to be readily available to Hellenic authorities and scientific community. It must be noted though that the data and outputs produced are also available in any of the existing Coordinate/Geodetic Reference Systems including the WGS 84 and the ETRS 89. In fact, all produced data and outputs will be available through the projects WebGIS platform using the WGS84 GRS.

2.3 Scope

Pilot implementation for LHA were scheduled and implemented by all partners their respective Pilot Implementation Areas (PIA) in order to evaluate the outputs of the selected methods, to assess their adaptability to specific conditions, to evaluate them by comparing their outputs to actual facts and to assess their dissemination potential in order to promote their use by the project’s stakeholders (Administration staff members, scientific community, engineers, geologists, planners etc).

An additional target is the development of landslide hazard maps which can be used by the State Regional and Local Administration to support strategic planning for landslide disaster prevention.

2.4 Activities

Implementation comprised of research activities and field work.

Research activities included:

- i) Review and analysis of published scientific research regarding landslide hazard assessment methods in order to select the ones that are feasible to implement without compromising reliability and accuracy of their outputs. Review also focused on the geologic and tectonic conditions of the PIA.
- ii) Evaluation of outputs by comparing them to actual facts.
- iii) Tectonic mapping using Remote Sensing techniques and Landsat TM & ETM+ data.
- iv) Calculation of the engineering properties of rock (rock mass strength analysis) using the generalized Hoek-Brown failure criterion.

Field work comprised of:

- i) Engineering geological surveys to record the respective characteristics of the geologic formations in the area.
- ii) Mapping of landslides.
- iii) Surveying in Serres PIA, in natural & cut slopes indicated as “High Landslide Hazard” by the regional LHA, in order to prepare large scale (1:250) topographic maps in order to apply slope stability analyses.

Office work included:

- i) Preparation of required digitized data (topographic and geologic maps, rainfall data, etc)
- ii) The development of a GIS to incorporate, analyze and further process the data, and
- iii) Application of the selected LHA models and production of the respective cartographic material (various maps, tables, graphs etc)
- iv) Evaluation of outputs by comparing them to actual landslides recorded in the field.

Hardware and software used

- v) A high performance Toshiba laptop, purchased in order to
 - a. cover the very high processing requirements both in the office, given the facts of the very large areas covered and the demand for high resolution outputs that can be readily applicable and

- b. in situ processing in order to reduce time in the field and the respective costs.
- vi) A field data collection device, water and dust proof, to measure all required parameters (geological planes, geotagged photos, database for data collection etc), store and deliver data to the GIS in real time.
- vii) Open Source GIS software including Quantum GIS (QGIS), SAGA GIS and Multispec[®].

2.5 Serres Pilot Implementation Area

Serres Pilot Implementation Area (PIA) covers a total area of approximately 495km² in the eastern part of Kentriki Makedonia (Central Macedonia), Hellas (Fig.2).

This specific PIA was selected for many reasons including:

- i) its proximity to the Lead Beneficiary basis; a fact that limits the costs of field work and implementation time;
- ii) its great importance for communication (transportation routes) of the border areas of Greece with the main urban centers of the area as well as the communication of Northern Greece and Bulgaria (transportation routes linking Kentriki Makedonia and Serres regional administration unit to Ilinden-Eksochi, Blagoevgrad);
- iii) the multitude of geologic formations outcropping in the area with varying engineering geological attributes and geotechnical behavior;
- iv) the presence of numerous landslides in certain parts of the area.

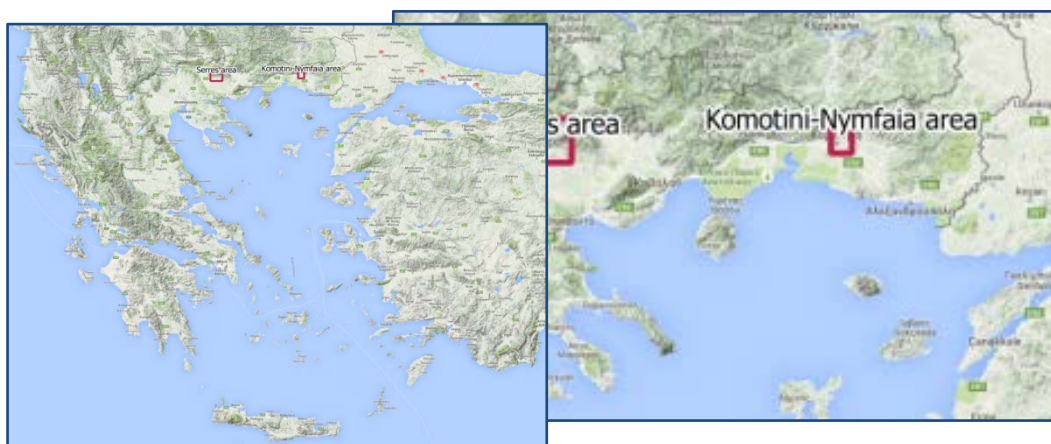


Fig. 2 Landslide Hazard Assessment Pilot Implementation Areas: Serres and Komotini-Nymfaia, Greece

2.5.1 Geomorphology

The natural processes that shape the morphology of an area, are closely linked to the geotechnical behavior of its geologic formations and therefore to the event of slope failures and intense erosion phenomena. In that aspect, the examination of the morphological characteristics of an area provides information regarding the processes of weathering and erosion related phenomena and helps estimating the expected geotechnical behavior of the outcropping geologic formations.

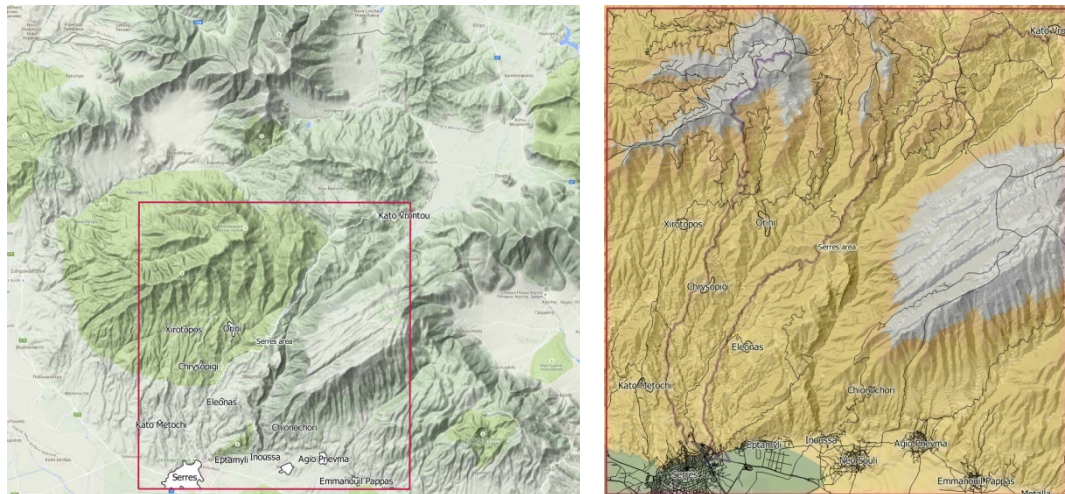


Fig. 3 Serres Pilot Implementation Area (PIA). A complex morphology is evident by steep slopes and abrupt slope changes in most of the area

The lowermost part of the area presents morphology with elongated hills having a N-S direction. In all natural slopes of this area there are indications of strong erosion processes leading to badland topography in certain cases.



Fig. 4 Intense erosional processes on natural slopes of the lowermost part of Serres PIA

The upper half of the Serres PIA presents an intense morphology, with high and steep natural slopes ranging from 25 to 50°.

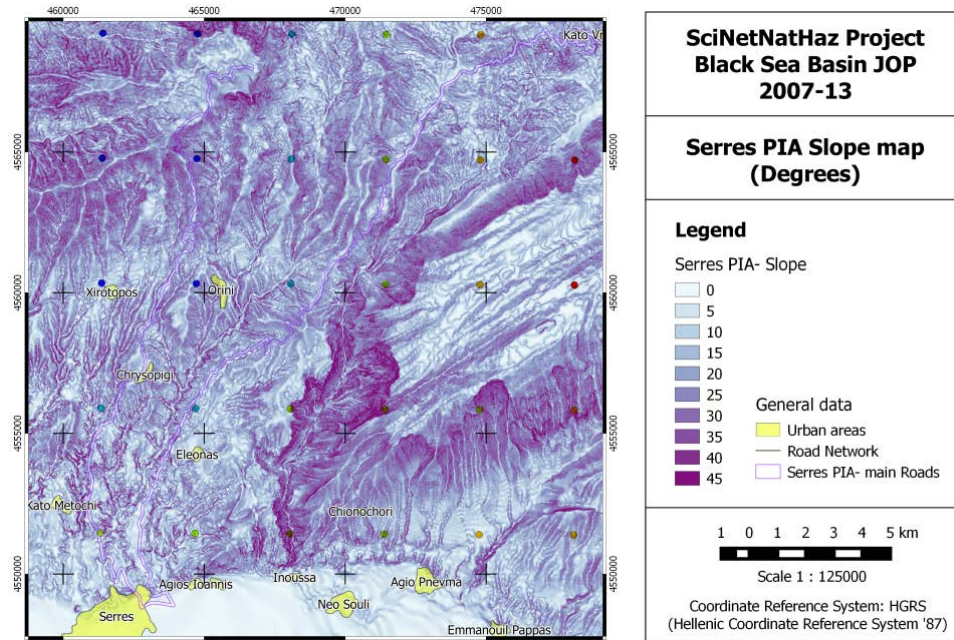


Fig. 5 Serres PIA natural slopes map

Serres PIA geological structure consists of Quaternary deposits which cover the metamorphic rocks of Rodopi massif and magmatic intrusions (granites). The presence of soil formations rich in clayey minerals, the presence of conglomerates with clayey cementing material which are extremely erodible, the intense tectonism of metamorphic and igneous rocks evident by plastic deformation and intense fracturing create an unfavorable geologic environment in respect to natural slope stability.

Intense tectonism of rocks combined with the presence of a thin (up to 1.5m), loose eluvia mantle and the action of surface and ground water cause numerous instability phenomena of limited extend, on the natural slopes of the area. Those natural slope failures are mainly slab slides and rock falls (limited extend failures), but there are also large circular slides especially within the conglomerates.

The intensive erosion phenomena abundant in the Miocenic and Quaternary formations of the area, are indicative of the mechanical characteristics of those formations and of their geotechnical behavior.

2.5.2 Engineering geologic mapping

The geotechnical behavior of the geologic formations with respect to landslide hazard depends on their natural properties, their mechanical characteristics and the presence of water. In order to better assess or even define the aforementioned parameters, an engineering geologic reconnaissance of the area was carried out.

Field work conducted, included engineering geologic mapping, systematic measurements of the orientation of geologic planes (schistosity, bedding, joints) especially along the major axes of the road network.

Engineering Geologic field work followed a remote sensing investigation in order to verify its results but also to take advantage of its respective findings. Areas, especially along major road axes, were investigated in order to evaluate the condition of the geologic formations in respect to weathering (degree, depth of weathered zone, nature of weathered material etc), to investigate the presence and depth of water, and to map landslides occurring in various parts of the PIA. Data collected were transferred to the GIS, they were processed, analyzed and used as input to apply the various LHA models.

A mixed team of experts including engineering geologists, civil engineers, remote sensing experts and surveyors coming from the LB and P1 teams were involved in this whole process.

In brief, the geologic formations outcropping in Serres PIA can be seen in the following geologic map of the area:

Neogene formations: Recent formations including the eluvial mantle, alluvial formations, alluvial fans, colluviums, talus cones, scree and terrestrial unconsolidated deposits in river/stream beds (torrential and fluvio-torrential deposits, terrace systems). These are loose formations comprising of clays and larger particle sized material (sand, gravel etc). In general, they are considered as permeable formations up to at least a depth of a few meters (5-6m).

Neogene formations are permeable and possess a high clay content. The presence of water affects negatively their geotechnical behavior. The presence of a permeable eluvial mantle which covers the theoretically impermeable metamorphic and igneous rocks of the area, causes the development of an unconfined superficial aquifer which is evident in many cut slopes along the local road network. Rainwater percolates through the eluvial mantle and flows along the contact of the less fractured

and weathered rock masses with the intensely fractured and weathered zone, reducing the mechanical properties of the materials and worsening their geotechnical behavior.

Miocenic deposits consist of clayey, sandy formations and conglomerates. Those formations include sandstones, clays and marls, conglomerates with varying cementing material (especially clayey), marine beds and lacustrine formations. These are in general, partially permeable or impermeable low strength formations due to the presence of clayey material.

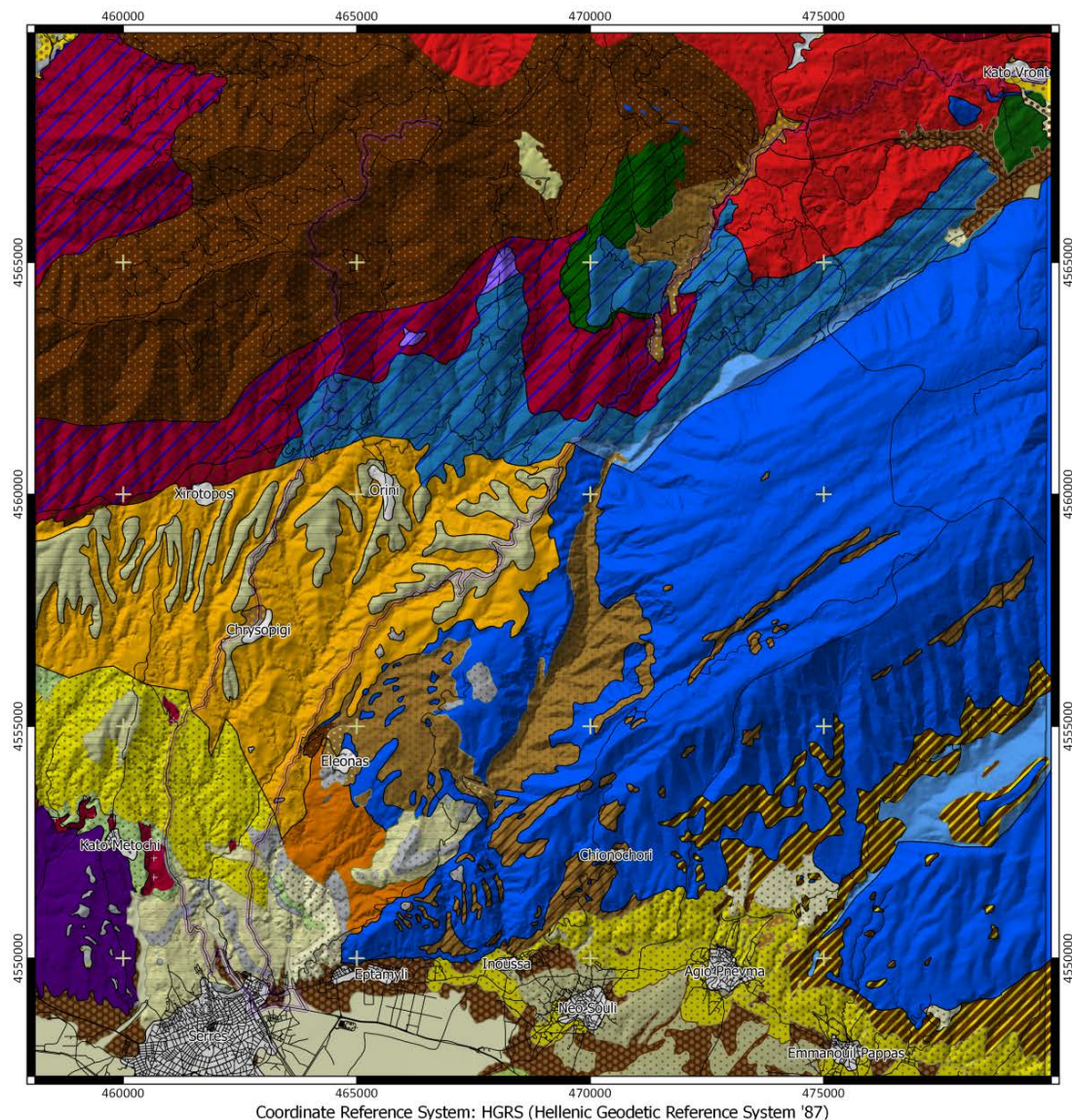
Miocenic formations (marls, conglomerates, sandstones) are erodible formations due to the presence of clay. Intense erosion in the natural slopes of streams in the area has created in many locations a “badland” topography. In areas where thick layers of conglomerates outcrop, slope failures including rock falls due to erosion of the cementing material, planar and circular landslides are abundant.

Gneisses and schists: a variety of gneisses, interchanging to mica schists or calcite schists (usually appear forming a transition zone between gneisses and marbles). These are intensely stressed and strained formations with permanent deformations evident by numerous folds and fractures. Weathering degree and schistosity of these formations largely affects their geotechnical behavior. Schistosity orientation combined with the orientation of natural and cut slopes, can be used to foresee failures in slopes due to shearing parallel to schistosity planes.

Amphibolites: low weathering degree, high strength, impermeable formations. Permeability depends on the degree of fracturing and is restricted up to a depth of a few meters (1-2m).

Marbles: High strength, highly permeable formations due to fracturing and carstic weathering.

Igneous rocks (granites, granodiorites and monzonites): very high strength, impermeable formations. Their mechanical (geotechnical) behavior strongly depends on weathering, fracturing and upon the orientation of joints as compared to the orientation of the natural and cut slopes.



SciNetNatHaz Project - Black Sea Basin JOP 2007-13

Geologic Map

Legend

Geologic Formations

- Alluvial formations
- Elouval mantle 1
- Elouval mantle 2
- Talus cones (2)
- Aluvial fans
- Talus cones (1)
- Torrenial deposits (sand, gravel, clay)
- Fluvio-torrenial deposits
- Torrenial-terrestrial deposits (conglomerates)
- Upper terrace system
- Middle terrace system
- Lower terrace system
- Sandstones, marles and organic limestones
- Clays, marls with sandy material and soft sandstones

- Sandstones, conglomerates
- Lacustrine-terrestrial formations (1)
- Lacustrine-terrestrial formations (2)
- Lacustrine-torrenial formation of Skala
- Lacustrine deposits
- Upper fine-grained lignite-bearing beds
- Sand, clays, clayey formations
- Marine beds of Metochi
- Lower torrenial beds (conglomerates)
- Terrestrial formation (breccio-conglomerates)
- Conglomerates, sandstones, clayey formations
- Red clays with loose conglomerate beds
- Marbles (thin layered)
- Marbles
- Gneissoid Monzonite
- Gneisses, Schists

- Gneisses, Marbles
- Gneisses, Amphibolites, Schists
- Gneisses, Amphibolites
- Schists
- Marbles (thin layered)
- Mica Schists
- Schists, Gneisses
- Granodiorite-quartz monzonite
- Gneissoid Granite
- Granite 1
- Granite 2
- Granodiorite-quartz monzonite brecciated
- Gneissoid quartz Monzonite
- Mylonitized quartz Monzonite-granite

General data

- Urban areas
- Serres PIA- main Roads
- Road Network

Map Scale 1 : 85.000

Fig. 6 Geologic Map of Serres Pilot Implementation Area (PIA)

2.5.3 Updating Serres PIA tectonic regime

Rock masses outcropping in Serres PIA appear to be badly fractured. The spatial distribution of the degree/density rocks in the area are fractured varies greatly within the PIA, making the reliable and accurate evaluation of the mechanical characteristics of the geological formations a very difficult task. Weathering is another process that plays an important role in the geotechnical behavior of the geologic formations and weathering processes are also greatly affected by fracturing. Inability to better define those factors renders any attempt to assess landslide hazard on a regional scale and provide accurate and reliable results, almost impossible. For those reasons, any assessment attempted may be from very accurate in the case of no fractured zones present in rocks, to very inaccurate in the opposite case. Thus, the tectonic regime of the area plays a very important role along with the geology in the, as accurate as possible, evaluation of the geotechnical behavior of rocks and the respective assessment of landslide hazard.

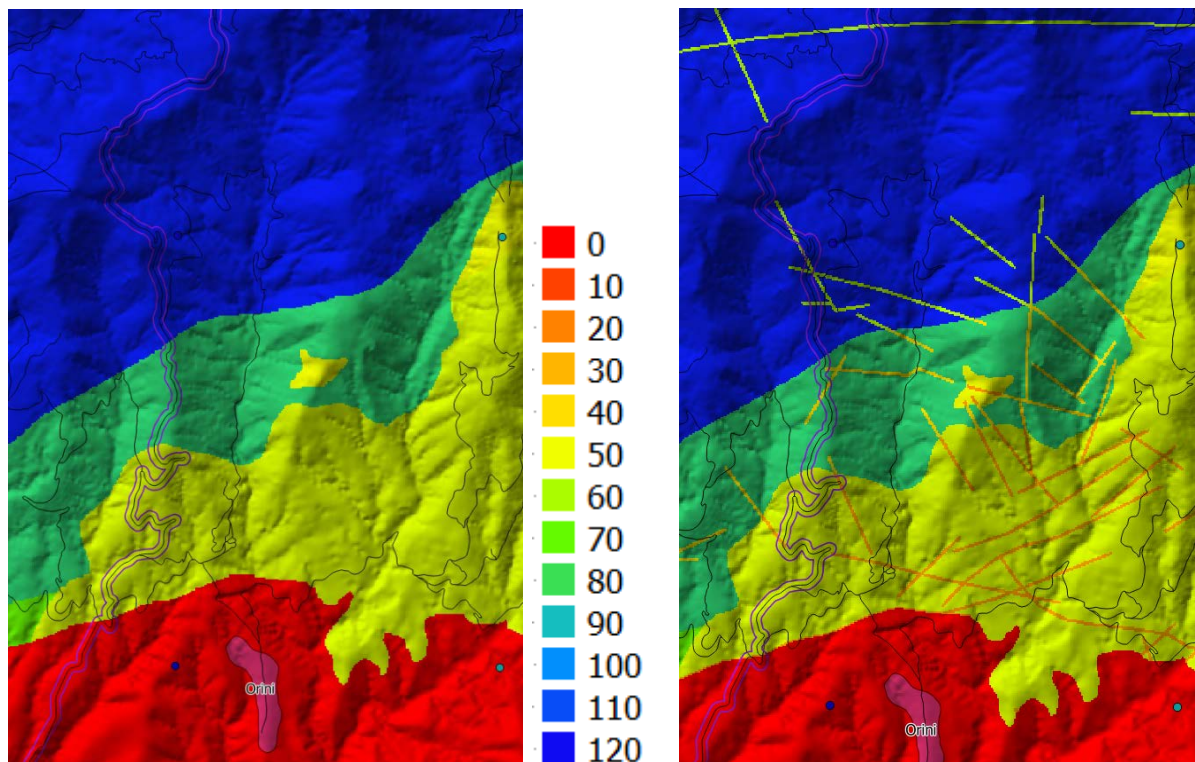


Fig. 7. Effective cohesion (c') values in (kPa) as estimated based on the geologic map of Serres PIA (left) and as supplemented by mapping lineaments considered as fractured zones

Geologic maps were used to map faults in the area, but these only contain a small number of faults mainly due to the fact that these maps were produced before 1980 when no contemporary

technologies were widely used so they represent a small number of the actual existing fractures in the area.

For those reasons remote sensing technologies were used to map lineaments in the area, most of which correspond to fractured zones as is evident by respective displacements registered. A buffer zone of 15m around those lineaments was considered to correspond to the potentially fractured zone within the rock, possessing different mechanical characteristics as those are described by the respective mechanical parameters, effective cohesion (c') and effective friction angle (ϕ).

A detailed description of the method used to map those lineaments using Landsat TM and ETM+ data, is given in the respective Activity A.1.10 deliverable (Remote Sensing Techniques in ELF Hazard Assessment).

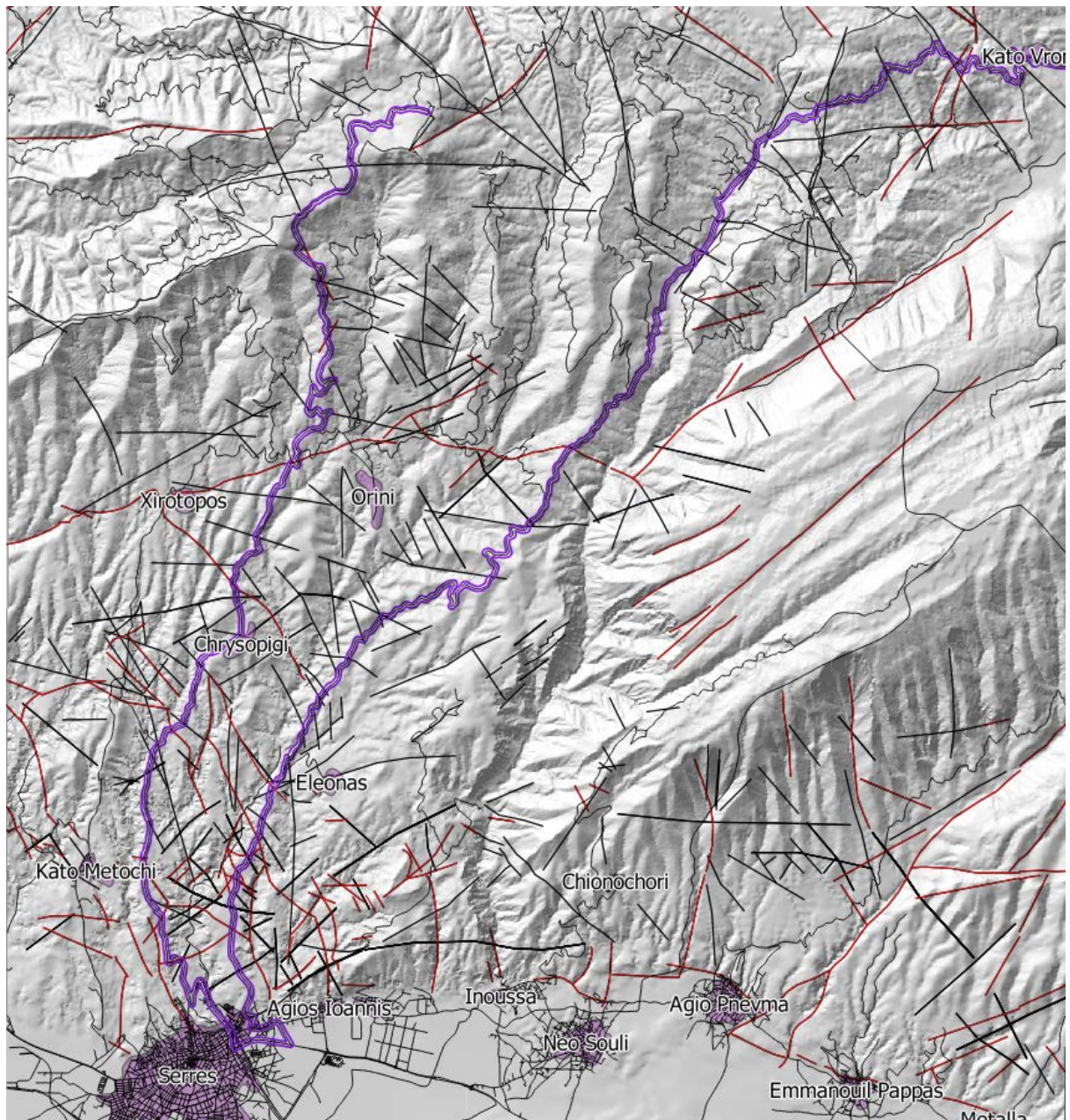


Fig. 8 Faults drawn from the geologic map of the area (scale 1:50.000, IGME) with red color and lineaments mapped using remote sensing techniques (black). Most of geologic map faults were also verified during this process and they overlap the respective lineaments drawn

The presence of low shear strength geologic surfaces as are bedding and schistosity, favors under certain conditions relating the orientation of these planes to that of the natural and cut slopes, slope failures due to sliding on those surfaces. Although in general those problems are restricted to small pieces of rock falling causing minor problems, in some cases larger parts of rock may slide and cause serious damage.

For that reason, an evaluation of the landslide susceptibility due to this reason was made. It was based on systematic measurements of the orientation of geologic planes and the mapping of locations with conditions favorable to sliding. The method used proposes the calculation of TOBIA Index (Topography Bedding Intersection Angle) proposed by [Meentemeyer et.al, 2000](#). According to this method, slopes intersected by geologic planes are classified into : 0. Underdip slopes; 1. Dip slopes; 2. Overdip slopes; 3. Steepened escarpments; 4. Normal escarpments; 5. Subdued escarpments; 6. Orthoclinal slopes (Fig.9).

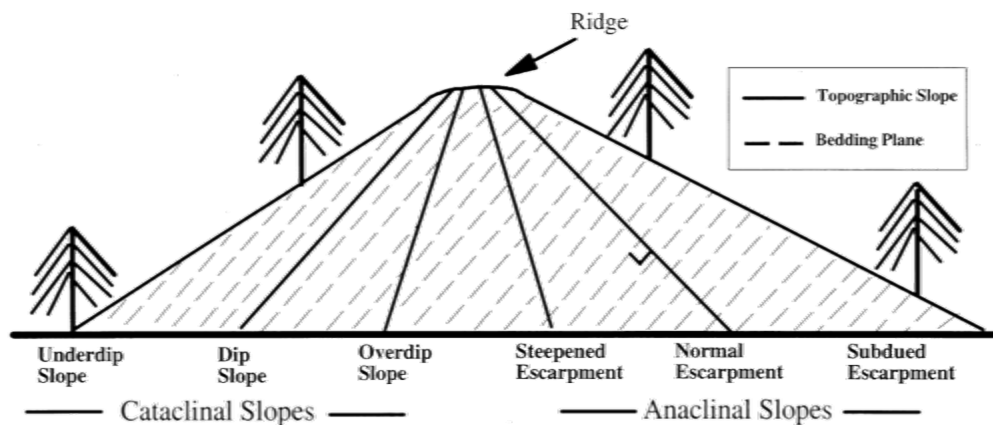


Fig. 10 TOBIA index classes (Meentemeyer et.al, 2000)

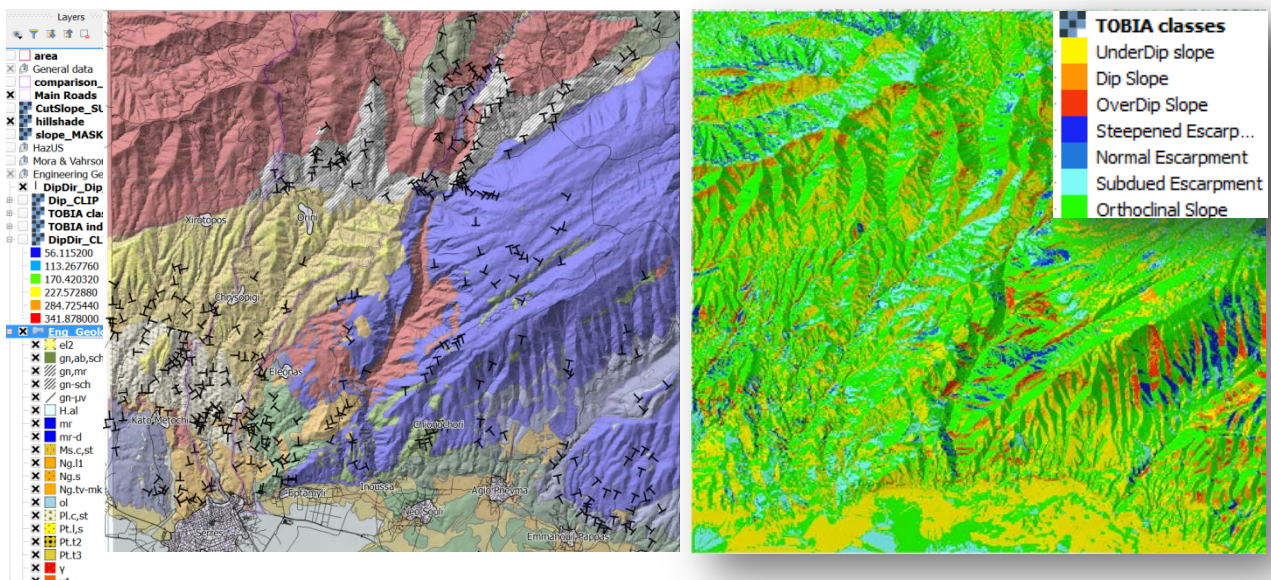


Fig. 9 Orientation of geologic planes on the geologic map (left) and TOBIA Slope classes (right)

2.6 Nymfaia Pilot Implementation Area

Nymfaia Pilot Implementation Area (PIA) covers a total area of approximately 195km² in the central part of Anatoliki Makedonia and Thraki (Eastern Macedonia and Thrace), Hellas (Fig.2).

This specific PIA was selected for many reasons including:

- i) its proximity to the P1 (Democritus University) basis; a fact that limits the costs of field work and implementation time;
 - ii) Its great importance for transportation as the main road axis which links the border areas of the eastern Hellenic mainland (Anatoliki Makedonia and Thraki) to the central part of Bulgaria forming also the main transportation route to the Black Sea coast. This road is also a vertical axis linking Egnatia Motorway running from the Ionian Sea coast to the Turkish border with the aforementioned areas.
 - iii) the multitude of geologic formations outcropping in the area with varying engineering geological attributes and geotechnical behavior;
 - iv) the presence of numerous high cut slopes a serious number of which have been strengthened with countermeasures, since otherwise they would present visible failure problems.
- The last two parameters convert this area to a natural laboratory for Landslide Hazard Assessment and evaluation of the outputs by comparison to actual facts.

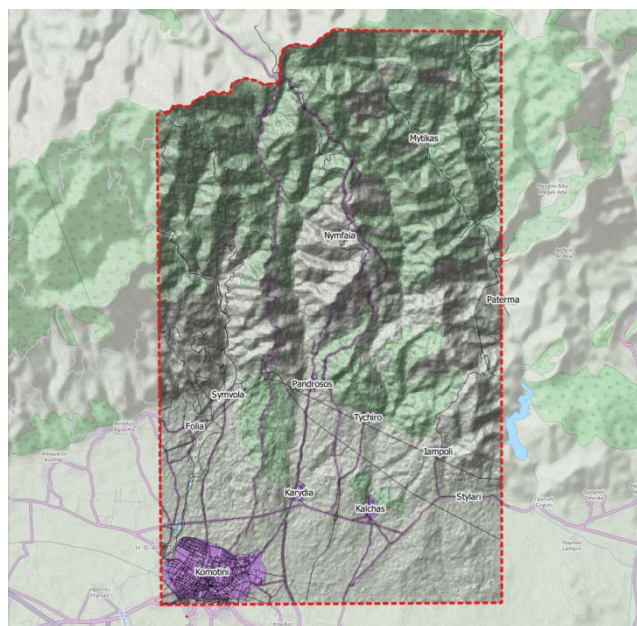


Fig. 11 Nymfaia PIA (red dotted line) on an Open Street Landscape Map

2.6.1 Geomorphology

As already mentioned, the morphologic characteristics of an area are closely related to geological and natural processes that took place and have defined the geotechnical behavior of its geologic formations which relates to slope failures and intense erosion phenomena. In that aspect, the examination of the morphological characteristics of an area can help estimate the expected geotechnical behavior of the outcropping geologic formations.

Nymfaia PIA covers an area of approximately 197000km², covering the area from the plain of Komotini to the Hellenic-Bulgarian border. Elevation ranges from 40 to 1115m. Natural slopes in the area range from horizontal to 51° (Fig.12)

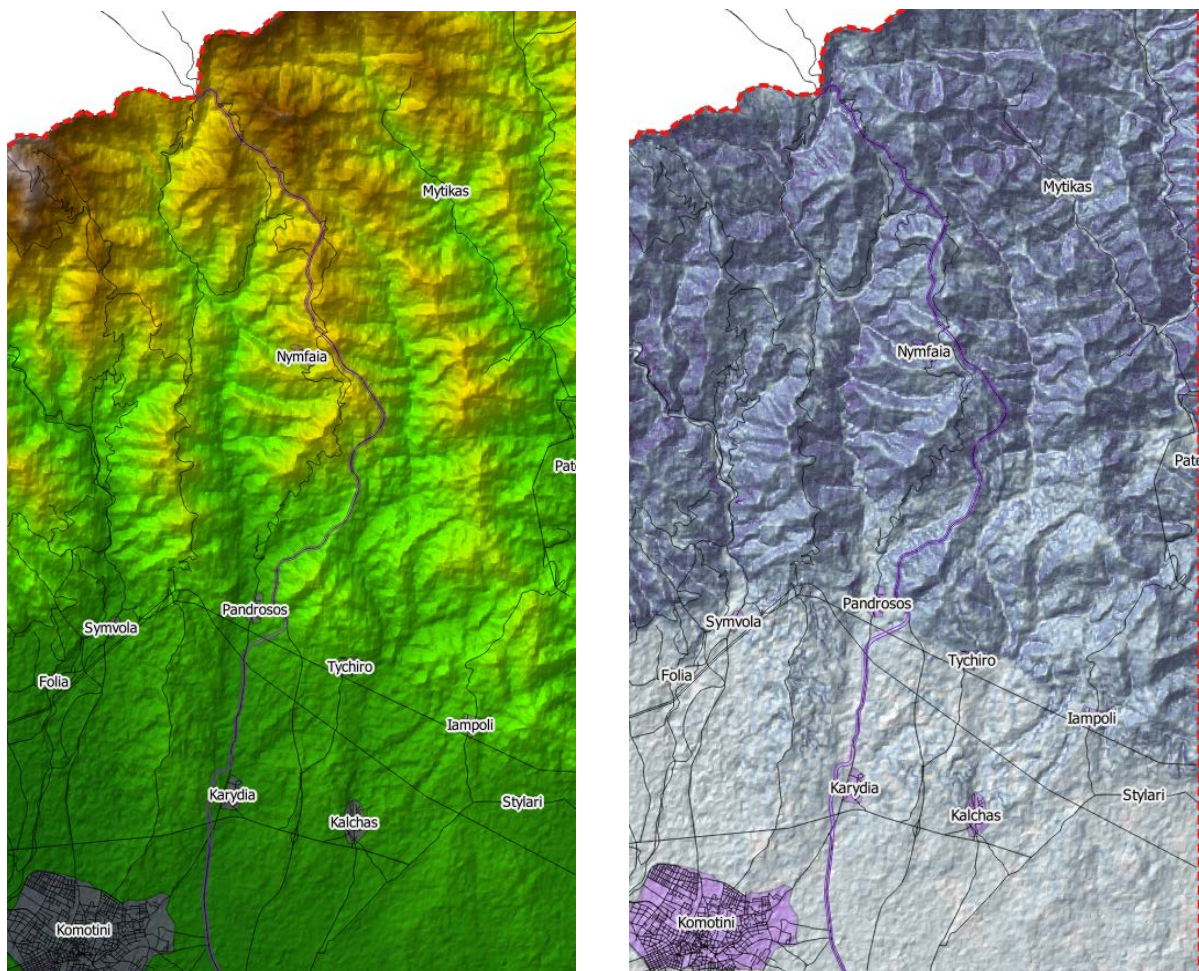


Fig. 12 Nymfaia PIA morphology: Digital Elevation Model on the left (elevation in m) and Slope map on the right (slope in degrees)

The southern part of the area present a smooth morphology with horizontal surfaces (plain) and small hills, whereas the northern half presents an intense morphology, with steep slopes and deep ravines. Most of this area is covered with dense vegetation which protects slopes from erosion and landslides.

2.6.2 Engineering geologic mapping

An engineering geological reconnaissance of the area was carried out in order to more accurately assess the mechanical characteristics of the geologic formations and their geotechnical behavior in respect to landslide hazard.

Field work conducted, included engineering geologic mapping and the evaluation of the geotechnical behavior based on failures recorded especially along the major axes of the road network.

Areas, especially along major road axes were investigated in order to evaluate the condition of the geologic formations in respect to weathering (degree, depth of weathered zone, nature of weathered material etc), to investigate the presence and depth of water, and to map landslides occurring in various parts of the PIA. Data collected were transferred to the GIS, they were processed, analyzed and used as input to apply the various LHA models.

Engineering Geologic field work was carried out on a second stage following the remote sensing investigation and the preliminary Landslide Hazard Assessment in order to verify the respective outputs.

A mixed team of experts including engineering geologists and geotechnical engineers, remote sensing experts and surveyors coming from the LB and P1 teams were involved in this entire process.

In brief, the geologic formations outcropping in Nymfaia PIA consist of (Fig. 13):

Recent (Quaternary) formations including:

- Alluvials consisting of clay and coarser material and their mixtures. Its permeability depends on the ratio of clay minerals against the coarser particles (sand, gravels, pebbles etc).
- Terrace systems and torrential sediments comprising of coarse particles with a smaller amount of clay. In general it is considered as a permeable formation.
- Clayey formations (marls, clay sandstones, lagoon sediments). Erodable, impermeable formations with a high clay content.

- Flysch: alternating layers of marls, sandstones and limestones with layers of tuffs. This formation presents an important vertical heterogeneity and anisotropy because of its structure. The presence of alternating permeable and impermeable layers controls the water infiltration and flow through them combined with the presence of clay rich formations, causing instabilities in natural and cut slopes.
- Volcano-sedimentary series consisting of tuffs, marls and sandstones. Thin layered formations presenting a very high vertical heterogeneity and anisotropy. The presence of clay rich strata combined with fracturing causes slope failures.
- Carbonate rocks (limestones and marbles) in the area are thick, well layered formations but they are heavily fractured so the main problems that appear are rock falls and in a few cases, slab slides.
- Amphibolites: low weathering degree, high strength, impermeable formations. Permeability depends on the degree of fracturing and is restricted up to a depth of a few meters (1-2m). The main parameter that defines their geotechnical behavior concerning landslide hazard is the degree of fracturing which is closely related to the degree of weathering. Fractured zones in amphibolites are clearly defined zones of rock with very poor mechanical characteristics differentiated by the rest of the formation which presents excellent characteristics and geotechnical behavior. This fact raises the necessity of mapping the fractured zones in order to more accurately define mechanical properties and assess the geotechnical behavior.
- Gneisses and schists: gneisses, interchanging to mica schists, are intensely stressed and strained formations with permanent deformations evident by numerous folds and fractures. Weathering degree and schistosity of these formations largely affects their geotechnical behavior. The orientation of schistosity planes combined with the orientation of natural and cut slopes, can be used to foresee failures in slopes due to shearing parallel to schistosity planes.
- The presence of fractured zones intersecting them also causes intense fracturing and weathering converting them to almost soil formations.
- Marbles: High strength, highly permeable formations due to fracturing and carstic weathering.
- Igneous rocks (granites, granodiorites): Very high strength, impermeable formations. Their geotechnical behavior strongly depends on weathering, fracturing and on the orientation of joints as compared to the orientation of the natural and cut slopes.

Hard rocks, with "theoretically" good to excellent mechanical properties cover the northern half of the area. Despite this, it must be taken into account the fact that their natural and mechanical properties as rock masses are very strongly dependent on fracturing and weathering (which also depends on fracturing). The orientation of fractures of any size (faults, large or even small joints) combined with the orientation of natural and cut slopes defines at large landslide problems related to rock falls or small slab slides. The density of fracturing on the other hand defines at large the degree of weathering, converts the rock into soil, in terms of geotechnical behavior and is related to large failures including planar and circular failures.

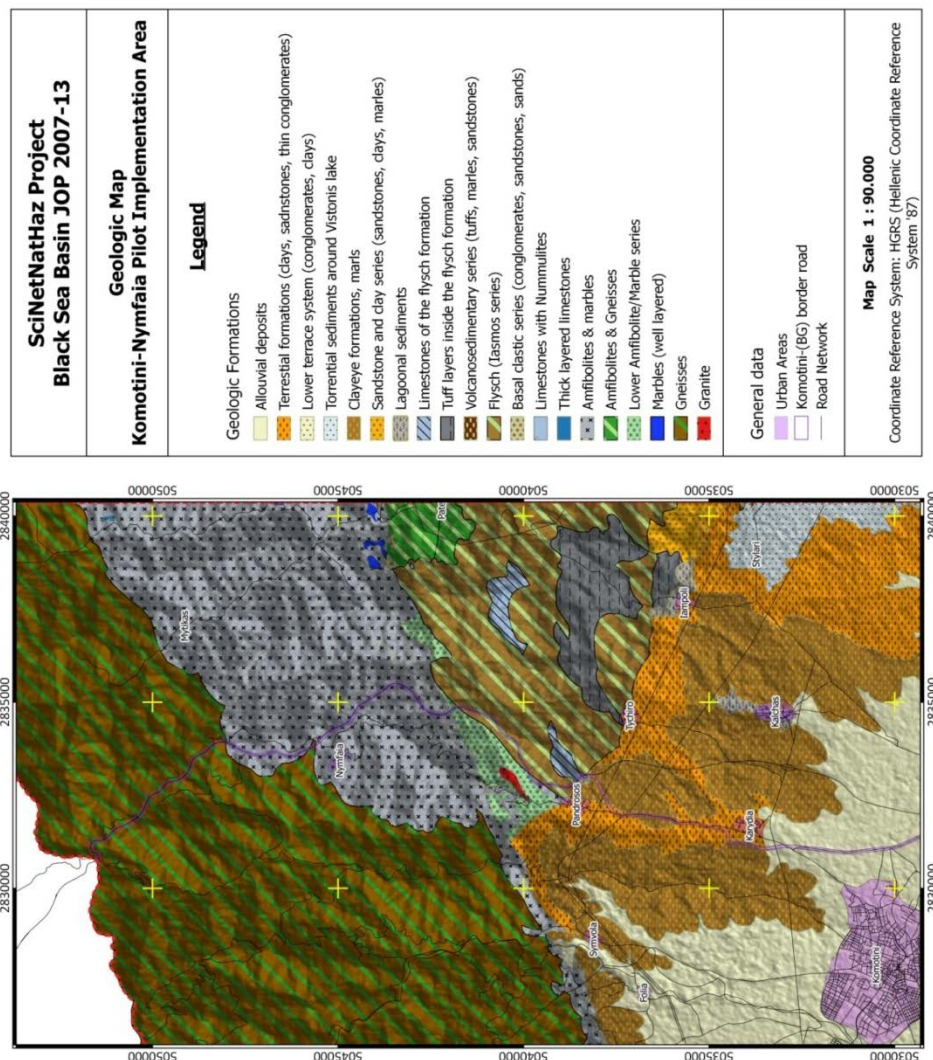


Fig. 13 Nymfaia PIA geologic Map digitized from the geologic Map of Greece 1:50000 (IGE) and updated using remote sensing techniques

2.6.3 Updating the Nymfaia PIA tectonic regime

Since fracturing is considered to play such an important role in the geotechnical behavior of rocks in the area and therefore on LHA, and in order to define as accurately as possible the mechanical properties of geologic formations, a remote sensing investigation to map potential large fractures in Nymfaia PIA was necessary.

The entire research conducted by LB personnel, was based on Landsat TM and ETM+ images and the use of the freeware Multispec[®] software and a high end Toshiba laptop. A detailed description of the research work conducted is given in the respective deliverable (Remote Sensing Techniques in ELF Hazard Assessment).

Remote sensing technologies were used to map lineaments in the area, most of which correspond to fractured zones as is evident by respective displacements registered. A buffer zone of 15m around those lineaments was considered to correspond to the potentially fractured zone within the rock, possessing different mechanical characteristics as those are described by the respective mechanical parameters, effective cohesion (c') and effective friction angle (ϕ').

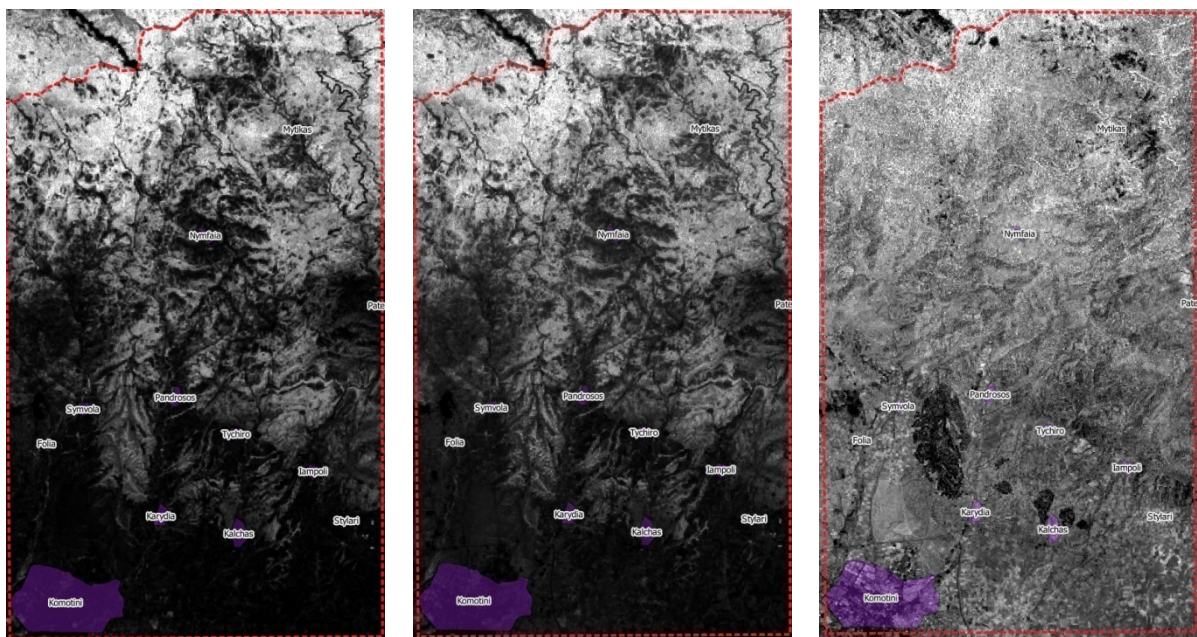


Fig. 14 Band ratios (left to right): TM4/TM3, TM5/TM3, TM7/TM3, showing large lineaments (center) with WSW-ENE; SW-NE and NW-SE directions. Landsat TM and ETM+ data (NASA) were downloaded from <http://glcf.umd.edu/data/landsat/>

Remote Sensing data processing included the creation of the multispectral image of the wider area, band ratios enhancing the features under investigation, false color composites (FCC) and visual analysis and interpretation.

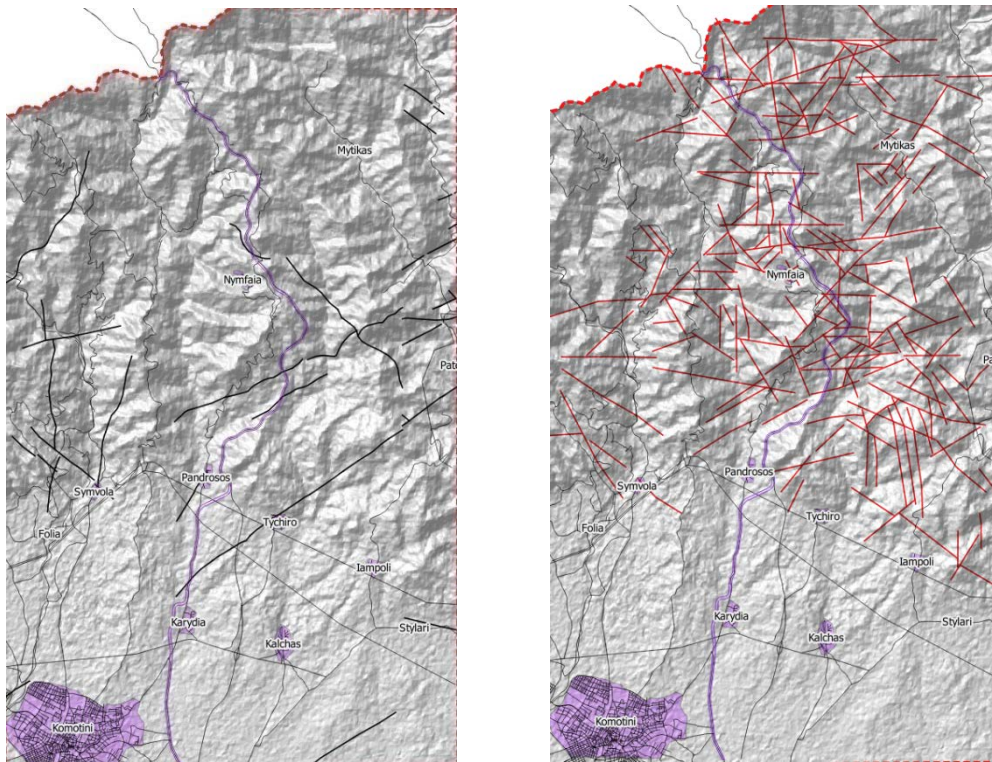


Fig. 15 Left image: Faults digitized from the geologic map 1:50.000 (IGME); right: Lineaments mapped using remote sensing technologies and Landsat TM and ETM+ data

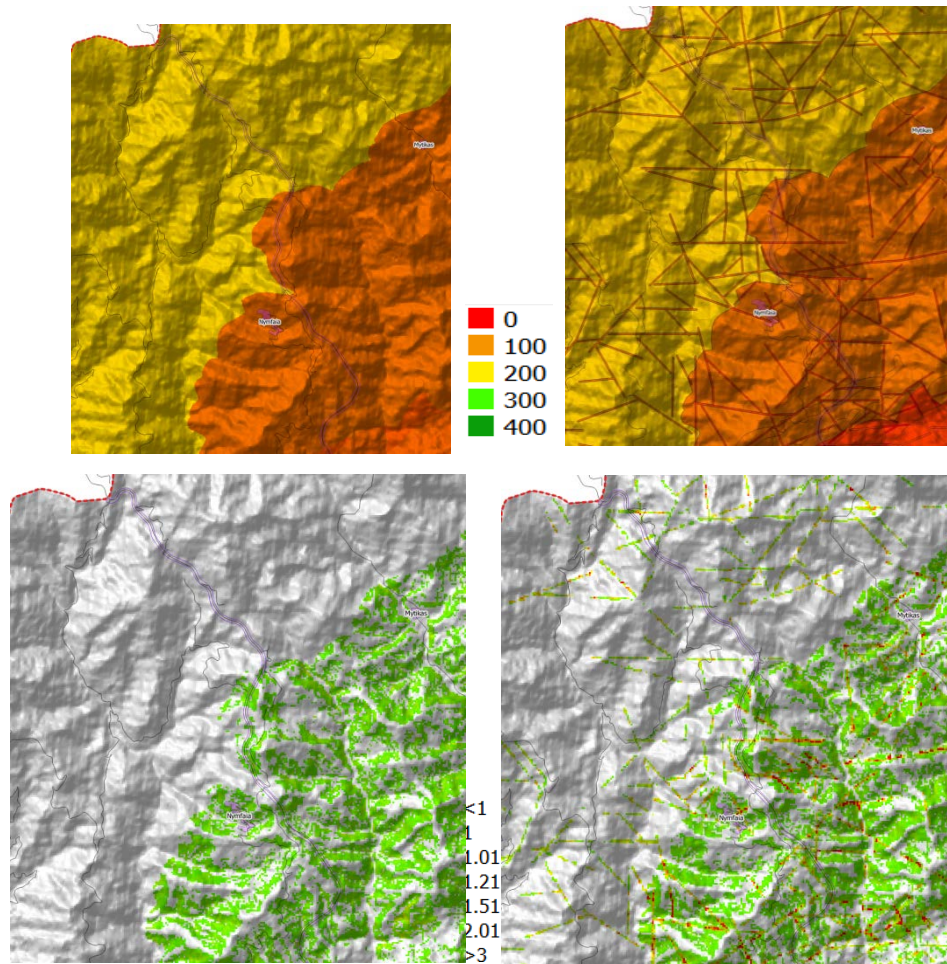


Fig. 16 Upper left: effective cohesion (c') before taking into consideration the mapped lineaments; upper right: c' with the effect of lineaments. Bottom: left and right the respective Factors of Safety calculated for a 5m thick sliding mass under “wet” conditions

3 Methods Used for Regional Landslide Hazard Assessment

3.1 Mora & Vahrson method

The method proposed by Mora and Vahrson (1994) for the prediction of susceptible zones was based on case studies of slope failures triggered both by earthquakes and by heavy rainfall. A detailed description of the method can be found in SciNetNatHaz projects deliverable D.01.02.

According to this method, three factors: relative relief, lithological conditions and soil moisture, are considered as the factors influencing the susceptibility to landslides. In addition, two factors: seismicity and rainfall intensity, are incorporated as the triggering factors.

By combining those factors, a degree of slope failure hazard (H_e) was defined as follows:

$H_e = \text{Susceptibility} * \text{Trigger or}$

$$H_e = (S_r * S_e * S_h) * (T_s * T_p) \quad (1)$$

Where (please look for further details into D.01.02),

H_e : landslide hazard index

S_r : value of relative relief index

S_e : value of lithological susceptibility

S_h : value of index of influence of natural humidity of the soil

T_s : value of influence of seismic intensity

T_p : value of influence of rainfall precipitation intensity

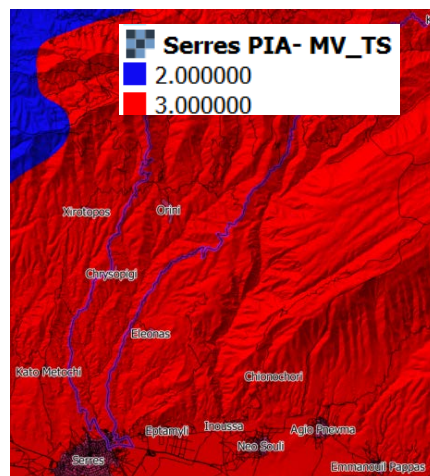
The slope factor S_r is defined based on relative relief $R_r = (h_{\max} - h_{\min})/\text{km}^2$

3.1.1 Data input

- Digital Elevation Model (DEM) created using elevation points and contours digitized from topographic maps (scale 1:50.000, contour interval 20m).
- Road network, urban areas, general information
- Geologic Maps
- Engineering geologic reconnaissance results
- Ground Motion data (PGA/100 yrs return period)
- Mean Monthly rainfall (mm) and maximum daily precipitations from seven meteorological stations within and around the area (Fig.9).

Data were harmonized, georeferenced and used as input into a GIS developed for the LHA. All rasters were produced with a pixel size of 15x15m.

Note: Factors given as numbers, have this value over the entire PIA):

$$T_p \text{ (value of influence of rainfall precipitation intensity)} = 2$$


Final Version
Page: 43 of 276

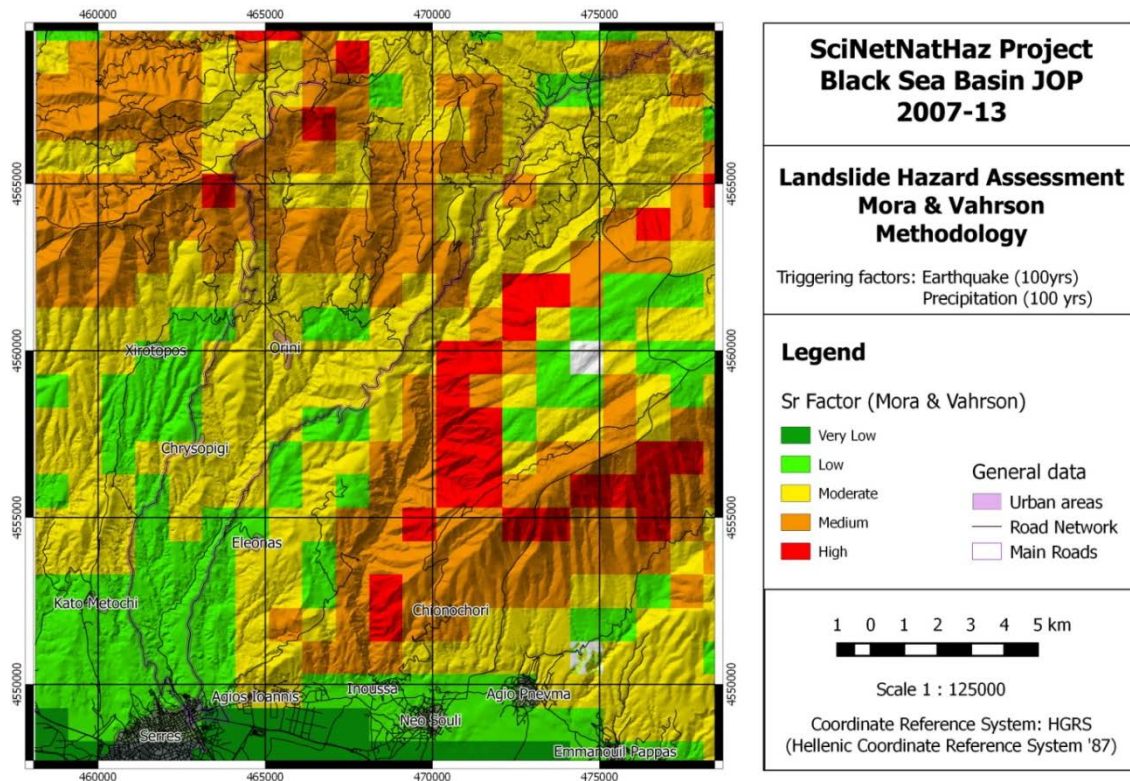


Fig. 19 Sr factor, Relative Relief Index

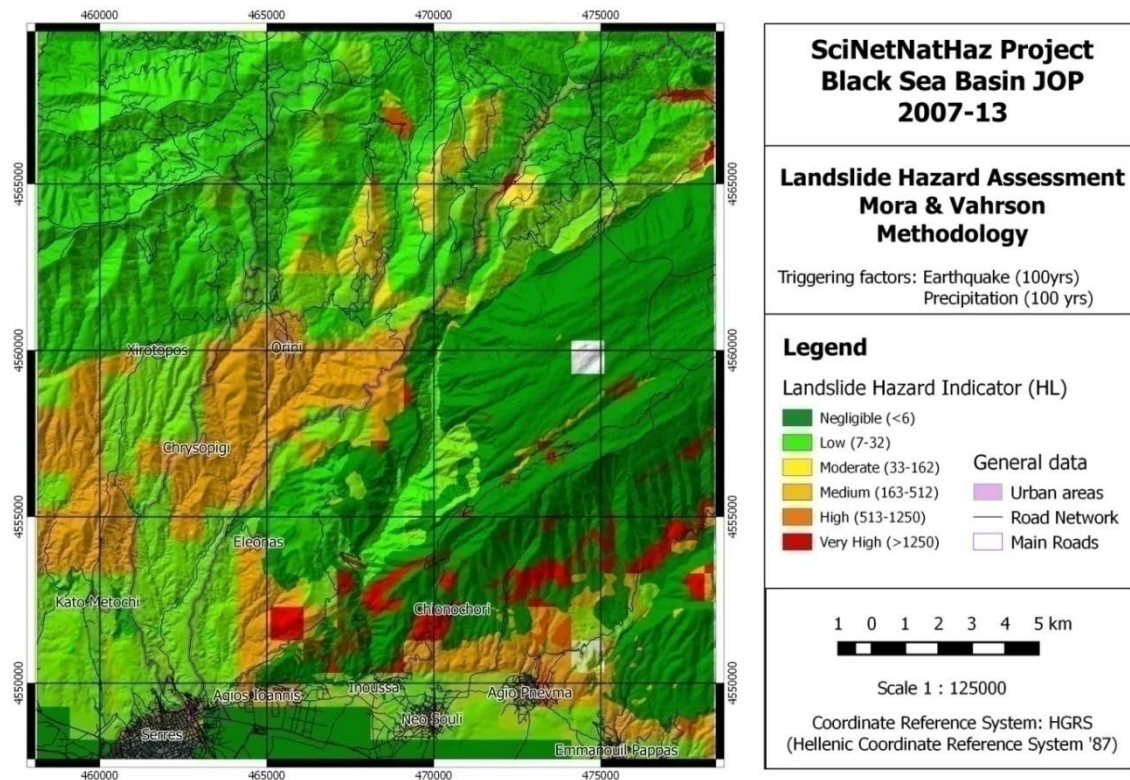


Fig. 20 H_e Landslide Hazard Indicator

Its of the Mora & Vahrson method implementation in **Nymfaia** PIA:

H_e (landslide hazard index)

S_r (value of relative relief index)

S_e (value of lithological susceptibility)

S_h (value of index of influence of natural humidity of the soil) = 1

T_s (value of influence of seismic intensity) = 2

T_p (value of influence of rainfall precipitation intensity) = 3

Note: Factors given as numbers, have this value over the entire PIA

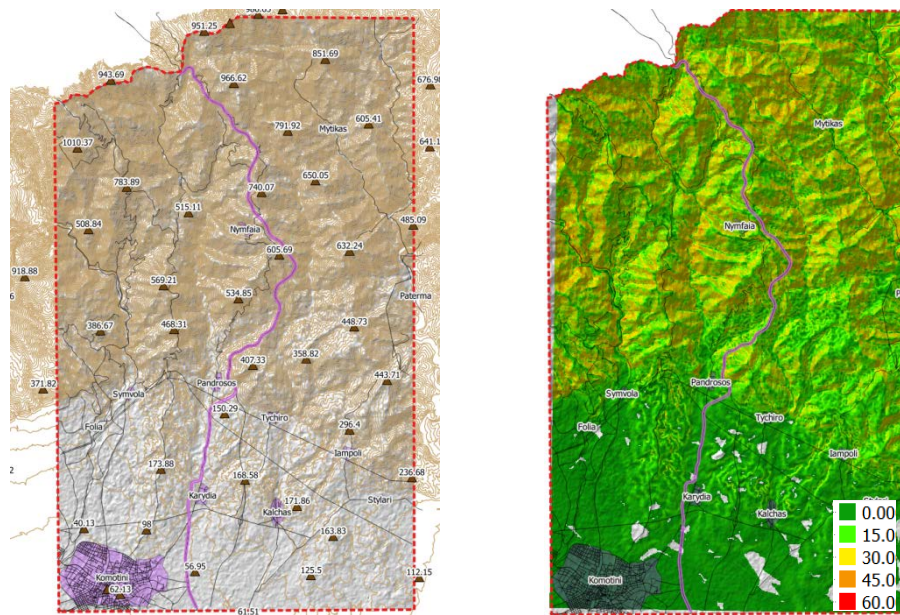


Fig. 21 Topographic map with elevation points (left) and slope map (right) of Nymfaia PIA

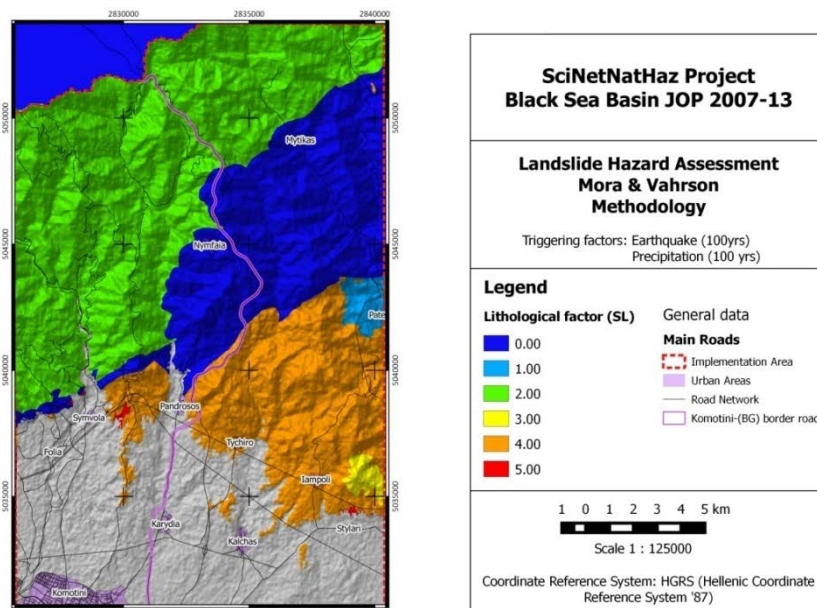


Fig. 22 Nymfaia PIA: Mora & Vahrson method Lithological Susceptibility Factor (S_e)

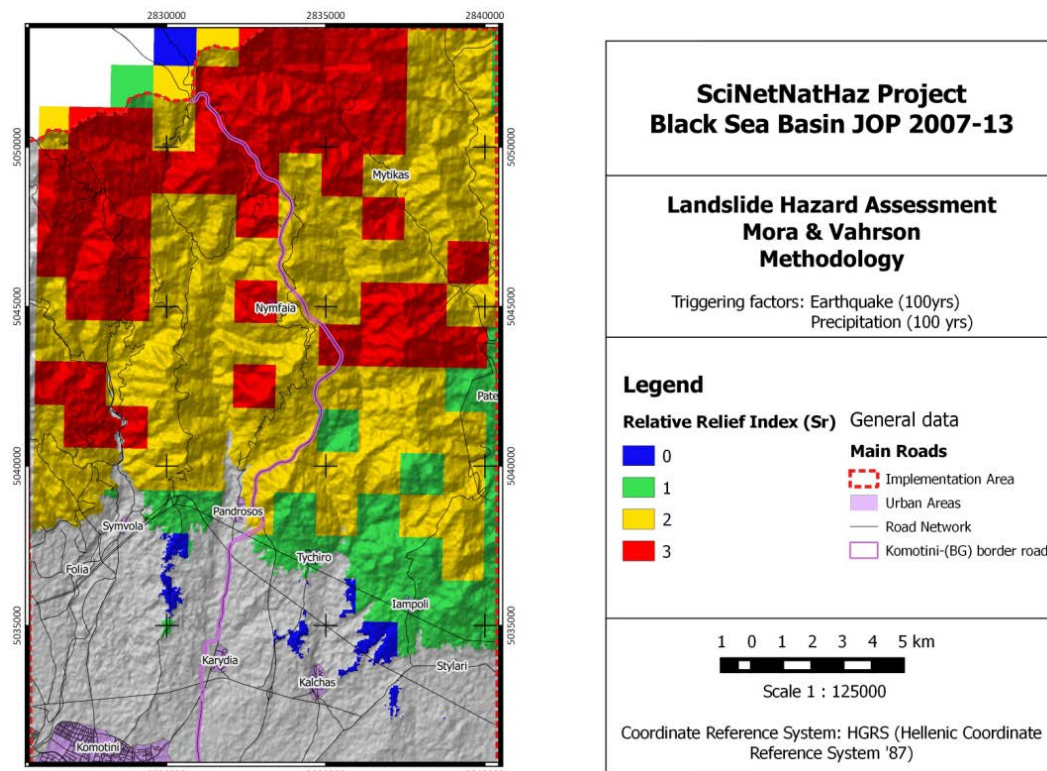


Fig. 23 Nymfaia PIA: Mora & Vahrson method Relative Relief Index (S_r)

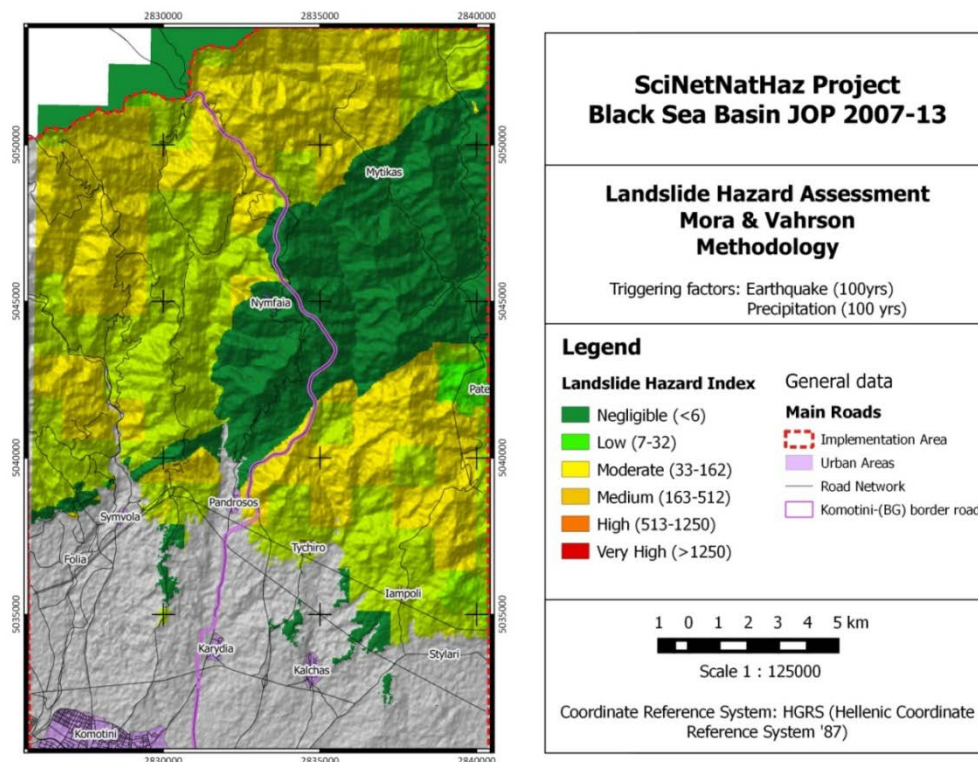


Fig. 24 Nymfaia PIA: Mora & Vahrson method Landslide Hazard Index (H_l)

3.2 FEMA method (HazUS)

The procedure proposed and used by the Federal Emergency Management Agency –FEMA (USA) to assess Landslide Hazard on regional scales is a three step procedure and it applies only when the triggering factor is a seismic event:

1. Assess Landslide Susceptibility
2. Assess the Critical Acceleration A_c , where “critical” is the seismic horizontal acceleration applied on a slope which produces a pseudostatic Factor of Safety equal to one ($F_s=1.0$).
3. Compare the A_c to the expected ground motion (Peak Ground Acceleration) by calculating the ratio A_c/PGA

All the above parameters are calculated for two different moisture/groundwater conditions: “dry” meaning that the groundwater level is below the level of sliding surface and “wet” meaning that the groundwater level is at ground surface (fully saturated).

3.2.1 Landslide susceptibility under static conditions (FEMA)

The Landslide susceptibility is evaluated taking into consideration the engineering geologic conditions, the slope angle for the two predefined moisture conditions (wet and dry) according to the following table (Fig.25).

Geologic Group		Slope Angle, degrees					
		0-10	10-15	15-20	20-30	30-40	≥40
(a) DRY (groundwater below level of sliding)							
A	Strongly Cemented Rocks (crystalline rocks and well-cemented sandstone, $c' = 300$ psf, $\phi' = 35^\circ$)	None	None	I	II	IV	VI
B	Weakly Cemented Rocks and Soils (sandy soils and poorly cemented sandstone, $c' = 0$, $\phi' = 35^\circ$)	None	III	IV	V	VI	VII
C	Argillaceous Rocks (shales, clayey soil, existing landslides, poorly compacted fills, $c' = 0$, $\phi' = 20^\circ$)	V	VI	VII	IX	IX	IX
(b) WET (groundwater level at ground surface)							
A	Strongly Cemented Rocks (crystalline rocks and well-cemented sandstone, $c' = 300$ psf, $\phi' = 35^\circ$)	None	III	VI	VII	VIII	VIII
B	Weakly Cemented Rocks and Soils (sandy soils and poorly cemented sandstone, $c' = 0$, $\phi' = 35^\circ$)	V	VIII	IX	IX	IX	X
C	Argillaceous Rocks (shales, clayey soil, existing landslides, poorly compacted fills, $c' = 0$, $\phi' = 20^\circ$)	VII	IX	X	X	X	X

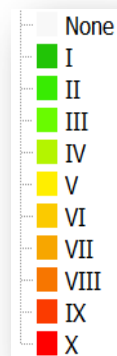


Fig. 25 Landslide susceptibility under static conditions, FEMA method, HazUS manual. Scale: I (green) less susceptible; X (red) most susceptible

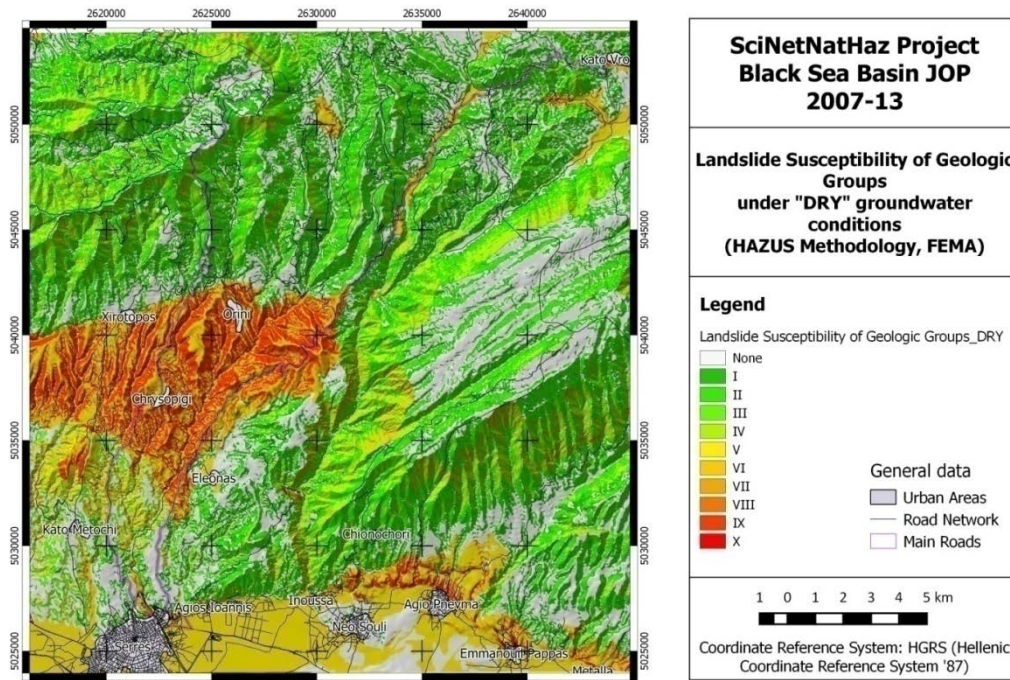


Fig. 26 Landslide susceptibility for “DRY” conditions (Serres PIA)

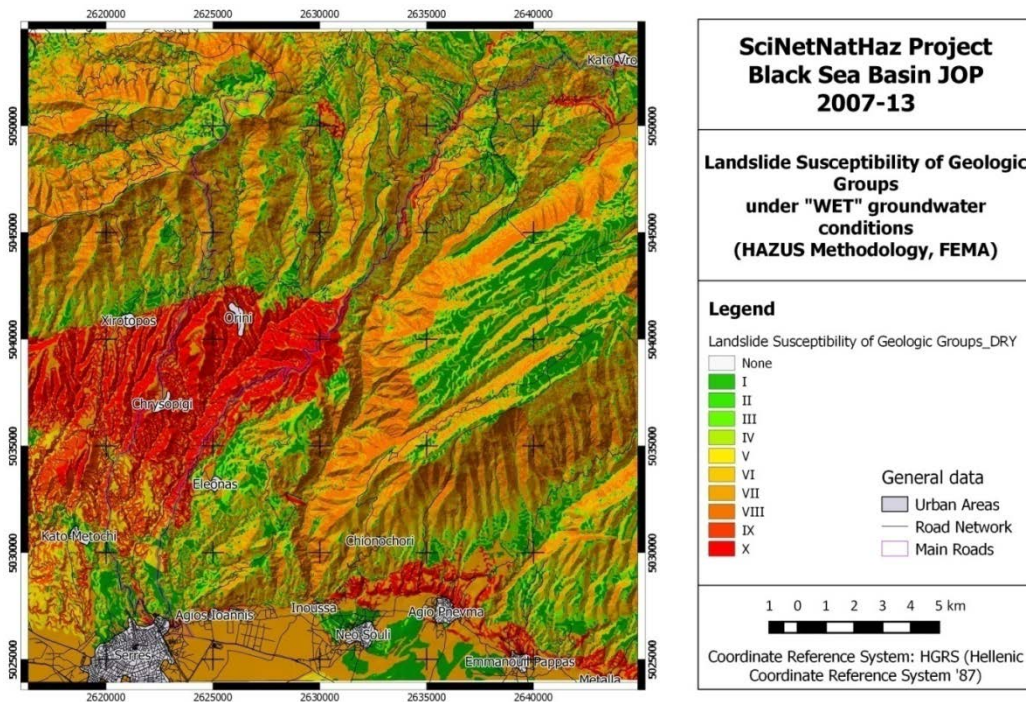


Fig. 27 Landslide susceptibility for “WET” conditions (Serres PIA)

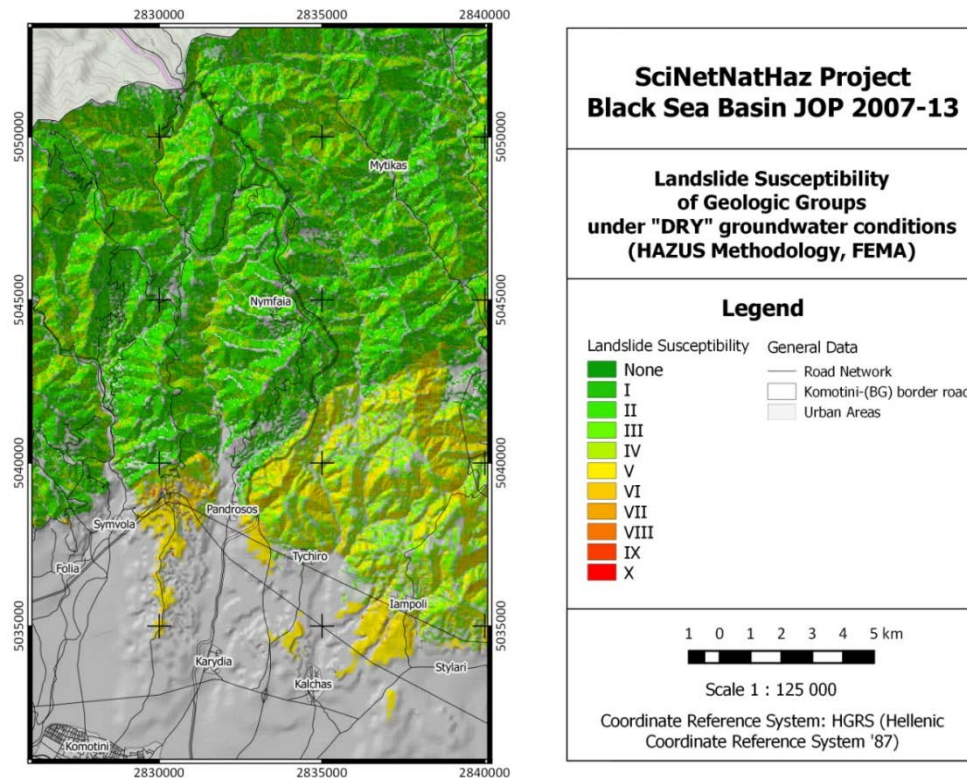


Fig. 28 Landslide susceptibility for “DRY” conditions (Nymfaia PIA)

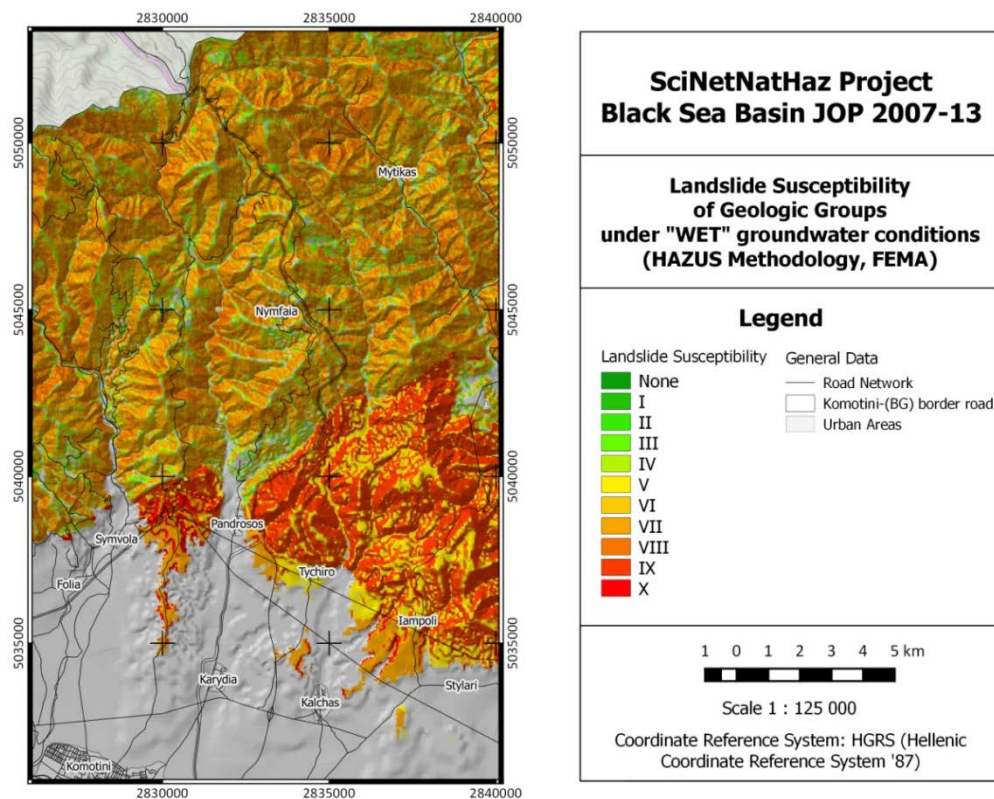


Fig. 29 Landslide susceptibility for “WET” conditions (Nymfaia PIA)

3.2.2 Landslide susceptibility under seismic conditions

Landslide susceptibility under seismic conditions is based on the limit equilibrium principle where an earthquake is considered as a horizontal force (seismic coefficient * weight of the potentially sliding mass of a slope). The crucial parameter is Critical Acceleration (A_c) which is defined as the seismic horizontal acceleration applied on a slope which produces a pseudostatic Factor of Safety $F_s=1.0$ on the slope.

The critical acceleration is calculated as a complex function of slope, geologic group, steepness, water table, type of land sliding and history of previous slope performance (Wilson and Keefer, 1985). There are certain bounds that limit the slope values for which a critical acceleration can be defined as shown in Fig.30.

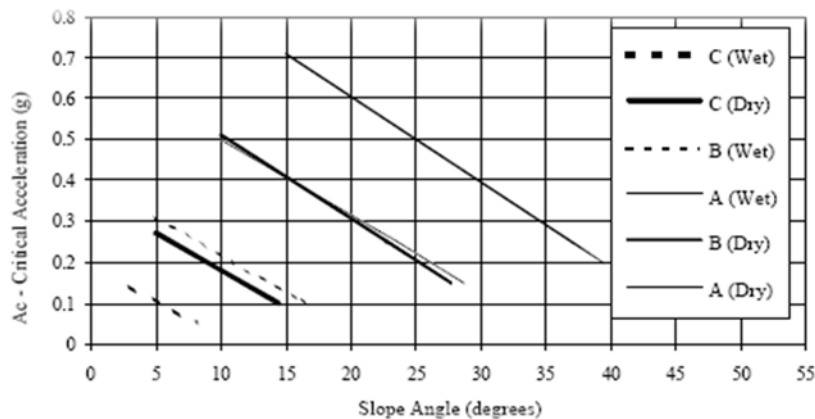


Fig.30 Critical acceleration (A_c) as a function of slope and geologic group (Wilson and Keefer, 1985)

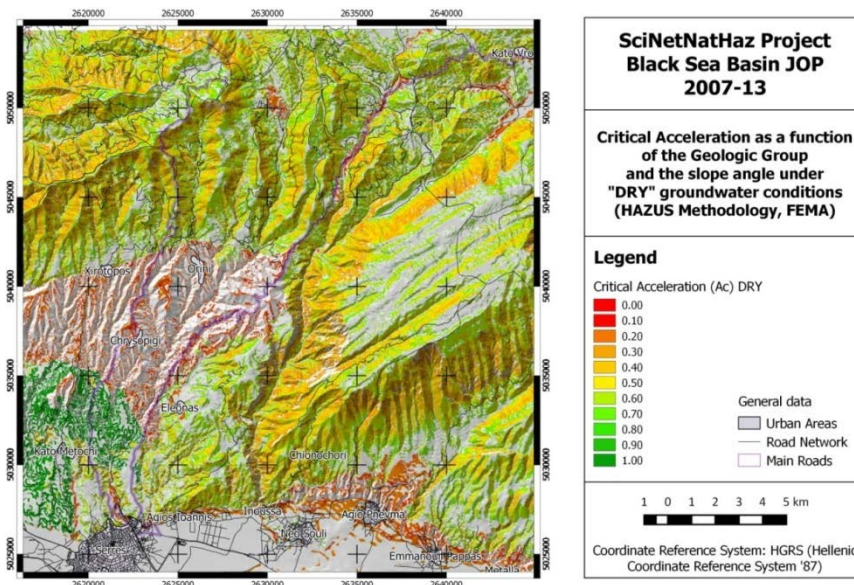
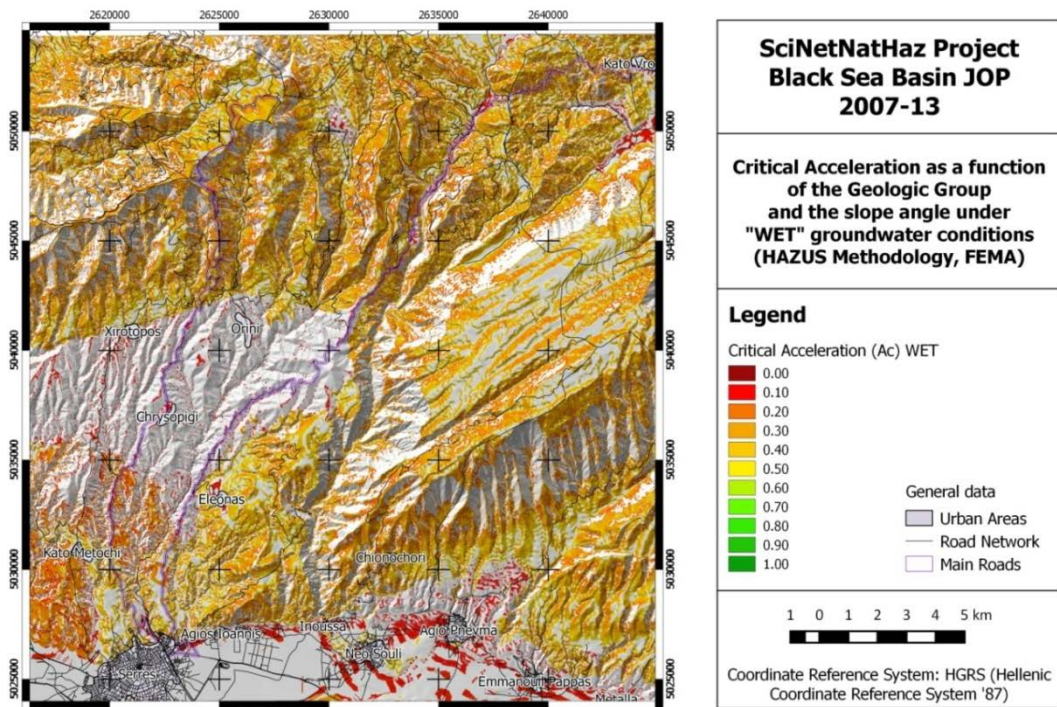


Fig.31 Critical acceleration (A_c) for “dry” conditions (Serres PIA)



Ground
Motion
(PGA) was
calculated
according
to the
Seismic
Hazard

Fig. 32 Critical acceleration (A_c) for “wet” conditions (Serres PIA)

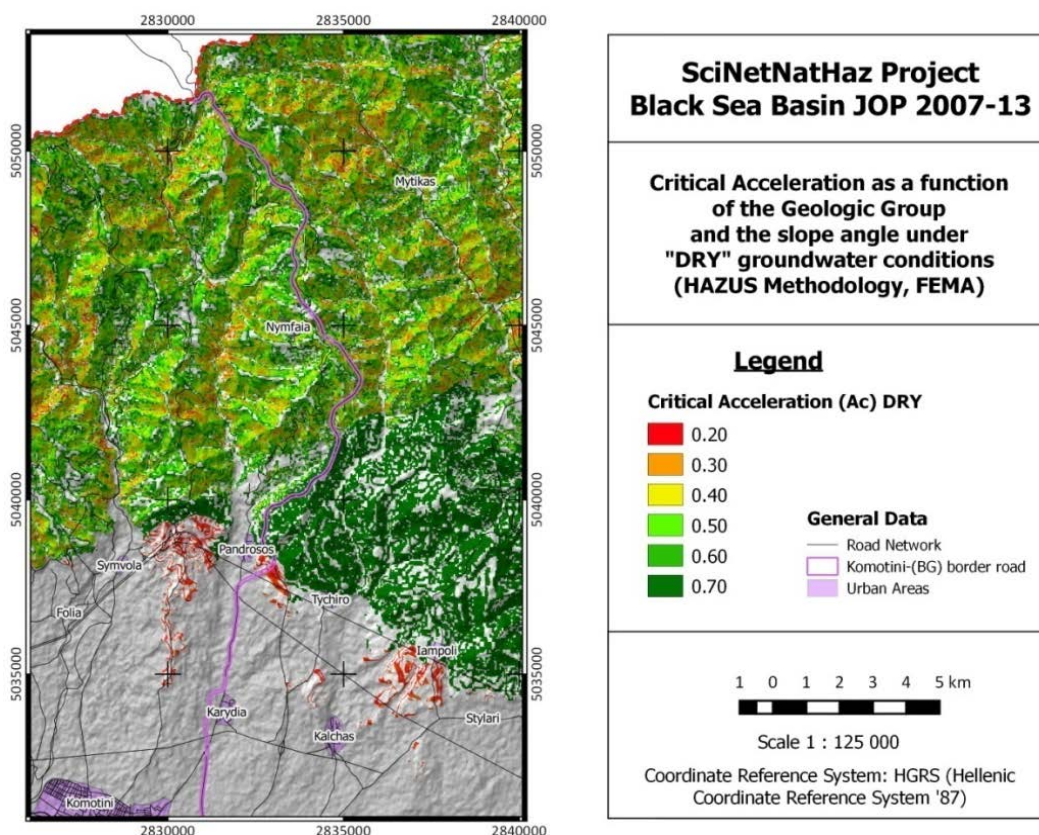


Fig. 33 Critical acceleration (A_c) for “dry” conditions (Nymfaia PIA)

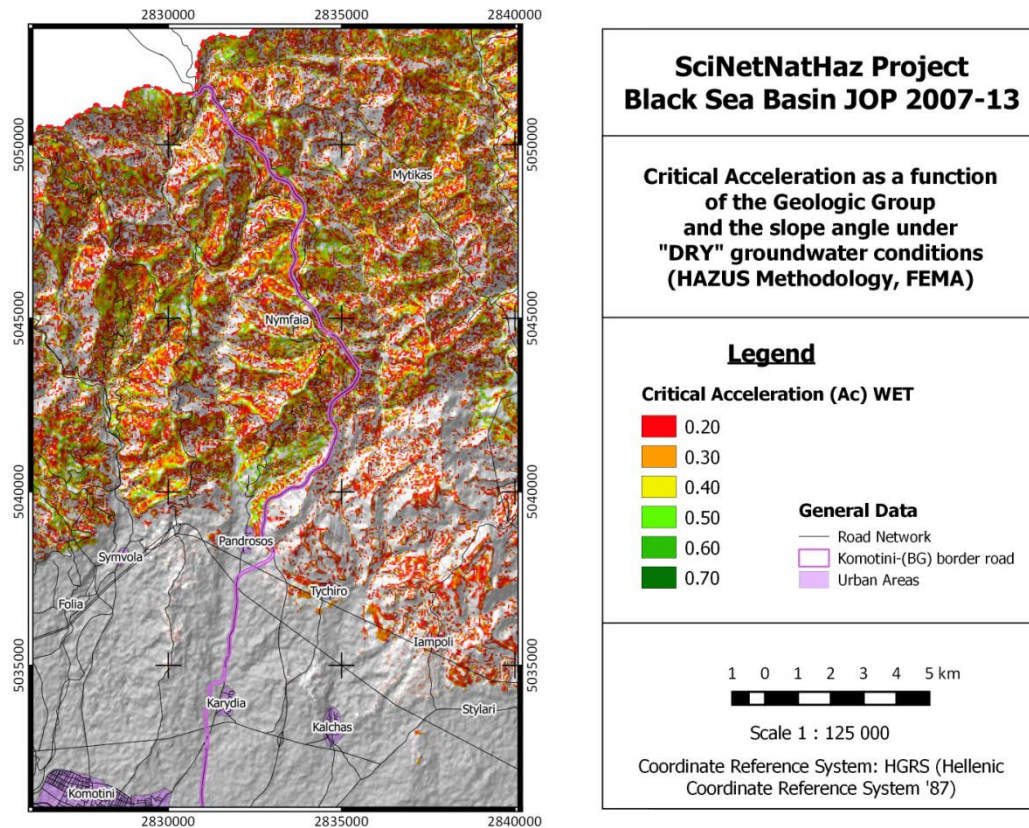


Fig. 34 Critical acceleration (A_c) for “wet” conditions (Nymfaia PIA)

Assessment for Serres PIA for 100, 200, 475 and 1000 years mean return period, using:

- the respective Ground Motion Prediction Equations (GMPEs) applicable in the specific region and soil types, or
- the respective GMPEs suitable for rock conditions, multiplied by an amplification factor ($PGA_i = PGA_R * F_{Ai}$) according to NEHRP 2000

The Ground Motion Prediction Equations (GMPEs) used for the local PGA calculations were the ones proposed by Scarlatoudis et al., (2003):

$$\log PGA = 1.07 + 0.45M - 1.35 \times \log(R+6) + 0.09F + 0.06S \pm 0.286$$

$$\log PGA = 0.86 + 0.45M - 1.27 \times \log(R^2 + h^2)^{1/2} + 0.10F + 0.06S \pm 0.286$$

PGA calculation taking into account soil amplification is calculated according to FEMA method as:

$$PGA_i = PGA_R * F_{Ai} \quad (2)$$

where PGA_i is the Peak Ground Acceleration for site class i (in units of g)
 PGA is the Peak Ground Acceleration for site class B (in units of g)
 F_{Ai} is the short period amplification factor for site class i as specified for spectral
 acceleration S_{as} (g)

Table 1 Soil amplification factors according to geologic formations and spectral
 acceleration Hazus 99-SR2 Technical Manual, Chapter 4-PESH)

Site Class B Spectral Acceleration	Site Class				
	A	B	C	D	E
Short-Period, S_{AS} (g)	Short-Period Amplification Factor, F_A				
≤ 0.25	0.8	1.0	1.2	1.6	2.5
0.50	0.8	1.0	1.2	1.4	1.7
0.75	0.8	1.0	1.1	1.2	1.2
1.0	0.8	1.0	1.0	1.1	0.9
≥ 1.25	0.8	1.0	1.0	1.0	0.8*

The ratio A_c/PGA provides an index of the potential that ground motion has, to trigger landslides.
 A_c/PGA ratio values are classified into six categories.

Criterion:

Index A_c/PGA and a
 “subjective” categorization

- ☐ Very high: < 0.3
- ☐ High: $0.3 - 0.6$
- ☐ Moderate: $0.6 - 0.8$
- ☐ Low: $0.8 - 1.0$
- ☐ Very Low: $1.0 - 3.0$
- ☐ None: > 3.0

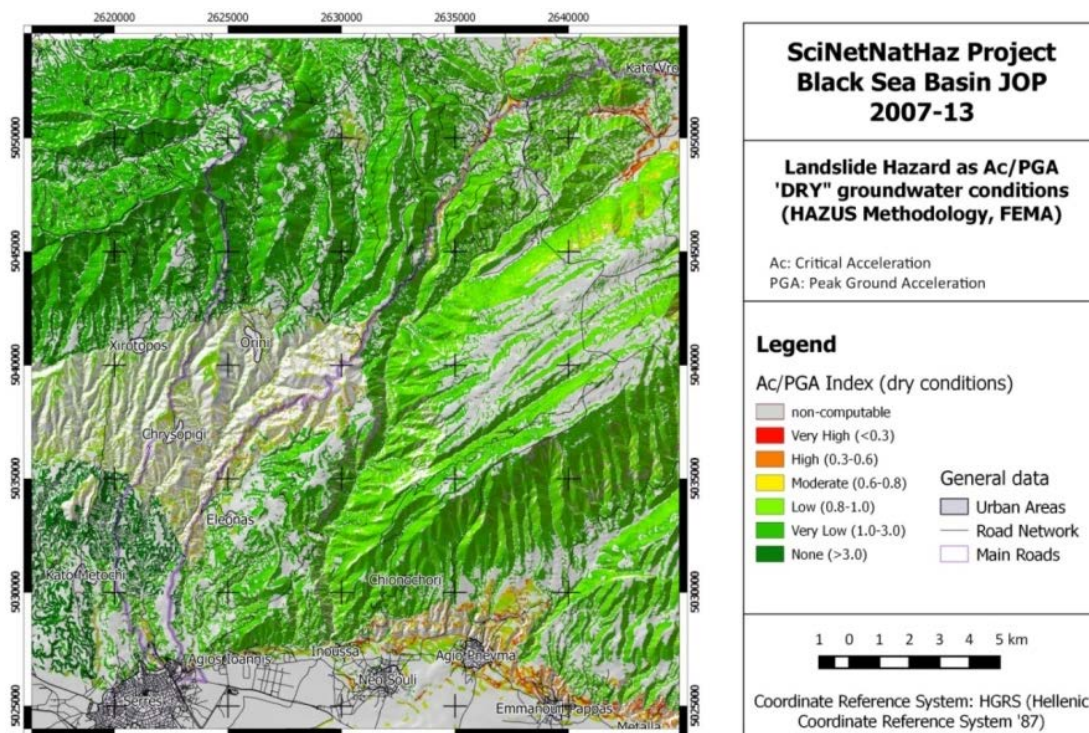


Fig. 35 Shallow Landslide Susceptibility (A_c /PGA index) under seismic “dry” conditions (Serres PIA)

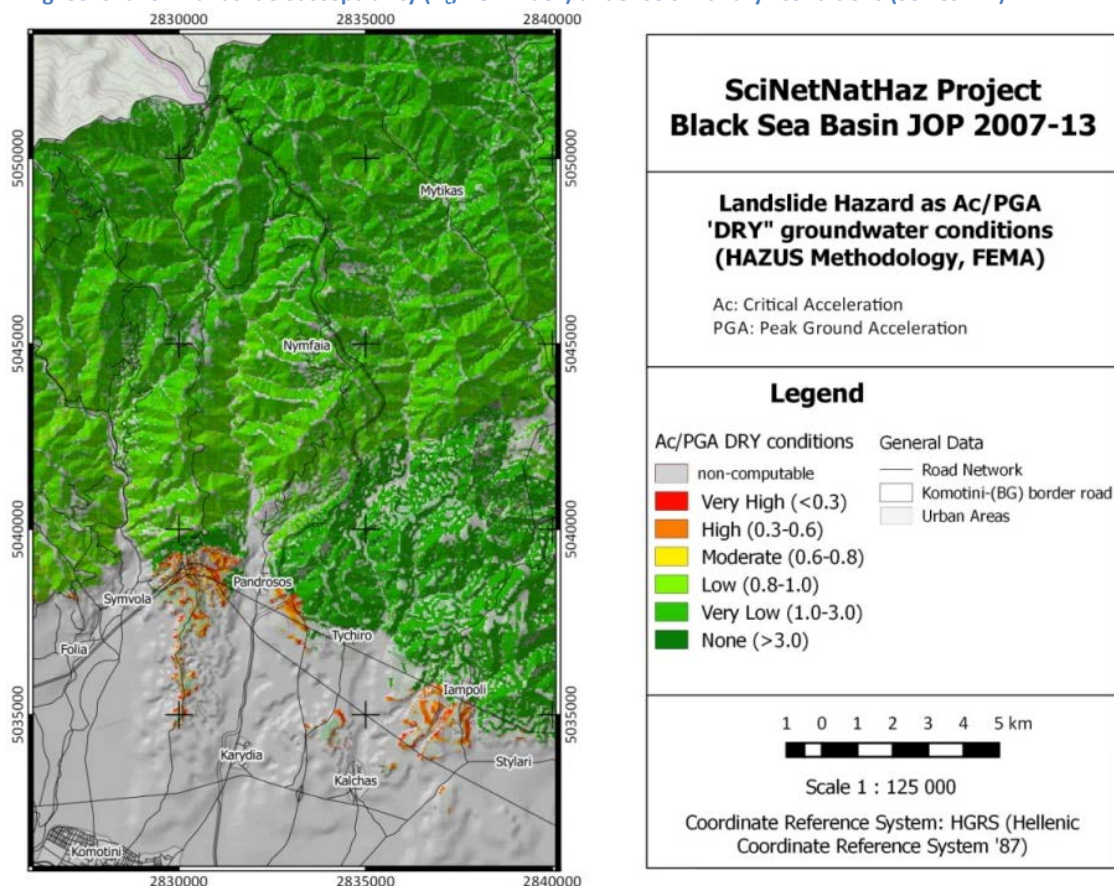


Fig. 36 Shallow Landslide Susceptibility (A_c /PGA index) under seismic “wet” conditions (Serres PIA)

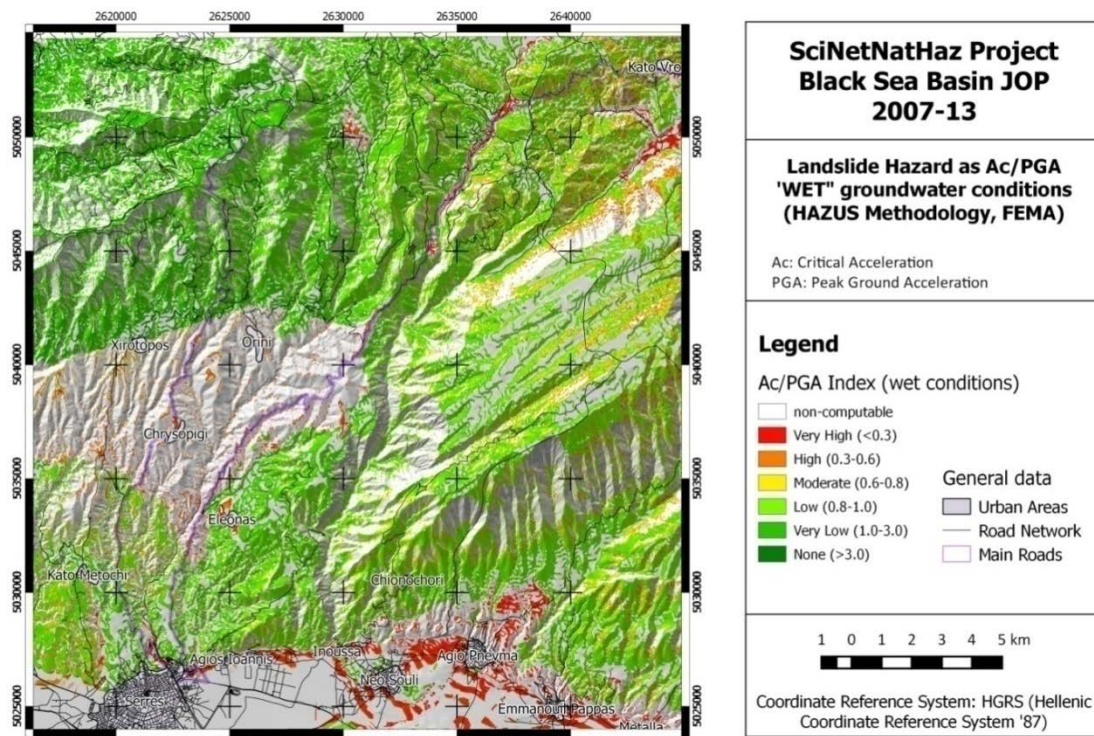


Fig. 37 Shallow Landslide Susceptibility (Ac/PGA index) under seismic “dry” conditions (Nymfaia PIA)

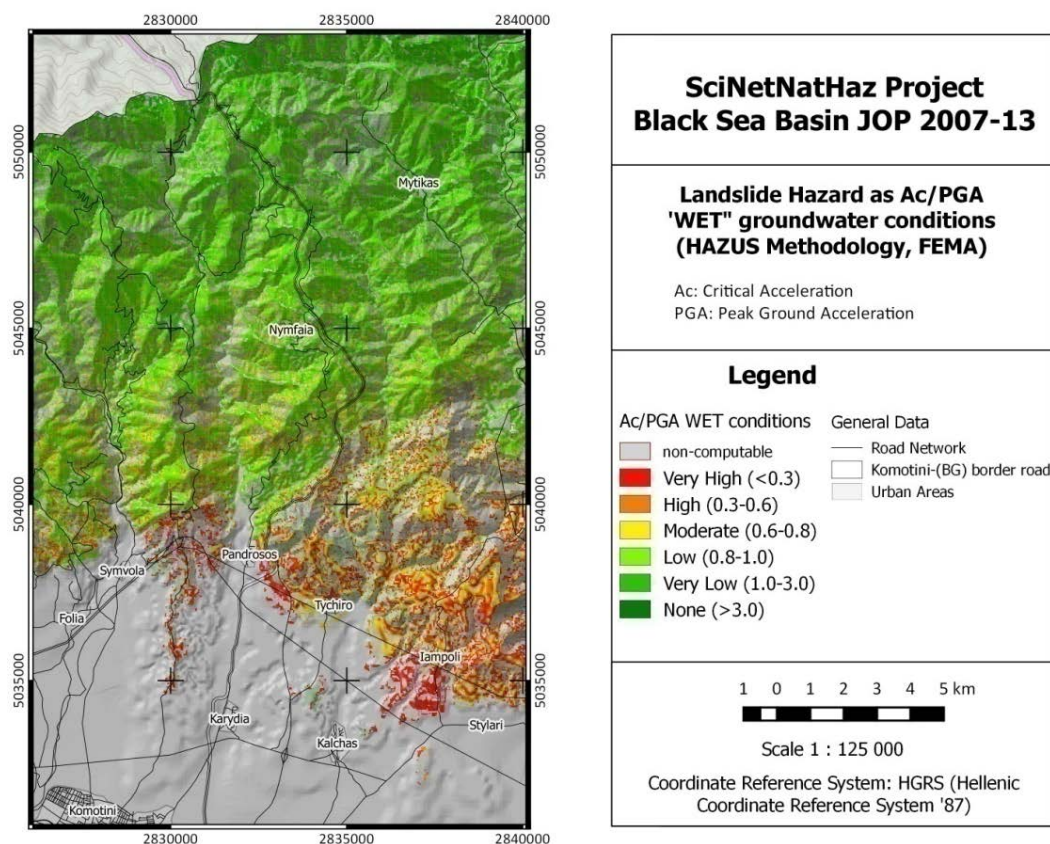


Fig. 38 Shallow Landslide Susceptibility (Ac/PGA index) under seismic “wet” conditions (Nymfaia PIA)

3.2.3 Landslide hazard under seismic conditions

Landslide Hazard Assessment under seismic conditions according to FEMA method is based on the calculation of Permanent Ground Displacements – PGD (Goodman and Seed, 1966). The method is applicable to the LHA for “shallow” landslides (depth of slip surface up to 8 or 10m max) which is the type of landslides in Serres and Komotini - Nymfaia PIA.

The idea behind this method is the fact that each shaking during the induced by the earthquake ground motion (A_{is}) may cause a permanent displacement of a sliding mass on a slope, in case peak ground acceleration (PGA) exceeds the Critical Acceleration (A_c). For each cycle, there is an expected permanent displacement ($E[d/A_{is}]$), so for a number (n) of cycles the total expected permanent displacement is:

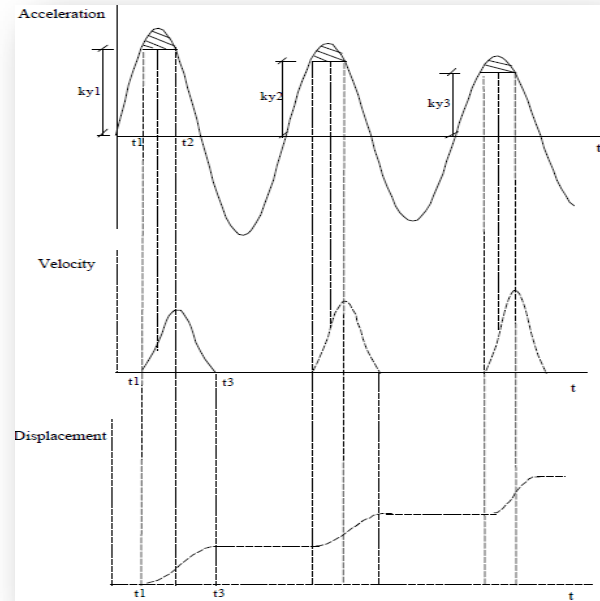


Fig. 39 Integration of accelerograms to determine downslope displacements (Goodman and Seed, 1996)

$$E[PGD] = E[d/A_{is}] \times A_{is} \times n \quad (3)$$

where A_{is} is the induced acceleration (in decimal fraction of g's)

A_{is} equals PGA for “shallow” landslides, whilst $A_{is} = (2/3)PGA$ for deep and large landslides

$E[d/A_{is}]$ the expected displacement factor per cycle, and

n the number of cycles which is calculated as a function of the Earthquake Moment Magnitude (M_w):

$$n = 0.3419M_w^3 - 5.5214M_w^2 + 33.6154M_w - 70.7692 \text{ (Seed and Idriss, 1982).}$$

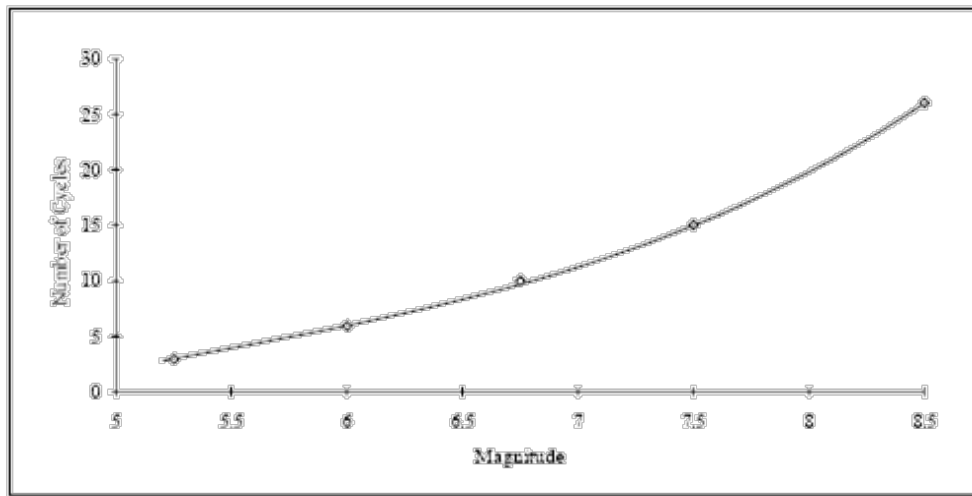


Fig. 40 Relationship between Earthquake Moment Magnitude and Number of Cycles (Hazus 99-SR2 Technical Manual, Chapter 4-PESH)

Moment Magnitudes were calculated for Serres and for Nymfaia PIAs respectively as: Serres PIA, $M_w = 6.2R$; Nymfaia PIA, $M_w = 6.7R$.

Those values were used to calculate the number of cycles (n) for each of the PIAs and in turn calculate the respective expected displacement factor $E[d/A_{is}]$ per cycle.

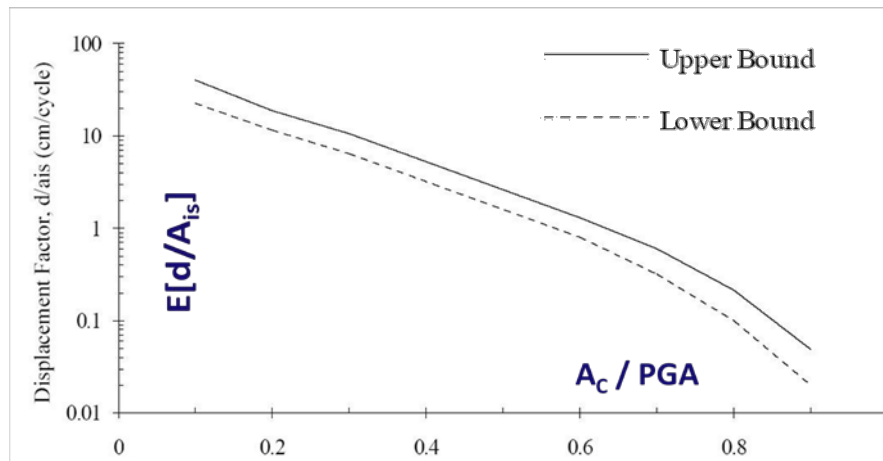


Fig. 41 Relationship between the displacement factor and the ratio A_c/PGA (Makdisi and Seed, 1978)

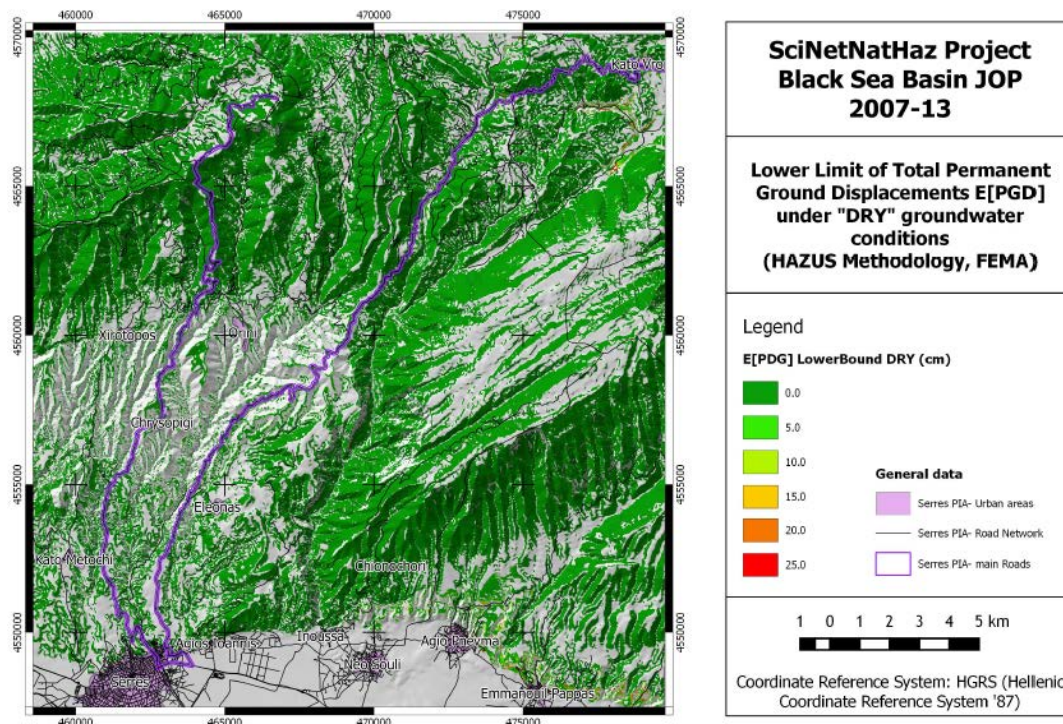


Fig. 42 Permanent Ground Displacements (E[PGD] lower limit, calculated for “dry” conditions on Serres PIA

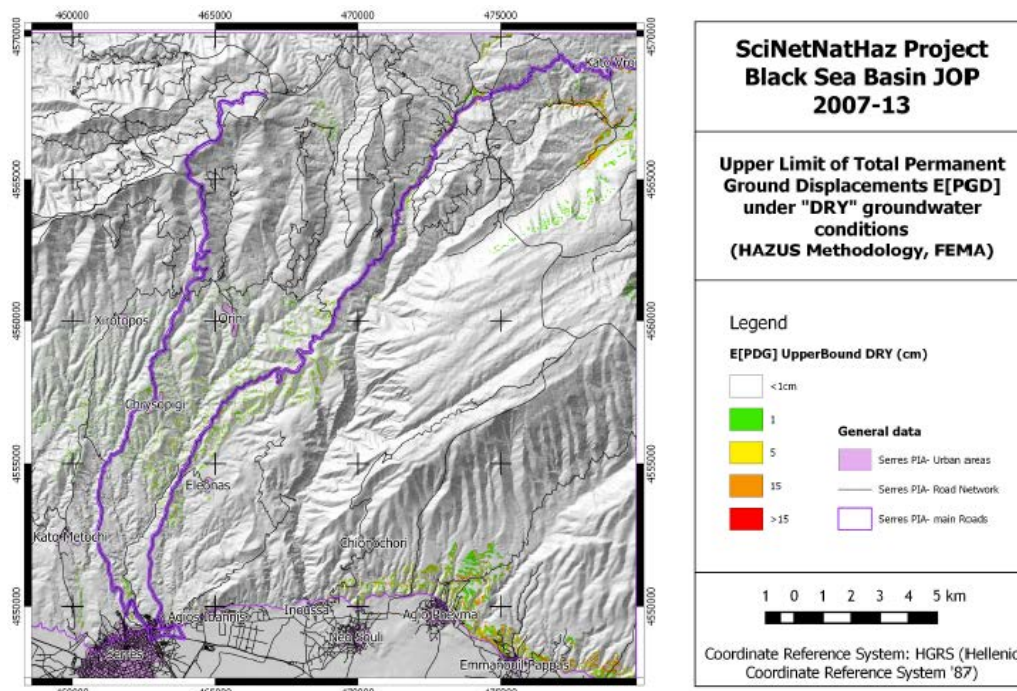


Fig. 43 Permanent Ground Displacements (E[PGD] upper limit, calculated for “dry” conditions on Serres PIA

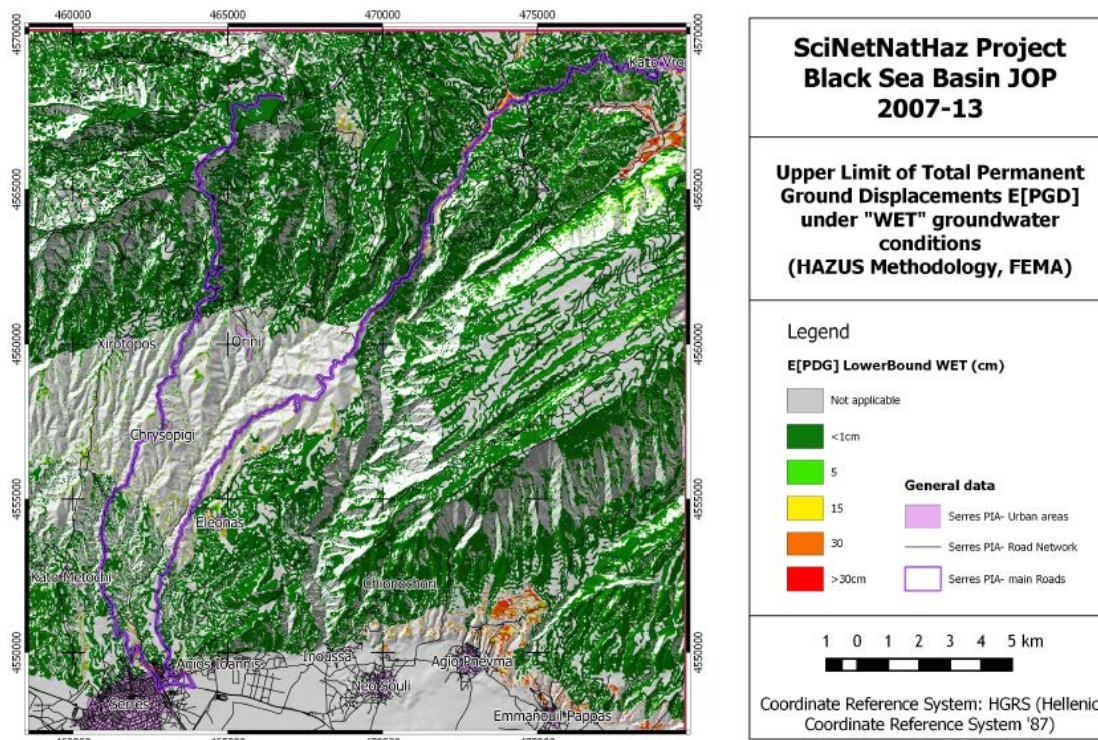


Fig. 44 Permanent Ground Displacements (E[PGD] lower limit, calculated for “wet” conditions on Serres PIA

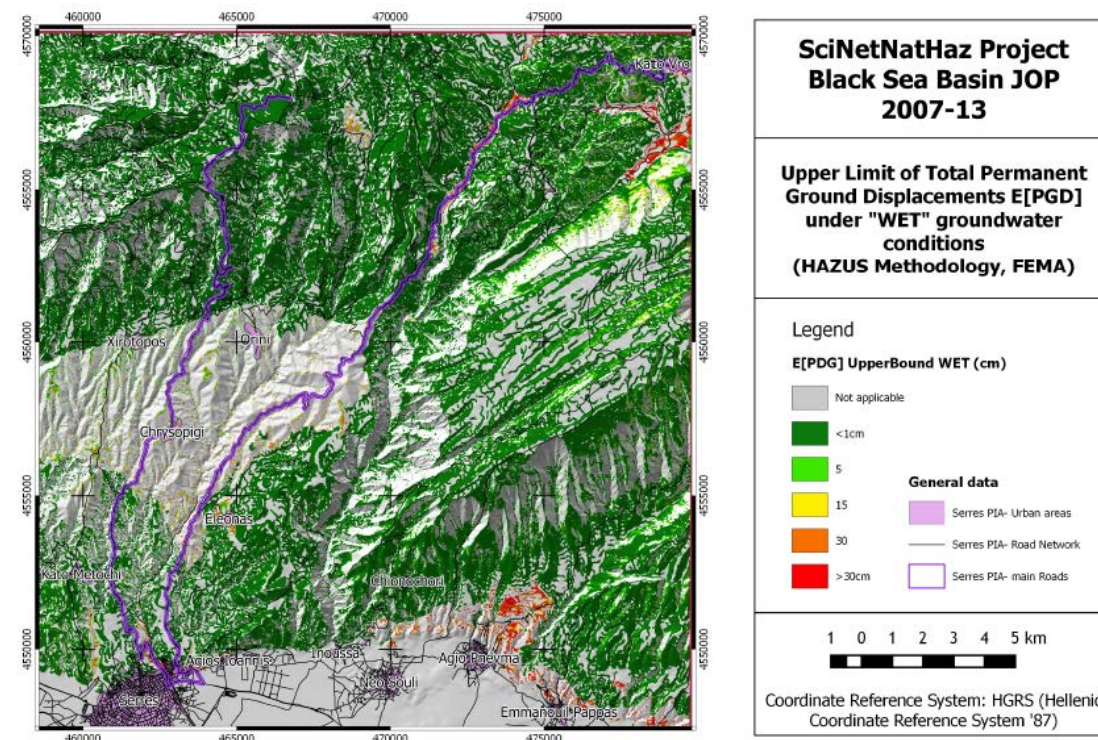


Fig. 45 Permanent Ground Displacements (E[PGD] upper limit, calculated for “wet” conditions on Serres PIA

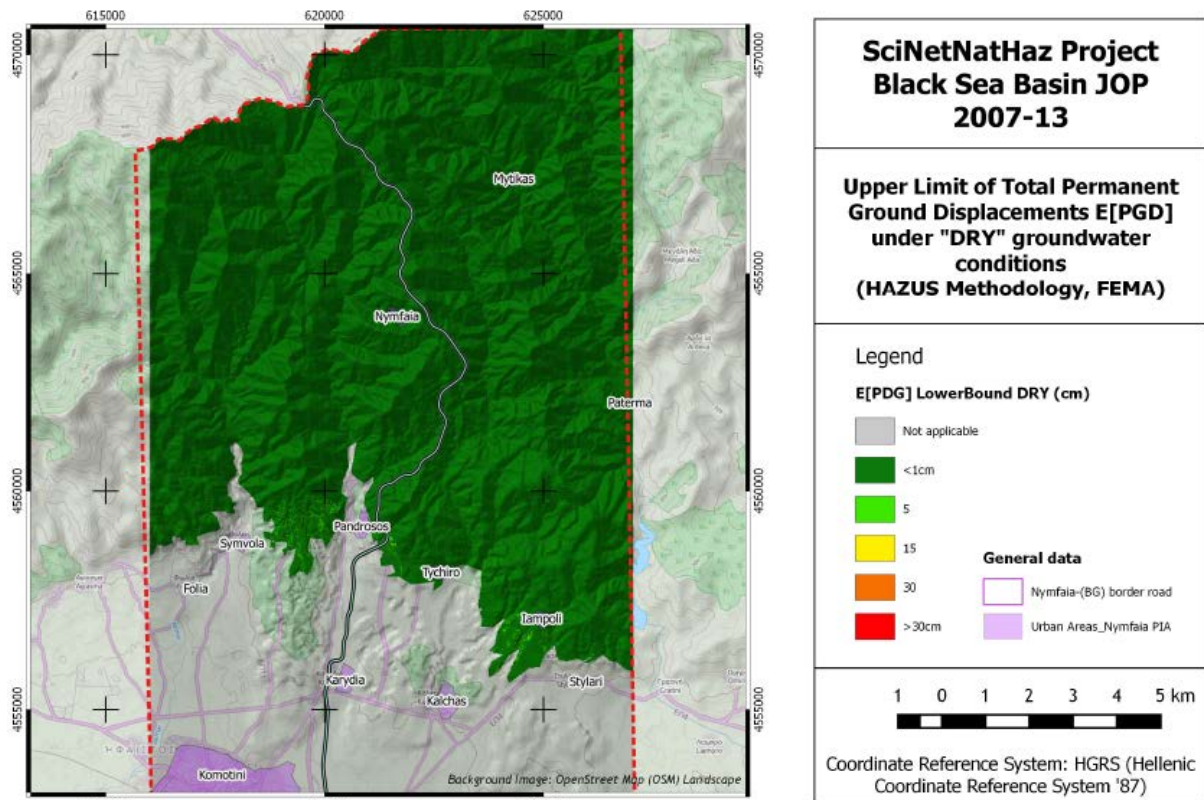


Fig. 46 Permanent Ground Displacements (E[PGD]) lower limit, calculated for “dry” conditions on Nymfaia PIA

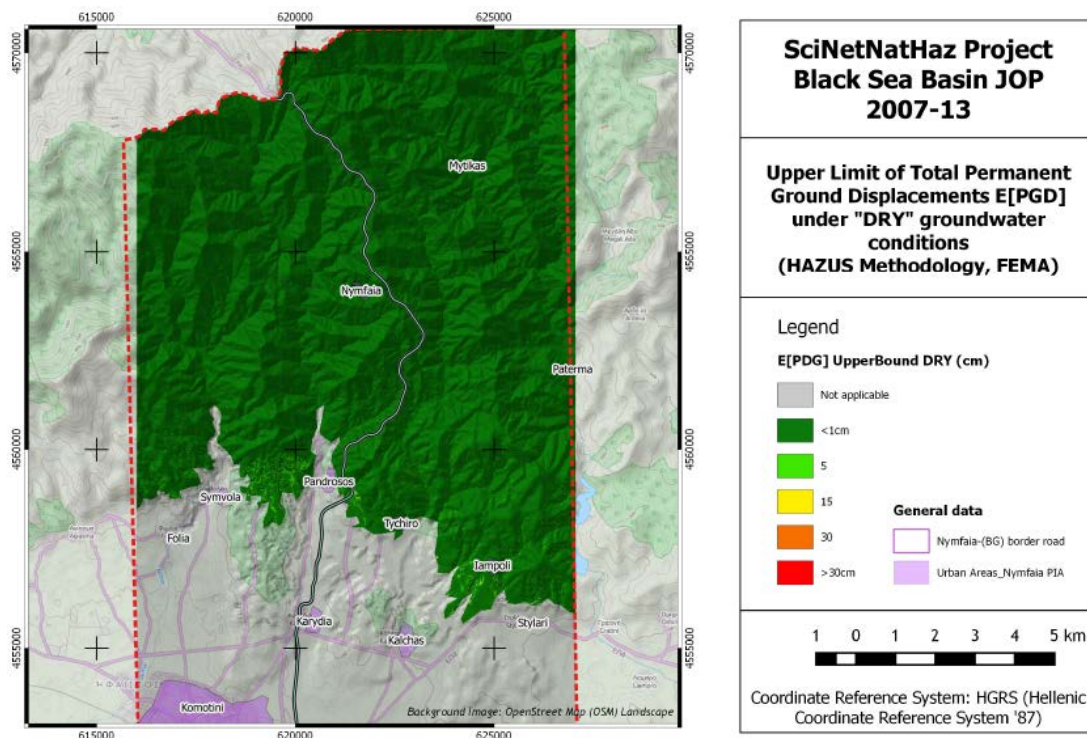


Fig. 47 Permanent Ground Displacements (E[PGD]) upper limit, calculated for “dry” conditions on Nymfaia PIA

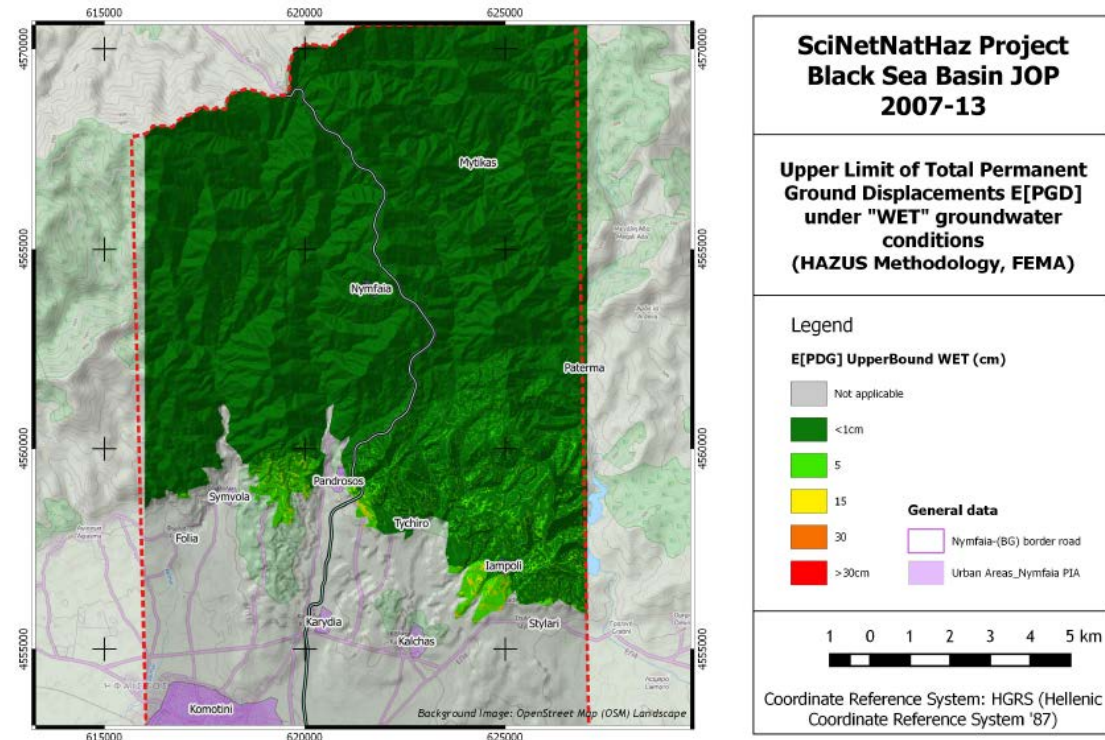


Fig. 48 Permanent Ground Displacements (E[PGD]) lower limit, calculated for “wet” conditions on Nymfaia PIA

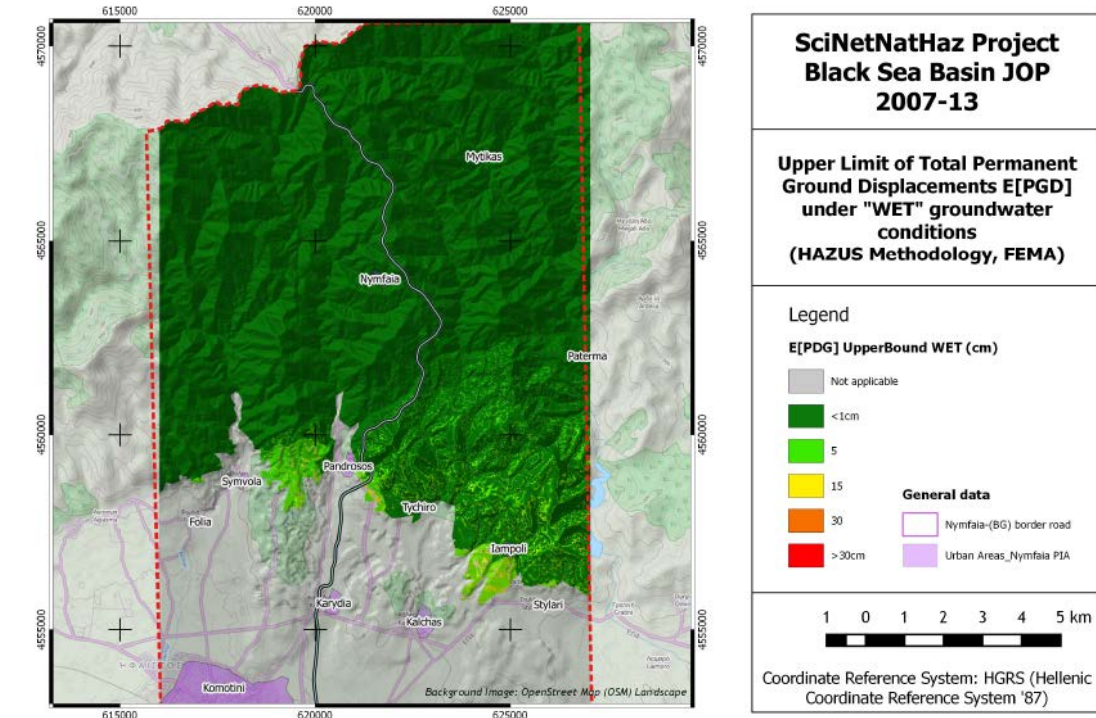


Fig. 49 Permanent Ground Displacements (E[PGD]) upper limit, calculated for “wet” conditions on Nymfaia PIA

3.3 Method of Factor of Safety

The LHA over the calculation of the Factor of Safety of natural and cut slopes falls into the physically based LHA methods which are based on modeling of slope failure processes (Montgomery and Dietrich, 1994; Ferentinou et al., 2006; Risklides, 2010).

This method is applicable over large areas provided that the geological and the geomorphological conditions are fairly homogeneous and the landslide types are relatively simple. This method is applicable in areas with incomplete or even non-existing landslide inventories.

Physically based LHA methods can be applied using the infinite slope model to model shallow landslides or the deterministic model for circular failures. Those methods take into account as triggering factors rainfall and transient groundwater response or the ground motion induced by earthquakes.

In both PIAs under investigation in Greece, the Factor of Safety calculation considering as triggering factors rainfall or earthquakes, was applied.

A geodatabase and a respective GIS were developed for hosting the required data and for the processing and the cartographic production activities that followed.

The scale of implementation, in terms of the specifications and analysis of the respective data input was 1:50,000, so elevation data were produced from topographic maps of 1:50,000 scale.

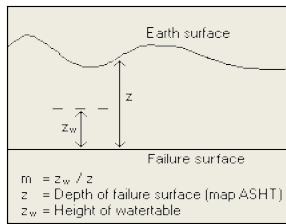
Additional data input and produced during the implementation phase included:

- Digitized Geologic Maps
- Calculation of the geotechnical properties of geologic formations (effective cohesion, effective friction angle, unit weight, hydraulic permeability) using RocLab software
- Mean monthly rainfall (mm), max daily precipitations (mm) and peak rainfall intensity (mm/hour)
- Ground Motion data (PGA values)
- Digital Elevation Model (DEM) with cell size of 15x15m
- Various maps related to the area morphology (slope, aspect, valley depth, hill shade etc) and numerous intermediate “products” during the processing phase and according to the requirements of the specific methods applied.
- Ancillary data (Corine 2000 Land use Maps, road network, urban areas etc)

It must be noted that all raster files were produced with a cell size of 15x15m which is considered as a high resolution analysis considering the regional scale of implementation. Reason for this decision was the commitment to produce outputs with the most effective spatial accuracy.

3.3.1 LHA - Infinite slope model under static and seismic conditions

Landslide Hazard Assessment method is based on the infinite slope model to model shallow landslides triggered by precipitation under static conditions:



$$F_S = \frac{c' + (\gamma_{app} - m * \gamma_w) * z * \cos^2 \beta * \tan \phi'}{\gamma_{app} * z * \sin \beta * \cos \beta} \quad (4)$$

where, ϕ' : effective angle of friction of geomaterial ($^{\circ}$)
 c' : effective cohesion of geomaterial (kPa),
 γ : specific weight (kN/m³),
 β : slope angle (Deg),
 γ_w : specific weight of the water (kN/m³),
 z : normal thickness of the failure slab (m)
 m : percentage of the water saturated failure slab (%)
 $\gamma_{app} = \gamma * (1 - m) + \gamma_{sat} * m$, if slope is dry then $\gamma_{app} = \gamma$ (m=0%), if completely saturated $\gamma_{app} = \gamma_{sat}$

The same physically based model (infinite slope) is used when the triggering factor is the earthquake. In this case the driving equation is modified as follows:

$$F_S = \frac{c' + (z * \gamma * (\cos \beta)^2 - z * \rho * a * \cos \beta * \sin \beta - \gamma_w * z_w * (\cos \beta)^2) * \tan \phi'}{z * \gamma * \sin \beta * \cos \beta + z * \rho * a * (\cos \beta)^2} \quad (5)$$

where, ϕ' : effective angle of friction of geomaterial ($^{\circ}$)
 c' : effective cohesion of geomaterial (kPa),
 γ : specific weight of geomaterial (kN/m³),
 ρ : bulk density (Kg/m³)
 β : slope angle (Deg),
 γ_w : specific weight of the water (kN/m³),
 z : normal thickness of the failure slab (m)
 m : percentage of the water saturated failure slab (%) and
 a : earthquake acceleration (m/sec²)

3.3.1.1 Data input

Basic data incorporated in the system are:

- The Digital Elevation Model with 15x15m cell size, created using elevation points and contours digitized from topographic maps (contour interval 20m).
- Polygons of geologic formations digitized from geologic maps of 1:50,000 scale (IGME, Greece).
- Weather station data regarding precipitation (mean annual, max daily and peak values).
- A grid of PGA values covering the entire area.

From that basic input, a number of information was produced and additional information was incorporated. Slope, aspect, relief maps; peak, mean annual and maximum daily precipitation; and PGA spatial distribution maps.

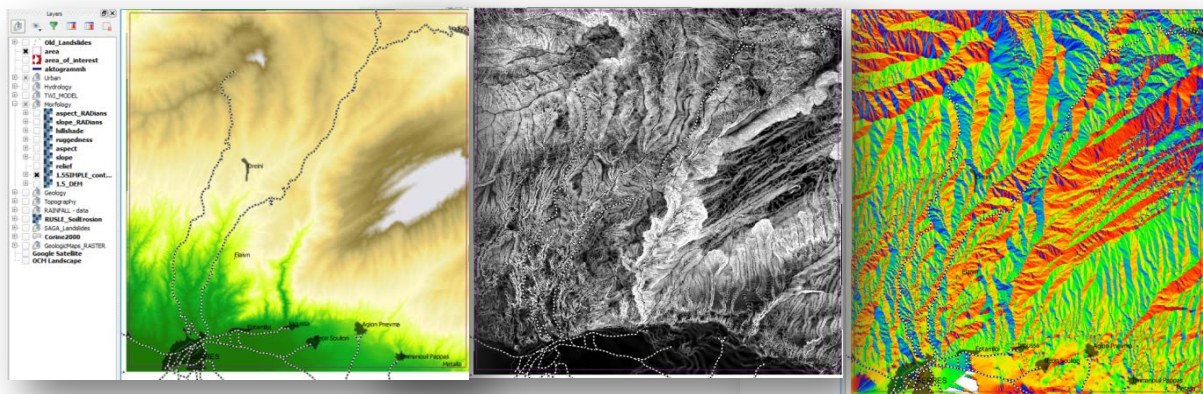


Fig. 50 Left to right: DEM, Slope and Aspect map of Serres PIA

Geotechnical parameters of rock and soil formations outcropping in the area were calculated using respectively the Hoek & Brown failure criterion for the former formations and the failure criterion of Mohr-Coulomb for the latter on. For each geologic formation, two pairs of effective cohesion (c') and effective angle of friction (ϕ') for low and high normal stresses (small slope and high slope respectively) were calculated. When the failure criterion of Mohr-Coulomb is applied on a sliding surface at a small slope (e.g. height of slope $H=5m$; low normal stresses on the sliding surface), then the corresponding pair of effective cohesion and angle of friction results in low values of effective cohesion and high values of effective angle of friction. When we apply the M-C failure criterion at a high slope (e.g. $H=50m$; high normal stresses over the sliding surface), then the corresponding pair of geotechnical parameters of shearing resistance results in high values of effective cohesion and low values of effective angle of friction. For the needs of the regional LHA on both PIAs we adopted the minimum values from each approach and we came up with a "conservative" pair of geotechnical

parameters describing shear resistance at a regional scale. The GSI (Geological Strength Index) and the Uniaxial Compressive Strength were also estimated according to rockmass lithology and the condition of the rockmass in terms of fracturing and weathering (Hoek, 2007; Marinos and Hoek, 1995; Marinos et al., 2005).

For soil geological formations, the respective values of c' and ϕ' were assigned according to data collected from previous studies in the area, working experience of the implementation team and even, in a few cases, the international bibliography.

In any case, the geotechnical parameters were either calculated or estimated in a conservative way in order to be on the “safe” side, given the big number of uncertainties at a regional scale.

	gn,ab		gn,ab,sch		gn,mr		gn-sch		gn-v		gn-uv		gn1		
Hoek Brown Classification	H=5m	H=50m	H=5m	H=50m	H=5m	H=50m	H=5m	H=50m	H=5m	H=50m	H=5m	H=50m	H=5m	H=50m	
sigci (Mpa)	100	100	100	100	100	100	100	100	120	120	175	175	100	100	
GSI	30	30	31	31	30	30	29	29	31	31	31	31	33	33	
mi	23	23	23	23	12	12	10	10	26	26	26	26	25	25	
D	1	1	1	1	1	1	1	1	1	1	1	1	1	1	
EI	40000	40000	30000	30000	85000	85000	30000	30000	48000	48000	70000	70000	30000	30000	
MR	400	400	300	300	850	850	300	300	400	400	400	400	300	300	
Hoek Brown Criterion															
mb	0.15497	0.15497	0.16645	0.16645	0.08086	0.08086	0.06273	0.06273	0.18816	0.18816	0.18816	0.18816	0.20870	0.20870	
s	8.57E-06	8.57E-06	1.01E-05	1.01E-05	8.57E-06	8.57E-06	7.26E-06	7.26E-06	1.01E-05	1.01E-05	1.01E-05	1.01E-05	1.41E-05	1.41E-05	
a	0.52234	0.52234	0.52089	0.52089	0.52234	0.52234	0.52390	0.52390	0.52089	0.52089	0.52089	0.52089	0.51826	0.51826	
Failure Envelope Range															
Application	Slopes	Slopes	Slopes	Slopes	Slopes	Slopes	Slopes	Slopes	Slopes	Slopes	Slopes	Slopes	Slopes	Slopes	
sig3max (Mpa)	0.12892	1.04787	0.12946	1.05227	0.12066	0.98074	0.12344	1.00331	0.13236	1.07584	0.13693	1.11300	0.13103	1.06504	
Unit Weight (MN/m3)	0.026	0.026	0.026	0.026	0.025	0.025	0.026	0.026	0.026	0.026	0.026	0.026	0.026	0.026	
Slope Height (m)	5	50	5	50	5	50	5	50	5	50	5	50	5	50	
Mohr-Coulomb Fit															
c (Mpa)	0.0587	0.2299	0.0616	0.2391	0.0530	0.1798	0.0500	0.1653	0.0685	0.2671	0.0827	0.3084	0.0688	0.2651	
phi (degrees)	51.6	35.1	52.3	35.9	46.3	29.9	43.6	27.4	54.4	38.3	56.7	41.1	54.3	38.0	
Rock Mass Parameters															
sigt (Mpa)	-0.0055	-0.0055	-0.0061	-0.0061	-0.0106	-0.0106	-0.0116	-0.0116	-0.0065	-0.0065	-0.0094	-0.0094	-0.0068	-0.0068	
sigc (Mpa)	0.2256	0.2256	0.2503	0.2503	0.2256	0.2256	0.2031	0.2031	0.3004	0.3004	0.4380	0.4380	0.3067	0.3067	
sigcm (Mpa)	4.5577	4.5577	4.7751	4.7751	3.2471	3.2471	2.8123	2.8123	6.1073	6.1073	8.9065	8.9065	5.4597	5.4597	
Erm (Mpa)	1128.98	1128.98	869.793	869.793	2399.08	2399.08	825.615	825.615	1391.67	1391.67	2029.52	2029.52	922.432	922.432	
Results															
	H(m)	φ	c (kPa)	H(m)	φ	c (kPa)	H(m)	φ	c (kPa)	H(m)	φ	c (kPa)	H(m)	φ	c (kPa)
	5	51.61	58.71	5	52.30	61.85	5	46.31	52.98	5	54.43	68.34	5	54.27	68.77
	50	35.14	229.90	50	35.88	239.11	50	29.90	179.85	50	38.29	267.10	50	38.04	265.11
Final Values		φ	c (kPa)		φ	c (kPa)		φ	c (kPa)		φ	c (kPa)		φ	c (kPa)
		35	59		36	62		30	53		38	69		38	69

Fig. 51 Mechanical properties of rocks masses calculated using the Hoek & Brown failure criterion

Mechanical and physical properties of geologic formations were attributed to the respective formations in the GIS for further processing and analysis. Respective maps of the spatial distribution

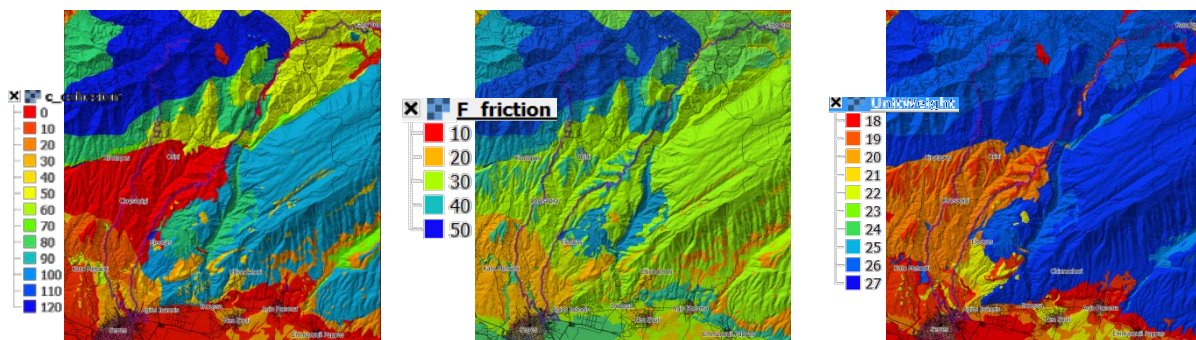
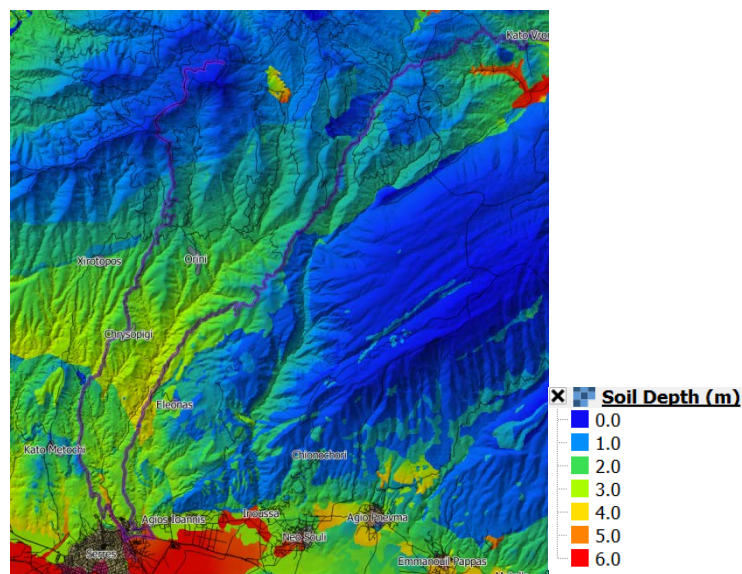


Fig. 52 Spatial distribution of mechanical properties of rocks: c' (kN/m^2), ϕ' ($^\circ$), Unit weight (kN/m^3)

As an alternative case, the “z” parameter was calculated using a physically based model that links it to soil and regolith development on natural slopes as has been suggested by previous researchers



The second, difficult to estimate, parameter is the percentage of saturation (m parameter). This parameter was correlated with rainfall values, the hydraulic conductivity of the respective geologic formation, the slope angle and the thickness of the sliding slab (z parameter), taking into

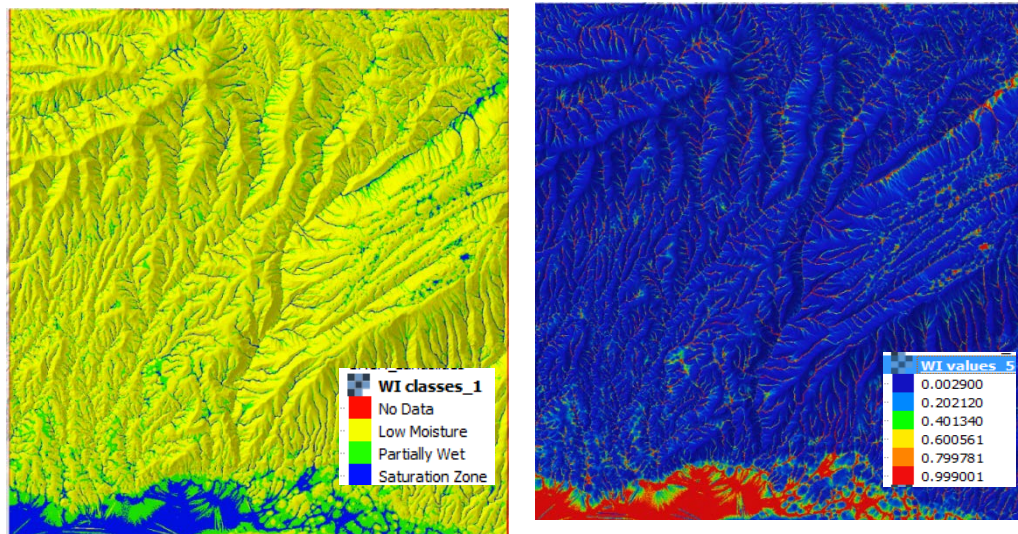


Fig. 54 Saturation classes (left) and saturation percentage (right) for a sliding slab 5m thick (SAGA GIS module)

consideration pre-existing research work (Beven & Kirkby, 1979 (Topmodel); Montgomery & Dietrich, 1994), using the respective module in SAGA GIS.

3.3.1.2 Serres PIA factor of safety of natural slopes

Factor of safety for natural slopes was calculated for various sliding slab normal thickness values: 1m, 5m, 10m and variable thickness calculated using the method described in previous paragraphs taking into consideration rainfall or earthquake or both of them. The respective maps are given in Annex A. An indicative number of maps is presented below in order to demonstrate changes in qualitative and quantitative characteristics in each of these outputs.

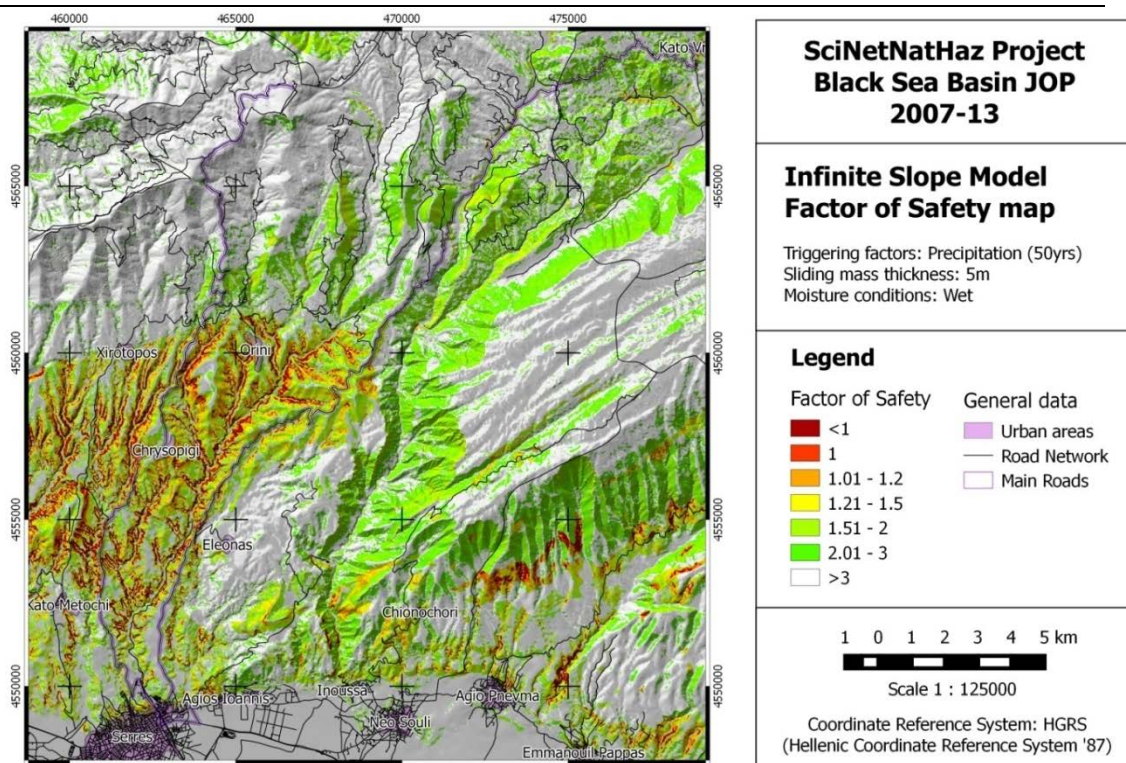


Fig. 55 Serres PIA Factor of Safety calculated for precipitation of 50yrs return period and for a five meters normal thickness sliding slab (z=5m)

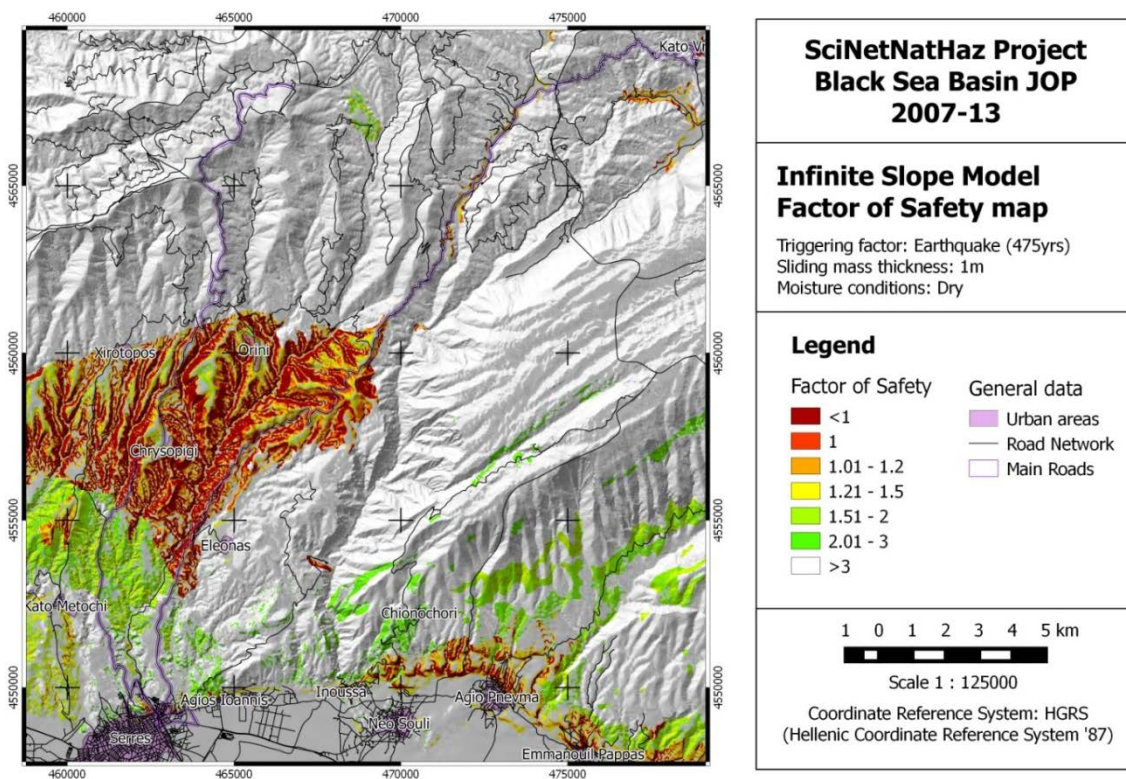


Fig. 26 Serres PIA Factor of Safety calculated for Earthquake of 475yrs return period and for a 1m normal thickness sliding slab (z=1m)

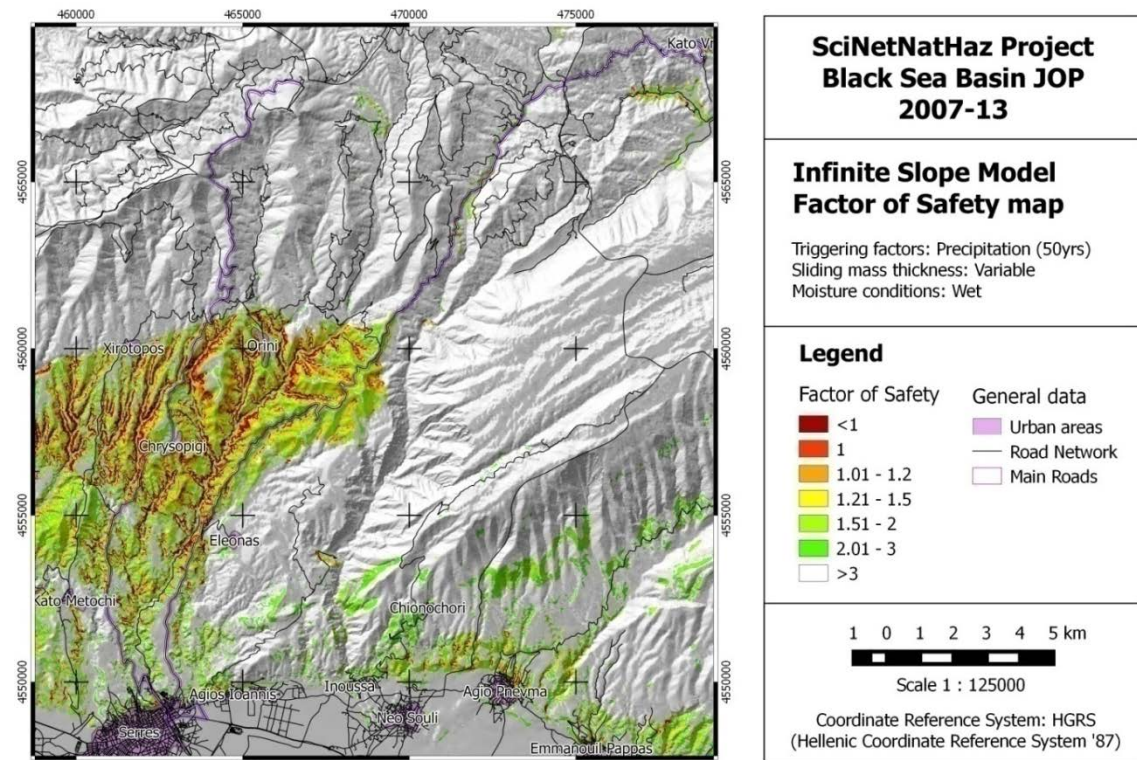


Fig. 57 Serres PIA Factor of Safety calculated for precipitation of 50yrs return period and for a variable normal thickness sliding slab calculated as described in previous paragraphs

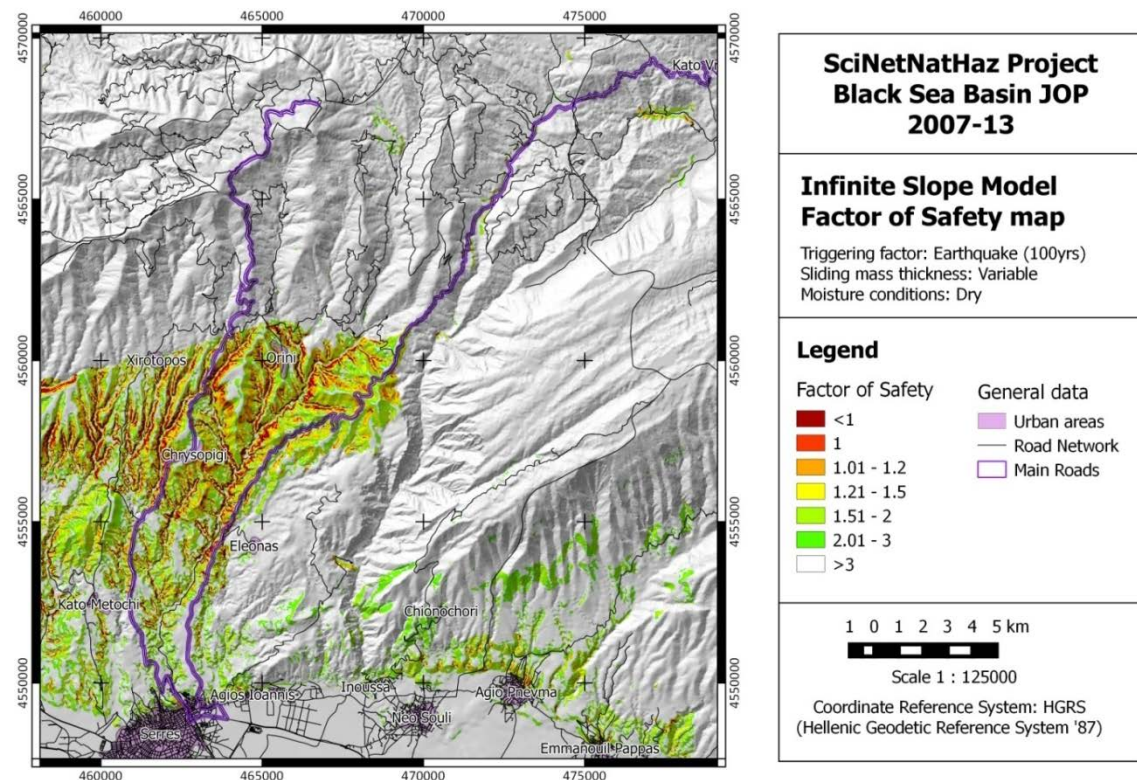


Fig. 58 Serres PIA Factor of Safety calculated for Earthquake of 100yrs return period and for a variable normal thickness sliding slab calculated as described in previous paragraphs

3.3.2 LHA - Deterministic model under static conditions for circular landslides

Landslide Hazard Assessment under static conditions method is using the deterministic model to model circular landslides triggered by precipitation was also applied (Ferentinou et al, 2006):

$$F_S = 4.32 * \left[\frac{c'}{\gamma * H * \sin \beta} \right] + 1.22 * (1 - r_u) * \frac{\tan \varphi'}{\tan \beta} + 0.005 \quad (6)$$

where

c' :	effective cohesion of geomaterial (kPa),
ϕ' :	effective angle of friction of geomaterial ($^{\circ}$)
γ :	specific weight (kN/m^3),
β :	slope angle (Deg),
γ_w :	specific weight of the water (kN/m^3),
H :	height of slope (m)
r_u :	percentage of the water saturated failure slab (γ_w/γ)

The slope height parameter (H) was parametrically set to 10m, 20m and 30m and the respective factors of safety were calculated for both PIAs.

In all cases, factors of safety were also calculated by taking into consideration the presence of fractured zones mapped by remote sensing techniques. As already mentioned, the effective cohesion value (c') was changed to correspond to such a fractured and weathered formation inside a buffer zone of 30m around each mapped lineament.

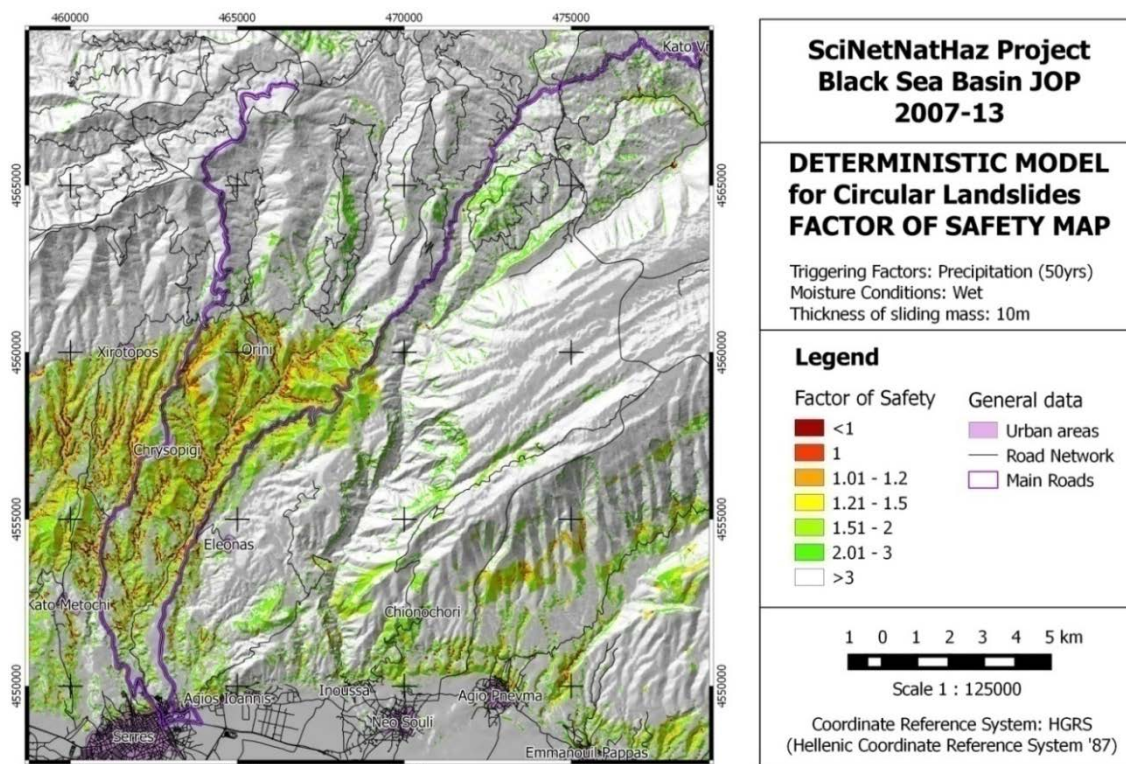


Fig. 59 Factor of Safety using the deterministic model for circular landslides, calculated for a 10m high slope

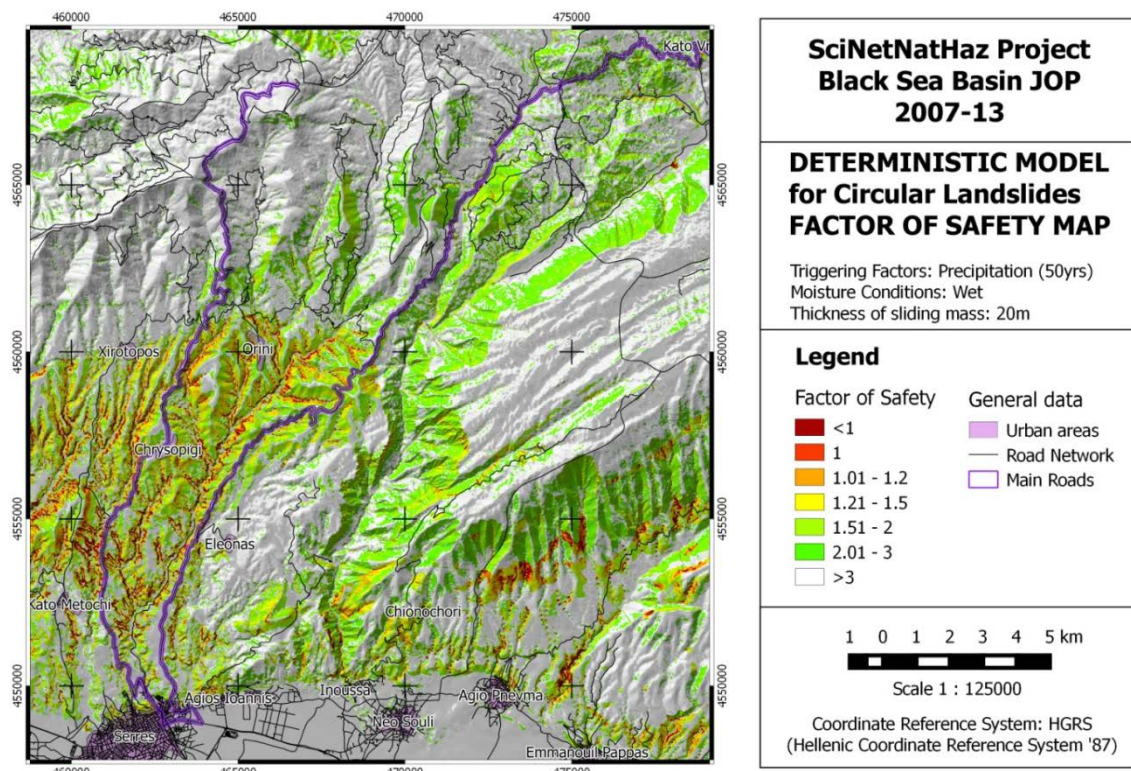


Fig. 60 Factor of Safety using the deterministic model for circular landslides, calculated for a 20m high slope

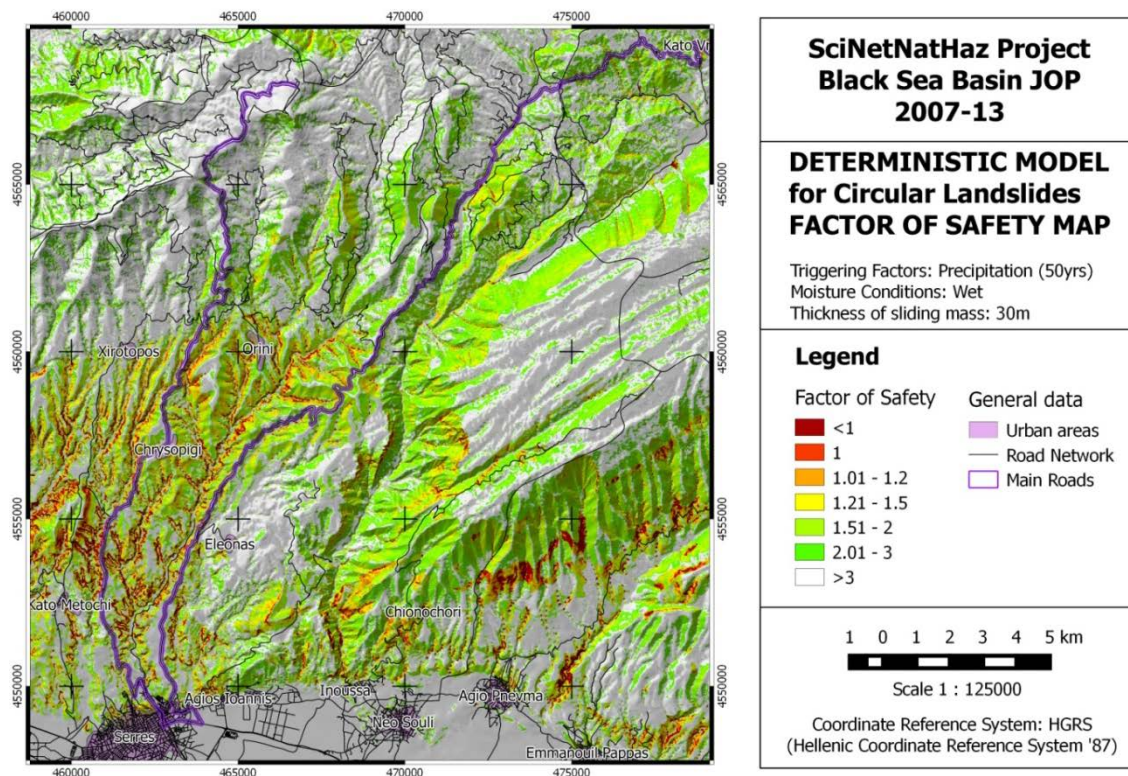


Fig. 61 Factor of Safety using the deterministic model for circular landslides, calculated for a 30m high slope

3.4 Evaluation of Methods used for Regional LHA

The evaluation of the methods used to assess Landslide Hazard in two Pilot Implementation Areas in Greece, was based on the comparison of field work data with their predictions.

Quality of results is always related to intrinsic weaknesses of the methods and the level of assumptions and generalizations during each of the processes followed.

The evaluation took into consideration, the reliability, accuracy and quality of results by comparing them to actual facts recorded in the field. Additional parameters were also considered included their ability to provide detailed information, the spatial resolution of their outputs, the compliance of their outputs with standing procedures (i.e. to classify LHA according to standing regulations), their complexity, and their requirements in terms of data and required processing. Finally, to assess their potential for dissemination and broader use by a network of scientists including personnel of state authorities, their “complexity” was also considered.

In terms of data requirements, all applied methods have almost the same requirements: digitized topographic map data, digitized geologic maps, rainfall data and ground motion data (PGA), to the exception of FEMA method which is more demanding.

If a classification and an evaluation in terms of: complexity of use, understanding and usefulness of the outputs and applicability for the 3 aforementioned methods to assess LH on a regional scale needs to be pronounced, our conclusions are as follows:

1. the method of **Mohra and Vahrson** could be considered as a crude and approximate method to assess regional LHA in a rather qualitative way for both triggering factors (water and earthquake), since hazard indicator is an arbitrary index denoting rather susceptibility than hazard to slide,
2. the method of **FEMA (HazUS)** is restricted to assess LH only if the triggering factor is an earthquake; it is quite demanding method in terms of data needed for its application and an important number of intermediate "products" (maps) has to be calculated in order to assess "Permanent Ground Displacements - PGD" which is the end-product of this method. Despite difficulties in application, complexity and understanding, this method can provide results in terms of permanent seismically-induced displacements, which is actually the only real way that the phenomenon of sliding is perceived,
3. the method of **Factor of Safety** is the most comprehensive among the 3 methods, since based on a physically based model. This method, applies to both static and seismic conditions, where water or earthquake are respectively the triggering factors and the results, i.e. maps with the factor of safety are well perceived by end users (usually engineers and geologists). Therefore, it is considered to be the most feasible when compared to the other ones and when tested to field in Serres and Nymfaia PIAs.

Hereafter, we present a number of figures where maps resulting from the above methods are compared among them (figs 62 and 63) and also with in-situ observations as existing in the PIAs of Serres (figs 64, 65 and 66) and Nymfaia.

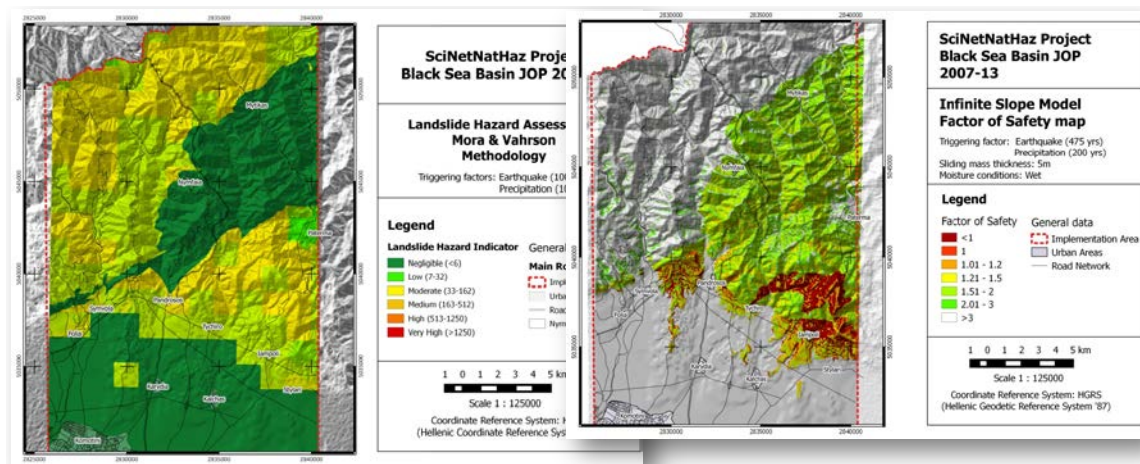


Fig. 62 Comparison of outputs from Mora and Vahrson method (left) to Factor of Safety method (right) based on the Infinite Slope Model in PIA of Serres

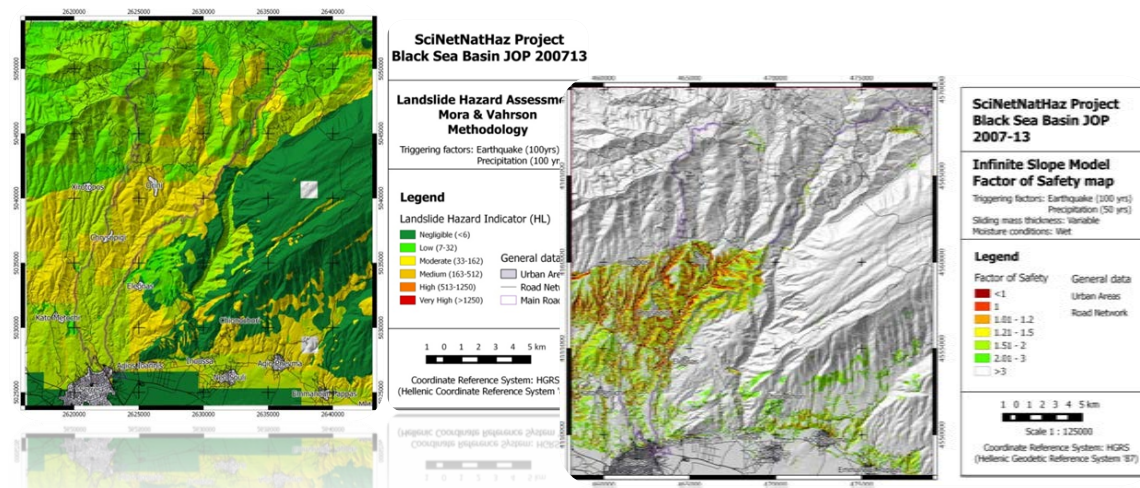


Fig. 63 Comparison of outputs from Mora and Vahrson method (left) to Factor of Safety method (right) based on the Infinite Slope Model in PIA of Nymfaia

The evaluation of reliability of outputs of Factor of Safety method, based on the Infinite Slope Model at a regional scale (1:50,000), has been tested initially by comparing predicted to recorded landslides in the PIA of Serres (figs 64 and 65).

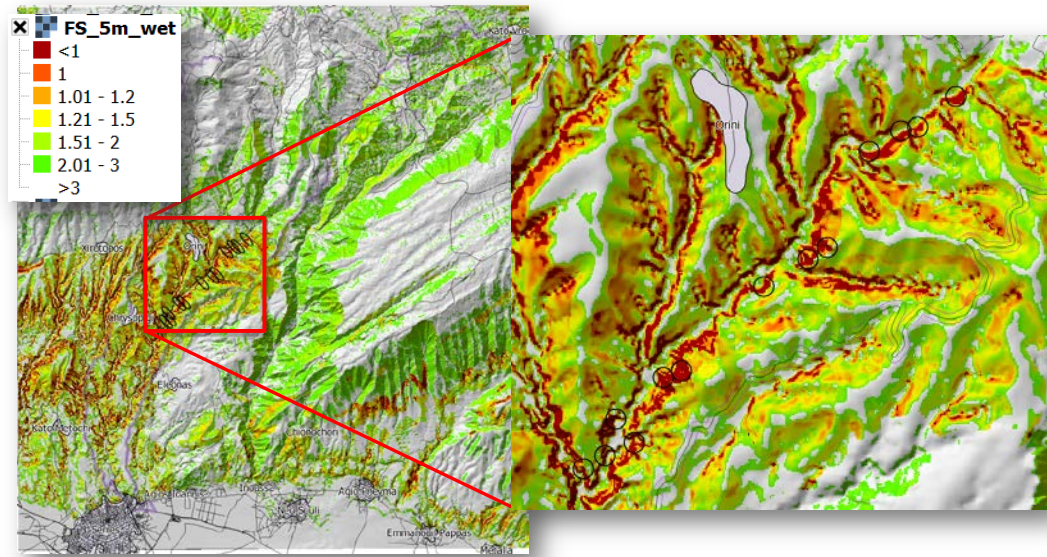


Fig. 64 Comparison of outputs from Factor of Safety method for "wet" conditions, with a thickness of a sliding slab of five meters ($z=5m$) on natural slopes in PIA of Serres. The black cycles (right part of the figure) are locations of landslides on natural slopes



Fig. 65 Prediction from Factor of Safety method for "wet" conditions, with a thickness of a sliding slab of five meters ($z=5m$) on natural slopes in PIA of Serres (left corner) and landslides on natural slopes in PIA of Serres

The evaluation of reliability and "relative accuracy" of outputs regarding implementation of the method of the Factor of Safety, based primarily on the Infinite Slope Model, has also been extended to Nymfaia PIA.

3.5 Improvement of Regional LHA performance with Remote Sensing

Initially the maps calculated for the F_s method, failed to describe in a reliable way reality as this is perceived by an in-situ visit along the vertical road axis from Komotini, through Nymfaia, to Hellenic-Bulgarian borders (implementation at Nymfaia PIA). Geologic formations of the examined area, are neither homogeneous, nor isotropic, over large areas, as they were considered by the Landslide Hazard Assessment at a regional scale. The reason for that are the inherent characteristics and the external affecting factors as fracturing and weathering.

Since rock formations in the PIA of Nymfaia were "in theory" of good quality (according to the geological maps of IGME at a scale of 1:50,000), the mechanical parameters that affect seriously Factor of Safety values, were largely over predicted and produced a very homogeneous map with high values of Factor of Safety, calculated according to the equations of the Infinite Slope Model.

Thus, LHA for Nymfaia PIA at a regional scale was not initially successful.

However, it is well known that:

- fracture zones, possess much poorer engineering properties (physical, mechanical and hydraulic) compared to intact rock, proportionally to the degree of fracturing or/and weathering,
- rain water infiltration (which is a triggering factor) and moisture is also related to fracturing
- weathering is in most cases, related to fracturing. Weathered zones, rich in clayey minerals with very poor geotechnical behavior, develop in fractured zones,

As is evident, the incorporation of a parameter that could differentiate the mechanical behavior between good quality rock masses and fractured zones or zones with a high degree of weathering, when calculating the Factor of Safety, could greatly improve final estimations.

Fractured zones can be detected using remote Sensing data. They correspond to “**lineaments**” in satellite images. Not all lineaments are fractures in rocks so there is a need for a detailed, visual interpretation.

Landsat TM and ETM+ data were used for both PI areas to map lineaments and detect fractured zones. Buffer zones of 15m were drawn around each lineament/fracture, representing a fractured zone of 30m width.

Rock Engineering parameters were assigned to those zones, taking into consideration the type of rock and its initial engineering properties. The new data were incorporated into the initial engineering geologic map and thus, a new map was created for calculations of the F_s .

An idea of how calculation of F_s has been modified / improved at Nymfaia PIA can be given by fig 66.

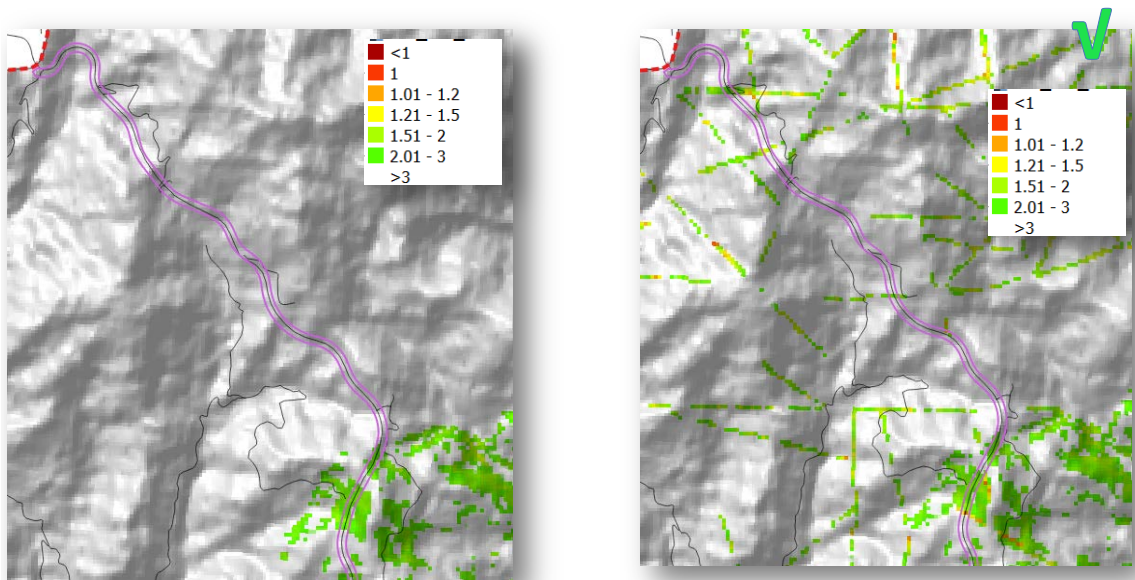


Fig. 66 Prediction of Factor of Safety method for a rainfall of 50 years, with a sliding slab thickness of five meters ($z=5m$) on natural slopes in Nymfaia PIA without (left) and with (right) fractured/weathered zones, located by remote sensing techniques used. Gray color corresponds to $F_s > 3$

Differences in calculation of F_s are obvious between left and right part of fig. 66, solely attributed to lineaments, representing fractured / weathered zones, as located by remote sensing techniques.

Regarding evaluation of predicted F_s values in terms of accuracy and reliability of the new map produced (fractured/weathered zones incorporated) at a regional scale, as implemented in Nymfaia PIA, along the vertical road axis, figs 67, 68, 69 and 70 can be used as an objective criterion.

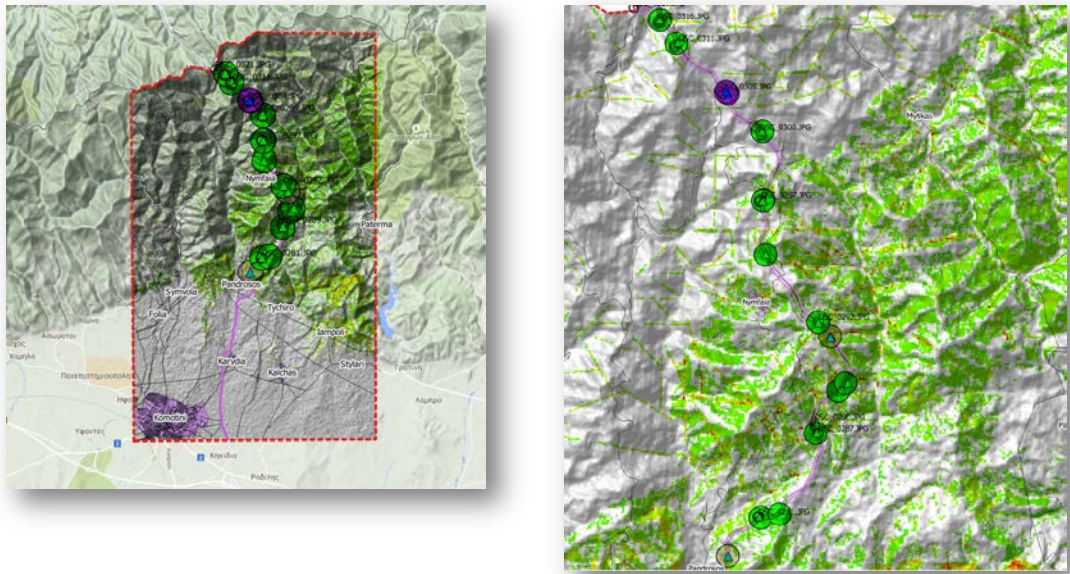


Fig. 67 Locations along the vertical road axis from Komotini - Nymfaia to Hellenic-Bulgarian, where predicted F_s values have been evaluated by in-situ observations. Green colored cycles denote successful prediction, whilst purple colored cycle represents failed prediction

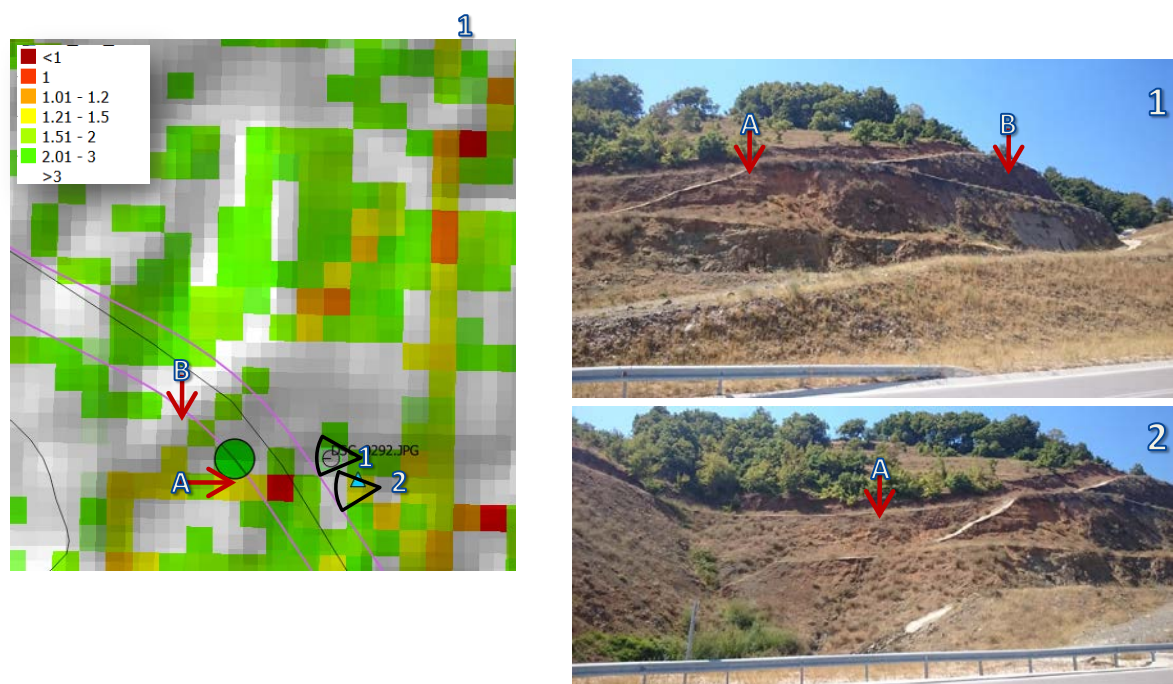


Fig. 68 Location No1 along the vertical road axis from Komotini - Nymfaia to Hellenic-Bulgarian, where predicted F_s values are evaluated by in-situ observations

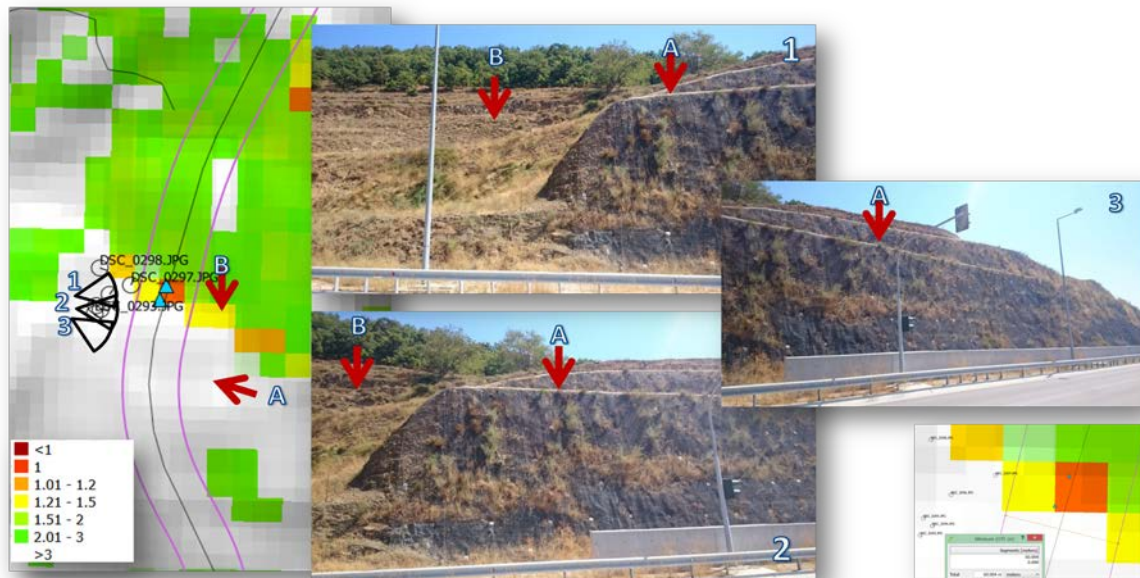


Fig. 69 Location No 2 along the vertical road axis from Komotini - Nymfaia to Hellenic-Bulgarian, where predicted F_s values are evaluated by in-situ observations

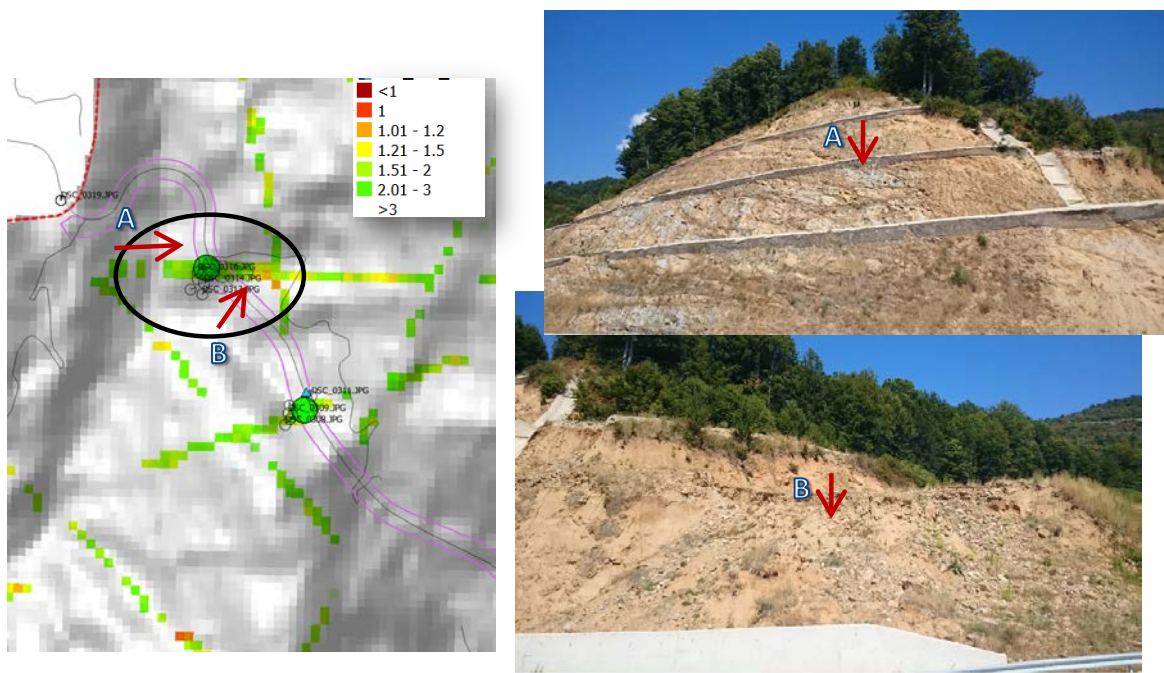


Fig. 70 Location No 3 along the vertical road axis from Komotini - Nymfaia to Hellenic-Bulgarian, where predicted F_s values are evaluated by in-situ observations

It is quite obvious that remote sensing assistance has greatly improved the map with predicted F_s values in Nymfaia PIA, after evaluation via in situ observations.

4 LANDSLIDE HAZARD ASSESSMENT ON A LOCAL SCALE - PILOT IMPLEMENTATIONS IN GREECE

The objective of the present part of the report is the presentation of 2D and 3D slope stability analyses on local scale on a number of natural slopes and cut slopes along the vertical road axis Komotini - Nymfaia - Greek / Bulgarian borders (PIA Nymfaia) and also cut slopes of Serres - Promahonas local road (PIA Serres).

In the present work representative geotechnical profiles per examined slope (natural or/and artificial) are elaborated, based on the geological and geotechnical data referring at the specific site. The goal of this part of the project is twofold: a) a direct comparison between regional and local LHA results in terms of safety factor both evaluated by field reality, and b) a proposal of countermeasures to enhance and assure the stability of the cut slopes along the examined road axes, based on local LHA calculations. We also investigate possible divergence of results between 2D and 3D slope analyses that have been performed in an attempt to define possible differentiations in geotechnical design.

4.1 Geological – Geotechnical Data

According to existing geological projects and, geotechnical investigation previously conducted which included drilling of boreholes and excavation of trial pits. The investigation concluded that in the PIA Nymfaia , formations of gray-gneiss, slightly to moderately weathered, with intercalations of highly weathered materials prevailed (Dimaras, 2006; Edafos s.a., 2007, 2008; Geoanalysis s.a., 2006, 2007; Tressos and Skempas, 2003).

However, the findings of the geotechnical investigation did not always reflect real conditions of the slopes, which were identified only during excavating operations and road construction. Therefore, the gneissic rock mass appears in different locations, either strongly disintegrated, or completely weathered, resembling rather to a soil formation, with an analogue mechanical behaviour regarding slope stability mechanisms.

As for the cut slopes examined at a local scale, located along the local road of Serres - Promahonas (PIA of Serres), geological investigation was based solely, on site observation and use of relevant geological maps of IGME at a scale of 1:50,000.

In the following paragraphs we present briefly geological and geotechnical data of every cut slope or natural slope examined in local scale, in PIAs. In fig 71 the total number of cut slopes of the vertical road axis (Nymfaia PIA) is presented.

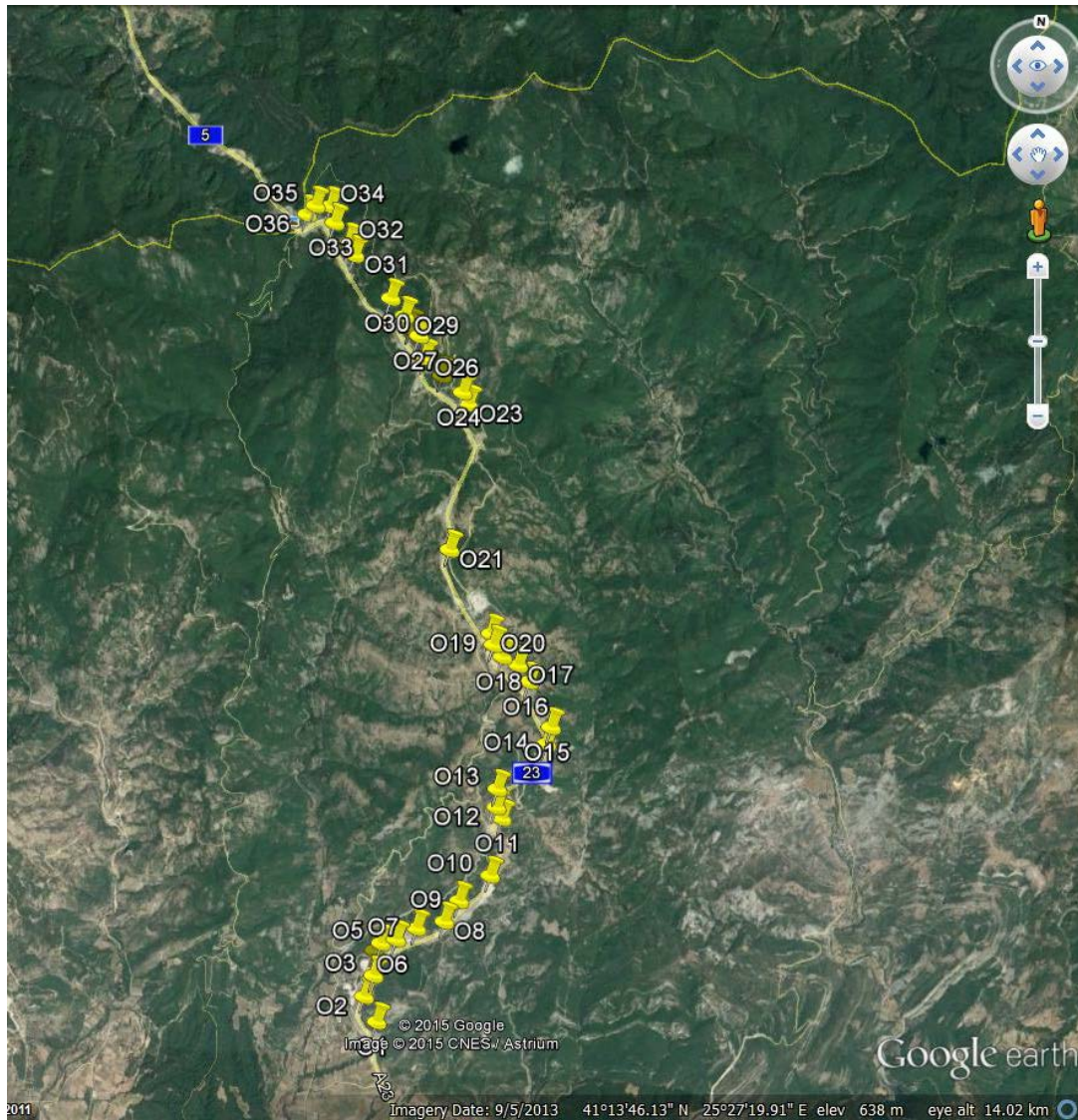


Fig. 71 The total number of cut slopes (O1 to O36) along the vertical road axis from Komotini - Nymfaia - Hellenic/Bulgarian borders (Nymfaia PIA)

4.1.1 PIA Nymfaia: Cut Slope O5

The area where cut slope O5 is located, between ch. 10+380km and ch. 10+460km, according to the existing geological studies and in-situ observation, consists of gneissic formations, slightly to moderately weathered, with intercalations of highly weathered material. Two soil layers can be distinguished. The superficial layer, starts from the ground level, and goes down to a depth of 5.0m

and is described as strongly disintegrated and fragmented gneiss (soil form in some areas). The underlying formation is a weak to strongly disintegrated rock. The physical and mechanical parameters of both formations are presented hereafter:

A. Strongly disintegrated and fragmented gneiss (depth 0.0m – 5.0m):

$$\gamma=21.0\text{kN/m}^3 \quad \varphi'=30^\circ \quad c'=0\text{kPa}$$

B. Weak to strongly disintegrated gneiss:

$$\gamma=22.0\text{kN/m}^3 \quad \varphi'=33^\circ \quad c'=5\text{kPa}$$

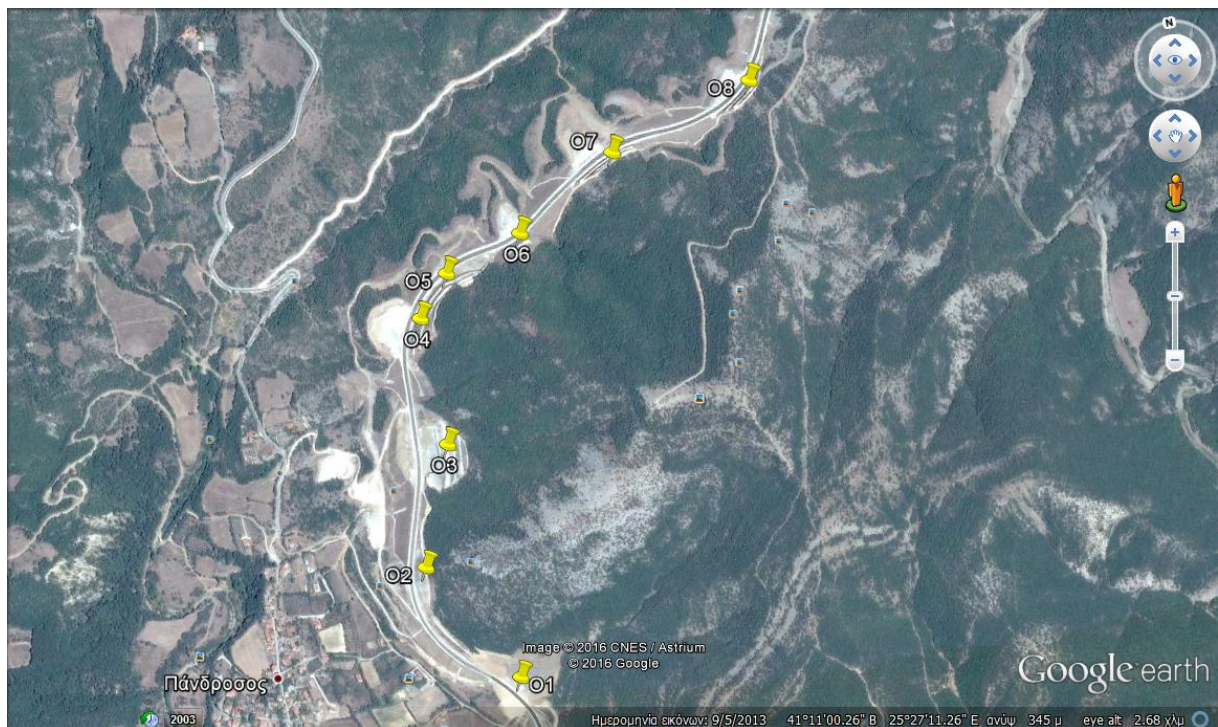


Fig. 72 Location of the examined cut slope O5

4.1.2 Nymfaia PIA: Cut Slope O14-O15

The examined cut slope is located between ch. 13+940km and ch. 14+400km and consists mainly of two geological formations. The superficial layer mainly of clayey SAND is found in a varying depth

along the cut slope (3.0-6.0m from the free surface). The second formation, which starts at a depth ranging from 3.0 to 6.0m, consists of highly weathered and fractured gneiss.

Since there were no geotechnical data for the precise cut slope, we used values of physical and mechanical parameters, from adjacent cut slopes, with similar geological formations as identified from existing geotechnical survey and geological observation, as well as in situ identification performed by P1 and LP research team.

The parameters of both formations are presented hereafter:

A. Clayey SAND (depth 0.0m – 6.0m):

$$\gamma=21.0 \text{ kN/m}^3 \quad \varphi'=34^\circ \quad c'=3 \text{ kPa}$$

B. Mantle of gneiss:

$$\gamma=26.4 \text{ kN/m}^3 \quad \varphi'=42^\circ \quad c'=150 \text{ kPa}$$

4.1.3 Nymfaia PIA: Cut Slope O16

Cut slope O16, is located between ch. 14+865km and ch. 15+000km and according to existing geological and geotechnical data it consists mainly of two geological formations. Rock mass formation below cut slope's toe, it is considered as a healthy gneiss (gneissic bedrock), whereas the rest forms a gneissic mantle described as weathered gneiss. The initial 18m from the weather mantle, whereas the 5m following underneath are characterized, as strongly disintegrated and fragmented gneiss. The physical and mechanical parameters of the three layers, described above, are presented as follows:

A. Weathered mantle (depth 0.0m – 18.0m):

$$\gamma=24.0 \text{ kN/m}^3 \quad \varphi'=38^\circ \quad c'=10 \text{ kPa}$$

B. Strongly disintegrated and fragmented gneiss (depth 18.0m – 23.0m):

$$\gamma=23.0 \text{ kN/m}^3 \quad \varphi'=34^\circ \quad c'=5 \text{ kPa}$$

C. Gneissic bedrock:

$$\gamma=26.0 \text{ kN/m}^3 \quad \varphi'=50^\circ \quad c'=200 \text{ kPa}$$

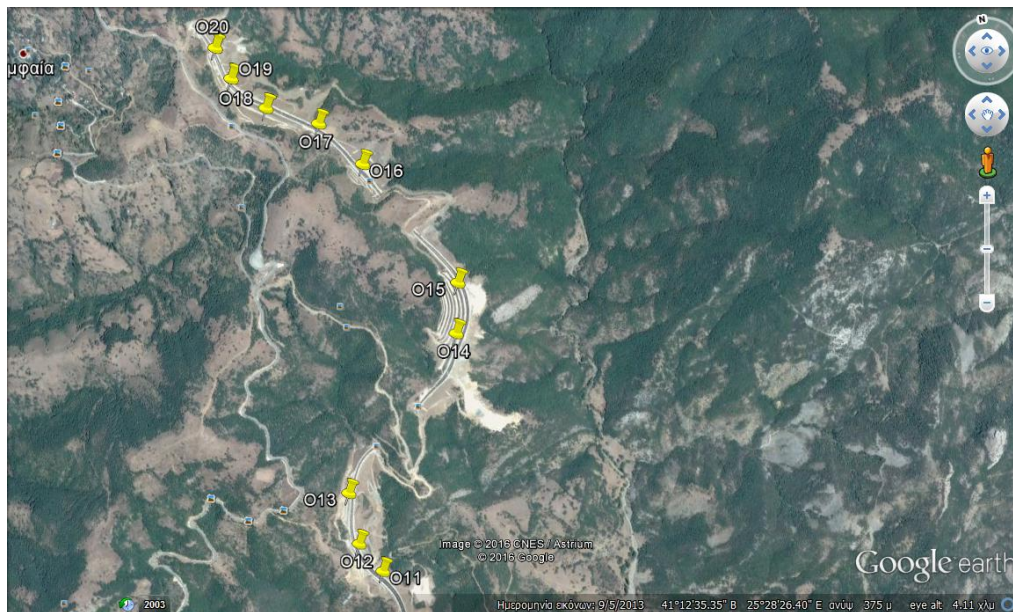


Fig. 73a Locations of the examined cut slopes O14-15 and O16

4.1.4 Nymfaia PIA: Cut Slope O21

Cut slope O21 is located between ch. 16+640km and ch. 17+080km and is divided into two parts, basically due to modification of the geological formations. During the excavation phase, the rock mass appeared strongly disintegrated and fragmented between ch.: 16+900 and ch.: 17+080 approximately (section B), whilst the rest part of the slope, ch.: 16+640 to ch.: 16+900 (section A), appeared completely weathered, as a residual soil formation.

According to the above statements, the following physical and mechanical parameters have been adopted herein for part A. The cut slope consists of a weathered mantle of about 12.0m thick from the surface. From the surface down to a depth of 5.0m poorer mechanical characteristics were

adopted, in order to simulate the effect of environmental conditions and surface runoff, while the rest 7.0m till the depth of 12.0m, values of shear strength parameters used for slope analysis were somewhat higher. The weathered mantle of gneiss bedrock throughout the examined area is quite homogeneous. For the intact (healthy) gneissic bedrock physical and mechanical values adopted for slope analysis were similar to those of the cut slope O21.

Section A geotechnical parameters:

A. Weathered mantle (depth 0.0m – 5.0m):

$$\gamma=20.5 \text{ kN/m}^3 \quad \varphi'=33^\circ \quad c'=3\text{kPa}$$

B. Mantle of gneiss (depth 5.0m – 12.0m):

$$\gamma=21.0 \text{ kN/m}^3 \quad \varphi'=34^\circ \quad c'=10\text{kPa}$$

C. Gneissic bedrock:

$$\gamma=24.9 \text{ kN/m}^3 \quad \varphi'=43^\circ \quad c'=150\text{kPa}$$

For the **section B** of the cut slope, also analyzed in the present report, the highly weathered and fractured gneiss extends to a depth of 12.0m, while deeper fresh gneissic bedrock is detected. The values of shear strength parameters of intact gneissic bedrock are identical to those of Section A, while for the weathered and highly fragmented gneiss the mechanical parameters have been assessed by use of the generalized criterion Hoek & Brown.

Physical and mechanical parameters of strongly weathered and fractured gneiss of **section B**:

$$\gamma=22.0 \text{ kN/m}^3 \quad \varphi'=36^\circ \quad c'=30\text{kPa}$$



Fig. 73b Location of cut slope O21

4.1.5 Nymfaia PIA: Cut Slope O32

Cut slope O32 is located between ch. 21+300km and ch. 21+460km close to Hellenic-Bulgarian borders. The geological survey revealed that the cut slope consists mainly of clayey sand with debris. This formation covers the majority of the terrain, under examination, with a variable thickness and lithological composition. The percentage of debris in the mass depends on the thickness of diluvium and the underlying parent rock which exists in high depth. Debris is mainly the product of red gneiss with variable granulation, mainly affected by physical and chemical processes of weathering.

The physical and mechanical parameters of the formation are presented hereafter:

$$\gamma=21.0\text{kN/m}^3 \quad \varphi'=36^\circ \quad c'=10\text{kPa}$$



Fig. 74 Location of cut slope O32, close to Hellenic-Bulgarian borders

4.1.6 Cut slope on Serres - Promahonas road (Serres PIA)

The examined area, consists mainly of two major geological formations. The superficial layer consists of clayey SAND with debris and its thickness varies along the cut slope from 3.0 to 9.0m from the surface. The underlying geological formation, detected at a depth ranging from 3.0 to 6.0m, is described as an interpolation of marls and conglomerates.

Since there are no data available leading to well documented values of physical and shear strength parameters, the present work was based on the determination of the mechanical characteristics on geological maps of the area and relevant national / international bibliography.

The geotechnical parameters for both formations are presented hereafter:

A. Clayey SAND (depth 0.0m – 9.0m):

$$\gamma=23.0 \text{ kN/m}^3 \quad \varphi'=34^\circ \quad c'=6\text{kPa}$$

B. Marls and conglomerates:

$$\gamma=27.0 \text{ kN/m}^3 \quad \varphi'=30^\circ \quad c'=53\text{kPa}$$

4.2 Hydraulic and Seismic Data at Nymfaia PIA

It is worthwhile noting that despite the fact that no water flows have been encountered during the time of the execution of the geological survey, local humidity was noted in the form of dark spots on the weathered mantle indicating possible water flows during the winter months.

For that reason, underground water table has not be used for slope analyses on the selected cut slopes. Instead, a pressure coefficient parameter was used, in the areas with high humidity, called "r_u". This parameter is defined as the ratio of the water pore pressure to the total overburden pressure.

$$r_u = \frac{u_w}{\sum(\gamma_t)_i * h_i} \quad (7)$$

where γ_t = total unit weight

h_i = thickness of each layer of overlying soil and

u_w = pore-water pressure

There is no theory available to predict the pore pressure coefficient. Rather, the value for the pore pressure coefficient is assumed, based on experiments.

As per the seismic data at Nymfaia PIA according to the New Seismic Hazard Map incorporated into the Hellenic Seismic Code (EAK 2000), the area under study is characterised as Zone I. The seismic coefficient is to be taken as $\alpha = 0.16$ and the seismic ground acceleration is equal to **A=α x g=0.16g**.

4.3 Slope Stability Analyses on Local Scale at Nymfaia and Serres PIAs

Slope Stability tests were performed, for each one of the selected cut slopes at Nymfaia PIA (cut slopes O5, O14-15, O21 and O32), in compliance to the proposed by the US Department of Transportation design guidelines (Federal Highway Administration Publication No. FHWA-SA-96-069R) assisted by the specialized software GSTABL7 with STEDwin. The aforementioned software uses limit equilibrium methods on two dimensions (2D analysis) to examine and determine the stability factor of safety for embankments, open pits, cut slopes etc.

4.3.1 Limit Equilibrium methods

Conventional limit equilibrium methods investigate the equilibrium of the soil mass tending to slide down under the influence of gravity. Transitional or rotational movement is considered on assumed or pre-defined potential slip surface below soil or rock mass. In rock slope engineering, methods may be highly significant to simple block failure along distinct discontinuities. All methods are based on comparison of forces (moments or stresses) resisting instability of the mass and those causing instability (disturbing forces). Two-dimensional sections are analyzed assuming plain strain conditions. These methods assume that shear strength of materials along the potential failure surface are governed by linear (Mohr-Coulomb) or non-linear relationships between shear strength and normal stress on the failure surface. Analysis provides a factor of safety, defined as a ratio of available shear resistance (capacity) to that required for equilibrium. If the value of factor of safety is less than 1.0, the slope is considered to be unstable. The most common limit equilibrium techniques are methods of slices where soil mass is discretized into vertical slices. Results (factor of safety) of particular methods can vary because methods differ in assumptions and satisfied equilibrium conditions.

4.3.2 Modified Bishop Limit Equilibrium method

One of the most common and widely used limit equilibrium methods is the one proposed by Alan W. Bishop. This method is an extension of the Method of Slices. By making some simplifying assumptions, the problem becomes statically determinate and suitable for hand calculations. The method has been shown to produce factor of safety values within a few percent of the "correct" values.

$$F = \frac{\sum \left[\frac{c' + ((W/b) - u) \tan \phi'}{\psi} \right]}{\sum [(W/b) \sin \alpha]} \quad (8)$$

where,

$$\psi = \cos \alpha + \frac{\sin \alpha \tan \phi}{F} \quad (9)$$

c' is the effective cohesion

ϕ' is the effective internal angle of friction

b is the width of each slice, assuming that all slices have the same width

W is the weight of each slice

u is the water pressure at the base of each slice

4.4 2D Analysis of Cut Slopes at Nymfaia and Serres PIAs

Using the aforementioned method (software GSTABL7 with STEDwin), stability analyses were performed for determining the Safety Factor of every cut slope separately. The results of all slope analyses results based on limit equilibrium methods are presented in the Appendix .

4.4.1 Cut Slope O5 at Nymfaia PIA

The most geologically unfavorable cross section of the examined cut slope, is of maximum height 20.0m and consists of two steps of 10.0m height with an inclination v:h=1:1, and a bench of 4.0m width with a transverse inclination of 6% towards the inner part of the excavation. In Fig 75 the cut slope is presented during excavation.



Fig. 75 Photo during excavation of cut slope O5 (Efraimidis, 2009)

4.4.1.1 Typical ground model of the cut slope O5

Based on the aforementioned, the typical ground model of the cut slope O5 that has been used for slope analyses, is displayed hereafter:

Depth (m)	Natural ground surface		
±0.00	<hr/>		
	Strongly disintegrated and fragmented gneiss		
	$\gamma=21.0 \text{ kN/m}^3$	$c'=0 \text{ kPa}$	$\phi'=30^\circ$
~5.00	<hr/>		
	Weak to strongly disintegrated gneiss		
	$\gamma=22.0 \text{ kN/m}^3$	$c'=5 \text{ kPa}$	$\phi'=33^\circ$
>5.0	<hr/>		

where

γ : unit weight (kN/m³)

c' : effective cohesion (kPa)

ϕ' : effective internal angle of friction (Deg)

4.4.1.2 Slope Stability Analysis Results on the cut slope O5

Based on the aforementioned typical ground model, slope stability analyses were performed in order to calculate cut slopes factor of safety. Specifically, 2500 failure circles were examined from which the ten (10) surfaces with the lower safety factor (F_s) are presented in Fig. 76. According to analyses results, the minimum safety factor value was estimated less than 1.0 ($F_s=0.992<1.0$), regarding static conditions. Therefore, the present cut slope is considered unstable without the use of stabilization or reinforcing measures.

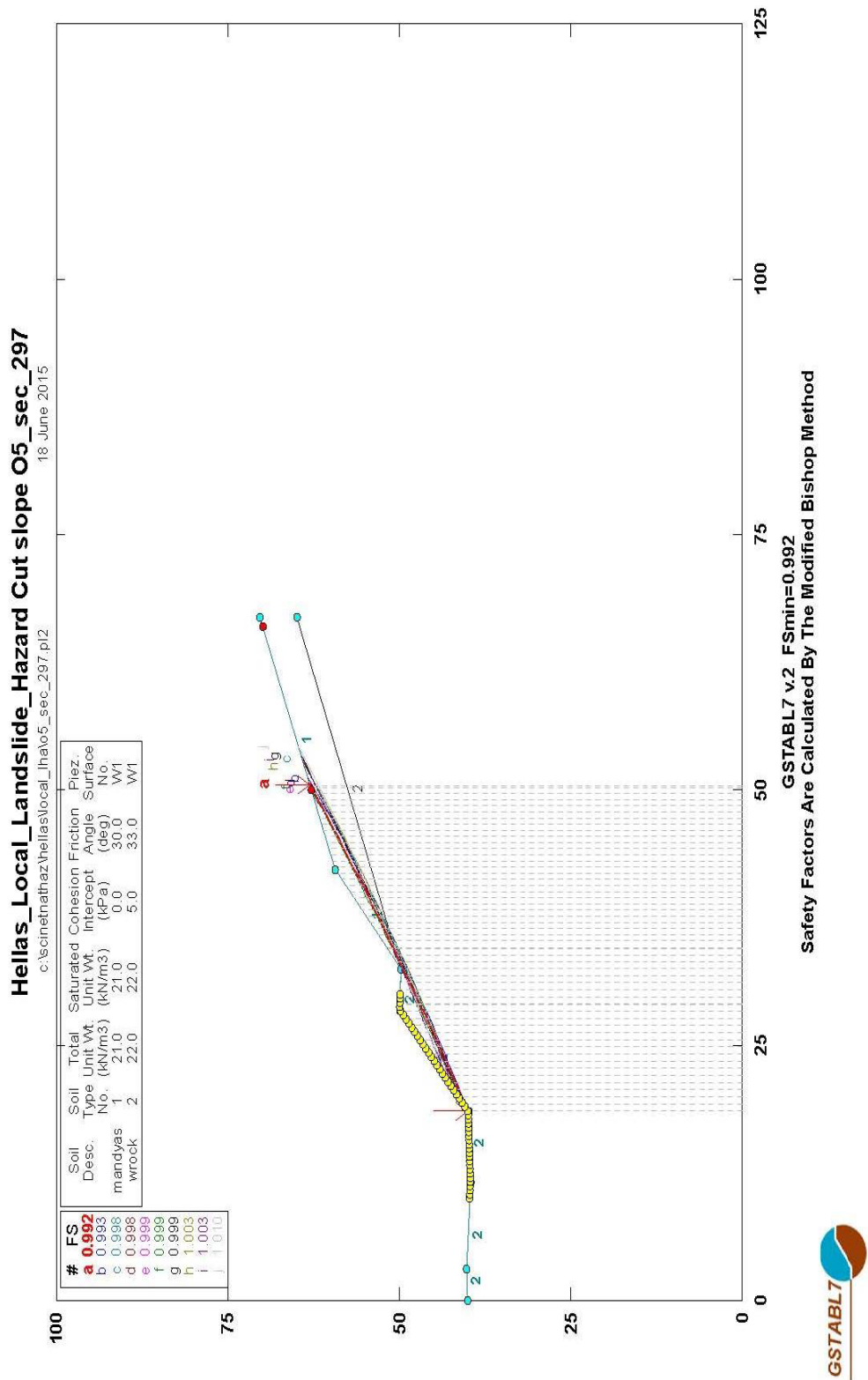


Fig. 76 2D analysis results (factor of safety) from GStabl7 with STEDwin software without any stabilization measures

For the stabilization of O5 cut slope, the most appropriate stabilizing measure is considered to be the use of passive anchors on the face of the slope placed on a grid.

Slope stability analysis is repeated, using the proposed support measures (passive anchors), in order to compute the revised safety factor and to provide the characteristics of the measures needed for stabilizing the cut slope. The analysis is presented in Fig. 77.

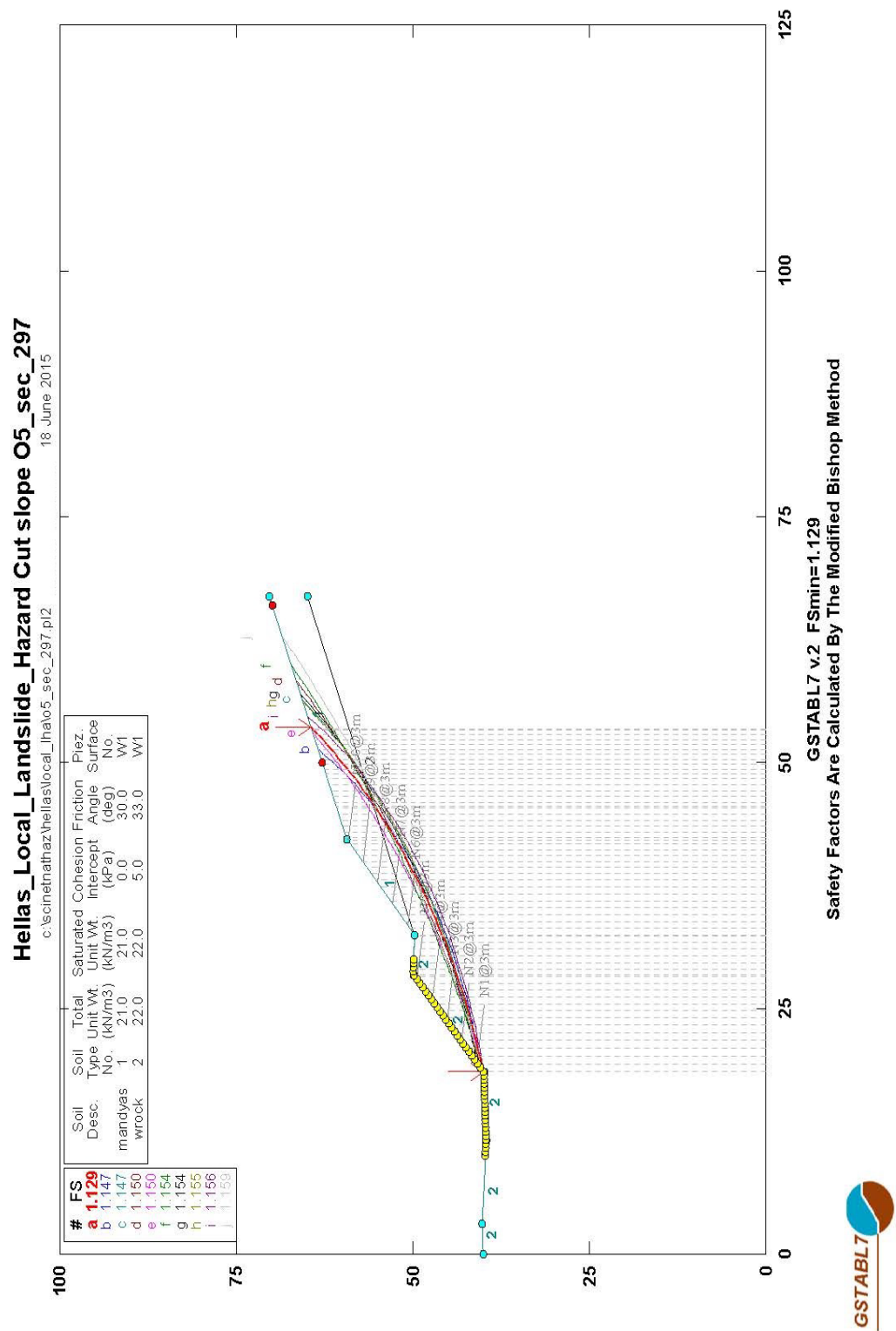


Fig. 77 2D analysis results from GSTabl7 with STEDwin software with the use of stabilizing measures (passive anchors)

It is concluded, that in order to stabilize O5 cut slope ($F_s=1.129>1.0$), fully bonded passive anchors are needed to be used, with a minimum length of 6.0m, placed in a staggered grid $S_v \times S_h=3.0 \times 3.0$ m at a downward inclination of 10 degrees with the horizontal.

4.4.2 Cut Slope O14 - O15 at Nymfaia PIA




The most geologically unfavorable section of the cut slope O14-O15, is of maximum height 57.0m and consists of seven steps of 10.0m height each one of them at an inclination of $v:h=1:1$, and six benches of width ranging from 2.0 to 4.0m, with transverse slope inclination of 6% towards the inner part of the excavation. In Figure 78 the cut slope is presented during excavation.



Fig. 78 Photo of the cut slope O14-O15 during excavation (Efraimidis, 2009)

4.4.2.1 Typical ground model of the cut slope O14-O15

Based on the aforementioned, a typical ground model of the studied area, is displayed hereafter in order to be used in all slope stability analyses that follow:

Depth (m)	Natural ground surface		
±0.00			
	Clayey SAND		
	$\gamma=21.0 \text{ kN/m}^3$	$c'=3 \text{ kPa}$	$\phi'=34^\circ$
~6.00			
	Gneiss		
	$\gamma=26.4 \text{ kN/m}^3$	$c'=150 \text{ kPa}$	$\phi'=42^\circ$
>20.0			

γ : unit weight (kN/m^3)

c' : effective cohesion (kPa)

ϕ' : effective internal angle of friction (Deg)

4.4.2.2 Slope Stability Analysis Results on the cut slope O14-O15

Based on geological and geotechnical investigation results and on the aforementioned typical ground model, stability analysis calculations were performed in order to decide cut slope's inclination in terms of a sufficient safety factor ($F_s > 1$). Specifically, 2500 failure circles were examined from which the ten (10) surfaces with the lower safety factor (F_s) are presented in Figure 79. According to slope analyses results, the minimum safety factor value was estimated to be less than 1.0 ($F_s = 0.970 < 1.0$), for static conditions. Therefore, the cut slope O14-O15 is considered to be unstable without the use of stabilization / reinforcing measures. For the stabilization of O14-O15 cut slope, the most appropriate solution was considered to be the use of passive anchors on the face of the slope placed on a grid.

The analysis is repeated, using the proposed support measures (passive anchors), in order to compute the value of safety factor and the characteristics of the measures needed for stabilization of the cut slope. The analysis is presented in Figure 80.

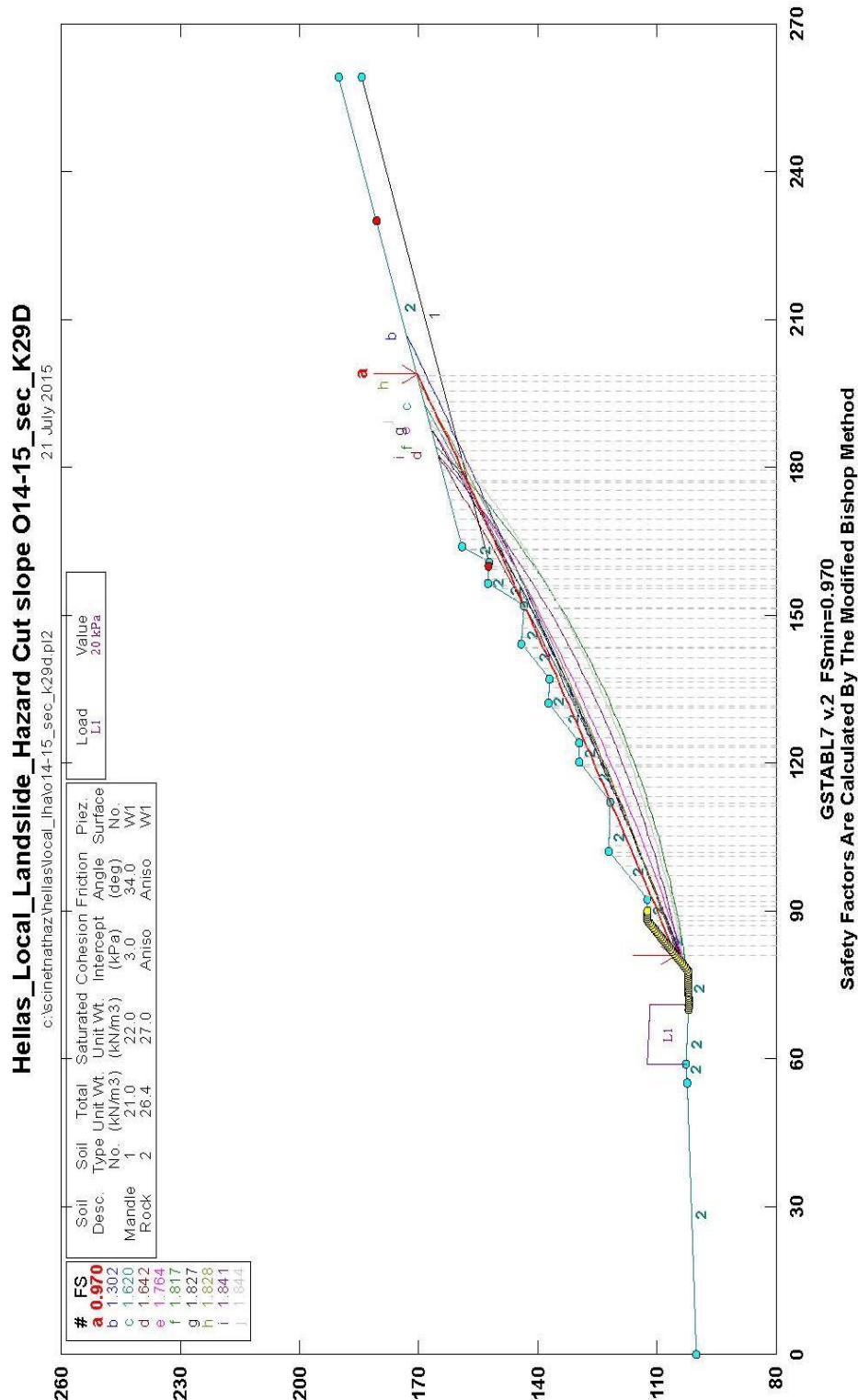
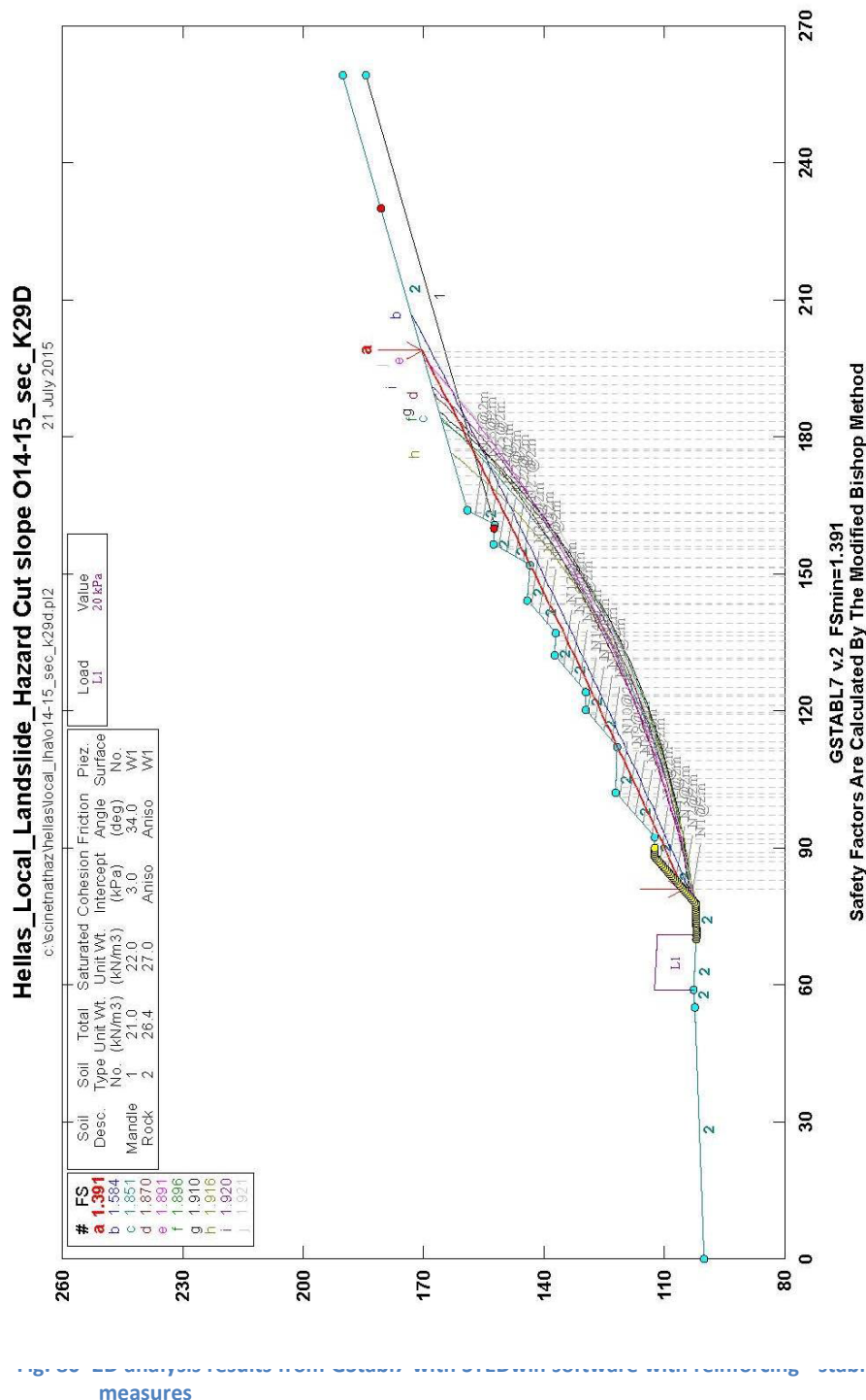


Fig. 79 2D analysis results from GStabl7 with STEDwin software without measures



It is concluded, from the 2D analysis, that in order to obtain a stable cut slope ($F_s=1.391>1.0$), fully bonded passive anchors are needed to be used, having a minimum length of 12.0m and placed on a staggered grid $S_v \times S_h=2.0 \times 2.0$ m at a downward inclination of 10 degrees with the horizontal.

4.4.3 Cut Slope O16 at Nymfaia PIA

The most geologically unfavorable cross section of the examined cut slope, is of maximum height 33.0m and consists of four steps of 10.0m height with an inclination v:h=2:3, and three benches (4.0m width) with a transverse inclination of 6% towards the inner part of the bench. In Figure 81 cut slope O16 is presented during excavation.



Fig. 81 Photo of O16 cut slope during excavation (Efraimidis, 2009)

4.4.3.1 Typical ground model of the cut slope O16

Based on the aforementioned, a representative ground model of O16 cut slope is proposed hereafter in order to be used in slope analyses calculations.

Depth (m)	Natural ground surface		
±0.00	<hr/>		
	Weathered mantle		
	$\gamma=24.0 \text{ kN/m}^3$	$c'=10 \text{ kPa}$	$\phi'=35^\circ$
~18.00	<hr/>		
	Strongly disintegrated and fragmented gneiss		
	$\gamma=23.0 \text{ kN/m}^3$	$c'=6 \text{ kPa}$	$\phi'=37^\circ$
~23.00	<hr/>		
	Gneissic bedrock		
	$\gamma=26.0 \text{ kN/m}^3$	$c'=200 \text{ kPa}$	$\phi'=36^\circ$

γ : unit weight (kN/m^3)

c' : effective cohesion (kPa)

ϕ' : effective internal angle of friction (Deg)

4.4.3.2 Slope Stability Analysis Results on cut slope O16

Based on the geological and geotechnical input data and on the aforementioned typical ground model, stability analyses calculations were performed in order to check the cut slope's safe inclination. Specifically, 2500 failure circles were examined, from which the ten (10) surfaces with the lower safety factor (F_s) are presented in Figure 82. According to the analyses results, the minimum safety factor value was calculated and found to be barely above 1.0 ($F_s=1.122>1.0$), for static conditions. Therefore, the slope is considered to be marginally stable without the use of stabilization or reinforcing measures. However, should calculations comply with regulations for safe road construction, then reinforcing and stabilization and reinforcing measures would be necessary to be adopted. As "design" is not the target of this project, but rather analysis on a local scale, we did not proceed further to design specifications.

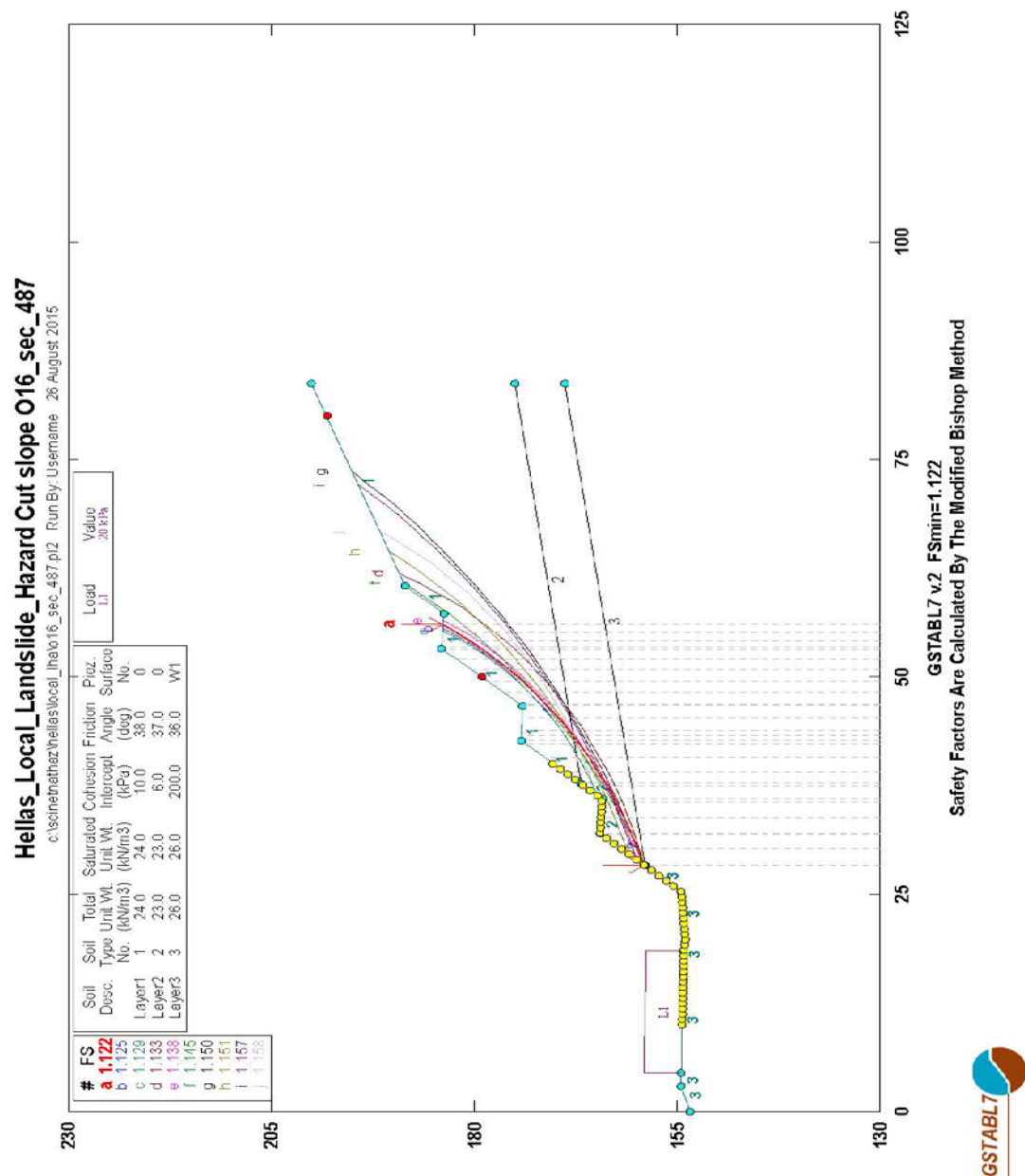


Fig. 82 2D analysis results from GSTabl7 with STEDwin software without any reinforcing - stabilizing measures

4.4.4 Cut Slope O21 at Nymfaia PIA

O21 cut slope has been divided into two parts (A and B) due to serious modification of the geological formations along the same cut slope and therefore both parts have been examined separately. The cross sections that have been selected for a 2D slope analysis have a maximum height of 29.90m and consist of three local slopes of maximum height 10.0 m and inclination $v:h=2.5:1$. Also, two 4.0m

width benches are designed with a slope inclination of 6% towards the inner of the slope. In Figure 83 the cut slope is presented during construction.



Fig. 83 Photo of cut slope O21 during excavation (part A, Efraimidis, 2009)

4.4.4.1 Typical ground model of the cut slope O21

Based on the aforementioned, the typical ground models of the two sections of cut slope O21, are displayed hereafter. Those typical ground models are representative of the two parts of the present cut slope and they have been subsequently used to carry for slope analyses on local scale.

Typical Ground Model (part A)

Depth (m)	Natural ground		
±0.00	<hr/>		
	Weathered mantle		
	$\gamma=20.5 \text{ kN/m}^3$	$c'=3 \text{ kPa}$	$\phi'=33^\circ$
~5.00	<hr/>		
	Mantle of Gneiss		
	$\gamma=21.0 \text{ kN/m}^3$	$c'=10 \text{ kPa}$	$\phi'=34^\circ$
~12.0	<hr/>		
	Fresh Gneiss bedrock		
	$\gamma=24.9 \text{ kN/m}^3$	$c'=150 \text{ kPa}$	$\phi'=43^\circ$
>20.0	<hr/>		

Typical Ground Model (part B)

Depth (m)	Natural ground		
±0.00	<hr/>		
	Strongly weathered and fractured gneiss		
	$\gamma=22.0 \text{ kN/m}^3$	$c'=30 \text{ kPa}$	$\phi'=36^\circ$
>20.0	<hr/>		

γ : unit weight (kN/m^3)

c' : effective cohesion (kPa)

ϕ' : effective internal angle of friction (Deg)

4.4.4.2 Slope Stability Analysis Results on the cut slope O21 (part A & B)

Based on geological-geotechnical investigation results and on the aforementioned typical ground models, stability analysis calculations were performed in order to check the cut slope's safe inclination. Specifically, 2500 failure circles were examined, from which ten (10) potential sliding surfaces with the lower safety factor (F_s) are presented in Figures 83 and 84. According to slope

analyses results, the minimum safety factor value was estimated to be less than 1.0 ($F_s=0.830$) in part A and equal to $F_s=1.218>1.0$ for part B, regarding the static conditions. Therefore the slopes have been considered to be unstable without the use of stabilization measures in part A and stable in part B.

For the stabilization of the cut slope's part A, the most appropriate solution was considered to be the use of passive anchors on the face of the slope placed in grid.

Slope analysis is repeated for part A, using the proposed support measures (passive anchors), in order to compute the value of revised safety factor and the characteristics of the measures necessary for stabilization and reinforcement of the slope. Analysis with the proposed reinforcing measures is presented in figure 85.

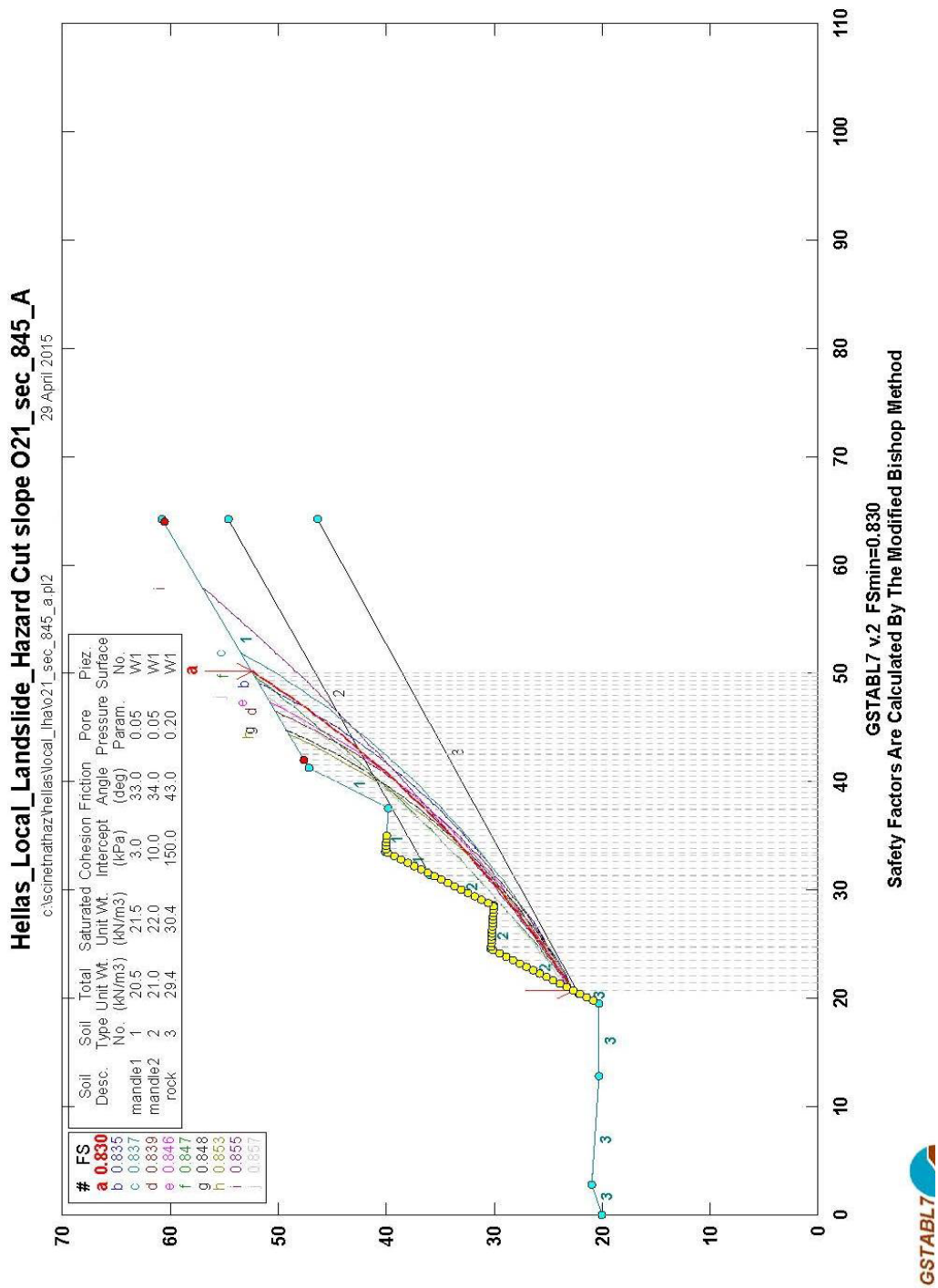


Fig. 83 2D analysis results from GSTabl7 with STEDwin software without measures (part A)

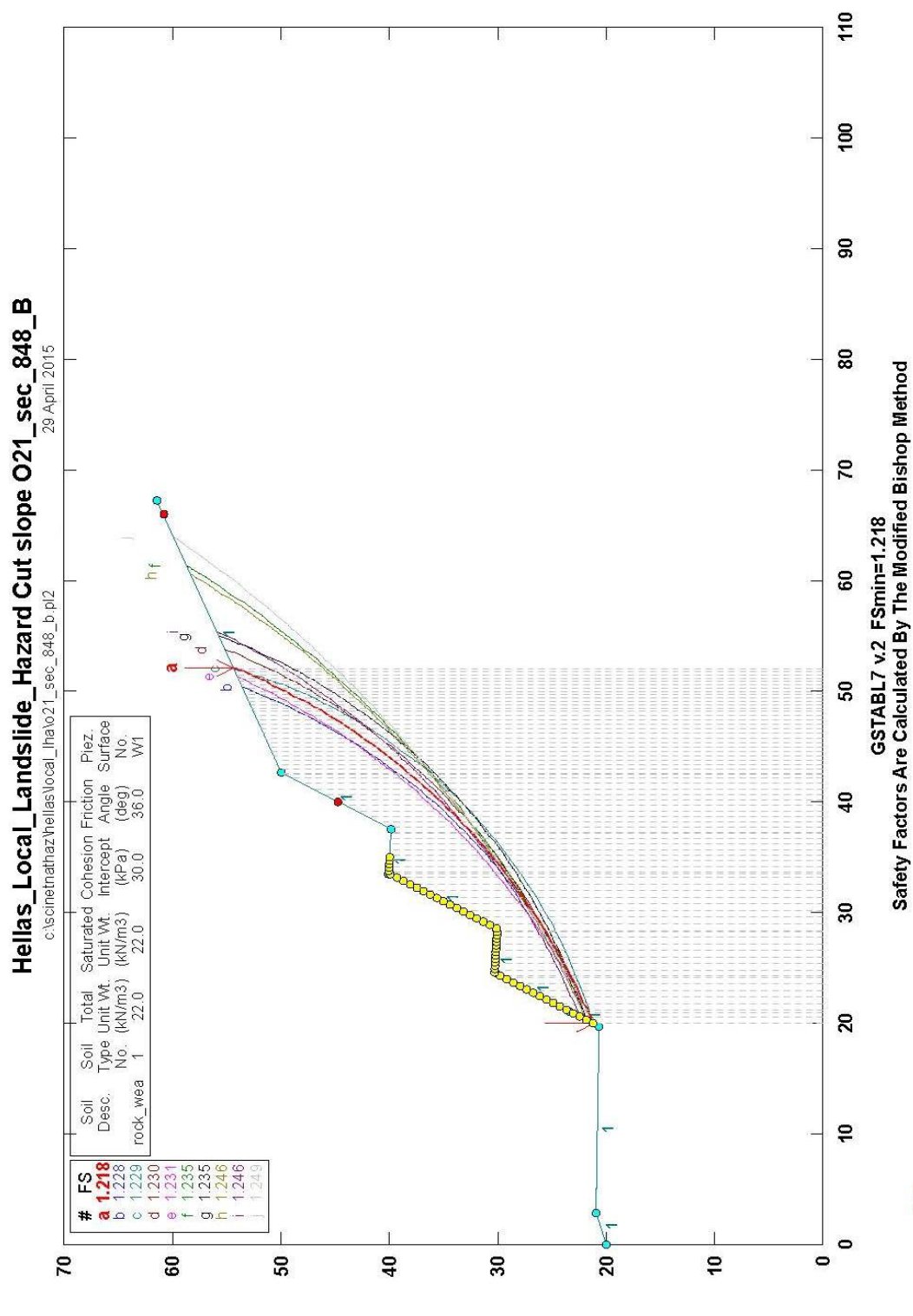


Fig. 84 2D analysis results from GSTabl7 with STEDwin software without measures (part B)

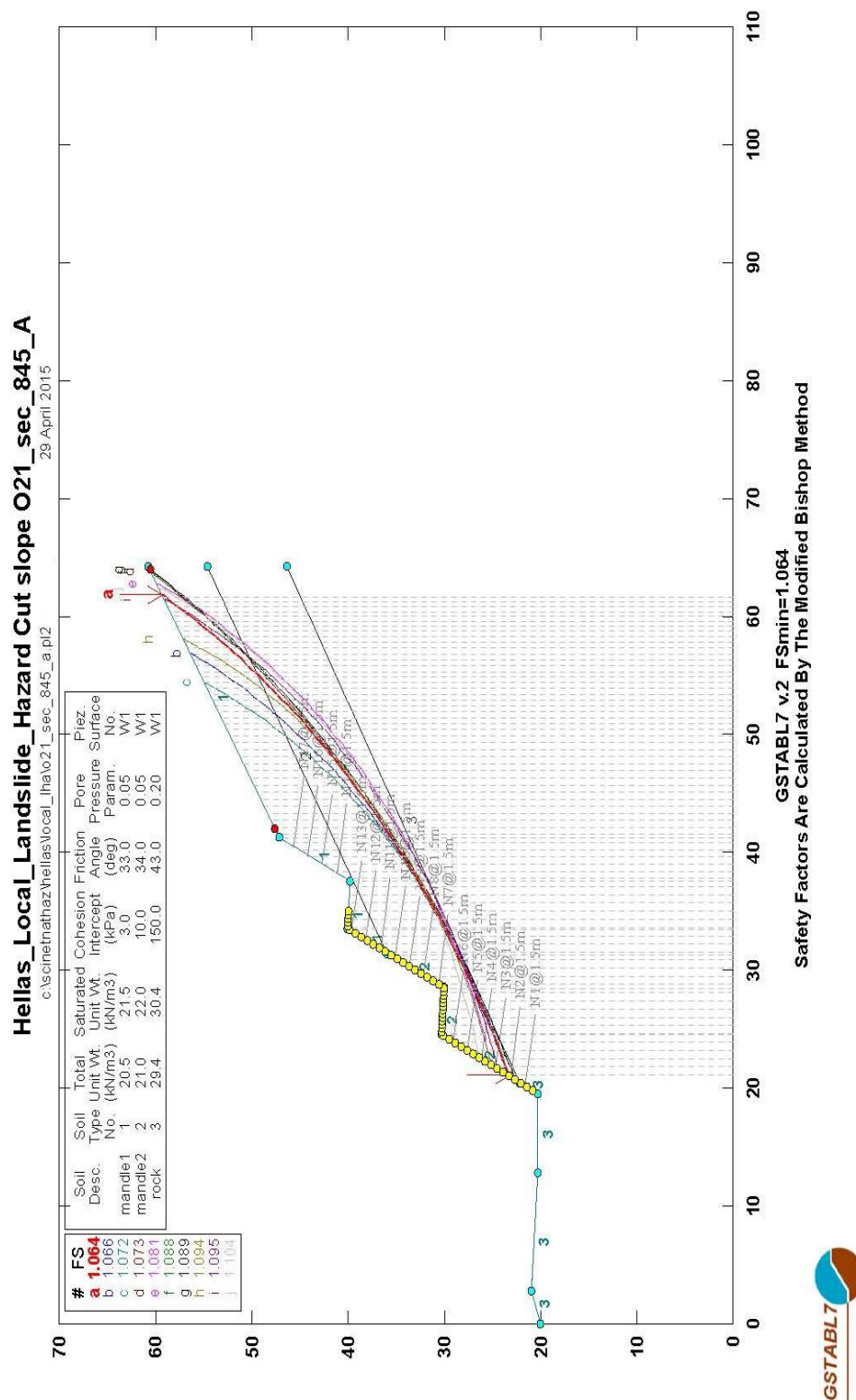


Fig. 85 2D analysis results from GStabl7 with STEDwin software with measures (part A)

Concluding from 2D slope analyses results concerning part A of the cut slope O21, measures to improve the existing factor of safety are deemed necessary ($F_s=1.064>1.0$). The proposed solution is use of fully bonded passive anchors with a minimum length of 6.0m, in a staggered grid $S_v \times S_h=2.0 \times 2.0$ m and at a downward inclination of 10 degrees to the horizontal.

4.4.5 Cut Slope O32 at Nymfaia PIA

We examined a cross section of maximum height of 27.70m since it represents the most demanding combination of geometrical features and most unfavorable geological-geotechnical conditions. The aforementioned cross section consists of three slopes of maximum height 10.0m with an inclination $v:h=2.5:1$ and two benches of 4.0m width constructed with a transverse slope inclination of 6% towards the inner part of the cut slope. Figure 86 the cut slope is presented during its construction.

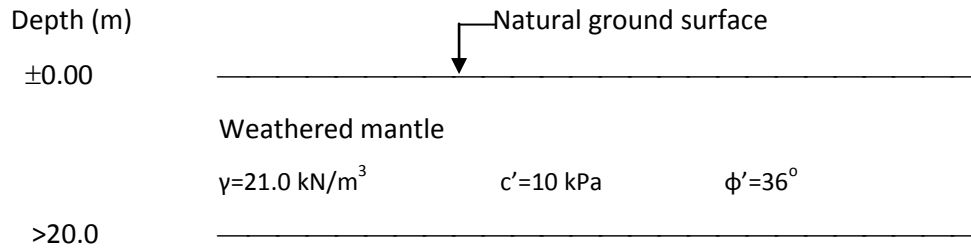


Fig. 86 Photo of cut slope O32 during construction (Efraimidis, 2009)

4.4.5.1 Typical ground model of cut slope O32

Based on the aforementioned, the typical ground model adopted hereafter is considered to be representative for stability calculations performed for the examined cut slope.

Typical Ground Model (cut slope O32)



γ : unit weight (kN/m^3)

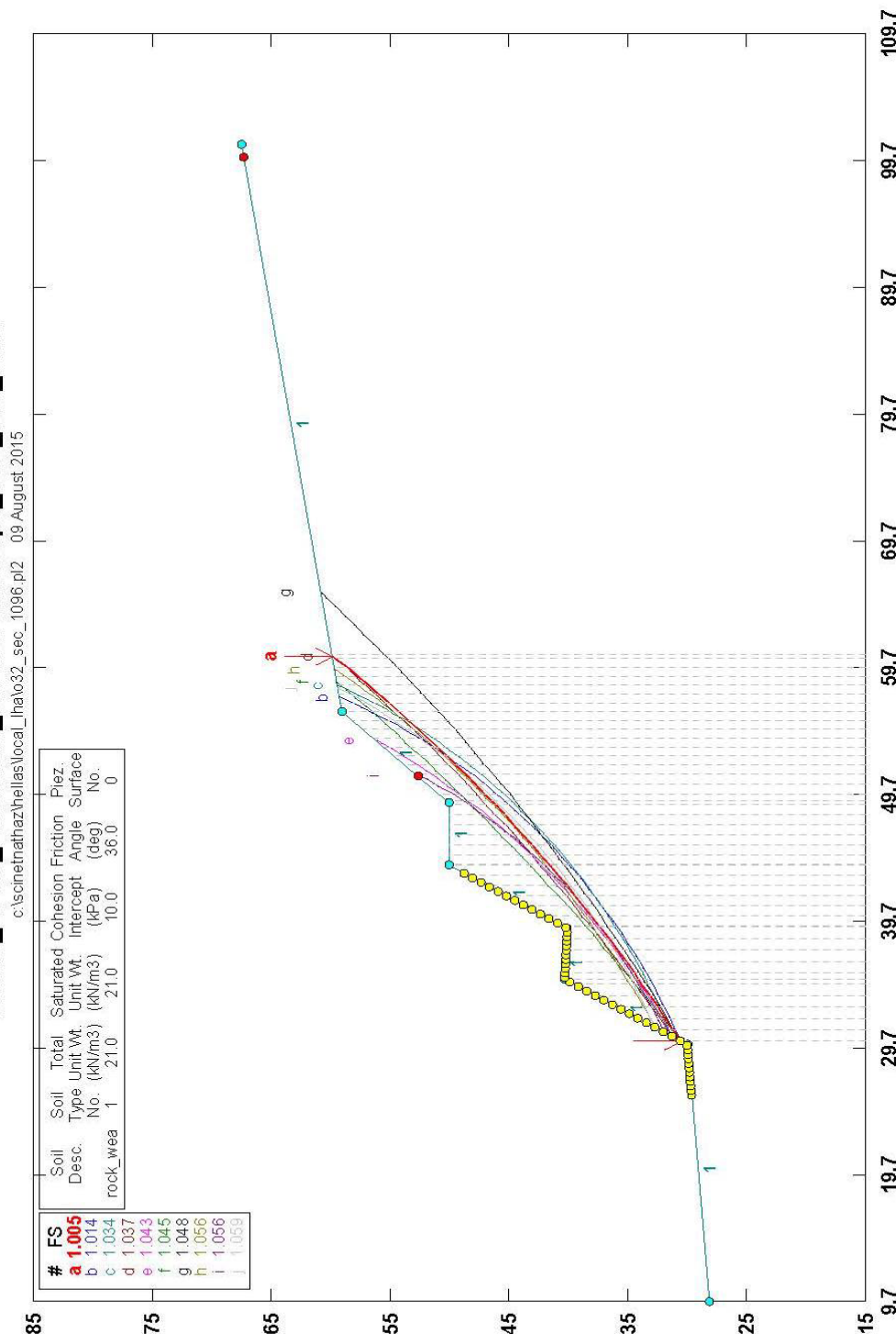
c' : effective cohesion (kPa)

ϕ' : effective internal angle of friction (Deg)

4.4.5.2 Slope Stability Analysis Results on the cut slope O32

Based on geological and geotechnical investigation results and on the aforementioned typical ground model, stability analysis calculations were performed in order to check the cut slope's safe inclination. Specifically, 2500 failure circles were examined, from which ten (10) potential sliding surfaces with the lower safety factor (F_s) are presented in Figure 86. According to slope stability analysis results, the minimum safety factor value was estimated to be marginally above 1.0 ($F_s=1.005 \geq 1.0$) for static conditions. Therefore the slope has been considered as marginally stable without the use of stabilization measures. We stress the attention to the fact that from a design point of view this is not admissible, but in the framework of the present deliverable we do not judge the result according to highway regulations, but only in terms of analysis where F_s values are solely judged on the criterion whether they exceed or not 1.0.

Hellas_Local_Landslide_Hazard Cut slope_O32_sec_1096



GSTABL7 v.2 FSmin=1.005
Safety Factors Are Calculated By The Modified Bishop Method



4.4.6 Slope along Serres - Promahonas road axis (Serres PIA)

The cross section of the slope, is of maximum total height of 82.0m and has an average inclination $v:h=2:5$. In Figure 87 the slope to be analyzed in local scale in Serres PIA is presented.



Fig. 87 Photo of the slope analyzed in Serres PIA

4.4.6.1 Typical ground model for a slope in Serres PIA

Based on the in situ geological investigation a typical ground model for slope stability analysis is displayed hereafter.

Depth (m)	Natural ground surface		
±0.00	<hr/>		
	Clayey sand		
	$\gamma=23.0 \text{ kN/m}^3$	$c'=6 \text{ kPa}$	$\phi'=34^\circ$
~3.0-6.0	<hr/>		
	Marls and conglomerates		
	$\gamma=27.0 \text{ kN/m}^3$	$c'=53 \text{ kPa}$	$\phi'=30^\circ$
>6.0	<hr/>		

γ : unit weight (kN/m^3)

c' : effective cohesion (kPa)

ϕ' : effective internal angle of friction (Deg)

4.4.6.2 Slope Stability Analysis Results on a Slope in Serres PIA

Based on the aforementioned typical ground model, slope analysis calculations were performed in order to check the cut slope's stability. Specifically, 2500 failure circles were examined from which ten (10) potential sliding surfaces with the lower safety factor (F_s) are presented in Figure 88. Due to the important height of the total slope, several analyses were performed referring to local sliding surfaces, as well as sliding surfaces running at the entire slope surface. According to analysis results, the safety factor corresponding to the most critical sliding surface was calculated marginally above 1.0 ($F_s=1.007>1.0$) as per static conditions.

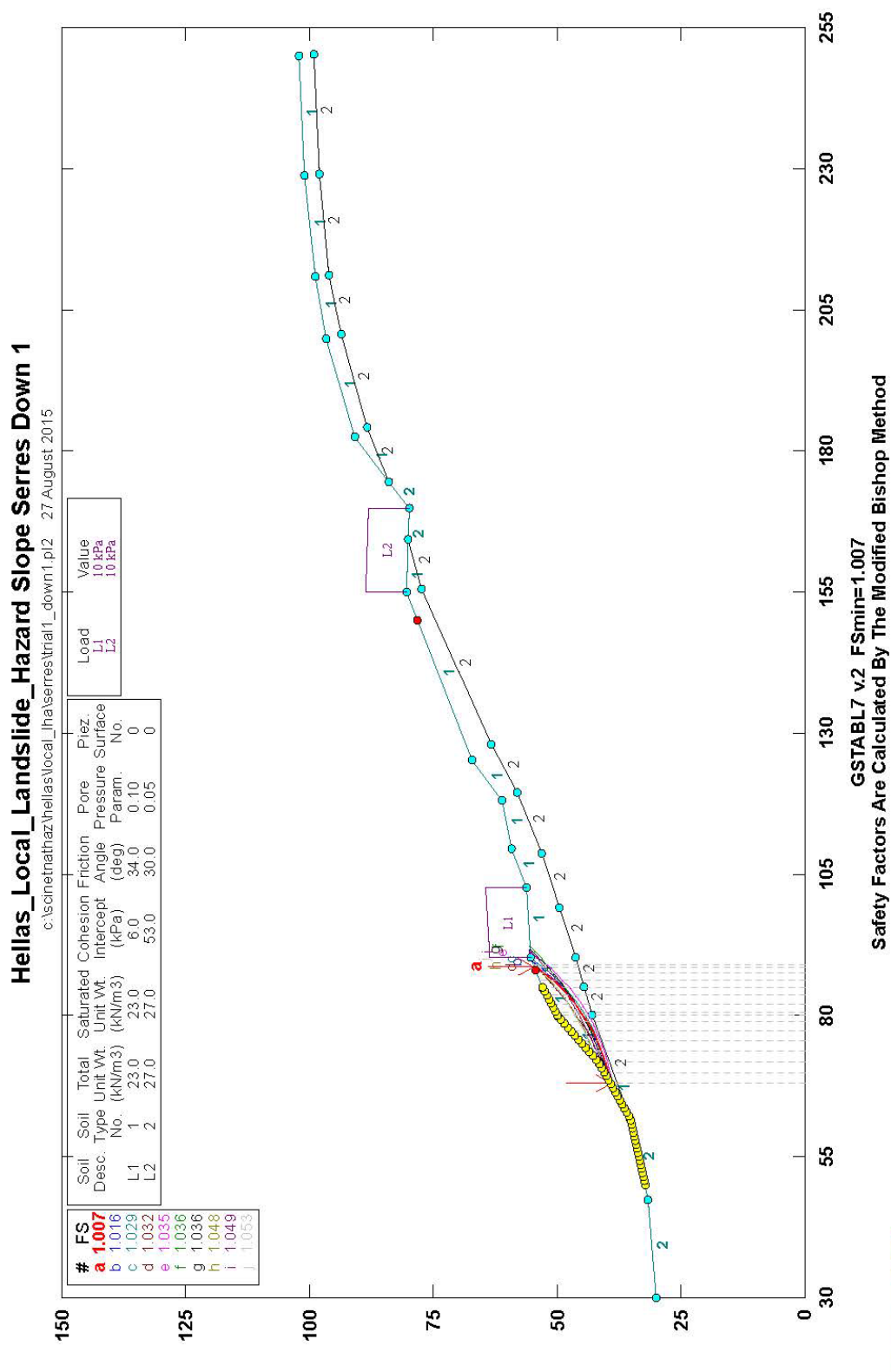


Fig. 88 2D analysis results from GStabl7 with STEDwin software for a slope at Serres PIA

4.5 Finite Difference Method

The finite difference method is among the oldest numerical techniques used for the solution of sets of differential equations, given initial values and/or boundary values. In the finite difference method, every derivative in the set of governing equations is replaced directly by an algebraic expression written in terms of the field variables (e.g., stress or displacement) at discrete points in space.

FLAC 3D is a software which uses the finite difference method, in three-dimensions, in order to simulate / analyze the behavior of structures built of soil, rock or other materials that may undergo plastic flow when their yield limits are reached. Materials are represented by elements, or zones, which form a grid that is adjusted by the user to fit the shape of the object to be modeled. Each element behaves according to a prescribed linear or nonlinear stress/strain law in response to the applied forces or boundary restraints. The material can yield and flow, and the grid can deform (in large-strain mode) and move with the material that is represented. The Lagrangian calculation scheme and the mixed-discretization zoning technique used in FLAC ensure that plastic collapse and flow are modeled very accurately.

4.5.1 3D Analysis of Cut Slopes O21 and O32 (Nymfaia PIA)

Actual slopes are not infinitely long and straight. Usually, they are curved in both plan and elevation. The effect of slope curvature can only be analyzed with a three-dimensional model. Taking this into consideration, in combination with the geometry of the examined cut slopes, analysis with FLAC 3D was considered necessary. In the next paragraphs are presented the results from the analysis of two areas, cut slope O21 and cut slope O32. From these two slopes, the first one, O21, was created using combined crude shapes, whilst the other, O32, was created in greater detail, by using 3D modeling software. Both analyses were executed in FLAC 3D.

4.5.2 3D Analysis of Cut Slope O21

FLAC 3D version 5.00 was used for the analysis of the cut slopes. In figure 89 the geometry of the model is presented; it consists of three radial-cylinder shapes and one brick shape, approximating reality in a rather crude way.

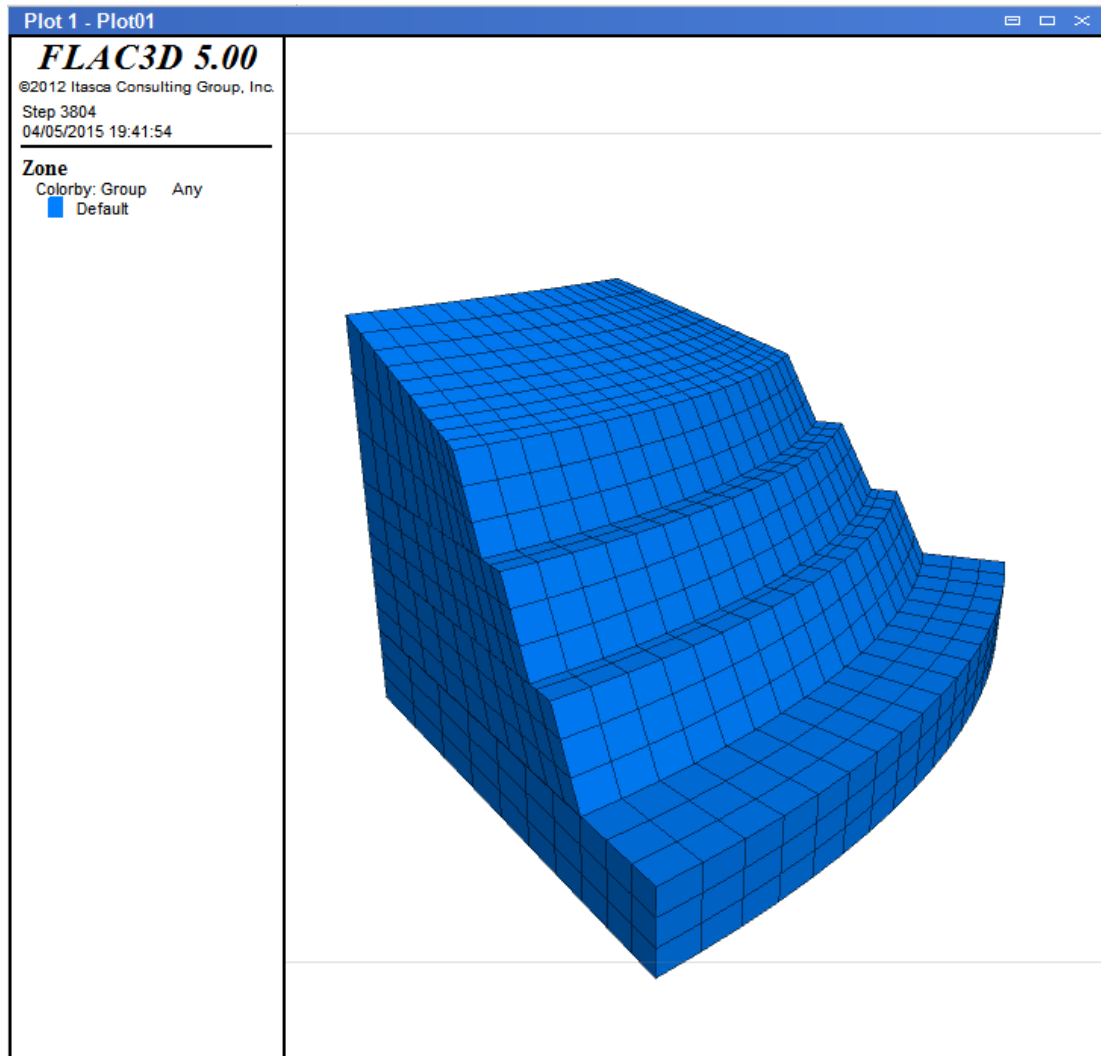


Fig. 89 Geometry of the model presented in FLAC 3D plot window to evaluate the influence of slope curvature

The model is assigned a Mohr-Coulomb material model with the following properties:

Modulus of elasticity: 350 MPa

Poisson ratio: 0.2

Bulk modulus: 194 MPa

Shear modulus: 145.83 MPa

Friction angle: 36°

Cohesion: 30 kPa

Tension limit: 30 kPa

The mass density of the material is 2400 kg/m^3 and the gravity is specified at 9.81 m/sec^2 acting in the negative z-direction.

The factor of safety is calculated by the strength reduction method using the SOLVE fos command. A value of 1.23 is calculated for F_s . This is slightly higher than the factor of safety produced by the 2D (Bishop) circular failure analysis ($F_s=1.218$), implying thus, that there is a very slight effect of slope curvature on the stability. The resulting failure surface is depicted by the displacement contour plot shown in Figure 90.

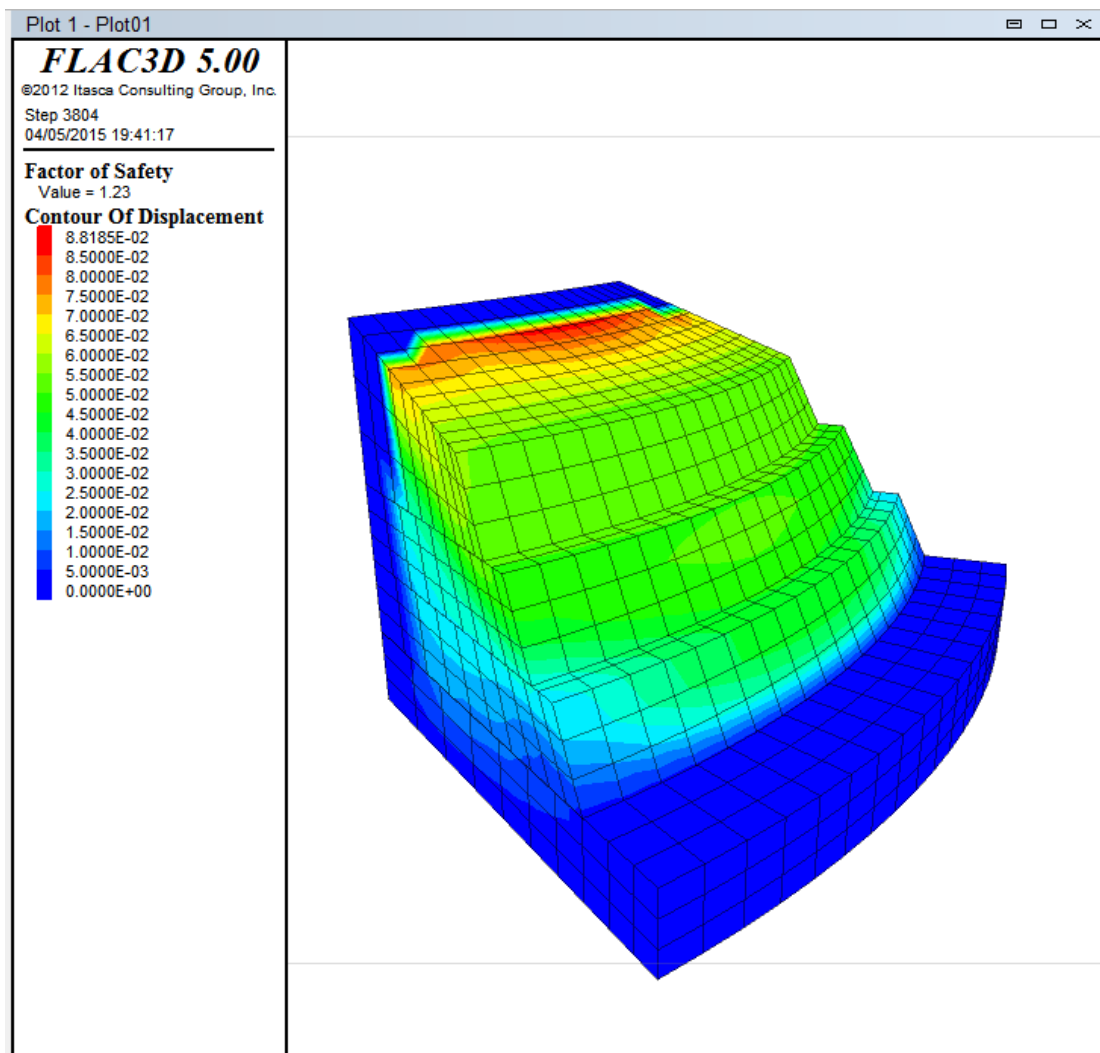


Fig. 90 Displacement contours and safety factor in FLAC 3D model at the failure state

4.5.3 3D Analysis of Cut Slope O32

This cut slope was analyzed in two different ways, as far as it concerns its geometry. In the first analysis, the model was created in a crude way by use of three radial shapes and one brick shape, as shown in figure 91.

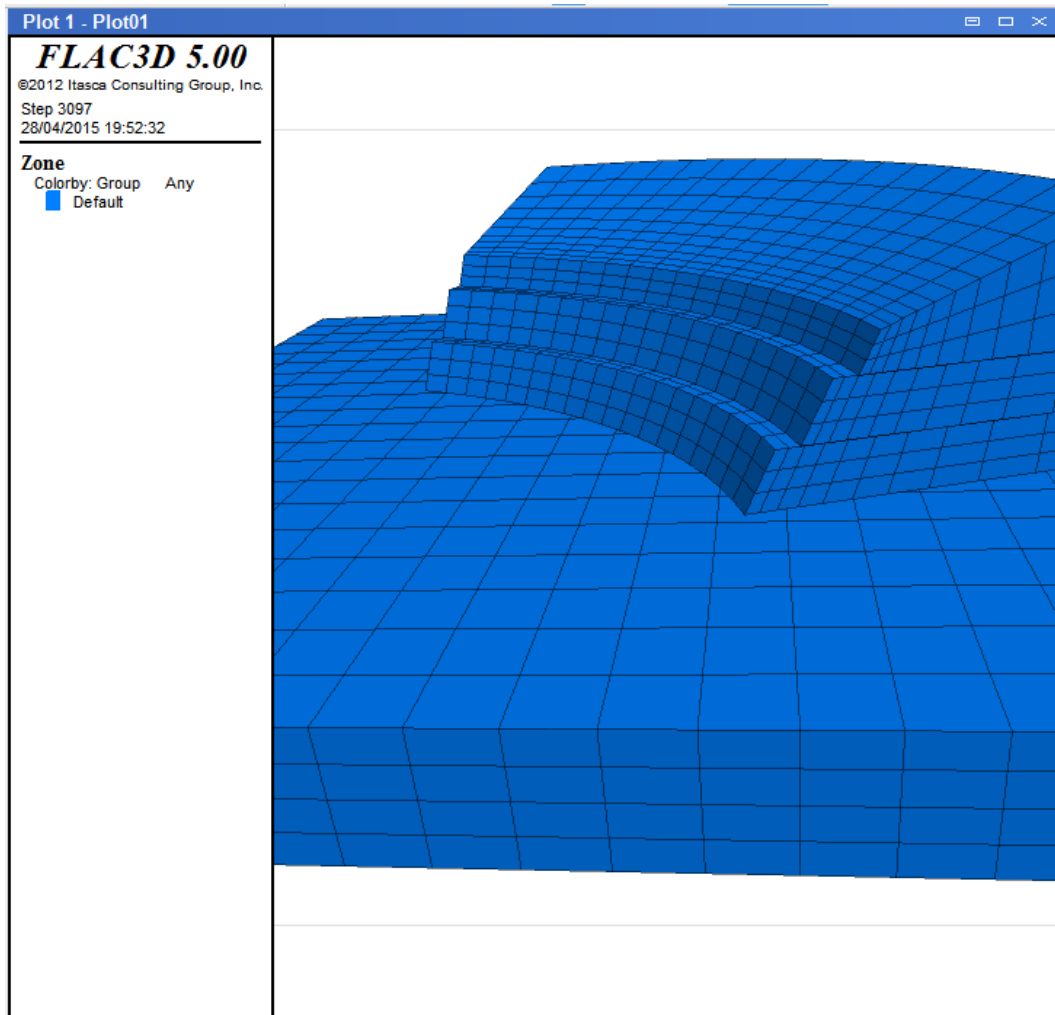


Fig. 91 Geometry of the model presented in FLAC 3D plot window to evaluate the influence of slope curvature

The model is assigned a Mohr-Coulomb material model with the following mechanical and deformational properties:

Modulus of elasticity: 250 MPa

Poisson ratio: 0.33

Bulk modulus: 250 MPa

Shear modulus: 93.75 MPa

Friction angle: 36°

Cohesion: 10 kPa

Tension limit: 10 kPa

The mass density of the material is 2100 kg/m^3 and the gravity is specified at 9.81 m/sec^2 acting in the negative z-direction.

The factor of safety is calculated by the strength reduction method using the SOLVE fos command. A value of 1.35 is calculated for F_s . This is much higher compared to the factor of safety calculated by the 2D (Bishop) circular failure analysis ($F_s=1.005$), which suggests that there is a considerable effect of slope curvature on slope stability. The resulting failure surface is depicted by the displacement contour plot shown in Figure 92.

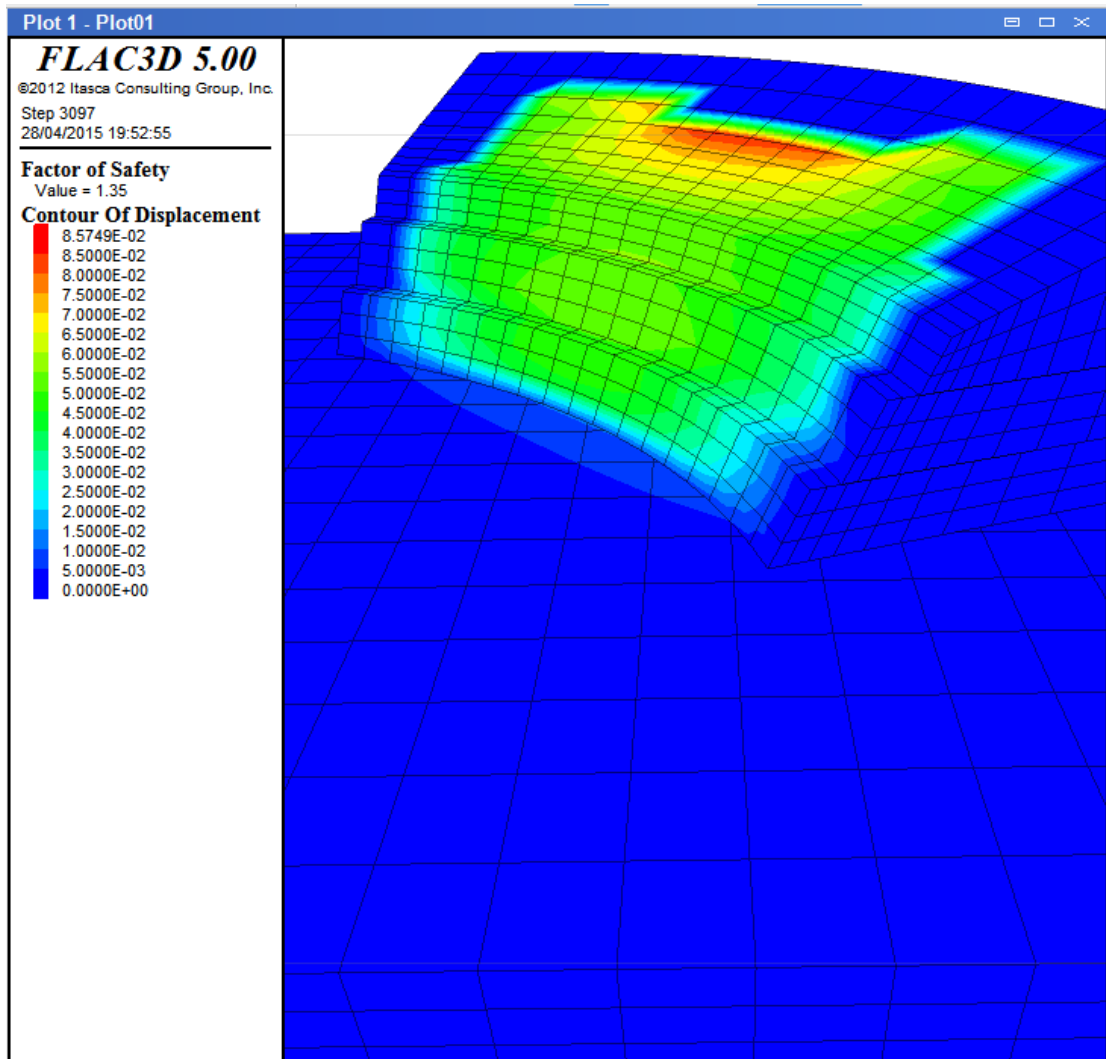


Fig. 92 Displacement contours and safety factor in FLAC 3D model at the failure state

For the second type analysis with Flac 3D software, a different modeling approach was followed. The model was initially created using 3D design software in which semantic detail could be achieved. In figures 93, 94 and 95 all stages from the "construction" of the model in this software are presented in detail, whilst in figure 96 the examined cut slope is presented as it is constructed in the present.

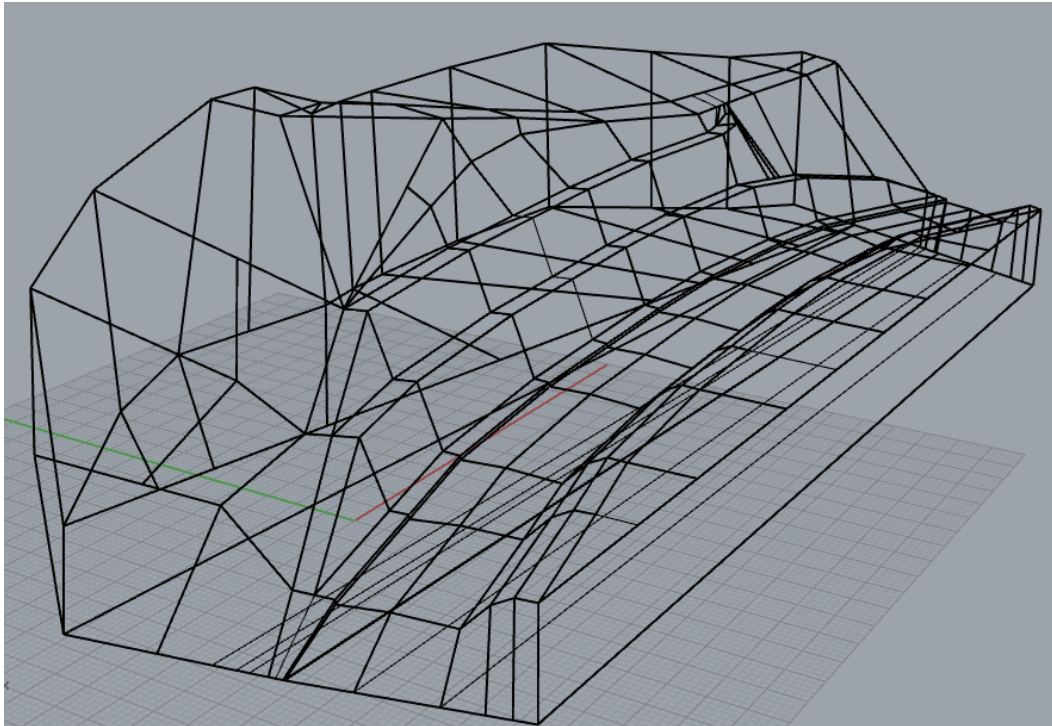


Fig. 93 Creating the frame of the model

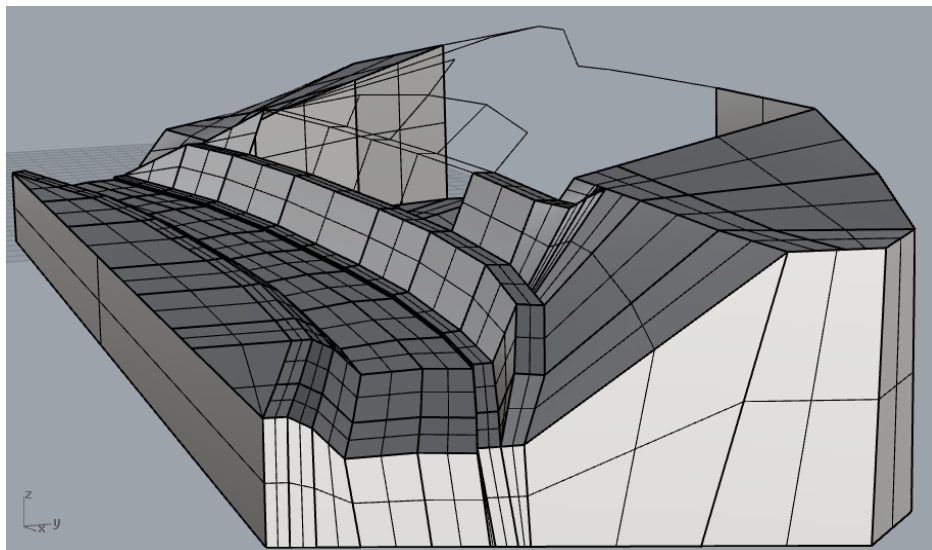


Fig. 94 Covering the frame of the model with surfaces

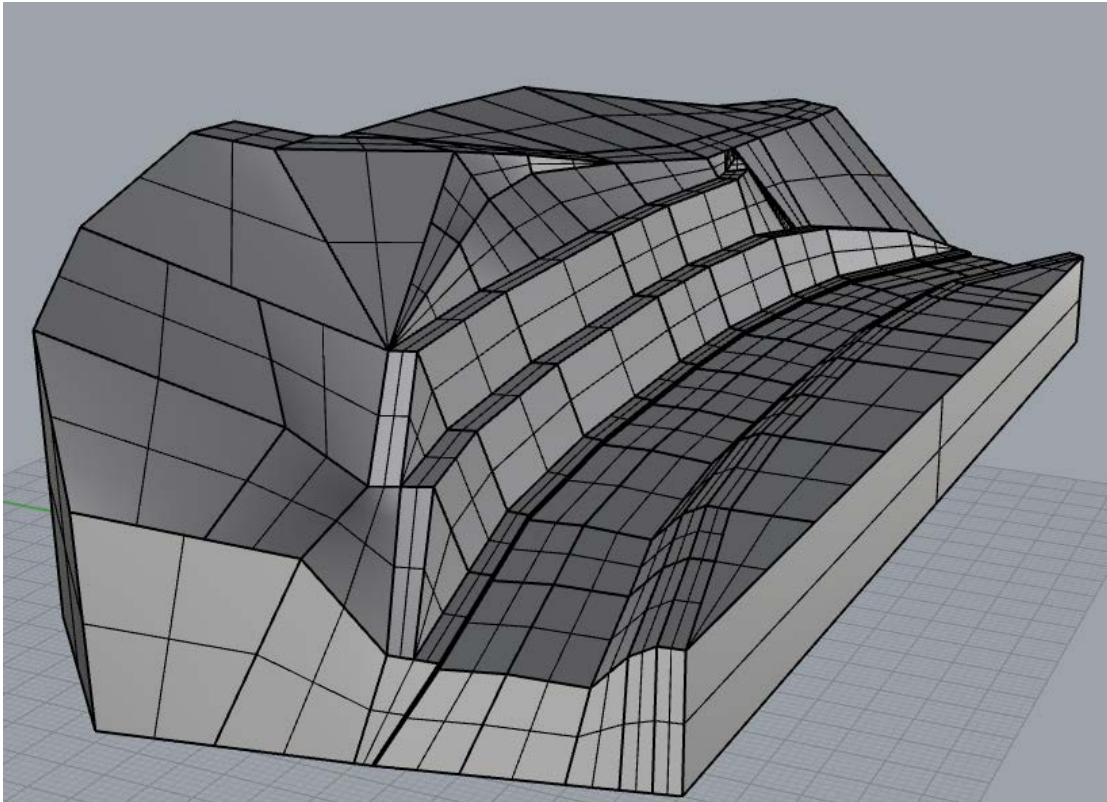


Fig. 95 The model in the final stage



Fig. 96 The cut slope as built in present

Once the model created, another software is used in order to create the 3D grid of the model which, finally will be analyzed by the software FLAC 3D. This software is Kubrix Geo Ver. 15. The latter, presented in figure 97, is a mesh generator for Itasca's FLAC 3D software. It has the ability to transform demanding geometrical shapes 2D or 3D, regular or irregular, into hexahedral, tetrahedral, octree and hybrid grid models, in order to be analyzed.

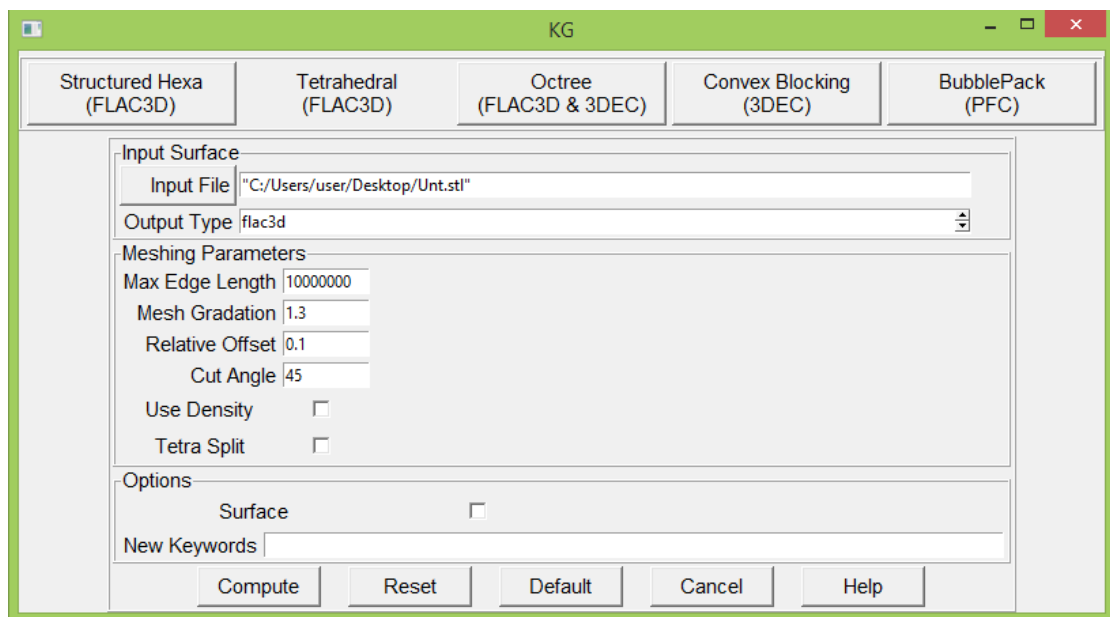


Fig. 97 Kubrix Geo Ver. 15 (a mesh generator for Flac 3D software)

By using Kubrix Geo Ver. 15, the model is transformed into a form which can be "understood" and analyzed by FLAC 3D (Figure 98).

The model is assigned a Mohr-Coulomb material model with the following mechanical and deformational properties:

Modulus of elasticity: 250 MPa

Poisson ratio: 0.33

Bulk modulus: 250 MPa

Shear modulus: 93.75 MPa

Friction angle: 36°

Cohesion: 10 kPa

Tension limit: 10 kPa

The mass density of the material is 2100 kg/m^3 and the gravity is specified at 9.81 m/sec^2 acting in the negative z-direction.

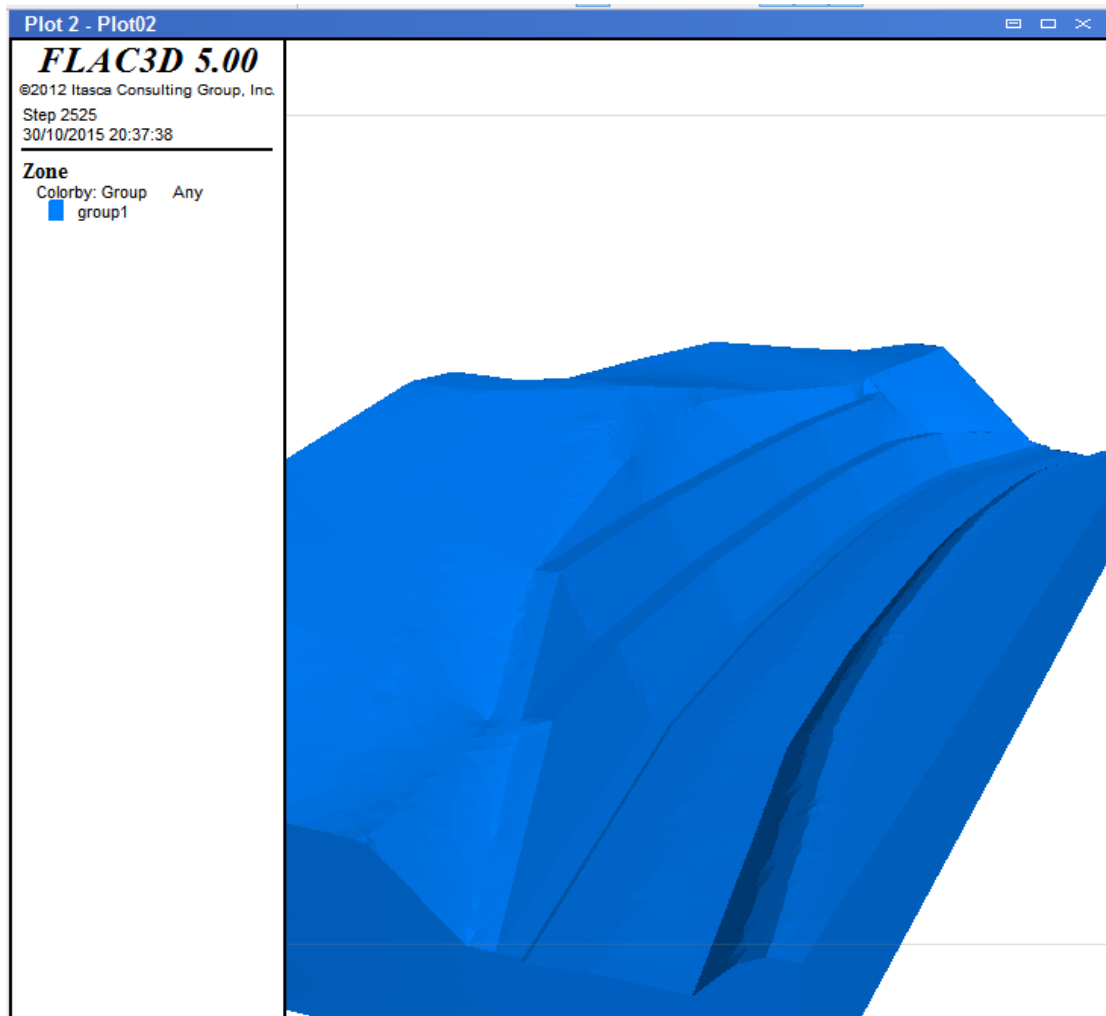


Fig. 98 Geometry of the model presented in FLAC 3D plot window

Initially, the model is analyzed in order to occur the maximum displacement by using the SOLVE command. In figure 99 results from this analysis are presented, which concluded that the maximum deflection is in the order of 5.0cm and occurred in the highest part of the slope.

The factor of safety is calculated by the strength reduction method using the SOLVE fos command. A value of 1.09 is calculated for F_s . This is slightly higher compared to the factor of safety calculated by the 2D (Bishop) circular failure analysis ($F_s=1.005$), which suggests that there is a slight effect of slope curvature on the stability. This result is significantly different from the previous one of Flac 3D, based on a crude approximation of the reality. Therefore, by comparison of the two different 3D analyses (the crude one and the detailed one), it is concluded that geometry of the model and its details, can

largely affect the calculated factor of safety and 3D approach, if deemed necessary to be used for slope stability problems, should be used with great care regarding real geometry of the slope. The resulting failure surface is depicted by the displacement contour plot as shown in Figures 100 and 101.

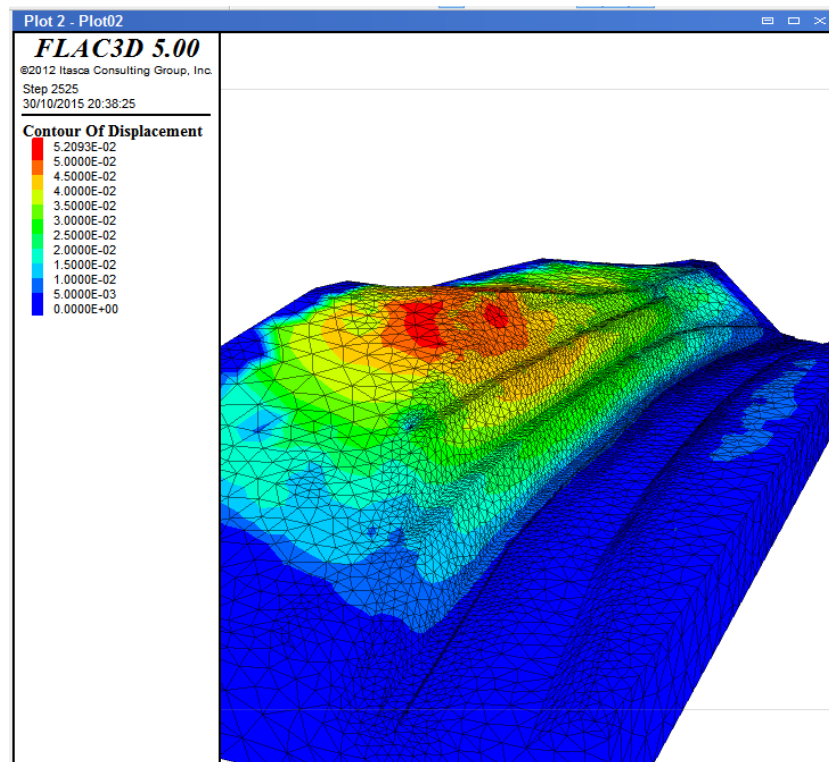


Fig. 99 Displacement contours in FLAC 3D model

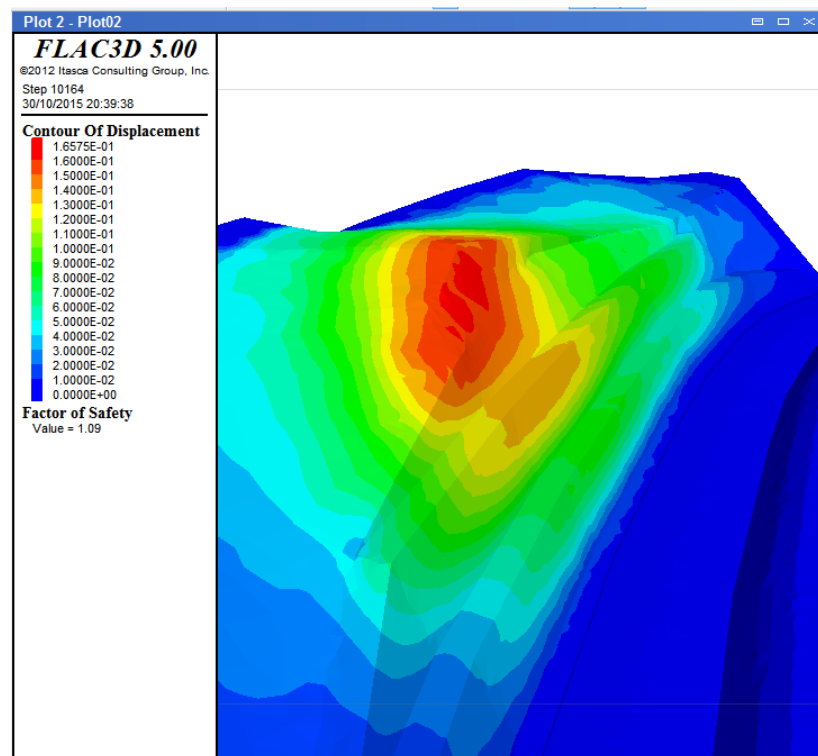


Fig. 100 Displacement contours and safety factor in FLAC 3D model at failure state

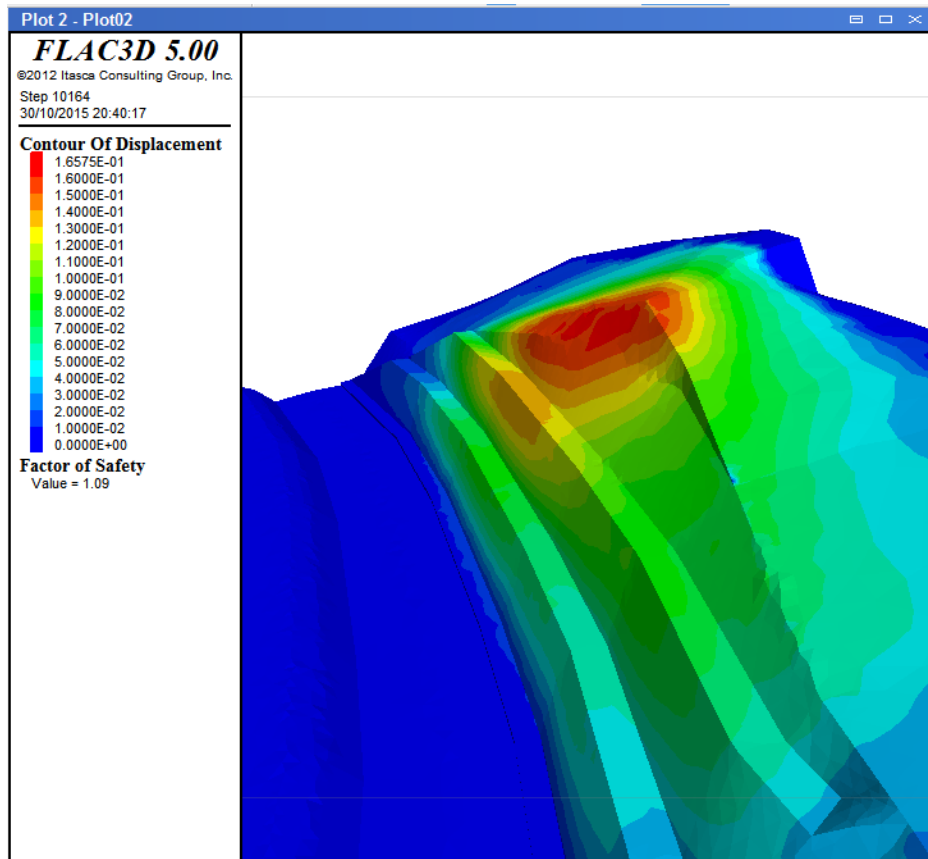


Fig. 101 Displacement contours and safety factor in FLAC 3D model at the failure state

4.5.4 Concluding Remarks

4.5.4.1 Comparison of 2D and 3D models

We have presented stability analysis of three cut slopes of maximum height of approximately 30m and a slope inclination $v:h=2.5:1$ with two different methods. The first one was a 2D limit equilibrium method while the second, was a finite difference method. Comparing results coming the above analyses, it is concluded that:

- Despite the fact that the two methods are totally different they both concluded to almost the same safety factor.
- Both 2D and 3D models predicted the same failure surface.
- The 3D effect at the model can be considered as minor to negligible.
- It is shown that the equivalent plane strain (2D) analysis is sufficient from a computational point of view.

4.5.4.2 Comparison of local (2D) and regional LHA models

Regional and local landslide hazard assessment deals with the same problem but at a different scale affecting thus largely the optic of each approach. Regional scale LHA should be mostly used in making rational decisions regarding strategic planning of developing regions or construction of large scale infrastructure, taking into account the level of hazard regarding landslides. Quantification of landslide hazard has been assessed upon physically-based models where topographical, geological, hydrological, and geotechnical data must be rationally used, according to the model of soil or rock failure adopted.

Local scale LHA approach refers to scales deemed for design; therefore, they cannot and should not be overlooked, regardless of existing regional scale LHA maps. Along the vertical road axis from Komotini to Nymfaia and Hellenic / Bulgarian borders, we produced maps with the factor of safety calculated at a regional scale (1:50,000), based on the "infinite slope model" or / and at the "circular slope model" on natural slopes under different conditions (wet, dry, seismic conditions for various mean return periods of the seismic event). As the bedrock was essentially gneissic exhibiting an important variation regarding the degree of weathering and fragmentation was stated, in very short distances, exhibiting thus a seriously heterogeneous rock mass shear resistance largely modified according to the local conditions.

Natural slopes in the examined area presented inclinations varying from 25° to almost 40° , whereas cut slopes of height ranging from 15 to 40m were constructed with inclinations v:h = 1:1 to 2.5:1. Factor of safety on natural slopes on a regional scale approach ranging from 1 to 2, presented factors of safety less than 1.4 on a local scale for the aforementioned inclinations. As a general trend for factors of safety resulting from a LHA at a regional scale exceeding the value of "3" ($F_s > 3$), resulted in rather safe cut slopes with a few or no need for countermeasures. As per regions with factors of safety calculated on natural slopes, between 2 and 3, the factor of safety for cut slopes was either marginally satisfactory ($F_s \geq 1.4$) for static conditions, or not satisfactory ($F_s < 1.4$) implying thus the need of reinforcing measures.

However, it has to be noted that even if a relationship could be established between factor of safety as calculated on a regional scale approach on natural slopes, with an equivalent factor of safety based on a local scale approach, this should be treated extremely carefully, as this relationship is not universal and is highly dependent on the geology, the topography and the hydrological conditions, at least.

5 LANDSLIDE HAZARD ASSESSMENT ON A REGIONAL SCALE - PILOT IMPLEMENTATIONS IN TURKEY

5.1 Introduction

Based on the conclusions of the meeting at Burgas, Bulgaria held on 23-25 October 2014, the consensus was achieved on the application of the Montgomery and Dietrich method (1994), Mora and Vahrson method (1994), FEMA method and Siyahi and Ansal (1993). After the application of the previously mentioned methods at the Tekirdag down town as the pilot region, the application of the methods for whole Tekirdag and Samsun provinces are performed. In this report, after a concise review of the applied 4 methods, the results of the local microzonation for Tekirdag and Samsun city centers and regional microzonation of the Tekirdag and Samsun provinces are presented.

5.2 Montgomery and Dietrich Method

In Montgomery and Dietrich method (1994), an attempt is made to develop a method, based on the logic proposed by O' Loughlin (1981, 1986) which is founded on the assumption that topography creates the most detrimental effect on slope stability. It is stated that since interested areas exhibit themselves as convergent or divergent topographical structures, it requires to introduce a method considering local surface topography as primary parameter, and that the water transmission capacity of soil should be determined to assess whether it is capable of conducting infiltrated rain water or not. Such an application enables one to derive a parameter, called wetness index, which can be given as:

$$W = \frac{I_z A}{b T \sin \theta} \quad (10)$$

where I_z , A/b , T , θ denote the net rainfall rate, specific catchment area, the soil transmissivity at saturation ($Kh.z.\cos\theta$) and slope angle, respectively. Where, ϕ is residual shear strength angle, γ_{sat} , is the saturated unit weight of soil.

In order to provide a criterion for microzonation of the region with respect to Montgomery and Dietrich method (1994), the estimated wetness index can be associated with the saturation ratio of the interested soil layer. As a result, this parameter can be included in the factor of safety equation in

the case of infinite slope stability. To get this done, the estimated wetness index given in Eq.(10) can be evaluated as:

$$W = \frac{K \sin \theta h \cos \theta}{K \sin \theta z \cos \theta} = \frac{h}{z} \quad (11)$$

where h and z are groundwater table height and soil depth, respectively.

Also, the factor of safety equation proposed for infinite slope case is given as;

$$FoS = \frac{c + (z\gamma_{sat} - h\gamma_w) \cos^2 \theta \tan \phi}{z\gamma_{sat} \cos \theta \sin \theta} \quad (12)$$

This parameter can be included in the factor of safety equation where c = 0 as;

$$FoS = \frac{\tan \phi}{\tan \theta} \left[1 - W \left(\frac{\gamma_w}{\gamma_{sat}} \right) \right] \quad (13)$$

where ϕ is residual shear strength angle and γ_{sat} , is the saturated unit weight of soil.

5.2.1 Calculation of terrain related parameters

This stage relates to the extraction of the DEM (Digital Elevation Model) from the contour map of the studied region, and the generation of the slope angle map and specific catchment area. The procedure is presented so that all needed parameters is obtained using the SAGA.

5.2.1.1 Extraction of the DEM using SAGA

The contour maps of the target regions are converted to DEM using the SAGA software. The appropriate cell resolution of the DEM for this work is 25m×25m. Special attention should be paid in the selection of the correct global coordinate system of the studied area during projection stage and the clipping of the region border.

5.2.1.2 The use of DEM for extraction of slope angle map

The resulted DEM is used to extract slope angle map of the region using SAGA utilities.

5.2.1.3 The use of the DEM for extraction of catchment are map

This process can be achieved using SAGA. The specific catchment area can be extracted from the generated DEM. At first, by preserving a minimum slope gradient between cells (0.01°), the extracted DEM is turned to a depression less DEM, a flow path grid and a grid with watershed basins. Then using this DEM, the Saga Wetness Index and Total Catchment Area is estimated. Finally, the process is completed by the extraction of the Specific Catchment Area.

5.2.2 Preparation of the rainfall data

The rainfall records of the region are obtained from the meteorological stations. The number of the selected region should be enough in order to reflect the behavior of the rainfall at different parts of the region. The records of the station usually consist of two parts. First part is the records which has been done using digital recording instruments (in our case recorded per 10 minutes from 2007-2014). The second part is the daily measurements (in our case daily rainfall amount from 1960-2007). In order to obtain hazard compatible data, the method proposed by Ven Te Chow(1953) was applied to calculate the different return period of the cumulative daily rainfall amount. In addition, a suitable distribution model was applied on the existing rainfall records to find the probability of exceedance of the most unfavorable rainfall conditions. Fig. 103 shows the application of the Ven Te Chow(1953) for calculation of the daily rainfall amount return periods of the Tekirdag region with respect to the annual exceedance values of the rainfall records.

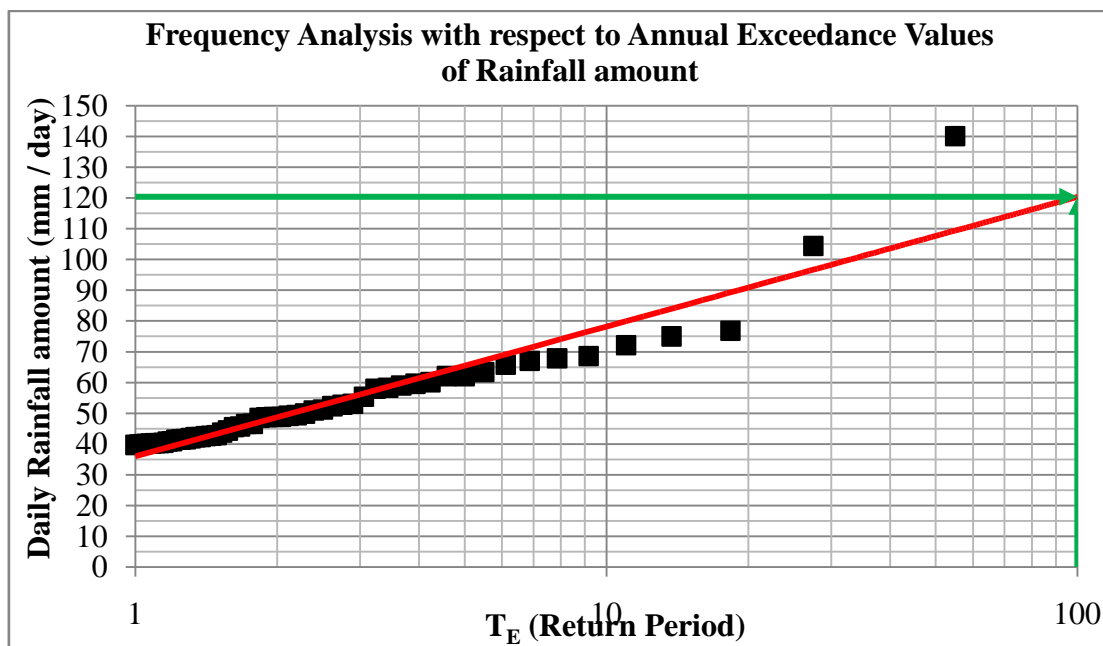


Fig. 102 Return period versus daily rainfall amount for Tekirdag region based on Ven Te Chow (1953) method

As can be seen in Figs 102 and 103, the daily rainfall amounts of the Tekirdag and Samsun Regions with return period of 100 years are about 120mm and 190 mm with respect to the Illinois University method, respectively (Ven Te Chow, 1953). In the case of the rainfall induced landslide investigations, the use of the daily rainfall amount with return periods well less than 100 years is recommended.

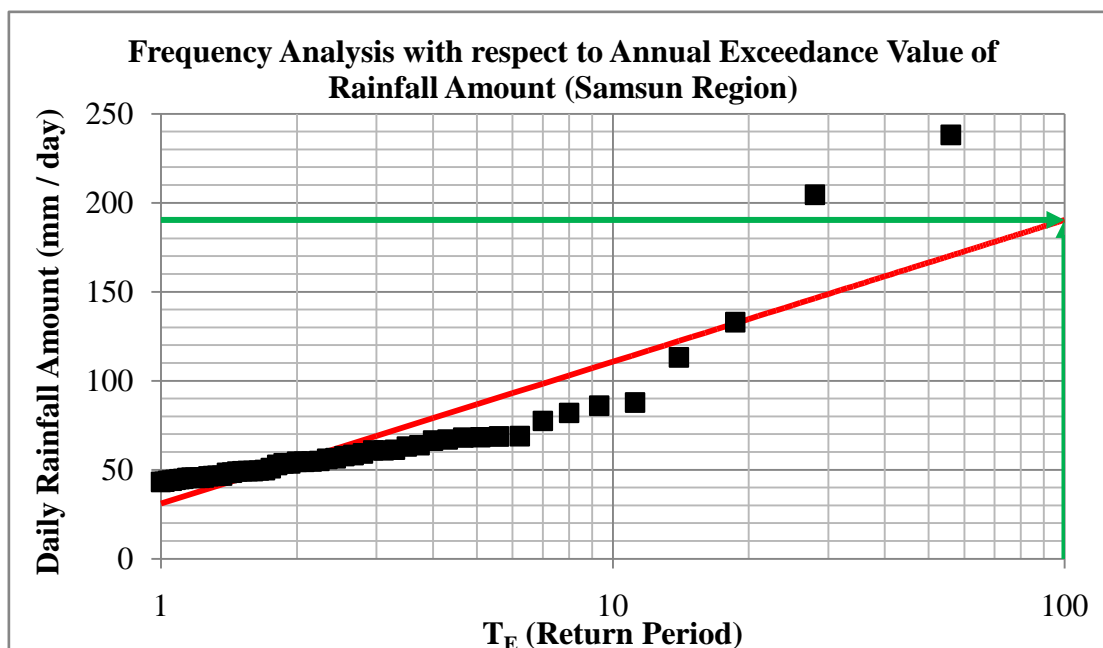


Fig. 103 Return period versus daily rainfall amount for Samsun region based on Ven Te Chow (1953) method

5.2.3 Compilation of the geotechnical properties of the region

Through the evaluation of the geotechnical and geological maps, reports, field investigations and all related sources, the information including layer thickness, soil permeability and its strength parameters were obtained. All these data were converted to excel sheets to be used in the analysis (Akinci et al., 2011, Faridfathi et al., 2012, Gazioglu et al., 2005, Gedik et al., 1984, Gedik et al., 1984, Gokasan et al., 2003, Sari, E., 2008, Şengüler, I, 2013, Yilmaz et al., 2010)

5.2.4 Other considerations and advices

In this step by step procedure, it is tired to obtain all needed parameters from the SAGA and use in the MAPINFO for making desired factor of safety map. The appropriate cell resolution of the DEM for this kind of works is 25m×25m. In some cases, if the grid dimensions of the certain parameters is more than 25m×25m, for example in the case of the geotechnical properties distribution map which can be 500m×500m, the grid can be refined in to the desired dimension by preserving the initial values of the properties.

5.3 Mora and Vahrson Method

This method is based on the visual inspection of the region for classification of the landslide hazard in seismically active tropical areas. A degree of slope failure hazard is introduced as;

$$H_l = |S_r * S_l * S_h| * |T_s + T_p| \quad (14)$$

Where, H_l , S_r , S_l and S_h denote the landslide hazard index, the value of relative relief index, the value of lithological susceptibility and the value of index of influence of natural humidity of the soil, respectively. These first three factors define the intrinsic land slide susceptibility. On the other hand, T_s and T_p denote the value of influence of seismic intensity and the value of influence of rainfall precipitation intensity, respectively. The combination of the rainfall and seismic intensity factors provide the triggering indicators.

5.3.1 Extraction of the DEM using Saga

The contour maps of the target regions are converted to the DEM using the SAGA software. The appropriate cell resolution of the DEM for this work is 25m×25m. Attention should be paid to the selection of the appropriate global coordinate system (projection stage) and the clipping of the region border.

5.3.2 Calculation of the relative relief index

In Mora and Vahrson method, the relative relief index is defined as the difference between summit level, the highest altitude for a given area, and base level, lowest altitude for each 1 km² of the given area. In order to use the advantage of high resolution DEM, the corresponding relative relief index table is corrected as gradient via dividing the each range by 1000. The corrected table is presented at Table . In this way, the distribution of the topographic gradient (tanθ) can be readily estimated from DEM using SAGA. Therefore the slope factors (S_r) can be determined with respect to gradient values.

Table 2 Corrected Relative Relief

Relative Relief	Susceptibility	Parameter, S _r
0 – 0.075m/km ²	Very Low	0
0.076 – 0.175	Low	1
0.176 – 0.3	Moderate	2
0.301 – 0.5	Medium	3
0.501 – 0.8	High	4
> 0.8	Very High	5

5.3.3 Selection of the lithological susceptibility value

Through the projection of the lithological map of the region on the 25m×25m discretized region grid, the corresponding lithological susceptibility value of each cell is selected with respect to classification introduced by Mora and Vahrson. Table 1 presents the lithological classification.

Table 1 *Classification of the lithological influence according to the general conditions, representative for Central America.*

Lithology	Susceptibility	Value, S_l
Permeable limestone, slightly fissured intrusions, basalt, andesites, granites, ignimbrite, gneiss, hornfels; low degree of weathering, low water table, clean – rugose fractures, high shear strength rocks	Low	1
High degree of weathering of above mentioned lithologies and of hard massive clastic sedimentary rocks; low shear strength; shearable structures	Moderate	2
Considerably weathered sedimentary, intrusive, metamorphic, volcanic rocks, compacted sandy regolith soils, considerable fracturing, fluctuating water tables, compacted colluvium and alluvium	Medium	3
Considerably weathered, hydrothermally altered rocks of any kind, strongly fractures and fissured, clay filled; poorly compacted pyroclastic and fluvio – lacustrine soils, shallow water tables	High	4
Extremely altered rocks, low shear resistance alluvial, colluvial and residual soils, shallow water tables	Very high	5

5.3.4 Selection of the soil natural humidity parameter (S_h)

To estimate this parameter, through the working on the rainfall data gathered from meteorological stations of the area, the monthly average precipitation value is estimated and the corresponding value is assigned with respect to the Table 2.

Table 2 The classes of average monthly precipitation.	
Average Monthly Precipitation (mm/month)	Assigned Value
< 125	0
125 - 250	1
250 <	2

Then, the sum of all twelve monthly assigned values for each analyzed station is evaluated and the corresponding moisture factor (S_h) is assigned with respect to the Table 3:

Table 3 Weighting for annual precipitation.		
Summation of Precipitation Averages	Susceptibility	Value, S_h
0 – 4	Very low	1
5 – 9	Low	2
10 – 14	Medium	3
15 – 19	High	4
20 – 24	Very high	5

5.4 Determination of Related Hazard Parameters

5.4.1 The value of influence of seismic intensity (T_s)

The seismic intensity factor is selected with respect to the Modified Mercalli Scale, which depend on the seismic characteristics of interested region. The pursued route in this study was the estimation of the PGA values through time independent seismic hazard analyses with respect to the 475 years return period and relating it to MMI using the following equation:

$$MMI = 3.0262 \log[PGA(\text{cm/sec}^2)] + 1.0195 \quad (15)$$

Thus, the related T_s factor with respect to MMI can be selected from Table 4:

Table 4 The influence of seismic intensity (Modified Mercalli Scale) as a triggering factor for landslide generation

Intensities (MM) $T_r = 100$ years	Susceptibility	Value, T_s
III	Slight	1
IV	Very low	2
V	Low	3
VI	Moderate	4
VII	Medium	5
VIII	Considerable	6
IX	Important	7
X	Strong	8
XI	Very Strong	9
XII	Extremely Strong	10

5.4.2 The value of influence of rainfall precipitation intensity (T_p)

The precipitation intensity factor (T_p) relies upon the probabilistic assessment of rainfall data provided that long records for meteorological stations are available. Annual maxima of daily rainfall amount (mm/day) for data set are modeled through an appropriate distribution function and the value for 100 years return period is calculated to obtain T_p . If rainfall records are shorter than 10 years, average of the yearly maximum values is proposed to attain T_p . In this study, the rainfall amounts corresponding to 100 years return period (T_M) (Fig. 104 and Fig. 105) are estimated with respect to the Illinois University method in order to obtain hazard compatible data (Ven Te Chow, 1953) using Eqs (16) and (17);

$$K = - \left(1.1 + 1.795 \log_{10} \log_{10} \frac{N+1}{N+1-m} \right) \quad (16)$$

$$T_M = \frac{N+1}{m} \quad (17)$$

N , is the number of years and m is the rank for each rainfall data.

The fact that K value of 3.05 corresponds to T_M amounting to 100 years is employed to find out the relevant values as 114 mm and 166.2 mm for Tekirdağ and Samsun Regions, respectively. The T_p factor can be found at Table 5.

Table 5 The influence of rainfall precipitation intensity as a triggering factor for landslides.

Maximum Rainfall $n > 10$ years: $T_r = 100$ years	Rainfall $n < 10$ years; Average	Susceptibility	Value, T_p
< 100 mm	< 50 mm	Very low	1
101 – 200	51 – 90	Low	2
201 – 300	91 – 130	Medium	3
301 – 400	131 – 175	High	4
> 400	> 175	Very High	5

Finally, the previously estimated susceptibility and triggering parameters are used to calculate the hazard index by Eq. (14) and classifying with respect to Table 6.

Table 6 The influence of rainfall precipitation intensity as a triggering factor for landslides.

Value from Eq. (5)	Class	Susceptibility of Hazard
0 – 6	I	Negligible
7 – 32	II	Low
33 – 162	III	Moderate
163 – 512	IV	Medium
513 – 1250	V	High
> 1250	VI	Very High

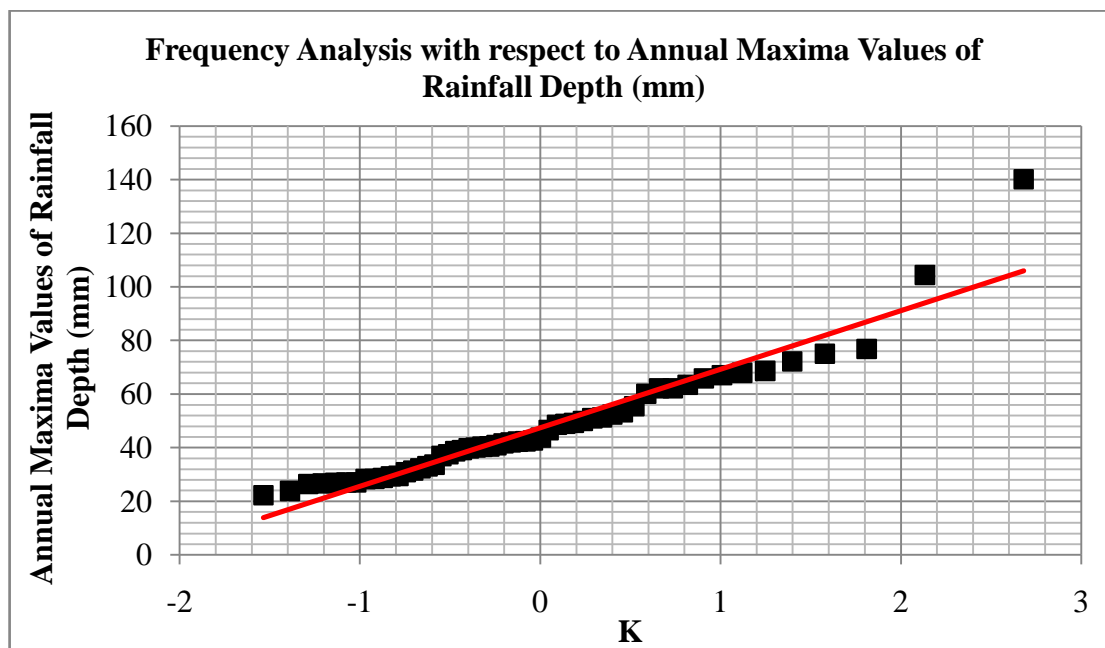


Fig. 104 Rainfall Frequency Analysis with respect to Annual Maxima of Rainfall Depth for Tekirdağ Region (Ven Te Chow, 1953)

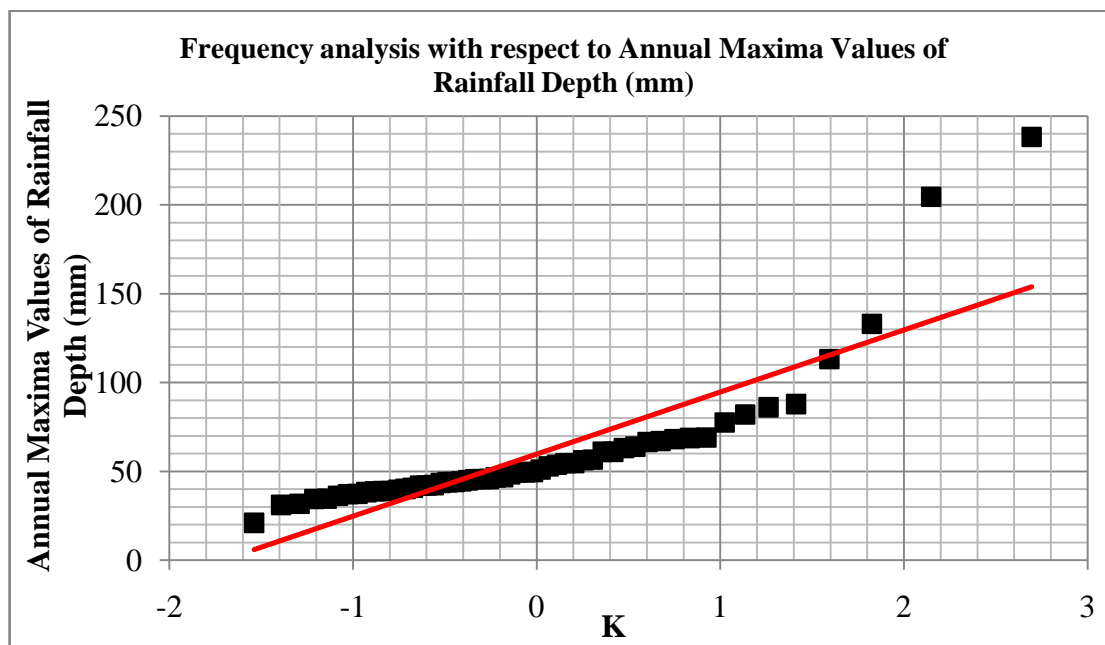


Fig. 105 Rainfall Frequency Analysis with respect to Annual Maxima of Rainfall Depth for Samsun Region (Ven Te Chow, 1953)

5.4.3 Other Considerations and Advice

In this step by step procedure, all the required parameters are determined from the SAGA software and used in the MAPINFO for plotting the hazard maps. The appropriate cell resolution of the DEM is 25m×25m. At some cases, if the grid dimensions of the certain parameters is more than 25m×25m, for example in the case of the geotechnical properties distribution map which can be 500m×500m, the grid can be refined in to the desired dimension by preserving the initial values of the properties.

5.5 FEMA Method

In this project, the FEMA (USA) method, which also known as (HAZUS-SR99, 1999) method for Landslide Susceptibility under static and seismic conditions, is also applied to the selected pilot regions. For static conditions, this method is applied for two different condition; Dry condition, which is applied for the condition that groundwater table is below the sliding level; and Wet condition, which is applied for conditions that the groundwater table is at the surface and is comparable to the after rain condition. In this method, landslide susceptibility classification of a site is done with respect to the geologic group, slope angle and the hydraulic condition of the site. The approximate effect of the hydraulic condition of the site is considered using the WET and DRY terms, as presented in the Table 7.

Table 7 Landslide susceptibility classification according to the FEMA method – HazUS99-SR2, Technical Manual, Chapter 4-PESH, 1999)

Geologic Group		Slope Angle, degrees					
		0-10	10-15	15-20	20-30	30-40	>40
(a) DRY (groundwater below level of sliding)							
A	Strongly Cemented Rocks (crystalline rocks and well-cemented sandstone, $c' = 300$ psf, $\phi' = 35^\circ$)	None	None	I	II	IV	VI
B	Weakly Cemented Rocks and Soils (sandy soils and poorly cemented sandstone, $c' = 0$, $\phi' = 35^\circ$)	None	III	IV	V	VI	VII
C	Argillaceous Rocks (shales, clayey soil, existing landslides, poorly compacted fills, $c' = 0$, $\phi' = 20^\circ$)	V	VI	VII	IX	IX	IX
(b) WET (groundwater level at ground surface)							
A	Strongly Cemented Rocks (crystalline rocks and well-cemented sandstone, $c' = 300$ psf, $\phi' = 35^\circ$)	None	III	VI	VII	VIII	VIII
B	Weakly Cemented Rocks and Soils (sandy soils and poorly cemented sandstone, $c' = 0$, $\phi' = 35^\circ$)	V	VIII	IX	IX	IX	X
C	Argillaceous Rocks (shales, clayey soil, existing landslides, poorly compacted fills, $c' = 0$, $\phi' = 20^\circ$)	VII	IX	X	X	X	X

5.6 Siyahi and Ansal Method

Siyahi and Ansal (1993) developed a microzonation method for slope instability based on the method proposed by Koppula (1984). The method originally proposed was a pseudo-static evaluation of slope stability utilizing a seismic coefficient A to account for the earthquake- induced horizontal forces. The variation in shear strength with depth is assumed linear and potential failure surface is taken as a circular arc as shown in Fig. 106.

Parameters α , β , λ and n are related to the geometry of the slope and configuration of sliding surface. As given below, the factor of safety, F_s , can be defined as;

$$F_s = \frac{a_0}{\gamma} N_1 + \frac{c_0}{\gamma H} N_2 \quad (18)$$

where,

$$N_1 = \frac{3(\alpha + \cot\lambda - \alpha \cot\alpha \cot\lambda)}{\text{DEN}} \quad (19)$$

$$N_2 = \frac{6\alpha}{\text{DEN}} \quad (20)$$

$$\text{DEN} = \sin^2\alpha \sin^2\lambda (D_1 + D_2) \quad (21)$$

$$D_1 = 1 - 2\cot^2\beta - 3\cot\alpha\cot\beta + 3\cot\beta\cot\lambda + 3\cot\lambda\cot\alpha - 6n\cot\beta - 6n^2 - 6n\cot\alpha + 6n\cot\lambda \quad (22)$$

$$D_2 = A(\cot\beta + \cot^3\lambda + 3\cot\alpha\cot^2\lambda - 3\cot\alpha\cot\beta\cot\lambda - 6n\cot\alpha\cot\lambda) \quad (23)$$

In Siyahi and Ansal (1993), a linear variation with depth is assumed regarding the shear strength of normally consolidated soils as follows;

$$c = a_0 z, \quad c_0 = 0 \quad (24)$$

$$c = \sigma \tan\phi = \gamma z \tan\phi \quad (25)$$

Then,

$$a_0 = \gamma \tan\phi \quad (26)$$

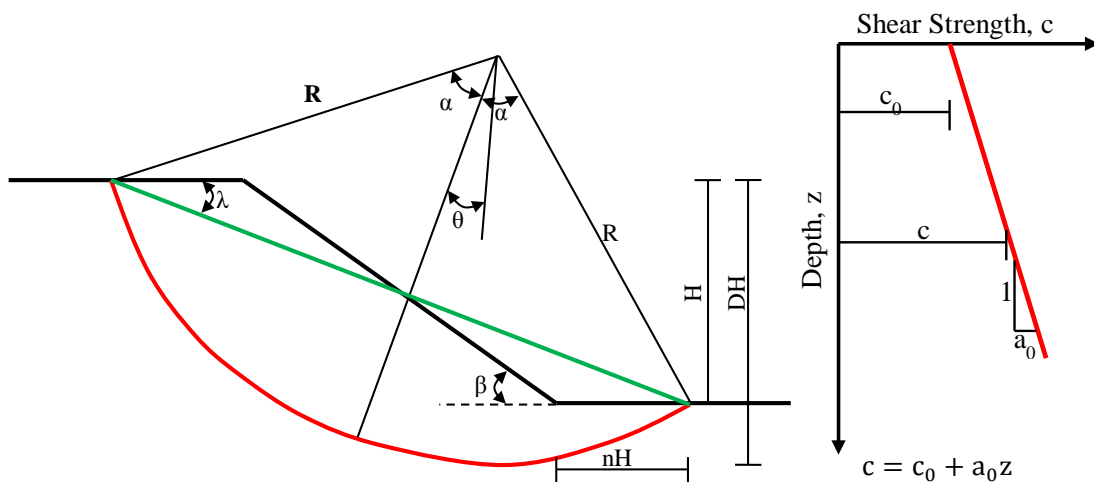


Fig. 106 A typical section of slope and shear strength variation with depth

$$F_s = \frac{a_0}{\gamma} N_1 = \frac{\gamma \tan \varphi}{\gamma} N_1 = \tan \varphi N_1 \quad (27)$$

Thus the factor of safety depends on the angle of shear strength and stability number, N_1 representing the configuration of the slope and failure surface. In this deliverable, the variation of parameters α , β , λ , n and A is specified as below in order to populate the N_1 (min) vs. β graph presented in Siyahi and Ansal Method (1993) and the results are given in Fig. 107.

$$\alpha = 5^\circ, \dots, 85^\circ$$

$$\beta = 10^\circ, 10.5^\circ, \dots, 60^\circ$$

$$\lambda = 10^\circ, \dots, 55^\circ$$

$$n = 0 \text{ (toe failure presumption)}$$

$$A \text{ (g)} = 0.00, 0.02, \dots, 1.00$$

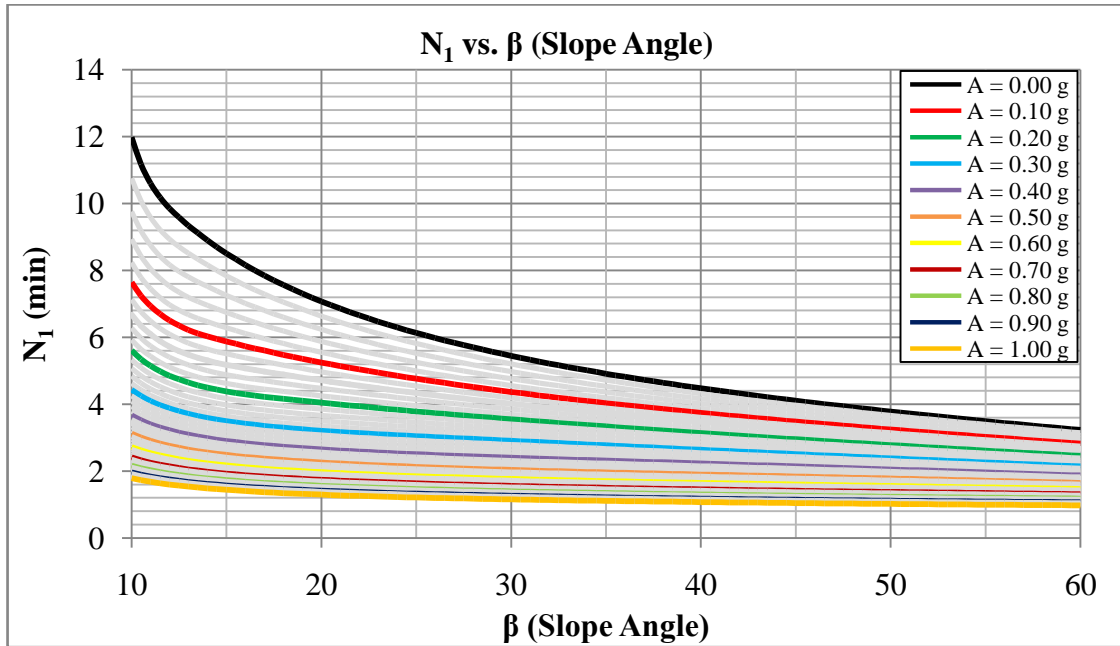


Fig. 107 N_1 vs β (Slope Angle)

5.7 Microzonation for Rainfall Induced Landslides

In this section, the results of the application of the Montgomery and Dietrich method (1994), Mora and Vahrson method (1994), FEMA method and Siyahi and Ansal (1993) are presented. The step by step preparation of the methods parameters and analysis stage are presented in Fig. 108.

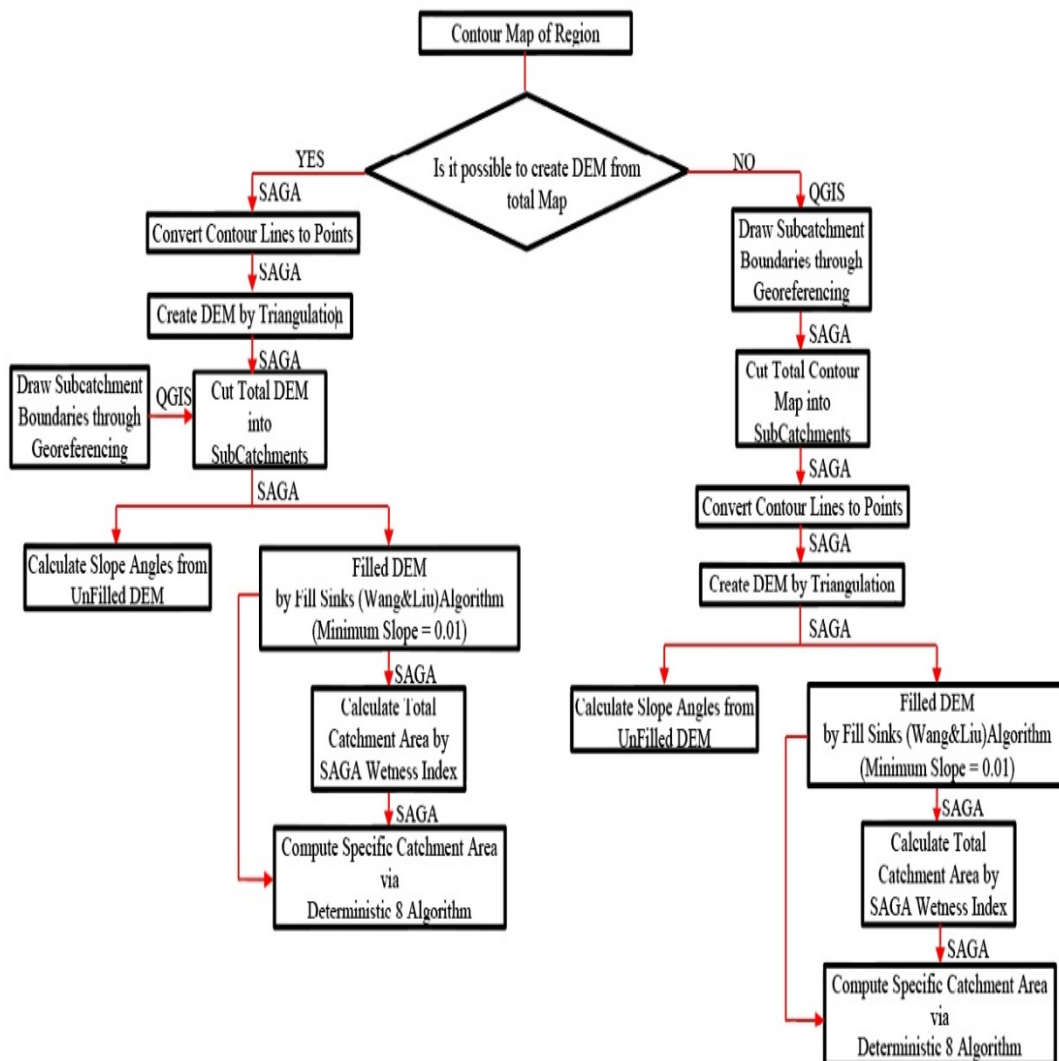


Fig. 108 Flow chart of the analysis

6 LOCAL MICROZONATION OF TEKİRDAĞ CITY CENTER

6.1 Geology

Tekirdag province is located at north of Marmara sea, north-west Turkey, with the total area of 6.218 km². Tekirdağ Municipality is situated onto 23.64 km² area with total perimeter of 64.15 km and its geology is governed by 6 different geologic formations; (1) Quaternary Alluvium, (2) Danişmen Formation alluvium, (3) Man-Made Fill, (4) Ergene Formation, (5) Trakya Formation, (6) Danişmen Formation sand (Ansal et al. 2005). The general geology of the region is shown at Fig. 102. The oldest geological unit in Tekirdağ and its vicinity is Danişmen Formation belonging to Tertiary. The bottom of this unit with thickness changing between 100-300m has been observed in the study area. The other units outcropping in Tekirdag are Ergene and Trakya Formations with their unconformable contacts. The Quaternary Alluvium overlies all these formations. In order to determine the geotechnical specification of the region, relatively detailed site investigation based on borings were conducted. The results of the laboratory test on soil samples and in-situ SPT tests have been evaluated and used to estimate required parameters such as permeability, shear strength angle, unit weight, underground water table etc. The estimated parameters have been compared to the USGS ranges defined for permeability of different types of soils.



Fig. 109 Tekirdag City Center Geology Map

The higher amount of clay and clayey formations and the presence of strongly weathered siltstone and sandstone levels with water bearing capacity over these formations are the factors that can produce the potential landsliding. Also, in order to perform slope stability evaluation, the distribution of the slope angle in the region is needed. The slope angle map of the region has been extracted using DEM (Digital Elevation Model) and shown in Fig. 110. The studies conducted at the region show that the critical slope angles occasionally show a general variation of 0°-20° in the slope maps. As can be seen, the areas with steeper slopes are generally dominant and concentrated at the middle part of the region. The rest of the coastal region has generally the mild slope of less than 10°.

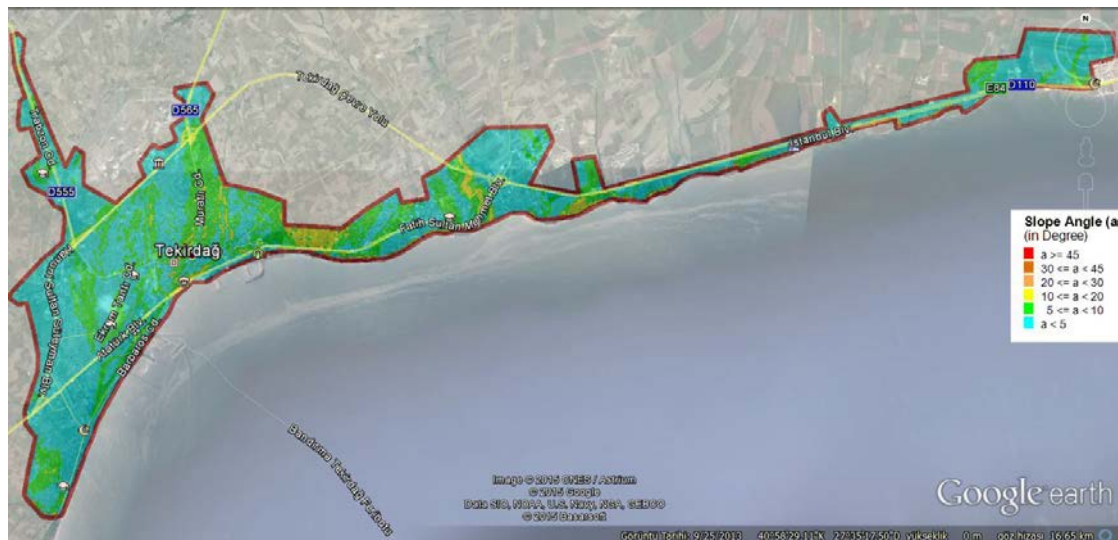


Fig. 110 The slope map of the Tekirdag City Center

6.2 Results of the microzonation of Tekirdag for rainfall induced landslide

At Fig. 111, the distribution of the safety factor is seen. It is seen that the failed cell concentration is at the middle and coastal parts of the region. About 4.37% of the cells (1726 cells out of 39454) in the region has the FOS less than 1, which is colored by red on the map.



Fig. 111 Microzonation of Tekirdag City Center by Montgomery & Dietrich (1994)

The results of the application of the Mora and Vahrson (1994) method on the selected pilot region (Tekirdag) are presented in the Fig. 112. As can be seen, the highest hazard index relates to the moderate level. There are rare points with medium hazard level, but these points lie on the boundaries of the region and likely they are resulted under the effect of the cut borders thus are negligible.



Fig. 112 Microzonation of Tekirdag City Center by Mora and Vahrson (1994)

The results of the application of the FEMA method on Tekirdag region are presented on Fig. 113 and Fig. 114 for both DRY and WET conditions. Because the aim of this investigation is the study of the rainfall induced landslide, the results of the application of the method under the wet condition can better approximate the region status under the rainfall. The parts of the Tekirdag region with high landslide susceptibility can be seen at Fig. 114.



Fig. 113 Microzonation of Tekirdag City Center by FEMA method (Dry condition)



Fig. 114 Microzonation of Tekirdag City Center by FEMA method (Wet condition)

Factor of Safety
(Siyahi & Ansal, 1990)

- FOS ≥ 1.5
- $1 \leq$ FOS < 1.5
- FOS < 1

Image © 2014 CNES / Airbus
© 2014 Google
Data SRTM, NGA, U.S. Navy, NSA, GEBCO
© 2014 Bing.com

Google earth

Görüntü Tarihi: 9/25/2016 40°53'29.86"N 27°35'16.64"E Yükseklik: 0 m Göz hizası: 16.60 km

Deliverable-No.	D.03.01, Vol. 2
Issue: I.01	Date: 04 February 2016

7 LOCAL MICROZONATION OF SAMSUN CITY CENTER

7.1 Geology

As can be seen in Fig. 116, the geology of Samsun City Center is governed by Permo – Triassic (pink), Quaternary (green) and Lower – Middle Eocene (brown). Also, The slope map of the Tekirdag region is presented in Fig. 117.

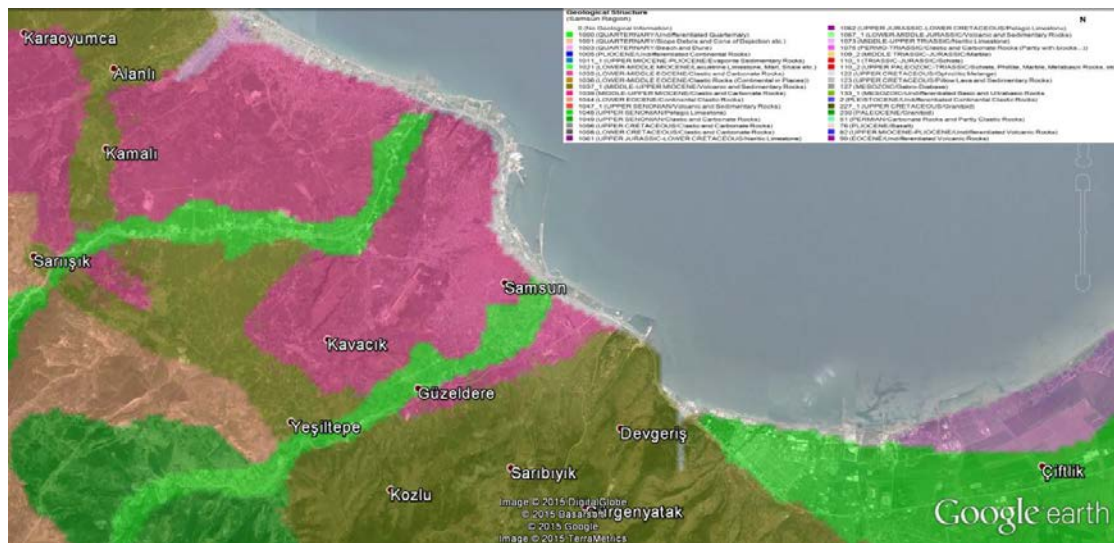


Fig. 116 Samsun City Center Geology Map



Fig. 117 The slope map of Samsun City Center

7.2 Results of the microzonation of Samsun for rainfall induced landslide

At Fig. 118, the microzonation of the Samsun City Center with respect to factor of safety by Montgomery and Dietrich (1994) are presented. The estimated factor of safety has been presented in 3 levels. The cells with FOS less than 1 have been colored by red which means that failure is likely to be occurred under the rainfall with exceedance probability of %1 within 1 year (return period of 100 years). The cells with yellow color represent the factor of safety range between 1 and 1.5, which is considered as the parts that are on the verge of failure under the assumed hazard level. The cells with FOS more than 1.5 are considered as safe area, and have been colored by green. It is seen that failed regions are generally concentrated on Devgeriş, Sarıbiyik, Kozlu and Gürgenyatak Districts. With respect to slope map, this region corresponds to the areas with slope angles generally greater than 30°.

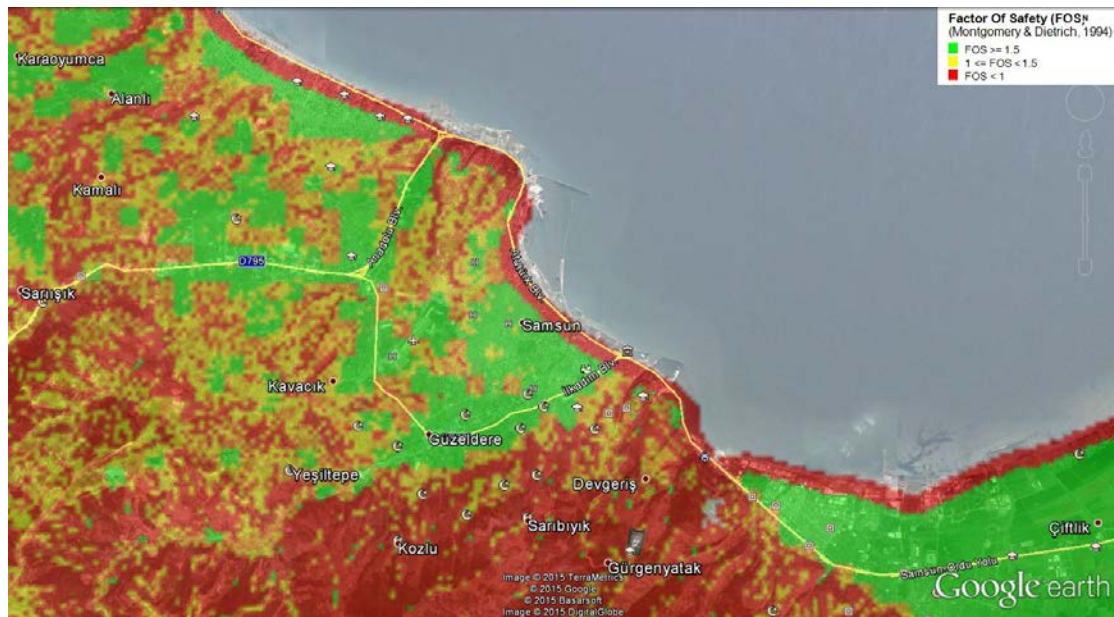


Fig. 118 Microzonation of Samsun City Center by Montgomery and Dietrich (1994)



Fig. 119 Microzonation of the Samsun City Center by Mora and Vahrson (1994)

The microzonation of the Samsun City Center by Mora and Wahrson (1994) has been presented at Fig. 119. While the Karaoyumca, Kamalı, Kavacık, Yeşiltepe, Devgeriş, Sarıbiyik, Kozlu and

Gürgenyatak Districts are generally dominated by the moderate hazard level index, negligible and low hazards have been observed at Çiftlik and Güzeldere.

Fig. 120 and Fig. 121 present the results of the application of the FEMA method for Samsun City Center. Although Fig. 120 show the microzonation of the region under dry condition, because of the existence of a band of high slope angles at Devgeriş, Sarıbiyik, Kozlu and Gürgenyatak Districts, such areas with high susceptibility (IX) has been detected. Other parts of the studied area have generally got susceptibility level of medium (V) and lower. Regarding the wet condition, Fig. 121, a tangible increase in the susceptibility level is seen.



Fig. 120 Microzonation of Samsun City Center by FEMA method (Dry condition)

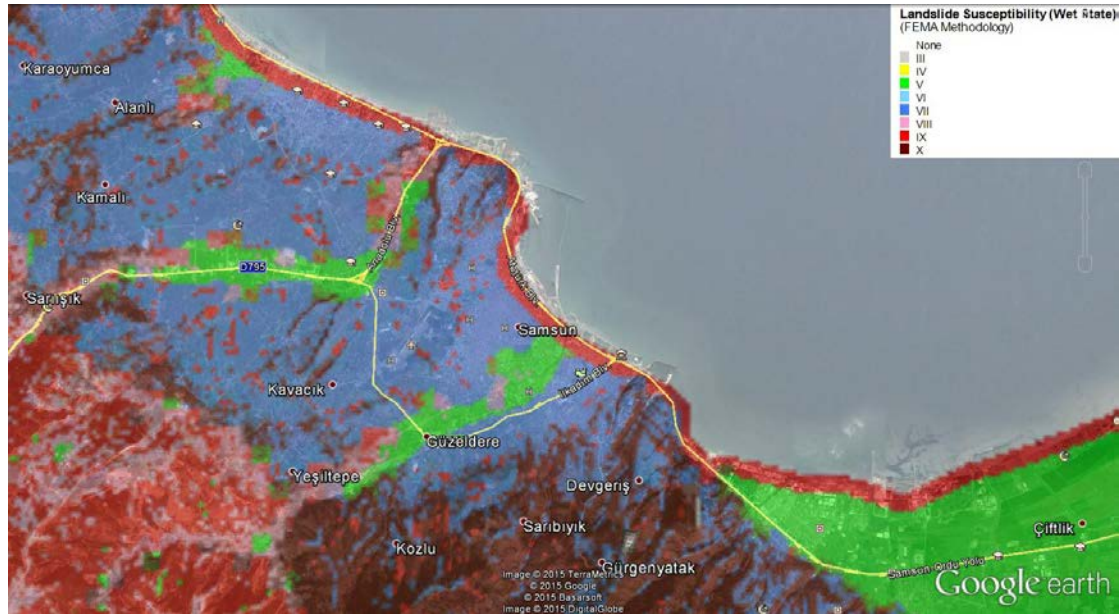


Fig. 121 Microzonation of Samsun City Center by FEMA method (Wet condition)

8 REGIONAL MICROZONATION OF TEKIRDAG PROVINCE

8.1 Geology

Tekirdag region is located at the west Marmara Sea, north-west Turkey, with the total area of 6339km². Tekirdağ geology is governed by 6 different geologic formations; (1) Quaternary Alluvium, (2) Danişmen Formation alluvium, (3) Man–Made Fill, (4) Ergene Formation, (5) Trakya Formation, (6) Danişmen Formation sand (Ansal et al., 2005). The general geology of the region is shown at Fig. 122

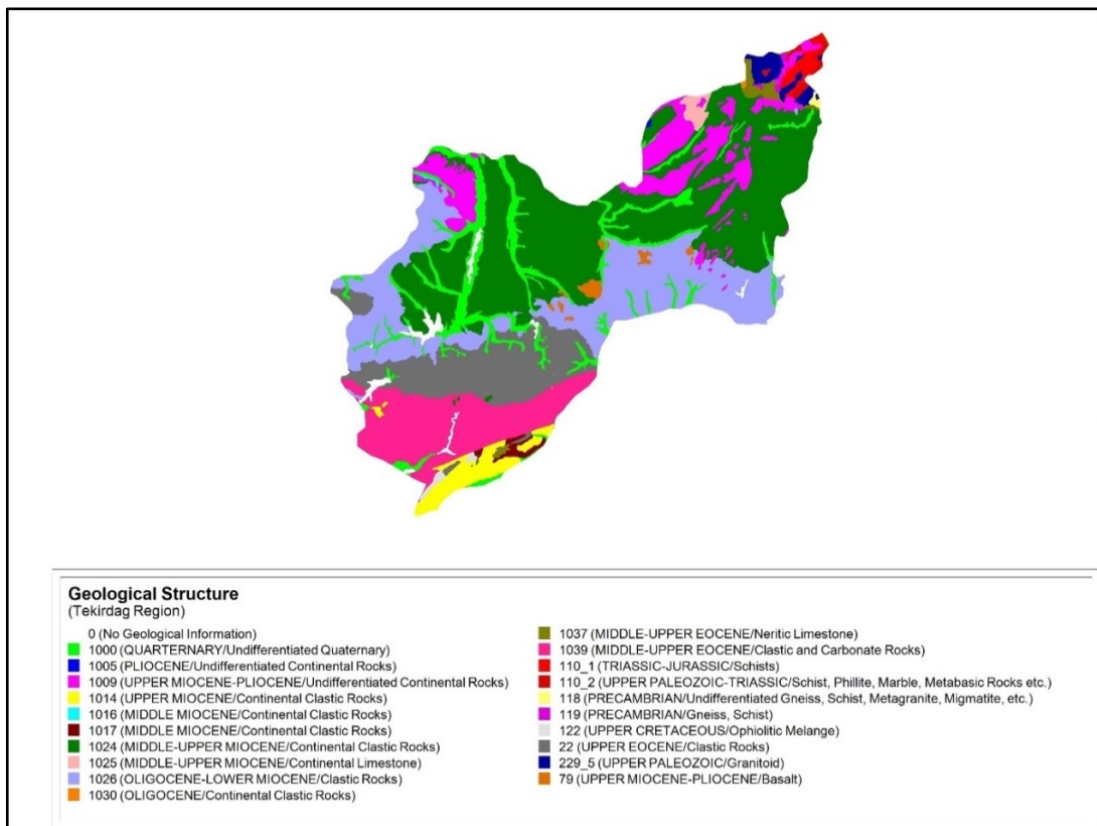
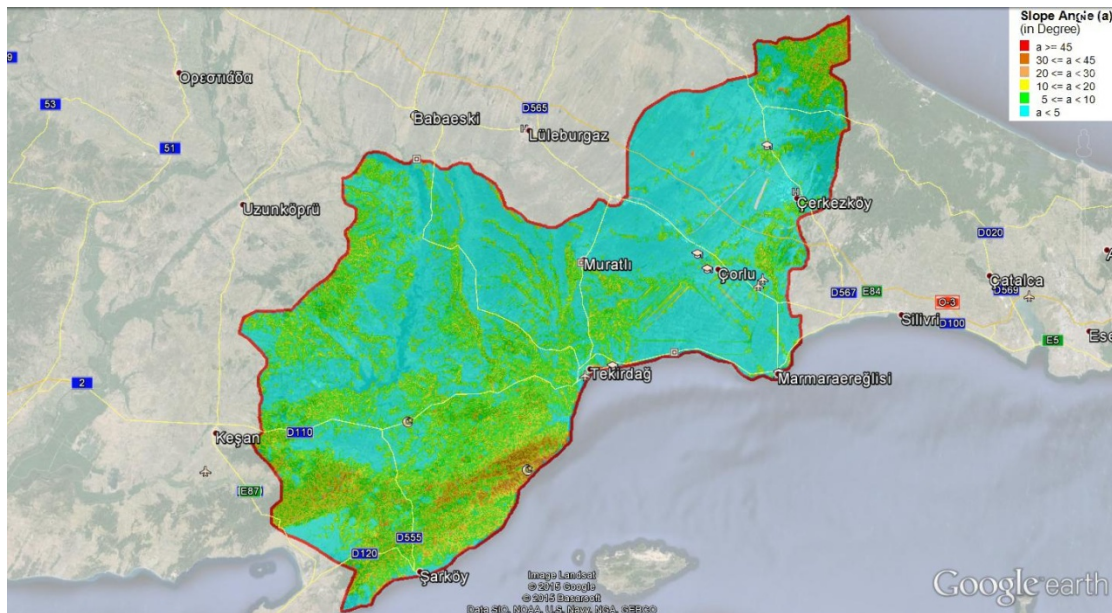


Fig. 122 Tekirdag province geological map

The geological evolution of the Tekirdag Basin is controlled by the active tectonic regime of the NAFZ, and it is continuing to form through transtension and transpression at a releasing bend of this zone whereby the age of this basin is considered as Pliocene (Yilmaz et al., 2010).

The oldest geological unit in Tekirdağ and its vicinity is Danişmen Formation belonging to Tertiary. The bottom of this unit with thickness changing between 100-300m is seen in study area. The other units outcropping in this are Ergene and Trakya Formations with their unconformable contacts. The Quaternary Alluvium overlies all these formations. The estimated parameters have been compared to the USGS boundaries defined for permeabilities of different types of soils. The higher amount of clay and clayey formations and the presence of strongly weathered siltstone and sandstone levels with water bearing capacity over these formations are the factors that can produce the potential land sliding.

The geological properties of the shallow layers of the studied area have been extracted from the geological maps of the General Directorate and of Mineral Research and Exploration (Scale: 1/500000) and the geotechnical reports and studies done at the region during different projects. (Ansal A. et al, 2005, Şengüler, 2013). The estimated parameters have been compared to the USGS boundaries defined for permeabilities of different types of soils. The slope map of the Tekirdağ region is presented in Fig. 123.



8.2 Results of the microzonation of Tekirdag for rainfall induced landslide

In this section, the microzonation of Tekirdag region for rainfall induced landslide by four different methods is presented. Fig. 124 shows the results of the application of the Montgomery and Dietrich method for Tekirdag region.

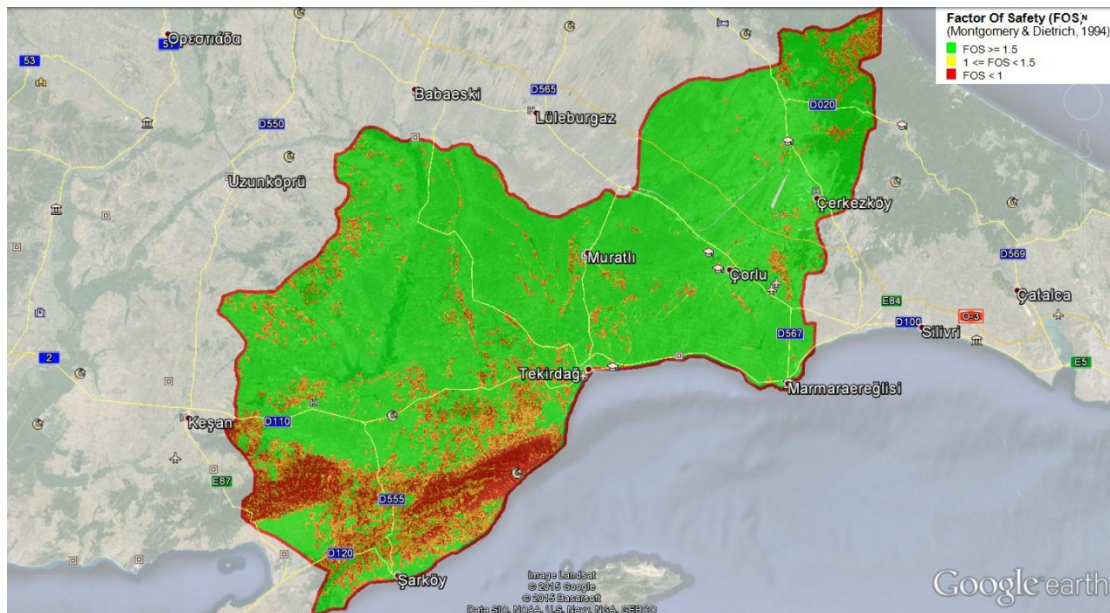


Fig. 124 Microzonation of the Tekirdag region by Montgomery and Dietrich (1994)

The estimated factor of safety has been classified in 3 groups. The cells colored by red have got FOS less than 1. These parts are considered as the area that most likely will failed under the rainfall with exceedance probability of 100 years. The cells with FOS between 1 and 1.5 are colored by yellow and are considered as the parts that are on the verge of failure under the rainfall with return period of 100 years. The cells with FOS more than 1.5 are considered as safe area, and have been colored by green. As can be seen, the concentration of the area with red color is at the south part of the Tekirdag. Also, with respect to the slopes map, the concentration of the area with higher slope are seen in the same part. There is also the slight distribution of region with red and yellow colors at the north, center and west of the Tekirdag. At these parts, the occurrence of the low scale rainfall induced landslide is expected.

As explained before, the Mora and Vahrson (1994) method is based on the visual inspection of the region for classification of the landslide hazard in seismically active tropical areas. Nevertheless, the proposed hazard index (HI) comprises, to some extent, the effects of the rainfall and earthquake. In this method, the hazard index of a site is assigned from “I” (negligible) to “VI” (very high).

Figure shows the microzonation of the Tekirdag by Mora and Vahrson (1994). With respect to these results, most of the Tekirdag area is indexed by low and moderate hazard index. Only the limited area at the south of the region has got yellow color (moderate hazard index).



Fig. 125 Microzonation of the Tekirdag region by Mora and Vahrson (1994)

The results of the application of the FEMA method are presented at Fig. 126 and Fig.127. The results of this method are presented for two different condition; Dry condition, which is applied for the condition that groundwater table is below the sliding level; and Wet condition, which is applied for conditions that the groundwater table is at the surface. Fig. 126 and Fig.127 show the microzonation of the Tekirdag by the FEMA method under dry and wet conditions, respectively.

In this method, the susceptibility of the sites for landslide are classified by levels from “none” to “IX” under dry condition, and from “III” to “X” under wet condition. As can be seen at Fig. 126, the concentration of the regions with susceptibility more than “v” are at the south of the Tekirdag. Also, a limited region with susceptibility of “V” and “VIII” can be seen at the north of the Tekirdag. These results are expectable under dry condition. Nevertheless, the best estimate of the rainfall induced landslide can be achieved by the application of the wet condition. Fig. 126 presents the microzonation of the Tekirdag by FEMA method under wet condition. It is seen that the susceptibility of the hazardous region in the south has been increased to “VII” and more with respect to the results of the dry condition. Also, a limited region with susceptibility about “VII” can be traced at the north of the Tekirdag. As is was seen in the results of the Montgomery and Dietrich method at Fig. 124, the region with high susceptibilities can be seen at the center and west of the Tekirdag. The occurrence of the low scale rainfall induced landslide is expected at these parts, too.

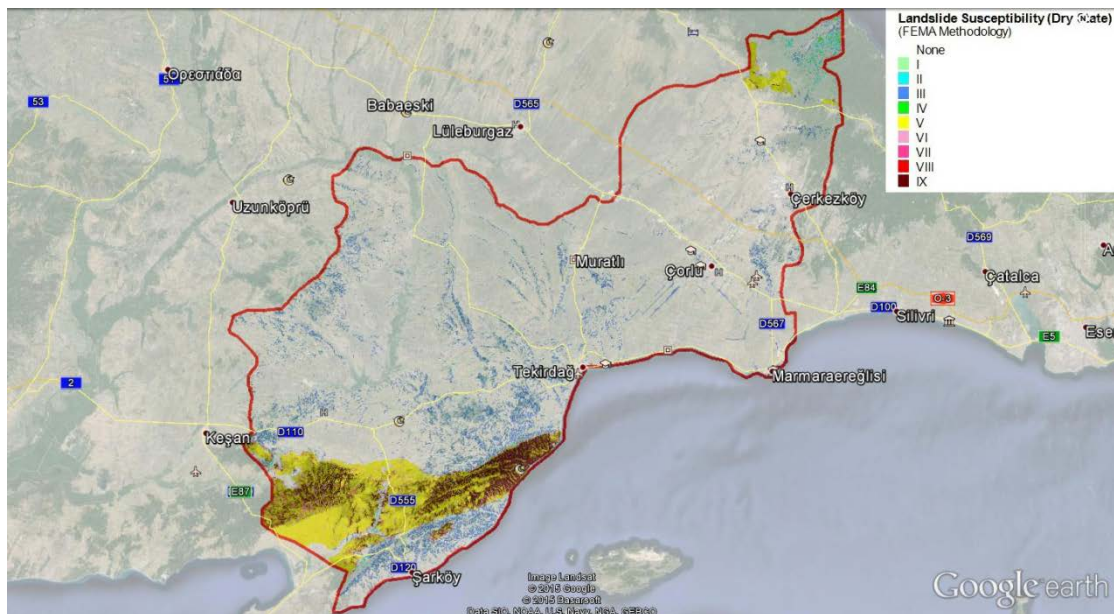


Fig. 126 Microzonation of Tekirdag region by FEMA method (Dry condition)

The last zoning method that has been applied at Tekirdag region is Siyahi and Ansal (1993) method. The effect of the rainfall has not been considered in this method and the method mainly classifies the region for earthquake induced landslide. Fig. 127 presents the microzonation of the Tekirdag for earthquake induced landslide. As can be seen, the concentration of the regions with FOS less than 1

is at the south of the Tekirdag. In fact, all of the applied microzonation methods have detected the southern part as a region with high hazard level. An important point about the results of the Siyahi and Ansal (1993) method is the condition of the southern part of the region (along the southern border).

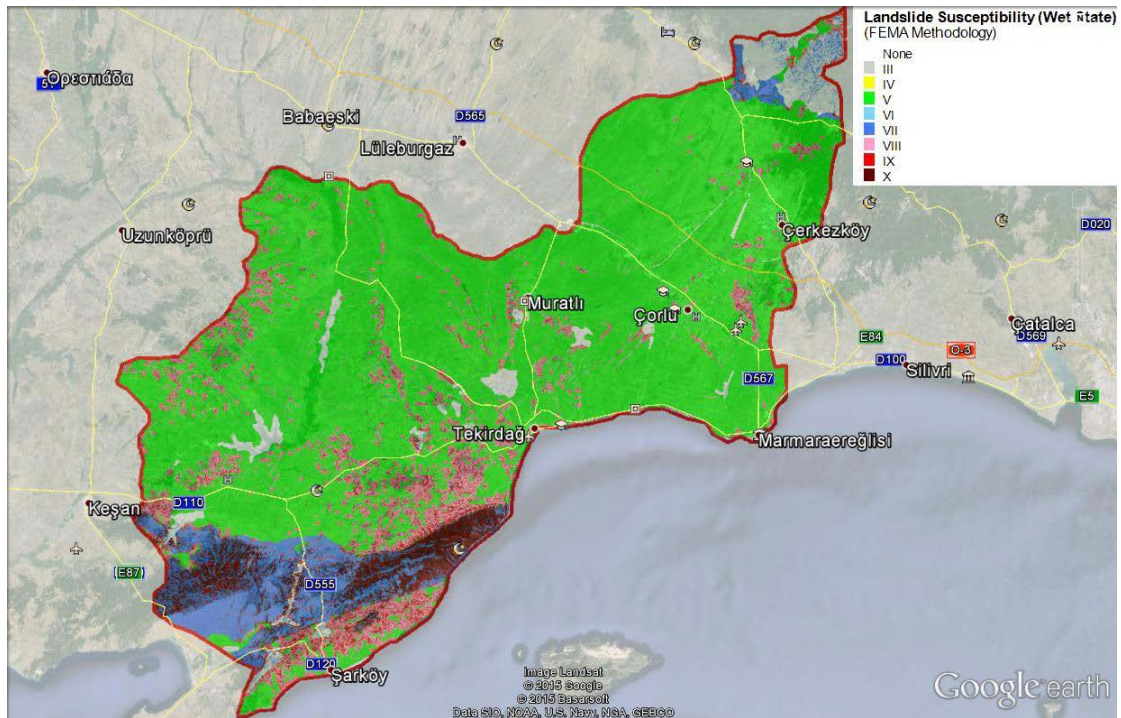


Fig. 127 Microzonation of Tekirdag region by FEMA method (Wet condition)

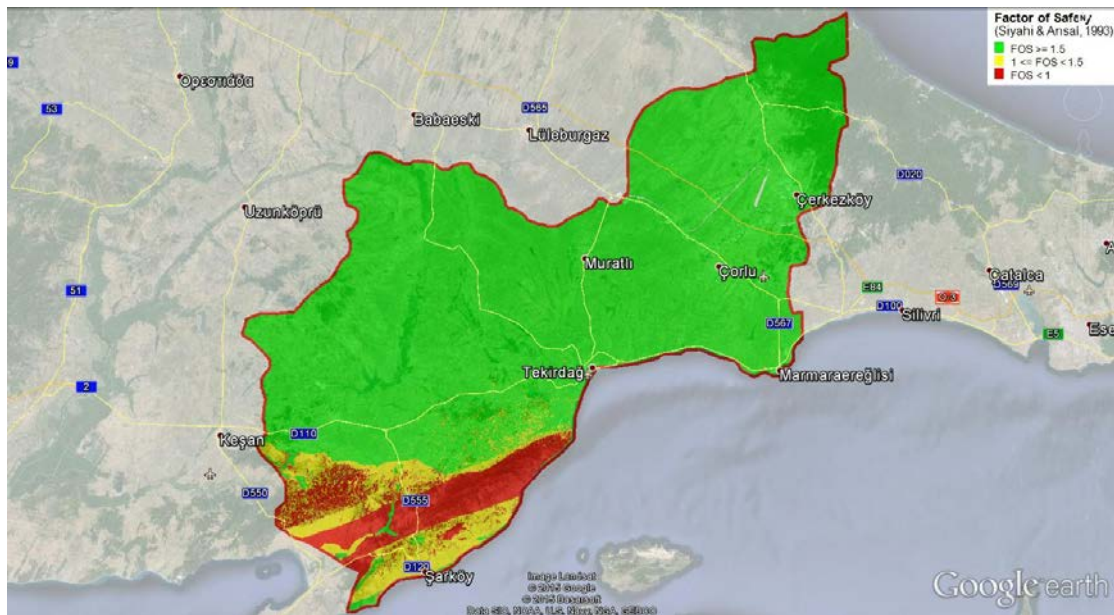


Fig. 128 Microzonation of the Tekirdag region by Siyahi and Ansal (1993)

While this region has been considered as safe or low susceptible zone by other methods, the Siyahi and Ansal (1993) method has identified it as the region on the verge of failure (FOS between 1 and 1.5). It means that although this region with rather low slope angle would be safe under the effects induced by rainfall, it may have higher hazard level under earthquake induced landslide.

9 REGIONAL MICROZONATION OF SAMSUN PROVINCE

9.1 Geology

Samsun province is located on the north coast of Turkey. The study area covers about 9352 km² with the geographical coordinates between northern latitudes 40° 05' and 41° 44' and between eastern longitudes 35° 30' and 37° 05'. The Samsun area comprises 6 different geological formations; (1) Tekkekoy formation, (2) Samsun formation, (3) Ilyas member, (4) Karasamsun member, (5) Old alluvium and (6) Flood-plain sediment. The general geology of the region is shown at Fig. 129.

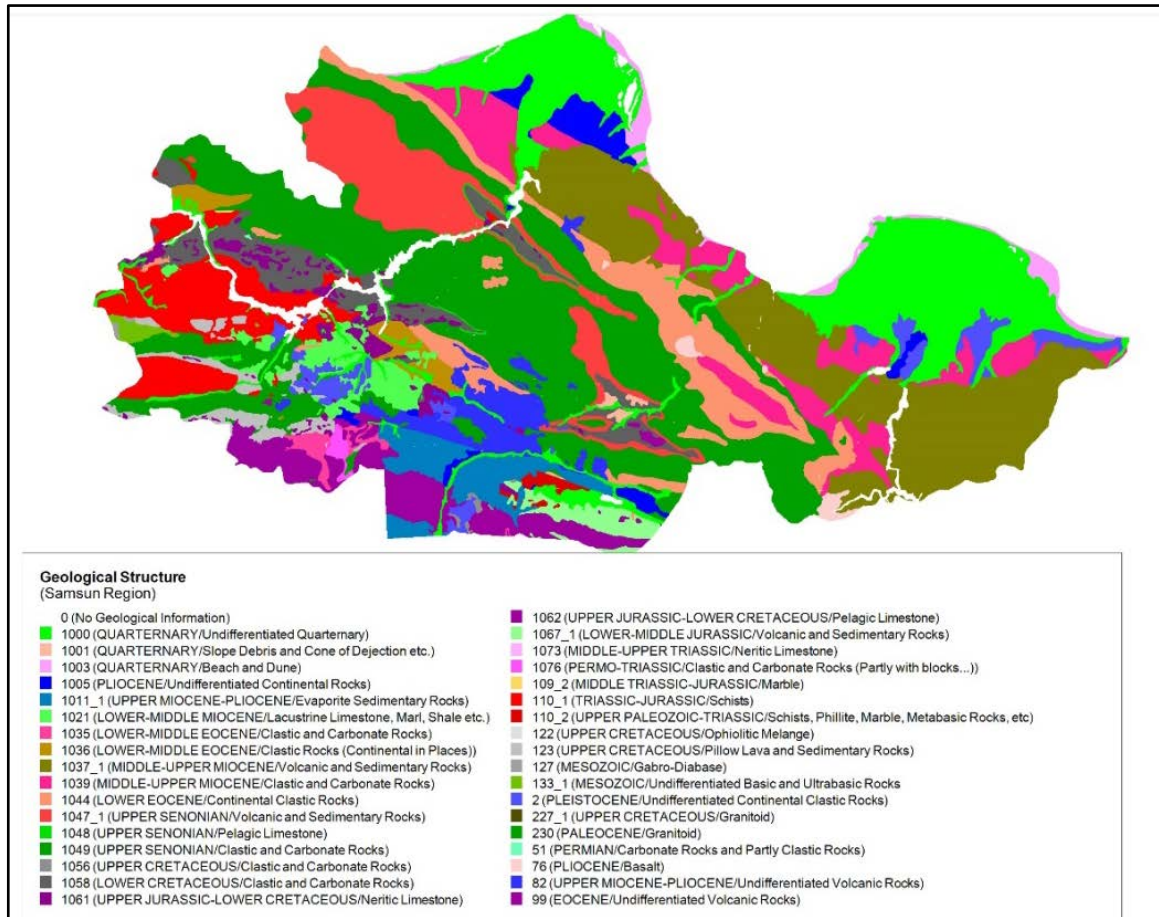


Fig. 129 Samsun province geological map

Tekkekoy formation is the oldest volcanic formation of the region, which consists of sandstone, marl, tuff inter-bedding, basalt and agglomerates. Samsun formation consists of grey-blue marls and is

mainly marine originated. The age of the Ilyas member lasts to Upper Miocene to Lower Pliocene. The Karasamsun unit consists of sandstone, siltstone and marl with lenses, in places mid-tight attached and also well-cemented conglomerates. Old alluvium unit consists of silt and irregularly composed sand of marine shells in the coastal plains of Atakum, and sand, gravel and silt along the Kürtün River. And finally, the Flood-plain sediment consists of gravel along the Mert River and very fine tiny sand and silts. Its thickness ranges between 10 to 20m (Akinci et. al. 2011^[2]).

The geological properties of the shallow layers of the studied area have been extracted from the revealed geological maps of the General Directorate of Mineral Research and Exploration (Scale: 1/500000) and the geotechnical reports and studies done at the region during different projects (Sari E., 2008; Gedik et al., 1984 and Gedik et al., 1984). The estimated parameters have been compared to the USGS boundaries defined for permeabilities of different types of soils. The slope map of the Tekirdag region is presented in Fig. 130.

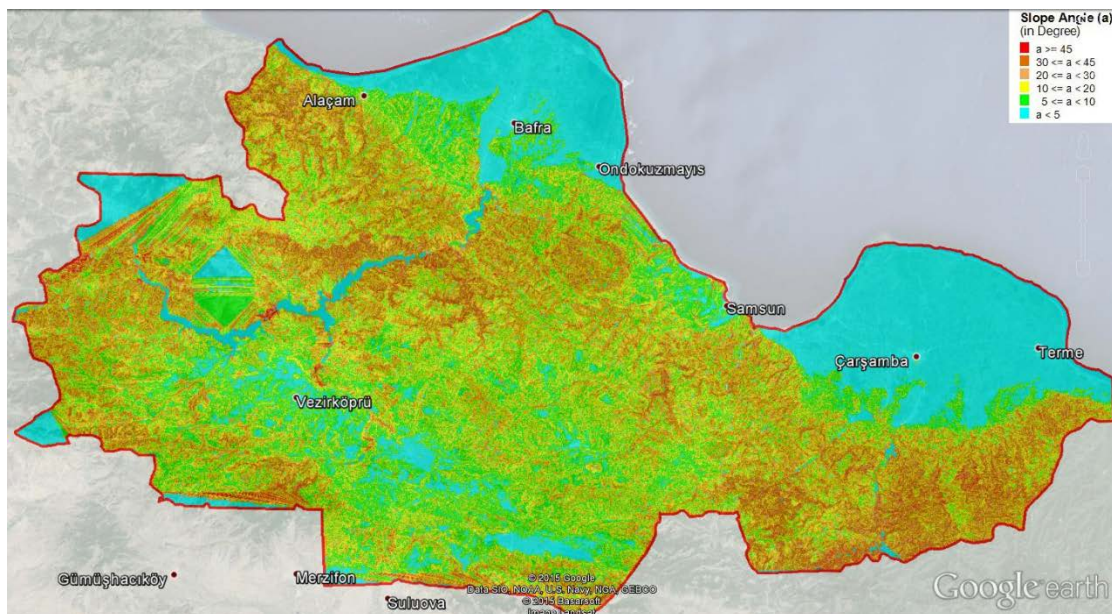


Fig. 130 The slope map of the Samsun region

9.2 Results of the microzonation of Samsun for rainfall induced landslide

The microzonation of Samsun region for rainfall induced landslide has been conducted based on Montgomery and Dietrich (1994), Mora and Vahrson (1994), FEMA method (1999) and Siyahi and Ansal (1993). At Fig. 131 the microzonation of the Samsun with respect to factor of safety by Montgomery and Dietrich (1994) are presented. The estimated factor of safety has been presented in 3 levels. The cells with FOS less than 1 have been colored by red which means that failure is likely to be occurred under the rainfall with exceedance probability of %1 within 1 year (return period of 100 years). The cells with yellow color represent the factor of safety range between 1 and 1.5, which is considered as the parts that are on the verge of failure under the assumed hazard level. The cells with FOS more than 1.5 are considered as safe area, and have been colored by green. It is seen that there is abound of likely failed region extending from North-West to South-East of Samsun province. With respect to slope map, this region corresponds to the areas with slope angles generally greater than 30°. Also, a region with FOS less than 1 can be identified at the West part of the Samsun. The other parts of the studied region, especially coastal parts, have mainly been estimated as safe with respect to Montgomery and Dietrich (1994).

The microzonation of the Samsun by Mora and Vahrson (1994) has been presented at Fig. 132. The obtained highest level of hazard is Medium (IV) with respect to the hazard index classification of the method. While Samsun province is generally dominated by the moderate hazard level index, the areas with medium hazard index (yellow color) have been scattered at the parts of the east and to some extent at the south-west of the region. As was seen in the previous methods, the coastal parts have got negligible hazard level. Regarding the low level hazard index, although the concentration of these area is mainly seen at the south-west of the region, the scattered distribution of this hazard level can be traced at the whole parts of region except the west.

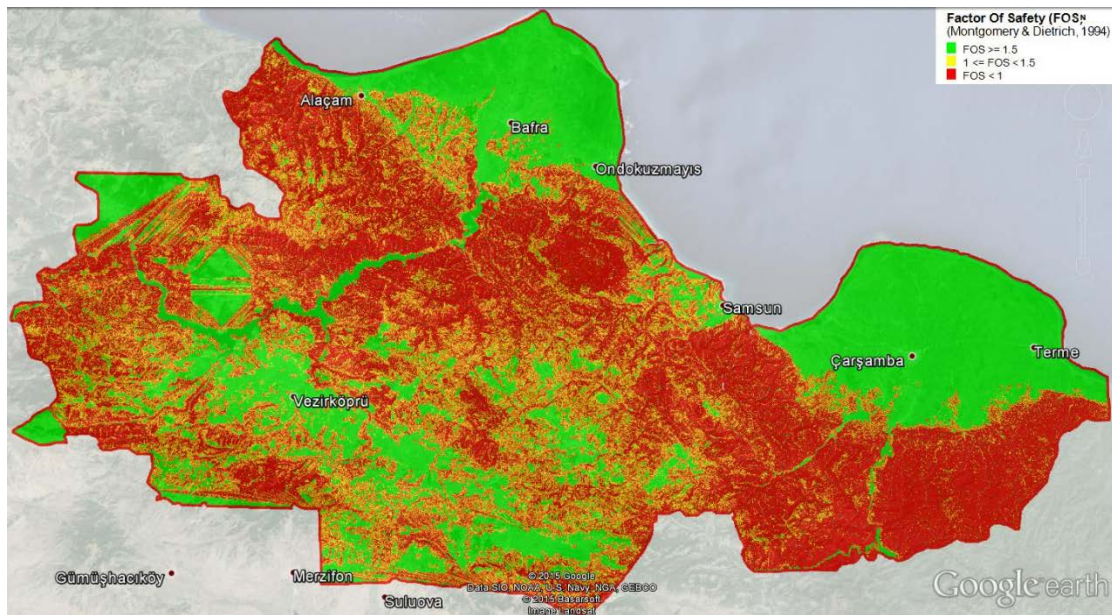


Fig. 131 Microzonation of Samsun region by Montgomery and Dietrich (1994)

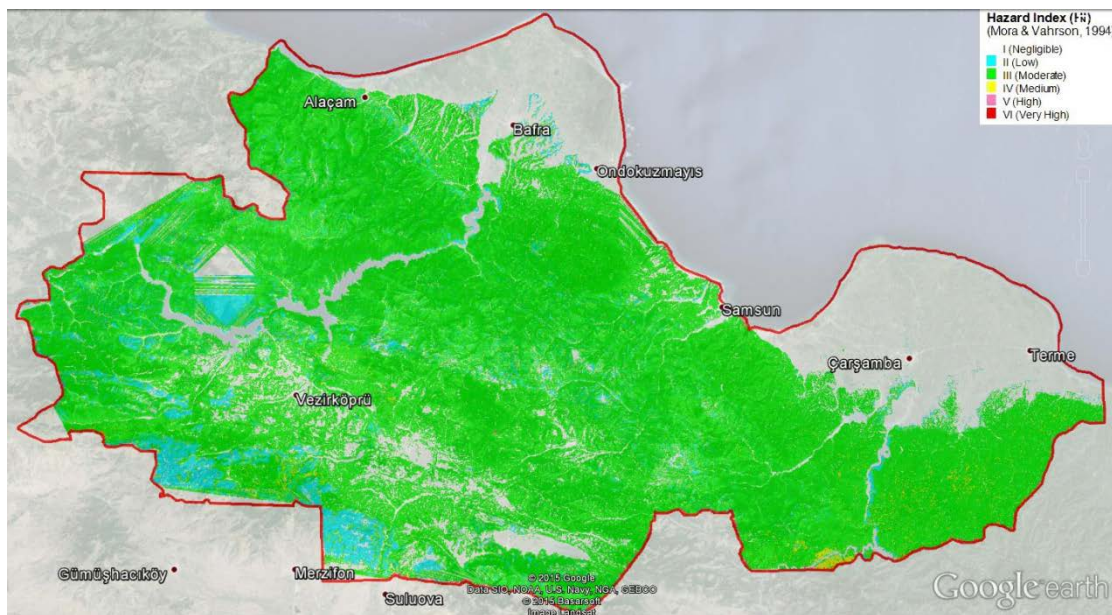


Fig. 132 Microzonation of Samsun region by Mora and Vahrson (1994)

Fig. 133 and fig. 134 present the results of the application of the FEMA method for Samsun region. Although fig. 133 shows the microzonation of the region under dry condition, because of the existence of a band of high slope angles, the region with high susceptibility, ranging from North-West

to South-East, has been detected. Except the limited regions at center and South-West of the Samsun, the other parts of the studied area have generally got susceptibility level of medium (V) and lower. Regarding the wet condition, fig. 134, a tangible increase in the susceptibility level is seen. Under the wet condition, the high susceptible narrow band seen at the dry condition has been widened so that it covers most of the central parts of the studied area. Although the susceptibility state of the coastal and South-West of the region have been promoted with respect to the dry condition, the susceptibility level of these parts are still in safe side.

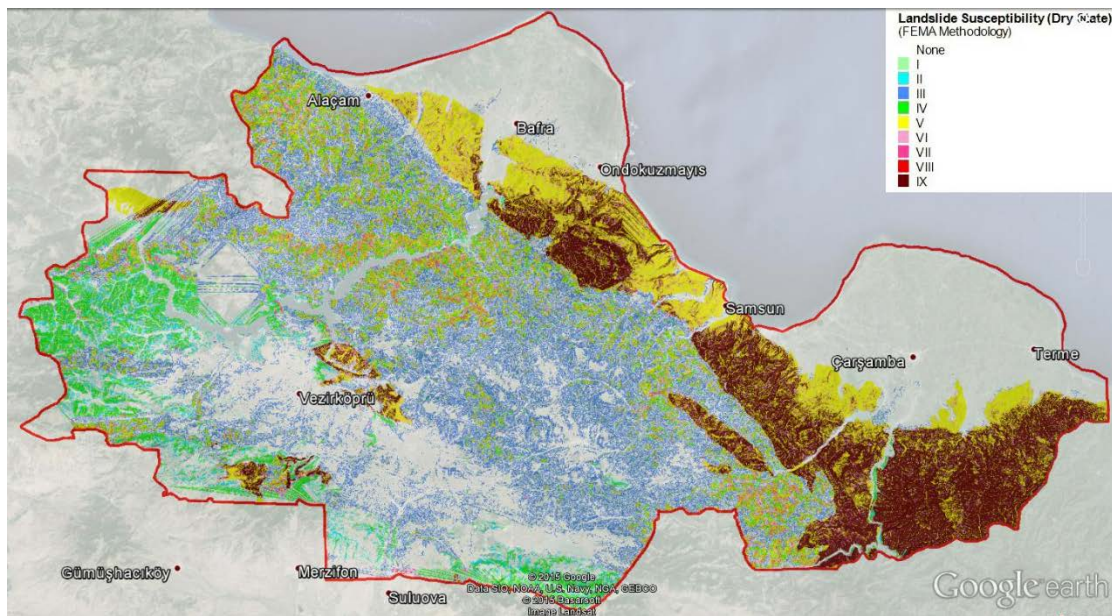


Fig. 133 Microzonation of Samsun region by FEMA method (Dry condition)

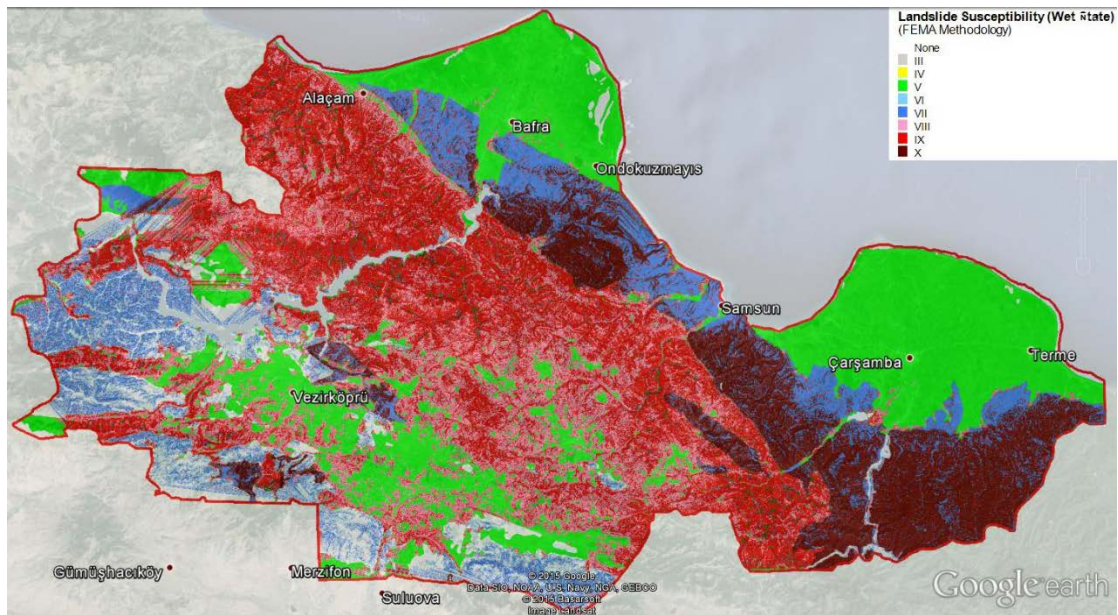


Fig. 134 Microzonation of Samsun region by FEMA method (Wet condition)

The microzonation of the Samsun region by Siyahi and Ansal (1993) has been presented at Fig. 135. Approximately more than two third of the Samsun area has been classified as safe area with respect to the method. The concentration of the regions on the verge of the failure are seen at the west, south and along a band begins from south-east and continues diagonally to the north. The areas with FOS less than 1 are mainly limited to the parts with high slope angles (greater than 30°).

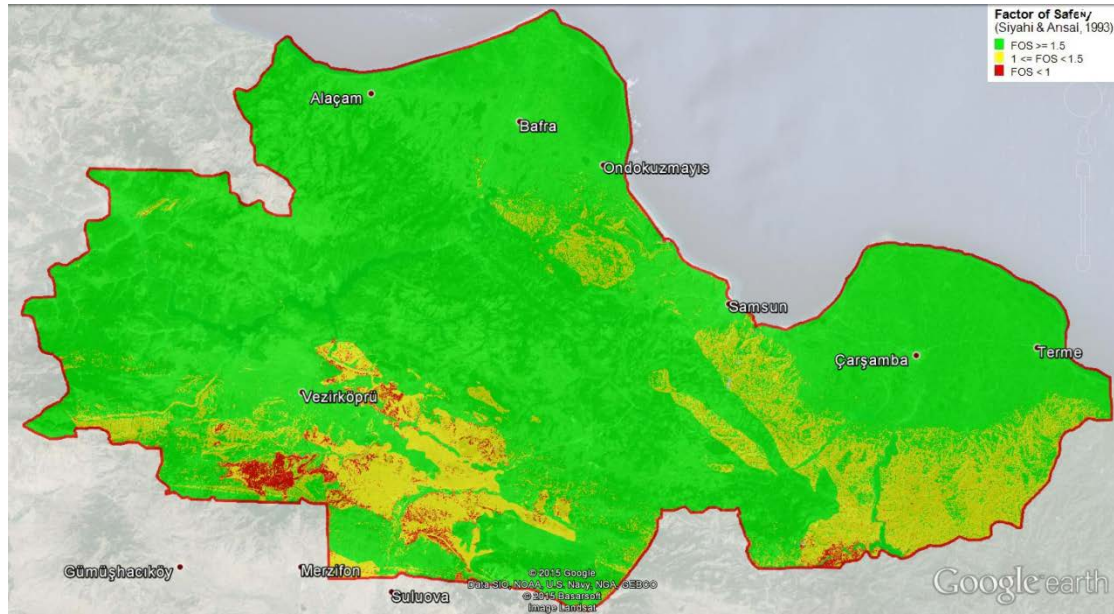


Fig. 135 Microzonation of the Samsun region by Siyahi and Ansal (1993)

10 CONCLUSIONS

Pilot studies for local and regional microzonation for rainfall and seismically induced landslide hazard are carried out for Tekirdag and Samsun city centers and provinces. The four methods adopted are Montgomery and Dietrich method (1994), Mora and Vahrson method (1994), FEMA method (1999) and Siyahi and Ansal (1994). In the case of regional and especially for local microzonation it became evident that the reliability and extent of the input geological and geotechnical data plays a very significant role. Thus in order for establishing realistic landslide hazard microzonation maps relatively comprehensive geological and geotechnical site investigations are necessary. It is also very important to have sufficient and detailed rainfall statistics for the region investigated as well as a comprehensive study concerning the regional seismic hazard for different hazard levels.

The results obtained from landslide hazard microzonation maps need to be considered to determine the priorities of the preventive measures that can be taken to prevent rainfall and seismically induced landslides to minimize the possible damages especially in residential areas. In addition in the case of rainfall induced landslide hazard microzonation, it appears possible to utilize the findings with respect to rainfall amount as an early warning method depending on the meteorological weather forecasts concerning the rainfall amount.

11 LANDSLIDE HAZARD ASSESSMENT ON A REGIONAL SCALE - PILOT IMPLEMENTATION IN BULGARIAN BLACK SEA COAST

The assessment of landslide susceptibility along the Bulgarian strip of Black Sea coast is made through the use of method of Mora and Vahrson (1994). Reasons for adoption of this approach are related to the severely complicated geological structure of the examined area and the resulting need for availability of a serious dataset of specific geotechnical properties corresponding to the various lithological units. There is a lapse of representative and authentic data of landslide activations for whole area and the available records are not enough for any estimation of statistical probability of occurrence (Wise et al., 2004).

Due to specific peculiarities of Bulgarian sea-side strip, we improved the method with adding to the original formula a new triggering factor related to **the abrasion and erosion activity** along the coast and rivers that has to be taken into consideration and it is marked as T_e . This factor is characteristic for Bulgaria and the coastal area. It is expressed as follows:

$$H = (S_r * S_l * S_h) * (T_s + T_p + T_e) \quad (28)$$

where:

S_r - slope factor, established by range of elevations per square unit area according to Mora and Vahrson (1994), layer is shown in Fig.136

S_l - lithology factor, shown in Table 9, layer is shown in Fig. 137

S_h - soil humidity factor, shown in Fig. 138

T_s —seismicity triggering factor, shown in Fig. 139

T_p —precipitation triggering factor, shown in Fig. 140

T_e —erosion/abrasion triggering factor, shown in Fig. 141

The slope factor is derived from free data obtained by NASA, 30m DEM. The classification is applied according to approach given by Mora and Vahrson (Table 9).

Table 9 Slope factor scores (Mora and Vahrson, 1994)

Slope value R_r , m/km ²	S_r
0 – 75	0
76 – 175	1
176 – 300	2
301 – 500	3
501 – 800	4
>800	5

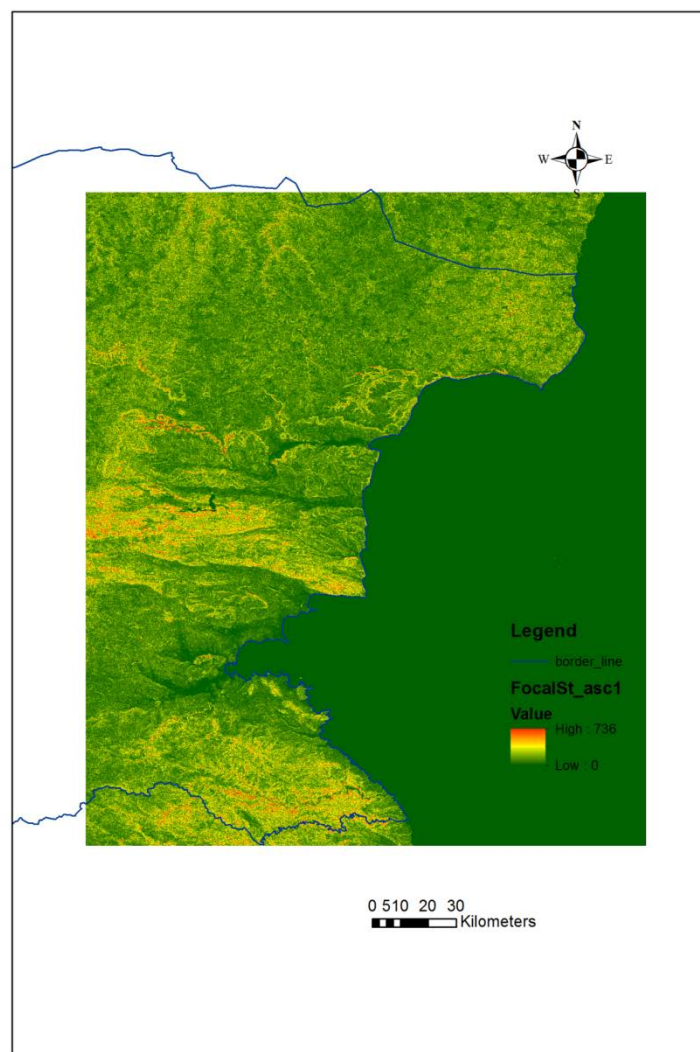


Fig. 136 Map of Black Sea coast according to slope factor S_r

The criteria applied for lithology factor are also closely to original approach. Geology of the sea side area is very complicated especially in the southern sector from Varna to Emine Cape, and also in Strandja Mts. Despite that, geological units can be qualified into 3 groups as it is shown in Table 10 and Fig. 137.

Table 10 Lithology factor criteria, classification and scores

Lithology	Qualification	S_l
All rocky formations: sedimentary, volcanic, etc. (Neogene, Paleogene, Cretaceous etc.)	Moderate	
Altered sediments, as flysch of Paleogene and Cretaceous age. Weathered rocks and loess. Availability of shallow water tables	High	
Diluvia, alluvial and clay formations of Quaternary and Neogene age	Very high	

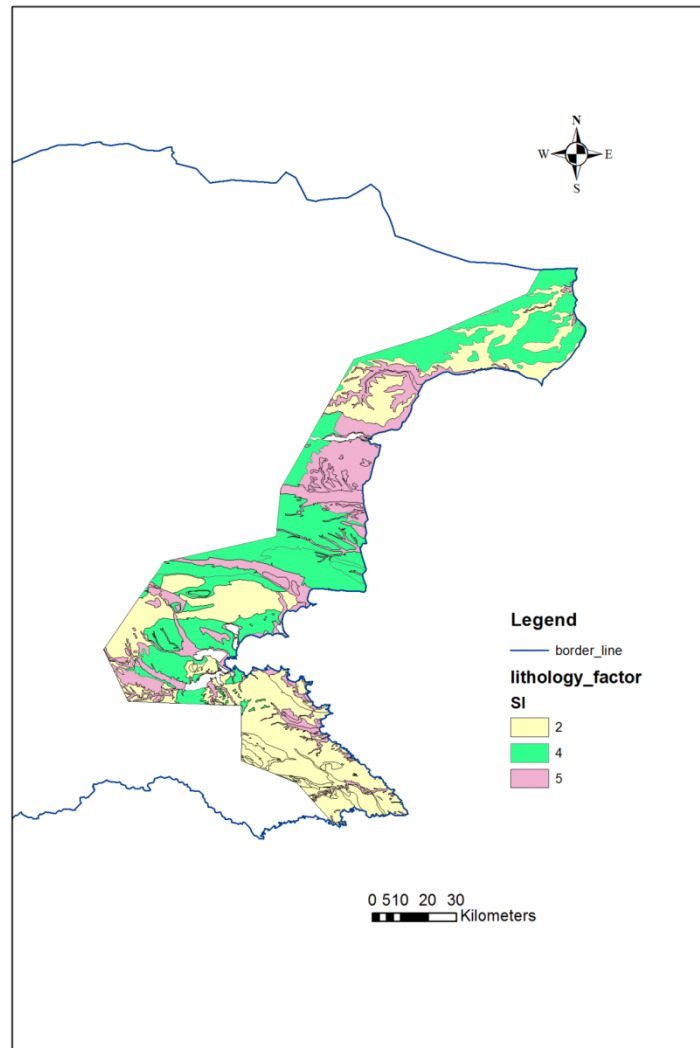


Fig. 137 Map of Black Sea coast according to lithological factor S_l

The soil humidity factor is taken from data published by Koleva and Peneva (1990) for 15 sites in Bulgaria. The range of raining time per 24 hours varies between 1 and 3 hours for territory of Bulgaria. For Black Sea coast area the range is mostly from 1 to 1.5 hours, but in southern part of Burgas region the values are less than 1 hour, namely Strandja Mts area (Fig 138). The data for precipitation are taken from the same source as well and are presented in Fig. 139. The most intense area is close to Varna City, and the most dry areas are in Dobroudja plateau northern to Balchiktown and in Burgas area.

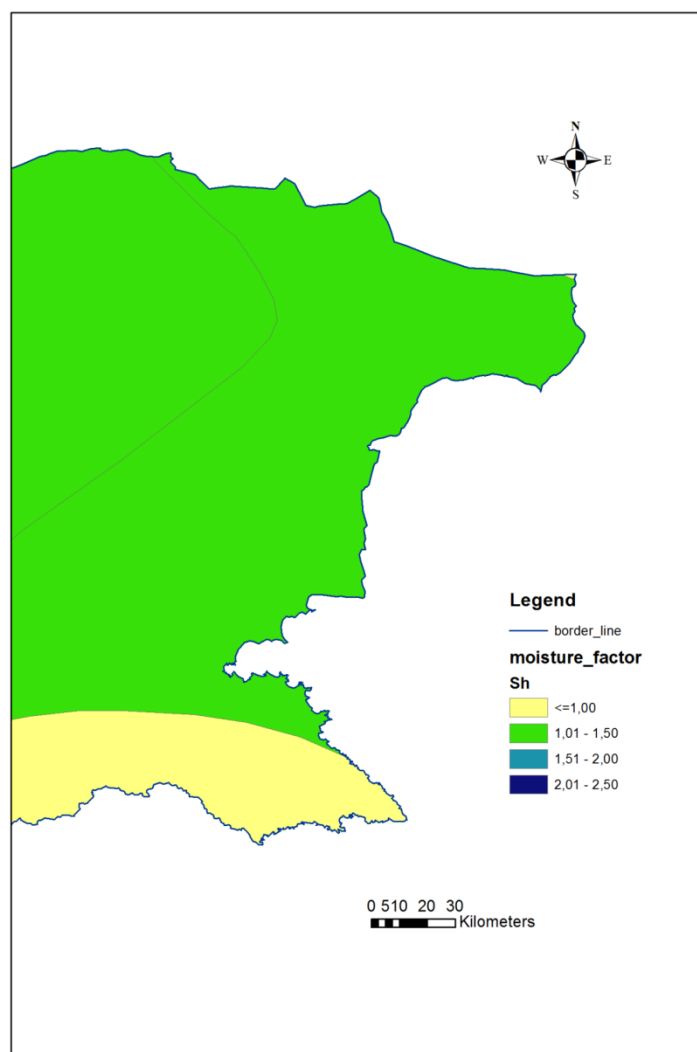


Fig. 138 Map of Black Sea coast according to moisture (humidity) factor S_h

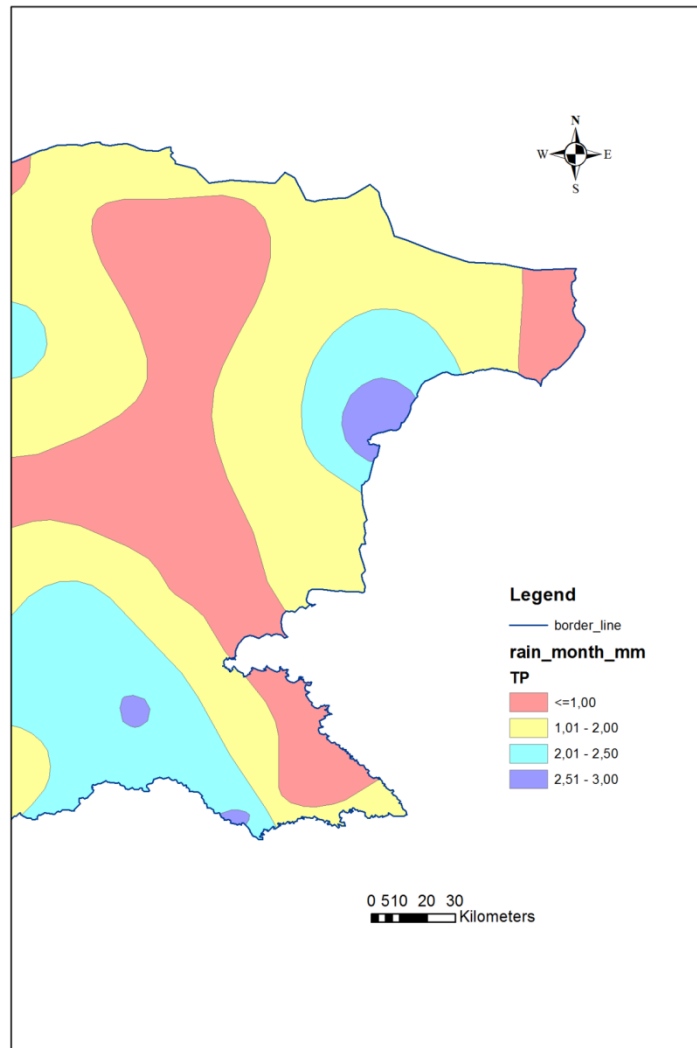


Fig. 139 Map of Black Sea coast according to precipitation triggering factor T_p

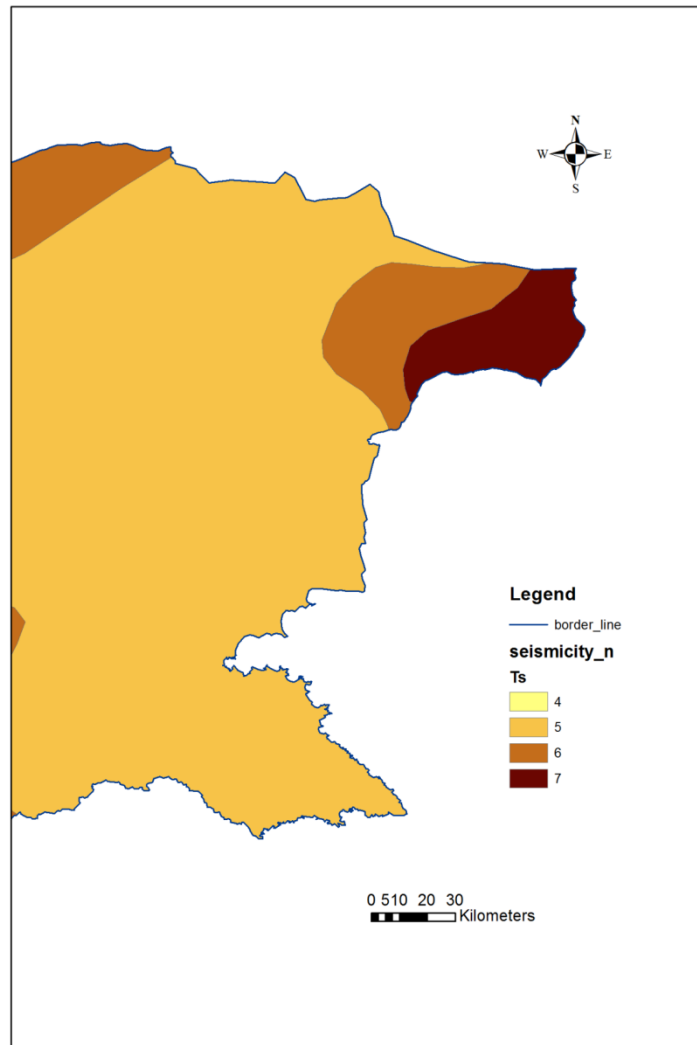


Fig. 140 Map of Black Sea coast according to seismicity triggering factor T_s

Seismicity triggering factor T_s varies on the territory of Bulgaria from 4 (VI degree) to 7 (IX degree). The data for seismicity have been taken from *Codes for design of buildings and facilities in earthquake regions* (1987) which are referred for 1000 year period. For example, the Burgas region has $T_s=5$, but Shabla-Kaliakra will have $T_s=7$ (Fig. 140). The most dangerous is the Shabla earthquake source zone, which is situated into Black Sea and parallel to the shoreline. The most impressive earthquake was recorded on 31 March 1901 with magnitude 7.2.

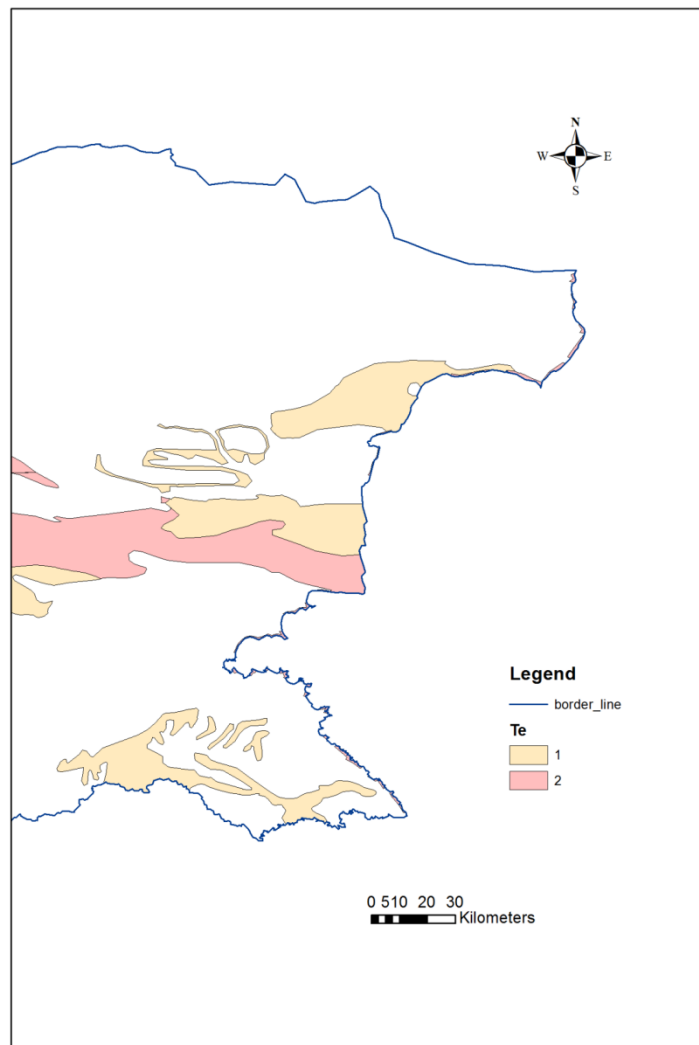


Fig. 141 Map of Black sea coast according to erosion/abrasion triggering factor T_e

Data about erosion (sheet and linear) and abrasion were taken from Map of geological hazards in Bulgaria: for erosion (Iliev-Bruchev, ed., 1994) and for abrasion (Shuiskij and Simeonova, 1976; Simeonova, 1989). We propose to add the following scores for erosion and abrasion triggering factor (Table 11):

Table 11 Classification of landslide hazard H

Description of sea-side strip and cliff	Erosion and abrasion factor T_e
Accumulation zone	0
Rocky cliff, with abrasion and erosion processes	1
Soft soils cliff, with abrasion and erosion processes	2

11.1 Susceptibility mapping

The compiled map using equation 30 is shown in Fig. 142. Six degrees are proposed for final classification, given in Table 12. The maximum class is IV – medium in accordance with the original classification proposed by Mora and Vahrson (1994). These levels correspond with real situation of landslide activity in Bulgarian Black Sea coast area. Due to this reason we could accept scores >162 (i.e. medium level according to the original method) as corresponding to high hazard level for a local use. The original method of Mora and Vahrson used a grid of area of 1 sq. km in the hazard assessment, as well as the first researchers applied this method (Berov 1996, Berov, Frangov, 1997). However in recent years, the accuracy for assessment of hazard degrees become more detailed (Salazar, 2007; Solano et al., 2013, and others). Many researchers apply statistical methods in interpolation of the data to determine the degree of hazard. Because of the terrain features (very rugged) and complicated geology, we also decided to use this approach in order to get a more representative map, and for this reason we used a more detailed net corresponding for used 30 m DEM, as well as additional subdivisions of some factors as T_p and S_h .

Table 12 Classification of landslide hazard H

H	Class	Classification of hazard of landslide potential
<6	I	Negligible
7-32	II	Low
33-162	III	Moderate
163-512	IV	Medium
513-1250	V	High
>1250	VI	Very high

11.2 Pilot area map

A pilot study was applied for an area in Southern Bulgarian Black sea coast in scale 1:25,000 (Fig. 143). This area around Tsarevo town is quite characteristic for the landslide hazard, since we have manifestation of many landslides along the coastal zone and banks of some rivers and gullies. The geology setting is composed by Miocene deposits of Galata Formation (gN_1^{t-k}) and Upper Cretaceous volcanic rocks (drK_2). The vast majority of landslides are formed in Miocene deposits having layers of fat clays dipped to sea direction. The relief is rather gentle. The western part of the examined area has low mountain character, but is built up of volcanic rocks and landslides rarely occur there. Landslides at Tsarevo area are shallow, of rotational type, with slip surfaces formed into fat clay layers. Final susceptibility map consists predominantly of 2 classes – low and moderate. Current landslide phenomena are distributed mainly in moderate level area. However, a group of landslides mapped from our team at northern part of Tsarevo are located outside the moderate level area. This is obviously connected with a wider distribution of Miocene sediments in North direction, which is not accounted in the geological literature used by us in the present study.

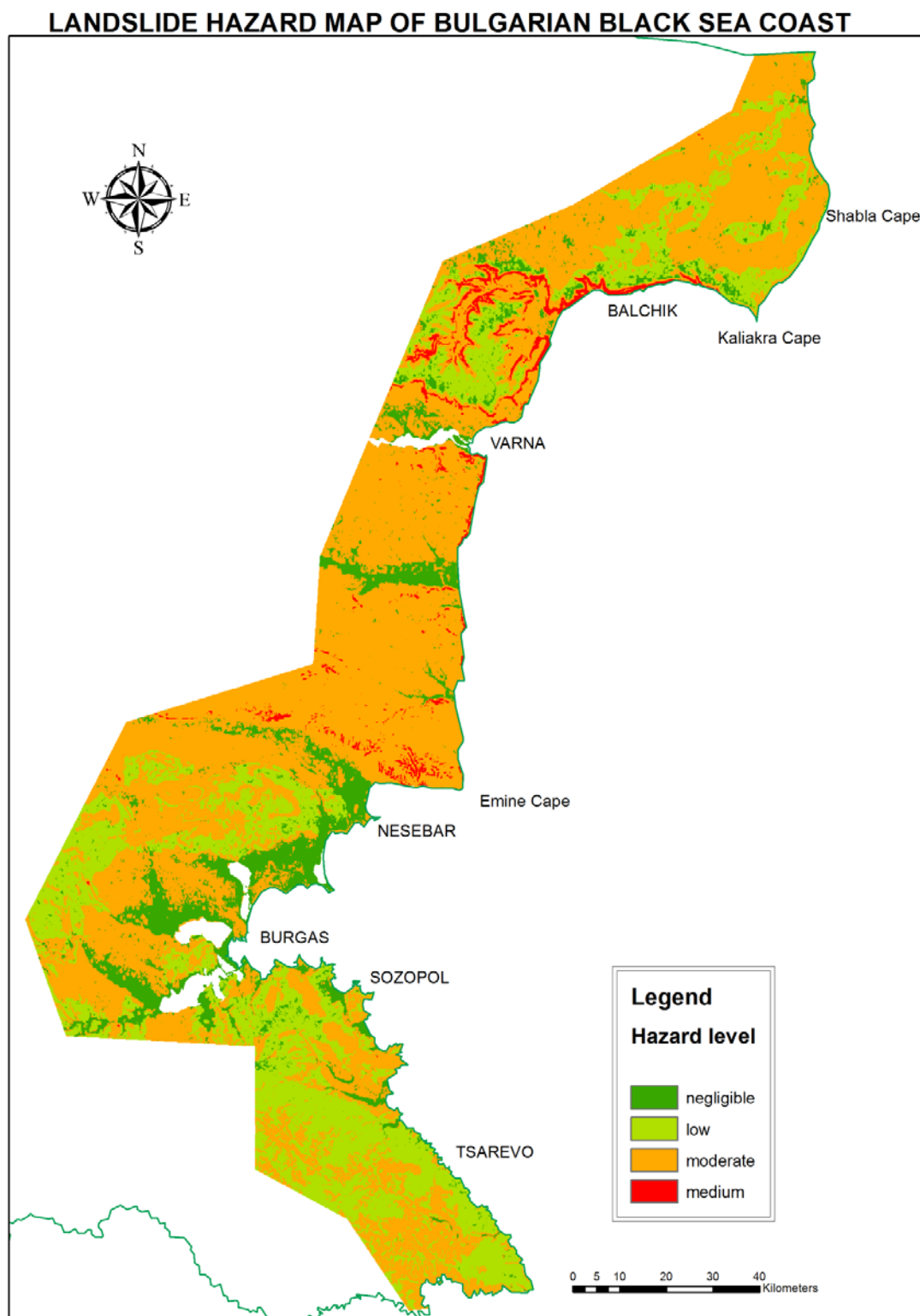


Fig.142 Landslide susceptibility map of the Bulgarian Black Sea coast according to the method of Mora and Vahrson (1993)

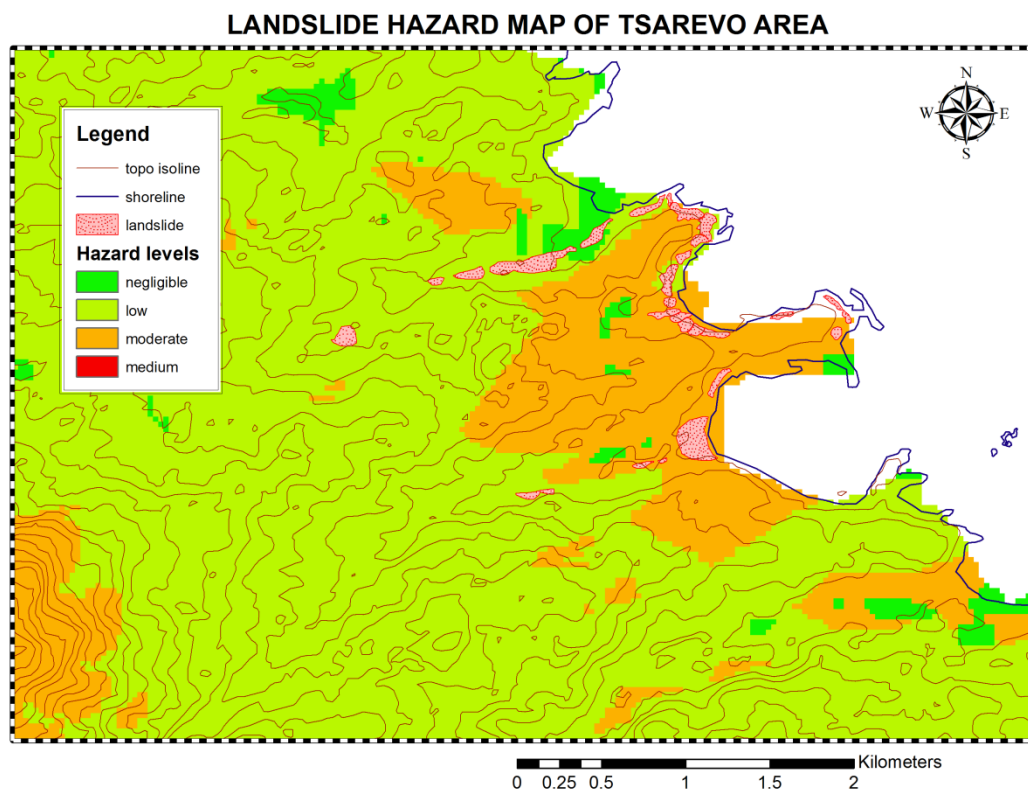


Fig. 143 Landslide susceptibility map of Tsarevo area and Bulgarian Black Sea coast, according to the method of Mora and Vahrson (1994)

12 LANDSLIDE HAZARD ASSESSMENT ON A REGIONAL SCALE - PILOT IMPLEMENTATIONS IN ROMANIA

12.1 Definition of the problem

Landslide, is defined as the movement of a mass of rock, debris or earth down a slope (Cruden, 1991); it is a local phenomenon controlled by different internal / external factors like topographic, geological, climate conditions, etc. Land use activities can contribute to the occurrence of landslide.

Earl E. Brabb, the pioneer in landslide mapping, in his publication entitled: “The World Landslide Problem” (1991) wrote: “[...] *Landsliding is a worldwide problem that probably results in thousands of deaths and tens of billions of dollars of damage each year. Much of this loss would be avoidable if the problems were recognized early, but less than one percent of the world has landslide-inventory maps that show where landslides have been a problem in the past, and even smaller areas have landslide susceptibility maps that show the severity of landslide problems in terms decision makers understand. Landslides are generally more manageable and predictable than earthquakes, volcanic eruptions, and some storms, but only a few countries have taken advantage of this knowledge to reduce landslide hazards.*”

Despite all the efforts the situation concerning the landslide cartography has not changed significantly.

Firstly, a controversy exists between the terms landslide “susceptibility” and landslide “hazard”. Landslide susceptibility is the likelihood of a landslide occurring in an area on the basis of local terrain conditions. (Brabb, 1984). Landslide susceptibility maps describe the relative likelihood of future landslide based solely on the intrinsic properties of a silt (USGS). Landslide hazard maps indicate the possibility of landslides occurring throughout a given area (USGS) or landslide hazard is the probability that a landslide of a given magnitude will occur in a given period and in a given area.

Different authors: Aleotti and Chowdhury, (1999), Carrara and Pike (2008), Carrara et al. (1991; 1995), Fell et al., (2008), Guzzetti et al. (2006), Hutchinson (1986; 1995), Soeters and van Westen (1996), VanWesten (2000; 2015), VanWesten et al., (2003; 2008), Varnes (1984), as well as, the Committee on the Review of the National Landslide Hazards Mitigation Strategy (2004), propose five categories of methods which can be schematized in Fig. 144: (i) direct geomorphologic mapping, (ii)

analysis of landslide inventories, (iii) heuristic or index based methods, (iv) statistical methods, including neural networks and expert systems, and (v) process based, conceptual models

The direct methods consist in the identification of landslide from aerial photographs or from satellite images.

The analysis of landslide inventories attempts to predict future patterns of instability directly from the past distribution of landslide deposits.

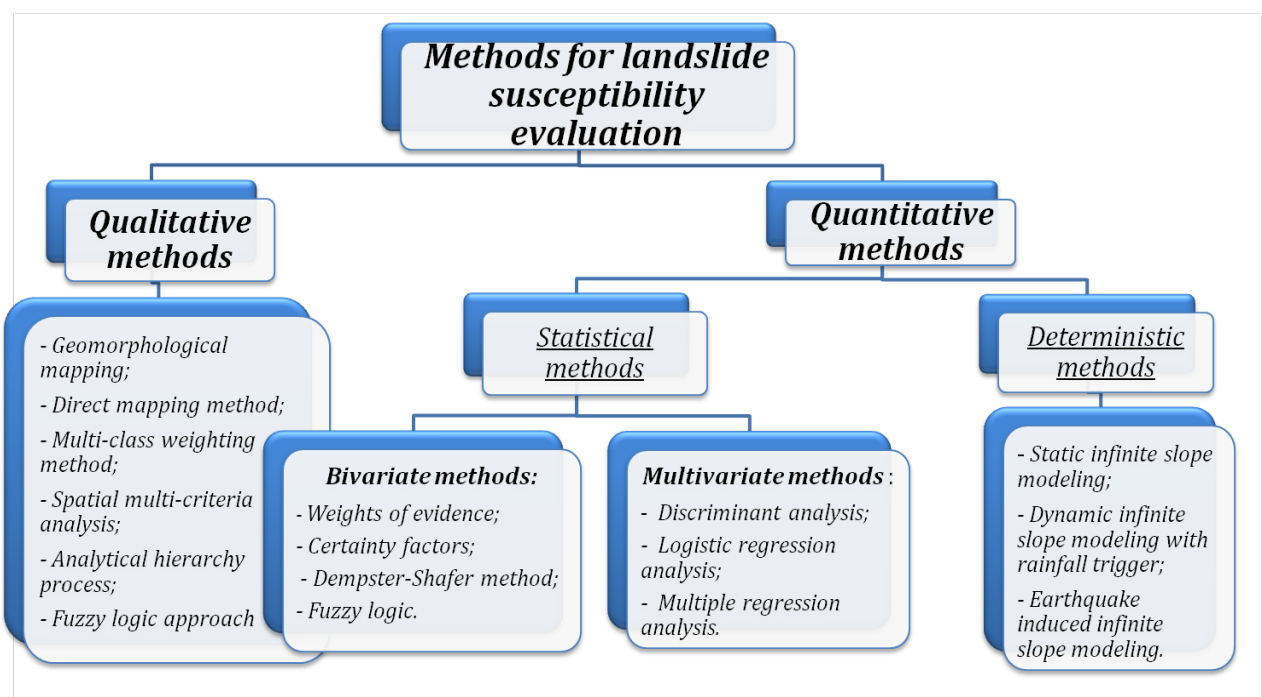


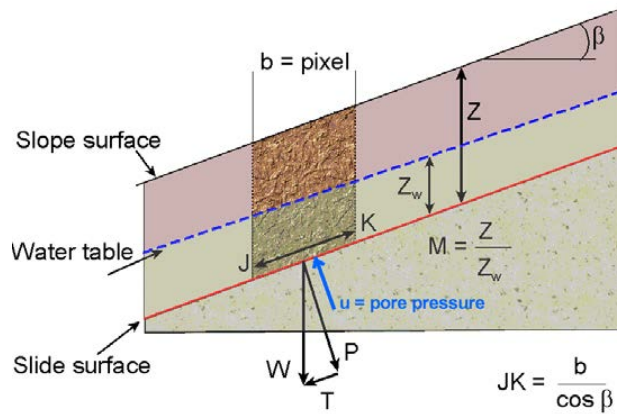
Fig. 144 Flow chart of methods for landslide susceptibility evaluation

The statistical methods consist into find a relationship between instability factors and the past and present distribution of slope failures (Carrara, 1991).

The deterministic methods are process based models. In fact those methods use physical laws controlling slope instability. Due to lack of information or poor understanding of the physical laws controlling landslide initiation and development, only simplified, “conceptual” models are considered. These models calculate the stability of a slope using parameters such as normal stress, angle of internal friction, cohesion, etc. As results we obtain an index named safety factor expressing the ratio between the local stabilizing and driving forces. When applied over large areas, local

stability conditions are generally evaluated by means of a static stability model, such as the well known “infinite slope model”, where the local equilibrium along a potential slip surface is considered.

The most common equation used by this model under static condition, are the following:



$$F_s = \frac{c' + (\gamma_{app} - m * \gamma_w) * z * \cos^2 \beta * \tan \phi'}{\gamma_{app} * z * \sin \beta * \cos \beta} \quad (29)$$

where:

ϕ' : effective angle of friction of geomaterial ($^\circ$)

c' : effective cohesion of geomaterial (kPa),

γ_{app} : specific weight (kN/m^3),

β : slope angle (deg),

γ_w : specific weight of the water (kN/m^3),

z : normal thickness of the failure slab (m)

m : percentage of the water saturated failure slab (%)

In dry conditions: $m=0\%$, then $\gamma_{app} = \gamma$

In saturated conditions: $m=100\%$, then $\gamma_{app} = \gamma_{sat}$

In wet conditions ($0 \leq m \leq 100\%$): $\gamma_{app} = \gamma * (1-m) + \gamma_{sat} * m$

The above one dimensional (1D) model describes the stability of slopes with an infinitely large failure plane. It can be used in a GIS, as the calculation can be done on a pixel basis. The pixels in the parameter maps can be considered as homogeneous units. The effect of the neighboring pixels is not considered, and the model can be used to calculate the stability of each individual pixel, resulting in a hazard map of safety factors. The infinite slope model can be used on profiles as well as on pixels. The entire analysis requires first the preparation of the data base.

To apply this model at a regional scale the necessary data are the following:

1. Geological maps of relevant scale (lithology per geologic group)
2. Topographic maps of relevant scale to define slope angle (β)

Some geotechnical parameters per geological formation must be estimated / calculated (ϕ' , c' , γ).

12.2 Loess distribution

Loess and loess-like sediments cover 10% of Earth's land surfaces. Geographically, loess is extensive in the North American Great Plains, south-central Europe, central Asia, and central East of South America. In Europe, loess and loess-like sediments cover almost 1/5 of its total land surface are common in areas that extend between the former Alpine and the Scandinavian ice sheets and in regions to the east, associated with major river systems (Fig.145).



Fig 145 Loess distribution in Europe. Loess distribution is related to the former extent of ice sheets and the

distribution of major river systems (Smalley et al., 2009)

Loessoid soils are very common in Romania, mainly in Romania Plain, Dobrogea County and Moldavia County (Figure 3).

The common feature of the three units of Dobrogea is the vast Quaternary cover, starting with Lower Pleistocene reddish clays and continuing up to Holocene with a sequence of various thicknesses (2-20 m) enclosing up to 6 couples of loess - paleosoil layers.

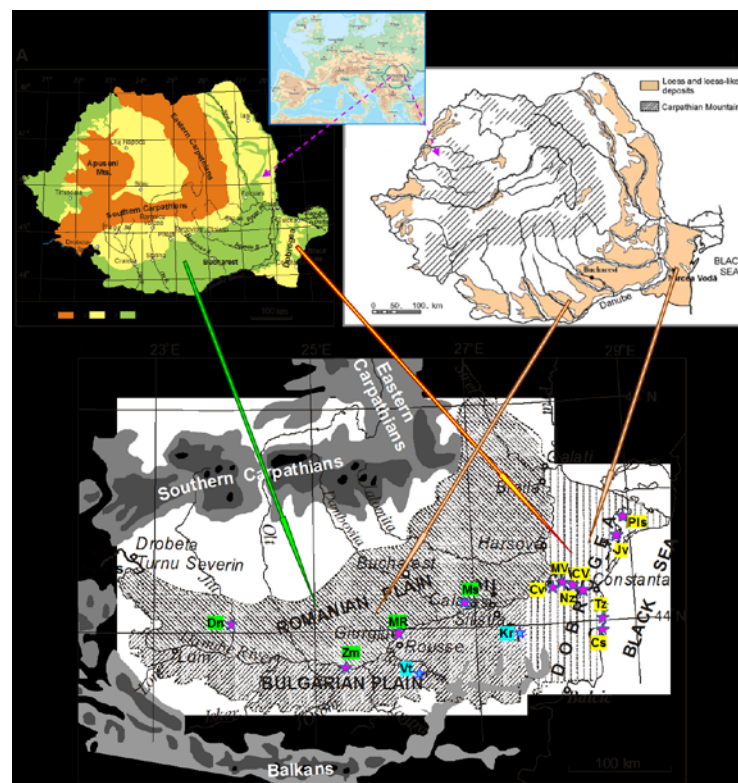


Fig. 146 Location of the most important loess - palaeosoil sections in the Romanian Plain and Dobrogea (Romania)

The types of loss and loss-like deposits function of grain-size are presented in figure 147.

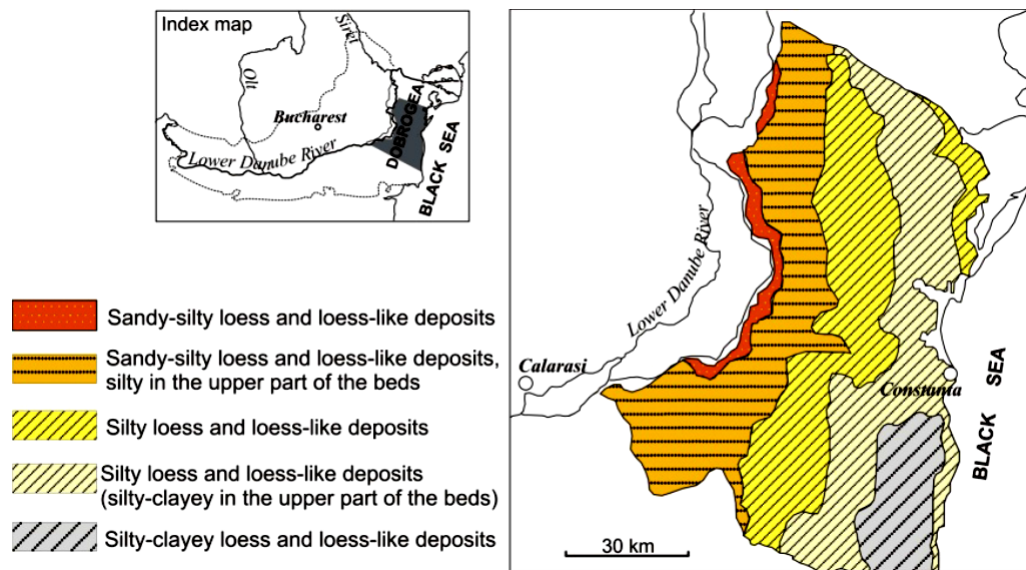


Fig. 147 Grain-size types of loess deposits representing the parental source of the modern soil in Dobrogea.
 From Conea (1970b)

In many studies published in the scientific literature there have been made no differences between loess and loess-like deposits, but there were often used the both terms for deposits with different textures.

The loess:

- is unconsolidated, yellow, unstratified and uniform rock;
- has silty texture (with prevailing dimensions ranging from 0,05 to 0,01mm), and without coarse particles;
- has high porosity (40-50%);
- has very low or without plasticity;
- has carbonates equally dispersed in rock and precipitates as limes concretions;
- favors subsidence and is easily erodable.

The loess-like deposits:

- are unconsolidated rocks, with different colors, sometimes with stratification and varying uniformity;

- present differentiated mechanical composition (clay, sand, silt), with coarse sand and / or gravel;
- have varying porosity, generally low;
- present varying plasticity, depending on mechanical composition;
- carbonates are dispersed;
- they can be quickly and radically transformed by secondary processes.

Loess has more than 60% particles between 0,01 and 0,1mm and loess-like deposits have less than 60% of those particles.

The textural analyses made for loess and loess-like deposits from main regions of the country stated that loess from Romania is similar, as far as mechanical composition is concerned, with that from Eastern and Central Europe (Gherghina, Grecu, Cotet, 2006).

Minimum and maximum values of **geotechnical parameters of loess** in natural state in Dobrogea region are presented in Table 13.

Table 13 Geotechnical parameters of loess

Param	Clay %	Silt %	Sand %	W_L %	W_p %	w %	n %	S_r	M_{2-3} kPa	i_{m3} cm/m	ϕ' (degree)	c' kPa
Min	14	50	3	32	12	7.8	46	0.4	1870	0.6	5	5
Max	29	80	18	40	17	28.5	54	1	10700	15	30	48

Legend of symbols used in Table 13

W_L liquid limit (lower limit of plasticity)

W_p limit of plasticity (upper limit of plasticity)

w moisture

n porosity

S_r degree of saturation

ϕ' internal friction angle

c' cohesion

M_{2-3} oedometric modulus in the pressure range 200-300 kPa

i_{m3} specific settlement index

12.3 Study case

Dobrogea region is situated between lower Danube and the Black Sea (Figure 148). The territory of the Romanian region Dobrogea is organized as the counties of Constanța and Tulcea, with a combined area of 15,500 km².

From the geo-morphological point of view, Dobrogea contains four morpho - structural units: the Danube alluvial and deltaic plain, the mountainous – hilly Hercynian-Kimeric unit of the Northern Dobrudja, the green schist Casimcea plateau or the Central Dobrudja, the plateau with Sarmatian structure or the Southern Dobrudja.

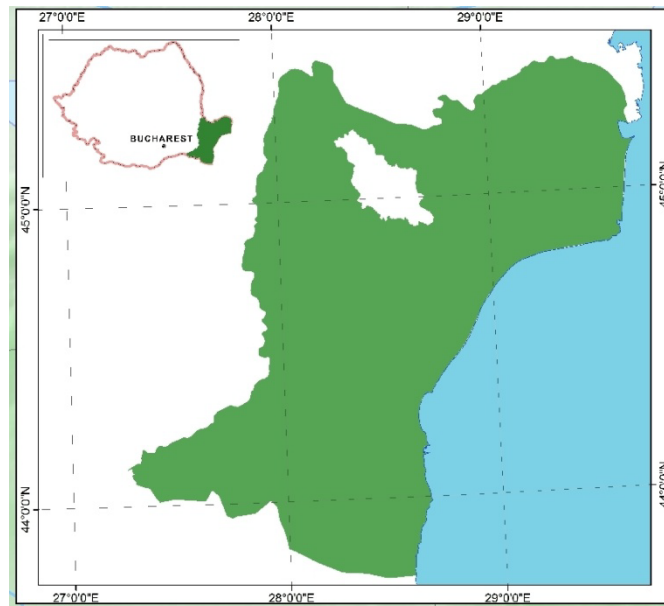


Fig. 148 The Dobrogea region

Dobrogea's climate is temperate - continental and is divided in 2 units (Paltineanu Cr., 2000): (I) the Eastern units which contains the Danube Delta, its south, two lagoons (Razim lake and Sinoe lake); whose extension varies from 20 to 50km to the littoral, depending on the warm/ cold season; II (II) The Western units, which contain the rest of territory where thermal inversion regime is emphasized only on the low lands and where the climate is temperate continental.

From a geological point of view, this area includes three tectonic units – Northern, Central and Southern Dobrogea (figure 149). The tectonic units are separated by two major crustal faults, approximately oriented NW-SE: Peceneaga-Camena (between North and Central Dobrogea) and Capidava-Ovidiu (between Central and the Southern units).

We investigated only the Littoral Coast line from Constanța to 2 Mai village, which is about 50 km along the Black Sea coast, crossing the Danube – Black Sea Channel at Agigea and passing through several resorts – Eforie Nord, Eforie Sud, Techirghiol, Costinești and Mangalia (Figure 149 - left)).

The common feature of the three units of Dobrogea is the vast Quaternary cover, having various thicknesses of loess layers (figure 149 - right). There are in small percentage: green schist, limestone and reddish clay.

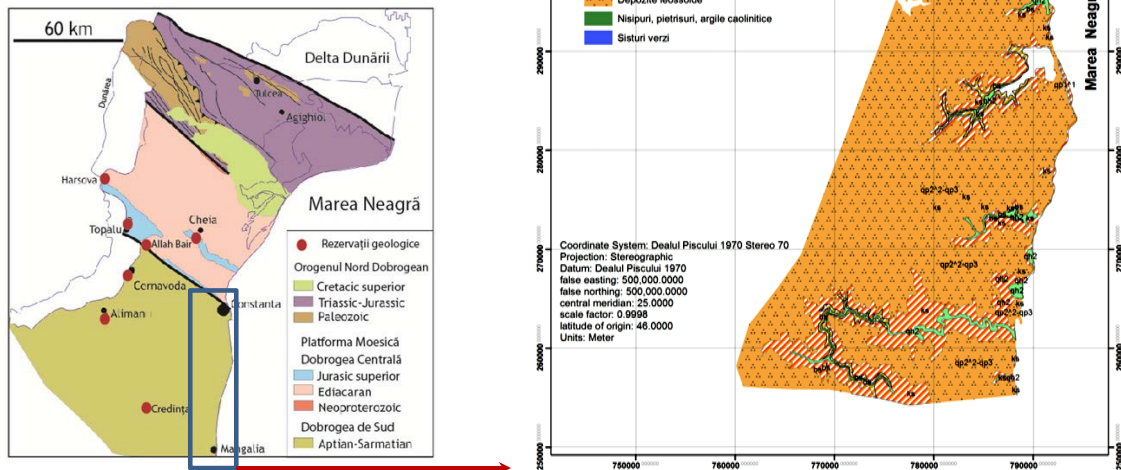


Fig. 149 Tectonic units

An ASTER DEM (resolution 30x30m) was used in order to generate the Digital Elevation Model which has been used for the processing that followed. Maximum elevation is 168.2 m.

12.4 Factor of safety method based on infinite slope model

In order to assess the LS factor of safety using infinite slope model under ArcView GIS, the methodology proposed is described in the following figure (figure 150): (i) derived slope from DEM (Figure 151); (ii) developed geology map and a raster for each geotechnical parameter described in table 14; (iii) applied formula (1) for $m=0$ and $m=100\%$ for different z .

All maps are presented in Stereo 70 projection.

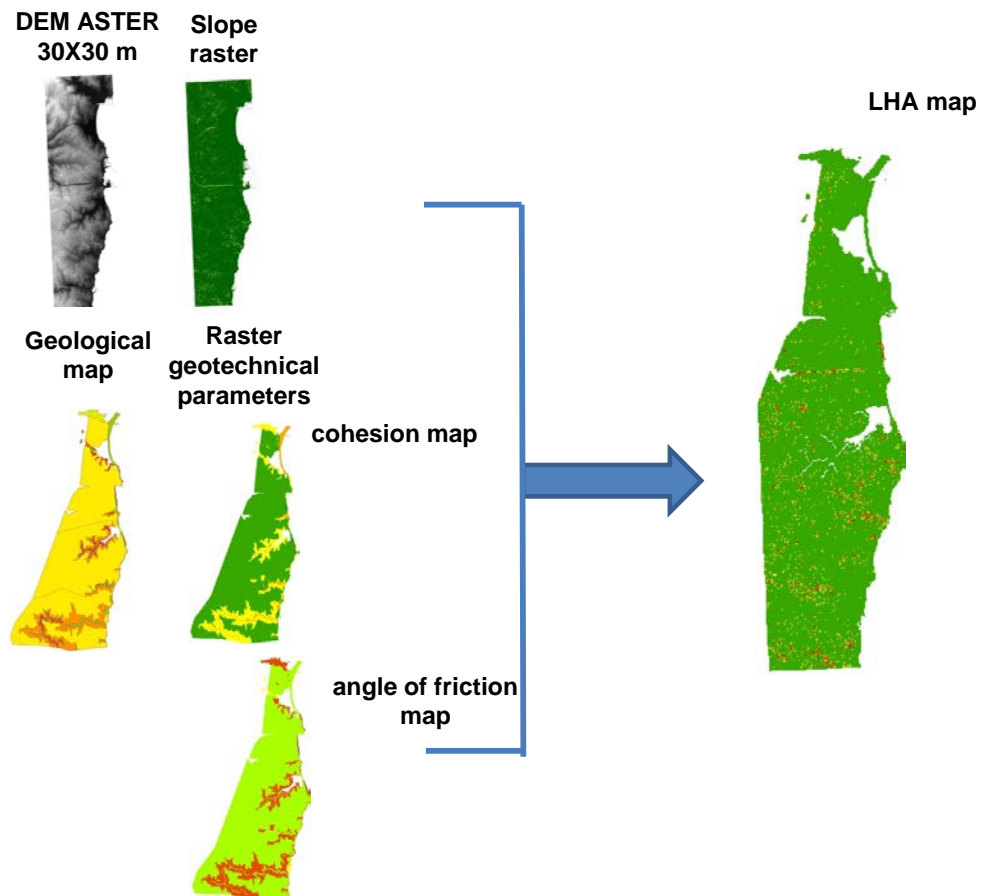


Fig. 150 Methodology to LHA map under ArcGis

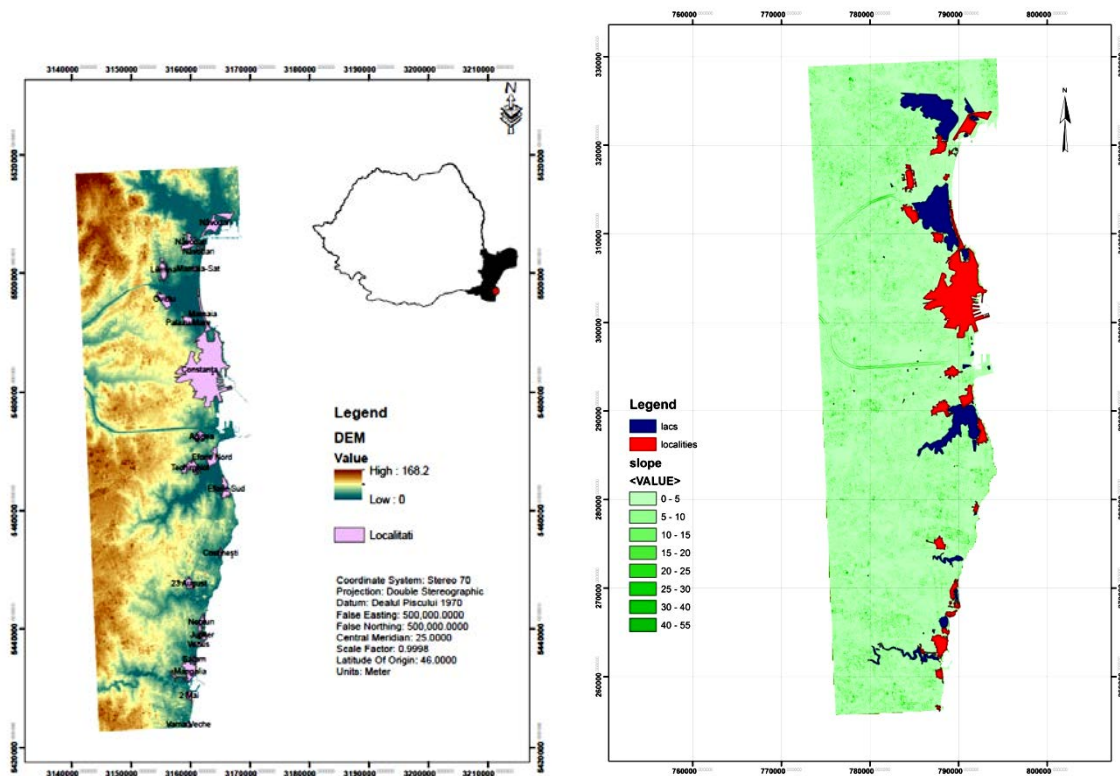


Fig. 151 DEM and slope map for the investigated area

The major part of the investigated area is flat (0-10 degree). The steeper slopes are on the coast line, on the Danube-Black Sea Canal and on the valey.

The geological map at 1:200,000 scale was digitized. The geotechnical parameters for every principal lithological group are presented in Table 14.

Geotechnical parameters are identified from various geotechnical studies conducted in Dobrogea region (Florea, 2010).

Table 14 Geotechnical parameters for the principal lithological groups

Id	Symbol	c'(kPa)	ϕ' (deg)	γ (kN/m ³)	γ_{sat} (kN/m ³)	Lithologic group
1	qh2	5.00	28.00	15.00	28.00	resedimented leoss, marine deposit
12	cp+ma	0.00	35.00	14.50	23.00	chalkstone with silex, limestone, marls
14	bs	0.00	35.00	17.50	26.50	limestone, clay, diatomit
16	qp1^1	23.00	19.70	20.37	27.20	Clay with gypsum
17	ks	0.00	35.00	17.50	26.50	limestone, oolitic limestone
48	qp2^2- qp3	16.00	31.00	15.64	20.08	Loess like deposit,
59	Pts	0.00	35.00	17.00	26.00	Green shiest
61	ox+km	0.00	29.00	15.00	25.50	dolomitic limestone, dolomite, clay
62	ap	0.00	31.00	17.00	21.50	Sand, gravel, caolinitic clay
65	br	0.00	28.00	17.50	26.50	Calcareous marl

For every geotechnical parameter a raster map was produced.

The final aim of large scale landslide hazard analysis is to create quantitative hazard maps. The hazard degree can be expressed by the Safety Factor, which is the ratio between the forces that make the slope fail and those that prevent the slope from failing. F-values larger than 1 indicate stable conditions, and F-values smaller than 1 unstable. At F=1 the slope is at the point of failure.

Using raster calculator we can build the F_s map for different z (thickness of the failure slab) and for different conditions (dry and wet). In this study we have calculated the safety factors for different scenarios where only rainfall is the triggering factor. We did not yet look at the influence of an earthquake.

In the following figures we presented the F_s map for different thickness of the failure slab $z(t)=1, 5, 10$ and 50m and for the saturated conditions ($m=100\%$). The F_s map let us see how much percent of the area is unstable under these conditions.

In order to know that we will first classify the F_s map into four classes:

- Unstable = safety factor lower than 1
- Critical (slope is at the point of failure)= safety factor between 1 and 1.3
- Medium stable= safety factor between 1.3 and 1.5
- Stable = safety factor above 1.5

The design static safety factor standard for Romania is 1.5.

When the thickness of the failure slab is equal 1m the F_s map did not shows a relevant results. In fact, we can conclude that the shallow landslides (Fig. 152 - left) are insignificant or at the regional scale used we cannot assess it.

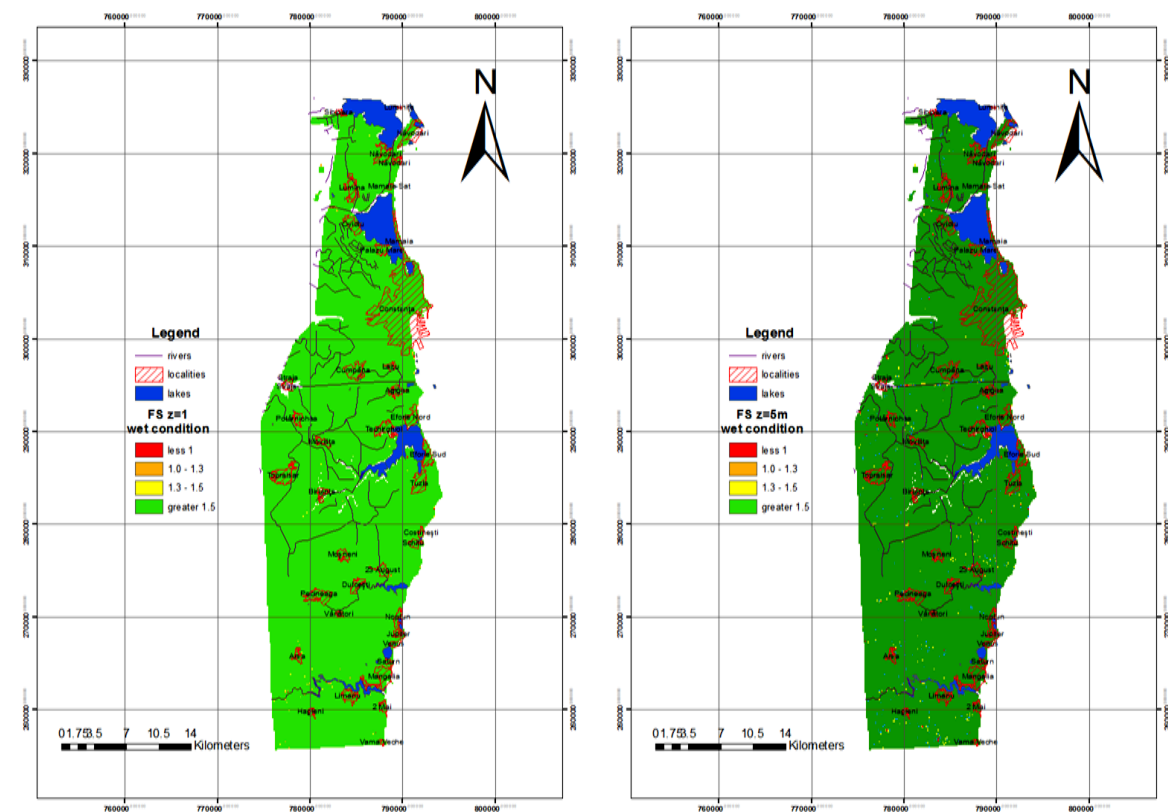


Fig. 152 F_s map for 1m (left) and 5m (right) thickness of the failure slab under saturated condition

When the thickness of the failure slab is equal 5m an unstable terrain appear only on cut slope of the Danube - Black Sea Channel, on the rivers valley and on few littoral zones (ex. South of Eforie City) - see fig. 152 right.

Taking a look to the FS map for the thickness of the failure slab equal with 10m and 50m we can observe that many areas from the study region are affected by landslide (fig. 153).

We used also a thickness of the failure slab equal with 50m because the thickness of loess layer in Dobrogea region varies from 5 to 60m (Conea, Ciurea, etc) and the landslides has as trigger factor the accumulation of water at contact zone between loess deposit and underlying layer (reddish clay).

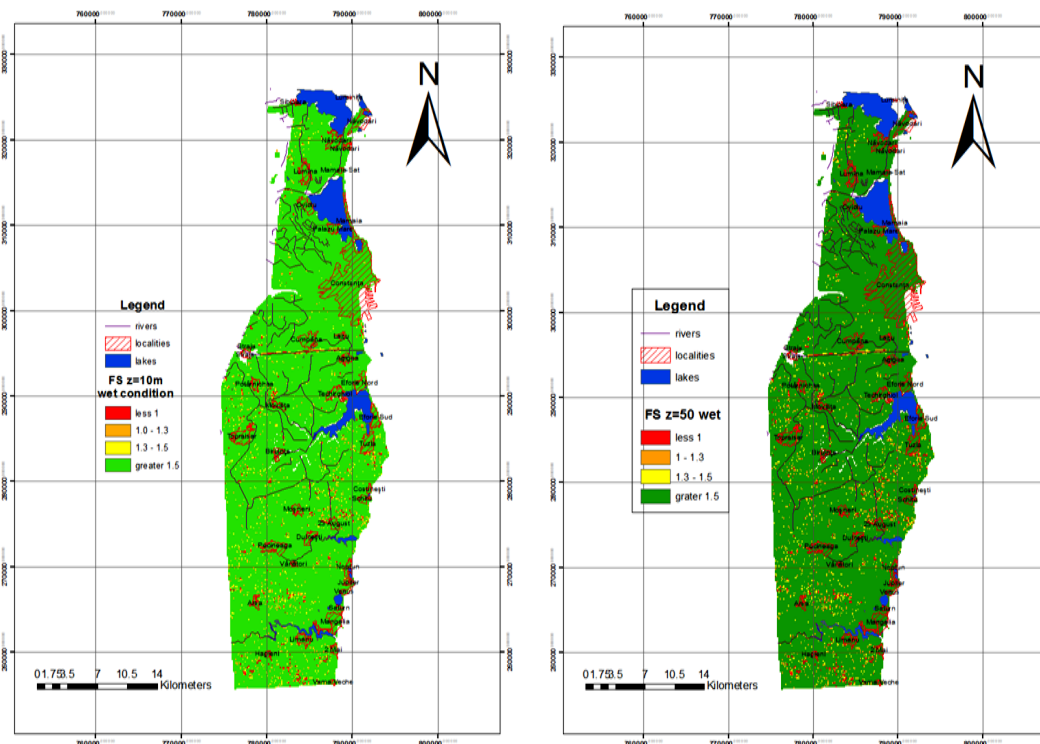


Fig. 153 FS map for 10m (left) and 50m (right) thickness of the failure slab under saturated condition

12.5 Conclusions

The scenario that we have evaluated in this research study was the condition in which the slopes are completely saturated. When we have a saturated soil, the m factor from the *infinite slope formula* is equal to 1. This means that the water table is at the surface. This is not a very realistic situation, but it will give us the most pessimistic estimation of slope stability, with only one triggering factor involved (rainfall leading to high perched watertables). There is also another parameter that will vary when the soil is completely saturated, which is $\gamma = \gamma_{app} = \gamma_{sat}$. We also used different values for cohesion, friction angle and unit weight of soils for different soil or lithological types. (Table 14).

First we have calculated the safety factor for the soils under the assumption that the soil is completely dry. In that case the parameter m is equal to zero. In this case the map F_s dry gives the most stable situation (Factor of Safety >1.5).

Based on the research results, the following understanding and conclusions can be drawn for large scale landslides and for the effect of the groundwater on the stability of the soils in the in the study area:

- Based on the F_s map (Fig. 152), as a general trend the vast majority of the area studied is rather stable (Factor of Safety >1.5);
- Most landslides on low- to moderate-gradient slopes (0-10deg.) have acceptable stability ($1.3 < F_s < 1.5$), even in fully saturated conditions;
- Factors of Safety approaching the threshold of stability (Factors of Safety = 1) are indicated where landslides lie on steep slopes (e.g. Coastal and littoral zone at South of Constanta City and West and South-West areas of Mangalia City), where water table seasonally reaches very high piezometric levels);
- Slopes of river banks or channels (Danube – Black Sea Channel) in the examined area are characterized as unstable (landslide is about to occur, $F_s < 1$);
- Regarding LHA maps, these could be great tools used in the creation of failure probability maps.
- Regarding Factor of Safety method (for static conditions: geologic maps + topography maps + hydraulic conditions (% of sliding slab saturation) + geotechnical parameters (ϕ' , c') + sliding slab normal thickness) seems to work fine for “shallow” landslides, but needs some improvement (*regarding assessment of sliding slab thickness*).
- Is better to work at local scale in order to quantify more precise the landslide areas (eg. 1:5000 scale).

13 LANDSLIDE HAZARD ASSESSMENT ON A REGIONAL SCALE - PILOT IMPLEMENTATIONS IN MOLDOVA

There are a lot of regions affected by landslides in Moldova (near 16000 lots). The intensity of landslides in the central part of Moldova, including Chisinau, considerably increased in end of twenty century. In total, 357 private households involving 1400 people were affected, 214 houses were destroyed, and 137 were damaged. The total national damage accounted for 44.3 million Lei (World Bank Report, 2007).

The Chisinau municipality region was selected as a pilot area for landslide hazard evaluation. The methodology of landslide vulnerability of Moldavian territory is based on the Mora and Vahrson approach (1994). Reasons for acceptance of this method are based on the complex geological structure of study area, geotechnical properties of local rocks, and there sensitivity to water impact. Calculations and construction of maps was carried out using the software QGIS 2.10, SAGA GIS2.1, with partial use of ArcGIS 9.3.1.

Landslide characteristics are influenced by slope susceptibility to failure, which depends, among other factors, on slope geometry, lithology, climatic conditions and human intervention. This methodology is required a specific dataset for physical and mechanical properties of the various lithological units. Earthquakes and rainfalls have been common triggers of landslides in Moldova; however, earthquake magnitude or rainfall intensity alone does not reflect the effects on landslides characteristics.

Estimation of landslides risk (H) is based on More`s theory. The calculations assume that landslide risk is directly proportional to susceptibility of the slope (**Su**) and trigger factor value (**Tr**). Common geological material related to landslides in studied area is Neogen sandy-clay formation. Intrinsic landslide susceptibility is formed by the following factors: Slope Factor (**Sr**), Lithology Factor (**Sl**), Soil Humidity Conditions (**Sh**). The trigger factor is included two components Precipitation factor (**Tp**) Seismic factor (**Ts**).

The selected method of landslide hazard evaluation uses a following equation:

$$H = (S_r * S_l * S_h) * (T_s + T_p) \quad (30)$$

The slope factor is derived from free data obtained from National Geospatial Data Fund which were made by SAR (**Synthetic Aperture Radar**) with the resolution 20 m. It was a base for DEM creation.

The classification is applied according to approach given by Mora and Vahrson: $R_r = (H_{max} - H_{min}) / km^2$ (Table 15).

Table 15 Slope factor classification

Relative Relief R_r (m/km ²)	Classification	Slope Factor S_r
0-75	Very Low	0
76-175	Low	1
176-300	Moderate	2
301-500	Medium	3
501-800	High	4
>800	Very High	5

The location of pilot area is presented in figure 154. DEM was build for this area by the respective modeling approach of ArcGIS 9.3.1 tools.



Fig. 154 Pilot area for landslide hazard evaluation (Durlesti village)

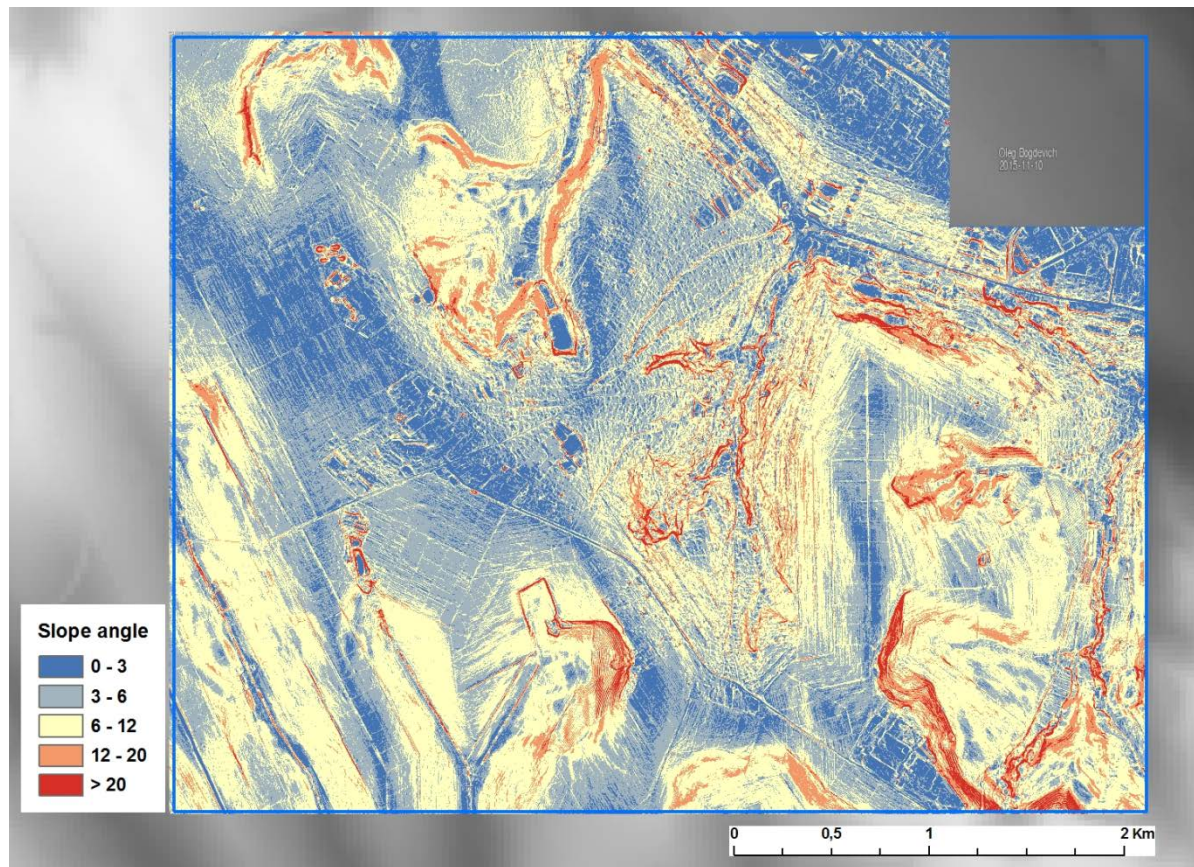


Fig. 155 DEM for pilot studied area

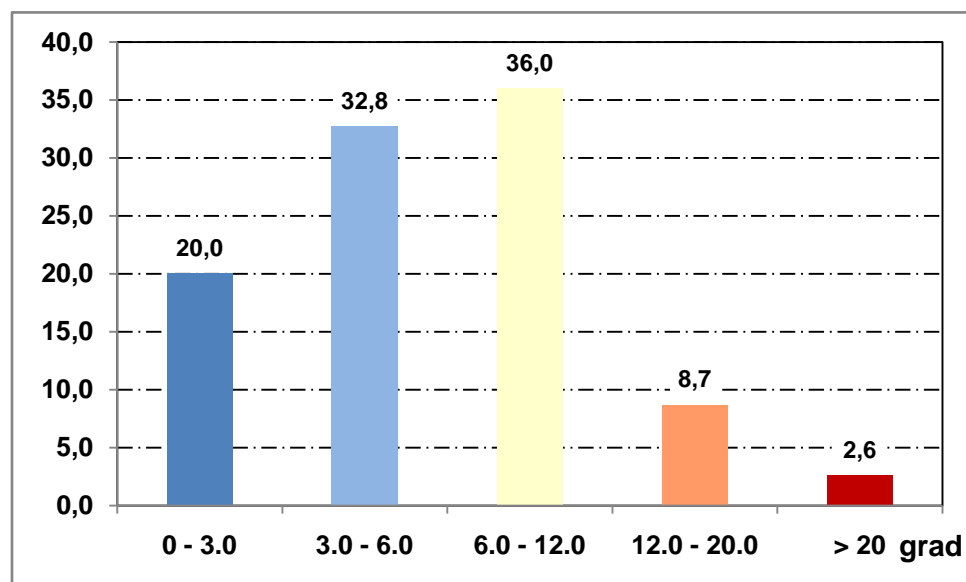


Fig. 156 Percentage distribution of slope angles (grad)

The figure 155 is demonstrated a calculated DEM from obtained data. The empirical evaluation of degree slope inclination to landslide activity in studied area determined that surface with the inclination up to 3 degree is not affected by landslide processes. The inclination in the interval 3 - 6 degree is not affected by the inclination more 6 degree is a critical for the studied area. Slopes with inclination more 6 degree, have landslides and erosion processes, as a rule. Near 53 % of the territory has an inclination below 6 degree, other territory more of this value. Territories with the inclination from 6 to 12 degree cover near 36 % of all territory. The inclination more 12 degree occupies 11,5% of the territory. The higher landslide frequency fall within the slope angles between 6° and 20 degree.

The influence of each factor is not equal ranking, and degree of influence of each factor can be empirically determined by means of studies of data about existing landslides.

The geological conditions are determined by the sand-clayey formation of neogen age. Very small thickness of quaternary deposits is situated in pilot area. The neogen formation is presented by four stratigraphic layers: N_1b-s_1 , N_1s_2 , N_1s_3 , N_2-Q .

The geological map of this area was obtained from regional geological map: figure 157. Three geological formations are situated in zones of landslide formation: N_2-Q , N_1s_3 , N_1s_2 . The landslide events are correlated more with slope inclination and lithology composition. Upper sarmatian deposits are characterized by rhythmical alluvial deposits of fine sands and clays. The thickness of this formation is up to 45 m. the Pliocene deposits of the Dniester River terraces.

Unfavorable factors are slope inclination more 6 degree and presents of clayey rock. All three geological formations from high part of geological section of this area have the similar geotechnical properties and can be classified into one group. The comparison of hills degree and geological map showed confirmed this fact. The landslide events are developed in all geological formations (figure 158). There are no correlation between geological formations (in studied area) and landslide events.

Humidity factor was calculated based on the number of precipitation for the year. This information was taken from recent studies in central part of Moldova. The precipitation distribution is illustrated in figure 6. Annual precipitation is in the interval 550 – 650 mm per year.

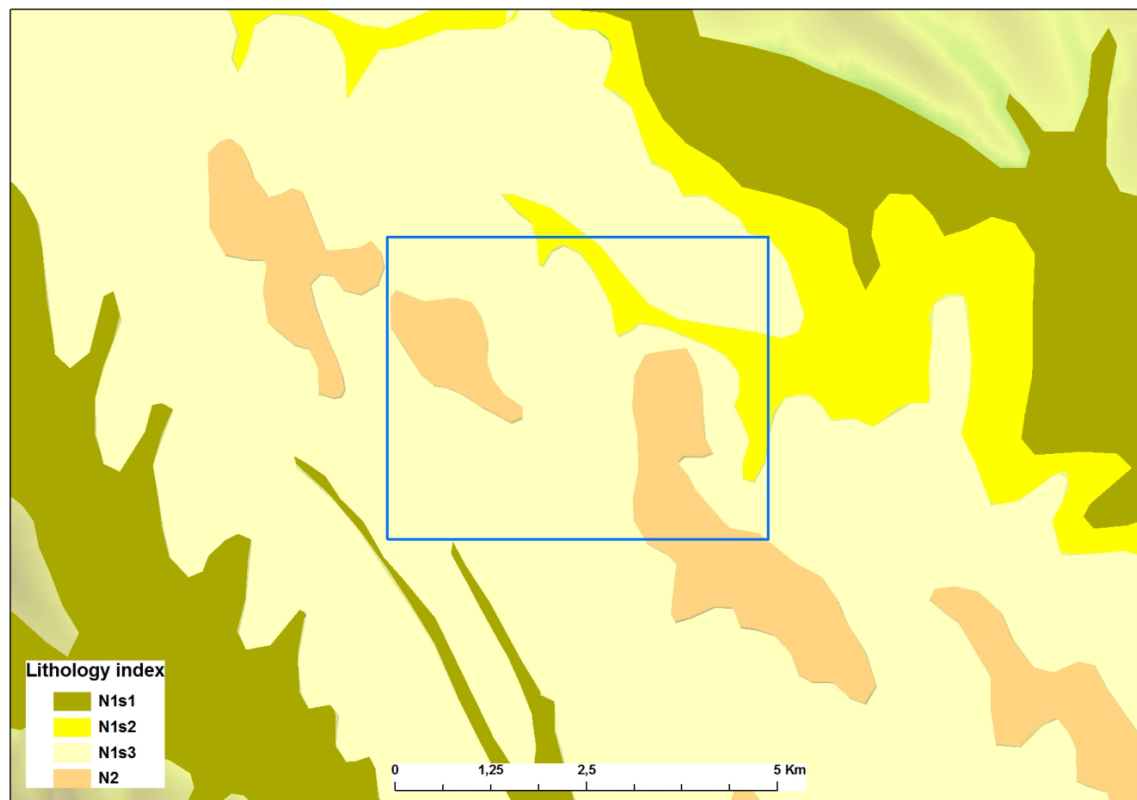


Fig. 157 Geological map of studied area (pilot area is indicated by quadrat)

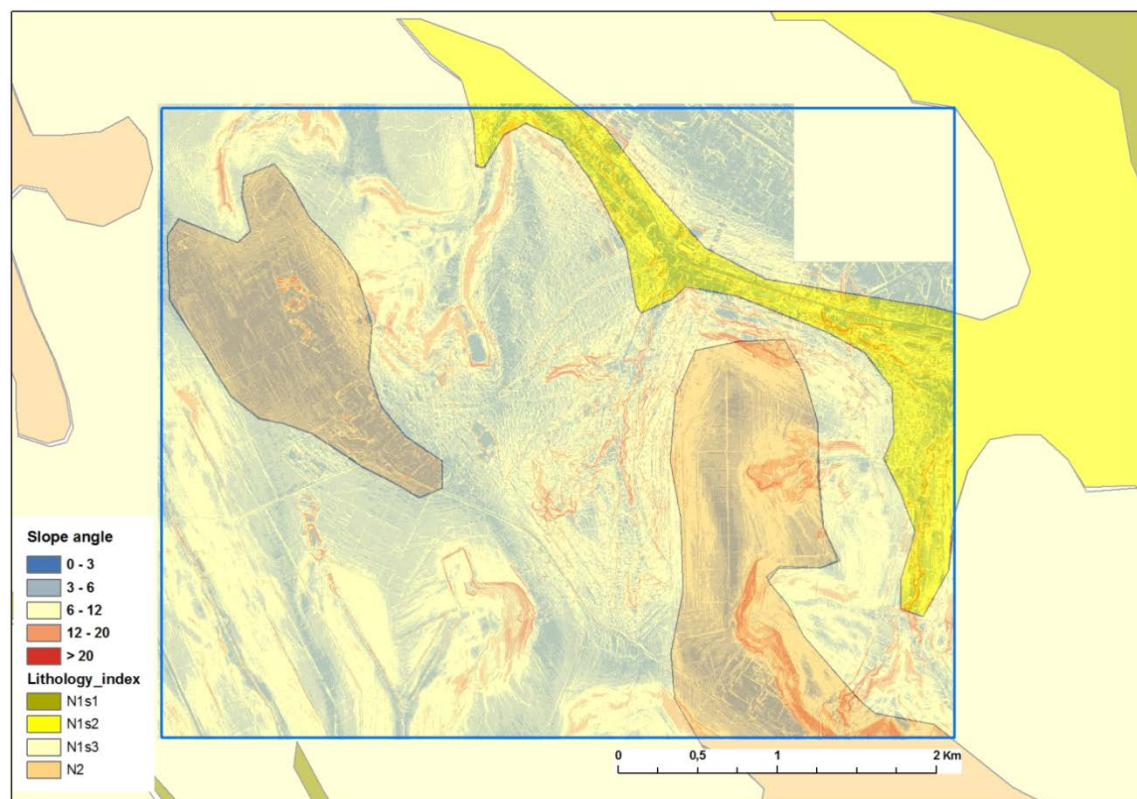


Fig. 158 The DEM in the comparison with geological layers

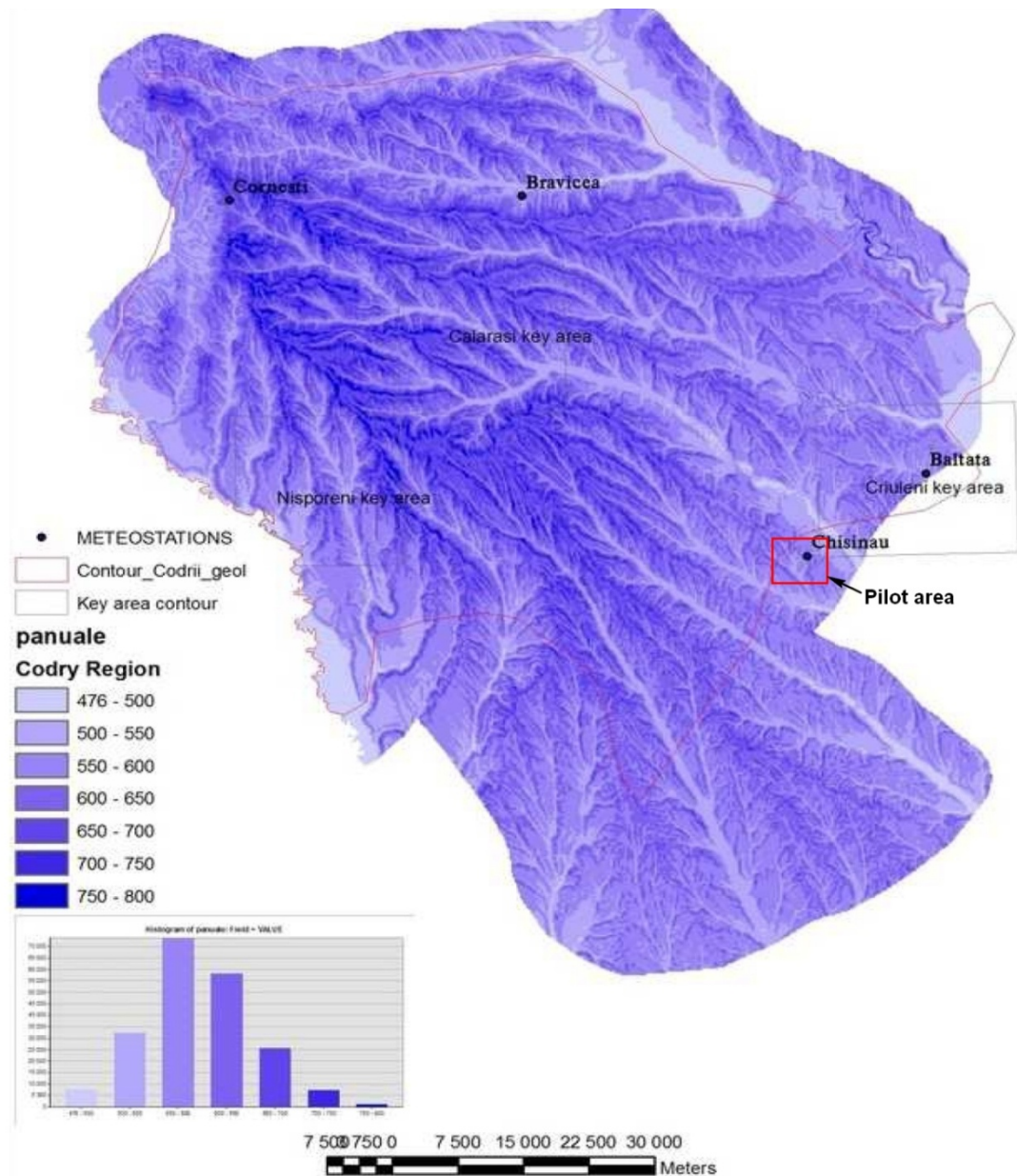


Fig. 159 Annual precipitation distribution in central Moldova (State Hydro Meteorological Services of Moldova)

The intensive atmospheric precipitation is a one of trigger factor. The predominant maximal intensity of torrential rains is in the interval 0,5 – 1,9 mm/min, only in exceptional cases more that 5 mm/min. The value 0,1 mm/min is accepted as a usual for torrential rains in the central part of Moldova. The

medium range of raining time is near 1,5 hour, maximal – 4 hours. Maximal value of the precipitation can be assessed as 50 mm for one hour.

Precipitation factor (Tp) originating from the classification of maximum daily precipitations over a return period in 100 yrs. An auxiliary classification based on the average yearly maximum values per day is given in column 2.

Maximum Rainfall n>10yrs, Tr = 100yrs	Rainfall n<10yrs; Average	Qualification	Tp Factor
<100mm	<50mm	Very Low	1
101-200mm	51-90mm	Low	2
201-300mm	91-130mm	Medium	3
301-400mm	131-175mm	High	4
>400mm	>175mm	Very High	5

The central part of Republic of Moldova present average maximum daily precipitations in the range up to 90mm, so they fall into the “Low” and “Very Low” category (Tp=1-2).

Seismic activity can make slopes unstable and lead to landslides intensification. Seismic zoning of Republic of Moldova (normative document) is a source of the information for the intensity of this factor. Seismicity triggering factor is in the interval between 6 and 8 degree of seismic intensity for territory of Republic of Moldova (figure 160).



Fig. 160 The map of seismic zoning of Republic of Moldova

Pilot area is situated in zone 7 degree of seismic intensity (MSK-64). The acceleration value for soil should be adopted as 0,2 g (200 Gall) by local normative documents for the construction design projects.

The value of trigger factor is determined by summation of the above listed values, which are expressed in points, with significance coefficients` application for each component of trigger factor.

$$Tr = P + 0,2(S\Delta) \quad (32)$$

Significance and value of the point of the constituents of trigger factor are listed below.

Slope factor (Sr) is the leading factor for landslides risk evaluation. This factor can be expressed by height amplitude per unit area, or by steepness of a ground relief. We propose following ranking of ground surface steepness, according to intervals: 0 - 3, 3 – 6, 6 - 12, 12 - 20, > 20 degree. These are the basic diapasons of the slope characteristics. This risk index interval following:

- 1 point – 0-3 degree,
- 2 points – 3 – 6 degree
- 5 points – 6 – 12 degree,
- 7 points – 12 - 20 degree,
- 9 points – > 20 degree.

Lithology Factor (Sl), is also very important factor. The presence of limestone, sandstone of neogen formation reduces risk to the minimum. Good geotechnical properties have sand formation. The inclination in the area of sandy rocks has a very intensive inclination. It means that landslides has low risk in area of sandy rocks distribution. Loam, clay, aleurites, stratified with clay sandy rocks have a high risk of the landslide formation. We propose the following index risks for lithology factor

- 1 point – neogen deposits of limestones and sandstones (N_1b-s_1 , N_1s_2 etc.);
- 2 points – neogen and quaternary sand deposits (N_1s_2 , N_1s_3-m , N_2-Q etc);
- 4 points – neogen and quaternary, clay, sandy clay, loam deposits (N_1s_2 , N_1s_3-m , N_2-Q etc).

Soil Humidity (Sh). Presents of low groundwater level close to surface, springs above of erosion basis is also unfavorable factor for landslide processes. Rise of underground water level, in most of the cases, leads to exogenous gravitational processes activation, including landslides. The studies of underground water level, in most of the cases, are carried out on a local scale; while on a regional scale can evaluate only regional aquifer levels and very difficult use for regional landslide risk evaluation. The first aquifer plays a principal part in landslide processes, as usual. This aquifer is related with atmospheric precipitation and lithology factor. Where clay rocks are developed the low groundwater level exists. We propose following risk indexes for this factor (local level risk evaluation):

- 1 point – groundwater level > 15 m and bellow of erosion basis;
- 1,5 point – water level in the interval 10 – 15 m, no springs on the hills;
- 2,0 points – water level in the interval 10 – 15 m. there springs on hills;
- 3,0 points - water level in the interval 5 – 10 m, there springs on hills;
- 4,0 points – water level above 5,0 m on intensity inclination hills.

Atmospheric precipitation intensity (P) is the crucial parameter for landslide intensification. Atmospheric precipitation intensity in most of the cases leads to underground water level rise, which leads to the changing of geotechnical properties and formation of landslide surfaces. Direct correlation between landslide intensification and the amount of atmospheric precipitation was proven in the course of numerous studies. The significance of the atmospheric precipitation also depends of the filtration parameters of the rocks. On a regional level for landslide risk estimation, atmospheric precipitation intensity can be used without correction to rocks filtering properties. It is taken into consideration in lithology and soil humidity factors. For the estimation of potential landslide risk is used quantity of average annual precipitation, this factor can be ranked as follows:

- 1 point – less than 550 mm per year,
- 2 points – 500- 650 mm per year,
- 3 points – 650- 800 mm per year,
- 4 points – 800-950 mm per year,

Seismic point of a territory assuming seismic activity amplification ($S+\Delta$). Seismic activity of a territory determines a degree of intensification of potentially dangerous areas. Seismic point of a territory is based on a general seismic zoning of Republic of Moldova (2010). According to this zoning, seismic intensity is varied from 6 to 8 degree. Moreover, due to local engineer-geological peculiarities of certain territories (mechanical properties and watering, geomorphological features) seismic points for distinct areas can be increased up to 1 point, which was shown by the results of microseismic zoning. That is why for the purposes of landslide risk estimation; seismic component is used assuming probable seismic activity amplification (Δ) for the regions, where microseismic zoning was carried out. Since seismic activity in Republic of Moldova is evaluated according to MSK-64 scale and expressed in points, there is no need to convert these values. Taking into account high values of the points in MSK-64 scale in relevance to other factors values, it is suggested to use this parameter with the coefficient 0.2.

14 LANDSLIDE HAZARD ASSESSMENT ON A REGIONAL SCALE - PILOT IMPLEMENTATIONS IN UKRAINE

14.1 Landslide hazard assessment of the southern Ukraine

It was used **Mora & Vahrson** methodology for regional landslide hazard assessment of the southern Ukraine (Mora & Vahrson, 1994).

Selecting a method is due to the availability of input data for the calculations. Calculations and construction of maps was carried out using the software QGIS 2.10, SAGA GIS2.1, with partial use of ArcGIS 10.2.

Landslide hazard assessment carried out within the south of Ukraine. The western border of the territory - the border line with the state of Moldova, the southern border - the Black Sea coast, the eastern - Nikolaev, the width of the area - 100 km from the coast of the Black Sea.

The spatial resolution of the digitized maps, and the resulting maps of 90 m (based on the accuracy of the data available on the factor of the slope).

Landslide hazard in a particular area is formed by two components - the intrinsic landslide susceptibility and the value of the trigger factor. Intrinsic landslide susceptibility is formed by the following factors: Slope Factor (**Sr**), Lithology Factor (**Sl**), Soil Humidity Conditions (**Sh**).

The susceptibility of the slope indicates potential danger of landslides on the slopes. Occurrence of a landslide on the slope can be triggered by an earthquake or a strong downpour in the presence of a potential hazard.

Seismic activity areas and frequency of occurrence of heavy rainfall is forming of the triggering factor. So **the leading factors influencing the risk of developing landslides are:** Slope Factor (**Sr**), Lithology Factor (**Sl**), Soil Humidity Conditions (**Sh**), Precipitation factor (**Tp**) Seismic factor (**Ts**),

The value of the landslide hazard in the south of Ukraine is calculated using the formula:

$$HI = S USC * TRIG = (Sr * Sl * Sh) * (Ts + Tp) \quad (33)$$

where:

Sr : “Slope” factor

Sl : Geology factor

Sh: Humidity factor

Ts: (Earthquake) Seismic triggering factor

Tp: Precipitation triggering factor

To calculate the landslide hazard of southern Ukraine the following data were used.

14.2 Slope factor (Sr)

For construction of maps topography slopes used SRTM data.

The Slope Factor is defined by the maximum difference in elevation per unit area R_r = Relative Relief per grid unit (square km), $R_r = (H_{max} - H_{min}) / km^2$

Data on slopes topography are expressed in points in accordance with Table 16.

Table 16 Slope factor classification

Relative Relief R_r (m/km ²)	Classification	Slope Factor S_r
0-75	Very Low	0
76-175	Low	1
176-300	Moderate	2
301-500	Medium	3
501-800	High	4
>800	Very High	5

Relief within the of southern Ukraine is characterized by a small relative, mostly moderate, low and medium, $R_r < 500$ m/km². Relative relief is expressed in points in accordance with Table 16. The map is made a slope factor (Fig.161).

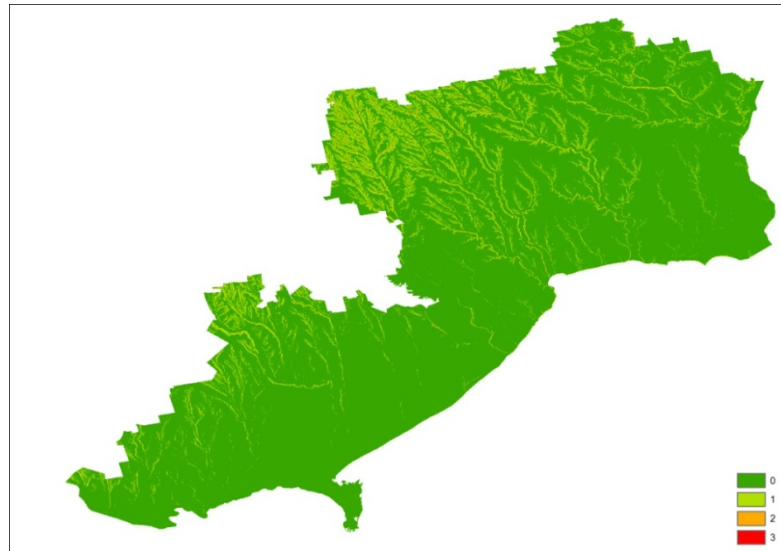


Fig. 161 The map of slope factor of southern Ukraine

The highest slopes relief (up to 500 mt / km²) are observed in the northern areas of the south of Ukraine, in the river valleys. Most of the area is characterized by slopes up to 175 m / km².

14.3 Geology factor (SI)

Map of geologic factors (lithology factor) is made by an expert evaluation. The main parameter of the geological factor is the shear strength. In compiling maps took into account the age of the rocks, the degree of lithification, genetic type, lithological composition, thickness non-lithified sediments. Geology factor is expressed in points in accordance with Table 17.

Table 17 Geology factor classification

Age and type of geological formations	Classification	Lithology Factor (SI)
All rocks	moderate	2
Non-lithified alluvial and limanical Neogene-Quaternary deposits (sandy and silt formation)	medium	3
Neogene-Quaternary loess and clay loam deposits, thickness <20 m	high	4
Neogene-Quaternary loess and clay loam deposits, thickness <20 m and intensely abrasive rocks and deposits of the coastal zone	very high	5

In the south of Ukraine are mainly distributed Neogene and Quaternary slightly lithified deposits of sand and silt and clay formations with low shear strength. The most susceptible landslides are loess rocks that consist of clay, silt and sand. Rock that destroyed the waters of rivers, limans and the sea in the coastal cliffs are intensively susceptible landslides also.

Map of geologic factors is presented in Fig. 162.

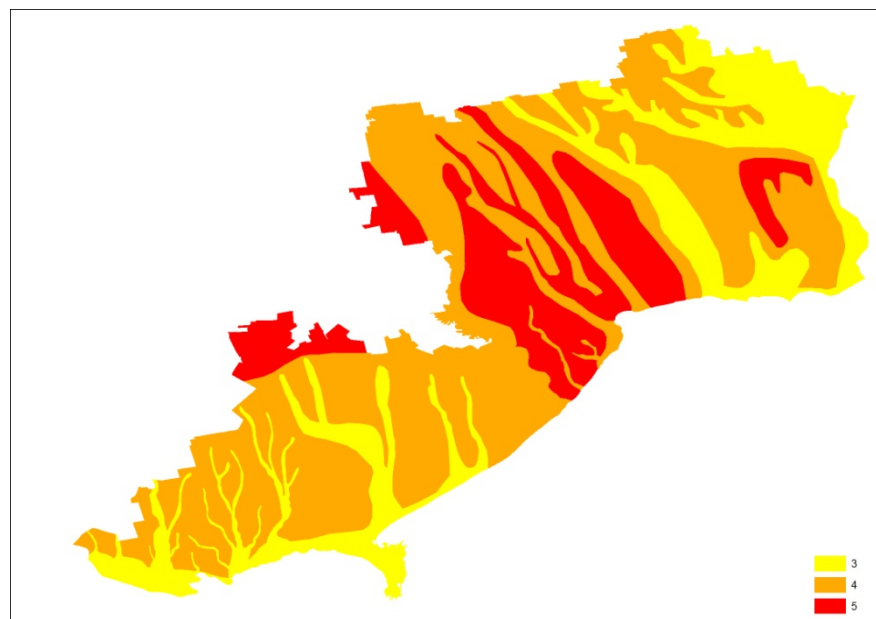


Fig. 162 The map of geology factor of southern Ukraine

To compile this map have been used and digitized geological and tectonic maps of regional geological enterprises and maps of the National Atlas of Ukraine (2010).

The most susceptible landslides on geology factors are the territory between the Dniester and Southern Bug, especially in watershed highlands. These areas prevalent non-lithified silty-clay deposits with high thickness.

14.4 Humidity factor (Sh)

Humidity factor was calculated based on the number of precipitation in every month of the year. We used maps of precipitation in summer (April-October) and winter (November-March) seasons

(National Atlas of Ukraine, 2010). It was assigned the index of precipitation at each map and every month of the year in accordance with Table 18.

Table 18 Average monthly rainfall values classification

Average Monthly Precipitation AMP (mm/month)	Assigned Value
<125	0
126-250	1
>250	2

The sum of index of 12 months of the year was moved to humidity factor points according to Table 19.

Table 19 Moisture factor (Sh) from accumulated AMP values

Accumulated value of Precipitation Indices	Qualification	Factor Sh
0-4	Very Low	1
5-9	Low	2
10-14	Medium	3
15-19	High	4
20-24	Very High	5

Number of precipitation is not more than 550 mm / year in the south of Ukraine, including in the warm season - 325 mm, and in the cold season - 225 mm. Number of precipitation in the south of Ukraine is <125 mm / month in most of the year, 4 months of the year - 126-250 mm / month. Thus, Humidity factor in the south of Ukraine is equal to 1. This figure was used in the formula for calculating the landslide hazard.

14.5 Seismic (earthquake) triggering factor (Ts)

It performed general seismic zoning (GSZ-2004) to the south of Ukraine on the basis of the intensity of earthquakes with a recurrence period of earthquakes - 500 years. According to the GSZ-2004 intensity of possible earthquakes in the south of Ukraine is from 6 points to the east, up to 8 points in the west, in the area of the Danube Delta (12-point scale).

Were digitized maps of probable seismic intensity to determine the seismic factor (Ts). Seismic factor (Ts) was determined by Table 20. There was a map of seismic factor (Ts) to of southern Ukraine (Fig. 163) as a result.

Table 20 Seismic Intensity factor

Intensities (MM) Tr=100yr	Qualification	Factor Ts
III	Slight	1
IV	Very Low	2
V	Low	3
VI	Moderate	4
VII	Medium	5
VIII	Considerable	6
IX	Important	7
X	Strong	8
XI	Very Strong	9
XII	Extremely Strong	10



Fig. 163 The map of seismic triggering factor of southern Ukraine

Meaning seismic factor (T_s) is in the range of from 4 to 6 in the south of Ukraine. The highest values are typical for the south-western region - the Danube Delta. This is due to the proximity of the Vrancea zone in Romania.

14.6 Precipitation triggering factor (T_p)

Were processed observations of hydrometeorological stations and maps of daily maximum precipitation (National Atlas of Ukraine) for determining precipitation triggering factor. The values of this factor is expressed in points from Table 21.

Table 21 Precipitation factor (Tp) originating from the classification of maximum daily precipitations over a return period of 100yrs. An auxiliary classification based on the average yearly maximum values per day is given in column 2

Maximum Rainfall n>10yrs, Tr = 100yrs	Rainfall n<10yrs; Average	Qualification	Tp Factor
<100mm	<50mm	Very Low	1
101-200mm	51-90mm	Low	2
201-300mm	91-130mm	Medium	3
301-400mm	131-175mm	High	4
>400mm	>175mm	Very High	5

The southern Ukraine areas present average maximum daily precipitations in the range up to 90mm, so they fall into the “Low” and “Very Low” category (Tp=1-2).

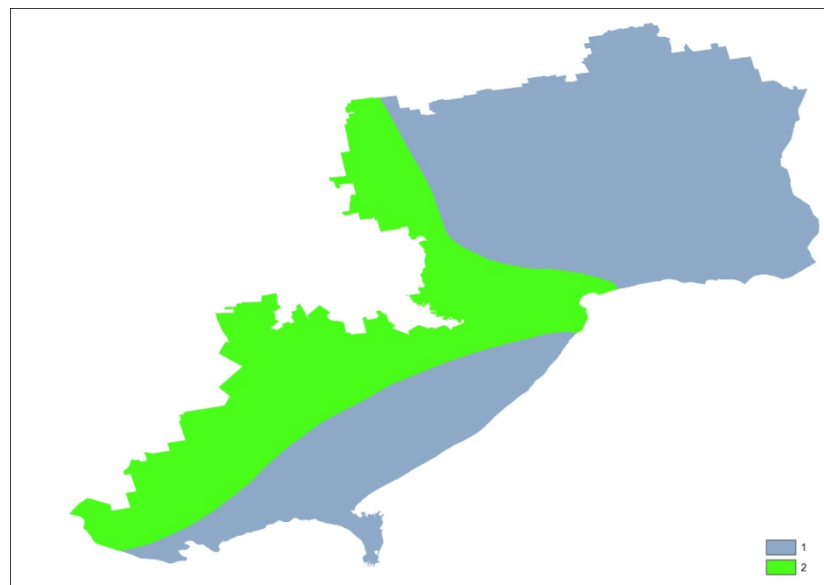


Fig. 164 The map of precipitation triggering factor of southern Ukraine

Thus, the results of calculations landslide hazard were calculated for the southern of Ukraine. The results are shown in points in accordance with Table 22.

Table 22 Classification of the Landslide Hazard HI parametric values.

Value of HI	Class	Classification of Hazard of Landslide Potential
<6	I	Negligible
7-32	II	Low
33-162	III	Moderate
163-512	IV	Medium
513-1250	V	High
>1250	VI	Very High

The resultant landslide hazard map of southern Ukraine is shown in Fig. 165.

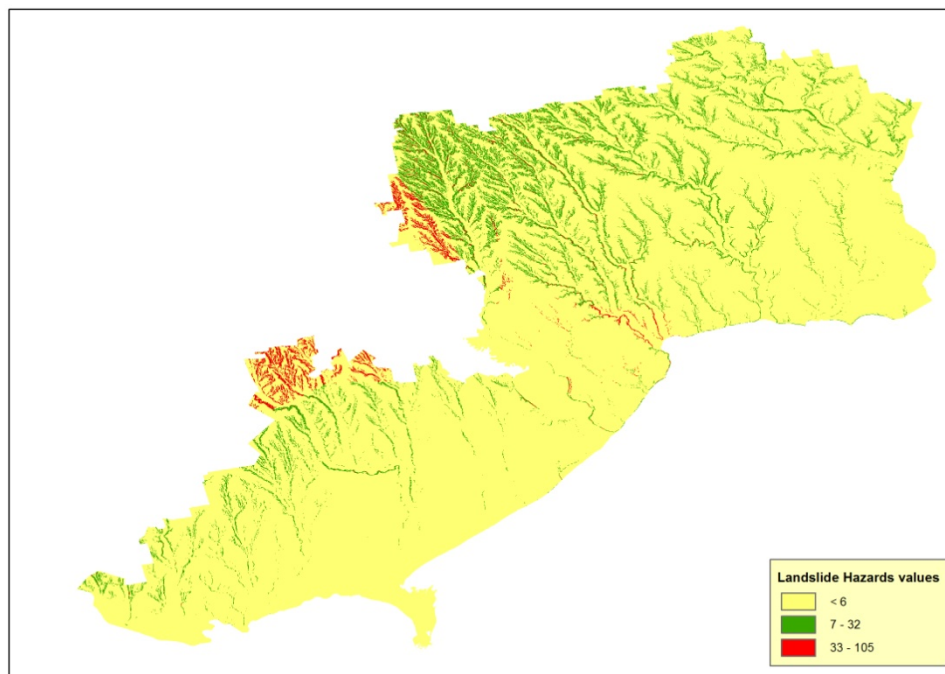


Fig. 165 The resultant map of landslide hazard of southern Ukraine

The obtained values of the potential landslides hazard is in range from <6 to 105 points. Landslide hazard of southern Ukraine is characterized mainly as "Negligible", "Low" and "Moderate". The most dangerous sites are located in the basin of the Dniester River, along the shores of the Black Sea estuaries and the coast of the Black Sea near the city of Odessa.

The results are in good agreement with Ukraine made in the national estimates of the potential danger of landslides and real data on manifestations of landslide processes on the territory of Ukraine.

15 GENERAL CONCLUSIONS

Regional and local landslide hazard assessment deal with the same problem but at a different scale affecting thus largely the optic of each approach. Regional scale LHA should be mostly used in making rational decisions regarding strategic planning of developing regions or construction of large scale infrastructure, taking into account the level of hazard regarding landslides. Quantification of landslide hazard has been assessed upon physically-based models where topographical, geological, hydrological, and geotechnical data must be used, according to the model of soil or rock failure adopted.

Local scale LHA approach refers to scales deemed for design or screening on slope stability issues in a detailed way. Therefore, they cannot and should not be overlooked, regardless of existing regional scale LHA maps. The physically-based models used herein are mostly the "infinite slope model" and occasionally the "circular slope model" on natural slopes under different conditions (wet, dry, seismic conditions for various mean return periods of the seismic event). A strong point regarding the choice of physically-based models is that the procedure for assessing landslide hazard is based on real failure mechanisms developed in nature and is not based on statistics. This means that the procedure for LHA can work even without inventory maps, or systematic registration of landslides of the examined area taking into account temporal and spatial variation in the past; this is a major asset, since usually this kind of information is missing.

However, on the other hand a major drawback of the physically-based models is that they are seriously dependent upon the geotechnical parameters used, which might spatially fluctuate upon their state; so, in large areas with spatial variability or intense heterogeneities, those models might be misleading, if those heterogeneities are not referred in the geological maps used. In such cases, assistance by remote sensing techniques, might be of considerable importance in order to define zones or areas tectonically disturbed, where often, hydrological and geotechnical parameters of the same geological formation are largely reduced. Such a case was investigated in one of the pilot areas in Greece (Nymfaia PIA).

Another important issue is the assessment of the thickness of the sliding slab (regolith depth), when the "infinite slope model" is adopted as the potential mechanism of failure, as well as, the percentage of saturation of the sliding slab. Nevertheless, despite the above shortcomings LHA at a regional scale when compared and tested to real cases in the PIAs (in Greece and Turkey) has proved to be successful when based on physically-based models.

The following three (3) methods have been used, and subsequently tested for LHA in the Hellenic PIAs: Mora and Vahrson, 1994 (rainfall and earthquake as triggering factors); FEMA, 1999 (earthquake as triggering factor); Factor of Safety for "Infinite Slope Model" (rainfall or earthquake as triggering factors).

In the Turkish PIAs four (4) methods have been used in order to assess Landslide Hazard triggered by rainfall or earthquakes: Montgomery and Dietrich, 1994 (calculation of factor of safety based on the infinite slope model triggered by rainfall), Mora and Vahrson, 1994 (rainfall and earthquake as triggering factors), FEMA, 1999 (earthquake as triggering factor; earthquake induced permanent ground displacement are calculated) and Siyahi and Ansal, 1994 (earthquake as triggering factor; a pseudostatic factor of safety is calculated, based on a circular slope model).

As for the rest of the partners, Bulgaria, Moldova and Ukraine have implemented the method of Mora and Vahrson (1994) at a regional scale, whilst Romania has implemented the method of factor of safety based on the "infinite slope model" at a regional scale.

A summary of the main conclusions from the LHA at regional and local scale, as implemented in the pilot areas, is as follows:

1. all partners have used the method of **Mora and Vahrson (1994)** for LHA at regional scale; it can be considered as an approximate method to assess regional LHA in a rather qualitative way for both triggering factors (rainfall and earthquake), since hazard indicator is an arbitrary index denoting rather susceptibility than landslide hazard. Even though less demanding in terms of input data, the results are qualitative and it has to be treated with care as the method was based on data coming solely from South America,
2. the method of **FEMA (1999)** has been implemented by Greece and Turkey in their PIAs; it is restricted to assess LHA only if the triggering factor is earthquake. The first step of the method is a qualitative approach of the Landslide Susceptibility; on a second step, this method estimates the earthquake induced Permanent Ground Displacements. This step is quite demanding due to the number and the kind of input data needed for its application, whereas an important number of intermediate "products" (maps) needs also to be calculated in order to assess "Permanent Ground Displacements - PGD", being the end-product of this method. Despite difficulties in implementation, complexity and understanding, this method can provide results in terms of permanent seismically-induced displacements, which is

- actually the most realistic way to evaluate the occurrence of an earthquake-induced landslide,
3. the method of **Factor of Safety** (included also the method of **Montgomery and Dietrich, 1994**), based on the "infinite slope model" (and occasionally based on the "circular slope model") is the most comprehensive among all methods implemented herein. This method, applies to both static (rainfall, as triggering factor) and seismic conditions (earthquake, as triggering factor) and the results, i.e. maps presenting values of the factor of safety are well perceived by end users (usually engineers and geologists). Therefore, it is considered to be the most feasible when compared to the other ones and to field data in the Hellenic and Turkish PIAs,
 4. the method of **Siyahi and Ansal (1994)**, calculates a pseudostatic factor of safety, based on a circular slope model; the triggering factor is earthquake and it is taken into consideration in terms of seismic acceleration. Results from this method can be directly compared to those of the factor of safety, provided that the physically-based model adopted is the "circular slope model". This method and the FEMA method can be used as complimentary methods, as the triggering factor, in both cases, is the earthquake.
 5. In the case of regional, and especially for local scale LHA, it became evident that reliability and extent of the input geological, hydrological and geotechnical data plays a very significant role. Thus, in order to establish realistic landslide hazard maps, relatively comprehensive geological and geotechnical site investigations are necessary. It is also very important to have sufficient and detailed rainfall statistics (hydrological data) for the region investigated as well as a comprehensive study concerning the regional seismic hazard for different hazard levels.
 6. The results obtained from landslide hazard maps at a regional scale should be considered as a "**useful and powerful tool**" to make decisions of strategic character and to determine the priorities of the measures that can be taken to prevent rainfall and seismically induced landslides aiming to minimize the possible damages in residential areas and infrastructure. Regarding LHA maps, these could be great tools used in the creation of failure probability maps. They should not be considered under any circumstances as a "**design tool**".
 7. In addition, in the case of rainfall induced landslide hazard assessment, it appears possible to utilize the findings with respect to rainfall amount, as an early warning method or an alert system depending on the weather forecasts concerning the rainfall amount; this, would imply reliable hydrological data.

8. LHA in regional scale at PIAs in Greece have been compared to in-situ "reality" and to 2D or even 3D approaches regarding slope stability at a much larger scale (even exceeding "local scale"). The results appear very promising and were close enough to real cases. The regional scale LHA was successful enough and slope stability analyses at different locations were within the results provided by regional scale in most of the cases.
9. In local scale, comparison between 2D limit equilibrium approach and 3D finite difference approach in terms of factor of safety, were almost similar. Both 2D and 3D slope stability models predicted the same failure surface and mainly the same failure mechanism adopted in the regional approach.

16 REFERENCES

- Akinci, Halil, et al., (2011): Production of landslide susceptibility map of Samsun (Turkey) City Center by using frequency ratio method., *International Journal of the Physical Sciences* 6.5: 1015-1025.
- Aleotti P., Chowdhury R., (1999): Landslide hazard assessment: summary review and new perspectives. – *Bull. Engng. Geol. Environm.*, 58: 21–44.
- Ansal, A., Tönük G. and Bayrakli Y., (2005): Microzonation for Site Conditions for Tekirdağ Municipality, Boğaziçi University, Kandilli Observatory and Earthquake Research Institute, Earthquake Engineering Department.
- Berov B., D. Frangov, (1997): Zoning of the Sofia valley by the degree of landslide hazard potential. In: *Proc. 4th National Scientific and Practical Conference on scientific support of the prevention activities and protection of the population in emergency situations*, Nov. 5-6 1997, Sofia, Vol.5, 207-215 (in Bulgarian). *Codes for design of buildings and facilities in earthquake regions*. 1987. Council for Territorial and Urban Planning, Construction and Architecture and Bulgarian Academy of Sciences, Sofia. 68 pages (in Bulgarian).
- Berov, B., (1996): *Geological hazard processes in Sofia kettle*. PhD Thesis, Geological Institute, Sofia.
- Beven, K.J., Kirkby, M.J., (1979): A physically-based variable contributing area model of basin hydrology. *Hydrology Science Bulletin*, 24, 43-69.
- Carrara A, Cardinali M., Detti R., Guzzetti F., Pasqui V., Reichenbach P., (1991): GIS Techniques and statistical models in evaluating landslide hazard. *Earth Surface Processes and Landform* 16, 427–445.
- Carrara A., Cardinali M., Guzzetti F., Reichenbach P., (1995): GIS technology in mapping landslide hazard. In: Carrara, A., Guzzetti, F. (Eds.), *Geographical Information Systems in Assessing Natural Hazards*. Kluwer Academic Publisher, Dordrecht, The Netherlands, pp. 135–175.
- Carrara A., Pike R.J., (2008): GIS technology and models for assessing landslide hazard and risk. *Geomorphology*, 94(3-4), 257-260.
- Catani et.al., (2010): An empirical geomorphology-based approach to the spatial prediction of soil thickness at catchment scale. *Water resources research* Vol. 46.

- Conea, A., Depozitelecuaternare din Dobrogea. Editura Academiei, București, 1970.
- Cruden D. M., (1991): A simple definition of a landslide, Bulletin of the International Association of Engineering Geology, Volume 43, Issue 1, pp 27-29, April 1991.
- Dimaras, K., (2006): Updating of the final geological study of national road (Vertical axis 75 of Egnatia Odos) Komotini - Nymfaia - Greek / Bulgarian Borders.
- EDAFOS Ltd., (2007): Presentation report of geotechnical survey on Vertical Axis 75 of Egnatia Odos, Komotini - Nymfaia - Greek/Bulgarian Borders.
- EDAFOS Ltd., (2008): Geotechnical preliminary design of the embankments and cut slopes of Vertical Axis 75 of Egnatia Odos, from ch. 4+900 km to ch. 6+840 km.
- Efraimidis Ch., 2009 Personal communication.
- Faridfathi, Füsün Yiğit, and Mustafa Ergin., (2012): Holocene sedimentation in the tectonically active Tekirdağ Basin, western Marmara Sea, Turkey., Quaternary International 261: 75-90.
- Fell, R. et al., (2008): Guidelines for landslide susceptibility, hazard and risk zoning for land use planning. Engineering Geology, 102(3-4): 85-98.
- Ferentinou et al., (2006): An introduced methodology for estimating landslide hazard for seismic and rainfall induced landslides in geographical information system environment. ECI Conference on Geohazards, Lillehammer, Norway.
- Florea, N., (2010): Loess was formed, but not sedimented, Rev. Roum. Géogr./Rom. Journ. Geogr., 54, (2), 159–169, București.
- Gazioğlu, Cem, Zeki Yasar Yücel, and Ertuğrul Doğan., (2005): Morphological features of major submarine landslides of Marmara Sea using multibeam data., Journal of Coastal Research: 664-673.
- Gedik A., Ercan T. , Korkmaz S., (1984): Orta Karadeniz (Samsun-Sinop) Havzasinin Jeolojisi Ve Volkanik Kayaçların Petrolojisi, Maden Tetkik ve Arama Dergisi, cilt.99-100, ss.34-50.
- Gedik A., Korkmaz S., (1984): Sinop Havzasinin Jeolojisi Ve Petrol Olanakları, Jeoloji Mühendisliği Dergisi, cilt.19, ss.53-79.

- Geoanalysis S.A., (2007): Support of Egnatia Odos S.A. Design Department on the Final Road Design for the optimization of the alignment of the Vertical Axis 75 of Egnatia Odos, Komotini - Nymfaia - Greek/Bulgarian Borders.
- Gokaşan, Erkan, et al., (2003): Morphotectonic evolution of the Marmara Sea inferred from multi-beam bathymetric and seismic data., *Geo-Marine Letters* 23.1: 19-33.
- Goodman and Seed, 1966 Goodman RE and Seed HB, (1966): Earthquake-induced displacements in sand embankments. *Journal of the Soil Mechanics and Foundation Division, ASCE* 92(SM2), p.: 125–146.
- Goodman E. Richard, (1993): *Engineering Geology. Rock in Engineering Construction*. J. Wiley & Sons.
- GSTABL7 v.2 with STEDwin 3.57, (2003): Gregory Geotechnical Engineering Software & STEDwin, by Annapolis Geotechnical Engineering Software.
- Guzzetti F, Reichenbach P, Ardizzone F, Cardinali M, Galli M., (2006): Estimating the quality of landslide susceptibility models. *Geomorphology* 81(1-2): 166-184.
- Guzzetti F., Reichenbach P., Cardinali M., Galli M. & Ardizzone F, (2005): Probabilistic landslide hazard assessment at the basin scale. *Geomorphology* 72: 272-299.
- HAZUS99-SR2 Technical Manual, Chapter 4 Potential Earth Science Hazards (PESH).
- Hoek E., (2007): *Practical Rock Engineering.*, Chapter 11, pp. 50. [Hoek's Corner \(Rock Science\)](#)
- Hutchinson J.N., (1986): A sliding-consolidation model for flow slides. *Can. Geotech J.* 23:115–126.
- Hutchinson J.N., (1995): Keynote paper: landslide hazard assessment. In: Bell (Ed.), *Landslides*. Balkema, Rotterdam, pp.1805–1841.
- Iliev-Bruchev, Il. (Ed.) et al., (1994): *Map of geological hazards in Bulgaria. Scale 1:500,000*. Committee of Geology and Mineral Resources, Bulgarian Academy of Sciences, Sofia, designed and printed by MTS, Troyan.
- Institute of Geologic and Mineral Exploration-IGME, (1978): *Geologic Map of Greece 1:50000*, map sheets: Sidirokastro, Serres, Angistro, Nevrokopi, Drama.
- Itasca, Inc (2015): *FLAC 3D - Fast Lagrangian Analysis of Continua in 3 Dimensions - Version 5.0, Manual*

- Japan International Cooperation Agency (JICA), (2007): The Study on Protection and Rehabilitation of the Southern Romanian Black Sea Shore in Romania. Volume 1 - Basic Study and Coastal Protection Plan. Japan International Cooperation Agency: ECOH Corp.
- Koleva, E., R. Peneva., (1991): *Climatic guide. Rainfalls in Bulgaria*. BAS, Sofia (in Bulgarian).
- Koppula, S. D. (1984): Pseudo-static analysis of clay slopes subjected to earthquakes., *Geotechnique* 34.1: 71-79.
- Makdisi and Seed, (1978): Simplified procedure for estimating dam and embankment earthquake induced deformations. *Journal of geotechnical engineering* 104(7), p.: 849-867.
- Marinos P. and Hoek E., (1995): A geologically friendly tool for rock mass strength estimation.
- Marinos V., Marinos P. and Hoek E., (2005): The Geological Strength Index: applications and limitations. *Bulletin of Eng. Geol. Environ.* (2005) 64: 55-65, DOI 10.1007/s10064-004-0270-5.
- Montgomery & Dietrich, (1994): A physically-based model for the topographic control. *Water Resources Research* Vol. 30, No4, p.1153-1171.
- Mora, S. and Vahrson W-G, (1994): Macrozonation methodology for landslide hazard determination. *Bulletin of the Association of Engineering Geologists*, v. 31, n. 1, p. 49-58.
- National Atlas of Ukraine, (2010), Kiev, Ukraine.
- O'loughlin, E. M., (1981): Saturation regions in catchments and their relations to soil and topographic properties." *Journal of hydrology* 53.3: 229-246.
- O'loughlin, E. M., (1986): Prediction of surface saturation zones in natural catchments by topographic analysis., *Water Resources Research* 22.5: 794-804.
- Pelletier et al, (2009): Tectonic and structural control of fluvial channel morphology in metamorphic core complexes: The example of the Catalina-Rincon core complex, Arizona. *Geosphere* 5(4), p.: 363-384
- RISKSLIDES: Risk management of natural and anthropogenic landslides in the Greek-Bulgarian cross-border area. European territorial Cooperation, Operational Programme Greece-Bulgaria (2010). Technical report.
- Salazar M., L.G., (1991): Modelaje de la amenaza al deslizamiento mediante el sistema de informacion geografico - ILWIS - utilizando el metodo Mora &Vahrson.

- Sari, E., (2008): Samsun’ un genel jeolojisi ve imar planina ait çalışmalar.
- Saulnier et al, (1997): Including spatially variable effective soil depths in TOPMODEL, J. Hydrol., p. 158–172
- Seed, H. B., and Idriss, I. M. (1982): Ground motions and soil liquefaction during earthquakes. Earthquake Engineering Research Institute Monograph, Oakland, Calif.
- Şengüler, İ., (2013): Ergene (Trakya) Havzasinin Jeolojisi ve Kömür Potansiyeli, MTA Doğal Kaynaklar ve Ekonomi Bülteni, 16. Sayı: 109 – 115.
- Shafique, M., van der Mejde, M., and Rossiter, D.G. (2011): Geophysical and remote sensing-based approach to model regolith thickness in a data-sparse environment, Catena, 87, p.11-19.
- Shuiskij, J., G. Simeonova, (1976): About the influence of geological structures along sea-side banks on the abrasion processes. *Comptes rendus ac. bulg. des sciences*, 29, 241-243 (in Russian).
- Simeonova, G., (1989): Formation of coastal zone of water reservoirs at various engineering geological conditions in Bulgaria. PhD Thesis, GI-BAS, Sofia, 234 p. (in Bulgarian).
- Siyahi, B.G. and Ansal, A. (1993): Manual for Zonation on Seismic Geotechnical Hazard, TC4 Committee of ISSMFE, Japanese Society of Soil Mechanics and Foundation Engineering, pp.55-57.
- Soeters R, Van Westen C.J., (1996): Slope stability recognition, analysis and zonation. In Landslides: Investigation and Mitigation, Transportation Research Board, National Research Council Special Report 247, Turner AK, Shuster RL (eds); 129 –177.
- Tesfa, K.T., Tarboton, D.G., Chandler, D.G, McNamara, J.P. (2009): Modelling soil depth from topographic and land cover attributes, Water Resources Research, Vol.45.
- Tressos, N., Skempas, M., (2003): Geotechnical evaluation of national road Komotini - Nymfaia - Greek/Bulgarian Borders, Section from ch. 4+000 km to ch. 12+000 km.
- United States Geological Service (USGS), (1997): Standards for digital elevation models. Mid-Continent Mapping Center, Branch of Research, Technology and Applications, 67p.
- VanWesten C.J., (2015): Deterministic landslide hazard zonation, International Institute for Geo-Information Science and Earth Observation (ITC), <http://www.itc.nl/ilwis/applications/application06.asp>.

- VanWesten, C.J., (2000): The modeling of landslide hazards using GIS, *Surveys in Geophysics* 21 (2–3), 241–255.
- VanWesten, C.J., Castellanos, E. and Kuriakose, S.L., (2008): Spatial data for landslide susceptibility, hazard, and vulnerability assessment: An overview. *Engineering Geology*, 102(3-4): 112-131.
- VanWesten, C.J., Rengers, N. and Soeters, R., (2003): Use of Geomorphological Information in Indirect Landslide Susceptibility Assessment. *Natural Hazards*, 30(3): 399-419.
- VanWesten, van Duren, I., Kruse, H.M.G. and Terlien, M.T.J. GISSIZ., (1993): training package for geographic information systems in slope instability zonation. ITC Publication number 15, 2 volumes, ITC, Enschede, The Netherlands.
- Varnes (1984), Varnes, D.J., 1984. *Landslide Hazard Zonation: A Review of Principles and Practice*. Unesco, Paris.
- Yilmaz, Y., Gökas, an, E., Erbay, A.Y., (2010): Morphotectonic development of the Marmara Region. *Tectonophysics* 488 (1e4), 51e70.

17 ADDITIONAL BIBLIOGRAPHY

- Brabb E.E., (1984): Innovative approaches to landslide hazard and risk mapping, Proceedings of the 4th International Symposium on Landslides, 16–21 September, Toronto, Ontario, Canada (Canadian Geotechnical Society, Toronto, Ontario, Canada), 1:307–324.
- Clark Ian, European Commission, (2012): EU Civil Protection policy Priorities 2011-2013. European Commission, DG Humanitarian Aid and Civil Protection, ECHO A5, Civil Protection Policy, Prevention and Preparedness.
- Clark Ian, European Commission, (2012): The EU Contribution to the Implementation of the Hyogo Framework in Europe. European Commission, DG Humanitarian Aid and Civil Protection, ECHO A5, Civil Protection Policy, Prevention and Preparedness.
- Clark Ian, European Commission, (2012): Towards an EU Policy on Disaster Management. European Commission, DG Humanitarian Aid and Civil Protection, ECHO A5, Civil Protection Policy, Prevention and Preparedness.
- Commission communication [P7_TA(2010)0326], (2010): A community approach on the prevention of natural and man-made disasters. European Parliament resolution of 21 September 2010 on the Commission communication: A Community approach on the prevention of natural and man-made disasters (2009/2151(INI)).
- Commission DG Environment, (2008): Assessing the Potential for a Comprehensive Community Strategy for the prevention of Natural and Manmade Disasters., Final Report, March 2008.
- Commission of the European Communities, (2009): Communication from the Commission to the Council and the European Parliament on EU Strategy for supporting Disaster Risk Reduction in developing countries, COM (2009) 84 Final, Brussels, 23.2.2009.
- Conrad, O., Bechtel, B., Bock, M., Dietrich, H., Fischer, E., Gerlitz, L., Wehberg, J., Wichmann, V., and Böhner, J., (2015): System for Automated Geoscientific Analyses (SAGA) v. 2.1.4, Geosci. Model Dev., 8, 1991-2007, doi:10.5194/gmd-8-1991-2015, 2015. Available online for free <http://www.geosci-model-dev.net/8/1991/2015/gmd-8-1991-2015.html>

Council of the European Union, (2009): Council Conclusions on a Community framework on disaster prevention within the EU 2979th JUSTICE and HOME AFFAIRS Council meeting, Brussels, 30 November 2009.

Dietrich, W.E., Reiss, R., Hus. M.L. and Montgomery, D.R. (1995) A Process-Based Model for Colluvial Soil Depth and Shallow Landsliding Using Digital Elevation Data. *Hydrological Processes*, 9, 383-400.

Directorate General for Research, (2005): Extract of the DG RTD Unit I.4. Catalogue of Contracts topic: Natural hazards Flood Related EU Hazard Research Projects (Framework Programme 5 (1998 – 2002) “PROGRAMME ENVIRONMENT AND SUSTAINABLE DEVELOPMENT” and Framework Programme 6 (2002 – 2006): “PROGRAMME SUSTAINABLE DEVELOPMENT, GLOBAL CHANGE AND ECOSYSTEMS”).

ESRI, ArcGIS Desktop Help 10.1, Available at: <http://webhelp.esri.com/arcgisdesktop/10.1/index.cfm>, 2012.

ESRI, ArcGIS Desktop Help 9.3, Available at: <http://webhelp.esri.com/arcgisdesktop/9.3/index.cfm>, 2009.

European Commission DG Environment, (2008): Member States' Approaches towards Prevention Policy – a Critical Analysis. Final Report. March 2008.

Garrett J., (2010): GIS-based landslide susceptibility analysis of southwestern Colorado Springs, El Paso County, Colorado.

GT 019-98, Slope Landslide Risk Map Elaboration Guide for Building Stability, Institute of Studies and Projects for Territorial Planning, I.S.P.I.F. S.A., Approved by M.L.P.A.T. by order no. 80/N of 19.10.1998, [Published in Romanian], 1998.

Jipa, D.C., (2013): Overview of the loess accumulation sedimentary features in the romanian plain and dobrogea, Field Trip Guidebook, National Institute of Marine Geology and Geoecology GeoEcoMar, Meeting of INQUA – Section on European Quaternary Stratigraphy (SEQS) 23-27th September 2013, Constanța (Romania).

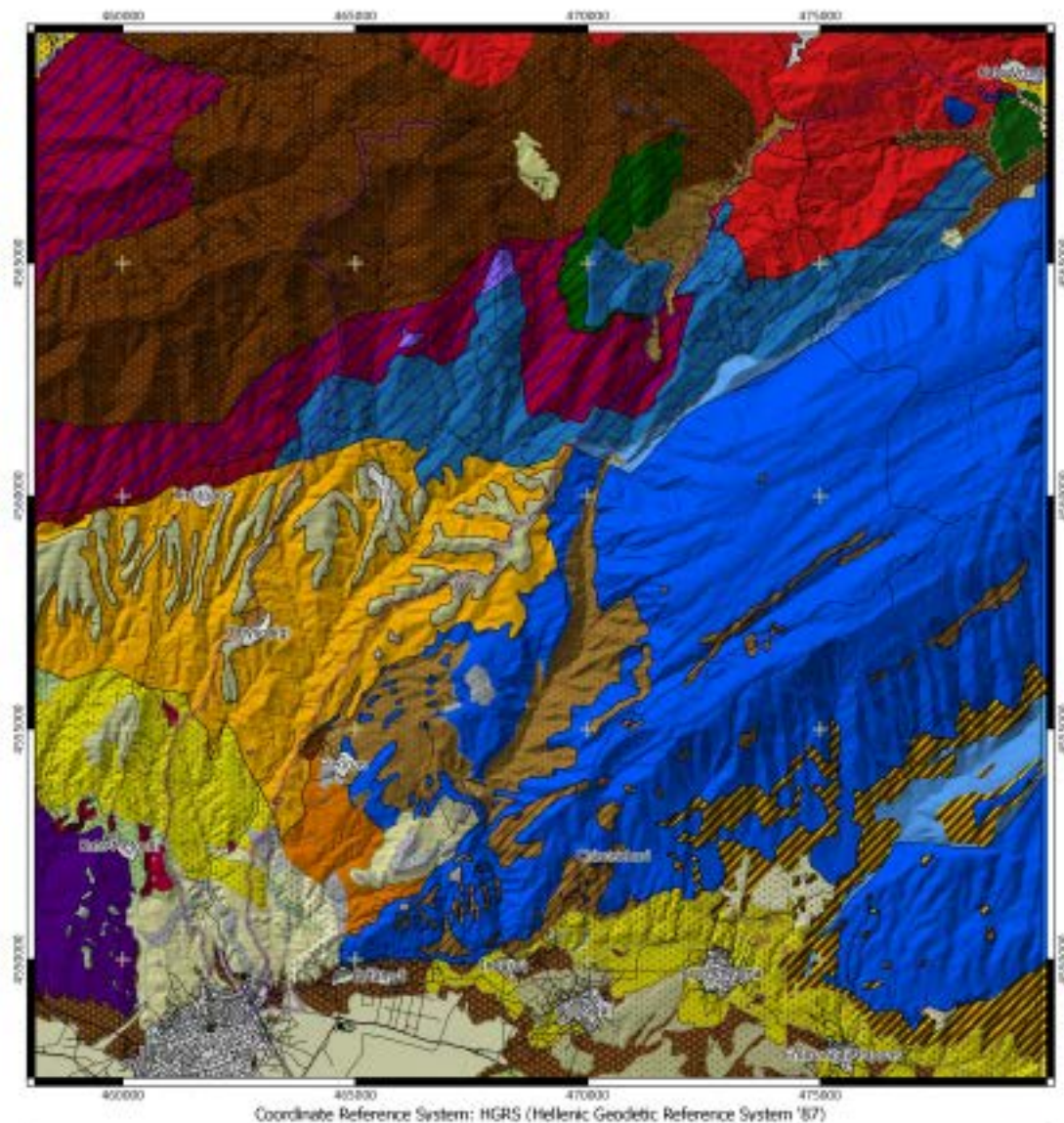
K. Papatheodorou, N. Klimis, B. Margaris, K. Ntoulos, K. Evangelidis, A. Konstantinidis, (2014): “An Overview of the EU Actions towards Natural Hazard Prevention and Management: Current Status and Future Trends”, *Journal of Environmental Protection and Ecology (JEPE)*, Vol. 15, No.2.

- Klimchuk, L. M., Blinov, P.V., Velichko, V. F., Prymushko, S. I., Fesenko, O.V., Shestopalov, V. M., (2008): Modern engineering-geological conditions of Ukraine as a part of life safety. Kiev, Ukraine.
- Li Y., Chen G., Tang C., Zhou G., Zheng L., (2012): Rainfall and earthquake-induced landslide susceptibility assessment using GIS and Artificial Neural Network. *Nat. Hazards Earth Syst. Sci.*, 12, 2719–2729.
- Papatheodorou K., (2001): Engineering Geological Applications. Civil Engineering department, University of Thessaly, pp272.
- Pustovitenko, B. G., Ulomov, V. I., (2004): Maps of general seismic zoning of Ukraine.
- Săndulescu et al, (1978): Geological map of Romania sc. 1:1,000,000, edited by the Geological Institute of Romania.
- Smalley I., O’Hara-Dhand K., Wint J., Machalett B., Jary Z., Jefferson I., Rivers and loess, (2009): The significance of long river transportation in the complex event-sequence approach to loess deposit formation. *Quaternary International*, 198/1–2, 7–18.
- Solano J.G.R., C. D. Q. Cabeza, H. U. R. Alarcón, J. M. Tellez, (2013): Landslide hazard zoning in urban areas by the Mora & Vahrson analysis method: Case of study. *Revista ambiental agua, aire y suelo*. Universidad de Pamplona Vol.4, 1, 13-22. ISSN 1900-9178.
- Yalcin, A., (2008): GIS-based landslide susceptibility mapping using analytical hierarchy process and bivariate statistics in Ardesen (Turkey): Comparisons of results and confirmations. *CATENA*, 72(1): 1-12.
- Zagorcev, I. (1992): Neotectonic development of the Strumna (Kraistid) lineament, southwest Bulgaria and northern Greece, *Geol. Mag.*, 129, 197-222.

ANNEX A

Landslide Hazard Maps at Regional Scale in Greece (Serres and Nymfaia Pilot Implementation Areas)

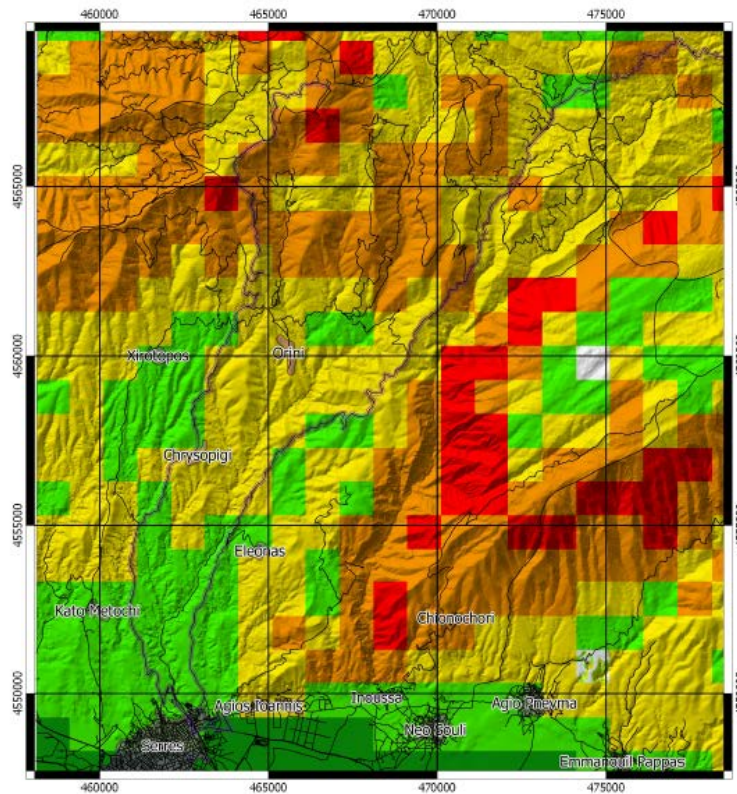
SERRES PIA



SciNetNatHaz Project - Black Sea Basin JOP 2007-13

Geologic Map





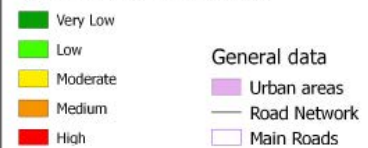
**SciNetNatHaz Project
Black Sea Basin JOP
2007-13**

**Landslide Hazard Assessment
Mora & Vahrson
Methodology**

Triggering factors: Earthquake (100yrs)
Precipitation (100 yrs)

Legend

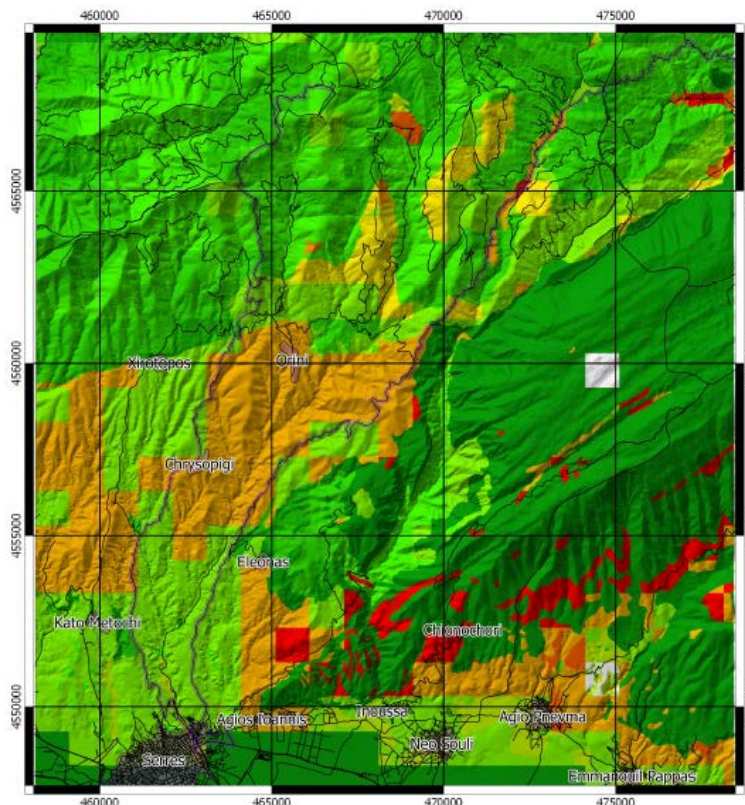
Sr Factor (Mora & Vahrson)



1 0 1 2 3 4 5 km

Scale 1 : 125000

Coordinate Reference System: HGRS
(Hellenic Coordinate Reference System '87)



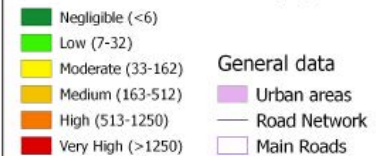
**SciNetNatHaz Project
Black Sea Basin JOP
2007-13**

**Landslide Hazard Assessment
Mora & Vahrson
Methodology**

Triggering factors: Earthquake (100yrs)
Precipitation (100 yrs)

Legend

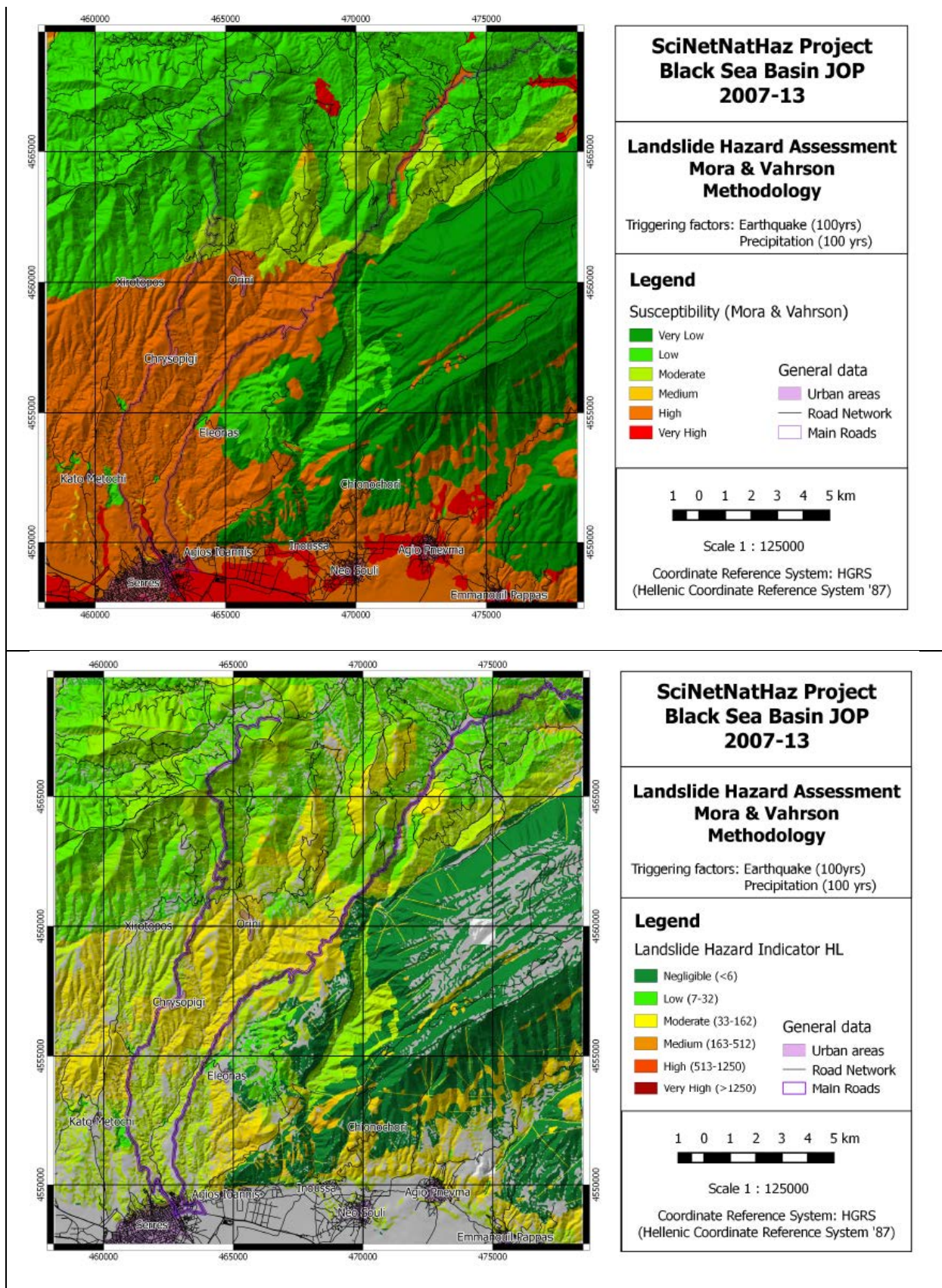
Landslide Hazard Indicator (HL)

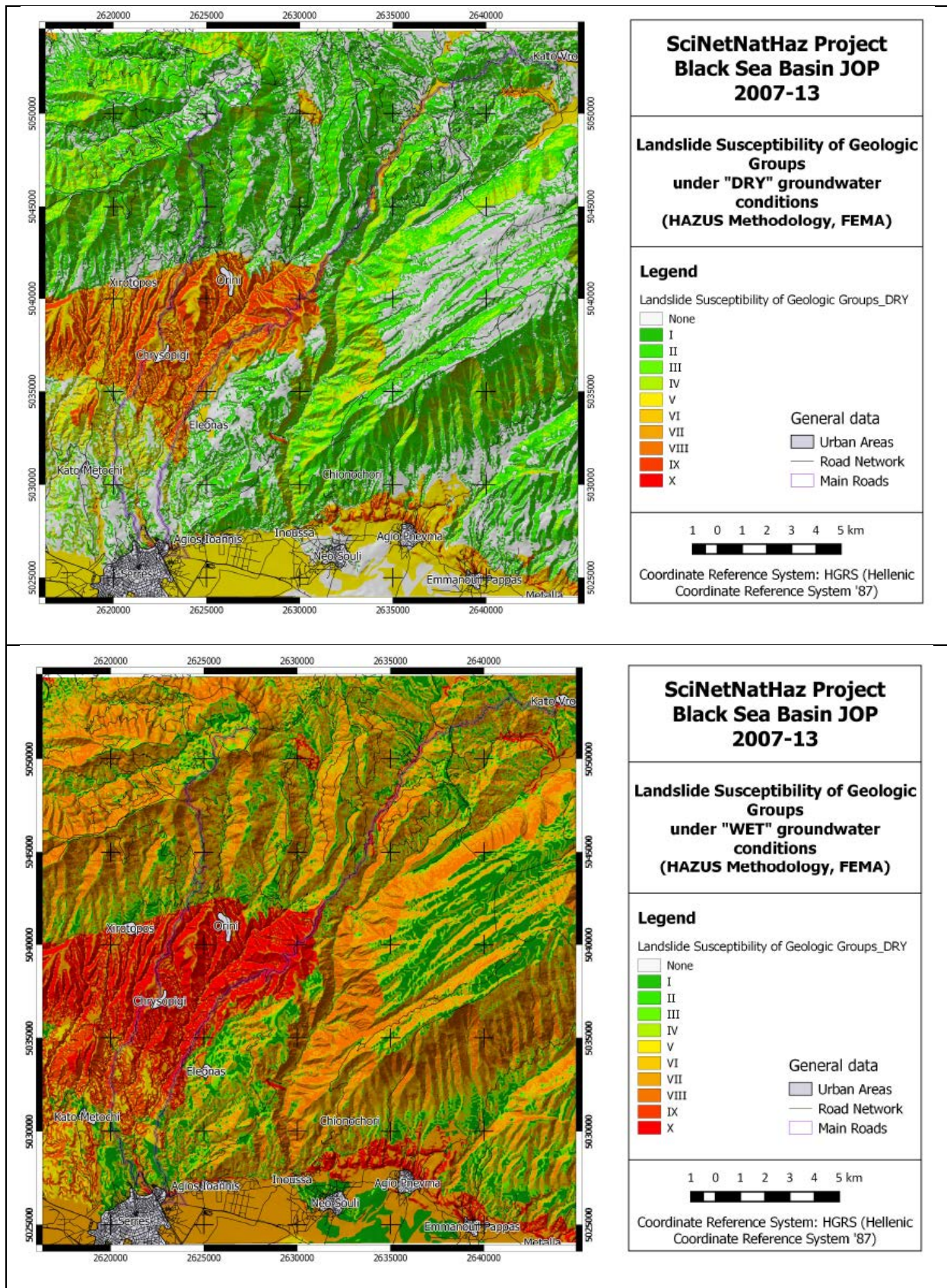


1 0 1 2 3 4 5 km

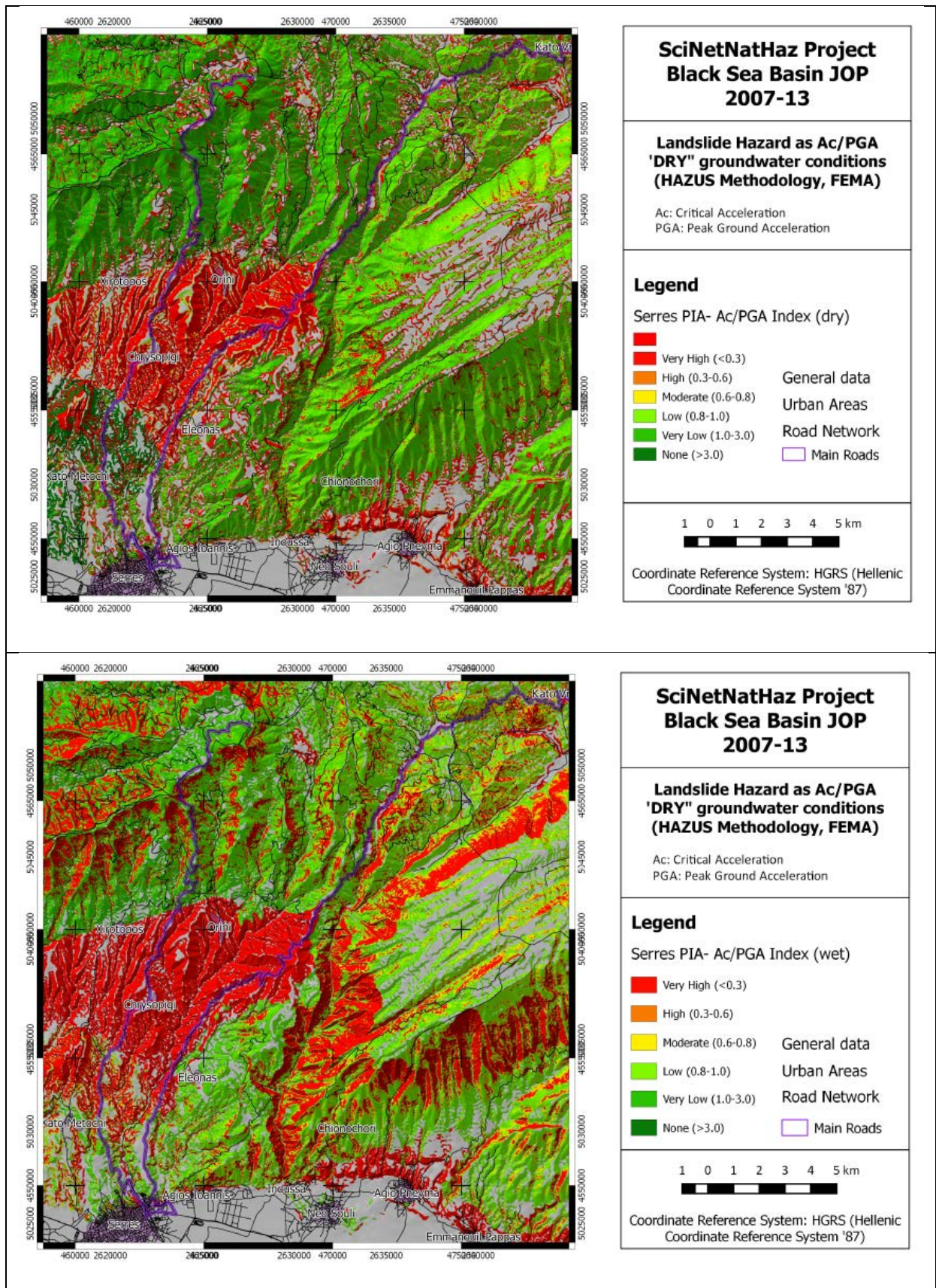
Scale 1 : 125000

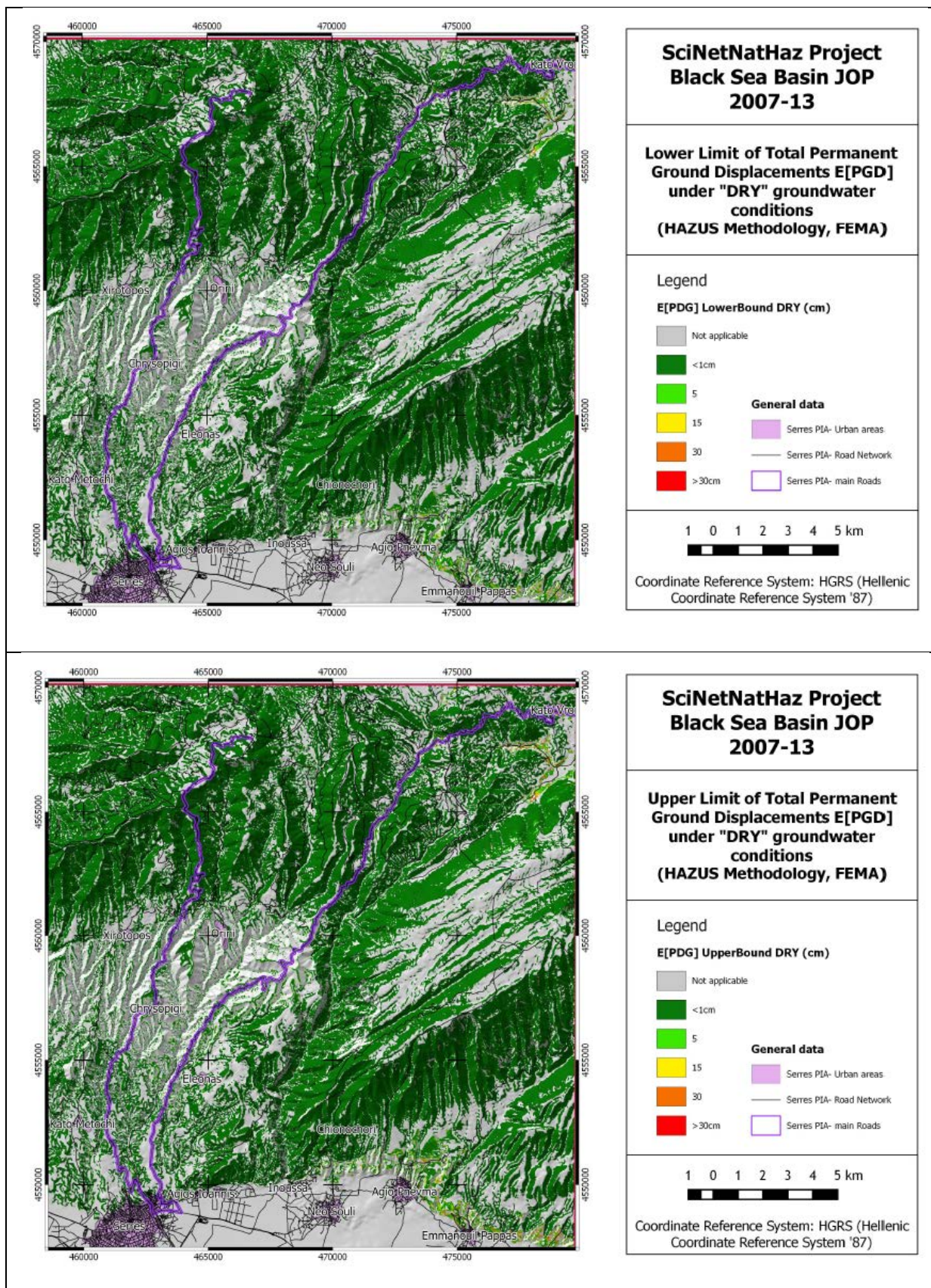
Coordinate Reference System: HGRS
(Hellenic Coordinate Reference System '87)

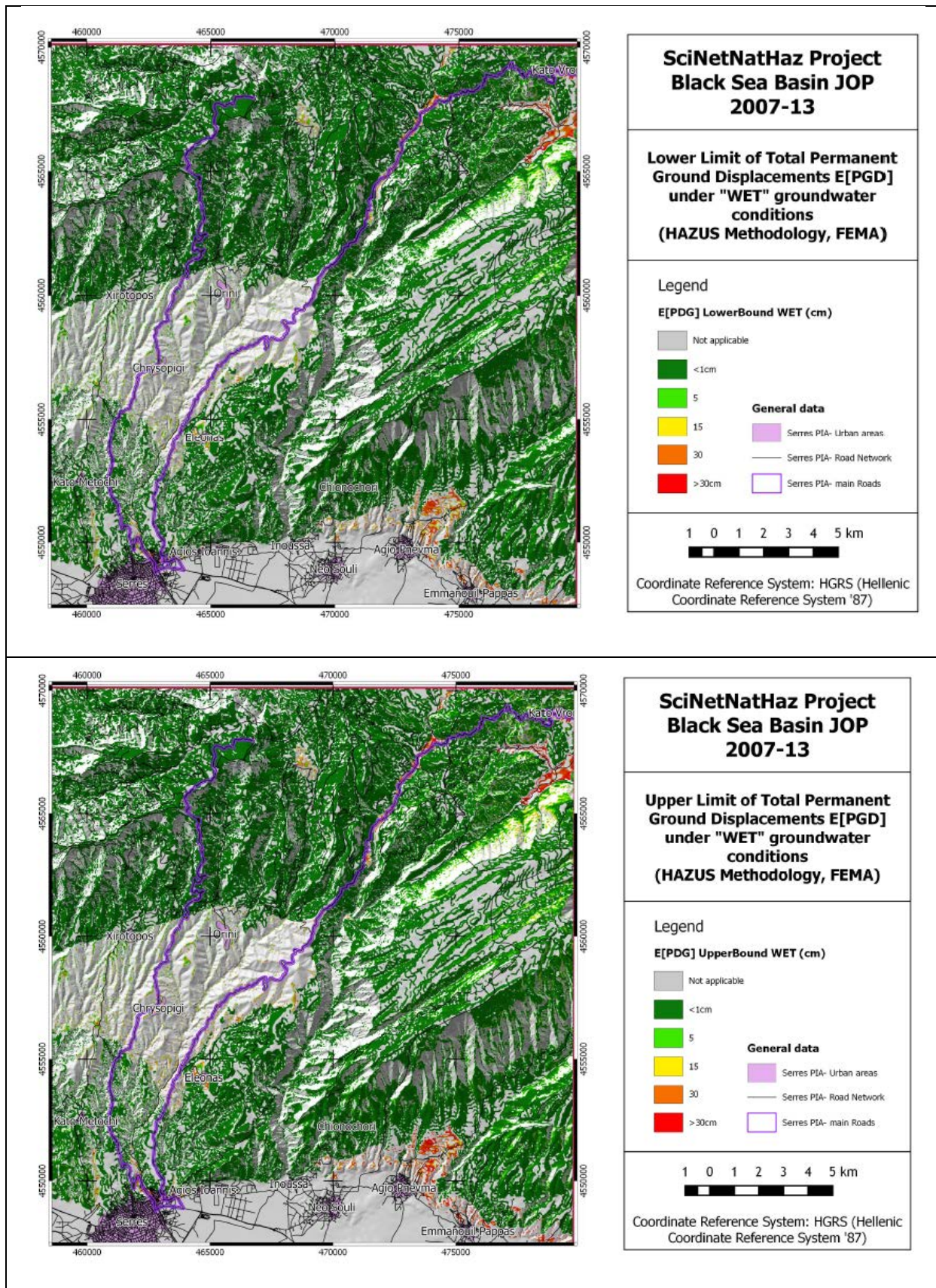


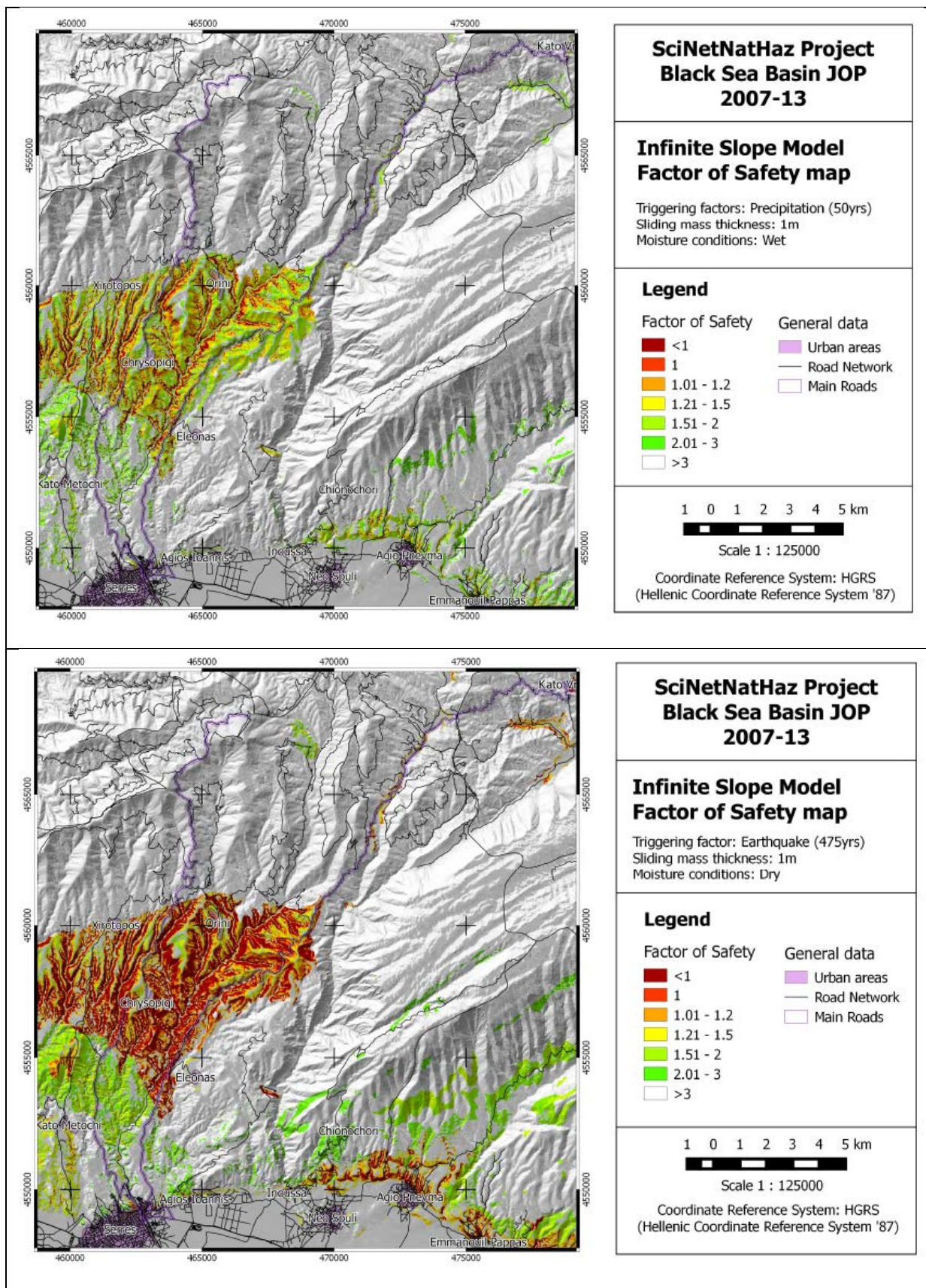


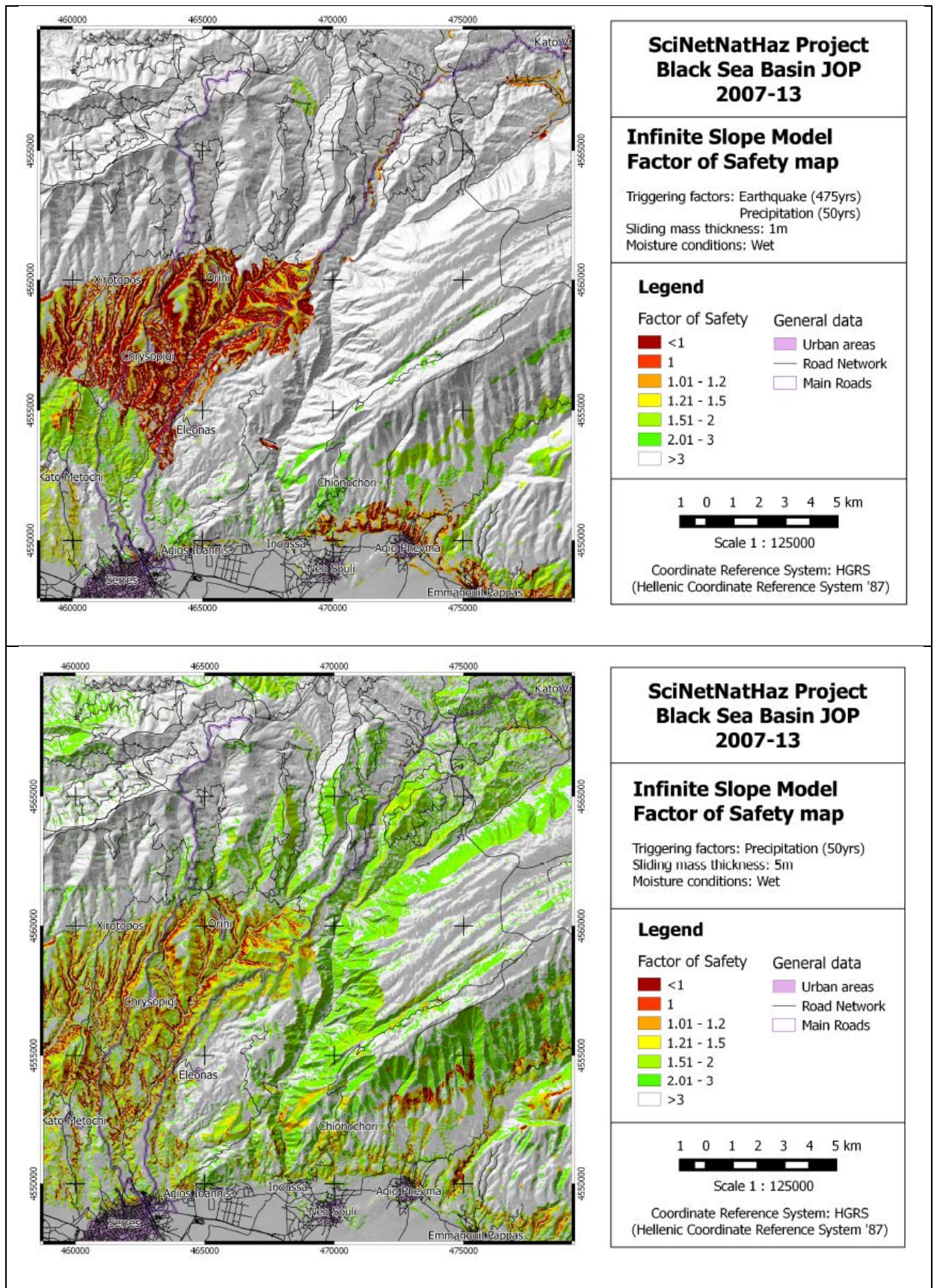
**“Black Sea JOP, “SciNet NatHaz”
Earthquake, Landslide and Flood Hazard
Assessment: Implementation at Regional and
Local Scales**

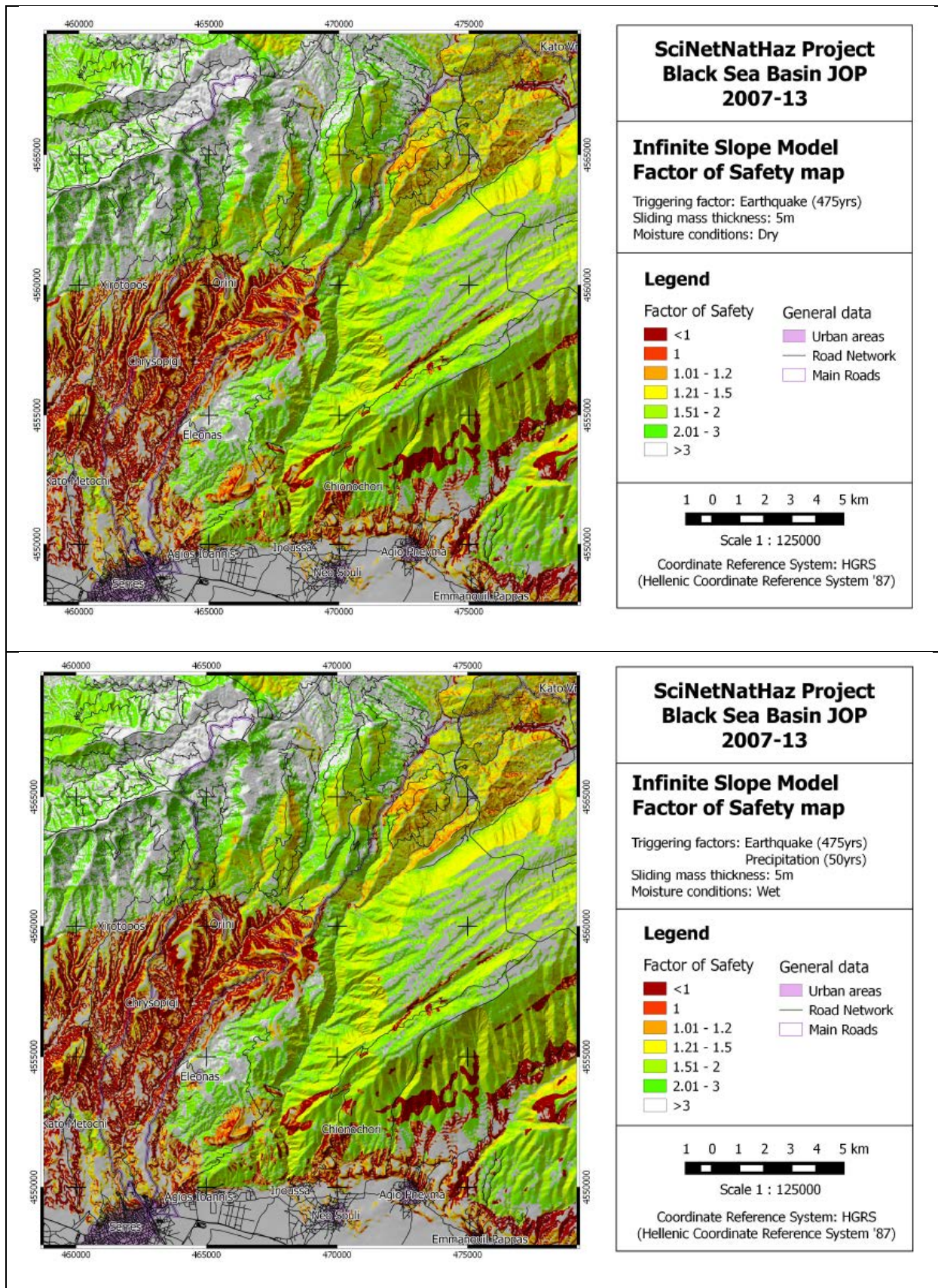


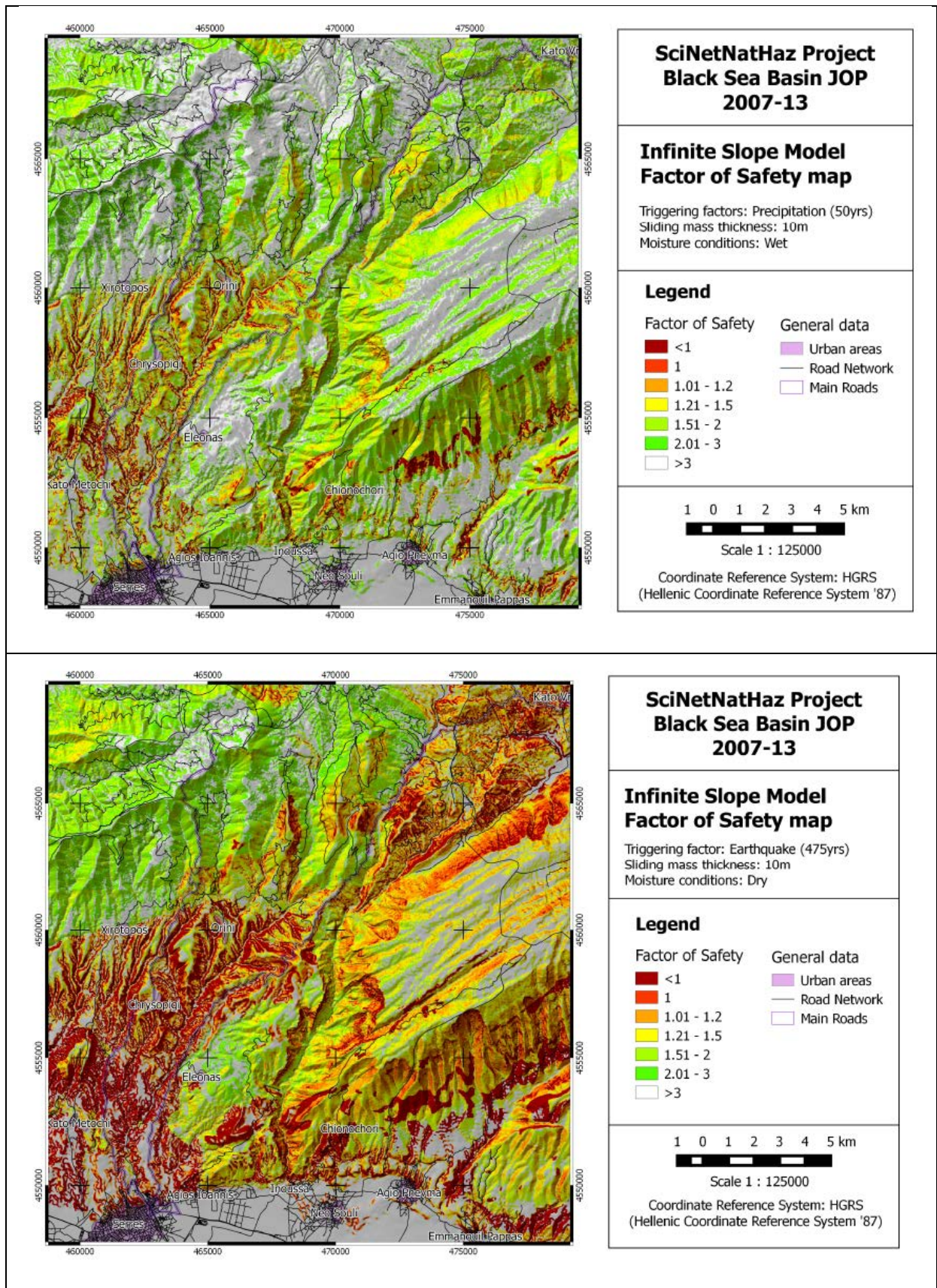


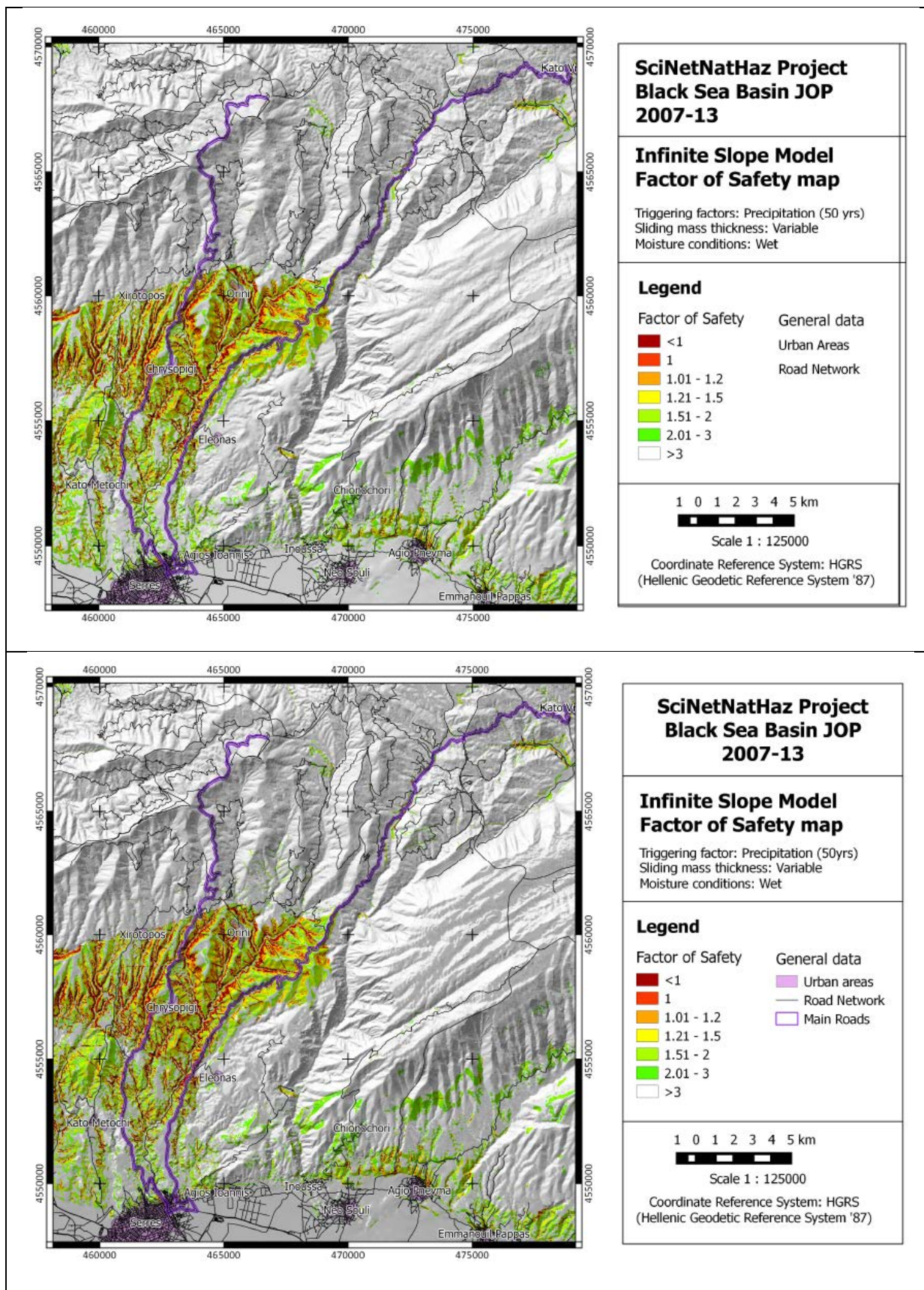


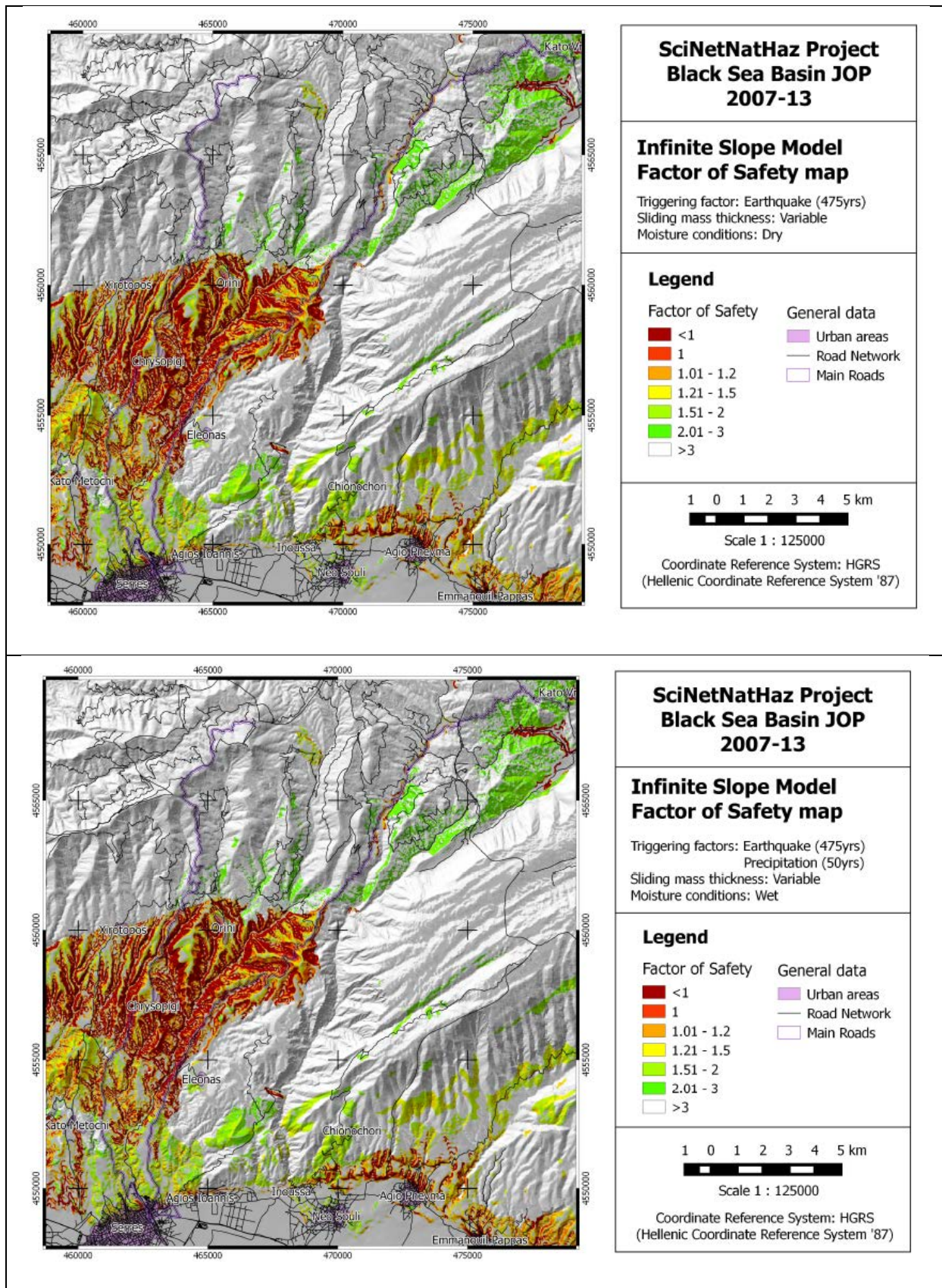


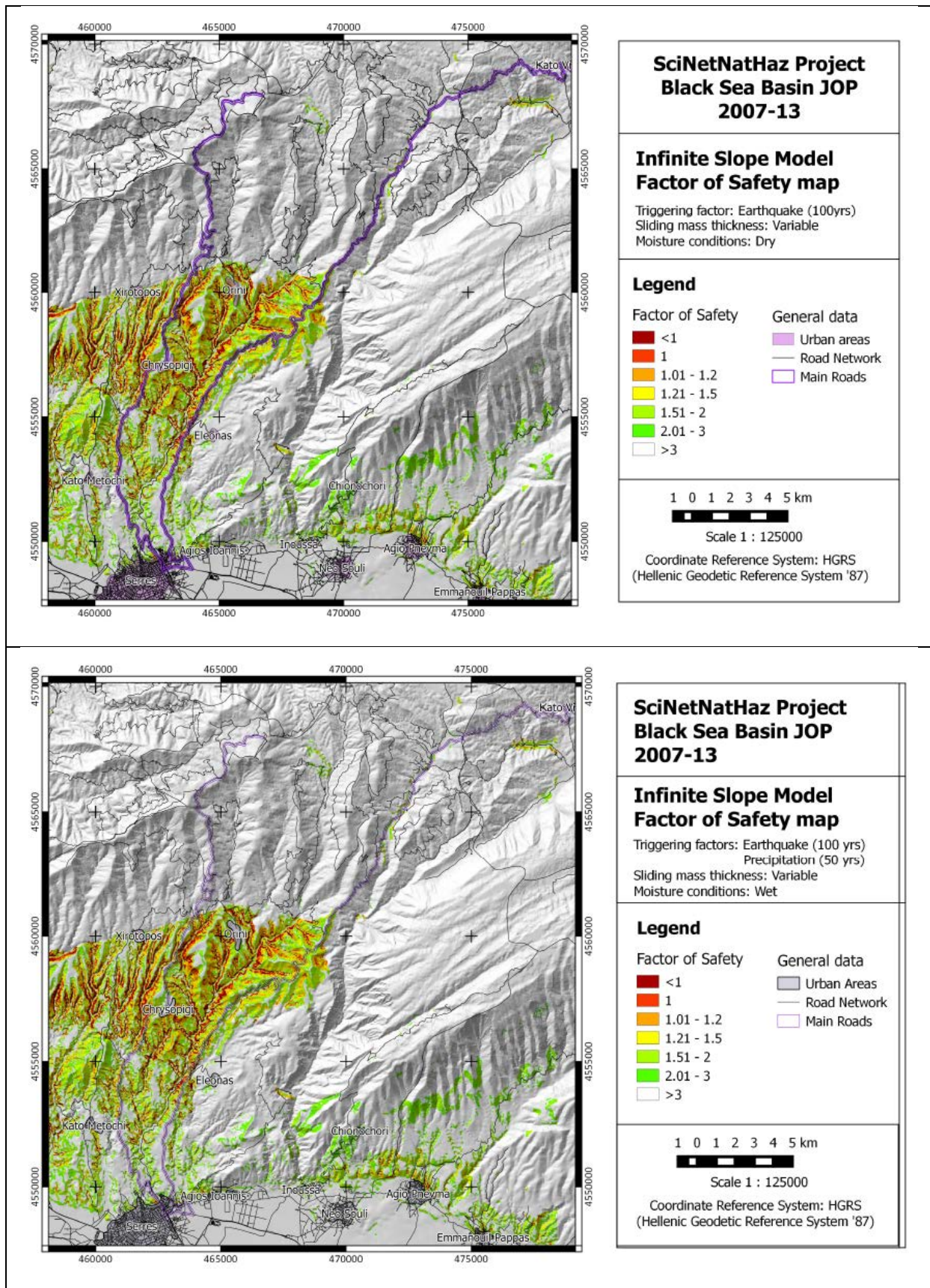


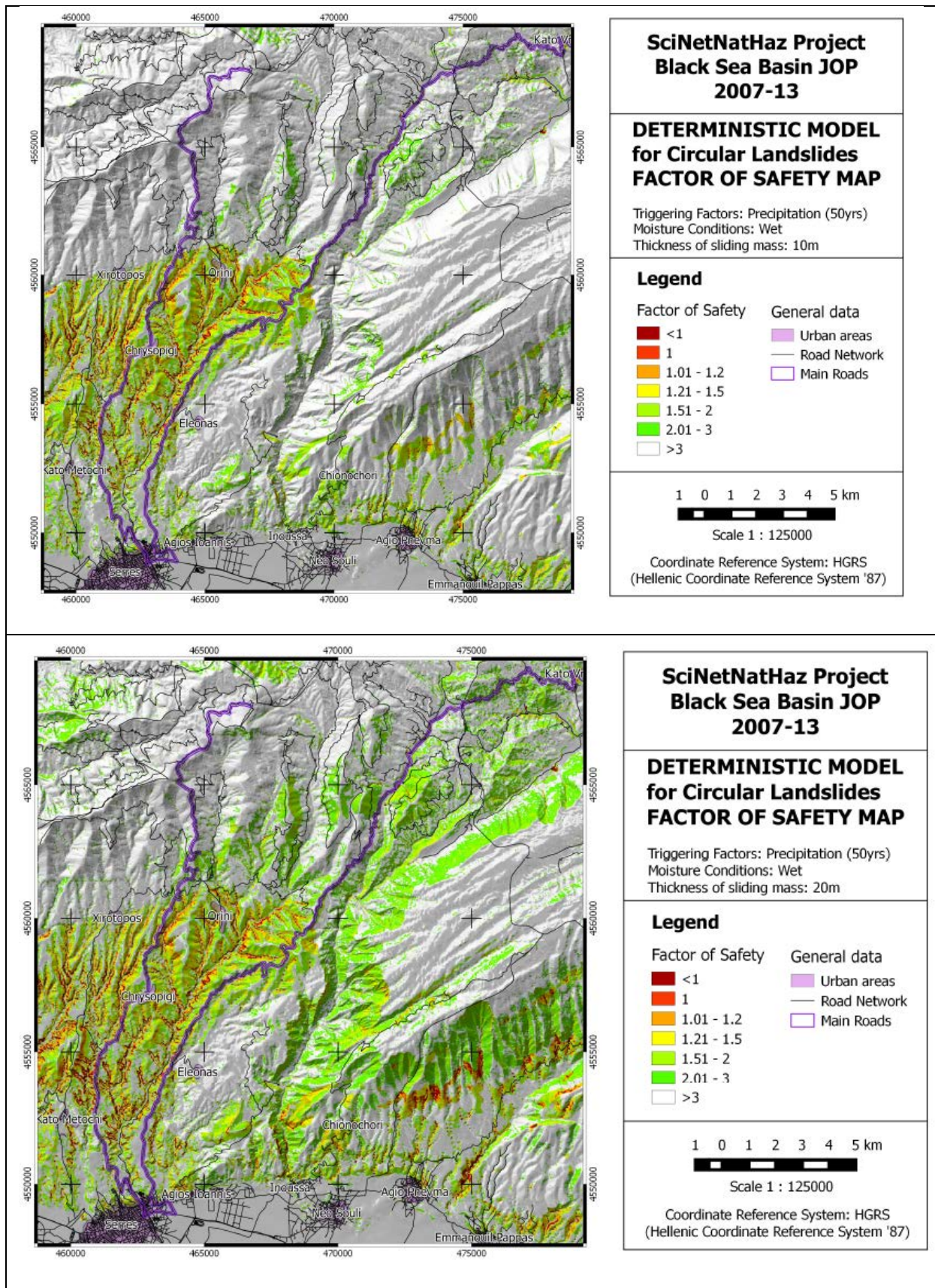


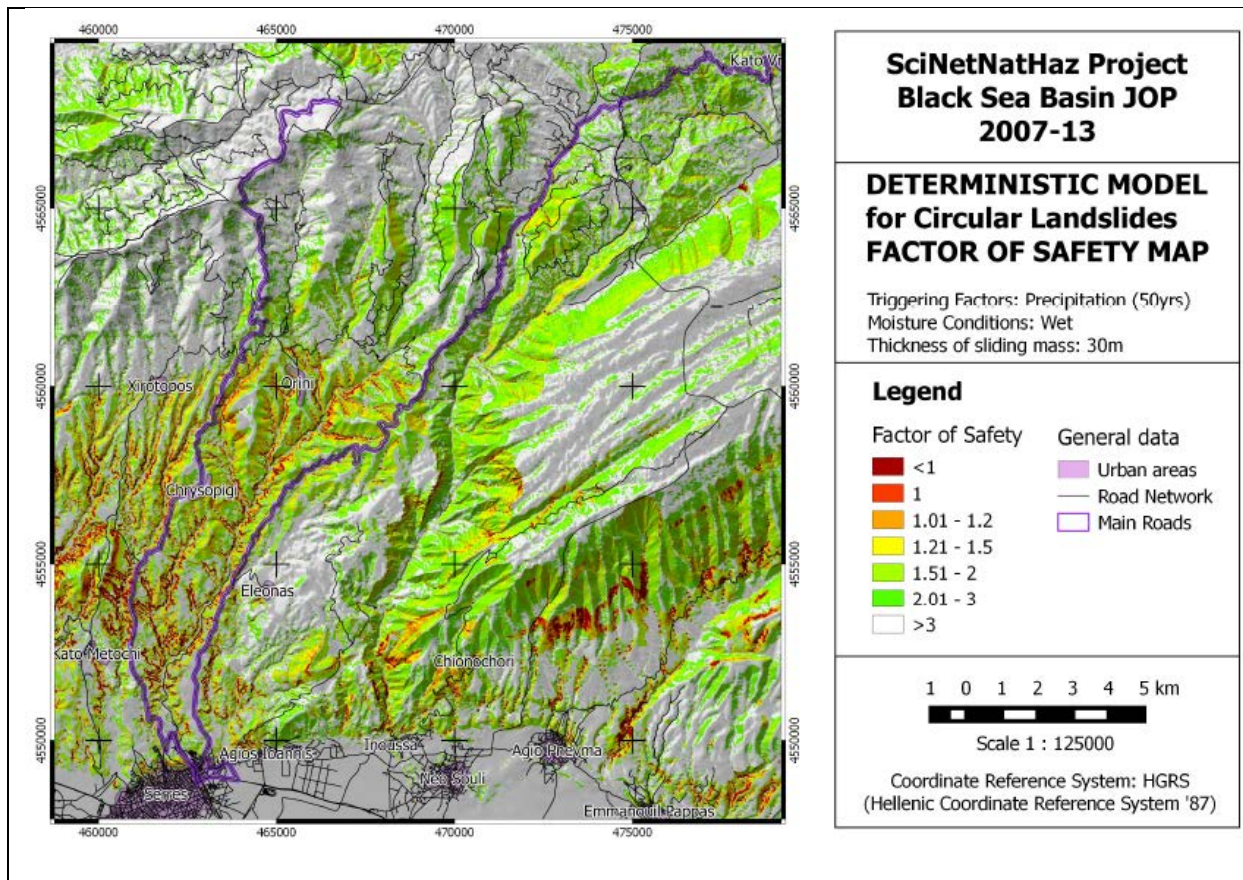


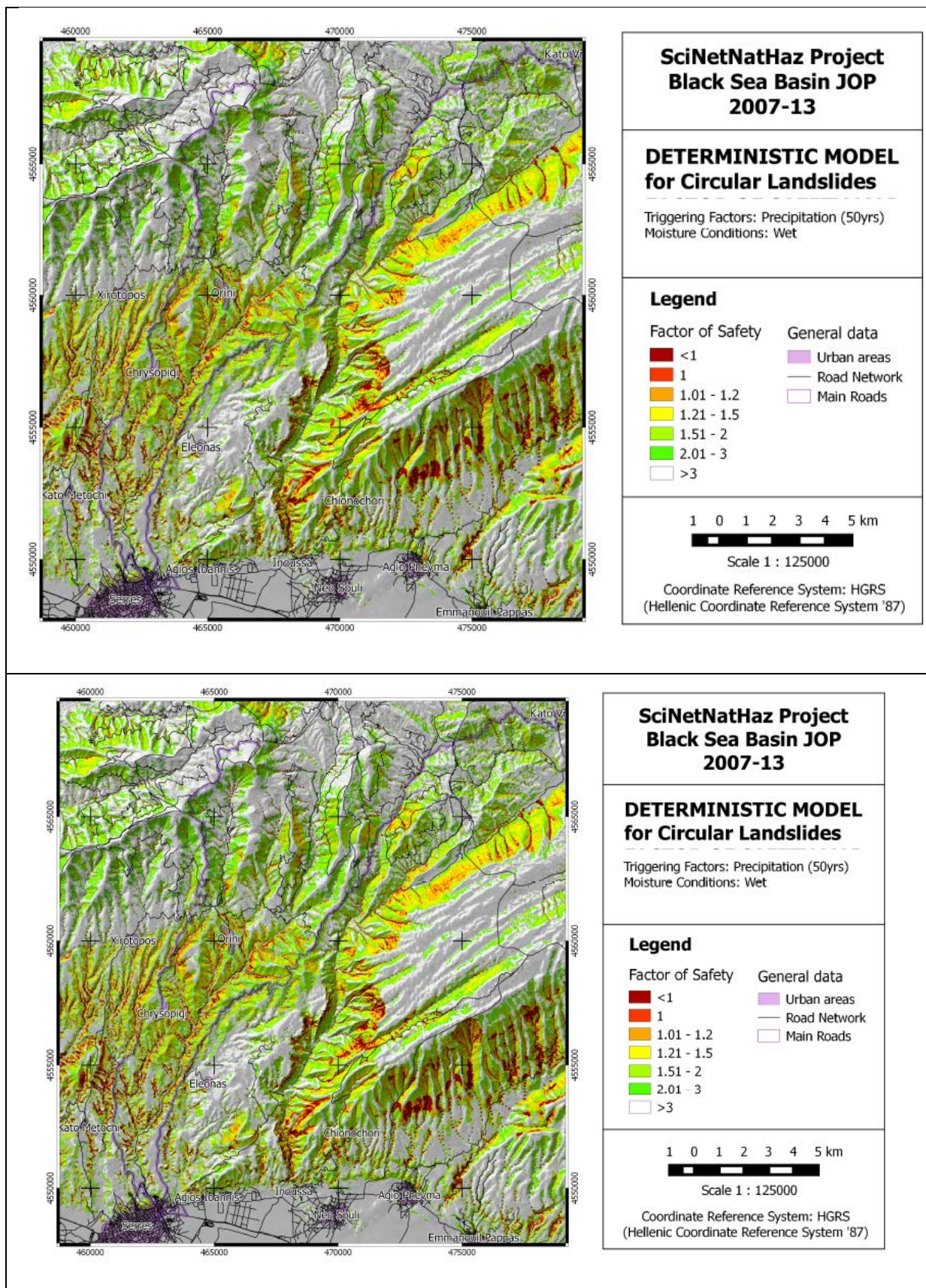




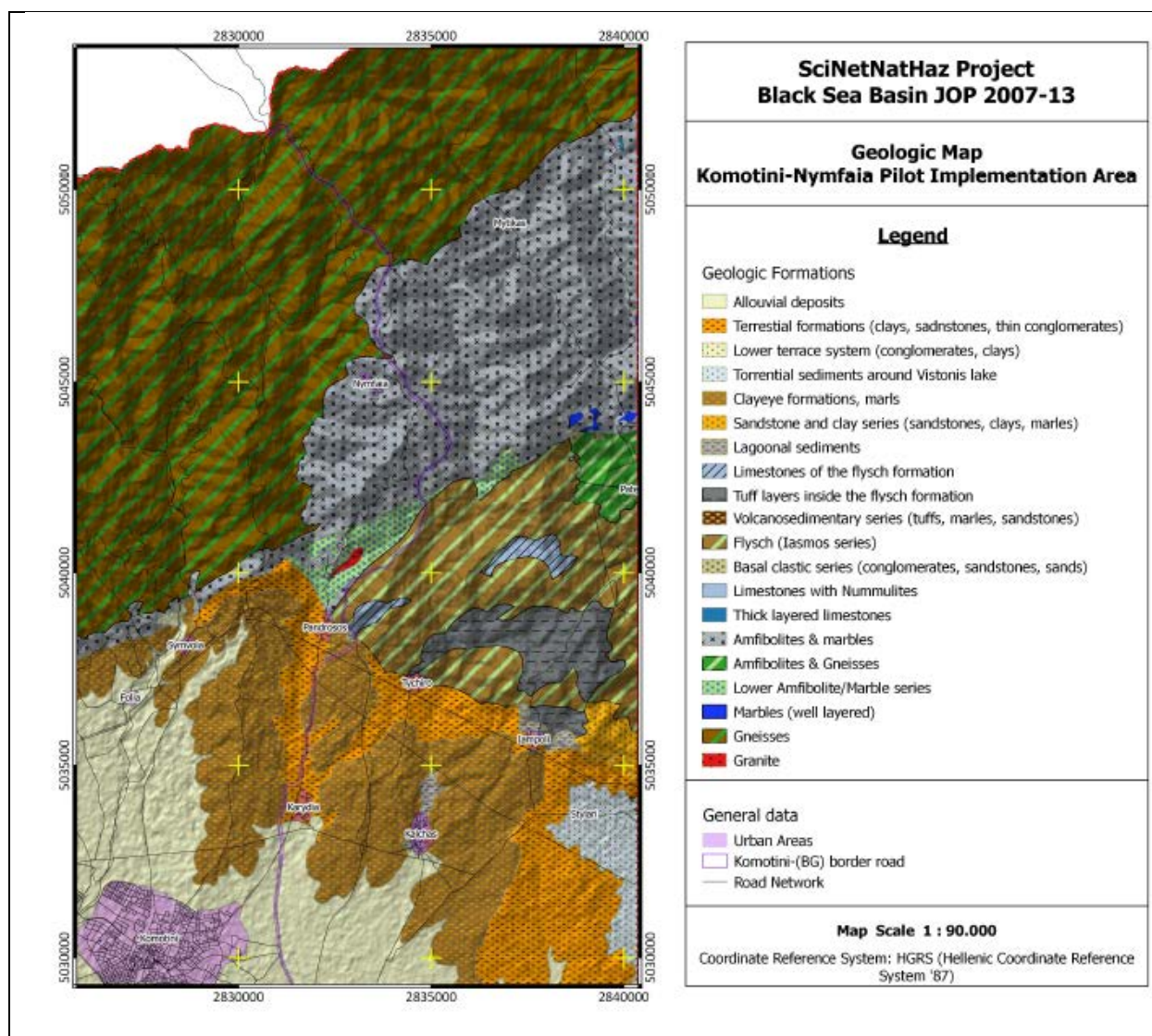


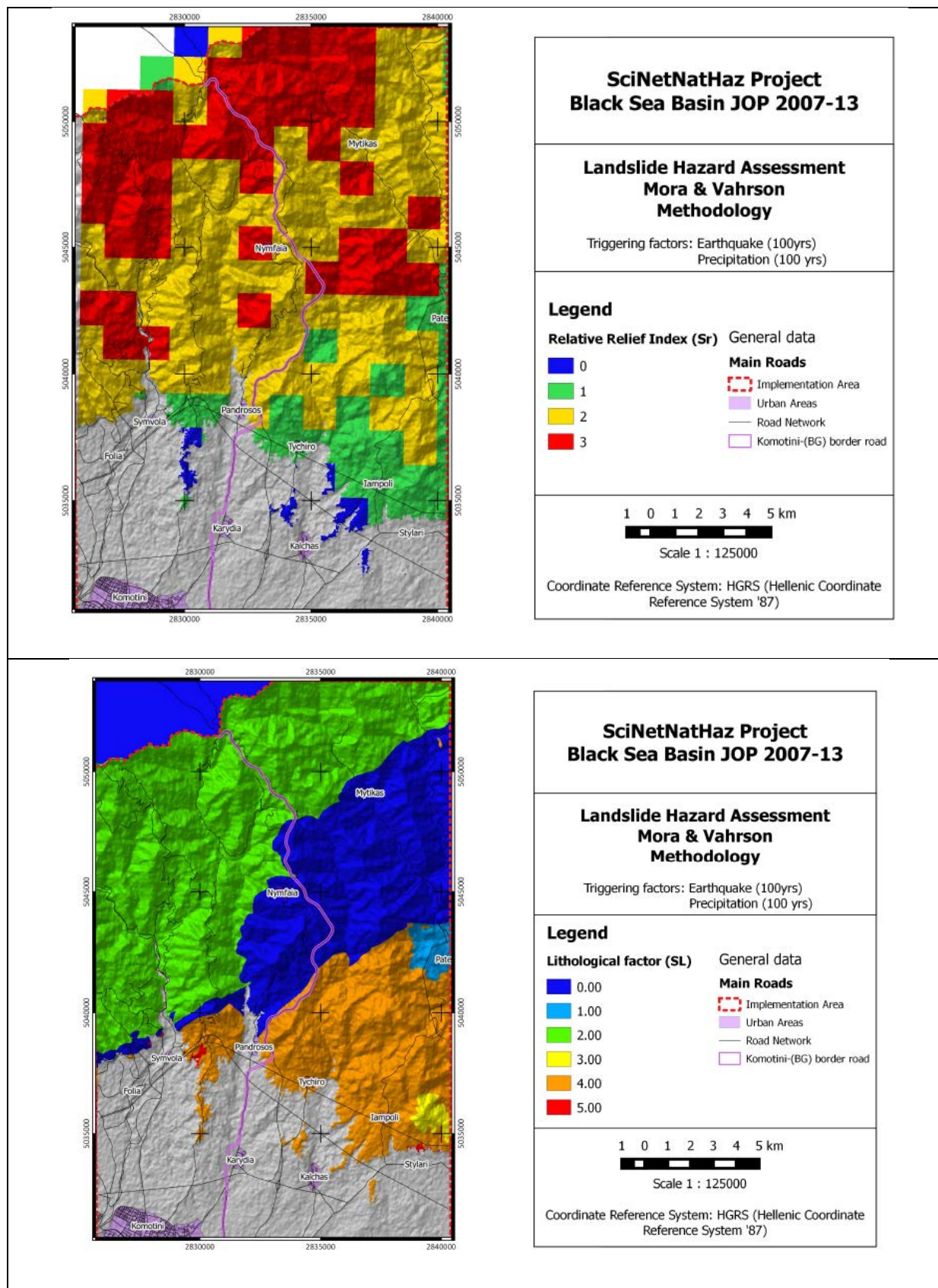


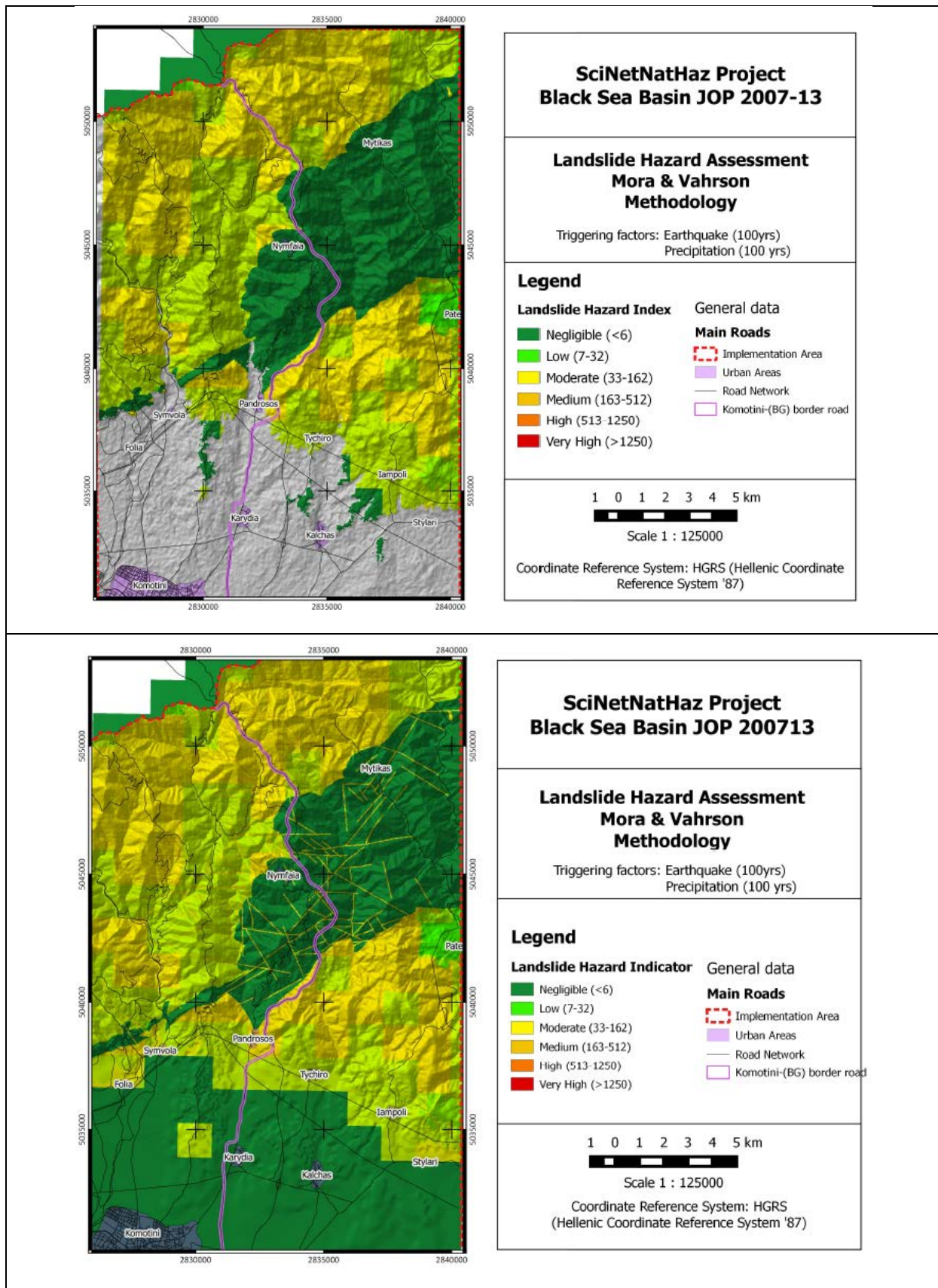


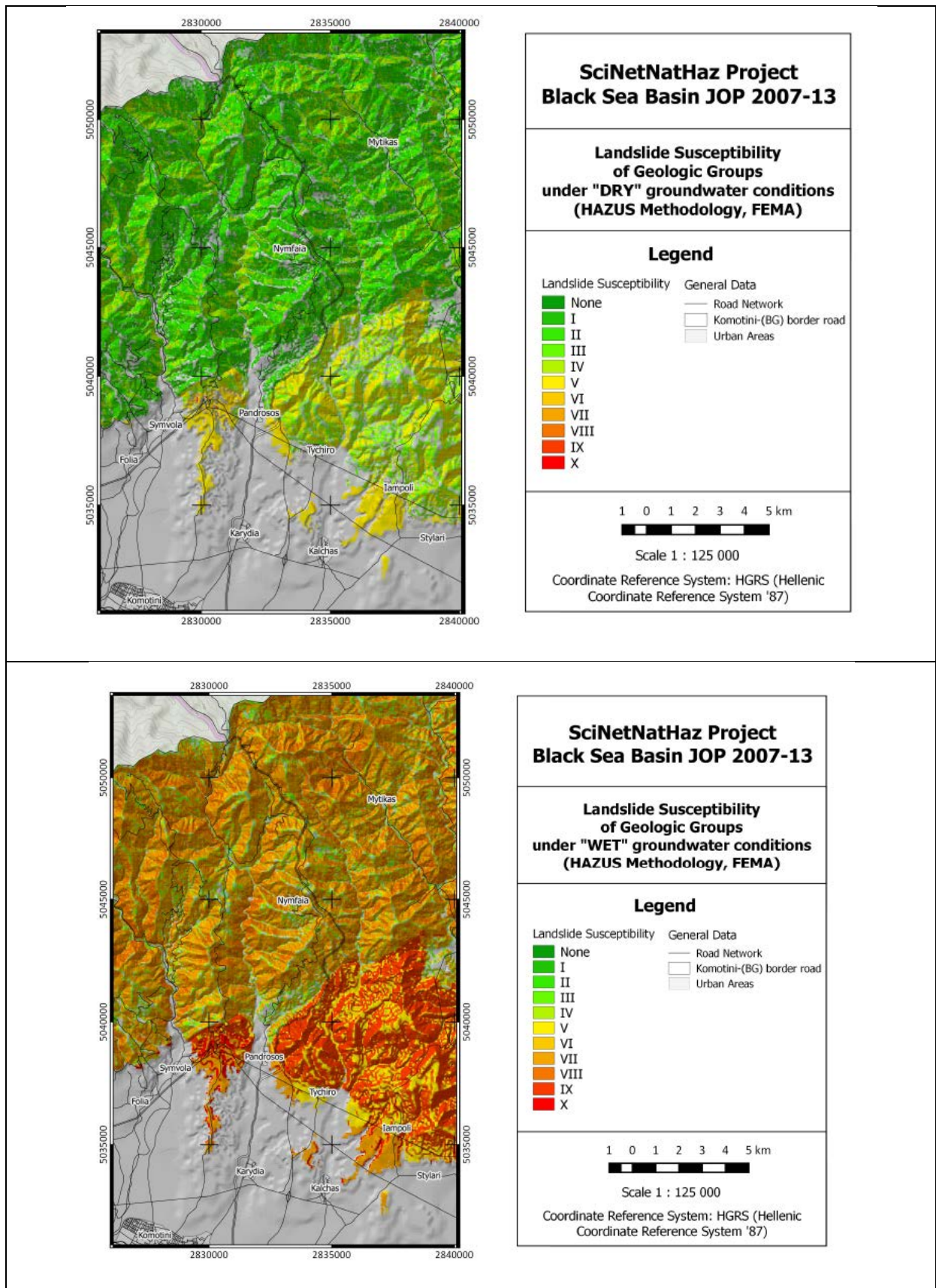


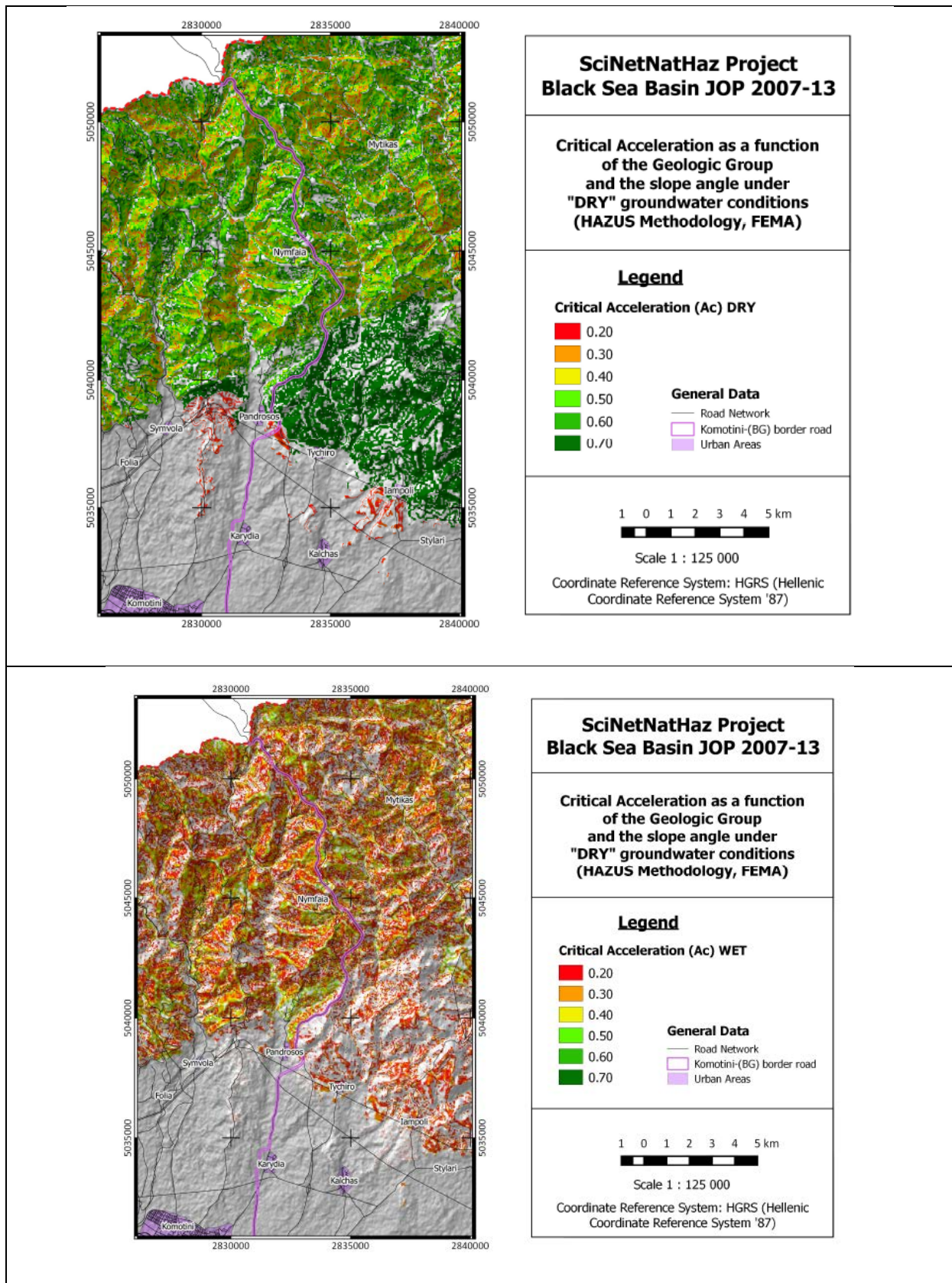
NYMFAIA PIA

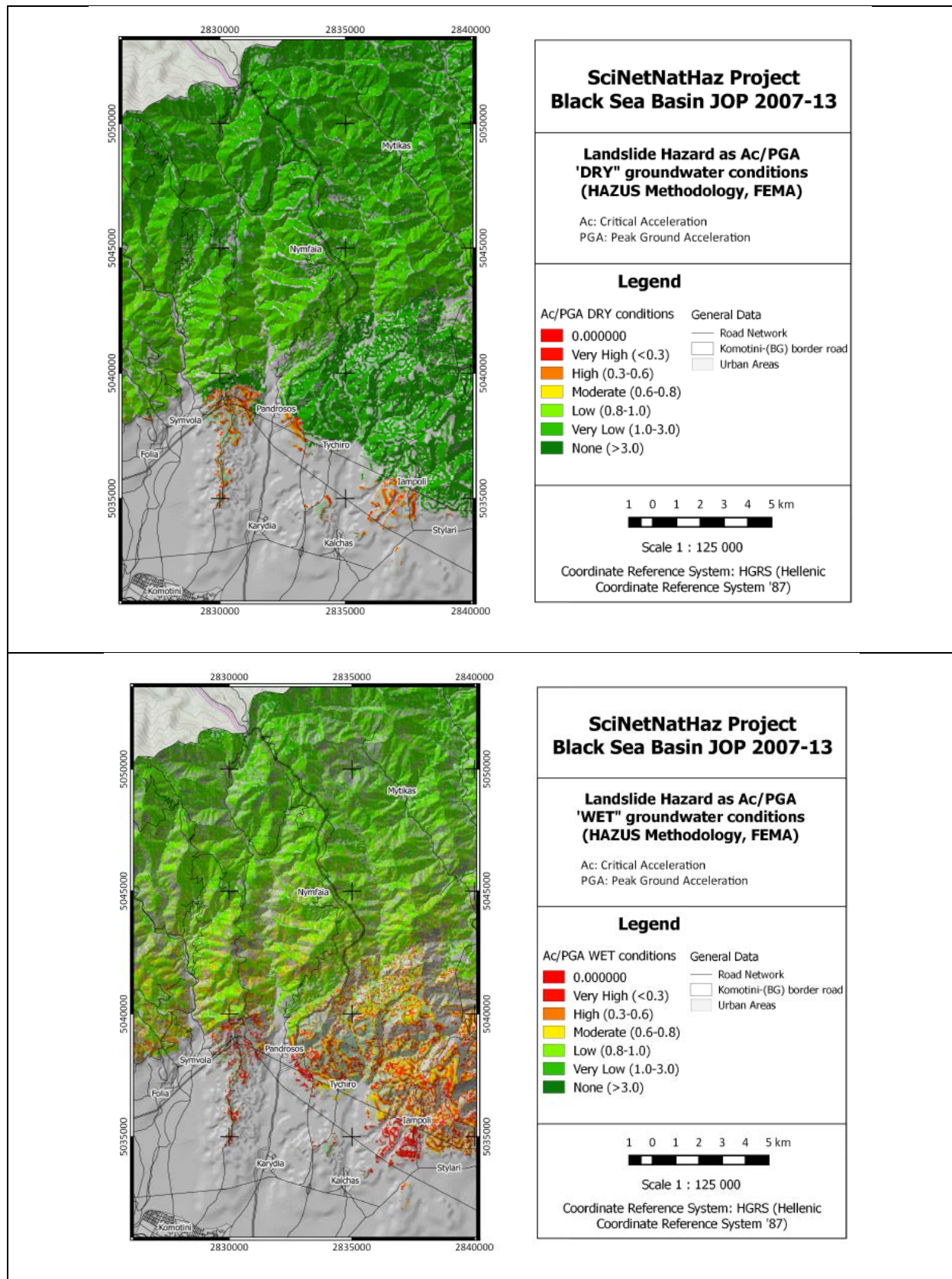


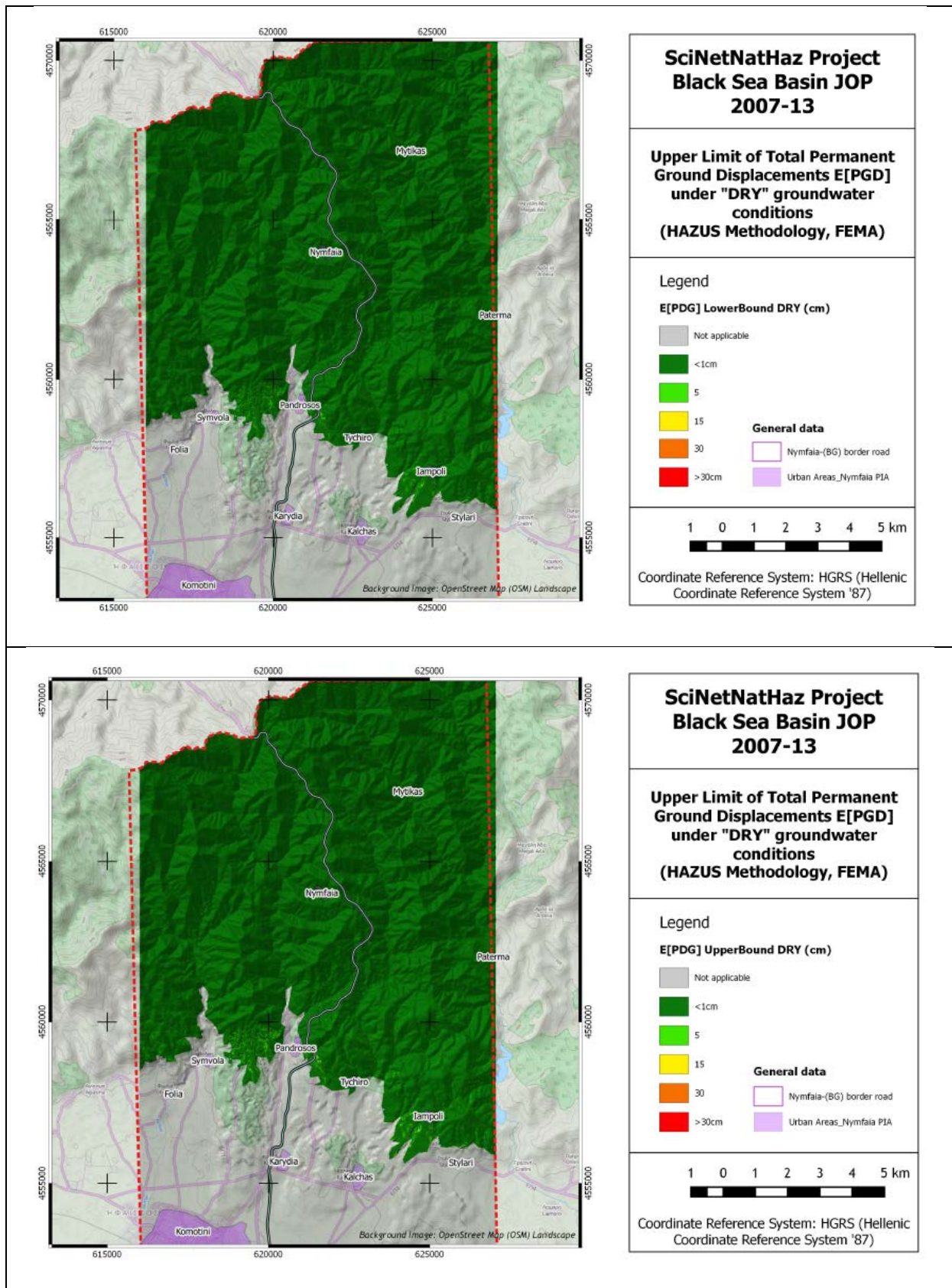


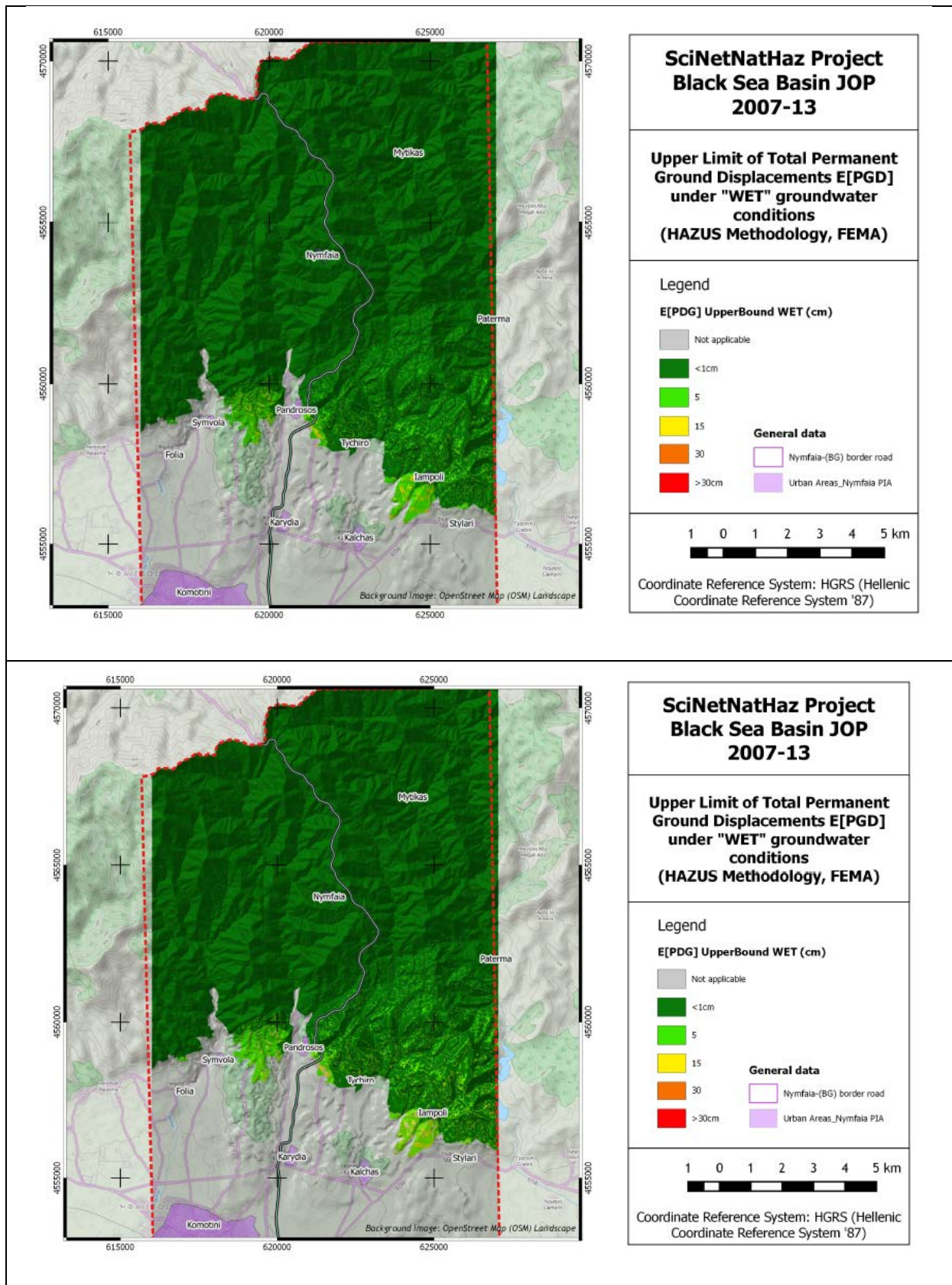


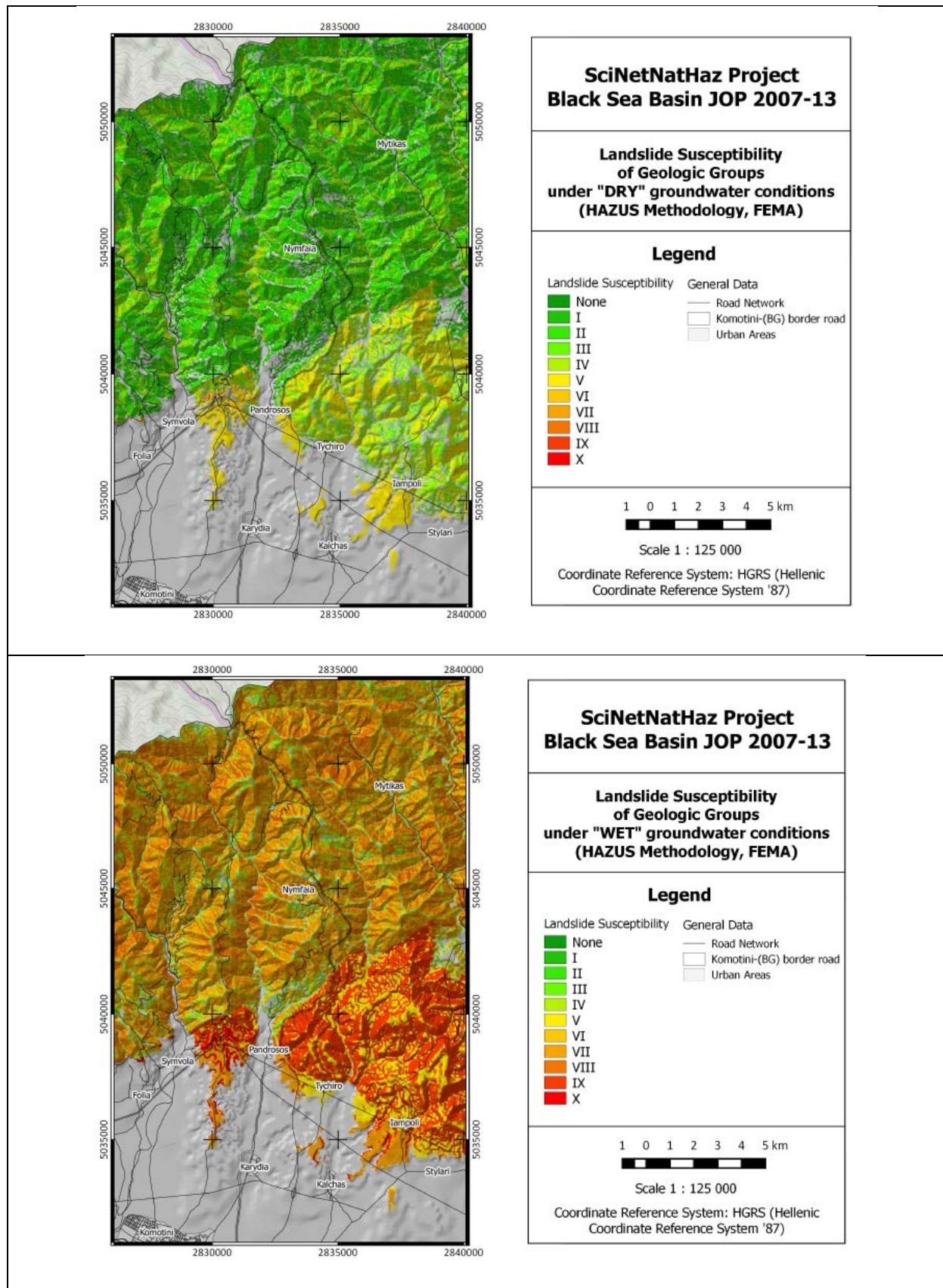


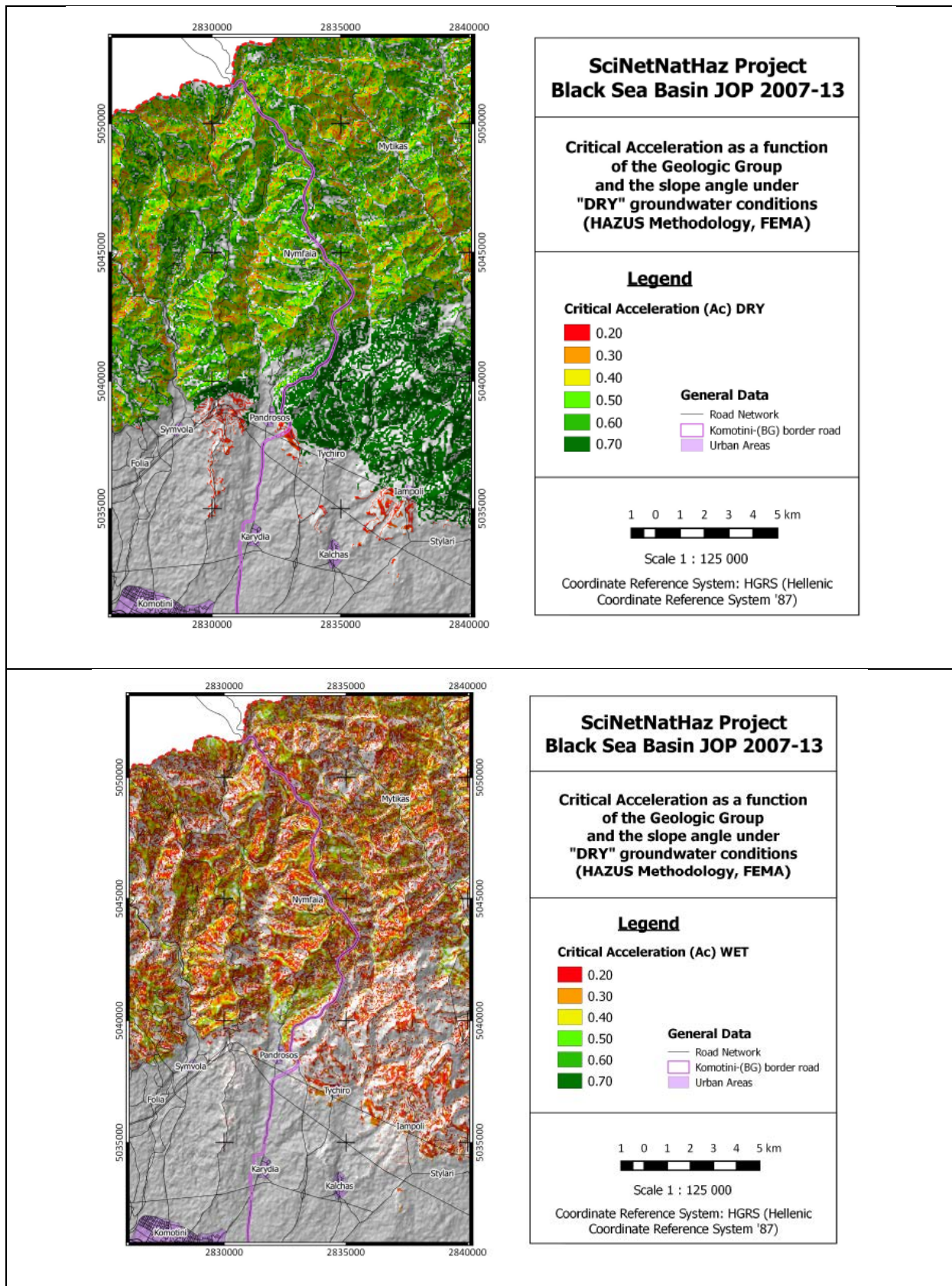


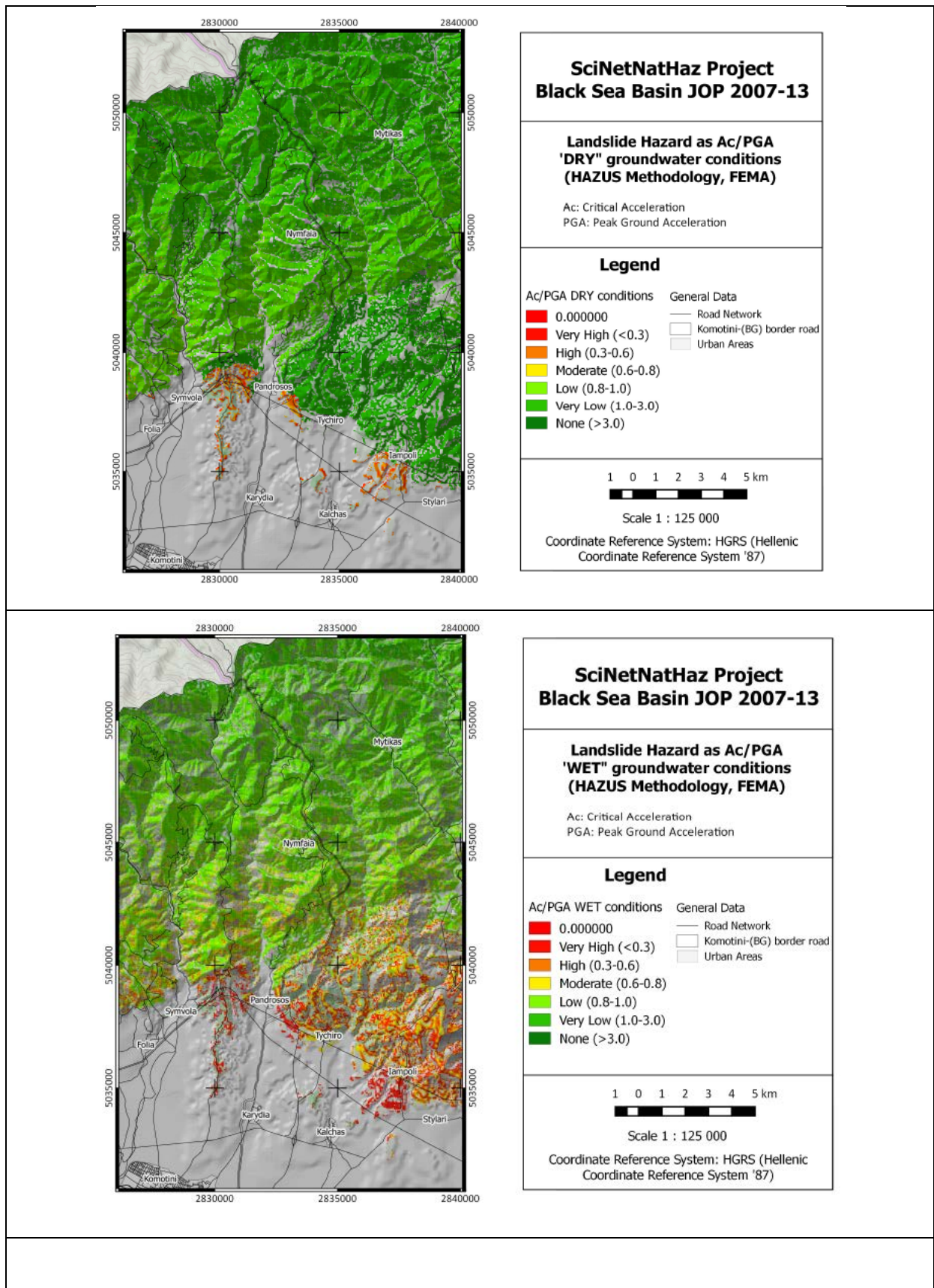


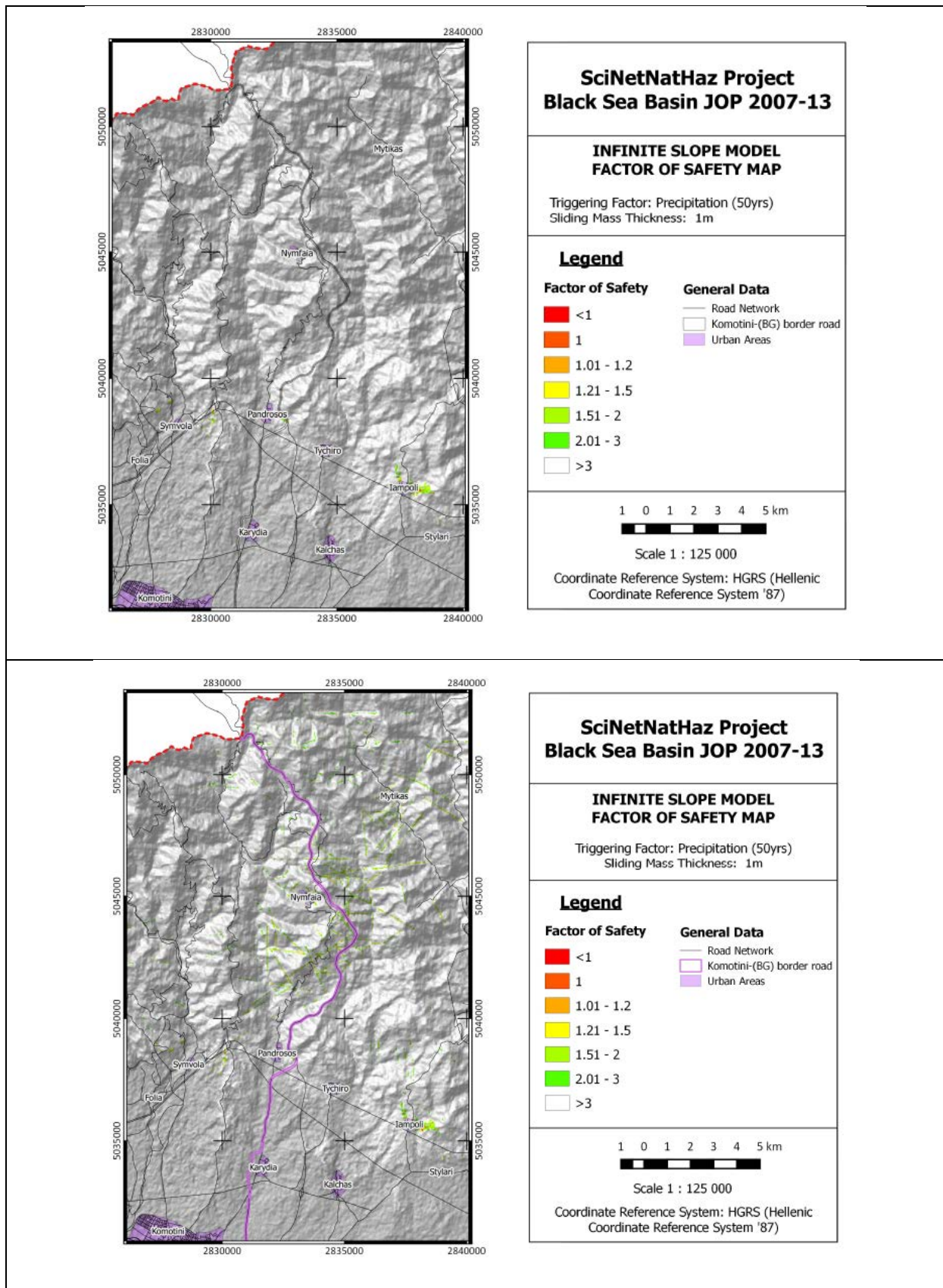


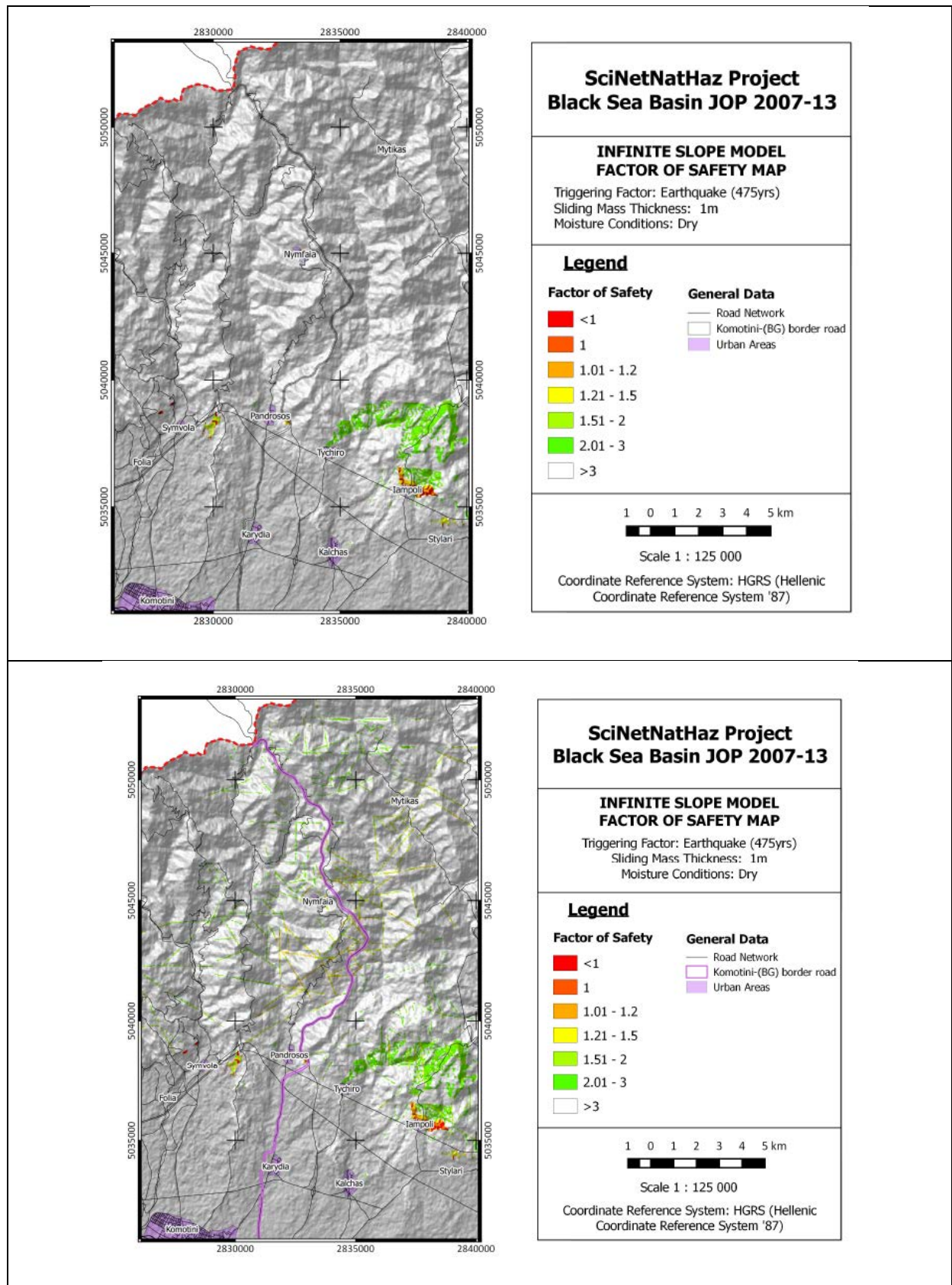


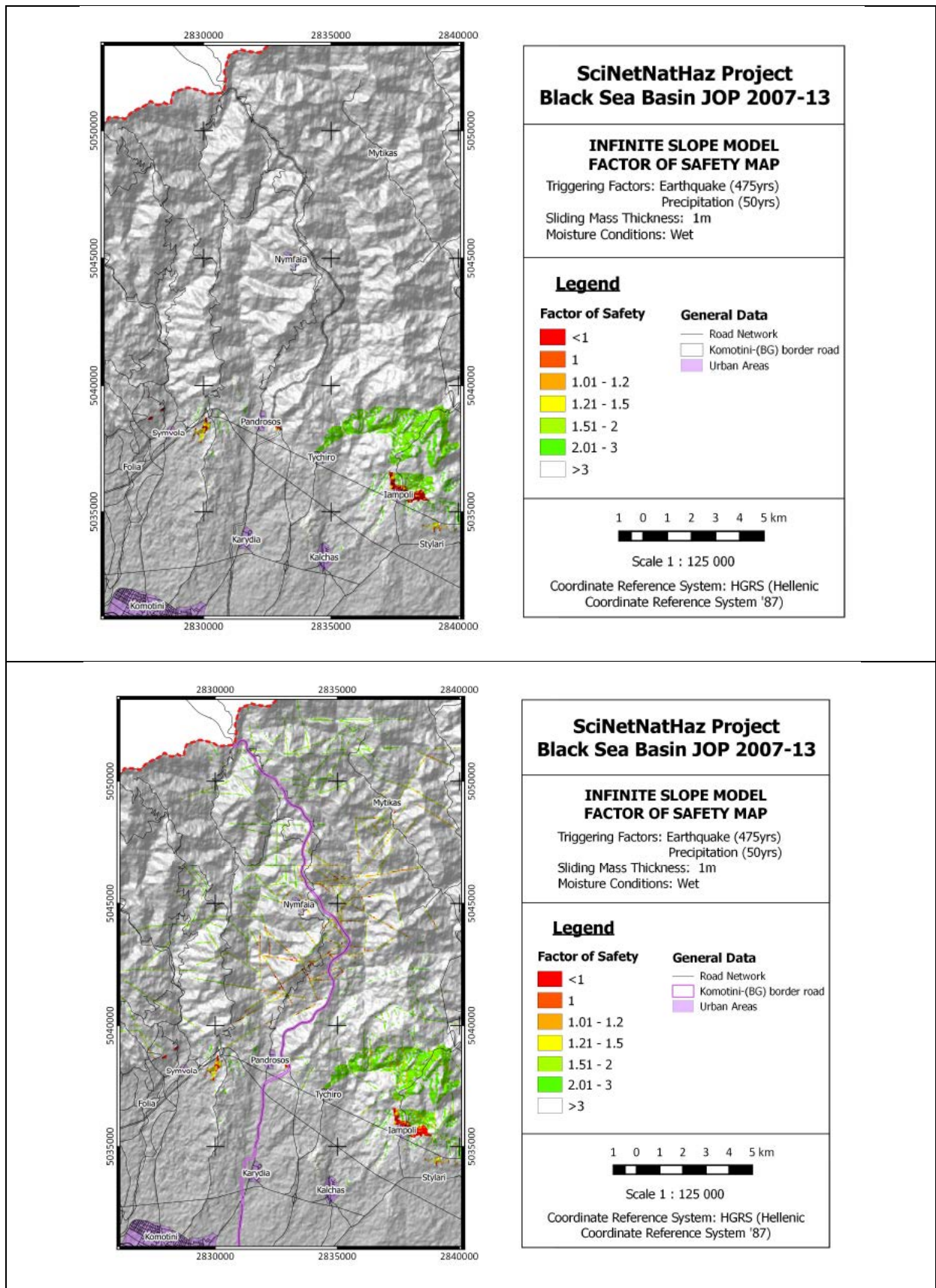


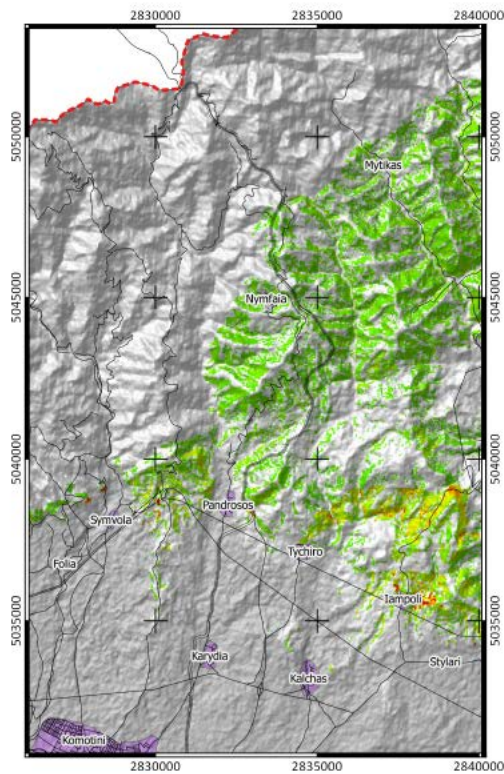












SciNetNatHaz Project Black Sea Basin JOP 2007-13

INFINITE SLOPE MODEL FACTOR OF SAFETY MAP

Triggering Factor: Precipitation (50yrs)
Sliding Mass Thickness: 5m

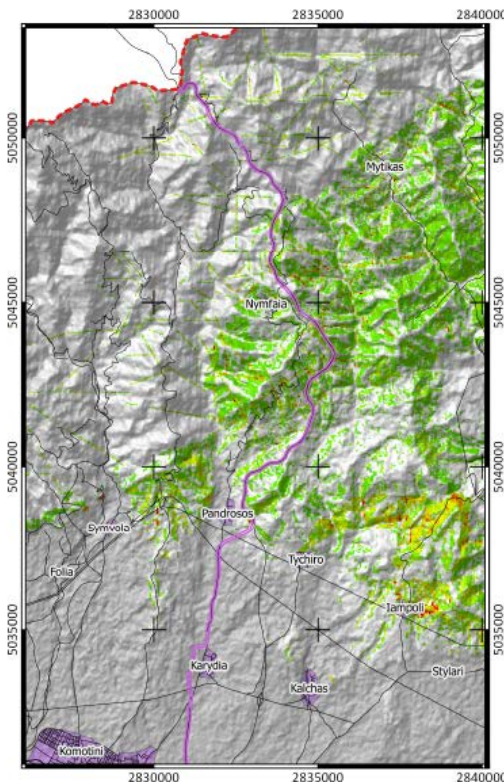
Legend

Factor of Safety	General Data
■ <1	— Road Network
■ 1	— Komotini-(BG) border road
■ 1.01 - 1.2	■ Urban Areas
■ 1.21 - 1.5	
■ 1.51 - 2	
■ 2.01 - 3	
■ >3	

1 0 1 2 3 4 5 km

Scale 1 : 125 000

Coordinate Reference System: HGRS (Hellenic
Coordinate Reference System '87)



SciNetNatHaz Project Black Sea Basin JOP 2007-13

INFINITE SLOPE MODEL FACTOR OF SAFETY MAP

Triggering Factor: Precipitation (50yrs)
Sliding Mass Thickness: 5m

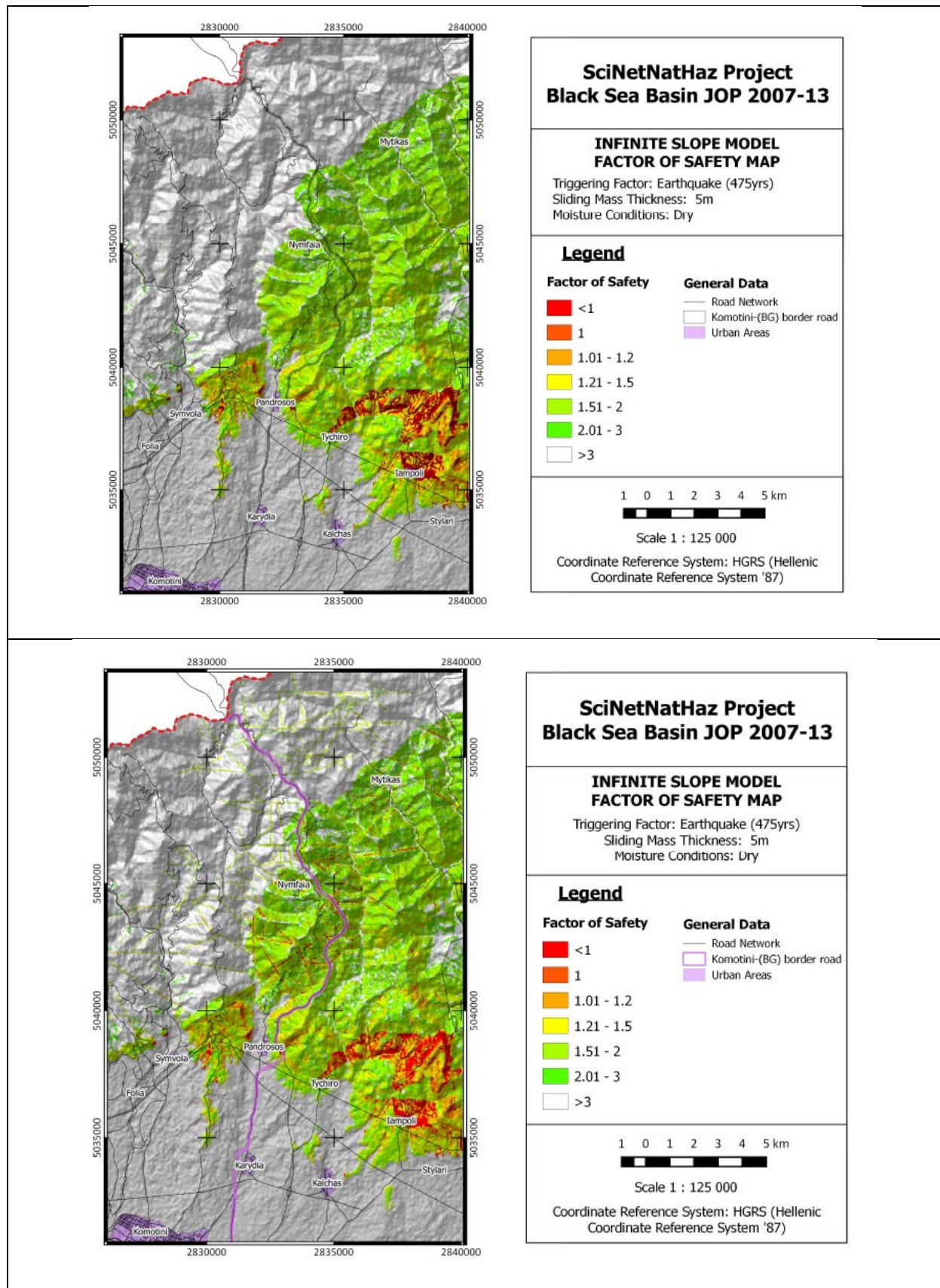
Legend

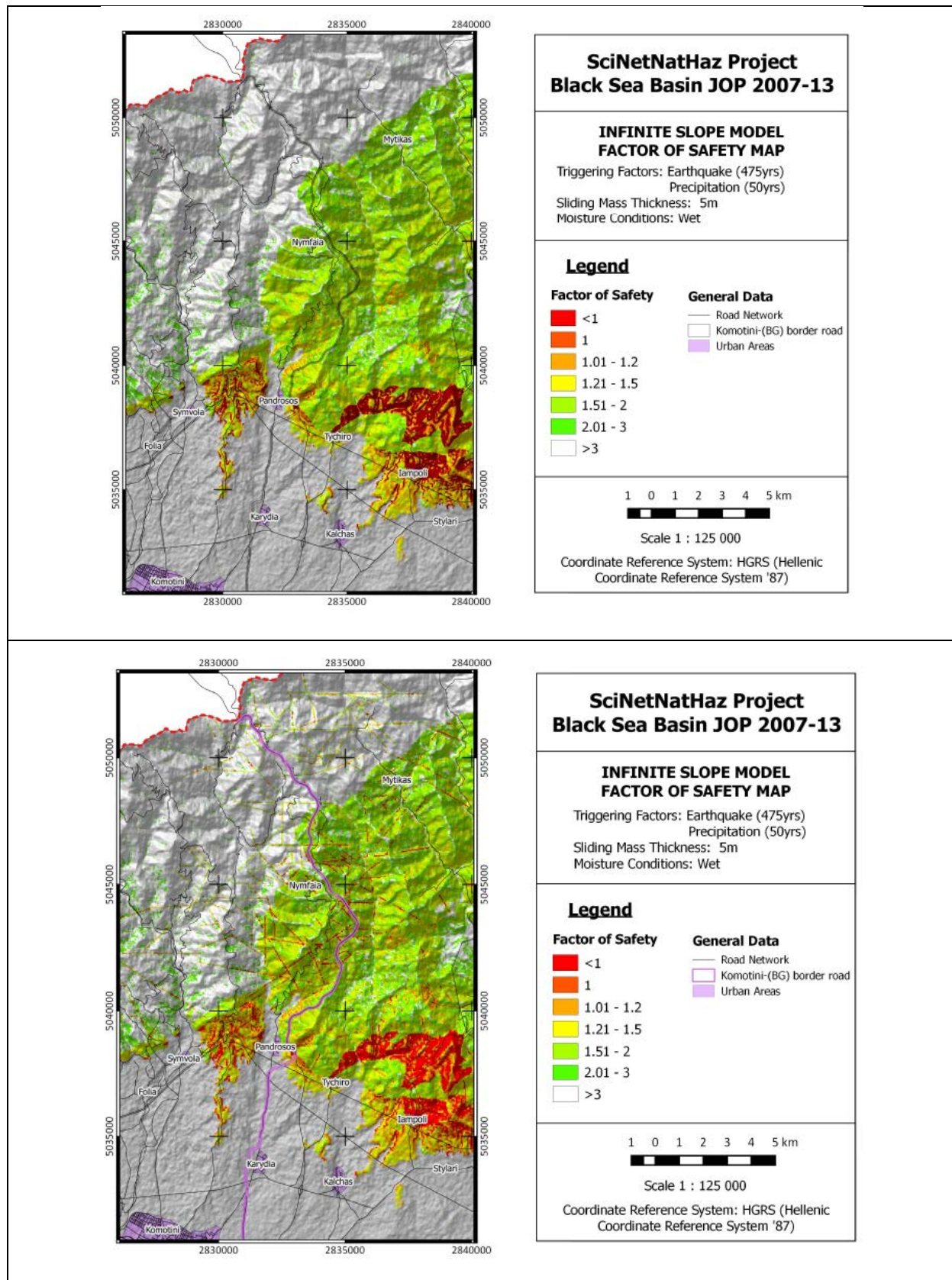
Factor of Safety	General Data
■ <1	— Road Network
■ 1	— Komotini-(BG) border road
■ 1.01 - 1.2	■ Urban Areas
■ 1.21 - 1.5	
■ 1.51 - 2	
■ 2.01 - 3	
■ >3	

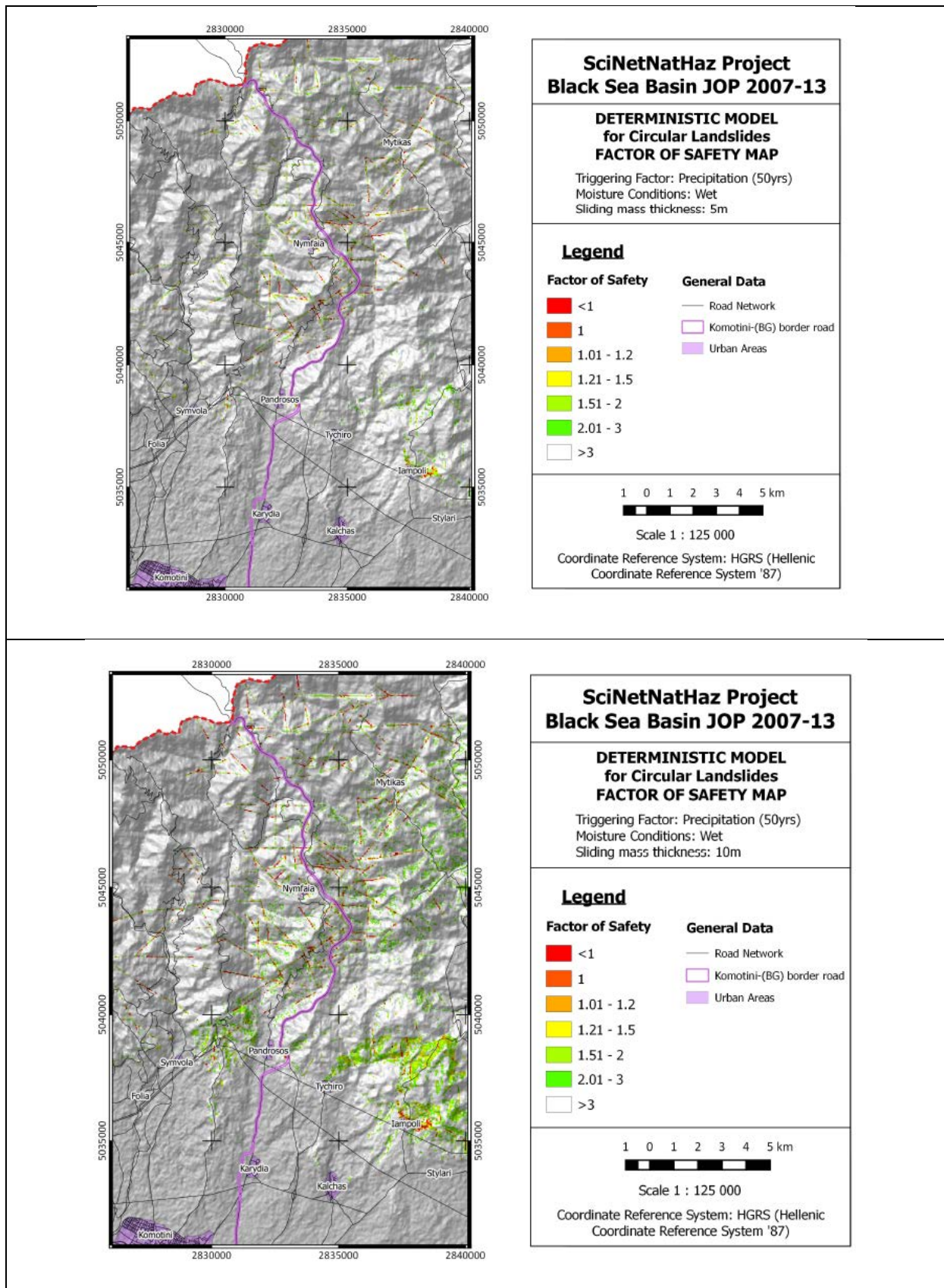
1 0 1 2 3 4 5 km

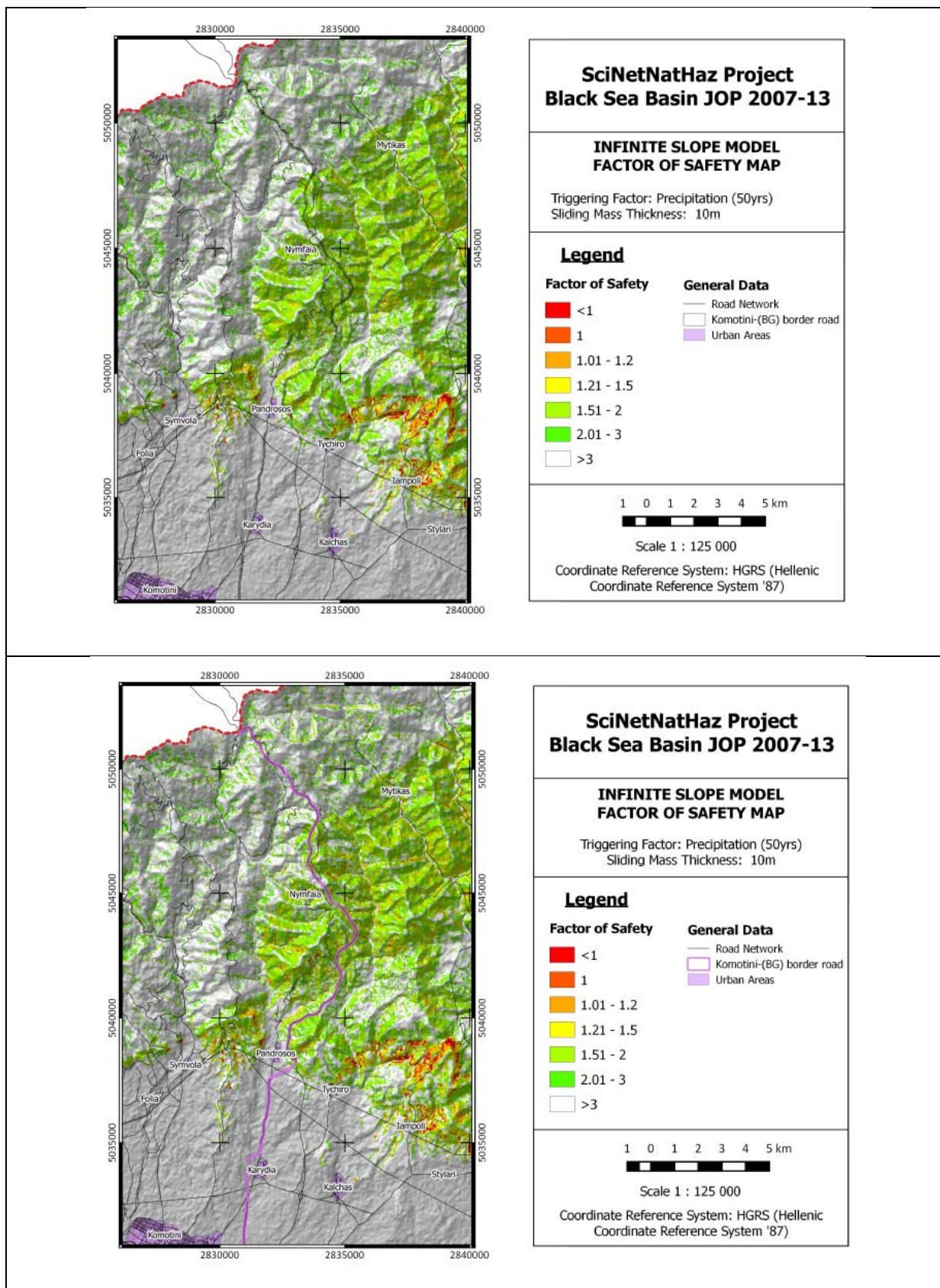
Scale 1 : 125 000

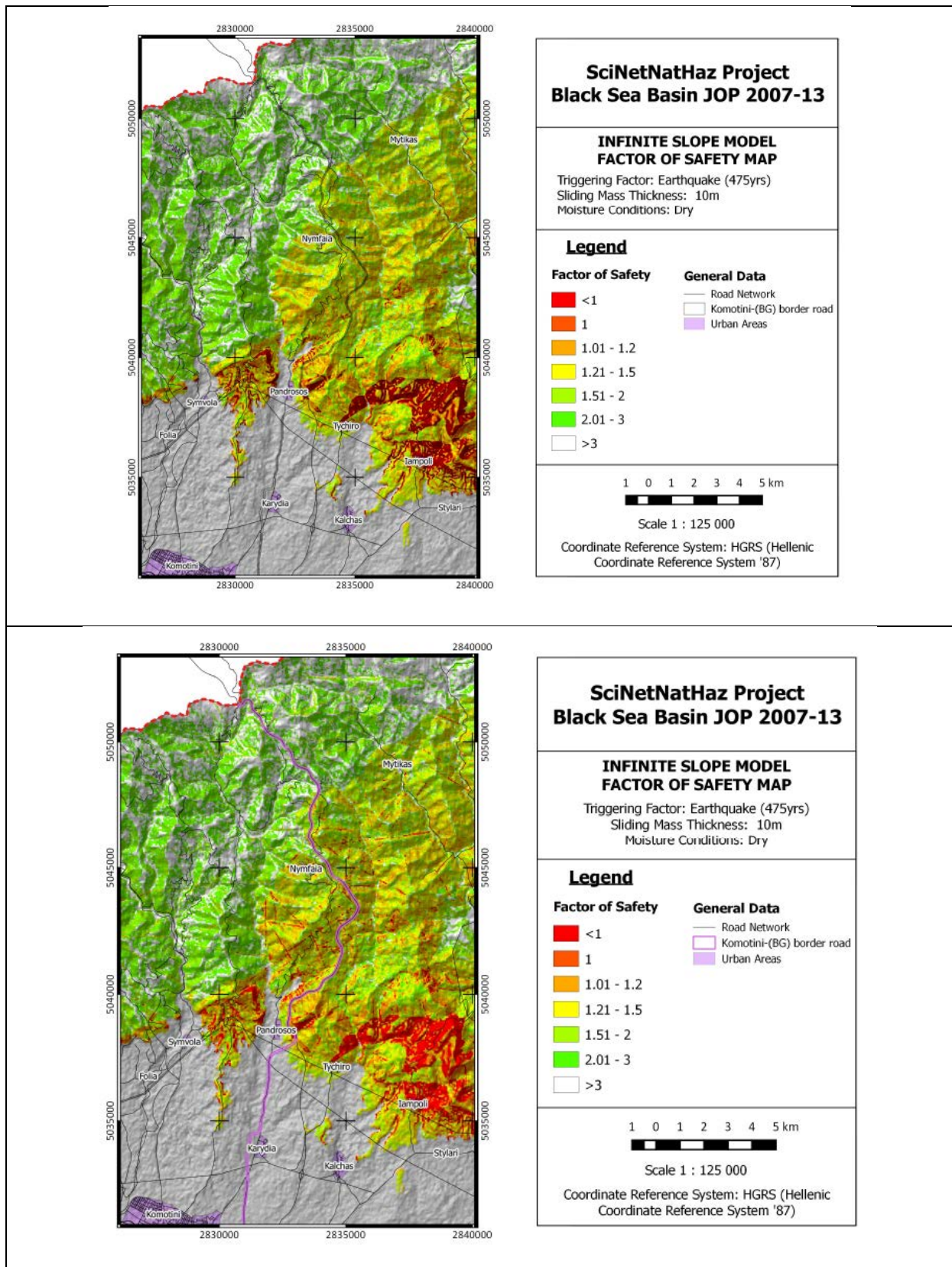
Coordinate Reference System: HGRS (Hellenic
Coordinate Reference System '87)

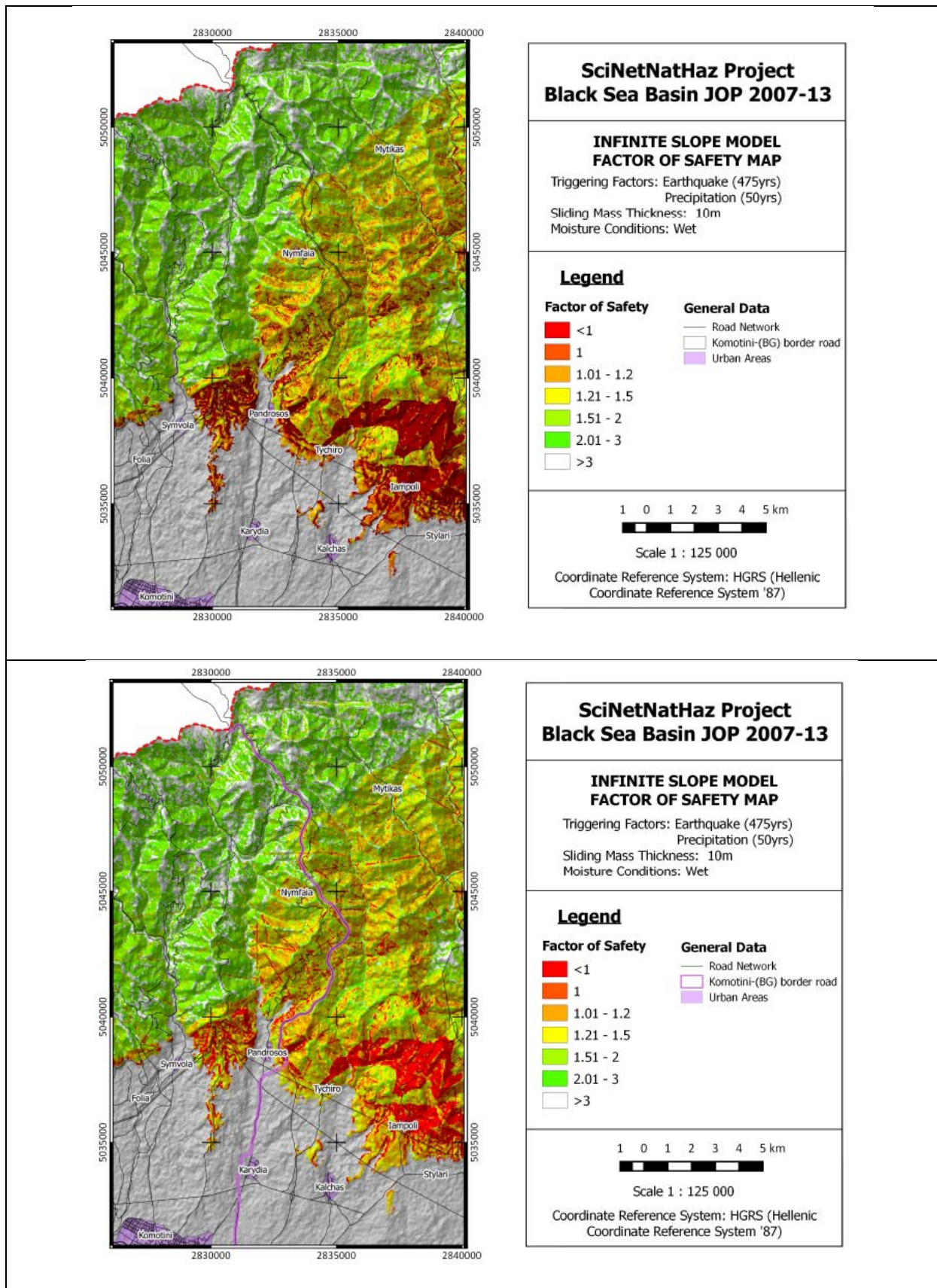


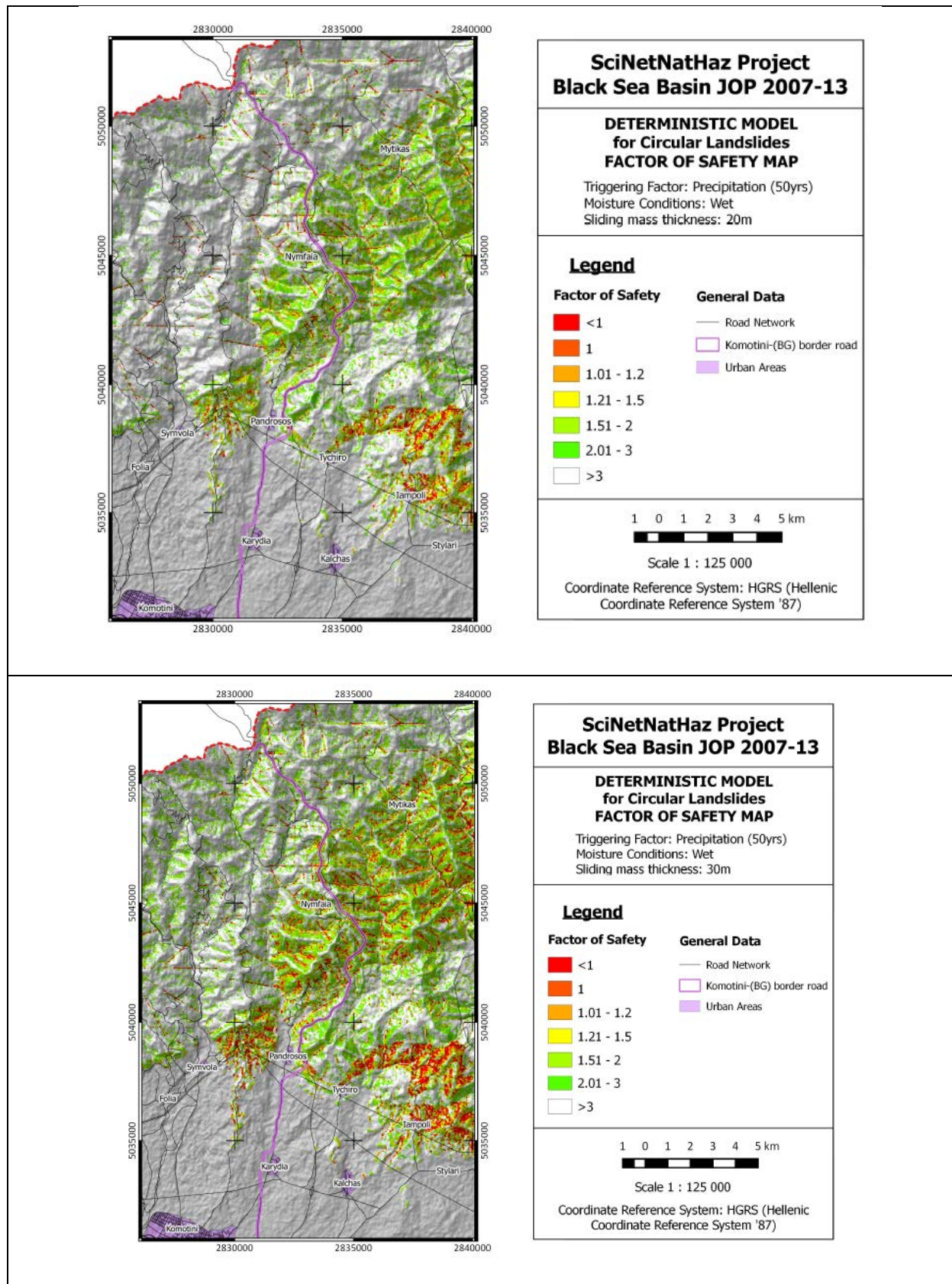












ANNEX B

Geotechnical Parameters for Samsun and Tekirdag Regions - Turkey

GEOTECHNICAL PARAMETERS FOR SAMSUN REGION

Table 23 Geotechnical parameters for Samsun Region

KOD	ϕ	UNIT WEIGHT (kN/m ³)	K _{sat} (m/sec)	Z	S _i
1000	28	19	0.0001	1.5	4
1001	28	19	0.0001	1.5	4
1002	28	19	0.0001	1.5	4
1003	28	19	0.0001	1.5	4
1005	28	19	0.0001	1.5	4
1011_1	22	20	0.00001	1.5	4
1018	22	20	0.00001	1.5	4
1019	22	20	0.00001	1.5	4
102	30	20	0.00003	1.5	4
1027	25	21	0.00001	1.5	4
1036	12	21	0.000001	1.5	5
1037_1	12	21	0.000001	1.5	5
1038	12	21	0.000001	1.5	5
1039	12	21	0.000001	1.5	5
1043	30	20	0.00003	1.5	4
1043_1	30	20	0.00003	1.5	4
1044	30	20	0.00003	1.5	4
1046	30	20	0.00003	1.5	4
1047_1	30	20	0.00003	1.5	4
1049	30	20	0.00003	1.5	4
1054_1	30	20	0.00003	1.5	4
1055	30	20	0.00003	1.5	4
1058	30	20	0.00003	1.5	4
1061	35	22	0.00001	1.5	2
1062	35	22	0.00001	1.5	2
1067_1	35	22	0.00001	1.5	2
1076	22	20	0.00001	1.5	4
110	35	22	0.00001	1.5	2

Table 24 Geotechnical parameters for Samsun Region (Cont' d)

KOD	ϕ	UNIT WEIGHT (kN/m ³)	K _{sat} (m/sec)	Z	S _i
110_1	35	22	0.00001	1.5	2
110_2	35	22	0.00001	1.5	2
112	35	22	0.00001	1.5	2
112	35	22	0.00001	1.5	2
133_1	35	22	0.00001	1.5	2
19	35	22	0.000003	1.5	1
2	28	19	0.0001	1.5	4
224	30	20	0.00003	1.5	4
229_1	30	20	0.00003	1.5	4
2302	35	22	0.000003	1.5	1
245	35	22	0.000003	1.5	1
51	22	20	0.00001	1.5	4
76	22	20	0.00001	1.5	4
77	22	20	0.00001	1.5	4
82	22	20	0.00001	1.5	4
100	35	22	0.000001	1.5	1
1012_1	22	20	0.00001	1.5	4
1021	28	20	0.0001	1.5	4
1023	28	20	0.0001	1.5	4
1028_1	28	20	0.0001	1.5	4
1034	12	21	0.000001	1.5	5
1035	12	21	0.000001	1.5	5
1037	12	21	0.000001	1.5	5
1041	30	20	0.00003	1.5	4
1042	30	20	0.00003	1.5	4
1045	30	20	0.00003	1.5	4
1048	30	20	0.00003	1.5	4
1051	30	20	0.00003	1.5	4
1052	30	20	0.00003	1.5	4
1056	30	20	0.00003	1.5	4
1068	35	22	0.00001	1.5	2
1073	35	22	0.00001	1.5	2

Table 25 Geotechnical parameters for Samsun Region (Cont' d)

KOD	ϕ	UNIT WEIGHT (kN/m ³)	K _{sat} (m/sec)	Z	S _i
1075	22	20	0.00001	1.5	4
1079	28	19	0.0001	1.5	4
1080	28	19	0.0001	1.5	4
109_2	35	22	0.000001	1.5	1
109_5	35	22	0.000001	1.5	1
118	35	22	0.000001	1.5	1
122	35	22	0.000001	1.5	1
123	35	22	0.000001	1.5	1
127	35	22	0.000001	1.5	1
133	35	22	0.00001	1.5	2
160	35	22	0.000001	1.5	1
163_1	35	22	0.000001	1.5	1
227_1	35	22	0.000001	1.5	1
230	35	22	0.000001	1.5	1
231	35	22	0.000001	1.5	1
39	28	19	0.0001	1.5	4
57	22	20	0.00001	1.5	4
59	22	20	0.00001	1.5	4
84	35	22	0.000001	1.5	1
94	35	22	0.000001	1.5	1
95	35	22	0.000001	1.5	1
99	35	22	0.000001	1.5	1
0	45	24	0.0000001	1.5	1

GEOTECHNICAL PARAMETERS FOR TEKIRDAG REGION

Table 26 Geotechnical parameters for Tekirdag Region

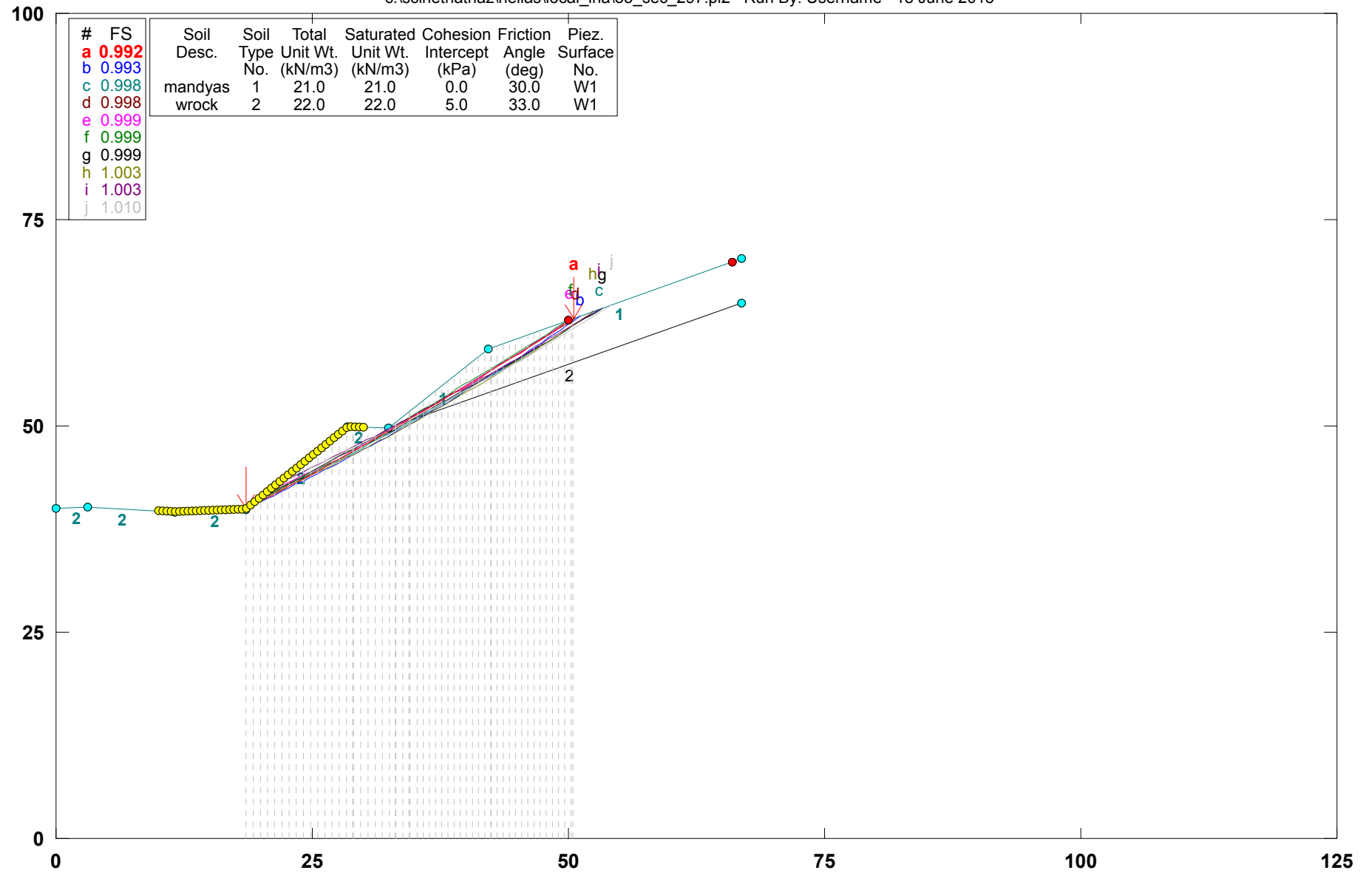
KOD	ϕ	UNIT WEIGHT (kN/m ³)	K _{sat} (m/sec)	Z	S _i
22	28	19	0.0001	1.5	4
79	35	22	0.000001	1.5	1
118	35	22	0.000001	1.5	1
119	35	22	0.000001	1.5	1
122	35	22	0.000001	1.5	1
1000	28	19	0.0001	1.5	4
1005	28	19	0.0001	1.5	4
1009	28	20	0.0001	1.5	4
1014	28	20	0.0001	1.5	4
1016	30	20	0.00003	1.5	4
1017	30	20	0.00003	1.5	4
1024	28	20	0.0001	1.5	4
1025	30	20	0.00003	1.5	4
1026	28	20	0.0001	1.5	4
1030	28	19	0.0001	1.5	4
1037	12	21	0.000001	1.5	5
1039	12	21	0.000001	1.5	5
1026_1	28	20	0.0001	1.5	4
107_2	35	22	0.000001	1.5	1
110_1	35	22	0.00001	1.5	2
110_2	35	22	0.00001	1.5	2
229_5	35	22	0.000001	1.5	1

APPENDIX

Landslide Hazard Assessment at Local Scale in Greece (Serres and Nymfaia Pilot Implementation Areas)

Hellas_Local_Landslide_Hazard Cut slope O5_sec_297

c:\scinetnathaz\hellas\local_lha\o5_sec_297.pl2 Run By: Username 18 June 2015



GSTABL7 v.2 FSmin=0.992

Safety Factors Are Calculated By The Modified Bishop Method



*** GSTABL7 ***

** GSTABL7 by Garry H. Gregory, P.E. **

** Original Version 1.0, January 1996; Current Version 2.003, June 2002 **

(All Rights Reserved-Unauthorized Use Prohibited)

SLOPE STABILITY ANALYSIS SYSTEM

Modified Bishop, Simplified Janbu, or GLE Method of Slices.

(Includes Spencer & Morgenstern-Price Type Analysis)

Including Pier/Pile, Reinforcement, Soil Nail, Tieback,

Nonlinear Undrained Shear Strength, Curved Phi Envelope,

Anisotropic Soil, Fiber-Reinforced Soil, Boundary Loads, Water

Surfaces, Pseudo-Static & Newmark Earthquake, and Applied Forces.

Analysis Run Date: 18 June 2015

Time of Run:

Run By: Username

Input Data Filename: C:\SciNetNatHaz\Hellas\Local_LHA\05_sec_297.in

Output Filename: C:\SciNetNatHaz\Hellas\Local_LHA\05_sec_297.OUT

Unit System: SI

Plotted Output Filename: C:\SciNetNatHaz\Hellas\Local_LHasec_297.PLT

PROBLEM DESCRIPTION: Hellas_Local_Landslide_Hazard

Cut slope 05_sec_297

BOUNDARY COORDINATES

7 Top Boundaries

8 Total Boundaries

Boundary No.	X-Left (m)	Y-Left (m)	X-Right (m)	Y-Right (m)	Soil Type Below Bnd
1	0.00	40.00	3.10	40.22	2
2	3.10	40.22	11.60	39.62	2
3	11.60	39.62	18.50	39.93	2
4	18.50	39.93	28.50	49.93	2
5	28.50	49.93	32.50	49.69	2

6	32.50	49.69	42.20	59.39	1
7	42.20	59.39	66.85	70.22	1
8	32.50	49.69	66.85	64.82	2

Default Y-Origin = 0.00(m)

Default X-Plus Value = 0.00(m)

Default Y-Plus Value = 0.00(m)

ISOTROPIC SOIL PARAMETERS

2 Type(s) of Soil

Soil Type No.	Total Unit Wt. (kN/m3)	Saturated Unit Wt. (kN/m3)	Cohesion Intercept (kPa)	Friction Angle (deg)	Pore Pressure Param. (kPa)	Pressure Constant (kPa)	Piez. Surface No.
1	21.0	21.0	0.0	30.0	0.00	0.0	1
2	22.0	22.0	5.0	33.0	0.00	0.0	1

SOIL NAIL LOAD(S)

10 SOIL NAIL LOAD(S) SPECIFIED

Nail No.	X-Pos (m)	Y-Pos (m)	Nail Dia (mm)	Tendon Dia (mm)	Spacing (m)	Inclin. (deg)	Length (m)
1	19.50	40.93	89.0	25.0	3.00	10.00	6.00
2	21.62	43.05	89.0	25.0	3.00	10.00	6.00
3	23.74	45.17	89.0	25.0	3.00	10.00	6.00
4	25.86	47.29	89.0	25.0	3.00	10.00	6.00
5	27.98	49.41	89.0	25.0	3.00	10.00	6.00
6	33.50	50.69	89.0	25.0	3.00	10.00	6.00
7	35.62	52.81	89.0	25.0	3.00	10.00	6.00
8	37.74	54.93	89.0	25.0	3.00	10.00	6.00
9	39.86	57.05	89.0	25.0	3.00	10.00	6.00
10	41.98	59.17	89.0	25.0	3.00	10.00	6.00

SOIL NAIL LOAD DATA

Soil Nail No. 1 3 Load Points Apply to This Nail

Load Diagram Type = 3

POINT NO.	X-COORD.(m)	Y-COORD.(m)	FORCE(kN)
1	19.50	40.93	10.00
2	21.72	40.49	38.55
3	25.41	39.89	0.00

Allowable Pullout Stress = 120.0(kPa)

Allowable Tendon Stress = 434782.6

Allowable Nail Head Load = 30.0(kN)

Soil Nail No. 2 3 Load Points Apply to This Nail

Load Diagram Type = 3

POINT NO.	X-COORD.(m)	Y-COORD.(m)	FORCE(kN)
1	21.62	43.05	10.00
2	23.81	42.61	38.55
3	27.53	42.01	0.00

Allowable Pullout Stress = 120.0(kPa)

Allowable Tendon Stress = 434782.6

Allowable Nail Head Load = 30.0(kN)

Soil Nail No. 3 3 Load Points Apply to This Nail

Load Diagram Type = 3

POINT NO.	X-COORD.(m)	Y-COORD.(m)	FORCE(kN)
1	23.74	45.17	10.00
2	25.89	44.73	38.55
3	29.65	44.13	0.00

Allowable Pullout Stress = 120.0(kPa)

Allowable Tendon Stress = 434782.6

Allowable Nail Head Load = 30.0(kN)

Soil Nail No. 4 3 Load Points Apply to This Nail

Load Diagram Type = 3

POINT NO.	X-COORD.(m)	Y-COORD.(m)	FORCE(kN)
1	25.86	47.29	10.00
2	27.98	46.85	38.55
3	31.77	46.25	0.00

Allowable Pullout Stress = 120.0(kPa)

Allowable Tendon Stress = 434782.6

Allowable Nail Head Load = 30.0(kN)

Soil Nail No. 5 3 Load Points Apply to This Nail

Load Diagram Type = 3

POINT NO.	X-COORD.(m)	Y-COORD.(m)	FORCE(kN)
1	27.98	49.41	10.00
2	30.07	48.97	38.55
3	33.89	48.37	0.00

Allowable Pullout Stress = 120.0(kPa)

Allowable Tendon Stress = 434782.6

Allowable Nail Head Load = 30.0(kN)

Soil Nail No. 6 3 Load Points Apply to This Nail

Load Diagram Type = 3

POINT NO.	X-COORD.(m)	Y-COORD.(m)	FORCE(kN)
1	33.50	50.69	10.00
2	35.51	50.25	38.55
3	39.41	49.65	0.00

Allowable Pullout Stress = 120.0(kPa)

Allowable Tendon Stress = 434782.6

Allowable Nail Head Load = 30.0(kN)

Soil Nail No. 7 3 Load Points Apply to This Nail

Load Diagram Type = 3

POINT NO.	X-COORD.(m)	Y-COORD.(m)	FORCE(kN)
1	35.62	52.81	10.00
2	37.59	52.37	38.55
3	41.53	51.77	0.00

Allowable Pullout Stress = 120.0(kPa)

Allowable Tendon Stress = 434782.6

Allowable Nail Head Load = 30.0(kN)

Soil Nail No. 8 3 Load Points Apply to This Nail

Load Diagram Type = 3

POINT NO.	X-COORD.(m)	Y-COORD.(m)	FORCE(kN)
1	37.74	54.93	10.00
2	39.68	54.49	38.55
3	43.65	53.89	0.00

Allowable Pullout Stress = 120.0(kPa)

Allowable Tendon Stress = 434782.6

Allowable Nail Head Load = 30.0(kN)

Soil Nail No. 9 3 Load Points Apply to This Nail

Load Diagram Type = 3

POINT NO.	X-COORD.(m)	Y-COORD.(m)	FORCE(kN)
1	39.86	57.05	10.00
2	41.77	56.61	38.55
3	45.77	56.01	0.00

Allowable Pullout Stress = 120.0(kPa)

Allowable Tendon Stress = 434782.6

Allowable Nail Head Load = 30.0(kN)

Soil Nail No. 10 3 Load Points Apply to This Nail

Load Diagram Type = 3

POINT NO.	X-COORD.(m)	Y-COORD.(m)	FORCE(kN)
1	41.98	59.17	10.00
2	43.86	58.73	38.55
3	47.89	58.13	0.00

Allowable Pullout Stress = 120.0(kPa)

Allowable Tendon Stress = 434782.6

Allowable Nail Head Load = 30.0(kN)

NOTE - An Equivalent Line Load Is Calculated For Each Row Of Soil Nails
Assuming A Uniform Distribution Of Load Horizontally Between
Individual Nails.

SOIL NAIL LOAD DATA HAS BEEN SUPPRESSED

A Critical Failure Surface Searching Method, Using A Random
Technique For Generating Circular Surfaces, Has Been Specified.
2500 Trial Surfaces Have Been Generated.

50 Surface(s) Initiate(s) From Each Of 50 Points Equally Spaced
Along The Ground Surface Between X = 10.00(m)

and X = 30.00(m)

Each Surface Terminates Between X = 50.00(m)

and X = 66.00(m)

Unless Further Limitations Were Imposed, The Minimum Elevation

At Which A Surface Extends Is Y = 0.00(m)

0.80(m) Line Segments Define Each Trial Failure Surface.

Following Are Displayed The Ten Most Critical Of The Trial

Failure Surfaces Evaluated. They Are

Ordered - Most Critical First.

* * Safety Factors Are Calculated By The Modified Bishop Method * *

Total Number of Trial Surfaces Evaluated = 2500

Statistical Data On All Valid FS Values:

FS Max = 2.117 FS Min = 0.992 FS Ave = 1.587

Standard Deviation = 0.257 Coefficient of Variation = 16.17 %

Failure Surface Specified By 51 Coordinate Points

Point No.	X-Surf (m)	Y-Surf (m)
1	18.57	40.00
2	19.25	40.43
3	19.92	40.86
4	20.59	41.29
5	21.26	41.73
6	21.94	42.17

7	22.61	42.60
8	23.27	43.04
9	23.94	43.48
10	24.61	43.93
11	25.27	44.37
12	25.94	44.82
13	26.60	45.26
14	27.26	45.71
15	27.92	46.16
16	28.58	46.61
17	29.24	47.07
18	29.90	47.52
19	30.56	47.98
20	31.21	48.44
21	31.87	48.90
22	32.52	49.36
23	33.17	49.82
24	33.83	50.29
25	34.48	50.75
26	35.12	51.22
27	35.77	51.69
28	36.42	52.16
29	37.06	52.63
30	37.71	53.11
31	38.35	53.58
32	38.99	54.06
33	39.64	54.54
34	40.28	55.02
35	40.91	55.50
36	41.55	55.98
37	42.19	56.47
38	42.82	56.96
39	43.46	57.44
40	44.09	57.93
41	44.72	58.42
42	45.35	58.92
43	45.98	59.41
44	46.61	59.91
45	47.24	60.40
46	47.86	60.90
47	48.49	61.40
48	49.11	61.90
49	49.73	62.41
50	50.35	62.91
51	50.52	63.04

Circle Center At X = -159.70 ; Y = 320.83 ; and Radius = 332.63

Factor of Safety

*** 0.992 ***

Individual data on the					54 slices		Earthquake		
Slice No.	Width (m)	Weight (kN)	Water Force Top	Water Force Bot	Tie Force Norm	Tie Force Tan	Force Hor	Force Ver	Surcharge Load
			(kN)	(kN)	(kN)	(kN)	(kN)	(kN)	(kN)
1	0.7	1.8	0.0	0.0	0.	0.	0.0	0.0	0.0
2	0.7	5.4	0.0	0.0	0.	0.	0.0	0.0	0.0
3	0.7	9.0	0.0	0.0	0.	0.	0.0	0.0	0.0
4	0.7	12.5	0.0	0.0	0.	0.	0.0	0.0	0.0
5	0.7	16.0	0.0	0.0	0.	0.	0.0	0.0	0.0
6	0.7	19.4	0.0	0.0	0.	0.	0.0	0.0	0.0
7	0.7	22.8	0.0	0.0	0.	0.	0.0	0.0	0.0
8	0.7	26.1	0.0	0.0	0.	0.	0.0	0.0	0.0
9	0.7	29.3	0.0	0.0	0.	0.	0.0	0.0	0.0
10	0.7	32.5	0.0	0.0	0.	0.	0.0	0.0	0.0
11	0.7	35.7	0.0	0.0	0.	0.	0.0	0.0	0.0
12	0.7	38.8	0.0	0.0	0.	0.	0.0	0.0	0.0
13	0.7	41.9	0.0	0.0	0.	0.	0.0	0.0	0.0
14	0.7	44.9	0.0	0.0	0.	0.	0.0	0.0	0.0
15	0.6	41.6	0.0	0.0	0.	0.	0.0	0.0	0.0
16	0.1	6.2	0.0	0.0	0.	0.	0.0	0.0	0.0
17	0.7	44.4	0.0	0.0	0.	0.	0.0	0.0	0.0
18	0.7	37.2	0.0	0.0	0.	0.	0.0	0.0	0.0
19	0.7	30.0	0.0	0.0	0.	0.	0.0	0.0	0.0
20	0.7	22.8	0.0	0.0	0.	0.	0.0	0.0	0.0
21	0.7	15.5	0.0	0.0	0.	0.	0.0	0.0	0.0
22	0.6	8.2	0.0	0.0	0.	0.	0.0	0.0	0.0

23	0.0	0.2	0.0	0.0	0.	0.	0.0	0.0	0.0
24	0.7	6.3	0.0	0.0	0.	0.	0.0	0.0	0.0
25	0.6	8.0	0.0	0.0	0.	0.	0.0	0.0	0.0
26	0.1	0.8	0.0	0.0	0.	0.	0.0	0.0	0.0
27	0.7	11.2	0.0	0.0	0.	0.	0.0	0.0	0.0
28	0.6	13.7	0.0	0.0	0.	0.	0.0	0.0	0.0
29	0.6	16.1	0.0	0.0	0.	0.	0.0	0.0	0.0
30	0.6	18.5	0.0	0.0	0.	0.	0.0	0.0	0.0
31	0.6	20.8	0.0	0.0	0.	0.	0.0	0.0	0.0
32	0.6	23.1	0.0	0.0	0.	0.	0.0	0.0	0.0
33	0.6	25.3	0.0	0.0	0.	0.	0.0	0.0	0.0
34	0.6	27.5	0.0	0.0	0.	0.	0.0	0.0	0.0
35	0.6	29.7	0.0	0.0	0.	0.	0.0	0.0	0.0
36	0.6	31.8	0.0	0.0	0.	0.	0.0	0.0	0.0
37	0.6	33.9	0.0	0.0	0.	0.	0.0	0.0	0.0
38	0.6	35.9	0.0	0.0	0.	0.	0.0	0.0	0.0
39	0.6	37.9	0.0	0.0	0.	0.	0.0	0.0	0.0
40	0.0	0.7	0.0	0.0	0.	0.	0.0	0.0	0.0
41	0.6	36.8	0.0	0.0	0.	0.	0.0	0.0	0.0
42	0.6	34.7	0.0	0.0	0.	0.	0.0	0.0	0.0
43	0.6	31.8	0.0	0.0	0.	0.	0.0	0.0	0.0
44	0.6	28.9	0.0	0.0	0.	0.	0.0	0.0	0.0
45	0.6	26.0	0.0	0.0	0.	0.	0.0	0.0	0.0
46	0.6	23.1	0.0	0.0	0.	0.	0.0	0.0	0.0
47	0.6	20.2	0.0	0.0	0.	0.	0.0	0.0	0.0
48	0.6	17.3	0.0	0.0	0.	0.	0.0	0.0	0.0
49	0.6	14.3	0.0	0.0	0.	0.	0.0	0.0	0.0
50	0.6	11.3	0.0	0.0	0.	0.	0.0	0.0	0.0
51	0.6	8.3	0.0	0.0	0.	0.	0.0	0.0	0.0
52	0.6	5.3	0.0	0.0	0.	0.	0.0	0.0	0.0
53	0.6	2.3	0.0	0.0	0.	0.	0.0	0.0	0.0
54	0.2	0.1	0.0	0.0	0.	0.	0.0	0.0	0.0

Failure Surface Specified By 52 Coordinate Points

Point No.	X-Surf (m)	Y-Surf (m)
1	18.57	40.00
2	19.26	40.40
3	19.95	40.81
4	20.64	41.22
5	21.33	41.63
6	22.01	42.04
7	22.70	42.46
8	23.38	42.87
9	24.06	43.29
10	24.74	43.72
11	25.41	44.14
12	26.09	44.57
13	26.76	45.00
14	27.44	45.44
15	28.11	45.87
16	28.78	46.31
17	29.44	46.76
18	30.11	47.20
19	30.77	47.65
20	31.43	48.10
21	32.09	48.55
22	32.75	49.00
23	33.41	49.46
24	34.06	49.92
25	34.72	50.38
26	35.37	50.84
27	36.02	51.31
28	36.67	51.78
29	37.31	52.25
30	37.96	52.73
31	38.60	53.20
32	39.24	53.68
33	39.88	54.16
34	40.52	54.65
35	41.15	55.13
36	41.78	55.62
37	42.42	56.11
38	43.04	56.61
39	43.67	57.10
40	44.30	57.60

41	44.92	58.10
42	45.54	58.61
43	46.16	59.11
44	46.78	59.62
45	47.40	60.13
46	48.01	60.64
47	48.62	61.16
48	49.23	61.68
49	49.84	62.20
50	50.45	62.72
51	51.05	63.24
52	51.14	63.32

Circle Center At X = -86.07 ; Y = 220.56 ; and Radius = 208.69

Factor of Safety
*** 0.993 ***

Failure Surface Specified By 53 Coordinate Points

Point No.	X-Surf (m)	Y-Surf (m)
1	18.98	40.41
2	19.66	40.83
3	20.35	41.24
4	21.03	41.66
5	21.71	42.08
6	22.39	42.50
7	23.07	42.93
8	23.74	43.35
9	24.42	43.78
10	25.09	44.21
11	25.77	44.64
12	26.44	45.07
13	27.11	45.51
14	27.78	45.94
15	28.45	46.38
16	29.12	46.82
17	29.79	47.26
18	30.46	47.70
19	31.12	48.15
20	31.79	48.59
21	32.45	49.04
22	33.11	49.49
23	33.77	49.94
24	34.44	50.39
25	35.09	50.84
26	35.75	51.30
27	36.41	51.75
28	37.06	52.21
29	37.72	52.67
30	38.37	53.13
31	39.02	53.60
32	39.68	54.06
33	40.33	54.53
34	40.97	55.00
35	41.62	55.47
36	42.27	55.94
37	42.91	56.41
38	43.56	56.88
39	44.20	57.36
40	44.84	57.84
41	45.48	58.32
42	46.12	58.80
43	46.76	59.28
44	47.40	59.76
45	48.04	60.25
46	48.67	60.74
47	49.30	61.22
48	49.94	61.71
49	50.57	62.21
50	51.20	62.70
51	51.83	63.19
52	52.45	63.69
53	53.03	64.15

Circle Center At X = -150.32 ; Y = 319.56 ; and Radius = 326.48

Factor of Safety
*** 0.998 ***

Failure Surface Specified By 49 Coordinate Points

Point No.	X-Surf (m)	Y-Surf (m)
1	19.80	41.23
2	20.47	41.65
3	21.15	42.08
4	21.82	42.51
5	22.50	42.94
6	23.17	43.37
7	23.84	43.81
8	24.51	44.24
9	25.18	44.68
10	25.85	45.12
11	26.52	45.56
12	27.19	46.00
13	27.85	46.44
14	28.52	46.89
15	29.18	47.34
16	29.84	47.78
17	30.51	48.23
18	31.17	48.68
19	31.83	49.14
20	32.48	49.59
21	33.14	50.05
22	33.80	50.51
23	34.45	50.97
24	35.11	51.43
25	35.76	51.89
26	36.41	52.35
27	37.06	52.82
28	37.71	53.28
29	38.36	53.75
30	39.01	54.22
31	39.65	54.70
32	40.30	55.17
33	40.94	55.64
34	41.59	56.12
35	42.23	56.60
36	42.87	57.08
37	43.51	57.56
38	44.15	58.04
39	44.78	58.52
40	45.42	59.01
41	46.05	59.50
42	46.69	59.98
43	47.32	60.47
44	47.95	60.96
45	48.58	61.46
46	49.21	61.95
47	49.84	62.45
48	50.46	62.95
49	50.68	63.11

Circle Center At X = -159.00 ; Y = 326.20 ; and Radius = 336.42

Factor of Safety
*** 0.998 ***

Failure Surface Specified By 47 Coordinate Points

Point No.	X-Surf (m)	Y-Surf (m)
1	20.20	41.63
2	20.89	42.05
3	21.58	42.46
4	22.26	42.87
5	22.94	43.29
6	23.62	43.71
7	24.30	44.14
8	24.98	44.56
9	25.65	44.99
10	26.33	45.42
11	27.00	45.85
12	27.67	46.29
13	28.34	46.72
14	29.01	47.16
15	29.68	47.60
16	30.35	48.05
17	31.01	48.49
18	31.67	48.94

19	32.33	49.39
20	32.99	49.85
21	33.65	50.30
22	34.31	50.76
23	34.96	51.22
24	35.61	51.68
25	36.26	52.14
26	36.91	52.61
27	37.56	53.08
28	38.21	53.55
29	38.85	54.03
30	39.50	54.50
31	40.14	54.98
32	40.78	55.46
33	41.42	55.94
34	42.05	56.43
35	42.69	56.91
36	43.32	57.40
37	43.95	57.89
38	44.58	58.39
39	45.21	58.88
40	45.84	59.38
41	46.46	59.88
42	47.09	60.38
43	47.71	60.88
44	48.33	61.39
45	48.94	61.90
46	49.56	62.41
47	50.10	62.86

Circle Center At X = -97.97 ; Y = 239.73 ; and Radius = 230.67

Factor of Safety

*** 0.999 ***

Failure Surface Specified By 49 Coordinate Points

Point No.	X-Surf (m)	Y-Surf (m)
1	19.39	40.82
2	20.06	41.25
3	20.73	41.69
4	21.40	42.13
5	22.07	42.57
6	22.73	43.01
7	23.40	43.45
8	24.07	43.90
9	24.73	44.34
10	25.40	44.79
11	26.06	45.23
12	26.72	45.68
13	27.38	46.13
14	28.04	46.58
15	28.70	47.04
16	29.36	47.49
17	30.02	47.95
18	30.67	48.40
19	31.33	48.86
20	31.98	49.32
21	32.64	49.78
22	33.29	50.25
23	33.94	50.71
24	34.59	51.17
25	35.25	51.64
26	35.89	52.11
27	36.54	52.58
28	37.19	53.05
29	37.84	53.52
30	38.48	53.99
31	39.13	54.46
32	39.77	54.94
33	40.41	55.42
34	41.05	55.89
35	41.70	56.37
36	42.33	56.85
37	42.97	57.33
38	43.61	57.82
39	44.25	58.30
40	44.88	58.79

41	45.52	59.27
42	46.15	59.76
43	46.79	60.25
44	47.42	60.74
45	48.05	61.23
46	48.68	61.73
47	49.31	62.22
48	49.94	62.72
49	50.14	62.88

Circle Center At X = -197.27 ; Y = 375.31 ; and Radius = 398.53

Factor of Safety

*** 0.999 ***

Failure Surface Specified By 53 Coordinate Points

Point No.	X-Surf (m)	Y-Surf (m)
1	19.39	40.82
2	20.07	41.24
3	20.75	41.66
4	21.43	42.08
5	22.11	42.51
6	22.78	42.93
7	23.46	43.36
8	24.13	43.79
9	24.81	44.22
10	25.48	44.65
11	26.15	45.08
12	26.83	45.52
13	27.50	45.95
14	28.17	46.39
15	28.84	46.83
16	29.51	47.27
17	30.17	47.71
18	30.84	48.15
19	31.50	48.60
20	32.17	49.04
21	32.83	49.49
22	33.50	49.94
23	34.16	50.39
24	34.82	50.84
25	35.48	51.29
26	36.14	51.74
27	36.79	52.20
28	37.45	52.65
29	38.11	53.11
30	38.76	53.57
31	39.42	54.03
32	40.07	54.49
33	40.72	54.96
34	41.37	55.42
35	42.03	55.89
36	42.67	56.35
37	43.32	56.82
38	43.97	57.29
39	44.62	57.76
40	45.26	58.24
41	45.91	58.71
42	46.55	59.18
43	47.19	59.66
44	47.84	60.14
45	48.48	60.62
46	49.12	61.10
47	49.76	61.58
48	50.39	62.06
49	51.03	62.55
50	51.67	63.03
51	52.30	63.52
52	52.93	64.01
53	53.23	64.24

Circle Center At X = -183.95 ; Y = 370.82 ; and Radius = 387.62

Factor of Safety

*** 0.999 ***

Failure Surface Specified By 52 Coordinate Points

Point No.	X-Surf (m)	Y-Surf (m)
1	19.39	40.82

2	20.09	41.21
3	20.78	41.60
4	21.48	42.00
5	22.17	42.40
6	22.86	42.80
7	23.55	43.21
8	24.24	43.62
9	24.92	44.03
10	25.61	44.44
11	26.29	44.86
12	26.97	45.28
13	27.65	45.70
14	28.33	46.12
15	29.01	46.55
16	29.68	46.98
17	30.36	47.41
18	31.03	47.85
19	31.70	48.28
20	32.37	48.72
21	33.03	49.17
22	33.70	49.61
23	34.36	50.06
24	35.02	50.51
25	35.68	50.96
26	36.34	51.42
27	36.99	51.88
28	37.65	52.34
29	38.30	52.80
30	38.95	53.27
31	39.60	53.74
32	40.24	54.21
33	40.89	54.68
34	41.53	55.16
35	42.17	55.64
36	42.81	56.12
37	43.45	56.61
38	44.08	57.09
39	44.71	57.58
40	45.34	58.07
41	45.97	58.57
42	46.60	59.06
43	47.23	59.56
44	47.85	60.07
45	48.47	60.57
46	49.09	61.08
47	49.71	61.58
48	50.32	62.10
49	50.94	62.61
50	51.55	63.13
51	52.16	63.64
52	52.44	63.89

Circle Center At X = -79.19 ; Y = 217.25 ; and Radius = 202.11

Factor of Safety
*** 1.003 ***

Failure Surface Specified By 49 Coordinate Points

Point No.	X-Surf (m)	Y-Surf (m)
1	21.43	42.86
2	22.12	43.26
3	22.81	43.67
4	23.49	44.08
5	24.18	44.49
6	24.86	44.91
7	25.55	45.32
8	26.23	45.74
9	26.91	46.16
10	27.59	46.58
11	28.27	47.00
12	28.95	47.43
13	29.63	47.85
14	30.30	48.28
15	30.98	48.71
16	31.65	49.14
17	32.33	49.57
18	33.00	50.01

19	33.67	50.44
20	34.34	50.88
21	35.00	51.32
22	35.67	51.76
23	36.34	52.21
24	37.00	52.65
25	37.67	53.10
26	38.33	53.55
27	38.99	54.00
28	39.65	54.45
29	40.31	54.90
30	40.97	55.36
31	41.62	55.82
32	42.28	56.27
33	42.93	56.74
34	43.59	57.20
35	44.24	57.66
36	44.89	58.13
37	45.54	58.59
38	46.18	59.06
39	46.83	59.53
40	47.48	60.01
41	48.12	60.48
42	48.76	60.96
43	49.41	61.43
44	50.05	61.91
45	50.69	62.39
46	51.32	62.88
47	51.96	63.36
48	52.60	63.85
49	52.94	64.11

Circle Center At X = -134.12 ; Y = 307.50 ; and Radius = 306.97

Factor of Safety
*** 1.003 ***

Failure Surface Specified By 50 Coordinate Points

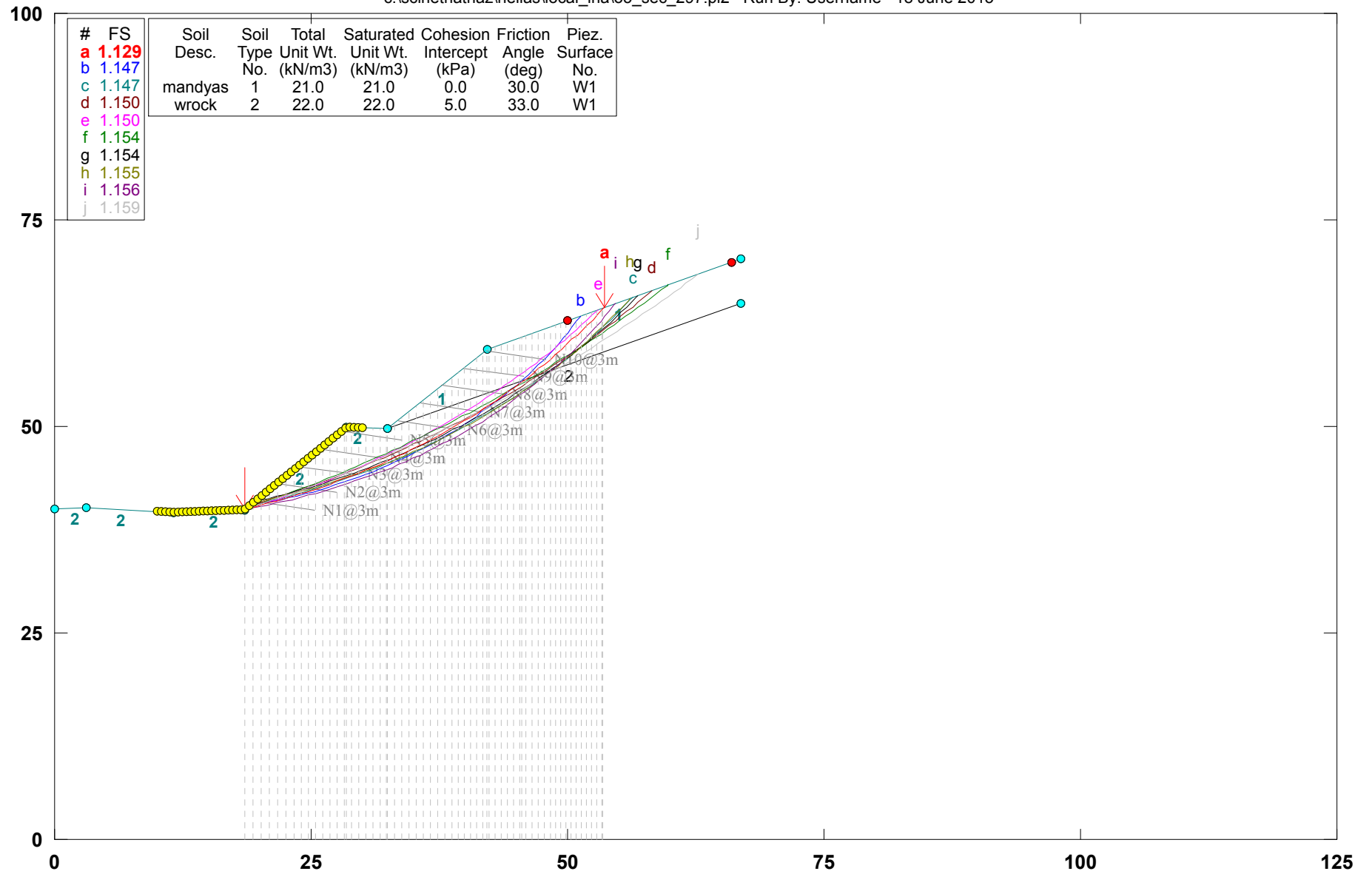
Point No.	X-Surf (m)	Y-Surf (m)
1	21.84	43.27
2	22.54	43.65
3	23.24	44.04
4	23.94	44.43
5	24.63	44.82
6	25.33	45.22
7	26.02	45.61
8	26.72	46.01
9	27.41	46.41
10	28.10	46.82
11	28.79	47.22
12	29.48	47.63
13	30.16	48.05
14	30.85	48.46
15	31.53	48.87
16	32.21	49.29
17	32.89	49.71
18	33.57	50.14
19	34.25	50.56
20	34.93	50.99
21	35.60	51.42
22	36.27	51.85
23	36.94	52.29
24	37.61	52.72
25	38.28	53.16
26	38.95	53.60
27	39.62	54.05
28	40.28	54.49
29	40.94	54.94
30	41.60	55.39
31	42.26	55.85
32	42.92	56.30
33	43.58	56.76
34	44.23	57.22
35	44.89	57.68
36	45.54	58.14
37	46.19	58.61
38	46.84	59.08

39	47.48	59.55
40	48.13	60.02
41	48.77	60.50
42	49.41	60.98
43	50.05	61.46
44	50.69	61.94
45	51.33	62.42
46	51.96	62.91
47	52.60	63.40
48	53.23	63.89
49	53.86	64.38
50	54.23	64.68

Circle Center At X = -89.75 ; Y = 247.33 ; and Radius = 232.58
Factor of Safety
*** 1.010 ***
**** END OF GSTABL7 OUTPUT ****

Hellas_Local_Landslide_Hazard Cut slope O5_sec_297

c:\scinetnathaz\hellas\local_lha\o5_sec_297.pl2 Run By: Username 18 June 2015



GSTABL7 v.2 FSmin=1.129

Safety Factors Are Calculated By The Modified Bishop Method



*** GSTABL7 ***

** GSTABL7 by Garry H. Gregory, P.E. **

** Original Version 1.0, January 1996; Current Version 2.003, June 2002 **

(All Rights Reserved-Unauthorized Use Prohibited)

SLOPE STABILITY ANALYSIS SYSTEM

Modified Bishop, Simplified Janbu, or GLE Method of Slices.

(Includes Spencer & Morgenstern-Price Type Analysis)

Including Pier/Pile, Reinforcement, Soil Nail, Tieback,

Nonlinear Undrained Shear Strength, Curved Phi Envelope,

Anisotropic Soil, Fiber-Reinforced Soil, Boundary Loads, Water

Surfaces, Pseudo-Static & Newmark Earthquake, and Applied Forces.

Analysis Run Date: 18 June 2015

Time of Run:

Run By: Username

Input Data Filename: C:\SciNetNatHaz\Hellas\Local_LHA\05_sec_297.in

Output Filename: C:\SciNetNatHaz\Hellas\Local_LHA\05_sec_297.OUT

Unit System: SI

Plotted Output Filename: C:\SciNetNatHaz\Hellas\Local_LHasec_297.PLT

PROBLEM DESCRIPTION: Hellas_Local_Landslide_Hazard

Cut slope 05_sec_297

BOUNDARY COORDINATES

7 Top Boundaries

8 Total Boundaries

Boundary No.	X-Left (m)	Y-Left (m)	X-Right (m)	Y-Right (m)	Soil Type Below Bnd
1	0.00	40.00	3.10	40.22	2
2	3.10	40.22	11.60	39.62	2
3	11.60	39.62	18.50	39.93	2
4	18.50	39.93	28.50	49.93	2
5	28.50	49.93	32.50	49.69	2

6	32.50	49.69	42.20	59.39	1
7	42.20	59.39	66.85	70.22	1
8	32.50	49.69	66.85	64.82	2

Default Y-Origin = 0.00(m)

Default X-Plus Value = 0.00(m)

Default Y-Plus Value = 0.00(m)

ISOTROPIC SOIL PARAMETERS

2 Type(s) of Soil

Soil Type No.	Total Unit Wt. (kN/m ³)	Saturated Unit Wt. (kN/m ³)	Cohesion Intercept (kPa)	Friction Angle (deg)	Pore Pressure Param. (kPa)	Pressure Constant (kPa)	Piez. Surface No.
1	21.0	21.0	0.0	30.0	0.00	0.0	1
2	22.0	22.0	5.0	33.0	0.00	0.0	1

SOIL NAIL LOAD(S)

10 SOIL NAIL LOAD(S) SPECIFIED

Nail No.	X-Pos (m)	Y-Pos (m)	Nail Dia (mm)	Tendon Dia (mm)	Spacing (m)	Inclin. (deg)	Length (m)
1	19.50	40.93	89.0	25.0	3.00	10.00	6.00
2	21.62	43.05	89.0	25.0	3.00	10.00	6.00
3	23.74	45.17	89.0	25.0	3.00	10.00	6.00
4	25.86	47.29	89.0	25.0	3.00	10.00	6.00
5	27.98	49.41	89.0	25.0	3.00	10.00	6.00
6	33.50	50.69	89.0	25.0	3.00	10.00	6.00
7	35.62	52.81	89.0	25.0	3.00	10.00	6.00
8	37.74	54.93	89.0	25.0	3.00	10.00	6.00
9	39.86	57.05	89.0	25.0	3.00	10.00	6.00
10	41.98	59.17	89.0	25.0	3.00	10.00	6.00

SOIL NAIL LOAD DATA

Soil Nail No. 1 3 Load Points Apply to This Nail

Load Diagram Type = 3

POINT NO.	X-COORD.(m)	Y-COORD.(m)	FORCE(kN)
1	19.50	40.93	10.00
2	21.72	40.49	38.55
3	25.41	39.89	0.00

Allowable Pullout Stress = 120.0(kPa)

Allowable Tendon Stress = 434782.6

Allowable Nail Head Load = 30.0(kN)

Soil Nail No. 2 3 Load Points Apply to This Nail

Load Diagram Type = 3

POINT NO.	X-COORD.(m)	Y-COORD.(m)	FORCE(kN)
1	21.62	43.05	10.00
2	23.81	42.61	38.55
3	27.53	42.01	0.00

Allowable Pullout Stress = 120.0(kPa)

Allowable Tendon Stress = 434782.6

Allowable Nail Head Load = 30.0(kN)

Soil Nail No. 3 3 Load Points Apply to This Nail

Load Diagram Type = 3

POINT NO.	X-COORD.(m)	Y-COORD.(m)	FORCE(kN)
1	23.74	45.17	10.00
2	25.89	44.73	38.55
3	29.65	44.13	0.00

Allowable Pullout Stress = 120.0(kPa)

Allowable Tendon Stress = 434782.6

Allowable Nail Head Load = 30.0(kN)

Soil Nail No. 4 3 Load Points Apply to This Nail

Load Diagram Type = 3

POINT NO.	X-COORD.(m)	Y-COORD.(m)	FORCE(kN)
1	25.86	47.29	10.00
2	27.98	46.85	38.55
3	31.77	46.25	0.00

Allowable Pullout Stress = 120.0(kPa)

Allowable Tendon Stress = 434782.6

Allowable Nail Head Load = 30.0(kN)

Soil Nail No. 5 3 Load Points Apply to This Nail

Load Diagram Type = 3

POINT NO.	X-COORD.(m)	Y-COORD.(m)	FORCE(kN)
1	27.98	49.41	10.00
2	30.07	48.97	38.55
3	33.89	48.37	0.00

Allowable Pullout Stress = 120.0(kPa)

Allowable Tendon Stress = 434782.6

Allowable Nail Head Load = 30.0(kN)

Soil Nail No. 6 3 Load Points Apply to This Nail

Load Diagram Type = 3

POINT NO.	X-COORD.(m)	Y-COORD.(m)	FORCE(kN)
1	33.50	50.69	10.00
2	35.51	50.25	38.55
3	39.41	49.65	0.00

Allowable Pullout Stress = 120.0(kPa)

Allowable Tendon Stress = 434782.6

Allowable Nail Head Load = 30.0(kN)

Soil Nail No. 7 3 Load Points Apply to This Nail

Load Diagram Type = 3

POINT NO.	X-COORD.(m)	Y-COORD.(m)	FORCE(kN)
1	35.62	52.81	10.00
2	37.59	52.37	38.55
3	41.53	51.77	0.00

Allowable Pullout Stress = 120.0(kPa)

Allowable Tendon Stress = 434782.6

Allowable Nail Head Load = 30.0(kN)

Soil Nail No. 8 3 Load Points Apply to This Nail

Load Diagram Type = 3

POINT NO.	X-COORD.(m)	Y-COORD.(m)	FORCE(kN)
1	37.74	54.93	10.00
2	39.68	54.49	38.55
3	43.65	53.89	0.00

Allowable Pullout Stress = 120.0(kPa)

Allowable Tendon Stress = 434782.6

Allowable Nail Head Load = 30.0(kN)

Soil Nail No. 9 3 Load Points Apply to This Nail

Load Diagram Type = 3

POINT NO.	X-COORD.(m)	Y-COORD.(m)	FORCE(kN)
1	39.86	57.05	10.00
2	41.77	56.61	38.55
3	45.77	56.01	0.00

Allowable Pullout Stress = 120.0(kPa)

Allowable Tendon Stress = 434782.6

Allowable Nail Head Load = 30.0(kN)

Soil Nail No. 10 3 Load Points Apply to This Nail

Load Diagram Type = 3

POINT NO.	X-COORD.(m)	Y-COORD.(m)	FORCE(kN)
1	41.98	59.17	10.00
2	43.86	58.73	38.55
3	47.89	58.13	0.00

Allowable Pullout Stress = 120.0(kPa)

Allowable Tendon Stress = 434782.6

Allowable Nail Head Load = 30.0(kN)

NOTE - An Equivalent Line Load Is Calculated For Each Row Of Soil Nails
Assuming A Uniform Distribution Of Load Horizontally Between
Individual Nails.

A Critical Failure Surface Searching Method, Using A Random
Technique For Generating Circular Surfaces, Has Been Specified.
2500 Trial Surfaces Have Been Generated.

50 Surface(s) Initiate(s) From Each Of 50 Points Equally Spaced
Along The Ground Surface Between X = 10.00(m)

and X = 30.00(m)

Each Surface Terminates Between X = 50.00(m)

and X = 66.00(m)

Unless Further Limitations Were Imposed, The Minimum Elevation
At Which A Surface Extends Is Y = 0.00(m)

0.80(m) Line Segments Define Each Trial Failure Surface.

Following Are Displayed The Ten Most Critical Of The Trial

Failure Surfaces Evaluated. They Are
Ordered - Most Critical First.

* * Safety Factors Are Calculated By The Modified Bishop Method * *

Total Number of Trial Surfaces Evaluated = 2500

Statistical Data On All Valid FS Values:

FS Max = 2.117 FS Min = 1.129 FS Ave = 1.602

Standard Deviation = 0.236 Coefficient of Variation = 14.76 %

Failure Surface Specified By 56 Coordinate Points

Point No.	X-Surf (m)	Y-Surf (m)
1	18.57	40.00
2	19.34	40.23
3	20.10	40.47
4	20.86	40.72
5	21.62	40.97
6	22.38	41.24
7	23.13	41.51

8	23.88	41.79
9	24.62	42.09
10	25.36	42.39
11	26.10	42.70
12	26.83	43.02
13	27.56	43.34
14	28.29	43.68
15	29.01	44.02
16	29.73	44.38
17	30.44	44.74
18	31.15	45.11
19	31.86	45.49
20	32.56	45.88
21	33.25	46.27
22	33.94	46.68
23	34.63	47.09
24	35.31	47.51
25	35.98	47.94
26	36.65	48.37
27	37.32	48.82
28	37.98	49.27
29	38.63	49.73
30	39.28	50.20
31	39.92	50.67
32	40.56	51.16
33	41.19	51.65
34	41.82	52.15
35	42.44	52.65
36	43.05	53.17
37	43.66	53.69
38	44.26	54.22
39	44.85	54.75
40	45.44	55.29
41	46.02	55.84
42	46.60	56.40
43	47.17	56.96
44	47.73	57.53
45	48.28	58.11
46	48.83	58.69
47	49.37	59.28
48	49.90	59.88
49	50.43	60.48
50	50.95	61.09
51	51.46	61.70
52	51.97	62.33
53	52.46	62.95
54	52.95	63.58
55	53.43	64.22
56	53.55	64.37

Circle Center At X = -0.15 ; Y = 104.14 ; and Radius = 66.82

Factor of Safety

*** 1.129 ***

Slice No.	Width (m)	Weight (kN)	Individual data on the		59 slices		Earthquake		Surcharge Load (kN)
			Water Force Top (kN)	Water Force Bot (kN)	Tie Force Norm (kN)	Tie Force Tan (kN)	Force Hor (kN)	Force Ver (kN)	
1	0.8	4.5	0.0	0.0	0.	0.	0.0	0.0	0.0
2	0.8	13.5	0.0	0.0	0.	0.	0.0	0.0	0.0
3	0.8	22.1	0.0	0.0	0.	0.	0.0	0.0	0.0
4	0.8	30.5	0.0	0.0	0.	0.	0.0	0.0	0.0
5	0.8	38.6	0.0	0.0	0.	0.	0.0	0.0	0.0
6	0.8	46.4	0.0	0.0	0.	0.	0.0	0.0	0.0
7	0.7	54.0	0.0	0.0	0.	0.	0.0	0.0	0.0
8	0.7	61.2	0.0	0.0	0.	0.	0.0	0.0	0.0
9	0.7	68.2	0.0	0.0	0.	0.	0.0	0.0	0.0
10	0.7	74.9	0.0	0.0	0.	0.	0.0	0.0	0.0
11	0.7	81.4	0.0	0.0	0.	0.	0.0	0.0	0.0
12	0.7	87.5	0.0	0.0	0.	0.	0.0	0.0	0.0
13	0.7	93.3	0.0	0.0	0.	0.	0.0	0.0	0.0
14	0.2	28.4	0.0	0.0	0.	0.	0.0	0.0	0.0
15	0.5	67.5	0.0	0.0	0.	0.	0.0	0.0	0.0
16	0.7	89.6	0.0	0.0	0.	0.	0.0	0.0	0.0
17	0.7	82.8	0.0	0.0	0.	0.	0.0	0.0	0.0
18	0.7	75.9	0.0	0.0	0.	0.	0.0	0.0	0.0

19	0.7	69.0	0.0	0.0	0.	0.	0.0	0.0	0.0
20	0.6	57.4	0.0	0.0	0.	0.	0.0	0.0	0.0
21	0.1	4.7	0.0	0.0	0.	0.	0.0	0.0	0.0
22	0.7	61.3	0.0	0.0	0.	0.	0.0	0.0	0.0
23	0.7	65.1	0.0	0.0	0.	0.	0.0	0.0	0.0
24	0.7	68.6	0.0	0.0	0.	0.	0.0	0.0	0.0
25	0.7	71.8	0.0	0.0	0.	0.	0.0	0.0	0.0
26	0.7	74.8	0.0	0.0	0.	0.	0.0	0.0	0.0
27	0.7	77.5	0.0	0.0	0.	0.	0.0	0.0	0.0
28	0.7	80.0	0.0	0.0	0.	0.	0.0	0.0	0.0
29	0.7	82.2	0.0	0.0	0.	0.	0.0	0.0	0.0
30	0.7	84.2	0.0	0.0	0.	0.	0.0	0.0	0.0
31	0.6	85.9	0.0	0.0	0.	0.	0.0	0.0	0.0
32	0.6	87.4	0.0	0.0	0.	0.	0.0	0.0	0.0
33	0.6	88.6	0.0	0.0	0.	0.	0.0	0.0	0.0
34	0.6	89.6	0.0	0.0	0.	0.	0.0	0.0	0.0
35	0.6	90.4	0.0	0.0	0.	0.	0.0	0.0	0.0
36	0.4	55.9	0.0	0.0	0.	0.	0.0	0.0	0.0
37	0.2	34.7	0.0	0.0	0.	0.	0.0	0.0	0.0
38	0.6	87.3	0.0	0.0	0.	0.	0.0	0.0	0.0
39	0.6	83.1	0.0	0.0	0.	0.	0.0	0.0	0.0
40	0.6	78.8	0.0	0.0	0.	0.	0.0	0.0	0.0
41	0.6	74.5	0.0	0.0	0.	0.	0.0	0.0	0.0
42	0.6	70.1	0.0	0.0	0.	0.	0.0	0.0	0.0
43	0.2	21.9	0.0	0.0	0.	0.	0.0	0.0	0.0
44	0.4	43.7	0.0	0.0	0.	0.	0.0	0.0	0.0
45	0.6	61.3	0.0	0.0	0.	0.	0.0	0.0	0.0
46	0.6	56.9	0.0	0.0	0.	0.	0.0	0.0	0.0
47	0.6	52.4	0.0	0.0	0.	0.	0.0	0.0	0.0
48	0.6	48.0	0.0	0.0	0.	0.	0.0	0.0	0.0
49	0.5	43.5	0.0	0.0	0.	0.	0.0	0.0	0.0
50	0.5	39.0	0.0	0.0	0.	0.	0.0	0.0	0.0
51	0.5	34.5	0.0	0.0	0.	0.	0.0	0.0	0.0
52	0.5	30.0	0.0	0.0	0.	0.	0.0	0.0	0.0
53	0.5	25.5	0.0	0.0	0.	0.	0.0	0.0	0.0
54	0.5	21.0	0.0	0.0	0.	0.	0.0	0.0	0.0
55	0.5	16.5	0.0	0.0	0.	0.	0.0	0.0	0.0
56	0.5	12.0	0.0	0.0	0.	0.	0.0	0.0	0.0
57	0.5	7.6	0.0	0.0	0.	0.	0.0	0.0	0.0
58	0.5	3.2	0.0	0.0	0.	0.	0.0	0.0	0.0
59	0.1	0.1	0.0	0.0	0.	0.	0.0	0.0	0.0

Failure Surface Specified By 53 Coordinate Points

Point No.	X-Surf (m)	Y-Surf (m)
1	18.98	40.41
2	19.76	40.57
3	20.54	40.75
4	21.32	40.94
5	22.09	41.15
6	22.86	41.36
7	23.63	41.59
8	24.39	41.83
9	25.15	42.09
10	25.91	42.35
11	26.66	42.63
12	27.40	42.92
13	28.14	43.23
14	28.88	43.54
15	29.61	43.87
16	30.33	44.21
17	31.05	44.56
18	31.76	44.92
19	32.47	45.29
20	33.17	45.68
21	33.87	46.08
22	34.55	46.49
23	35.23	46.91
24	35.91	47.34
25	36.58	47.78
26	37.23	48.23
27	37.89	48.69
28	38.53	49.17
29	39.17	49.65
30	39.80	50.15
31	40.42	50.65

32	41.03	51.17
33	41.63	51.70
34	42.23	52.23
35	42.81	52.78
36	43.39	53.33
37	43.96	53.89
38	44.51	54.47
39	45.06	55.05
40	45.60	55.64
41	46.13	56.24
42	46.65	56.85
43	47.16	57.47
44	47.66	58.09
45	48.15	58.72
46	48.63	59.36
47	49.09	60.01
48	49.55	60.67
49	50.00	61.33
50	50.43	62.01
51	50.86	62.68
52	51.27	63.37
53	51.27	63.38

Circle Center At X = 9.31 ; Y = 88.20 ; and Radius = 48.76

Factor of Safety

*** 1.147 ***

Failure Surface Specified By 59 Coordinate Points

Point No.	X-Surf (m)	Y-Surf (m)
1	18.98	40.41
2	19.75	40.62
3	20.52	40.84
4	21.29	41.06
5	22.05	41.30
6	22.81	41.54
7	23.57	41.80
8	24.33	42.06
9	25.08	42.33
10	25.83	42.61
11	26.58	42.90
12	27.32	43.20
13	28.06	43.51
14	28.79	43.82
15	29.53	44.14
16	30.25	44.48
17	30.98	44.82
18	31.70	45.16
19	32.41	45.52
20	33.13	45.89
21	33.83	46.26
22	34.54	46.64
23	35.23	47.03
24	35.93	47.43
25	36.62	47.84
26	37.30	48.25
27	37.98	48.67
28	38.65	49.10
29	39.32	49.54
30	39.99	49.99
31	40.65	50.44
32	41.30	50.90
33	41.95	51.37
34	42.59	51.85
35	43.23	52.33
36	43.86	52.82
37	44.49	53.32
38	45.11	53.83
39	45.72	54.34
40	46.33	54.86
41	46.93	55.39
42	47.52	55.92
43	48.11	56.46
44	48.70	57.01
45	49.27	57.57
46	49.84	58.13
47	50.41	58.70

48	50.96	59.27
49	51.51	59.85
50	52.06	60.44
51	52.59	61.03
52	53.12	61.63
53	53.64	62.24
54	54.16	62.85
55	54.67	63.47
56	55.17	64.09
57	55.66	64.72
58	56.15	65.36
59	56.32	65.59

Circle Center At X = 1.45 ; Y = 106.67 ; and Radius = 68.54

Factor of Safety

*** 1.147 ***

Failure Surface Specified By 61 Coordinate Points

Point No.	X-Surf (m)	Y-Surf (m)
1	18.98	40.41
2	19.73	40.68
3	20.48	40.96
4	21.23	41.25
5	21.97	41.54
6	22.71	41.84
7	23.45	42.15
8	24.19	42.46
9	24.93	42.77
10	25.66	43.10
11	26.39	43.42
12	27.11	43.76
13	27.84	44.10
14	28.56	44.44
15	29.28	44.79
16	29.99	45.15
17	30.71	45.51
18	31.42	45.88
19	32.12	46.26
20	32.83	46.64
21	33.53	47.02
22	34.23	47.42
23	34.92	47.81
24	35.61	48.22
25	36.30	48.62
26	36.99	49.04
27	37.67	49.46
28	38.34	49.88
29	39.02	50.31
30	39.69	50.75
31	40.36	51.19
32	41.02	51.64
33	41.68	52.09
34	42.34	52.54
35	42.99	53.01
36	43.64	53.47
37	44.29	53.95
38	44.93	54.42
39	45.56	54.91
40	46.20	55.40
41	46.83	55.89
42	47.45	56.39
43	48.08	56.89
44	48.69	57.40
45	49.31	57.91
46	49.92	58.43
47	50.52	58.96
48	51.12	59.48
49	51.72	60.02
50	52.31	60.55
51	52.90	61.10
52	53.48	61.64
53	54.06	62.20
54	54.64	62.75
55	55.21	63.31
56	55.77	63.88
57	56.33	64.45

58 56.89 65.02
 59 57.44 65.60
 60 57.99 66.19
 61 58.20 66.42
 Circle Center At X = -14.67 ; Y = 133.72 ; and Radius = 99.19
 Factor of Safety
 *** 1.150 ***

Failure Surface Specified By 55 Coordinate Points

Point No.	X-Surf (m)	Y-Surf (m)
1	18.57	40.00
2	19.32	40.28
3	20.07	40.57
4	20.81	40.86
5	21.55	41.17
6	22.29	41.47
7	23.02	41.79
8	23.76	42.11
9	24.49	42.44
10	25.21	42.78
11	25.93	43.13
12	26.65	43.48
13	27.37	43.84
14	28.08	44.20
15	28.79	44.57
16	29.49	44.95
17	30.19	45.34
18	30.89	45.73
19	31.58	46.13
20	32.27	46.54
21	32.96	46.95
22	33.64	47.37
23	34.31	47.80
24	34.99	48.23
25	35.66	48.67
26	36.32	49.11
27	36.98	49.57
28	37.63	50.02
29	38.29	50.49
30	38.93	50.96
31	39.57	51.44
32	40.21	51.92
33	40.84	52.41
34	41.47	52.91
35	42.09	53.41
36	42.71	53.92
37	43.32	54.43
38	43.93	54.95
39	44.54	55.48
40	45.13	56.01
41	45.73	56.55
42	46.31	57.09
43	46.89	57.64
44	47.47	58.20
45	48.04	58.76
46	48.61	59.32
47	49.17	59.89
48	49.72	60.47
49	50.27	61.05
50	50.81	61.64
51	51.35	62.23
52	51.88	62.83
53	52.41	63.43
54	52.93	64.04
55	53.01	64.14

Circle Center At X = -9.85 ; Y = 117.19 ; and Radius = 82.25
 Factor of Safety
 *** 1.150 ***

Failure Surface Specified By 64 Coordinate Points

Point No.	X-Surf (m)	Y-Surf (m)
1	18.57	40.00
2	19.31	40.31
3	20.04	40.63
4	20.77	40.95

5	21.50	41.28
6	22.23	41.61
7	22.96	41.95
8	23.68	42.28
9	24.41	42.63
10	25.13	42.97
11	25.85	43.33
12	26.56	43.68
13	27.28	44.04
14	27.99	44.41
15	28.70	44.78
16	29.41	45.15
17	30.11	45.52
18	30.82	45.91
19	31.52	46.29
20	32.22	46.68
21	32.91	47.07
22	33.61	47.47
23	34.30	47.87
24	34.99	48.28
25	35.68	48.69
26	36.36	49.10
27	37.04	49.52
28	37.72	49.94
29	38.40	50.37
30	39.08	50.80
31	39.75	51.23
32	40.42	51.67
33	41.08	52.11
34	41.75	52.55
35	42.41	53.00
36	43.07	53.46
37	43.73	53.91
38	44.38	54.38
39	45.03	54.84
40	45.68	55.31
41	46.33	55.78
42	46.97	56.26
43	47.61	56.74
44	48.25	57.22
45	48.88	57.71
46	49.51	58.20
47	50.14	58.69
48	50.77	59.19
49	51.39	59.70
50	52.01	60.20
51	52.62	60.71
52	53.24	61.22
53	53.85	61.74
54	54.46	62.26
55	55.06	62.79
56	55.66	63.31
57	56.26	63.84
58	56.86	64.38
59	57.45	64.92
60	58.04	65.46
61	58.62	66.00
62	59.20	66.55
63	59.78	67.10
64	59.81	67.13

Circle Center At X = -34.27 ; Y = 165.24 ; and Radius = 135.93

Factor of Safety
*** 1.154 ***

Failure Surface Specified By 59 Coordinate Points

Point No.	X-Surf (m)	Y-Surf (m)
1	19.39	40.82
2	20.16	41.04
3	20.92	41.27
4	21.68	41.51
5	22.45	41.76
6	23.20	42.02
7	23.96	42.28
8	24.71	42.56
9	25.46	42.84

10	26.20	43.13
11	26.95	43.42
12	27.69	43.73
13	28.42	44.04
14	29.16	44.36
15	29.88	44.69
16	30.61	45.03
17	31.33	45.38
18	32.05	45.73
19	32.76	46.09
20	33.47	46.46
21	34.18	46.83
22	34.88	47.22
23	35.58	47.61
24	36.27	48.01
25	36.96	48.41
26	37.65	48.83
27	38.33	49.25
28	39.00	49.68
29	39.67	50.11
30	40.34	50.56
31	41.00	51.01
32	41.66	51.46
33	42.31	51.93
34	42.95	52.40
35	43.60	52.88
36	44.23	53.36
37	44.86	53.86
38	45.49	54.36
39	46.11	54.86
40	46.72	55.37
41	47.33	55.89
42	47.93	56.42
43	48.53	56.95
44	49.12	57.49
45	49.71	58.04
46	50.29	58.59
47	50.86	59.14
48	51.43	59.71
49	51.99	60.28
50	52.54	60.85
51	53.09	61.44
52	53.63	62.03
53	54.17	62.62
54	54.70	63.22
55	55.22	63.82
56	55.74	64.44
57	56.25	65.05
58	56.75	65.67
59	56.88	65.84

Circle Center At X = -0.82 ; Y = 111.70 ; and Radius = 73.71

Factor of Safety

*** 1.154 ***

Failure Surface Specified By 58 Coordinate Points

Point No.	X-Surf (m)	Y-Surf (m)
1	19.39	40.82
2	20.16	41.02
3	20.94	41.22
4	21.71	41.44
5	22.47	41.66
6	23.24	41.90
7	24.00	42.15
8	24.76	42.40
9	25.51	42.66
10	26.27	42.94
11	27.01	43.22
12	27.76	43.51
13	28.50	43.81
14	29.24	44.12
15	29.97	44.44
16	30.70	44.77
17	31.43	45.10
18	32.15	45.45
19	32.87	45.80

20	33.58	46.17
21	34.29	46.54
22	34.99	46.92
23	35.69	47.31
24	36.38	47.71
25	37.07	48.12
26	37.75	48.53
27	38.43	48.96
28	39.11	49.39
29	39.77	49.83
30	40.44	50.28
31	41.09	50.73
32	41.74	51.20
33	42.39	51.67
34	43.03	52.15
35	43.66	52.64
36	44.29	53.14
37	44.91	53.64
38	45.53	54.15
39	46.13	54.67
40	46.74	55.20
41	47.33	55.73
42	47.92	56.27
43	48.50	56.82
44	49.08	57.38
45	49.65	57.94
46	50.21	58.51
47	50.76	59.09
48	51.31	59.67
49	51.85	60.26
50	52.38	60.86
51	52.91	61.46
52	53.42	62.07
53	53.93	62.69
54	54.44	63.31
55	54.93	63.94
56	55.42	64.58
57	55.90	65.22
58	56.10	65.50

Circle Center At X = 3.80 ; Y = 103.65 ; and Radius = 64.74

Factor of Safety

*** 1.155 ***

Failure Surface Specified By 58 Coordinate Points

Point No.	X-Surf (m)	Y-Surf (m)
1	18.57	40.00
2	19.35	40.17
3	20.13	40.35
4	20.91	40.54
5	21.69	40.74
6	22.46	40.95
7	23.23	41.17
8	23.99	41.40
9	24.75	41.65
10	25.51	41.90
11	26.27	42.17
12	27.02	42.44
13	27.76	42.73
14	28.51	43.03
15	29.24	43.33
16	29.98	43.65
17	30.71	43.98
18	31.43	44.32
19	32.15	44.67
20	32.87	45.03
21	33.58	45.40
22	34.28	45.78
23	34.98	46.17
24	35.67	46.57
25	36.36	46.98
26	37.04	47.40
27	37.72	47.82
28	38.39	48.26
29	39.05	48.71
30	39.71	49.17

31	40.36	49.63
32	41.00	50.11
33	41.64	50.59
34	42.27	51.09
35	42.89	51.59
36	43.51	52.10
37	44.11	52.62
38	44.71	53.15
39	45.31	53.68
40	45.89	54.23
41	46.47	54.78
42	47.04	55.34
43	47.60	55.91
44	48.16	56.49
45	48.70	57.08
46	49.24	57.67
47	49.77	58.27
48	50.29	58.88
49	50.80	59.49
50	51.30	60.12
51	51.79	60.74
52	52.28	61.38
53	52.75	62.02
54	53.22	62.67
55	53.68	63.33
56	54.13	63.99
57	54.56	64.66
58	54.70	64.88

Circle Center At X = 7.19 ; Y = 95.21 ; and Radius = 56.37
Factor of Safety
*** 1.156 ***

Failure Surface Specified By 68 Coordinate Points

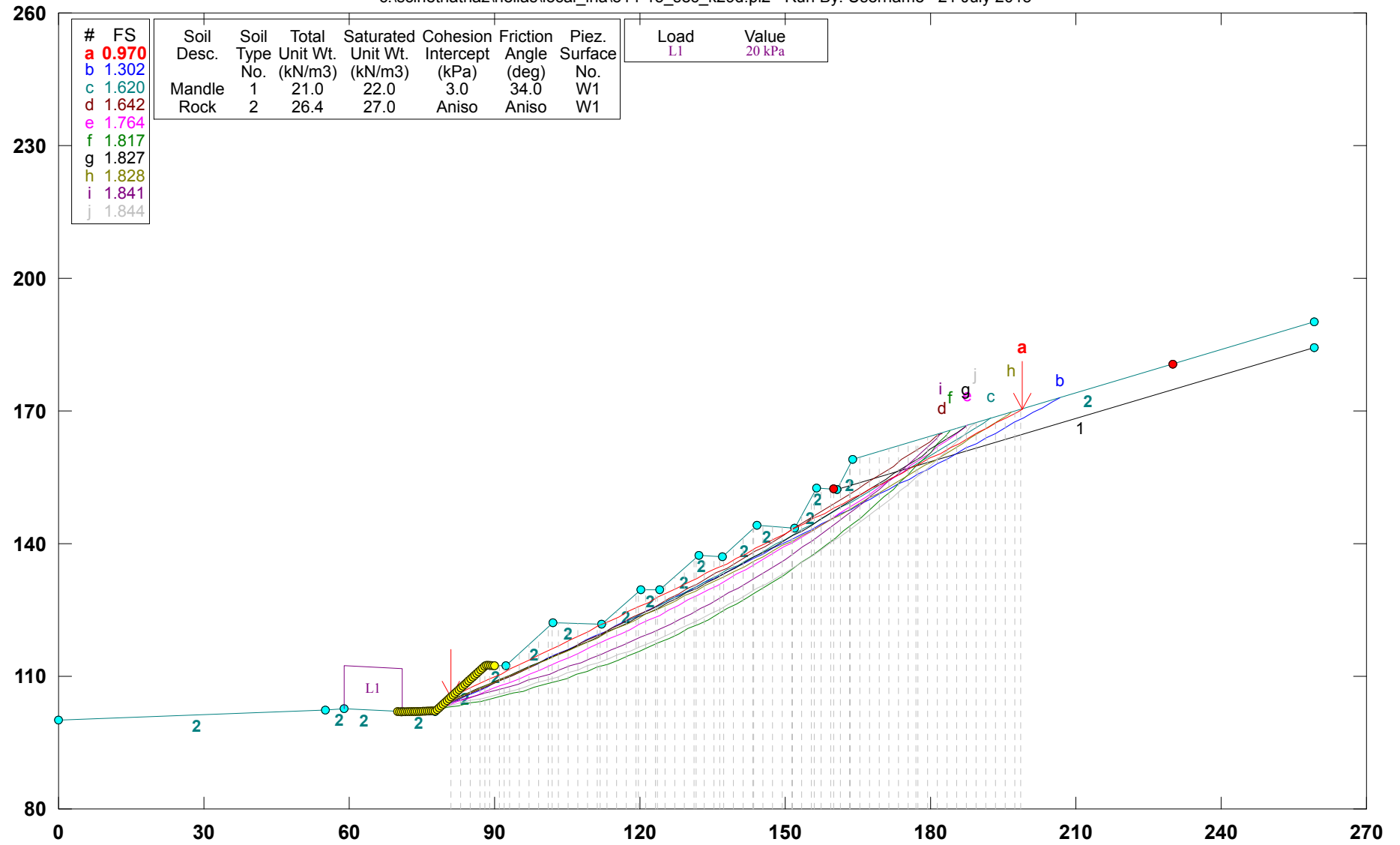
Point No.	X-Surf (m)	Y-Surf (m)
1	18.57	40.00
2	19.31	40.30
3	20.05	40.61
4	20.79	40.92
5	21.52	41.23
6	22.26	41.55
7	22.99	41.88
8	23.72	42.20
9	24.45	42.53
10	25.18	42.87
11	25.90	43.21
12	26.62	43.55
13	27.34	43.90
14	28.06	44.25
15	28.78	44.61
16	29.49	44.97
17	30.20	45.33
18	30.92	45.70
19	31.62	46.07
20	32.33	46.45
21	33.03	46.83
22	33.74	47.21
23	34.44	47.60
24	35.13	47.99
25	35.83	48.39
26	36.52	48.79
27	37.21	49.19
28	37.90	49.60
29	38.59	50.01
30	39.27	50.42
31	39.95	50.84
32	40.63	51.27
33	41.31	51.69
34	41.98	52.12
35	42.65	52.56
36	43.32	53.00
37	43.99	53.44
38	44.65	53.89
39	45.31	54.34
40	45.97	54.79
41	46.63	55.25

42	47.28	55.71
43	47.93	56.17
44	48.58	56.64
45	49.23	57.11
46	49.87	57.59
47	50.51	58.07
48	51.15	58.55
49	51.78	59.04
50	52.42	59.53
51	53.04	60.02
52	53.67	60.52
53	54.30	61.02
54	54.92	61.53
55	55.53	62.03
56	56.15	62.55
57	56.76	63.06
58	57.37	63.58
59	57.98	64.10
60	58.58	64.63
61	59.18	65.16
62	59.78	65.69
63	60.37	66.22
64	60.96	66.76
65	61.55	67.30
66	62.14	67.85
67	62.72	68.40
68	62.73	68.41

Circle Center At X = -34.15 ; Y = 170.47 ; and Radius = 140.72
Factor of Safety
*** 1.159 ***
**** END OF GSTABL7 OUTPUT ****

Hellas_Local_Landslide_Hazard Cut slope O14-15_sec_K29D

c:\scinet\nathaz\hellas\local_lha\o14-15_sec_k29d.pl2 Run By: Username 21 July 2015



GSTABL7 v.2 FSmin=0.970

Safety Factors Are Calculated By The Modified Bishop Method



```

*** GSTABL7 ***
** GSTABL7 by Garry H. Gregory, P.E. **
** Original Version 1.0, January 1996; Current Version 2.003, June 2002 **
  (All Rights Reserved-Unauthorized Use Prohibited)
*****
      SLOPE STABILITY ANALYSIS SYSTEM
      Modified Bishop, Simplified Janbu, or GLE Method of Slices.
      (Includes Spencer & Morgenstern-Price Type Analysis)
      Including Pier/Pile, Reinforcement, Soil Nail, Tieback,
      Nonlinear Undrained Shear Strength, Curved Phi Envelope,
      Anisotropic Soil, Fiber-Reinforced Soil, Boundary Loads, Water
      Surfaces, Pseudo-Static & Newmark Earthquake, and Applied Forces.
*****
Analysis Run Date:      21 July 2015
Time of Run:
Run By:                  Username
Input Data Filename:    C:\SciNetNatHaz\Hellas\Local_LHA\014-15_sec_k29d.in
Output Filename:        C:\SciNetNatHaz\Hellas\Local_LHA\014-15_sec_k29d.OUT
Unit System:            SI
Plotted Output Filename: C:\SciNetNatHaz\Hellas\Local_LHA-15_sec_k29d.PLT
PROBLEM DESCRIPTION:    Hellas_Local_Landslide_Hazard
                        Cut slope 014-15_sec_K29D

BOUNDARY COORDINATES
  18 Top      Boundaries
  19 Total Boundaries
Boundary      X-Left      Y-Left      X-Right      Y-Right      Soil Type
No.           (m)         (m)         (m)         (m)         Below Bnd
  1             0.00       100.00       55.22       102.21        2
  2             55.22       102.21       58.86       102.79        2
  3             58.86       102.79       70.86       101.95        2
  4             70.86       101.95       77.87       102.18        2
  5             77.87       102.18       88.19       112.50        2
  6             88.19       112.50       92.19       112.26        2

```

7	92.19	112.26	102.19	122.26	2
8	102.19	122.26	112.19	121.66	2
9	112.19	121.66	120.19	129.66	2
10	120.19	129.66	124.19	129.42	2
11	124.19	129.42	132.19	137.42	2
12	132.19	137.42	137.08	137.12	2
13	137.08	137.12	144.08	144.12	2
14	144.08	144.12	152.08	143.64	2
15	152.08	143.64	156.57	152.62	2
16	156.57	152.62	160.57	152.38	2
17	160.57	152.38	163.89	159.01	2
18	163.89	159.01	259.19	190.07	2
19	160.57	152.38	259.03	184.48	1

User Specified Y-Origin = 80.00(m)

Default X-Plus Value = 0.00(m)

Default Y-Plus Value = 0.00(m)

ISOTROPIC SOIL PARAMETERS

2 Type(s) of Soil

Soil Type	Total Unit Wt.	Saturated Unit Wt.	Cohesion Intercept	Friction Angle	Pore Pressure Param.	Pressure Constant	Piez. Surface
No.	(kN/m3)	(kN/m3)	(kPa)	(deg)		(kPa)	No.
1	21.0	22.0	3.0	34.0	0.00	0.0	1
2	26.4	27.0	150.0	42.0	0.00	0.0	1

ANISOTROPIC STRENGTH PARAMETERS

1 soil type(s)

Soil Type 2 Is Anisotropic

Number Of Direction Ranges Specified = 3

Direction Range	Counterclockwise Direction Limit	Cohesion Intercept	Friction Angle
No.	(deg)	(kPa)	(deg)
1	27.0	150.00	42.00
2	60.0	1.00	25.00
3	90.0	150.00	42.00

ANISOTROPIC SOIL NOTES:

- (1) An input value of 0.01 for C and/or Phi will cause Aniso C and/or Phi to be ignored in that range.
- (2) An input value of 0.02 for Phi will set both Phi and C equal to zero, with no water weight in the tension crack.
- (3) An input value of 0.03 for Phi will set both Phi and C equal to zero, with water weight in the tension crack.

BOUNDARY LOAD(S)

1 Load(s) Specified

Load No.	X-Left (m)	X-Right (m)	Intensity (kPa)	Deflection (deg)
1	58.86	70.86	20.0	0.0

NOTE - Intensity Is Specified As A Uniformly Distributed Force Acting On A Horizontally Projected Surface.

SOIL NAIL LOAD(S)

27 SOIL NAIL LOAD(S) SPECIFIED

Nail No.	X-Pos (m)	Y-Pos (m)	Nail Dia (mm)	Tendon Dia (mm)	Spacing (m)	Inclin. (deg)	Length (m)
1	78.87	103.18	89.0	22.0	2.00	10.00	12.00
2	80.87	105.18	89.0	22.0	2.00	10.00	12.00
3	82.87	107.18	89.0	22.0	2.00	10.00	12.00
4	84.87	109.18	89.0	22.0	2.00	10.00	12.00
5	86.87	111.18	89.0	22.0	2.00	10.00	12.00
6	93.11	113.18	89.0	22.0	2.00	10.00	12.00
7	95.11	115.18	89.0	22.0	2.00	10.00	12.00
8	97.11	117.18	89.0	22.0	2.00	10.00	12.00
9	99.11	119.18	89.0	22.0	2.00	10.00	12.00
10	101.11	121.18	89.0	22.0	2.00	10.00	12.00
11	113.71	123.18	89.0	22.0	2.00	10.00	12.00
12	115.71	125.18	89.0	22.0	2.00	10.00	12.00
13	117.71	127.18	89.0	22.0	2.00	10.00	12.00
14	119.71	129.18	89.0	22.0	2.00	10.00	12.00
15	125.95	131.18	89.0	22.0	2.00	10.00	12.00
16	127.95	133.18	89.0	22.0	2.00	10.00	12.00
17	129.95	135.18	89.0	22.0	2.00	10.00	12.00
18	139.14	139.18	89.0	22.0	2.00	10.00	12.00
19	141.14	141.18	89.0	22.0	2.00	10.00	12.00
20	143.14	143.18	89.0	22.0	2.00	10.00	12.00
21	152.85	145.18	89.0	22.0	2.00	10.00	12.00
22	153.85	147.18	89.0	22.0	2.00	10.00	12.00
23	154.85	149.18	89.0	22.0	2.00	10.00	12.00
24	155.85	151.18	89.0	22.0	2.00	10.00	12.00

25	160.97	153.18	89.0	22.0	2.00	10.00	12.00
26	161.97	155.18	89.0	22.0	2.00	10.00	12.00
27	162.97	157.18	89.0	22.0	2.00	10.00	12.00

SOIL NAIL LOAD DATA

Soil Nail No. 1 4 Load Points Apply to This Nail

Load Diagram Type = 1

POINT NO.	X-COORD.(m)	Y-COORD.(m)	FORCE(kN)
1	78.87	103.18	25.00
2	80.49	102.90	82.64
3	88.54	101.50	82.64
4	90.69	101.10	0.00

Allowable Pullout Stress = 250.0(kPa)

Allowable Tendon Stress = 434782.6

Allowable Nail Head Load = 50.0(kN)

Soil Nail No. 2 4 Load Points Apply to This Nail

Load Diagram Type = 1

POINT NO.	X-COORD.(m)	Y-COORD.(m)	FORCE(kN)
1	80.87	105.18	25.00
2	82.49	104.90	82.64
3	90.54	103.50	82.64
4	92.69	103.10	0.00

Allowable Pullout Stress = 250.0(kPa)

Allowable Tendon Stress = 434782.6

Allowable Nail Head Load = 50.0(kN)

Soil Nail No. 3 4 Load Points Apply to This Nail

Load Diagram Type = 1

POINT NO.	X-COORD.(m)	Y-COORD.(m)	FORCE(kN)
1	82.87	107.18	25.00
2	84.49	106.90	82.64
3	92.54	105.50	82.64
4	94.69	105.10	0.00

Allowable Pullout Stress = 250.0(kPa)

Allowable Tendon Stress = 434782.6

Allowable Nail Head Load = 50.0(kN)

Soil Nail No. 4 4 Load Points Apply to This Nail

Load Diagram Type = 1

POINT NO.	X-COORD.(m)	Y-COORD.(m)	FORCE(kN)
1	84.87	109.18	25.00
2	86.49	108.90	82.64
3	94.54	107.50	82.64
4	96.69	107.10	0.00

Allowable Pullout Stress = 250.0(kPa)

Allowable Tendon Stress = 434782.6

Allowable Nail Head Load = 50.0(kN)

Soil Nail No. 5 4 Load Points Apply to This Nail

Load Diagram Type = 1

POINT NO.	X-COORD.(m)	Y-COORD.(m)	FORCE(kN)
1	86.87	111.18	25.00
2	88.49	110.90	82.64
3	96.54	109.50	82.64
4	98.69	109.10	0.00

Allowable Pullout Stress = 250.0(kPa)

Allowable Tendon Stress = 434782.6

Allowable Nail Head Load = 50.0(kN)

Soil Nail No. 6 4 Load Points Apply to This Nail

Load Diagram Type = 1

POINT NO.	X-COORD.(m)	Y-COORD.(m)	FORCE(kN)
1	93.11	113.18	25.00
2	94.73	112.90	82.64
3	102.78	111.50	82.64
4	104.93	111.10	0.00

Allowable Pullout Stress = 250.0(kPa)

Allowable Tendon Stress = 434782.6

Allowable Nail Head Load = 50.0(kN)

Soil Nail No. 7 4 Load Points Apply to This Nail

Load Diagram Type = 1

POINT NO.	X-COORD.(m)	Y-COORD.(m)	FORCE(kN)
1	95.11	115.18	25.00
2	96.73	114.90	82.64
3	104.78	113.50	82.64
4	106.93	113.10	0.00

Allowable Pullout Stress = 250.0(kPa)

Allowable Tendon Stress = 434782.6

Allowable Nail Head Load = 50.0(kN)

Soil Nail No. 8 4 Load Points Apply to This Nail

Load Diagram Type = 1

POINT NO.	X-COORD.(m)	Y-COORD.(m)	FORCE(kN)
1	97.11	117.18	25.00
2	98.73	116.90	82.64
3	106.78	115.50	82.64
4	108.93	115.10	0.00

Allowable Pullout Stress = 250.0(kPa)
 Allowable Tendon Stress = 434782.6
 Allowable Nail Head Load = 50.0(kN)
 Soil Nail No. 9 4 Load Points Apply to This Nail

Load Diagram Type = 1

POINT NO.	X-COORD.(m)	Y-COORD.(m)	FORCE(kN)
1	99.11	119.18	25.00
2	100.73	118.90	82.64
3	108.78	117.50	82.64
4	110.93	117.10	0.00

Allowable Pullout Stress = 250.0(kPa)
 Allowable Tendon Stress = 434782.6
 Allowable Nail Head Load = 50.0(kN)
 Soil Nail No. 10 4 Load Points Apply to This Nail

Load Diagram Type = 1

POINT NO.	X-COORD.(m)	Y-COORD.(m)	FORCE(kN)
1	101.11	121.18	25.00
2	102.73	120.90	82.64
3	110.78	119.50	82.64
4	112.93	119.10	0.00

Allowable Pullout Stress = 250.0(kPa)
 Allowable Tendon Stress = 434782.6
 Allowable Nail Head Load = 50.0(kN)
 Soil Nail No. 11 4 Load Points Apply to This Nail

Load Diagram Type = 1

POINT NO.	X-COORD.(m)	Y-COORD.(m)	FORCE(kN)
1	113.71	123.18	25.00
2	115.33	122.90	82.64
3	123.38	121.50	82.64
4	125.53	121.10	0.00

Allowable Pullout Stress = 250.0(kPa)
 Allowable Tendon Stress = 434782.6
 Allowable Nail Head Load = 50.0(kN)
 Soil Nail No. 12 4 Load Points Apply to This Nail

Load Diagram Type = 1

POINT NO.	X-COORD.(m)	Y-COORD.(m)	FORCE(kN)
1	115.71	125.18	25.00
2	117.33	124.90	82.64
3	125.38	123.50	82.64
4	127.53	123.10	0.00

Allowable Pullout Stress = 250.0(kPa)
 Allowable Tendon Stress = 434782.6
 Allowable Nail Head Load = 50.0(kN)
 Soil Nail No. 13 4 Load Points Apply to This Nail

Load Diagram Type = 1

POINT NO.	X-COORD.(m)	Y-COORD.(m)	FORCE(kN)
1	117.71	127.18	25.00
2	119.33	126.90	82.64
3	127.38	125.50	82.64
4	129.53	125.10	0.00

Allowable Pullout Stress = 250.0(kPa)
 Allowable Tendon Stress = 434782.6
 Allowable Nail Head Load = 50.0(kN)
 Soil Nail No. 14 4 Load Points Apply to This Nail

Load Diagram Type = 1

POINT NO.	X-COORD.(m)	Y-COORD.(m)	FORCE(kN)
1	119.71	129.18	25.00
2	121.33	128.90	82.64
3	129.38	127.50	82.64
4	131.53	127.10	0.00

Allowable Pullout Stress = 250.0(kPa)
 Allowable Tendon Stress = 434782.6
 Allowable Nail Head Load = 50.0(kN)
 Soil Nail No. 15 4 Load Points Apply to This Nail

Load Diagram Type = 1

POINT NO.	X-COORD.(m)	Y-COORD.(m)	FORCE(kN)
1	125.95	131.18	25.00
2	127.57	130.90	82.64
3	135.62	129.50	82.64

4 137.77 129.10 0.00
 Allowable Pullout Stress = 250.0(kPa)
 Allowable Tendon Stress = 434782.6
 Allowable Nail Head Load = 50.0(kN)
 Soil Nail No. 16 4 Load Points Apply to This Nail
 Load Diagram Type = 1

POINT NO.	X-COORD.(m)	Y-COORD.(m)	FORCE(kN)
1	127.95	133.18	25.00
2	129.57	132.90	82.64
3	137.62	131.50	82.64
4	139.77	131.10	0.00

 Allowable Pullout Stress = 250.0(kPa)
 Allowable Tendon Stress = 434782.6
 Allowable Nail Head Load = 50.0(kN)
 Soil Nail No. 17 4 Load Points Apply to This Nail
 Load Diagram Type = 1

POINT NO.	X-COORD.(m)	Y-COORD.(m)	FORCE(kN)
1	129.95	135.18	25.00
2	131.57	134.90	82.64
3	139.62	133.50	82.64
4	141.77	133.10	0.00

 Allowable Pullout Stress = 250.0(kPa)
 Allowable Tendon Stress = 434782.6
 Allowable Nail Head Load = 50.0(kN)
 Soil Nail No. 18 4 Load Points Apply to This Nail
 Load Diagram Type = 1

POINT NO.	X-COORD.(m)	Y-COORD.(m)	FORCE(kN)
1	139.14	139.18	25.00
2	140.76	138.90	82.64
3	148.81	137.50	82.64
4	150.96	137.10	0.00

 Allowable Pullout Stress = 250.0(kPa)
 Allowable Tendon Stress = 434782.6
 Allowable Nail Head Load = 50.0(kN)
 Soil Nail No. 19 4 Load Points Apply to This Nail
 Load Diagram Type = 1

POINT NO.	X-COORD.(m)	Y-COORD.(m)	FORCE(kN)
1	141.14	141.18	25.00
2	142.76	140.90	82.64
3	150.81	139.50	82.64
4	152.96	139.10	0.00

 Allowable Pullout Stress = 250.0(kPa)
 Allowable Tendon Stress = 434782.6
 Allowable Nail Head Load = 50.0(kN)
 Soil Nail No. 20 4 Load Points Apply to This Nail
 Load Diagram Type = 1

POINT NO.	X-COORD.(m)	Y-COORD.(m)	FORCE(kN)
1	143.14	143.18	25.00
2	144.76	142.90	82.64
3	152.81	141.50	82.64
4	154.96	141.10	0.00

 Allowable Pullout Stress = 250.0(kPa)
 Allowable Tendon Stress = 434782.6
 Allowable Nail Head Load = 50.0(kN)
 Soil Nail No. 21 4 Load Points Apply to This Nail
 Load Diagram Type = 1

POINT NO.	X-COORD.(m)	Y-COORD.(m)	FORCE(kN)
1	152.85	145.18	25.00
2	154.47	144.90	82.64
3	162.52	143.50	82.64
4	164.67	143.10	0.00

 Allowable Pullout Stress = 250.0(kPa)
 Allowable Tendon Stress = 434782.6
 Allowable Nail Head Load = 50.0(kN)
 Soil Nail No. 22 4 Load Points Apply to This Nail
 Load Diagram Type = 1

POINT NO.	X-COORD.(m)	Y-COORD.(m)	FORCE(kN)
1	153.85	147.18	25.00
2	155.47	146.90	82.64
3	163.52	145.50	82.64
4	165.67	145.10	0.00

 Allowable Pullout Stress = 250.0(kPa)
 Allowable Tendon Stress = 434782.6
 Allowable Nail Head Load = 50.0(kN)
 Soil Nail No. 23 4 Load Points Apply to This Nail

Load Diagram Type = 1

POINT NO.	X-COORD.(m)	Y-COORD.(m)	FORCE(kN)
1	154.85	149.18	25.00
2	156.47	148.90	82.64
3	164.52	147.50	82.64
4	166.67	147.10	0.00

Allowable Pullout Stress = 250.0(kPa)

Allowable Tendon Stress = 434782.6

Allowable Nail Head Load = 50.0(kN)

Soil Nail No. 24 4 Load Points Apply to This Nail

Load Diagram Type = 1

POINT NO.	X-COORD.(m)	Y-COORD.(m)	FORCE(kN)
1	155.85	151.18	25.00
2	157.47	150.90	82.64
3	165.52	149.50	82.64
4	167.67	149.10	0.00

Allowable Pullout Stress = 250.0(kPa)

Allowable Tendon Stress = 434782.6

Allowable Nail Head Load = 50.0(kN)

Soil Nail No. 25 4 Load Points Apply to This Nail

Load Diagram Type = 1

POINT NO.	X-COORD.(m)	Y-COORD.(m)	FORCE(kN)
1	160.97	153.18	25.00
2	162.59	152.90	82.64
3	170.64	151.50	82.64
4	172.79	151.10	0.00

Allowable Pullout Stress = 250.0(kPa)

Allowable Tendon Stress = 434782.6

Allowable Nail Head Load = 50.0(kN)

Soil Nail No. 26 4 Load Points Apply to This Nail

Load Diagram Type = 1

POINT NO.	X-COORD.(m)	Y-COORD.(m)	FORCE(kN)
1	161.97	155.18	25.00
2	166.03	154.47	82.64
3	168.15	154.11	82.64
4	173.79	153.10	0.00

Allowable Pullout Stress = 100.0(kPa)

Allowable Tendon Stress = 434782.6

Allowable Nail Head Load = 50.0(kN)

Soil Nail No. 27 4 Load Points Apply to This Nail

Load Diagram Type = 1

POINT NO.	X-COORD.(m)	Y-COORD.(m)	FORCE(kN)
1	162.97	157.18	25.00
2	167.03	156.47	82.64
3	169.15	156.11	82.64
4	174.79	155.10	0.00

Allowable Pullout Stress = 100.0(kPa)

Allowable Tendon Stress = 434782.6

Allowable Nail Head Load = 50.0(kN)

NOTE - An Equivalent Line Load Is Calculated For Each Row Of Soil Nails
Assuming A Uniform Distribution Of Load Horizontally Between
Individual Nails.

SOIL NAIL LOAD DATA HAS BEEN SUPPRESSED

A Critical Failure Surface Searching Method, Using A Random
Technique For Generating Circular Surfaces, Has Been Specified.
2500 Trial Surfaces Have Been Generated.

50 Surface(s) Initiate(s) From Each Of 50 Points Equally Spaced
Along The Ground Surface Between X = 70.00(m)
and X = 90.00(m)

Each Surface Terminates Between X = 160.00(m)
and X = 230.00(m)

Unless Further Limitations Were Imposed, The Minimum Elevation
At Which A Surface Extends Is Y = 0.00(m)

2.30(m) Line Segments Define Each Trial Failure Surface.
Following Are Displayed The Ten Most Critical Of The Trial

Failure Surfaces Evaluated. They Are
Ordered - Most Critical First.

* * Safety Factors Are Calculated By The Modified Bishop Method * *

Total Number of Trial Surfaces Evaluated = 2500

Statistical Data On All Valid FS Values:

FS Max = 3.597 FS Min = 0.970 FS Ave = 2.795

Standard Deviation = 0.485 Coefficient of Variation = 17.36 %

Failure Surface Specified By 60 Coordinate Points

Point No.	X-Surf (m)	Y-Surf (m)
--------------	---------------	---------------

1	81.02	105.33
2	83.07	106.38
3	85.11	107.43
4	87.15	108.49
5	89.20	109.55
6	91.24	110.61
7	93.28	111.67
8	95.32	112.73
9	97.36	113.80
10	99.39	114.87
11	101.43	115.94
12	103.46	117.01
13	105.50	118.08
14	107.53	119.16
15	109.56	120.24
16	111.59	121.32
17	113.62	122.40
18	115.65	123.49
19	117.68	124.57
20	119.70	125.66
21	121.73	126.75
22	123.75	127.85
23	125.77	128.94
24	127.79	130.04
25	129.81	131.14
26	131.83	132.24
27	133.85	133.34
28	135.87	134.45
29	137.88	135.56
30	139.90	136.67
31	141.91	137.78
32	143.92	138.89
33	145.93	140.01
34	147.94	141.13
35	149.95	142.25
36	151.96	143.37
37	153.97	144.49
38	155.97	145.62
39	157.98	146.75
40	159.98	147.88
41	161.98	149.01
42	163.98	150.15
43	165.98	151.29
44	167.98	152.42
45	169.98	153.57
46	171.97	154.71
47	173.97	155.85
48	175.96	157.00
49	177.95	158.15
50	179.94	159.30
51	181.93	160.45
52	183.92	161.61
53	185.91	162.77
54	187.90	163.93
55	189.88	165.09
56	191.86	166.25
57	193.85	167.42
58	195.83	168.59
59	197.81	169.76
60	198.97	170.44

Circle Center At X = -933.59 ; Y = 2082.63 ; and Radius = 2222.42

Factor of Safety

*** 0.970 ***

		Individual data on the 73 slices									
		Water		Tie		Tie		Earthquake		Surcharge	
		Force	Force	Force	Force	Force	Force	Force	Force	Force	Force
		Top	Bot	Norm	Tan	Hor	Ver	Hor	Ver	Load	Load
Slice	Width	Weight	(kN)	(kN)	(kN)	(kN)	(kN)	(kN)	(kN)	(kN)	(kN)
No.	(m)	(kN)	(kN)	(kN)	(kN)	(kN)	(kN)	(kN)	(kN)	(kN)	(kN)
1	2.0	26.9	0.0	0.0	0.	0.	0.0	0.0	0.0	0.0	0.0
2	2.0	80.5	0.0	0.0	0.	0.	0.0	0.0	0.0	0.0	0.0
3	2.0	133.8	0.0	0.0	0.	0.	0.0	0.0	0.0	0.0	0.0
4	1.0	88.1	0.0	0.0	0.	0.	0.0	0.0	0.0	0.0	0.0
5	1.0	84.6	0.0	0.0	0.	0.	0.0	0.0	0.0	0.0	0.0
6	2.0	124.0	0.0	0.0	0.	0.	0.0	0.0	0.0	0.0	0.0
7	1.0	36.0	0.0	0.0	0.	0.	0.0	0.0	0.0	0.0	0.0

8	1.1	40.8	0.0	0.0	0.	0.	0.0	0.0	0.0
9	2.0	116.7	0.0	0.0	0.	0.	0.0	0.0	0.0
10	2.0	169.0	0.0	0.0	0.	0.	0.0	0.0	0.0
11	2.0	221.1	0.0	0.0	0.	0.	0.0	0.0	0.0
12	2.0	273.0	0.0	0.0	0.	0.	0.0	0.0	0.0
13	0.8	115.4	0.0	0.0	0.	0.	0.0	0.0	0.0
14	1.3	186.6	0.0	0.0	0.	0.	0.0	0.0	0.0
15	2.0	245.7	0.0	0.0	0.	0.	0.0	0.0	0.0
16	2.0	181.3	0.0	0.0	0.	0.	0.0	0.0	0.0
17	2.0	116.9	0.0	0.0	0.	0.	0.0	0.0	0.0
18	2.0	52.5	0.0	0.0	0.	0.	0.0	0.0	0.0
19	0.6	3.2	0.0	0.0	0.	0.	0.0	0.0	0.0
20	1.4	13.5	0.0	0.0	0.	0.	0.0	0.0	0.0
21	2.0	62.2	0.0	0.0	0.	0.	0.0	0.0	0.0
22	2.0	112.5	0.0	0.0	0.	0.	0.0	0.0	0.0
23	2.0	162.7	0.0	0.0	0.	0.	0.0	0.0	0.0
24	0.5	46.7	0.0	0.0	0.	0.	0.0	0.0	0.0
25	1.5	132.9	0.0	0.0	0.	0.	0.0	0.0	0.0
26	2.0	117.9	0.0	0.0	0.	0.	0.0	0.0	0.0
27	0.4	17.0	0.0	0.0	0.	0.	0.0	0.0	0.0
28	1.6	71.0	0.0	0.0	0.	0.	0.0	0.0	0.0
29	2.0	134.6	0.0	0.0	0.	0.	0.0	0.0	0.0
30	2.0	183.8	0.0	0.0	0.	0.	0.0	0.0	0.0
31	2.0	232.6	0.0	0.0	0.	0.	0.0	0.0	0.0
32	0.4	46.2	0.0	0.0	0.	0.	0.0	0.0	0.0
33	1.7	196.5	0.0	0.0	0.	0.	0.0	0.0	0.0
34	2.0	178.9	0.0	0.0	0.	0.	0.0	0.0	0.0
35	1.2	76.0	0.0	0.0	0.	0.	0.0	0.0	0.0
36	0.8	46.4	0.0	0.0	0.	0.	0.0	0.0	0.0
37	2.0	149.9	0.0	0.0	0.	0.	0.0	0.0	0.0
38	2.0	197.8	0.0	0.0	0.	0.	0.0	0.0	0.0
39	2.0	245.5	0.0	0.0	0.	0.	0.0	0.0	0.0
40	0.2	21.1	0.0	0.0	0.	0.	0.0	0.0	0.0
41	1.9	223.7	0.0	0.0	0.	0.	0.0	0.0	0.0
42	2.0	179.3	0.0	0.0	0.	0.	0.0	0.0	0.0
43	2.0	113.5	0.0	0.0	0.	0.	0.0	0.0	0.0
44	2.0	47.6	0.0	0.0	0.	0.	0.0	0.0	0.0
45	0.1	0.8	0.0	0.0	0.	0.	0.0	0.0	0.0
46	1.9	77.8	0.0	0.0	0.	0.	0.0	0.0	0.0
47	2.0	230.9	0.0	0.0	0.	0.	0.0	0.0	0.0
48	0.6	98.4	0.0	0.0	0.	0.	0.0	0.0	0.0
49	1.4	231.1	0.0	0.0	0.	0.	0.0	0.0	0.0
50	2.0	272.9	0.0	0.0	0.	0.	0.0	0.0	0.0
51	0.6	67.8	0.0	0.0	0.	0.	0.0	0.0	0.0
52	1.4	162.3	0.0	0.0	0.	0.	0.0	0.0	0.0
53	1.9	343.4	0.0	0.0	0.	0.	0.0	0.0	0.0
54	0.1	19.8	0.0	0.0	0.	0.	0.0	0.0	0.0
55	2.0	423.0	0.0	0.0	0.	0.	0.0	0.0	0.0
56	2.0	402.4	0.0	0.0	0.	0.	0.0	0.0	0.0
57	2.0	381.6	0.0	0.0	0.	0.	0.0	0.0	0.0
58	2.0	360.8	0.0	0.0	0.	0.	0.0	0.0	0.0
59	2.0	339.9	0.0	0.0	0.	0.	0.0	0.0	0.0
60	2.0	318.9	0.0	0.0	0.	0.	0.0	0.0	0.0
61	1.6	238.1	0.0	0.0	0.	0.	0.0	0.0	0.0
62	0.4	59.6	0.0	0.0	0.	0.	0.0	0.0	0.0
63	2.0	272.9	0.0	0.0	0.	0.	0.0	0.0	0.0
64	2.0	246.3	0.0	0.0	0.	0.	0.0	0.0	0.0
65	2.0	219.6	0.0	0.0	0.	0.	0.0	0.0	0.0
66	2.0	192.7	0.0	0.0	0.	0.	0.0	0.0	0.0
67	2.0	165.8	0.0	0.0	0.	0.	0.0	0.0	0.0
68	2.0	138.8	0.0	0.0	0.	0.	0.0	0.0	0.0
69	2.0	111.7	0.0	0.0	0.	0.	0.0	0.0	0.0
70	2.0	84.5	0.0	0.0	0.	0.	0.0	0.0	0.0
71	2.0	57.2	0.0	0.0	0.	0.	0.0	0.0	0.0
72	2.0	29.8	0.0	0.0	0.	0.	0.0	0.0	0.0
73	1.2	4.7	0.0	0.0	0.	0.	0.0	0.0	0.0

Failure Surface Specified By 65 Coordinate Points

Point No.	X-Surf (m)	Y-Surf (m)
1	78.16	102.47
2	80.22	103.50
3	82.28	104.53
4	84.33	105.56
5	86.39	106.60
6	88.44	107.64

7	90.49	108.68
8	92.54	109.72
9	94.59	110.77
10	96.64	111.81
11	98.68	112.87
12	100.73	113.92
13	102.77	114.97
14	104.81	116.03
15	106.85	117.09
16	108.89	118.15
17	110.93	119.22
18	112.97	120.29
19	115.00	121.36
20	117.04	122.43
21	119.07	123.51
22	121.10	124.58
23	123.13	125.66
24	125.16	126.75
25	127.19	127.83
26	129.22	128.92
27	131.24	130.01
28	133.27	131.10
29	135.29	132.20
30	137.31	133.29
31	139.33	134.39
32	141.35	135.50
33	143.37	136.60
34	145.38	137.71
35	147.40	138.82
36	149.41	139.93
37	151.42	141.04
38	153.43	142.16
39	155.44	143.28
40	157.45	144.40
41	159.46	145.53
42	161.46	146.65
43	163.47	147.78
44	165.47	148.91
45	167.47	150.05
46	169.47	151.18
47	171.47	152.32
48	173.46	153.47
49	175.46	154.61
50	177.45	155.76
51	179.45	156.90
52	181.44	158.05
53	183.43	159.21
54	185.42	160.36
55	187.40	161.52
56	189.39	162.68
57	191.37	163.85
58	193.36	165.01
59	195.34	166.18
60	197.32	167.35
61	199.30	168.52
62	201.27	169.70
63	203.25	170.88
64	205.22	172.06
65	206.78	172.99

Circle Center At X = -766.29 ; Y = 1795.27 ; and Radius = 1891.73

Factor of Safety

*** 1.302 ***

Failure Surface Specified By 58 Coordinate Points

Point No.	X-Surf (m)	Y-Surf (m)
1	78.98	103.29
2	81.06	104.26
3	83.14	105.25
4	85.22	106.23
5	87.29	107.23
6	89.37	108.23
7	91.43	109.23
8	93.50	110.24
9	95.56	111.26
10	97.62	112.29

11	99.68	113.32
12	101.73	114.35
13	103.78	115.39
14	105.83	116.44
15	107.87	117.50
16	109.91	118.56
17	111.95	119.62
18	113.99	120.70
19	116.02	121.77
20	118.05	122.86
21	120.07	123.95
22	122.09	125.05
23	124.11	126.15
24	126.13	127.26
25	128.14	128.37
26	130.15	129.49
27	132.15	130.62
28	134.15	131.75
29	136.15	132.89
30	138.15	134.03
31	140.14	135.18
32	142.13	136.34
33	144.11	137.50
34	146.10	138.67
35	148.07	139.84
36	150.05	141.02
37	152.02	142.21
38	153.99	143.40
39	155.95	144.60
40	157.91	145.80
41	159.87	147.01
42	161.82	148.22
43	163.77	149.44
44	165.72	150.67
45	167.66	151.90
46	169.60	153.14
47	171.53	154.38
48	173.46	155.63
49	175.39	156.88
50	177.32	158.14
51	179.24	159.41
52	181.15	160.68
53	183.07	161.96
54	184.97	163.24
55	186.88	164.53
56	188.78	165.82
57	190.68	167.12
58	192.38	168.29

Circle Center At X = -249.16 ; Y = 807.13 ; and Radius = 776.57

Factor of Safety

*** 1.620 ***

Failure Surface Specified By 54 Coordinate Points

Point No.	X-Surf (m)	Y-Surf (m)
1	78.98	103.29
2	81.07	104.24
3	83.16	105.21
4	85.25	106.18
5	87.33	107.16
6	89.40	108.15
7	91.48	109.14
8	93.54	110.15
9	95.61	111.17
10	97.67	112.19
11	99.72	113.23
12	101.77	114.27
13	103.82	115.32
14	105.86	116.38
15	107.89	117.45
16	109.92	118.53
17	111.95	119.62
18	113.97	120.71
19	115.99	121.82
20	118.00	122.93
21	120.01	124.05

22	122.01	125.18
23	124.01	126.32
24	126.01	127.47
25	127.99	128.63
26	129.98	129.79
27	131.95	130.96
28	133.93	132.15
29	135.90	133.34
30	137.86	134.54
31	139.82	135.74
32	141.77	136.96
33	143.71	138.18
34	145.66	139.42
35	147.59	140.66
36	149.52	141.91
37	151.45	143.17
38	153.37	144.43
39	155.28	145.71
40	157.19	146.99
41	159.10	148.28
42	160.99	149.58
43	162.89	150.89
44	164.77	152.20
45	166.65	153.53
46	168.53	154.86
47	170.40	156.20
48	172.26	157.55
49	174.12	158.91
50	175.97	160.27
51	177.82	161.64
52	179.66	163.02
53	181.49	164.41
54	182.26	165.00

Circle Center At X = -140.29 ; Y = 587.56 ; and Radius = 531.60

Factor of Safety

*** 1.642 ***

Failure Surface Specified By 57 Coordinate Points

Point No.	X-Surf (m)	Y-Surf (m)
1	78.16	102.47
2	80.30	103.32
3	82.43	104.18
4	84.56	105.06
5	86.68	105.94
6	88.80	106.84
7	90.91	107.75
8	93.02	108.67
9	95.12	109.60
10	97.22	110.55
11	99.31	111.50
12	101.40	112.47
13	103.48	113.45
14	105.56	114.44
15	107.63	115.44
16	109.69	116.46
17	111.75	117.49
18	113.80	118.52
19	115.85	119.57
20	117.89	120.63
21	119.92	121.71
22	121.95	122.79
23	123.97	123.88
24	125.99	124.99
25	128.00	126.11
26	130.00	127.24
27	132.00	128.38
28	133.99	129.53
29	135.98	130.69
30	137.96	131.87
31	139.93	133.05
32	141.89	134.25
33	143.85	135.46
34	145.80	136.67
35	147.74	137.90
36	149.68	139.14

37	151.61	140.39
38	153.53	141.66
39	155.45	142.93
40	157.36	144.21
41	159.26	145.50
42	161.15	146.81
43	163.04	148.12
44	164.92	149.45
45	166.79	150.79
46	168.66	152.13
47	170.51	153.49
48	172.36	154.86
49	174.20	156.24
50	176.04	157.63
51	177.86	159.02
52	179.68	160.43
53	181.49	161.85
54	183.29	163.28
55	185.09	164.72
56	186.87	166.17
57	187.54	166.72

Circle Center At X = -71.75 ; Y = 482.92 ; and Radius = 408.92

Factor of Safety

*** 1.764 ***

Failure Surface Specified By 56 Coordinate Points

Point No.	X-Surf (m)	Y-Surf (m)
1	78.16	102.47
2	80.42	102.90
3	82.68	103.36
4	84.92	103.85
5	87.17	104.36
6	89.40	104.91
7	91.63	105.48
8	93.85	106.09
9	96.06	106.72
10	98.26	107.38
11	100.46	108.07
12	102.64	108.79
13	104.82	109.54
14	106.98	110.31
15	109.14	111.12
16	111.28	111.95
17	113.41	112.81
18	115.54	113.69
19	117.65	114.61
20	119.74	115.55
21	121.83	116.52
22	123.90	117.52
23	125.96	118.54
24	128.01	119.59
25	130.04	120.67
26	132.06	121.77
27	134.06	122.90
28	136.05	124.05
29	138.03	125.23
30	139.98	126.44
31	141.93	127.67
32	143.85	128.93
33	145.76	130.21
34	147.65	131.52
35	149.53	132.85
36	151.39	134.21
37	153.23	135.59
38	155.05	136.99
39	156.85	138.42
40	158.64	139.87
41	160.40	141.35
42	162.15	142.84
43	163.87	144.36
44	165.58	145.91
45	167.27	147.47
46	168.93	149.06
47	170.58	150.66
48	172.20	152.29

49	173.80	153.94
50	175.38	155.61
51	176.94	157.30
52	178.48	159.02
53	179.99	160.75
54	181.48	162.50
55	182.95	164.27
56	184.00	165.56

Circle Center At X = 46.44 ; Y = 276.01 ; and Radius = 176.41

Factor of Safety

*** 1.817 ***

Failure Surface Specified By 55 Coordinate Points

Point No.	X-Surf (m)	Y-Surf (m)
1	80.20	104.51
2	82.32	105.41
3	84.43	106.32
4	86.54	107.24
5	88.65	108.17
6	90.75	109.10
7	92.84	110.05
8	94.94	111.01
9	97.02	111.98
10	99.10	112.95
11	101.18	113.94
12	103.25	114.94
13	105.32	115.94
14	107.39	116.96
15	109.44	117.98
16	111.50	119.02
17	113.55	120.07
18	115.59	121.12
19	117.63	122.18
20	119.66	123.26
21	121.69	124.34
22	123.72	125.44
23	125.73	126.54
24	127.75	127.65
25	129.76	128.77
26	131.76	129.90
27	133.76	131.04
28	135.75	132.19
29	137.73	133.35
30	139.71	134.52
31	141.69	135.70
32	143.66	136.89
33	145.62	138.08
34	147.58	139.29
35	149.53	140.51
36	151.48	141.73
37	153.42	142.96
38	155.36	144.21
39	157.29	145.46
40	159.21	146.72
41	161.13	147.99
42	163.04	149.27
43	164.95	150.56
44	166.85	151.85
45	168.74	153.16
46	170.63	154.47
47	172.51	155.80
48	174.38	157.13
49	176.25	158.47
50	178.11	159.82
51	179.97	161.18
52	181.82	162.55
53	183.66	163.92
54	185.50	165.31
55	187.21	166.61

Circle Center At X = -109.24 ; Y = 554.20 ; and Radius = 487.96

Factor of Safety

*** 1.827 ***

Failure Surface Specified By 60 Coordinate Points

Point No.	X-Surf (m)	Y-Surf (m)
--------------	---------------	---------------

1	79.80	104.11
2	81.90	105.03
3	84.01	105.96
4	86.11	106.89
5	88.20	107.84
6	90.30	108.79
7	92.39	109.75
8	94.48	110.71
9	96.56	111.69
10	98.64	112.67
11	100.72	113.65
12	102.79	114.65
13	104.86	115.65
14	106.93	116.66
15	108.99	117.68
16	111.05	118.70
17	113.11	119.73
18	115.16	120.77
19	117.21	121.81
20	119.26	122.86
21	121.30	123.92
22	123.34	124.99
23	125.37	126.06
24	127.40	127.14
25	129.43	128.22
26	131.45	129.32
27	133.47	130.42
28	135.49	131.53
29	137.50	132.64
30	139.51	133.76
31	141.51	134.89
32	143.51	136.03
33	145.51	137.17
34	147.50	138.32
35	149.49	139.47
36	151.48	140.63
37	153.46	141.80
38	155.43	142.98
39	157.40	144.16
40	159.37	145.35
41	161.34	146.55
42	163.30	147.75
43	165.25	148.96
44	167.20	150.18
45	169.15	151.41
46	171.10	152.64
47	173.03	153.87
48	174.97	155.12
49	176.90	156.37
50	178.82	157.63
51	180.75	158.89
52	182.66	160.16
53	184.58	161.44
54	186.48	162.72
55	188.39	164.01
56	190.29	165.31
57	192.18	166.61
58	194.07	167.92
59	195.96	169.24
60	196.56	169.66

Circle Center At X = -186.26 ; Y = 714.77 ; and Radius = 666.10

Factor of Safety

*** 1.828 ***

Failure Surface Specified By 54 Coordinate Points

Point No.	X-Surf (m)	Y-Surf (m)
1	79.39	103.70
2	81.61	104.28
3	83.83	104.88
4	86.05	105.51
5	88.25	106.16
6	90.45	106.84
7	92.64	107.54
8	94.82	108.27
9	97.00	109.01

10	99.16	109.79
11	101.32	110.58
12	103.47	111.40
13	105.61	112.24
14	107.74	113.11
15	109.86	114.00
16	111.97	114.91
17	114.08	115.85
18	116.17	116.81
19	118.25	117.79
20	120.32	118.79
21	122.37	119.82
22	124.42	120.87
23	126.46	121.94
24	128.48	123.03
25	130.49	124.14
26	132.49	125.28
27	134.48	126.44
28	136.45	127.62
29	138.41	128.82
30	140.36	130.05
31	142.29	131.29
32	144.21	132.56
33	146.12	133.84
34	148.01	135.15
35	149.89	136.48
36	151.76	137.83
37	153.60	139.19
38	155.44	140.58
39	157.26	141.99
40	159.06	143.42
41	160.85	144.87
42	162.62	146.34
43	164.37	147.82
44	166.11	149.33
45	167.83	150.85
46	169.54	152.40
47	171.23	153.96
48	172.90	155.54
49	174.55	157.14
50	176.19	158.75
51	177.81	160.39
52	179.41	162.04
53	180.99	163.71
54	182.15	164.96

Circle Center At X = 27.40 ; Y = 307.72 ; and Radius = 210.54

Factor of Safety

*** 1.841 ***

Failure Surface Specified By 58 Coordinate Points

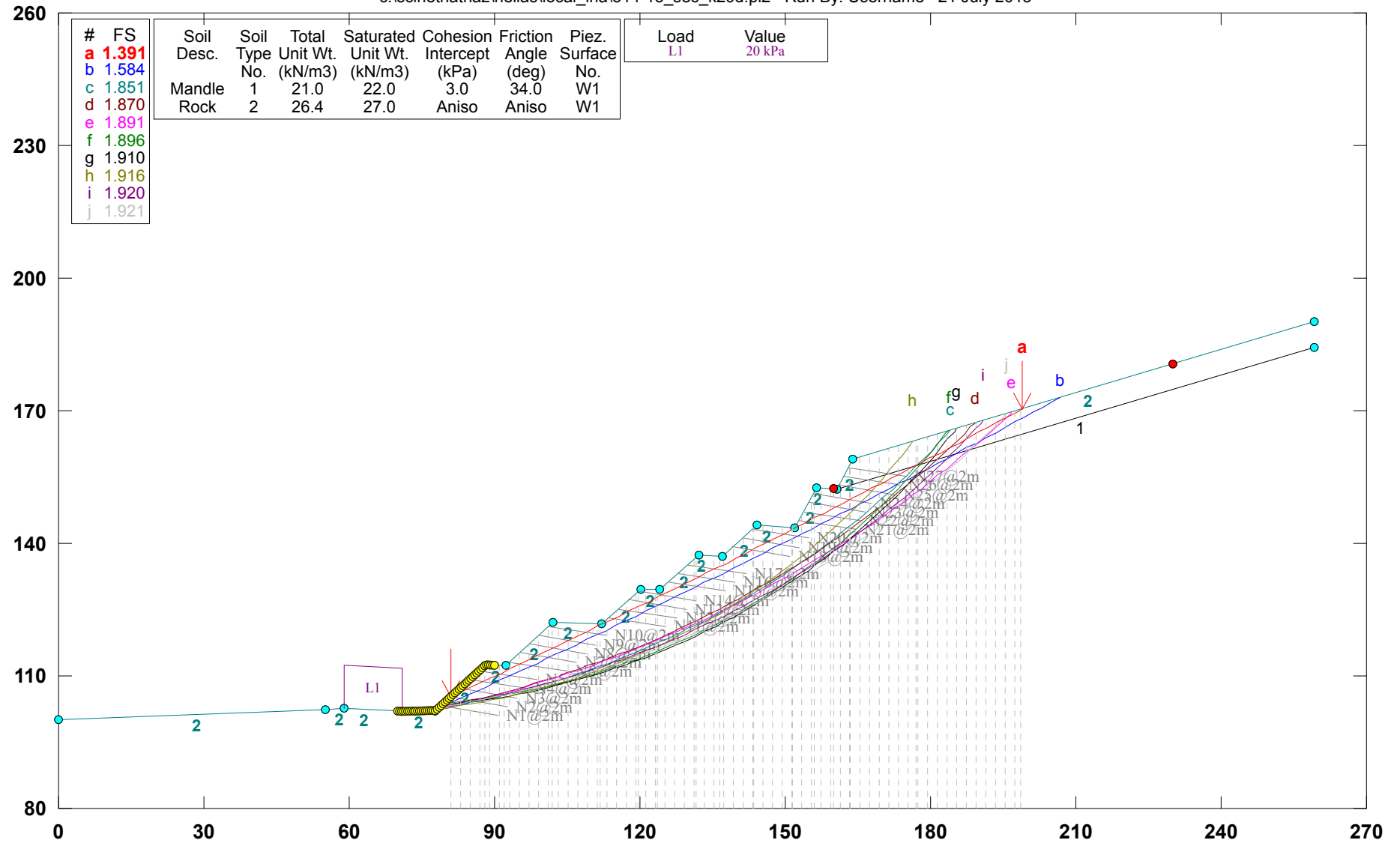
Point No.	X-Surf (m)	Y-Surf (m)
1	78.57	102.88
2	80.81	103.39
3	83.05	103.93
4	85.28	104.49
5	87.50	105.08
6	89.72	105.69
7	91.93	106.32
8	94.14	106.98
9	96.33	107.66
10	98.52	108.37
11	100.70	109.10
12	102.88	109.85
13	105.04	110.63
14	107.20	111.43
15	109.35	112.25
16	111.48	113.10
17	113.61	113.97
18	115.73	114.86
19	117.84	115.78
20	119.94	116.72
21	122.03	117.68
22	124.11	118.67
23	126.18	119.68
24	128.23	120.71

25	130.28	121.76
26	132.31	122.83
27	134.33	123.93
28	136.34	125.05
29	138.34	126.19
30	140.32	127.35
31	142.30	128.53
32	144.26	129.74
33	146.20	130.96
34	148.13	132.21
35	150.05	133.48
36	151.96	134.77
37	153.85	136.08
38	155.72	137.41
39	157.59	138.76
40	159.43	140.13
41	161.26	141.52
42	163.08	142.93
43	164.88	144.36
44	166.67	145.81
45	168.44	147.28
46	170.19	148.77
47	171.93	150.28
48	173.65	151.81
49	175.35	153.35
50	177.04	154.91
51	178.71	156.50
52	180.36	158.10
53	182.00	159.71
54	183.61	161.35
55	185.21	163.00
56	186.79	164.67
57	188.36	166.36
58	189.16	167.25

Circle Center At X = 32.61 ; Y = 309.04 ; and Radius = 211.22
Factor of Safety
*** 1.844 ***
**** END OF GSTABL7 OUTPUT ****

Hellas_Local_Landslide_Hazard Cut slope O14-15_sec_K29D

c:\scinetnathaz\hellas\local_lha\o14-15_sec_k29d.pl2 Run By: Username 21 July 2015



GSTABL7 v.2 FSmin=1.391

Safety Factors Are Calculated By The Modified Bishop Method



*** GSTABL7 ***

** GSTABL7 by Garry H. Gregory, P.E. **

** Original Version 1.0, January 1996; Current Version 2.003, June 2002 **

(All Rights Reserved-Unauthorized Use Prohibited)

SLOPE STABILITY ANALYSIS SYSTEM

Modified Bishop, Simplified Janbu, or GLE Method of Slices.

(Includes Spencer & Morgenstern-Price Type Analysis)

Including Pier/Pile, Reinforcement, Soil Nail, Tieback,

Nonlinear Undrained Shear Strength, Curved Phi Envelope,

Anisotropic Soil, Fiber-Reinforced Soil, Boundary Loads, Water

Surfaces, Pseudo-Static & Newmark Earthquake, and Applied Forces.

Analysis Run Date: 21 July 2015

Time of Run:

Run By: Username

Input Data Filename: C:\SciNetNatHaz\Hellas\Local_LHA\014-15_sec_k29d.in

Output Filename: C:\SciNetNatHaz\Hellas\Local_LHA\014-15_sec_k29d.OUT

Unit System: SI

Plotted Output Filename: C:\SciNetNatHaz\Hellas\Local_LHA-15_sec_k29d.PLT

PROBLEM DESCRIPTION: Hellas_Local_Landslide_Hazard

Cut slope 014-15_sec_K29D

BOUNDARY COORDINATES

18 Top Boundaries

19 Total Boundaries

Boundary No.	X-Left (m)	Y-Left (m)	X-Right (m)	Y-Right (m)	Soil Type Below Bnd
1	0.00	100.00	55.22	102.21	2
2	55.22	102.21	58.86	102.79	2
3	58.86	102.79	70.86	101.95	2
4	70.86	101.95	77.87	102.18	2
5	77.87	102.18	88.19	112.50	2
6	88.19	112.50	92.19	112.26	2
7	92.19	112.26	102.19	122.26	2
8	102.19	122.26	112.19	121.66	2
9	112.19	121.66	120.19	129.66	2
10	120.19	129.66	124.19	129.42	2
11	124.19	129.42	132.19	137.42	2
12	132.19	137.42	137.08	137.12	2
13	137.08	137.12	144.08	144.12	2
14	144.08	144.12	152.08	143.64	2
15	152.08	143.64	156.57	152.62	2
16	156.57	152.62	160.57	152.38	2
17	160.57	152.38	163.89	159.01	2
18	163.89	159.01	259.19	190.07	2
19	160.57	152.38	259.03	184.48	1

User Specified Y-Origin = 80.00(m)

Default X-Plus Value = 0.00(m)

Default Y-Plus Value = 0.00(m)

ISOTROPIC SOIL PARAMETERS

2 Type(s) of Soil

Soil Type No.	Total Unit Wt. (kN/m3)	Saturated Unit Wt. (kN/m3)	Cohesion Intercept (kPa)	Friction Angle (deg)	Pore Pressure Param. (kPa)	Pressure Constant (kPa)	Piez. Surface No.
1	21.0	22.0	3.0	34.0	0.00	0.0	1
2	26.4	27.0	150.0	42.0	0.00	0.0	1

ANISOTROPIC STRENGTH PARAMETERS

1 soil type(s)

Soil Type 2 Is Anisotropic

Number Of Direction Ranges Specified = 3

Direction Range No.	Counterclockwise Direction Limit (deg)	Cohesion Intercept (kPa)	Friction Angle (deg)
1	27.0	150.00	42.00
2	60.0	1.00	25.00
3	90.0	150.00	42.00

ANISOTROPIC SOIL NOTES:

- (1) An input value of 0.01 for C and/or Phi will cause Aniso C and/or Phi to be ignored in that range.
- (2) An input value of 0.02 for Phi will set both Phi and C equal to zero, with no water weight in the tension crack.
- (3) An input value of 0.03 for Phi will set both Phi and C equal to zero, with water weight in the tension crack.

BOUNDARY LOAD(S)

1 Load(s) Specified

Load No.	X-Left (m)	X-Right (m)	Intensity (kPa)	Deflection (deg)
1	58.86	70.86	20.0	0.0

NOTE - Intensity Is Specified As A Uniformly Distributed Force Acting On A Horizontally Projected Surface.

SOIL NAIL LOAD(S)

27 SOIL NAIL LOAD(S) SPECIFIED

Nail No.	X-Pos (m)	Y-Pos (m)	Nail Dia (mm)	Tendon Dia (mm)	Spacing (m)	Inclin. (deg)	Length (m)
1	78.87	103.18	89.0	22.0	2.00	10.00	12.00
2	80.87	105.18	89.0	22.0	2.00	10.00	12.00
3	82.87	107.18	89.0	22.0	2.00	10.00	12.00
4	84.87	109.18	89.0	22.0	2.00	10.00	12.00
5	86.87	111.18	89.0	22.0	2.00	10.00	12.00
6	93.11	113.18	89.0	22.0	2.00	10.00	12.00
7	95.11	115.18	89.0	22.0	2.00	10.00	12.00
8	97.11	117.18	89.0	22.0	2.00	10.00	12.00
9	99.11	119.18	89.0	22.0	2.00	10.00	12.00
10	101.11	121.18	89.0	22.0	2.00	10.00	12.00
11	113.71	123.18	89.0	22.0	2.00	10.00	12.00
12	115.71	125.18	89.0	22.0	2.00	10.00	12.00
13	117.71	127.18	89.0	22.0	2.00	10.00	12.00
14	119.71	129.18	89.0	22.0	2.00	10.00	12.00
15	125.95	131.18	89.0	22.0	2.00	10.00	12.00
16	127.95	133.18	89.0	22.0	2.00	10.00	12.00
17	129.95	135.18	89.0	22.0	2.00	10.00	12.00
18	139.14	139.18	89.0	22.0	2.00	10.00	12.00
19	141.14	141.18	89.0	22.0	2.00	10.00	12.00
20	143.14	143.18	89.0	22.0	2.00	10.00	12.00
21	152.85	145.18	89.0	22.0	2.00	10.00	12.00
22	153.85	147.18	89.0	22.0	2.00	10.00	12.00
23	154.85	149.18	89.0	22.0	2.00	10.00	12.00
24	155.85	151.18	89.0	22.0	2.00	10.00	12.00
25	160.97	153.18	89.0	22.0	2.00	10.00	12.00
26	161.97	155.18	89.0	22.0	2.00	10.00	12.00
27	162.97	157.18	89.0	22.0	2.00	10.00	12.00

SOIL NAIL LOAD DATA

Soil Nail No. 1 4 Load Points Apply to This Nail

Load Diagram Type = 1

POINT NO.	X-COORD.(m)	Y-COORD.(m)	FORCE(kN)
1	78.87	103.18	25.00
2	80.49	102.90	82.64
3	88.54	101.50	82.64
4	90.69	101.10	0.00

Allowable Pullout Stress = 250.0(kPa)

Allowable Tendon Stress = 434782.6

Allowable Nail Head Load = 50.0(kN)

Soil Nail No. 2 4 Load Points Apply to This Nail

Load Diagram Type = 1

POINT NO.	X-COORD.(m)	Y-COORD.(m)	FORCE(kN)
1	80.87	105.18	25.00
2	82.49	104.90	82.64
3	90.54	103.50	82.64
4	92.69	103.10	0.00

Allowable Pullout Stress = 250.0(kPa)

Allowable Tendon Stress = 434782.6

Allowable Nail Head Load = 50.0(kN)

Soil Nail No. 3 4 Load Points Apply to This Nail

Load Diagram Type = 1

POINT NO.	X-COORD.(m)	Y-COORD.(m)	FORCE(kN)
1	82.87	107.18	25.00
2	84.49	106.90	82.64
3	92.54	105.50	82.64
4	94.69	105.10	0.00

Allowable Pullout Stress = 250.0(kPa)

Allowable Tendon Stress = 434782.6

Allowable Nail Head Load = 50.0(kN)

Soil Nail No. 4 4 Load Points Apply to This Nail

Load Diagram Type = 1

POINT NO.	X-COORD.(m)	Y-COORD.(m)	FORCE(kN)
1	84.87	109.18	25.00
2	86.49	108.90	82.64
3	94.54	107.50	82.64
4	96.69	107.10	0.00

Allowable Pullout Stress = 250.0(kPa)
 Allowable Tendon Stress = 434782.6
 Allowable Nail Head Load = 50.0(kN)
 Soil Nail No. 5 4 Load Points Apply to This Nail
 Load Diagram Type = 1

POINT NO.	X-COORD.(m)	Y-COORD.(m)	FORCE(kN)
1	86.87	111.18	25.00
2	88.49	110.90	82.64
3	96.54	109.50	82.64
4	98.69	109.10	0.00

 Allowable Pullout Stress = 250.0(kPa)
 Allowable Tendon Stress = 434782.6
 Allowable Nail Head Load = 50.0(kN)
 Soil Nail No. 6 4 Load Points Apply to This Nail
 Load Diagram Type = 1

POINT NO.	X-COORD.(m)	Y-COORD.(m)	FORCE(kN)
1	93.11	113.18	25.00
2	94.73	112.90	82.64
3	102.78	111.50	82.64
4	104.93	111.10	0.00

 Allowable Pullout Stress = 250.0(kPa)
 Allowable Tendon Stress = 434782.6
 Allowable Nail Head Load = 50.0(kN)
 Soil Nail No. 7 4 Load Points Apply to This Nail
 Load Diagram Type = 1

POINT NO.	X-COORD.(m)	Y-COORD.(m)	FORCE(kN)
1	95.11	115.18	25.00
2	96.73	114.90	82.64
3	104.78	113.50	82.64
4	106.93	113.10	0.00

 Allowable Pullout Stress = 250.0(kPa)
 Allowable Tendon Stress = 434782.6
 Allowable Nail Head Load = 50.0(kN)
 Soil Nail No. 8 4 Load Points Apply to This Nail
 Load Diagram Type = 1

POINT NO.	X-COORD.(m)	Y-COORD.(m)	FORCE(kN)
1	97.11	117.18	25.00
2	98.73	116.90	82.64
3	106.78	115.50	82.64
4	108.93	115.10	0.00

 Allowable Pullout Stress = 250.0(kPa)
 Allowable Tendon Stress = 434782.6
 Allowable Nail Head Load = 50.0(kN)
 Soil Nail No. 9 4 Load Points Apply to This Nail
 Load Diagram Type = 1

POINT NO.	X-COORD.(m)	Y-COORD.(m)	FORCE(kN)
1	99.11	119.18	25.00
2	100.73	118.90	82.64
3	108.78	117.50	82.64
4	110.93	117.10	0.00

 Allowable Pullout Stress = 250.0(kPa)
 Allowable Tendon Stress = 434782.6
 Allowable Nail Head Load = 50.0(kN)
 Soil Nail No. 10 4 Load Points Apply to This Nail
 Load Diagram Type = 1

POINT NO.	X-COORD.(m)	Y-COORD.(m)	FORCE(kN)
1	101.11	121.18	25.00
2	102.73	120.90	82.64
3	110.78	119.50	82.64
4	112.93	119.10	0.00

 Allowable Pullout Stress = 250.0(kPa)
 Allowable Tendon Stress = 434782.6
 Allowable Nail Head Load = 50.0(kN)
 Soil Nail No. 11 4 Load Points Apply to This Nail
 Load Diagram Type = 1

POINT NO.	X-COORD.(m)	Y-COORD.(m)	FORCE(kN)
1	113.71	123.18	25.00
2	115.33	122.90	82.64
3	123.38	121.50	82.64
4	125.53	121.10	0.00

 Allowable Pullout Stress = 250.0(kPa)
 Allowable Tendon Stress = 434782.6
 Allowable Nail Head Load = 50.0(kN)
 Soil Nail No. 12 4 Load Points Apply to This Nail
 Load Diagram Type = 1

POINT NO.	X-COORD.(m)	Y-COORD.(m)	FORCE(kN)
1	115.71	125.18	25.00
2	117.33	124.90	82.64
3	125.38	123.50	82.64
4	127.53	123.10	0.00
Allowable Pullout Stress = 250.0(kPa)			
Allowable Tendon Stress = 434782.6			
Allowable Nail Head Load = 50.0(kN)			
Soil Nail No. 13 4 Load Points Apply to This Nail			
Load Diagram Type = 1			
POINT NO.	X-COORD.(m)	Y-COORD.(m)	FORCE(kN)
1	117.71	127.18	25.00
2	119.33	126.90	82.64
3	127.38	125.50	82.64
4	129.53	125.10	0.00
Allowable Pullout Stress = 250.0(kPa)			
Allowable Tendon Stress = 434782.6			
Allowable Nail Head Load = 50.0(kN)			
Soil Nail No. 14 4 Load Points Apply to This Nail			
Load Diagram Type = 1			
POINT NO.	X-COORD.(m)	Y-COORD.(m)	FORCE(kN)
1	119.71	129.18	25.00
2	121.33	128.90	82.64
3	129.38	127.50	82.64
4	131.53	127.10	0.00
Allowable Pullout Stress = 250.0(kPa)			
Allowable Tendon Stress = 434782.6			
Allowable Nail Head Load = 50.0(kN)			
Soil Nail No. 15 4 Load Points Apply to This Nail			
Load Diagram Type = 1			
POINT NO.	X-COORD.(m)	Y-COORD.(m)	FORCE(kN)
1	125.95	131.18	25.00
2	127.57	130.90	82.64
3	135.62	129.50	82.64
4	137.77	129.10	0.00
Allowable Pullout Stress = 250.0(kPa)			
Allowable Tendon Stress = 434782.6			
Allowable Nail Head Load = 50.0(kN)			
Soil Nail No. 16 4 Load Points Apply to This Nail			
Load Diagram Type = 1			
POINT NO.	X-COORD.(m)	Y-COORD.(m)	FORCE(kN)
1	127.95	133.18	25.00
2	129.57	132.90	82.64
3	137.62	131.50	82.64
4	139.77	131.10	0.00
Allowable Pullout Stress = 250.0(kPa)			
Allowable Tendon Stress = 434782.6			
Allowable Nail Head Load = 50.0(kN)			
Soil Nail No. 17 4 Load Points Apply to This Nail			
Load Diagram Type = 1			
POINT NO.	X-COORD.(m)	Y-COORD.(m)	FORCE(kN)
1	129.95	135.18	25.00
2	131.57	134.90	82.64
3	139.62	133.50	82.64
4	141.77	133.10	0.00
Allowable Pullout Stress = 250.0(kPa)			
Allowable Tendon Stress = 434782.6			
Allowable Nail Head Load = 50.0(kN)			
Soil Nail No. 18 4 Load Points Apply to This Nail			
Load Diagram Type = 1			
POINT NO.	X-COORD.(m)	Y-COORD.(m)	FORCE(kN)
1	139.14	139.18	25.00
2	140.76	138.90	82.64
3	148.81	137.50	82.64
4	150.96	137.10	0.00
Allowable Pullout Stress = 250.0(kPa)			
Allowable Tendon Stress = 434782.6			
Allowable Nail Head Load = 50.0(kN)			
Soil Nail No. 19 4 Load Points Apply to This Nail			
Load Diagram Type = 1			
POINT NO.	X-COORD.(m)	Y-COORD.(m)	FORCE(kN)
1	141.14	141.18	25.00
2	142.76	140.90	82.64
3	150.81	139.50	82.64
4	152.96	139.10	0.00

Allowable Pullout Stress = 250.0(kPa)
 Allowable Tendon Stress = 434782.6
 Allowable Nail Head Load = 50.0(kN)
 Soil Nail No. 20 4 Load Points Apply to This Nail
 Load Diagram Type = 1

POINT NO.	X-COORD.(m)	Y-COORD.(m)	FORCE(kN)
1	143.14	143.18	25.00
2	144.76	142.90	82.64
3	152.81	141.50	82.64
4	154.96	141.10	0.00

 Allowable Pullout Stress = 250.0(kPa)
 Allowable Tendon Stress = 434782.6
 Allowable Nail Head Load = 50.0(kN)
 Soil Nail No. 21 4 Load Points Apply to This Nail
 Load Diagram Type = 1

POINT NO.	X-COORD.(m)	Y-COORD.(m)	FORCE(kN)
1	152.85	145.18	25.00
2	154.47	144.90	82.64
3	162.52	143.50	82.64
4	164.67	143.10	0.00

 Allowable Pullout Stress = 250.0(kPa)
 Allowable Tendon Stress = 434782.6
 Allowable Nail Head Load = 50.0(kN)
 Soil Nail No. 22 4 Load Points Apply to This Nail
 Load Diagram Type = 1

POINT NO.	X-COORD.(m)	Y-COORD.(m)	FORCE(kN)
1	153.85	147.18	25.00
2	155.47	146.90	82.64
3	163.52	145.50	82.64
4	165.67	145.10	0.00

 Allowable Pullout Stress = 250.0(kPa)
 Allowable Tendon Stress = 434782.6
 Allowable Nail Head Load = 50.0(kN)
 Soil Nail No. 23 4 Load Points Apply to This Nail
 Load Diagram Type = 1

POINT NO.	X-COORD.(m)	Y-COORD.(m)	FORCE(kN)
1	154.85	149.18	25.00
2	156.47	148.90	82.64
3	164.52	147.50	82.64
4	166.67	147.10	0.00

 Allowable Pullout Stress = 250.0(kPa)
 Allowable Tendon Stress = 434782.6
 Allowable Nail Head Load = 50.0(kN)
 Soil Nail No. 24 4 Load Points Apply to This Nail
 Load Diagram Type = 1

POINT NO.	X-COORD.(m)	Y-COORD.(m)	FORCE(kN)
1	155.85	151.18	25.00
2	157.47	150.90	82.64
3	165.52	149.50	82.64
4	167.67	149.10	0.00

 Allowable Pullout Stress = 250.0(kPa)
 Allowable Tendon Stress = 434782.6
 Allowable Nail Head Load = 50.0(kN)
 Soil Nail No. 25 4 Load Points Apply to This Nail
 Load Diagram Type = 1

POINT NO.	X-COORD.(m)	Y-COORD.(m)	FORCE(kN)
1	160.97	153.18	25.00
2	162.59	152.90	82.64
3	170.64	151.50	82.64
4	172.79	151.10	0.00

 Allowable Pullout Stress = 250.0(kPa)
 Allowable Tendon Stress = 434782.6
 Allowable Nail Head Load = 50.0(kN)
 Soil Nail No. 26 4 Load Points Apply to This Nail
 Load Diagram Type = 1

POINT NO.	X-COORD.(m)	Y-COORD.(m)	FORCE(kN)
1	161.97	155.18	25.00
2	166.03	154.47	82.64
3	168.15	154.11	82.64
4	173.79	153.10	0.00

 Allowable Pullout Stress = 100.0(kPa)
 Allowable Tendon Stress = 434782.6
 Allowable Nail Head Load = 50.0(kN)
 Soil Nail No. 27 4 Load Points Apply to This Nail
 Load Diagram Type = 1

POINT NO.	X-COORD.(m)	Y-COORD.(m)	FORCE(kN)
1	162.97	157.18	25.00
2	167.03	156.47	82.64
3	169.15	156.11	82.64
4	174.79	155.10	0.00

Allowable Pullout Stress = 100.0(kPa)

Allowable Tendon Stress = 434782.6

Allowable Nail Head Load = 50.0(kN)

NOTE - An Equivalent Line Load Is Calculated For Each Row Of Soil Nails
Assuming A Uniform Distribution Of Load Horizontally Between
Individual Nails.

A Critical Failure Surface Searching Method, Using A Random
Technique For Generating Circular Surfaces, Has Been Specified.
2500 Trial Surfaces Have Been Generated.

50 Surface(s) Initiate(s) From Each Of 50 Points Equally Spaced
Along The Ground Surface Between X = 70.00(m)

and X = 90.00(m)

Each Surface Terminates Between X = 160.00(m)

and X = 230.00(m)

Unless Further Limitations Were Imposed, The Minimum Elevation
At Which A Surface Extends Is Y = 0.00(m)

2.30(m) Line Segments Define Each Trial Failure Surface.

Following Are Displayed The Ten Most Critical Of The Trial

Failure Surfaces Evaluated. They Are
Ordered - Most Critical First.

* * Safety Factors Are Calculated By The Modified Bishop Method * *

Total Number of Trial Surfaces Evaluated = 2500

Statistical Data On All Valid FS Values:

FS Max = 3.601 FS Min = 1.391 FS Ave = 2.807

Standard Deviation = 0.473 Coefficient of Variation = 16.85 %

Failure Surface Specified By 60 Coordinate Points

Point No.	X-Surf (m)	Y-Surf (m)
1	81.02	105.33
2	83.07	106.38
3	85.11	107.43
4	87.15	108.49
5	89.20	109.55
6	91.24	110.61
7	93.28	111.67
8	95.32	112.73
9	97.36	113.80
10	99.39	114.87
11	101.43	115.94
12	103.46	117.01
13	105.50	118.08
14	107.53	119.16
15	109.56	120.24
16	111.59	121.32
17	113.62	122.40
18	115.65	123.49
19	117.68	124.57
20	119.70	125.66
21	121.73	126.75
22	123.75	127.85
23	125.77	128.94
24	127.79	130.04
25	129.81	131.14
26	131.83	132.24
27	133.85	133.34
28	135.87	134.45
29	137.88	135.56
30	139.90	136.67
31	141.91	137.78
32	143.92	138.89
33	145.93	140.01
34	147.94	141.13
35	149.95	142.25
36	151.96	143.37
37	153.97	144.49
38	155.97	145.62
39	157.98	146.75
40	159.98	147.88
41	161.98	149.01
42	163.98	150.15

43	165.98	151.29
44	167.98	152.42
45	169.98	153.57
46	171.97	154.71
47	173.97	155.85
48	175.96	157.00
49	177.95	158.15
50	179.94	159.30
51	181.93	160.45
52	183.92	161.61
53	185.91	162.77
54	187.90	163.93
55	189.88	165.09
56	191.86	166.25
57	193.85	167.42
58	195.83	168.59
59	197.81	169.76
60	198.97	170.44

Circle Center At X = -933.59 ; Y = 2082.63 ; and Radius = 2222.42

Factor of Safety

*** 1.391 ***

Slice No.	Width (m)	Weight (kN)	Individual data on the		73 slices		Earthquake		Surcharge Load (kN)
			Water Force Top (kN)	Water Force Bot (kN)	Tie Force Norm (kN)	Tie Force Tan (kN)	Force Hor (kN)	Force Ver (kN)	
1	2.0	26.9	0.0	0.0	0.	0.	0.0	0.0	0.0
2	2.0	80.5	0.0	0.0	0.	0.	0.0	0.0	0.0
3	2.0	133.8	0.0	0.0	0.	0.	0.0	0.0	0.0
4	1.0	88.1	0.0	0.0	0.	0.	0.0	0.0	0.0
5	1.0	84.6	0.0	0.0	0.	0.	0.0	0.0	0.0
6	2.0	124.0	0.0	0.0	0.	0.	0.0	0.0	0.0
7	1.0	36.0	0.0	0.0	0.	0.	0.0	0.0	0.0
8	1.1	40.8	0.0	0.0	0.	0.	0.0	0.0	0.0
9	2.0	116.7	0.0	0.0	0.	0.	0.0	0.0	0.0
10	2.0	169.0	0.0	0.0	0.	0.	0.0	0.0	0.0
11	2.0	221.1	0.0	0.0	0.	0.	0.0	0.0	0.0
12	2.0	273.0	0.0	0.0	0.	0.	0.0	0.0	0.0
13	0.8	115.4	0.0	0.0	0.	0.	0.0	0.0	0.0
14	1.3	186.6	0.0	0.0	0.	0.	0.0	0.0	0.0
15	2.0	245.7	0.0	0.0	0.	0.	0.0	0.0	0.0
16	2.0	181.3	0.0	0.0	0.	0.	0.0	0.0	0.0
17	2.0	116.9	0.0	0.0	0.	0.	0.0	0.0	0.0
18	2.0	52.5	0.0	0.0	0.	0.	0.0	0.0	0.0
19	0.6	3.2	0.0	0.0	0.	0.	0.0	0.0	0.0
20	1.4	13.5	0.0	0.0	0.	0.	0.0	0.0	0.0
21	2.0	62.2	0.0	0.0	0.	0.	0.0	0.0	0.0
22	2.0	112.5	0.0	0.0	0.	0.	0.0	0.0	0.0
23	2.0	162.7	0.0	0.0	0.	0.	0.0	0.0	0.0
24	0.5	46.7	0.0	0.0	0.	0.	0.0	0.0	0.0
25	1.5	132.9	0.0	0.0	0.	0.	0.0	0.0	0.0
26	2.0	117.9	0.0	0.0	0.	0.	0.0	0.0	0.0
27	0.4	17.0	0.0	0.0	0.	0.	0.0	0.0	0.0
28	1.6	71.0	0.0	0.0	0.	0.	0.0	0.0	0.0
29	2.0	134.6	0.0	0.0	0.	0.	0.0	0.0	0.0
30	2.0	183.8	0.0	0.0	0.	0.	0.0	0.0	0.0
31	2.0	232.6	0.0	0.0	0.	0.	0.0	0.0	0.0
32	0.4	46.2	0.0	0.0	0.	0.	0.0	0.0	0.0
33	1.7	196.5	0.0	0.0	0.	0.	0.0	0.0	0.0
34	2.0	178.9	0.0	0.0	0.	0.	0.0	0.0	0.0
35	1.2	76.0	0.0	0.0	0.	0.	0.0	0.0	0.0
36	0.8	46.4	0.0	0.0	0.	0.	0.0	0.0	0.0
37	2.0	149.9	0.0	0.0	0.	0.	0.0	0.0	0.0
38	2.0	197.8	0.0	0.0	0.	0.	0.0	0.0	0.0
39	2.0	245.5	0.0	0.0	0.	0.	0.0	0.0	0.0
40	0.2	21.1	0.0	0.0	0.	0.	0.0	0.0	0.0
41	1.9	223.7	0.0	0.0	0.	0.	0.0	0.0	0.0
42	2.0	179.3	0.0	0.0	0.	0.	0.0	0.0	0.0
43	2.0	113.5	0.0	0.0	0.	0.	0.0	0.0	0.0
44	2.0	47.6	0.0	0.0	0.	0.	0.0	0.0	0.0
45	0.1	0.8	0.0	0.0	0.	0.	0.0	0.0	0.0
46	1.9	77.8	0.0	0.0	0.	0.	0.0	0.0	0.0
47	2.0	230.9	0.0	0.0	0.	0.	0.0	0.0	0.0
48	0.6	98.4	0.0	0.0	0.	0.	0.0	0.0	0.0
49	1.4	231.1	0.0	0.0	0.	0.	0.0	0.0	0.0

50	2.0	272.9	0.0	0.0	0.	0.	0.0	0.0	0.0
51	0.6	67.8	0.0	0.0	0.	0.	0.0	0.0	0.0
52	1.4	162.3	0.0	0.0	0.	0.	0.0	0.0	0.0
53	1.9	343.4	0.0	0.0	0.	0.	0.0	0.0	0.0
54	0.1	19.8	0.0	0.0	0.	0.	0.0	0.0	0.0
55	2.0	423.0	0.0	0.0	0.	0.	0.0	0.0	0.0
56	2.0	402.4	0.0	0.0	0.	0.	0.0	0.0	0.0
57	2.0	381.6	0.0	0.0	0.	0.	0.0	0.0	0.0
58	2.0	360.8	0.0	0.0	0.	0.	0.0	0.0	0.0
59	2.0	339.9	0.0	0.0	0.	0.	0.0	0.0	0.0
60	2.0	318.9	0.0	0.0	0.	0.	0.0	0.0	0.0
61	1.6	238.1	0.0	0.0	0.	0.	0.0	0.0	0.0
62	0.4	59.6	0.0	0.0	0.	0.	0.0	0.0	0.0
63	2.0	272.9	0.0	0.0	0.	0.	0.0	0.0	0.0
64	2.0	246.3	0.0	0.0	0.	0.	0.0	0.0	0.0
65	2.0	219.6	0.0	0.0	0.	0.	0.0	0.0	0.0
66	2.0	192.7	0.0	0.0	0.	0.	0.0	0.0	0.0
67	2.0	165.8	0.0	0.0	0.	0.	0.0	0.0	0.0
68	2.0	138.8	0.0	0.0	0.	0.	0.0	0.0	0.0
69	2.0	111.7	0.0	0.0	0.	0.	0.0	0.0	0.0
70	2.0	84.5	0.0	0.0	0.	0.	0.0	0.0	0.0
71	2.0	57.2	0.0	0.0	0.	0.	0.0	0.0	0.0
72	2.0	29.8	0.0	0.0	0.	0.	0.0	0.0	0.0
73	1.2	4.7	0.0	0.0	0.	0.	0.0	0.0	0.0

Failure Surface Specified By 65 Coordinate Points

Point No.	X-Surf (m)	Y-Surf (m)
1	78.16	102.47
2	80.22	103.50
3	82.28	104.53
4	84.33	105.56
5	86.39	106.60
6	88.44	107.64
7	90.49	108.68
8	92.54	109.72
9	94.59	110.77
10	96.64	111.81
11	98.68	112.87
12	100.73	113.92
13	102.77	114.97
14	104.81	116.03
15	106.85	117.09
16	108.89	118.15
17	110.93	119.22
18	112.97	120.29
19	115.00	121.36
20	117.04	122.43
21	119.07	123.51
22	121.10	124.58
23	123.13	125.66
24	125.16	126.75
25	127.19	127.83
26	129.22	128.92
27	131.24	130.01
28	133.27	131.10
29	135.29	132.20
30	137.31	133.29
31	139.33	134.39
32	141.35	135.50
33	143.37	136.60
34	145.38	137.71
35	147.40	138.82
36	149.41	139.93
37	151.42	141.04
38	153.43	142.16
39	155.44	143.28
40	157.45	144.40
41	159.46	145.53
42	161.46	146.65
43	163.47	147.78
44	165.47	148.91
45	167.47	150.05
46	169.47	151.18
47	171.47	152.32
48	173.46	153.47

49	175.46	154.61
50	177.45	155.76
51	179.45	156.90
52	181.44	158.05
53	183.43	159.21
54	185.42	160.36
55	187.40	161.52
56	189.39	162.68
57	191.37	163.85
58	193.36	165.01
59	195.34	166.18
60	197.32	167.35
61	199.30	168.52
62	201.27	169.70
63	203.25	170.88
64	205.22	172.06
65	206.78	172.99

Circle Center At X = -766.29 ; Y = 1795.27 ; and Radius = 1891.73

Factor of Safety

*** 1.584 ***

Failure Surface Specified By 56 Coordinate Points

Point No.	X-Surf (m)	Y-Surf (m)
1	78.16	102.47
2	80.42	102.90
3	82.68	103.36
4	84.92	103.85
5	87.17	104.36
6	89.40	104.91
7	91.63	105.48
8	93.85	106.09
9	96.06	106.72
10	98.26	107.38
11	100.46	108.07
12	102.64	108.79
13	104.82	109.54
14	106.98	110.31
15	109.14	111.12
16	111.28	111.95
17	113.41	112.81
18	115.54	113.69
19	117.65	114.61
20	119.74	115.55
21	121.83	116.52
22	123.90	117.52
23	125.96	118.54
24	128.01	119.59
25	130.04	120.67
26	132.06	121.77
27	134.06	122.90
28	136.05	124.05
29	138.03	125.23
30	139.98	126.44
31	141.93	127.67
32	143.85	128.93
33	145.76	130.21
34	147.65	131.52
35	149.53	132.85
36	151.39	134.21
37	153.23	135.59
38	155.05	136.99
39	156.85	138.42
40	158.64	139.87
41	160.40	141.35
42	162.15	142.84
43	163.87	144.36
44	165.58	145.91
45	167.27	147.47
46	168.93	149.06
47	170.58	150.66
48	172.20	152.29
49	173.80	153.94
50	175.38	155.61
51	176.94	157.30
52	178.48	159.02

53 179.99 160.75
 54 181.48 162.50
 55 182.95 164.27
 56 184.00 165.56
 Circle Center At X = 46.44 ; Y = 276.01 ; and Radius = 176.41
 Factor of Safety
 *** 1.851 ***

Failure Surface Specified By 58 Coordinate Points

Point No.	X-Surf (m)	Y-Surf (m)
1	78.57	102.88
2	80.81	103.39
3	83.05	103.93
4	85.28	104.49
5	87.50	105.08
6	89.72	105.69
7	91.93	106.32
8	94.14	106.98
9	96.33	107.66
10	98.52	108.37
11	100.70	109.10
12	102.88	109.85
13	105.04	110.63
14	107.20	111.43
15	109.35	112.25
16	111.48	113.10
17	113.61	113.97
18	115.73	114.86
19	117.84	115.78
20	119.94	116.72
21	122.03	117.68
22	124.11	118.67
23	126.18	119.68
24	128.23	120.71
25	130.28	121.76
26	132.31	122.83
27	134.33	123.93
28	136.34	125.05
29	138.34	126.19
30	140.32	127.35
31	142.30	128.53
32	144.26	129.74
33	146.20	130.96
34	148.13	132.21
35	150.05	133.48
36	151.96	134.77
37	153.85	136.08
38	155.72	137.41
39	157.59	138.76
40	159.43	140.13
41	161.26	141.52
42	163.08	142.93
43	164.88	144.36
44	166.67	145.81
45	168.44	147.28
46	170.19	148.77
47	171.93	150.28
48	173.65	151.81
49	175.35	153.35
50	177.04	154.91
51	178.71	156.50
52	180.36	158.10
53	182.00	159.71
54	183.61	161.35
55	185.21	163.00
56	186.79	164.67
57	188.36	166.36
58	189.16	167.25

Circle Center At X = 32.61 ; Y = 309.04 ; and Radius = 211.22
 Factor of Safety
 *** 1.870 ***

Failure Surface Specified By 62 Coordinate Points

Point No.	X-Surf (m)	Y-Surf (m)
1	78.16	102.47

2	80.40	103.01
3	82.63	103.57
4	84.86	104.15
5	87.08	104.75
6	89.29	105.38
7	91.50	106.02
8	93.70	106.68
9	95.90	107.37
10	98.08	108.07
11	100.27	108.80
12	102.44	109.55
13	104.61	110.32
14	106.77	111.10
15	108.92	111.91
16	111.07	112.74
17	113.21	113.59
18	115.34	114.46
19	117.46	115.35
20	119.57	116.26
21	121.67	117.19
22	123.77	118.14
23	125.86	119.11
24	127.93	120.09
25	130.00	121.10
26	132.06	122.13
27	134.10	123.18
28	136.14	124.24
29	138.17	125.33
30	140.19	126.43
31	142.19	127.56
32	144.19	128.70
33	146.18	129.86
34	148.15	131.04
35	150.11	132.24
36	152.06	133.46
37	154.00	134.70
38	155.93	135.95
39	157.85	137.22
40	159.75	138.51
41	161.64	139.82
42	163.52	141.15
43	165.39	142.49
44	167.24	143.85
45	169.08	145.23
46	170.91	146.63
47	172.73	148.04
48	174.53	149.47
49	176.31	150.92
50	178.09	152.38
51	179.85	153.86
52	181.59	155.36
53	183.32	156.88
54	185.04	158.41
55	186.74	159.95
56	188.43	161.52
57	190.10	163.09
58	191.76	164.69
59	193.40	166.30
60	195.03	167.92
61	196.64	169.56
62	196.81	169.74

Circle Center At X = 22.36 ; Y = 339.18 ; and Radius = 243.20

Factor of Safety
 *** 1.891 ***

Failure Surface Specified By 56 Coordinate Points

Point No.	X-Surf (m)	Y-Surf (m)
1	79.39	103.70
2	81.67	103.96
3	83.95	104.25
4	86.23	104.58
5	88.50	104.95
6	90.76	105.36
7	93.02	105.79
8	95.27	106.27

9	97.52	106.78
10	99.75	107.33
11	101.98	107.91
12	104.19	108.52
13	106.40	109.18
14	108.59	109.86
15	110.78	110.58
16	112.95	111.34
17	115.11	112.13
18	117.26	112.95
19	119.39	113.81
20	121.51	114.70
21	123.62	115.63
22	125.71	116.58
23	127.78	117.58
24	129.84	118.60
25	131.89	119.66
26	133.91	120.74
27	135.92	121.86
28	137.91	123.02
29	139.88	124.20
30	141.84	125.41
31	143.77	126.66
32	145.68	127.94
33	147.58	129.24
34	149.45	130.58
35	151.30	131.94
36	153.13	133.34
37	154.94	134.76
38	156.72	136.21
39	158.48	137.69
40	160.22	139.20
41	161.93	140.73
42	163.62	142.29
43	165.28	143.88
44	166.92	145.50
45	168.53	147.14
46	170.12	148.80
47	171.68	150.49
48	173.21	152.21
49	174.72	153.95
50	176.20	155.71
51	177.65	157.49
52	179.07	159.30
53	180.46	161.13
54	181.82	162.99
55	183.16	164.86
56	183.54	165.41

Circle Center At X = 64.16 ; Y = 248.14 ; and Radius = 145.25

Factor of Safety

*** 1.896 ***

Failure Surface Specified By 57 Coordinate Points

Point No.	X-Surf (m)	Y-Surf (m)
1	78.98	103.29
2	81.26	103.55
3	83.55	103.85
4	85.82	104.18
5	88.09	104.54
6	90.36	104.95
7	92.62	105.38
8	94.87	105.85
9	97.11	106.36
10	99.35	106.90
11	101.57	107.47
12	103.79	108.08
13	106.00	108.72
14	108.20	109.40
15	110.38	110.11
16	112.56	110.86
17	114.73	111.63
18	116.88	112.45
19	119.02	113.29
20	121.14	114.17
21	123.26	115.08

22	125.35	116.02
23	127.44	116.99
24	129.51	118.00
25	131.56	119.04
26	133.59	120.11
27	135.61	121.21
28	137.62	122.34
29	139.60	123.50
30	141.57	124.70
31	143.51	125.92
32	145.44	127.17
33	147.35	128.46
34	149.24	129.77
35	151.11	131.11
36	152.96	132.48
37	154.78	133.88
38	156.59	135.30
39	158.37	136.76
40	160.13	138.24
41	161.87	139.75
42	163.58	141.28
43	165.27	142.84
44	166.93	144.43
45	168.57	146.04
46	170.19	147.68
47	171.78	149.34
48	173.34	151.03
49	174.88	152.74
50	176.39	154.47
51	177.88	156.23
52	179.33	158.01
53	180.76	159.81
54	182.16	161.63
55	183.54	163.48
56	184.88	165.34
57	185.34	166.00

Circle Center At X = 63.20 ; Y = 251.61 ; and Radius = 149.16

Factor of Safety
*** 1.910 ***

Failure Surface Specified By 53 Coordinate Points

Point No.	X-Surf (m)	Y-Surf (m)
1	78.16	102.47
2	80.44	102.81
3	82.71	103.18
4	84.97	103.58
5	87.23	104.03
6	89.48	104.51
7	91.72	105.02
8	93.95	105.57
9	96.18	106.16
10	98.39	106.78
11	100.60	107.44
12	102.79	108.13
13	104.97	108.86
14	107.14	109.63
15	109.30	110.42
16	111.44	111.26
17	113.57	112.13
18	115.69	113.03
19	117.79	113.96
20	119.87	114.93
21	121.94	115.93
22	124.00	116.97
23	126.03	118.04
24	128.05	119.14
25	130.05	120.27
26	132.04	121.44
27	134.00	122.64
28	135.94	123.87
29	137.87	125.13
30	139.77	126.42
31	141.65	127.74
32	143.51	129.09
33	145.35	130.47

34	147.17	131.88
35	148.96	133.32
36	150.73	134.79
37	152.48	136.29
38	154.20	137.81
39	155.90	139.36
40	157.57	140.94
41	159.22	142.55
42	160.84	144.18
43	162.43	145.84
44	164.00	147.52
45	165.54	149.23
46	167.05	150.96
47	168.54	152.72
48	169.99	154.50
49	171.42	156.31
50	172.82	158.13
51	174.19	159.98
52	175.52	161.85
53	176.37	163.08

Circle Center At X = 58.57 ; Y = 244.11 ; and Radius = 142.98

Factor of Safety

*** 1.916 ***

Failure Surface Specified By 59 Coordinate Points

Point No.	X-Surf (m)	Y-Surf (m)
1	78.98	103.29
2	81.25	103.68
3	83.51	104.11
4	85.76	104.56
5	88.01	105.04
6	90.25	105.54
7	92.49	106.08
8	94.72	106.64
9	96.94	107.23
10	99.16	107.85
11	101.37	108.50
12	103.57	109.17
13	105.76	109.87
14	107.94	110.59
15	110.11	111.35
16	112.28	112.13
17	114.43	112.94
18	116.57	113.77
19	118.71	114.63
20	120.83	115.52
21	122.94	116.43
22	125.04	117.38
23	127.12	118.34
24	129.20	119.33
25	131.26	120.35
26	133.31	121.39
27	135.35	122.46
28	137.37	123.56
29	139.38	124.67
30	141.38	125.82
31	143.36	126.99
32	145.32	128.18
33	147.28	129.40
34	149.21	130.64
35	151.13	131.90
36	153.04	133.19
37	154.93	134.51
38	156.80	135.84
39	158.65	137.20
40	160.49	138.58
41	162.31	139.99
42	164.12	141.42
43	165.90	142.87
44	167.67	144.34
45	169.42	145.83
46	171.15	147.35
47	172.86	148.88
48	174.55	150.44
49	176.22	152.02

50	177.88	153.62
51	179.51	155.24
52	181.12	156.88
53	182.72	158.54
54	184.29	160.22
55	185.84	161.92
56	187.37	163.64
57	188.87	165.37
58	190.36	167.13
59	190.93	167.82

Circle Center At X = 48.33 ; Y = 285.84 ; and Radius = 185.10

Factor of Safety

*** 1.920 ***

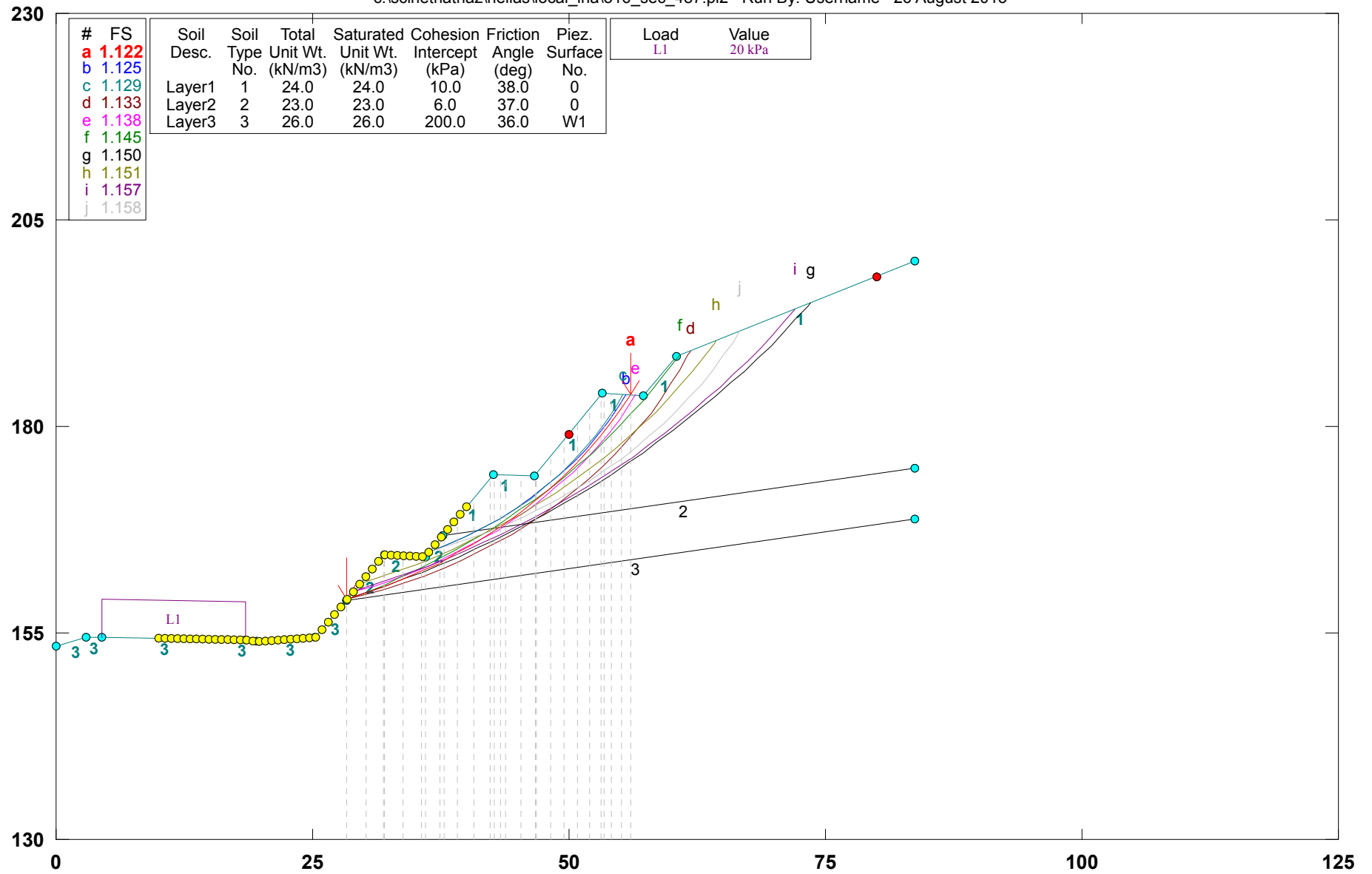
Failure Surface Specified By 61 Coordinate Points

Point No.	X-Surf (m)	Y-Surf (m)
1	78.57	102.88
2	80.84	103.28
3	83.10	103.71
4	85.35	104.16
5	87.60	104.64
6	89.85	105.14
7	92.08	105.67
8	94.32	106.22
9	96.54	106.81
10	98.76	107.41
11	100.97	108.05
12	103.17	108.71
13	105.37	109.39
14	107.56	110.10
15	109.74	110.84
16	111.91	111.60
17	114.07	112.38
18	116.22	113.20
19	118.36	114.03
20	120.50	114.89
21	122.62	115.78
22	124.73	116.69
23	126.83	117.62
24	128.92	118.58
25	131.00	119.57
26	133.07	120.57
27	135.13	121.61
28	137.17	122.66
29	139.20	123.74
30	141.22	124.84
31	143.22	125.97
32	145.22	127.12
33	147.19	128.29
34	149.16	129.49
35	151.11	130.70
36	153.05	131.94
37	154.97	133.21
38	156.88	134.49
39	158.77	135.80
40	160.65	137.13
41	162.51	138.48
42	164.35	139.85
43	166.18	141.25
44	168.00	142.66
45	169.79	144.10
46	171.57	145.56
47	173.33	147.03
48	175.08	148.53
49	176.81	150.05
50	178.52	151.59
51	180.21	153.15
52	181.88	154.72
53	183.54	156.32
54	185.17	157.94
55	186.79	159.57
56	188.39	161.23
57	189.97	162.90
58	191.53	164.59
59	193.07	166.30

```
60          194.59      168.02
61          195.77      169.40
Circle Center At X =    45.40 ; Y =    297.85 ; and Radius =    197.77
Factor of Safety
***      1.921      ***
**** END OF GSTABL7 OUTPUT ****
```

Hellas_Local_Landslide_Hazard Cut slope O16_sec_487

c:\scinetnathaz\hellas\local_lha\o16_sec_487.pl2 Run By: Username 26 August 2015



GSTABL7 v.2 FSmin=1.122

Safety Factors Are Calculated By The Modified Bishop Method



*** GSTABL7 ***

** GSTABL7 by Garry H. Gregory, P.E. **

** Original Version 1.0, January 1996; Current Version 2.003, June 2002 **

(All Rights Reserved-Unauthorized Use Prohibited)

SLOPE STABILITY ANALYSIS SYSTEM

Modified Bishop, Simplified Janbu, or GLE Method of Slices.

(Includes Spencer & Morgenstern-Price Type Analysis)

Including Pier/Pile, Reinforcement, Soil Nail, Tieback,

Nonlinear Undrained Shear Strength, Curved Phi Envelope,

Anisotropic Soil, Fiber-Reinforced Soil, Boundary Loads, Water

Surfaces, Pseudo-Static & Newmark Earthquake, and Applied Forces.

Analysis Run Date: 26 August 2015

Time of Run:

Run By: Username

Input Data Filename: C:\SciNetNatHaz\Hellas\Local_LHA\O16_sec_487.in

Output Filename: C:\SciNetNatHaz\Hellas\Local_LHA\O16_sec_487.OUT

Unit System: SI

Plotted Output Filename: C:\SciNetNatHaz\Hellas\Local_LHA_sec_487.PLT

PROBLEM DESCRIPTION: Hellas_Local_Landslide_Hazard

Cut slope O16_sec_487

BOUNDARY COORDINATES

15 Top Boundaries

17 Total Boundaries

Boundary No.	X-Left (m)	Y-Left (m)	X-Right (m)	Y-Right (m)	Soil Type Below Bnd
1	0.00	153.43	2.90	154.40	3
2	2.90	154.40	4.40	154.50	3
3	4.40	154.50	18.40	154.15	3
4	18.40	154.15	19.60	153.95	3
5	19.60	153.95	25.30	154.46	3

6	25.30	154.46	28.29	158.95	3
7	28.29	158.95	31.96	164.46	2
8	31.96	164.46	35.96	164.22	2
9	35.96	164.22	37.68	166.80	2
10	37.68	166.80	42.63	174.22	1
11	42.63	174.22	46.63	173.98	1
12	46.63	173.98	53.30	183.98	1
13	53.30	183.98	57.30	183.74	1
14	57.30	183.74	60.44	188.46	1
15	60.44	188.46	83.75	199.95	1
16	37.68	166.80	83.75	174.93	2
17	28.29	158.95	83.75	168.73	3

User Specified Y-Origin = 130.00(m)

Default X-Plus Value = 0.00(m)

Default Y-Plus Value = 0.00(m)

ISOTROPIC SOIL PARAMETERS

3 Type(s) of Soil

Soil Type No.	Total Unit Wt. (kN/m3)	Saturated Unit Wt. (kN/m3)	Cohesion Intercept (kPa)	Friction Angle (deg)	Pore Pressure Param.	Pressure Constant (kPa)	Piez. Surface No.
1	24.0	24.0	10.0	38.0	0.00	0.0	0
2	23.0	23.0	6.0	37.0	0.00	0.0	0
3	26.0	26.0	200.0	36.0	0.00	0.0	1

1 PIEZOMETRIC SURFACE(S) SPECIFIED

Unit Weight of Water = 9.81(kN/m3)

Piezometric Surface No. 1 Specified by 4 Coordinate Points

Pore Pressure Inclination Factor = 0.50

Point No.	X-Water (m)	Y-Water (m)
1	0.00	150.00
2	25.30	154.46
3	28.29	158.95
4	83.75	168.73

WATER SURFACE DATA HAS BEEN SUPPRESSED

BOUNDARY LOAD(S)

1 Load(s) Specified

Load No.	X-Left (m)	X-Right (m)	Intensity (kPa)	Deflection (deg)
1	4.40	18.40	20.0	0.0

NOTE - Intensity Is Specified As A Uniformly Distributed Force Acting On A Horizontally Projected Surface.

A Critical Failure Surface Searching Method, Using A Random Technique For Generating Circular Surfaces, Has Been Specified.

2500 Trial Surfaces Have Been Generated.

50 Surface(s) Initiate(s) From Each Of 50 Points Equally Spaced

Along The Ground Surface Between X = 10.00(m)

and X = 40.00(m)

Each Surface Terminates Between X = 50.00(m)

and X = 80.00(m)

Unless Further Limitations Were Imposed, The Minimum Elevation

At Which A Surface Extends Is Y = 0.00(m)

2.00(m) Line Segments Define Each Trial Failure Surface.

Following Are Displayed The Ten Most Critical Of The Trial

Failure Surfaces Evaluated. They Are

Ordered - Most Critical First.

* * Safety Factors Are Calculated By The Modified Bishop Method * *

Total Number of Trial Surfaces Evaluated = 2500

Statistical Data On All Valid FS Values:

FS Max = 4.164 FS Min = 1.122 FS Ave = 2.130

Standard Deviation = 0.554 Coefficient of Variation = 25.99 %

Failure Surface Specified By 20 Coordinate Points

Point No.	X-Surf (m)	Y-Surf (m)
1	28.37	159.07
2	30.23	159.80
3	32.05	160.61
4	33.85	161.50
5	35.61	162.45
6	37.33	163.47
7	39.01	164.55
8	40.64	165.71
9	42.23	166.92
10	43.77	168.20
11	45.26	169.54
12	46.69	170.93

13 48.07 172.38
 14 49.39 173.88
 15 50.65 175.44
 16 51.85 177.04
 17 52.98 178.69
 18 54.05 180.38
 19 55.05 182.11
 20 55.95 183.82

Circle Center At X = 10.57 ; Y = 206.64 ; and Radius = 50.79

Factor of Safety

*** 1.122 ***

Slice No.	Width (m)	Weight (kN)	Individual data on the		26 slices		Earthquake		Surcharge Load (kN)
			Water Force Top (kN)	Water Force Bot (kN)	Tie Force Norm (kN)	Tie Force Tan (kN)	Force Hor (kN)	Force Ver (kN)	
1	1.9	43.9	0.0	0.0	0.	0.	0.0	0.0	0.0
2	1.7	118.5	0.0	0.0	0.	0.	0.0	0.0	0.0
3	0.1	8.4	0.0	0.0	0.	0.	0.0	0.0	0.0
4	1.8	138.1	0.0	0.0	0.	0.	0.0	0.0	0.0
5	1.8	94.0	0.0	0.0	0.	0.	0.0	0.0	0.0
6	0.4	13.5	0.0	0.0	0.	0.	0.0	0.0	0.0
7	1.4	68.8	0.0	0.0	0.	0.	0.0	0.0	0.0
8	0.4	23.8	0.0	0.0	0.	0.	0.0	0.0	0.0
9	1.3	113.3	0.0	0.0	0.	0.	0.0	0.0	0.0
10	1.6	188.3	0.0	0.0	0.	0.	0.0	0.0	0.0
11	1.6	231.3	0.0	0.0	0.	0.	0.0	0.0	0.0
12	0.4	65.2	0.0	0.0	0.	0.	0.0	0.0	0.0
13	0.6	103.0	0.0	0.0	0.	0.	0.0	0.0	0.0
14	0.5	73.7	0.0	0.0	0.	0.	0.0	0.0	0.0
15	1.5	187.0	0.0	0.0	0.	0.	0.0	0.0	0.0
16	1.4	125.7	0.0	0.0	0.	0.	0.0	0.0	0.0
17	0.1	4.6	0.0	0.0	0.	0.	0.0	0.0	0.0
18	1.4	114.1	0.0	0.0	0.	0.	0.0	0.0	0.0
19	1.3	126.5	0.0	0.0	0.	0.	0.0	0.0	0.0
20	1.3	133.0	0.0	0.0	0.	0.	0.0	0.0	0.0
21	1.2	134.0	0.0	0.0	0.	0.	0.0	0.0	0.0
22	1.1	130.2	0.0	0.0	0.	0.	0.0	0.0	0.0
23	0.3	36.9	0.0	0.0	0.	0.	0.0	0.0	0.0
24	0.7	74.8	0.0	0.0	0.	0.	0.0	0.0	0.0
25	1.0	63.9	0.0	0.0	0.	0.	0.0	0.0	0.0
26	0.9	19.1	0.0	0.0	0.	0.	0.0	0.0	0.0

Failure Surface Specified By 15 Coordinate Points

Point No.	X-Surf (m)	Y-Surf (m)
1	36.33	164.77
2	38.13	165.64
3	39.88	166.61
4	41.58	167.66
5	43.22	168.80
6	44.80	170.02
7	46.32	171.33
8	47.77	172.71
9	49.14	174.16
10	50.44	175.68
11	51.66	177.27
12	52.79	178.91
13	53.84	180.62
14	54.80	182.37
15	55.51	183.85

Circle Center At X = 20.33 ; Y = 200.05 ; and Radius = 38.74

Factor of Safety

*** 1.125 ***

Failure Surface Specified By 15 Coordinate Points

Point No.	X-Surf (m)	Y-Surf (m)
1	36.33	164.77
2	38.13	165.63
3	39.89	166.59
4	41.59	167.64
5	43.23	168.78
6	44.81	170.01
7	46.32	171.32
8	47.76	172.71
9	49.12	174.18

10 50.39 175.72
 11 51.58 177.32
 12 52.69 178.99
 13 53.70 180.72
 14 54.61 182.50
 15 55.22 183.86
 Circle Center At X = 21.39 ; Y = 198.47 ; and Radius = 36.87
 Factor of Safety
 *** 1.129 ***

Failure Surface Specified By 25 Coordinate Points

Point No.	X-Surf (m)	Y-Surf (m)
1	28.37	159.07
2	30.28	159.66
3	32.16	160.34
4	34.02	161.08
5	35.84	161.89
6	37.64	162.78
7	39.40	163.73
8	41.12	164.75
9	42.80	165.83
10	44.43	166.98
11	46.03	168.19
12	47.57	169.47
13	49.06	170.80
14	50.50	172.18
15	51.89	173.62
16	53.22	175.12
17	54.49	176.66
18	55.70	178.25
19	56.85	179.89
20	57.94	181.57
21	58.96	183.29
22	59.91	185.05
23	60.80	186.84
24	61.61	188.67
25	61.80	189.13

Circle Center At X = 13.79 ; Y = 208.91 ; and Radius = 51.94
 Factor of Safety
 *** 1.133 ***

Failure Surface Specified By 20 Coordinate Points

Point No.	X-Surf (m)	Y-Surf (m)
1	28.98	159.99
2	30.86	160.66
3	32.72	161.41
4	34.54	162.24
5	36.32	163.14
6	38.07	164.12
7	39.77	165.16
8	41.43	166.28
9	43.04	167.47
10	44.60	168.72
11	46.10	170.04
12	47.55	171.42
13	48.94	172.86
14	50.26	174.36
15	51.53	175.91
16	52.73	177.51
17	53.85	179.16
18	54.91	180.86
19	55.90	182.60
20	56.51	183.79

Circle Center At X = 13.89 ; Y = 205.27 ; and Radius = 47.73
 Factor of Safety
 *** 1.138 ***

Failure Surface Specified By 24 Coordinate Points

Point No.	X-Surf (m)	Y-Surf (m)
1	28.37	159.07
2	30.17	159.92
3	31.96	160.83
4	33.71	161.79
5	35.44	162.79
6	37.14	163.85

7	38.81	164.95
8	40.45	166.10
9	42.06	167.29
10	43.63	168.52
11	45.16	169.80
12	46.67	171.13
13	48.13	172.49
14	49.55	173.89
15	50.94	175.34
16	52.28	176.82
17	53.58	178.33
18	54.84	179.89
19	56.06	181.48
20	57.23	183.10
21	58.36	184.75
22	59.43	186.44
23	60.46	188.15
24	60.72	188.60

Circle Center At X = -1.44 ; Y = 224.20 ; and Radius = 71.63
Factor of Safety
*** 1.145 ***

Failure Surface Specified By 31 Coordinate Points

Point No.	X-Surf (m)	Y-Surf (m)
1	28.37	159.07
2	30.21	159.83
3	32.04	160.64
4	33.86	161.48
5	35.66	162.35
6	37.44	163.27
7	39.20	164.21
8	40.94	165.19
9	42.67	166.20
10	44.37	167.25
11	46.06	168.33
12	47.72	169.45
13	49.36	170.59
14	50.97	171.77
15	52.57	172.98
16	54.13	174.22
17	55.68	175.49
18	57.20	176.79
19	58.69	178.12
20	60.16	179.48
21	61.60	180.87
22	63.01	182.28
23	64.40	183.73
24	65.75	185.20
25	67.08	186.69
26	68.38	188.22
27	69.64	189.76
28	70.88	191.34
29	72.09	192.93
30	73.26	194.55
31	73.50	194.90

Circle Center At X = -9.89 ; Y = 253.61 ; and Radius = 101.99
Factor of Safety
*** 1.150 ***

Failure Surface Specified By 25 Coordinate Points

Point No.	X-Surf (m)	Y-Surf (m)
1	29.59	160.90
2	31.45	161.64
3	33.29	162.43
4	35.10	163.28
5	36.89	164.18
6	38.65	165.13
7	40.38	166.13
8	42.08	167.18
9	43.75	168.28
10	45.39	169.43
11	46.99	170.63
12	48.55	171.87
13	50.08	173.16
14	51.57	174.49

15	53.03	175.87
16	54.44	177.29
17	55.80	178.75
18	57.13	180.24
19	58.41	181.78
20	59.64	183.35
21	60.83	184.96
22	61.97	186.61
23	63.06	188.28
24	64.11	189.99
25	64.33	190.38

Circle Center At X = 5.35 ; Y = 224.70 ; and Radius = 68.24

Factor of Safety

*** 1.151 ***

Failure Surface Specified By 29 Coordinate Points

Point No.	X-Surf (m)	Y-Surf (m)
1	28.98	159.99
2	30.84	160.72
3	32.69	161.49
4	34.51	162.30
5	36.32	163.16
6	38.11	164.05
7	39.88	164.98
8	41.63	165.95
9	43.35	166.96
10	45.06	168.01
11	46.74	169.10
12	48.39	170.22
13	50.03	171.38
14	51.63	172.57
15	53.21	173.80
16	54.76	175.06
17	56.28	176.36
18	57.78	177.69
19	59.24	179.05
20	60.67	180.45
21	62.07	181.87
22	63.44	183.33
23	64.78	184.82
24	66.09	186.33
25	67.36	187.87
26	68.60	189.45
27	69.80	191.05
28	70.96	192.67
29	71.97	194.15

Circle Center At X = -3.28 ; Y = 244.73 ; and Radius = 90.68

Factor of Safety

*** 1.157 ***

Failure Surface Specified By 22 Coordinate Points

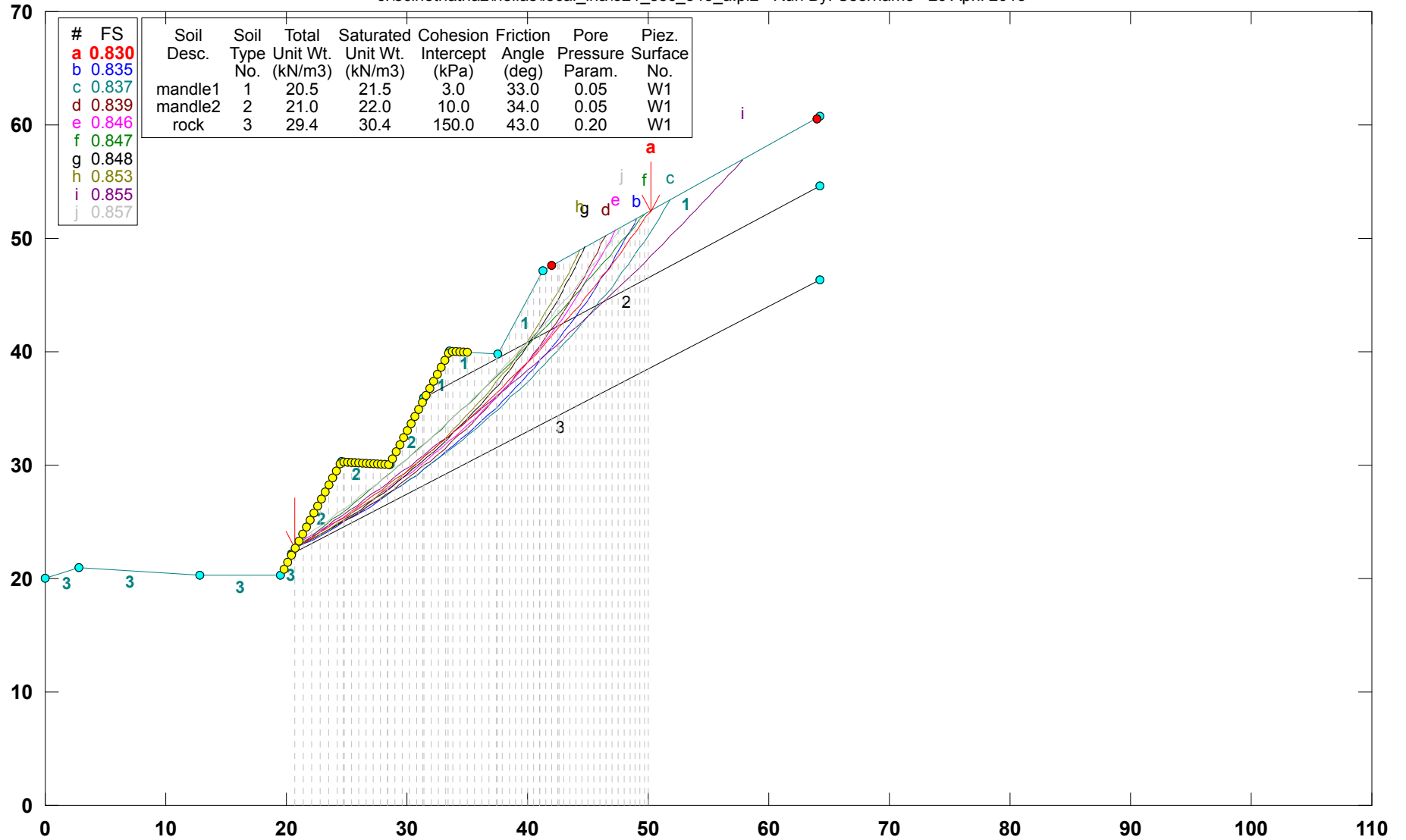
Point No.	X-Surf (m)	Y-Surf (m)
1	36.33	164.77
2	38.20	165.47
3	40.04	166.25
4	41.86	167.09
5	43.64	167.99
6	45.39	168.97
7	47.10	170.00
8	48.77	171.10
9	50.40	172.26
10	51.99	173.47
11	53.53	174.75
12	55.02	176.08
13	56.47	177.46
14	57.86	178.90
15	59.20	180.39
16	60.48	181.92
17	61.70	183.50
18	62.87	185.13
19	63.97	186.79
20	65.02	188.50
21	66.00	190.24
22	66.65	191.52

Circle Center At X = 18.14 ; Y = 215.96 ; and Radius = 54.32

Factor of Safety
*** 1.158 ***
**** END OF GSTABL7 OUTPUT ****

Hellas_Local_Landslide_Hazard Cut slope O21_sec_845_A

c:\scinetnathaz\hellas\local_lha\o21_sec_845_a.pl2 Run By: Username 29 April 2015



GSTABL7 v.2 FSmin=0.830

Safety Factors Are Calculated By The Modified Bishop Method



*** GSTABL7 ***

** GSTABL7 by Garry H. Gregory, P.E. **

** Original Version 1.0, January 1996; Current Version 2.003, June 2002 **

(All Rights Reserved-Unauthorized Use Prohibited)

SLOPE STABILITY ANALYSIS SYSTEM

Modified Bishop, Simplified Janbu, or GLE Method of Slices.

(Includes Spencer & Morgenstern-Price Type Analysis)

Including Pier/Pile, Reinforcement, Soil Nail, Tieback,

Nonlinear Undrained Shear Strength, Curved Phi Envelope,

Anisotropic Soil, Fiber-Reinforced Soil, Boundary Loads, Water

Surfaces, Pseudo-Static & Newmark Earthquake, and Applied Forces.

Analysis Run Date: 29 April 2015

Time of Run:

Run By: Username

Input Data Filename: C:\SciNetNatHaz\Hellas\Local_LHA\O21_sec_845_A.in

Output Filename: C:\SciNetNatHaz\Hellas\Local_LHA\O21_sec_845_A.OUT

Unit System: SI

Plotted Output Filename: C:\SciNetNatHaz\Hellas\Local_LHA_sec_845_A.PLT

PROBLEM DESCRIPTION: Hellas_Local_Landslide_Hazard

Cut slope O21_sec_845_A

BOUNDARY COORDINATES

11 Top Boundaries

13 Total Boundaries

Boundary No.	X-Left (m)	Y-Left (m)	X-Right (m)	Y-Right (m)	Soil Type Below Bnd
1	0.00	20.00	2.80	20.93	3
2	2.80	20.93	12.80	20.34	3
3	12.80	20.34	19.54	20.29	3
4	19.54	20.29	20.50	22.22	3
5	20.50	22.22	24.54	30.29	2
6	24.54	30.29	28.54	30.05	2
7	28.54	30.05	31.45	35.88	2

8	31.45	35.88	33.54	40.05	1
9	33.54	40.05	37.54	39.81	1
10	37.54	39.81	41.24	47.17	1
11	41.24	47.17	64.30	60.71	1
12	31.45	35.88	64.30	54.68	2
13	20.50	22.22	64.30	46.38	3

Default Y-Origin = 0.00(m)

Default X-Plus Value = 0.00(m)

Default Y-Plus Value = 0.00(m)

ISOTROPIC SOIL PARAMETERS

3 Type(s) of Soil

Soil Type No.	Total Unit Wt. (kN/m3)	Saturated Unit Wt. (kN/m3)	Cohesion Intercept (kPa)	Friction Angle (deg)	Pore Pressure Param. (kPa)	Pressure Constant (kPa)	Piez. Surface No.
1	20.5	21.5	3.0	33.0	0.05	0.0	1
2	21.0	22.0	10.0	34.0	0.05	0.0	1
3	29.4	30.4	150.0	43.0	0.20	0.0	1

SOIL NAIL LOAD(S)

17 SOIL NAIL LOAD(S) SPECIFIED

Nail No.	X-Pos (m)	Y-Pos (m)	Nail Dia (mm)	Tendon Dia (mm)	Spacing (m)	Inclin. (deg)	Length (m)
1	20.22	21.66	150.0	29.0	1.50	10.00	6.00
2	20.97	23.16	150.0	29.0	1.50	10.00	6.00
3	21.72	24.66	150.0	29.0	1.50	10.00	6.00
4	22.47	26.16	150.0	29.0	1.50	10.00	6.00
5	23.22	27.65	150.0	29.0	1.50	10.00	6.00
6	23.97	29.15	150.0	29.0	1.50	10.00	6.00
7	28.84	30.65	150.0	29.0	1.50	10.00	6.00
8	29.59	32.15	150.0	29.0	1.50	10.00	6.00
9	30.34	33.66	150.0	29.0	1.50	10.00	6.00
10	31.09	35.16	150.0	29.0	1.50	10.00	6.00
11	31.84	36.66	150.0	29.0	1.50	10.00	6.00
12	32.59	38.15	150.0	29.0	1.50	10.00	6.00
13	33.34	39.65	150.0	29.0	1.50	10.00	6.00
14	38.23	41.18	150.0	29.0	1.50	10.00	6.00
15	38.98	42.67	150.0	29.0	1.50	10.00	6.00
16	39.73	44.17	150.0	29.0	1.50	10.00	6.00
17	40.48	45.66	150.0	29.0	1.50	10.00	6.00

SOIL NAIL LOAD DATA

Soil Nail No. 1 4 Load Points Apply to This Nail

Load Diagram Type = 1

POINT NO.	X-COORD.(m)	Y-COORD.(m)	FORCE(kN)
1	20.22	21.66	140.00
2	21.03	21.52	191.46
3	23.22	21.14	191.46
4	26.13	20.62	0.00

Allowable Pullout Stress = 200.0(kPa)

Allowable Tendon Stress = 434782.6

Allowable Nail Head Load = 210.0(kN)

Soil Nail No. 2 4 Load Points Apply to This Nail

Load Diagram Type = 1

POINT NO.	X-COORD.(m)	Y-COORD.(m)	FORCE(kN)
1	20.97	23.16	140.00
2	21.78	23.02	191.46
3	23.97	22.64	191.46
4	26.88	22.12	0.00

Allowable Pullout Stress = 200.0(kPa)

Allowable Tendon Stress = 434782.6

Allowable Nail Head Load = 210.0(kN)

Soil Nail No. 3 4 Load Points Apply to This Nail

Load Diagram Type = 1

POINT NO.	X-COORD.(m)	Y-COORD.(m)	FORCE(kN)
1	21.72	24.66	140.00
2	22.53	24.52	191.46
3	24.72	24.14	191.46
4	27.63	23.62	0.00

Allowable Pullout Stress = 200.0(kPa)

Allowable Tendon Stress = 434782.6

Allowable Nail Head Load = 210.0(kN)

Soil Nail No. 4 4 Load Points Apply to This Nail

Load Diagram Type = 1

POINT NO.	X-COORD.(m)	Y-COORD.(m)	FORCE(kN)
1	22.47	26.16	140.00
2	23.55	25.97	191.46
3	24.47	25.81	191.46

4 28.38 25.11 0.00

Allowable Pullout Stress = 150.0(kPa)

Allowable Tendon Stress = 434782.6

Allowable Nail Head Load = 210.0(kN)

Soil Nail No. 5 4 Load Points Apply to This Nail

Load Diagram Type = 1

POINT NO.	X-COORD.(m)	Y-COORD.(m)	FORCE(kN)
1	23.22	27.65	140.00
2	24.30	27.47	191.46
3	25.22	27.31	191.46
4	29.13	26.61	0.00

Allowable Pullout Stress = 150.0(kPa)

Allowable Tendon Stress = 434782.6

Allowable Nail Head Load = 210.0(kN)

Soil Nail No. 6 4 Load Points Apply to This Nail

Load Diagram Type = 1

POINT NO.	X-COORD.(m)	Y-COORD.(m)	FORCE(kN)
1	23.97	29.15	140.00
2	25.05	28.96	191.46
3	25.97	28.80	191.46
4	29.88	28.11	0.00

Allowable Pullout Stress = 150.0(kPa)

Allowable Tendon Stress = 434782.6

Allowable Nail Head Load = 210.0(kN)

Soil Nail No. 7 3 Load Points Apply to This Nail

Load Diagram Type = 3

POINT NO.	X-COORD.(m)	Y-COORD.(m)	FORCE(kN)
1	28.84	30.65	140.00
2	29.53	30.45	183.10
3	34.75	29.61	0.00

Allowable Pullout Stress = 120.0(kPa)

Allowable Tendon Stress = 434782.6

Allowable Nail Head Load = 210.0(kN)

Soil Nail No. 8 3 Load Points Apply to This Nail

Load Diagram Type = 3

POINT NO.	X-COORD.(m)	Y-COORD.(m)	FORCE(kN)
1	29.59	32.15	140.00
2	30.27	31.96	183.10
3	35.50	31.11	0.00

Allowable Pullout Stress = 120.0(kPa)

Allowable Tendon Stress = 434782.6

Allowable Nail Head Load = 210.0(kN)

Soil Nail No. 9 3 Load Points Apply to This Nail

Load Diagram Type = 3

POINT NO.	X-COORD.(m)	Y-COORD.(m)	FORCE(kN)
1	30.34	33.66	140.00
2	31.00	33.46	183.10
3	36.25	32.61	0.00

Allowable Pullout Stress = 120.0(kPa)

Allowable Tendon Stress = 434782.6

Allowable Nail Head Load = 210.0(kN)

Soil Nail No. 10 3 Load Points Apply to This Nail

Load Diagram Type = 3

POINT NO.	X-COORD.(m)	Y-COORD.(m)	FORCE(kN)
1	31.09	35.16	140.00
2	31.74	34.96	183.10
3	37.00	34.12	0.00

Allowable Pullout Stress = 120.0(kPa)

Allowable Tendon Stress = 434782.6

Allowable Nail Head Load = 210.0(kN)

Soil Nail No. 11 3 Load Points Apply to This Nail

Load Diagram Type = 3

POINT NO.	X-COORD.(m)	Y-COORD.(m)	FORCE(kN)
1	31.84	36.66	140.00
2	32.32	36.49	173.67
3	37.75	35.62	0.00

Allowable Pullout Stress = 110.0(kPa)

Allowable Tendon Stress = 434782.6

Allowable Nail Head Load = 210.0(kN)

Soil Nail No. 12 3 Load Points Apply to This Nail

Load Diagram Type = 3

POINT NO.	X-COORD.(m)	Y-COORD.(m)	FORCE(kN)
1	32.59	38.15	140.00
2	33.05	37.99	173.67
3	38.50	37.11	0.00

Allowable Pullout Stress = 110.0(kPa)
 Allowable Tendon Stress = 434782.6
 Allowable Nail Head Load = 210.0(kN)
 Soil Nail No. 13 3 Load Points Apply to This Nail
 Load Diagram Type = 3

POINT NO.	X-COORD.(m)	Y-COORD.(m)	FORCE(kN)
1	33.34	39.65	140.00
2	33.79	39.48	173.67
3	39.25	38.61	0.00

Allowable Pullout Stress = 110.0(kPa)
 Allowable Tendon Stress = 434782.6
 Allowable Nail Head Load = 210.0(kN)
 Soil Nail No. 14 3 Load Points Apply to This Nail
 Load Diagram Type = 3

POINT NO.	X-COORD.(m)	Y-COORD.(m)	FORCE(kN)
1	38.23	41.18	140.00
2	38.41	41.05	164.25
3	44.14	40.14	0.00

Allowable Pullout Stress = 100.0(kPa)
 Allowable Tendon Stress = 434782.6
 Allowable Nail Head Load = 210.0(kN)
 Soil Nail No. 15 3 Load Points Apply to This Nail
 Load Diagram Type = 3

POINT NO.	X-COORD.(m)	Y-COORD.(m)	FORCE(kN)
1	38.98	42.67	140.00
2	39.15	42.54	164.25
3	44.89	41.63	0.00

Allowable Pullout Stress = 100.0(kPa)
 Allowable Tendon Stress = 434782.6
 Allowable Nail Head Load = 210.0(kN)
 Soil Nail No. 16 3 Load Points Apply to This Nail
 Load Diagram Type = 3

POINT NO.	X-COORD.(m)	Y-COORD.(m)	FORCE(kN)
1	39.73	44.17	140.00
2	39.89	44.03	164.25
3	45.64	43.12	0.00

Allowable Pullout Stress = 100.0(kPa)
 Allowable Tendon Stress = 434782.6
 Allowable Nail Head Load = 210.0(kN)
 Soil Nail No. 17 3 Load Points Apply to This Nail
 Load Diagram Type = 3

POINT NO.	X-COORD.(m)	Y-COORD.(m)	FORCE(kN)
1	40.48	45.66	140.00
2	40.63	45.52	164.25
3	46.39	44.62	0.00

Allowable Pullout Stress = 100.0(kPa)
 Allowable Tendon Stress = 434782.6
 Allowable Nail Head Load = 210.0(kN)

NOTE - An Equivalent Line Load Is Calculated For Each Row Of Soil Nails
 Assuming A Uniform Distribution Of Load Horizontally Between
 Individual Nails.

SOIL NAIL LOAD DATA HAS BEEN SUPPRESSED

A Critical Failure Surface Searching Method, Using A Random
 Technique For Generating Circular Surfaces, Has Been Specified.
 2500 Trial Surfaces Have Been Generated.

50 Surface(s) Initiate(s) From Each Of 50 Points Equally Spaced
 Along The Ground Surface Between X = 19.80(m)
 and X = 35.00(m)
 Each Surface Terminates Between X = 42.00(m)
 and X = 64.00(m)

Unless Further Limitations Were Imposed, The Minimum Elevation
 At Which A Surface Extends Is Y = 0.00(m)
 0.80(m) Line Segments Define Each Trial Failure Surface.

**** ERROR - RC11 ****

>>200 attempts to generate failure surface have failed. Revise limitations

Following Are Displayed The Ten Most Critical Of The Trial
 Failure Surfaces Evaluated. They Are
 Ordered - Most Critical First.

* * Safety Factors Are Calculated By The Modified Bishop Method * *

Total Number of Trial Surfaces Evaluated = 2500

Statistical Data On All Valid FS Values:

FS Max = 3.653 FS Min = 0.830 FS Ave = 1.117

Standard Deviation = 0.744 Coefficient of Variation = 66.59 %

Failure Surface Specified By 54 Coordinate Points

Point X-Surf Y-Surf

No.	(m)	(m)
1	20.73	22.68
2	21.40	23.12
3	22.06	23.57
4	22.73	24.02
5	23.38	24.47
6	24.04	24.93
7	24.69	25.40
8	25.33	25.87
9	25.98	26.35
10	26.61	26.83
11	27.25	27.31
12	27.88	27.81
13	28.51	28.30
14	29.13	28.81
15	29.75	29.31
16	30.36	29.82
17	30.97	30.34
18	31.58	30.86
19	32.18	31.39
20	32.78	31.92
21	33.37	32.46
22	33.96	33.00
23	34.55	33.55
24	35.13	34.10
25	35.70	34.65
26	36.27	35.21
27	36.84	35.78
28	37.40	36.35
29	37.96	36.92
30	38.51	37.50
31	39.06	38.08
32	39.61	38.67
33	40.15	39.26
34	40.68	39.85
35	41.21	40.45
36	41.73	41.06
37	42.25	41.67
38	42.77	42.28
39	43.28	42.90
40	43.78	43.52
41	44.28	44.14
42	44.77	44.77
43	45.26	45.40
44	45.75	46.04
45	46.23	46.68
46	46.70	47.32
47	47.17	47.97
48	47.63	48.63
49	48.09	49.28
50	48.54	49.94
51	48.99	50.60
52	49.43	51.27
53	49.87	51.94
54	50.18	52.42

Circle Center At X = -33.39 ; Y = 105.72 ; and Radius = 99.12

Factor of Safety
 *** 0.830 ***

Individual data on the 60 slices										
Slice No.	Width (m)	Weight (kN)	Water Force	Water Force	Tie Force	Tie Force	Earthquake Force		Surcharge Load	
			Top (kN)	Bot (kN)	Norm (kN)	Tan (kN)	Hor (kN)	Ver (kN)	(kN)	
1	0.7	6.3	0.0	0.4	0.	0.	0.0	0.0	0.0	0.0
2	0.7	18.7	0.0	1.1	0.	0.	0.0	0.0	0.0	0.0
3	0.7	30.7	0.0	1.9	0.	0.	0.0	0.0	0.0	0.0
4	0.7	42.5	0.0	2.6	0.	0.	0.0	0.0	0.0	0.0
5	0.7	54.0	0.0	3.3	0.	0.	0.0	0.0	0.0	0.0
6	0.5	49.4	0.0	3.0	0.	0.	0.0	0.0	0.0	0.0
7	0.1	15.2	0.0	0.9	0.	0.	0.0	0.0	0.0	0.0
8	0.6	62.8	0.0	3.9	0.	0.	0.0	0.0	0.0	0.0
9	0.6	55.5	0.0	3.5	0.	0.	0.0	0.0	0.0	0.0
10	0.6	48.3	0.0	3.0	0.	0.	0.0	0.0	0.0	0.0
11	0.6	41.0	0.0	2.6	0.	0.	0.0	0.0	0.0	0.0
12	0.6	33.8	0.0	2.1	0.	0.	0.0	0.0	0.0	0.0

13	0.6	26.5	0.0	1.7	0.	0.	0.0	0.0	0.0
14	0.0	1.2	0.0	0.1	0.	0.	0.0	0.0	0.0
15	0.6	25.7	0.0	1.6	0.	0.	0.0	0.0	0.0
16	0.6	36.3	0.0	2.3	0.	0.	0.0	0.0	0.0
17	0.6	45.4	0.0	3.0	0.	0.	0.0	0.0	0.0
18	0.6	54.2	0.0	3.6	0.	0.	0.0	0.0	0.0
19	0.5	48.6	0.0	3.2	0.	0.	0.0	0.0	0.0
20	0.1	14.2	0.0	0.9	0.	0.	0.0	0.0	0.0
21	0.6	70.8	0.0	4.7	0.	0.	0.0	0.0	0.0
22	0.6	78.4	0.0	5.2	0.	0.	0.0	0.0	0.0
23	0.6	85.7	0.0	5.8	0.	0.	0.0	0.0	0.0
24	0.2	25.5	0.0	1.7	0.	0.	0.0	0.0	0.0
25	0.4	63.6	0.0	4.3	0.	0.	0.0	0.0	0.0
26	0.6	82.0	0.0	5.6	0.	0.	0.0	0.0	0.0
27	0.6	74.3	0.0	5.1	0.	0.	0.0	0.0	0.0
28	0.6	66.8	0.0	4.6	0.	0.	0.0	0.0	0.0
29	0.6	59.2	0.0	4.1	0.	0.	0.0	0.0	0.0
30	0.6	51.8	0.0	3.7	0.	0.	0.0	0.0	0.0
31	0.6	44.4	0.0	3.2	0.	0.	0.0	0.0	0.0
32	0.1	9.7	0.0	0.7	0.	0.	0.0	0.0	0.0
33	0.4	31.1	0.0	2.2	0.	0.	0.0	0.0	0.0
34	0.6	45.9	0.0	3.3	0.	0.	0.0	0.0	0.0
35	0.5	51.3	0.0	3.7	0.	0.	0.0	0.0	0.0
36	0.5	56.3	0.0	4.1	0.	0.	0.0	0.0	0.0
37	0.5	61.2	0.0	4.5	0.	0.	0.0	0.0	0.0
38	0.5	65.7	0.0	4.9	0.	0.	0.0	0.0	0.0
39	0.5	70.0	0.0	5.3	0.	0.	0.0	0.0	0.0
40	0.0	4.3	0.0	0.3	0.	0.	0.0	0.0	0.0
41	0.5	66.3	0.0	5.1	0.	0.	0.0	0.0	0.0
42	0.5	66.7	0.0	5.1	0.	0.	0.0	0.0	0.0
43	0.5	62.7	0.0	4.9	0.	0.	0.0	0.0	0.0
44	0.1	14.4	0.0	1.1	0.	0.	0.0	0.0	0.0
45	0.4	44.4	0.0	3.5	0.	0.	0.0	0.0	0.0
46	0.5	54.9	0.0	4.4	0.	0.	0.0	0.0	0.0
47	0.5	51.0	0.0	4.1	0.	0.	0.0	0.0	0.0
48	0.5	47.1	0.0	3.8	0.	0.	0.0	0.0	0.0
49	0.5	43.2	0.0	3.5	0.	0.	0.0	0.0	0.0
50	0.5	39.3	0.0	3.2	0.	0.	0.0	0.0	0.0
51	0.5	35.3	0.0	3.0	0.	0.	0.0	0.0	0.0
52	0.5	31.4	0.0	2.7	0.	0.	0.0	0.0	0.0
53	0.5	27.5	0.0	2.3	0.	0.	0.0	0.0	0.0
54	0.5	23.6	0.0	2.0	0.	0.	0.0	0.0	0.0
55	0.5	19.8	0.0	1.7	0.	0.	0.0	0.0	0.0
56	0.5	15.9	0.0	1.4	0.	0.	0.0	0.0	0.0
57	0.4	12.1	0.0	1.1	0.	0.	0.0	0.0	0.0
58	0.4	8.3	0.0	0.8	0.	0.	0.0	0.0	0.0
59	0.4	4.5	0.0	0.4	0.	0.	0.0	0.0	0.0
60	0.3	0.9	0.0	0.1	0.	0.	0.0	0.0	0.0

Failure Surface Specified By 53 Coordinate Points

Point No.	X-Surf (m)	Y-Surf (m)
1	20.73	22.68
2	21.44	23.05
3	22.14	23.44
4	22.84	23.83
5	23.53	24.22
6	24.22	24.63
7	24.90	25.05
8	25.58	25.47
9	26.26	25.91
10	26.92	26.35
11	27.58	26.80
12	28.24	27.25
13	28.89	27.72
14	29.54	28.19
15	30.18	28.67
16	30.81	29.16
17	31.43	29.66
18	32.05	30.17
19	32.67	30.68
20	33.28	31.20
21	33.88	31.73
22	34.47	32.26
23	35.06	32.80
24	35.64	33.35

25	36.22	33.91
26	36.78	34.48
27	37.34	35.05
28	37.90	35.62
29	38.44	36.21
30	38.98	36.80
31	39.51	37.40
32	40.04	38.00
33	40.55	38.61
34	41.06	39.23
35	41.56	39.86
36	42.06	40.48
37	42.54	41.12
38	43.02	41.76
39	43.49	42.41
40	43.95	43.06
41	44.40	43.72
42	44.85	44.39
43	45.29	45.06
44	45.71	45.73
45	46.14	46.41
46	46.55	47.10
47	46.95	47.79
48	47.34	48.49
49	47.73	49.19
50	48.11	49.89
51	48.48	50.60
52	48.84	51.32
53	49.05	51.76

Circle Center At X = -9.01 ; Y = 79.98 ; and Radius = 64.55

Factor of Safety

*** 0.835 ***

Failure Surface Specified By 57 Coordinate Points

Point No.	X-Surf (m)	Y-Surf (m)
1	20.73	22.68
2	21.43	23.07
3	22.13	23.46
4	22.82	23.86
5	23.51	24.26
6	24.20	24.67
7	24.88	25.09
8	25.56	25.52
9	26.23	25.96
10	26.90	26.40
11	27.56	26.84
12	28.22	27.30
13	28.87	27.76
14	29.52	28.22
15	30.17	28.70
16	30.80	29.18
17	31.44	29.67
18	32.07	30.16
19	32.69	30.66
20	33.31	31.17
21	33.93	31.68
22	34.54	32.20
23	35.14	32.72
24	35.74	33.25
25	36.33	33.79
26	36.92	34.33
27	37.50	34.88
28	38.08	35.44
29	38.65	36.00
30	39.21	36.56
31	39.77	37.14
32	40.32	37.72
33	40.87	38.30
34	41.41	38.89
35	41.95	39.48
36	42.48	40.08
37	43.00	40.69
38	43.52	41.30
39	44.03	41.91
40	44.53	42.54

41	45.03	43.16
42	45.52	43.79
43	46.00	44.43
44	46.48	45.07
45	46.96	45.72
46	47.42	46.37
47	47.88	47.02
48	48.33	47.68
49	48.78	48.35
50	49.21	49.02
51	49.65	49.69
52	50.07	50.37
53	50.49	51.05
54	50.90	51.74
55	51.30	52.43
56	51.70	53.12
57	51.85	53.40

Circle Center At X = -16.64 ; Y = 91.67 ; and Radius = 78.46
Factor of Safety
*** 0.837 ***

Failure Surface Specified By 49 Coordinate Points

Point No.	X-Surf (m)	Y-Surf (m)
1	20.73	22.68
2	21.44	23.06
3	22.14	23.45
4	22.83	23.84
5	23.52	24.25
6	24.20	24.67
7	24.88	25.09
8	25.55	25.53
9	26.22	25.97
10	26.87	26.43
11	27.53	26.89
12	28.17	27.36
13	28.81	27.84
14	29.44	28.33
15	30.07	28.83
16	30.69	29.34
17	31.30	29.85
18	31.90	30.38
19	32.50	30.91
20	33.09	31.45
21	33.67	32.00
22	34.25	32.56
23	34.81	33.12
24	35.37	33.70
25	35.92	34.28
26	36.46	34.87
27	36.99	35.46
28	37.52	36.07
29	38.04	36.68
30	38.54	37.30
31	39.04	37.92
32	39.53	38.55
33	40.02	39.19
34	40.49	39.84
35	40.95	40.49
36	41.41	41.15
37	41.85	41.81
38	42.29	42.48
39	42.71	43.16
40	43.13	43.84
41	43.54	44.53
42	43.94	45.22
43	44.32	45.92
44	44.70	46.63
45	45.07	47.34
46	45.43	48.05
47	45.78	48.77
48	46.12	49.50
49	46.44	50.22

Circle Center At X = -5.93 ; Y = 73.33 ; and Radius = 57.24
Factor of Safety
*** 0.839 ***

Failure Surface Specified By 50 Coordinate Points

Point No.	X-Surf (m)	Y-Surf (m)
1	21.04	23.30
2	21.75	23.68
3	22.45	24.07
4	23.14	24.46
5	23.83	24.87
6	24.51	25.28
7	25.19	25.71
8	25.86	26.14
9	26.53	26.58
10	27.19	27.03
11	27.85	27.49
12	28.49	27.96
13	29.14	28.44
14	29.77	28.93
15	30.40	29.42
16	31.02	29.92
17	31.64	30.43
18	32.25	30.95
19	32.85	31.48
20	33.44	32.02
21	34.03	32.56
22	34.61	33.11
23	35.19	33.67
24	35.75	34.23
25	36.31	34.81
26	36.86	35.39
27	37.40	35.98
28	37.93	36.57
29	38.46	37.17
30	38.98	37.78
31	39.49	38.40
32	39.99	39.02
33	40.48	39.65
34	40.97	40.29
35	41.44	40.93
36	41.91	41.58
37	42.37	42.24
38	42.82	42.90
39	43.26	43.57
40	43.69	44.24
41	44.12	44.92
42	44.53	45.60
43	44.94	46.29
44	45.33	46.99
45	45.72	47.69
46	46.10	48.39
47	46.46	49.10
48	46.82	49.82
49	47.17	50.54
50	47.24	50.69
Circle Center At X = -6.89 ; Y = 76.24 ; and Radius = 59.86		
Factor of Safety		
*** 0.846 ***		

Failure Surface Specified By 53 Coordinate Points

Point No.	X-Surf (m)	Y-Surf (m)
1	20.73	22.68
2	21.36	23.18
3	21.98	23.68
4	22.60	24.18
5	23.22	24.69
6	23.84	25.20
7	24.46	25.71
8	25.07	26.22
9	25.68	26.74
10	26.28	27.26
11	26.89	27.79
12	27.49	28.31
13	28.09	28.84
14	28.69	29.38
15	29.28	29.91
16	29.87	30.45

17	30.46	30.99
18	31.05	31.54
19	31.63	32.08
20	32.21	32.63
21	32.79	33.19
22	33.37	33.74
23	33.94	34.30
24	34.51	34.86
25	35.08	35.43
26	35.64	35.99
27	36.20	36.56
28	36.76	37.13
29	37.32	37.71
30	37.87	38.29
31	38.42	38.87
32	38.97	39.45
33	39.52	40.03
34	40.06	40.62
35	40.60	41.21
36	41.13	41.81
37	41.67	42.40
38	42.20	43.00
39	42.73	43.60
40	43.25	44.21
41	43.77	44.81
42	44.29	45.42
43	44.81	46.03
44	45.32	46.65
45	45.83	47.26
46	46.34	47.88
47	46.84	48.50
48	47.34	49.13
49	47.84	49.75
50	48.33	50.38
51	48.83	51.01
52	49.31	51.65
53	49.68	52.13

Circle Center At X = -81.11 ; Y = 151.76 ; and Radius = 164.42

Factor of Safety
*** 0.847 ***

Failure Surface Specified By 47 Coordinate Points

Point No.	X-Surf (m)	Y-Surf (m)
1	20.73	22.68
2	21.43	23.07
3	22.12	23.48
4	22.80	23.89
5	23.48	24.32
6	24.15	24.75
7	24.82	25.19
8	25.48	25.65
9	26.13	26.11
10	26.78	26.58
11	27.42	27.06
12	28.05	27.55
13	28.68	28.05
14	29.29	28.56
15	29.90	29.07
16	30.51	29.60
17	31.10	30.13
18	31.69	30.68
19	32.27	31.23
20	32.84	31.79
21	33.41	32.35
22	33.96	32.93
23	34.51	33.51
24	35.05	34.10
25	35.58	34.70
26	36.10	35.31
27	36.61	35.92
28	37.12	36.54
29	37.61	37.17
30	38.10	37.81
31	38.58	38.45
32	39.04	39.10

33	39.50	39.75
34	39.95	40.42
35	40.39	41.08
36	40.82	41.76
37	41.24	42.44
38	41.65	43.13
39	42.05	43.82
40	42.44	44.52
41	42.82	45.22
42	43.19	45.93
43	43.55	46.65
44	43.90	47.37
45	44.24	48.09
46	44.57	48.82
47	44.74	49.23

Circle Center At X = -6.33 ; Y = 71.29 ; and Radius = 55.64

Factor of Safety

*** 0.848 ***

Failure Surface Specified By 46 Coordinate Points

Point No.	X-Surf (m)	Y-Surf (m)
1	20.73	22.68
2	21.42	23.09
3	22.10	23.50
4	22.78	23.92
5	23.46	24.36
6	24.12	24.80
7	24.78	25.25
8	25.43	25.72
9	26.08	26.19
10	26.72	26.67
11	27.35	27.16
12	27.98	27.65
13	28.60	28.16
14	29.21	28.67
15	29.82	29.20
16	30.41	29.73
17	31.00	30.27
18	31.59	30.82
19	32.16	31.38
20	32.73	31.94
21	33.29	32.51
22	33.84	33.09
23	34.38	33.68
24	34.91	34.28
25	35.44	34.88
26	35.96	35.49
27	36.46	36.11
28	36.96	36.73
29	37.46	37.36
30	37.94	38.00
31	38.41	38.65
32	38.87	39.30
33	39.33	39.96
34	39.77	40.62
35	40.21	41.29
36	40.64	41.97
37	41.05	42.65
38	41.46	43.34
39	41.86	44.04
40	42.25	44.74
41	42.62	45.44
42	42.99	46.15
43	43.35	46.87
44	43.70	47.59
45	44.04	48.31
46	44.34	48.99

Circle Center At X = -7.76 ; Y = 72.00 ; and Radius = 56.95

Factor of Safety

*** 0.853 ***

Failure Surface Specified By 65 Coordinate Points

Point No.	X-Surf (m)	Y-Surf (m)
1	20.73	22.68
2	21.38	23.15

3	22.03	23.62
4	22.67	24.09
5	23.31	24.57
6	23.95	25.05
7	24.59	25.53
8	25.23	26.01
9	25.87	26.50
10	26.50	26.99
11	27.13	27.48
12	27.76	27.97
13	28.39	28.47
14	29.02	28.96
15	29.64	29.46
16	30.26	29.97
17	30.88	30.47
18	31.50	30.98
19	32.12	31.49
20	32.73	32.00
21	33.35	32.52
22	33.96	33.03
23	34.57	33.55
24	35.17	34.07
25	35.78	34.60
26	36.38	35.12
27	36.98	35.65
28	37.58	36.18
29	38.18	36.71
30	38.77	37.25
31	39.36	37.79
32	39.95	38.33
33	40.54	38.87
34	41.13	39.41
35	41.71	39.96
36	42.29	40.51
37	42.87	41.06
38	43.45	41.61
39	44.03	42.17
40	44.60	42.73
41	45.17	43.29
42	45.74	43.85
43	46.31	44.41
44	46.87	44.98
45	47.44	45.55
46	48.00	46.12
47	48.56	46.69
48	49.11	47.26
49	49.67	47.84
50	50.22	48.42
51	50.77	49.00
52	51.32	49.59
53	51.86	50.17
54	52.41	50.76
55	52.95	51.35
56	53.48	51.94
57	54.02	52.53
58	54.55	53.13
59	55.09	53.73
60	55.62	54.33
61	56.14	54.93
62	56.67	55.53
63	57.19	56.14
64	57.71	56.75
65	57.87	56.94

Circle Center At X = -101.49 ; Y = 192.46 ; and Radius = 209.19

Factor of Safety

*** 0.855 ***

Failure Surface Specified By 50 Coordinate Points

Point No.	X-Surf (m)	Y-Surf (m)
1	21.04	23.30
2	21.68	23.77
3	22.33	24.25
4	22.96	24.74
5	23.60	25.23
6	24.23	25.72

7	24.85	26.22
8	25.48	26.72
9	26.10	27.22
10	26.71	27.73
11	27.33	28.25
12	27.93	28.77
13	28.54	29.29
14	29.14	29.82
15	29.74	30.35
16	30.33	30.88
17	30.92	31.42
18	31.51	31.97
19	32.09	32.52
20	32.67	33.07
21	33.25	33.63
22	33.82	34.19
23	34.38	34.75
24	34.95	35.32
25	35.51	35.89
26	36.06	36.47
27	36.61	37.05
28	37.16	37.63
29	37.70	38.22
30	38.24	38.81
31	38.77	39.41
32	39.30	40.01
33	39.83	40.61
34	40.35	41.22
35	40.87	41.83
36	41.38	42.44
37	41.89	43.06
38	42.39	43.68
39	42.89	44.31
40	43.39	44.93
41	43.88	45.57
42	44.36	46.20
43	44.84	46.84
44	45.32	47.48
45	45.79	48.13
46	46.26	48.78
47	46.73	49.43
48	47.18	50.08
49	47.64	50.74
50	47.85	51.05

Circle Center At X = -45.82 ; Y = 114.72 ; and Radius = 113.26

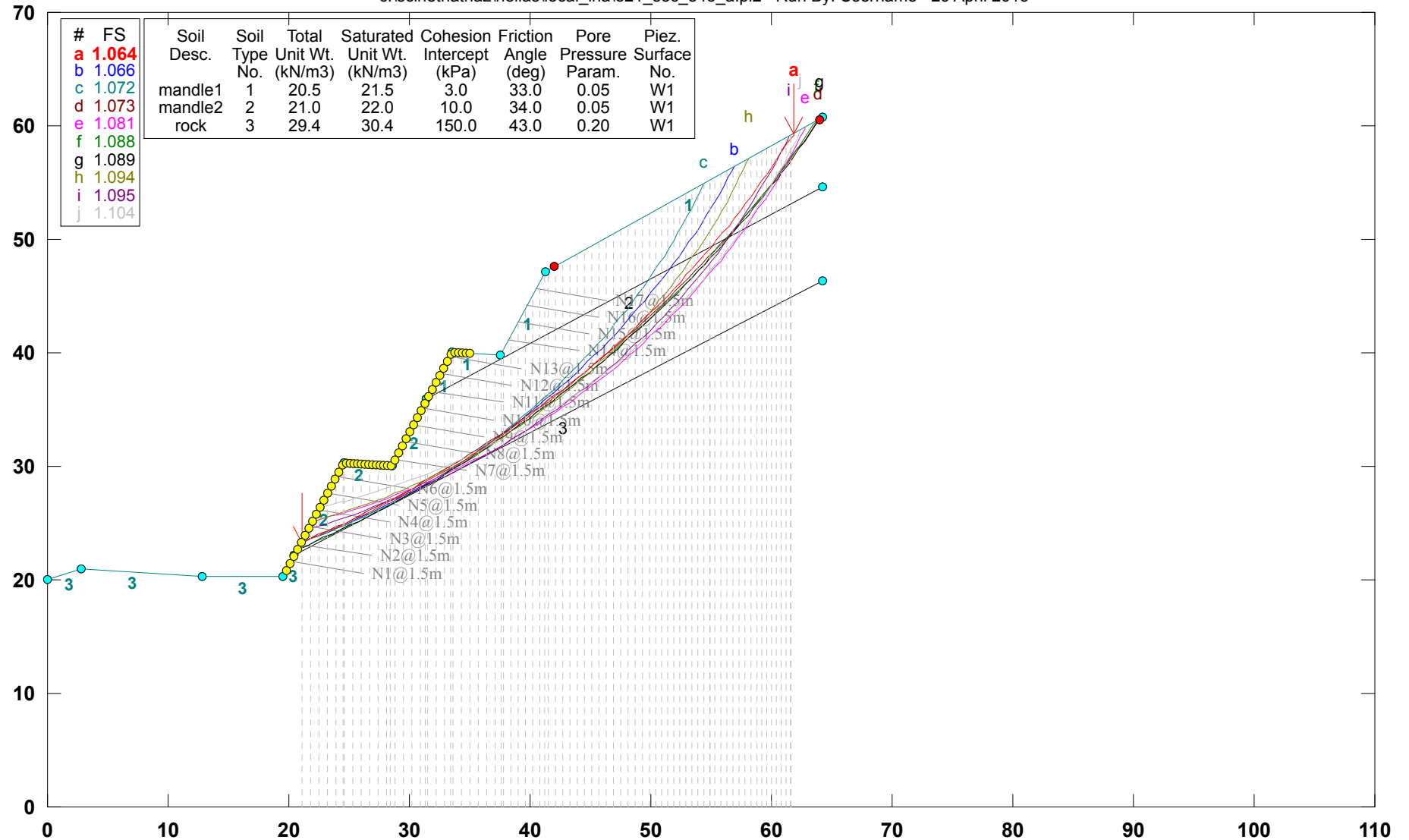
Factor of Safety

*** 0.857 ***

**** END OF GSTABL7 OUTPUT ****

Hellas_Local_Landslide_Hazard Cut slope O21_sec_845_A

c:\scinet\nathaz\hellas\local_lha\o21_sec_845_a.pl2 Run By: Username 29 April 2015



GSTABL7 v.2 FSmin=1.064

Safety Factors Are Calculated By The Modified Bishop Method



*** GSTABL7 ***

** GSTABL7 by Garry H. Gregory, P.E. **

** Original Version 1.0, January 1996; Current Version 2.003, June 2002 **

(All Rights Reserved-Unauthorized Use Prohibited)

SLOPE STABILITY ANALYSIS SYSTEM

Modified Bishop, Simplified Janbu, or GLE Method of Slices.

(Includes Spencer & Morgenstern-Price Type Analysis)

Including Pier/Pile, Reinforcement, Soil Nail, Tieback,

Nonlinear Undrained Shear Strength, Curved Phi Envelope,

Anisotropic Soil, Fiber-Reinforced Soil, Boundary Loads, Water

Surfaces, Pseudo-Static & Newmark Earthquake, and Applied Forces.

Analysis Run Date: 29 April 2015

Time of Run:

Run By: Username

Input Data Filename: C:\SciNetNatHaz\Hellas\Local_LHA\021_sec_845_A.in

Output Filename: C:\SciNetNatHaz\Hellas\Local_LHA\021_sec_845_A.OUT

Unit System: SI

Plotted Output Filename: C:\SciNetNatHaz\Hellas\Local_LHA_sec_845_A.PLT

PROBLEM DESCRIPTION: Hellas_Local_Landslide_Hazard

Cut slope 021_sec_845_A

BOUNDARY COORDINATES

11 Top Boundaries

13 Total Boundaries

Boundary No.	X-Left (m)	Y-Left (m)	X-Right (m)	Y-Right (m)	Soil Type Below Bnd
1	0.00	20.00	2.80	20.93	3
2	2.80	20.93	12.80	20.34	3
3	12.80	20.34	19.54	20.29	3
4	19.54	20.29	20.50	22.22	3
5	20.50	22.22	24.54	30.29	2
6	24.54	30.29	28.54	30.05	2
7	28.54	30.05	31.45	35.88	2
8	31.45	35.88	33.54	40.05	1
9	33.54	40.05	37.54	39.81	1
10	37.54	39.81	41.24	47.17	1
11	41.24	47.17	64.30	60.71	1
12	31.45	35.88	64.30	54.68	2
13	20.50	22.22	64.30	46.38	3

Default Y-Origin = 0.00(m)

Default X-Plus Value = 0.00(m)

Default Y-Plus Value = 0.00(m)

ISOTROPIC SOIL PARAMETERS

3 Type(s) of Soil

Soil Type No.	Total Unit Wt. (kN/m3)	Saturated Unit Wt. (kN/m3)	Cohesion Intercept (kPa)	Friction Angle (deg)	Pore Pressure Param.	Pressure Constant (kPa)	Piez. Surface No.
1	20.5	21.5	3.0	33.0	0.05	0.0	1
2	21.0	22.0	10.0	34.0	0.05	0.0	1
3	29.4	30.4	150.0	43.0	0.20	0.0	1

SOIL NAIL LOAD(S)

17 SOIL NAIL LOAD(S) SPECIFIED

Nail No.	X-Pos (m)	Y-Pos (m)	Nail Dia (mm)	Tendon Dia (mm)	Spacing (m)	Inclin. (deg)	Length (m)
1	20.22	21.66	150.0	29.0	1.50	10.00	6.00
2	20.97	23.16	150.0	29.0	1.50	10.00	6.00
3	21.72	24.66	150.0	29.0	1.50	10.00	6.00
4	22.47	26.16	150.0	29.0	1.50	10.00	6.00
5	23.22	27.65	150.0	29.0	1.50	10.00	6.00
6	23.97	29.15	150.0	29.0	1.50	10.00	6.00
7	28.84	30.65	150.0	29.0	1.50	10.00	6.00
8	29.59	32.15	150.0	29.0	1.50	10.00	6.00
9	30.34	33.66	150.0	29.0	1.50	10.00	6.00
10	31.09	35.16	150.0	29.0	1.50	10.00	6.00
11	31.84	36.66	150.0	29.0	1.50	10.00	6.00
12	32.59	38.15	150.0	29.0	1.50	10.00	6.00
13	33.34	39.65	150.0	29.0	1.50	10.00	6.00
14	38.23	41.18	150.0	29.0	1.50	10.00	6.00
15	38.98	42.67	150.0	29.0	1.50	10.00	6.00
16	39.73	44.17	150.0	29.0	1.50	10.00	6.00
17	40.48	45.66	150.0	29.0	1.50	10.00	6.00

SOIL NAIL LOAD DATA

Soil Nail No. 1 4 Load Points Apply to This Nail

Load Diagram Type = 1

POINT NO.	X-COORD.(m)	Y-COORD.(m)	FORCE(kN)
1	20.22	21.66	140.00
2	21.03	21.52	191.46
3	23.22	21.14	191.46
4	26.13	20.62	0.00

Allowable Pullout Stress = 200.0(kPa)
 Allowable Tendon Stress = 434782.6
 Allowable Nail Head Load = 210.0(kN)
 Soil Nail No. 2 4 Load Points Apply to This Nail
 Load Diagram Type = 1

POINT NO.	X-COORD.(m)	Y-COORD.(m)	FORCE(kN)
1	20.97	23.16	140.00
2	21.78	23.02	191.46
3	23.97	22.64	191.46
4	26.88	22.12	0.00

Allowable Pullout Stress = 200.0(kPa)
 Allowable Tendon Stress = 434782.6
 Allowable Nail Head Load = 210.0(kN)
 Soil Nail No. 3 4 Load Points Apply to This Nail
 Load Diagram Type = 1

POINT NO.	X-COORD.(m)	Y-COORD.(m)	FORCE(kN)
1	21.72	24.66	140.00
2	22.53	24.52	191.46
3	24.72	24.14	191.46
4	27.63	23.62	0.00

Allowable Pullout Stress = 200.0(kPa)
 Allowable Tendon Stress = 434782.6
 Allowable Nail Head Load = 210.0(kN)
 Soil Nail No. 4 4 Load Points Apply to This Nail
 Load Diagram Type = 1

POINT NO.	X-COORD.(m)	Y-COORD.(m)	FORCE(kN)
1	22.47	26.16	140.00
2	23.55	25.97	191.46
3	24.47	25.81	191.46
4	28.38	25.11	0.00

Allowable Pullout Stress = 150.0(kPa)
 Allowable Tendon Stress = 434782.6
 Allowable Nail Head Load = 210.0(kN)
 Soil Nail No. 5 4 Load Points Apply to This Nail
 Load Diagram Type = 1

POINT NO.	X-COORD.(m)	Y-COORD.(m)	FORCE(kN)
1	23.22	27.65	140.00
2	24.30	27.47	191.46
3	25.22	27.31	191.46
4	29.13	26.61	0.00

Allowable Pullout Stress = 150.0(kPa)
 Allowable Tendon Stress = 434782.6
 Allowable Nail Head Load = 210.0(kN)
 Soil Nail No. 6 4 Load Points Apply to This Nail
 Load Diagram Type = 1

POINT NO.	X-COORD.(m)	Y-COORD.(m)	FORCE(kN)
1	23.97	29.15	140.00
2	25.05	28.96	191.46
3	25.97	28.80	191.46
4	29.88	28.11	0.00

Allowable Pullout Stress = 150.0(kPa)
 Allowable Tendon Stress = 434782.6
 Allowable Nail Head Load = 210.0(kN)
 Soil Nail No. 7 3 Load Points Apply to This Nail
 Load Diagram Type = 3

POINT NO.	X-COORD.(m)	Y-COORD.(m)	FORCE(kN)
1	28.84	30.65	140.00
2	29.53	30.45	183.10
3	34.75	29.61	0.00

Allowable Pullout Stress = 120.0(kPa)
 Allowable Tendon Stress = 434782.6
 Allowable Nail Head Load = 210.0(kN)
 Soil Nail No. 8 3 Load Points Apply to This Nail
 Load Diagram Type = 3

POINT NO.	X-COORD.(m)	Y-COORD.(m)	FORCE(kN)
1	29.59	32.15	140.00
2	30.27	31.96	183.10
3	35.50	31.11	0.00

Allowable Pullout Stress = 120.0(kPa)
 Allowable Tendon Stress = 434782.6

Allowable Nail Head Load = 210.0(kN)
 Soil Nail No. 9 3 Load Points Apply to This Nail
 Load Diagram Type = 3

POINT NO.	X-COORD.(m)	Y-COORD.(m)	FORCE(kN)
1	30.34	33.66	140.00
2	31.00	33.46	183.10
3	36.25	32.61	0.00

 Allowable Pullout Stress = 120.0(kPa)
 Allowable Tendon Stress = 434782.6
 Allowable Nail Head Load = 210.0(kN)
 Soil Nail No. 10 3 Load Points Apply to This Nail
 Load Diagram Type = 3

POINT NO.	X-COORD.(m)	Y-COORD.(m)	FORCE(kN)
1	31.09	35.16	140.00
2	31.74	34.96	183.10
3	37.00	34.12	0.00

 Allowable Pullout Stress = 120.0(kPa)
 Allowable Tendon Stress = 434782.6
 Allowable Nail Head Load = 210.0(kN)
 Soil Nail No. 11 3 Load Points Apply to This Nail
 Load Diagram Type = 3

POINT NO.	X-COORD.(m)	Y-COORD.(m)	FORCE(kN)
1	31.84	36.66	140.00
2	32.32	36.49	173.67
3	37.75	35.62	0.00

 Allowable Pullout Stress = 110.0(kPa)
 Allowable Tendon Stress = 434782.6
 Allowable Nail Head Load = 210.0(kN)
 Soil Nail No. 12 3 Load Points Apply to This Nail
 Load Diagram Type = 3

POINT NO.	X-COORD.(m)	Y-COORD.(m)	FORCE(kN)
1	32.59	38.15	140.00
2	33.05	37.99	173.67
3	38.50	37.11	0.00

 Allowable Pullout Stress = 110.0(kPa)
 Allowable Tendon Stress = 434782.6
 Allowable Nail Head Load = 210.0(kN)
 Soil Nail No. 13 3 Load Points Apply to This Nail
 Load Diagram Type = 3

POINT NO.	X-COORD.(m)	Y-COORD.(m)	FORCE(kN)
1	33.34	39.65	140.00
2	33.79	39.48	173.67
3	39.25	38.61	0.00

 Allowable Pullout Stress = 110.0(kPa)
 Allowable Tendon Stress = 434782.6
 Allowable Nail Head Load = 210.0(kN)
 Soil Nail No. 14 3 Load Points Apply to This Nail
 Load Diagram Type = 3

POINT NO.	X-COORD.(m)	Y-COORD.(m)	FORCE(kN)
1	38.23	41.18	140.00
2	38.41	41.05	164.25
3	44.14	40.14	0.00

 Allowable Pullout Stress = 100.0(kPa)
 Allowable Tendon Stress = 434782.6
 Allowable Nail Head Load = 210.0(kN)
 Soil Nail No. 15 3 Load Points Apply to This Nail
 Load Diagram Type = 3

POINT NO.	X-COORD.(m)	Y-COORD.(m)	FORCE(kN)
1	38.98	42.67	140.00
2	39.15	42.54	164.25
3	44.89	41.63	0.00

 Allowable Pullout Stress = 100.0(kPa)
 Allowable Tendon Stress = 434782.6
 Allowable Nail Head Load = 210.0(kN)
 Soil Nail No. 16 3 Load Points Apply to This Nail
 Load Diagram Type = 3

POINT NO.	X-COORD.(m)	Y-COORD.(m)	FORCE(kN)
1	39.73	44.17	140.00
2	39.89	44.03	164.25
3	45.64	43.12	0.00

 Allowable Pullout Stress = 100.0(kPa)
 Allowable Tendon Stress = 434782.6
 Allowable Nail Head Load = 210.0(kN)
 Soil Nail No. 17 3 Load Points Apply to This Nail
 Load Diagram Type = 3

POINT NO.	X-COORD.(m)	Y-COORD.(m)	FORCE(kN)
1	40.48	45.66	140.00
2	40.63	45.52	164.25
3	46.39	44.62	0.00

Allowable Pullout Stress = 100.0(kPa)

Allowable Tendon Stress = 434782.6

Allowable Nail Head Load = 210.0(kN)

NOTE - An Equivalent Line Load Is Calculated For Each Row Of Soil Nails
Assuming A Uniform Distribution Of Load Horizontally Between
Individual Nails.

A Critical Failure Surface Searching Method, Using A Random
Technique For Generating Circular Surfaces, Has Been Specified.
2500 Trial Surfaces Have Been Generated.

50 Surface(s) Initiate(s) From Each Of 50 Points Equally Spaced

Along The Ground Surface Between X = 19.80(m)

and X = 35.00(m)

Each Surface Terminates Between X = 42.00(m)

and X = 64.00(m)

Unless Further Limitations Were Imposed, The Minimum Elevation

At Which A Surface Extends Is Y = 0.00(m)

0.80(m) Line Segments Define Each Trial Failure Surface.

**** ERROR - RC11 ****

>>200 attempts to generate failure surface have failed. Revise limitations

Following Are Displayed The Ten Most Critical Of The Trial

Failure Surfaces Evaluated. They Are

Ordered - Most Critical First.

* * Safety Factors Are Calculated By The Modified Bishop Method * *

Total Number of Trial Surfaces Evaluated = 2500

Statistical Data On All Valid FS Values:

FS Max = 4.221 FS Min = 1.064 FS Ave = 1.186

Standard Deviation = 0.743 Coefficient of Variation = 62.68 %

Failure Surface Specified By 71 Coordinate Points

Point No.	X-Surf (m)	Y-Surf (m)
1	21.04	23.30
2	21.77	23.62
3	22.50	23.95
4	23.23	24.28
5	23.95	24.62
6	24.68	24.97
7	25.39	25.32
8	26.11	25.68
9	26.82	26.05
10	27.53	26.42
11	28.23	26.80
12	28.93	27.19
13	29.63	27.58
14	30.32	27.98
15	31.01	28.39
16	31.70	28.80
17	32.38	29.22
18	33.06	29.64
19	33.73	30.07
20	34.40	30.51
21	35.07	30.95
22	35.73	31.40
23	36.39	31.85
24	37.05	32.31
25	37.70	32.78
26	38.34	33.25
27	38.98	33.73
28	39.62	34.21
29	40.25	34.70
30	40.88	35.20
31	41.50	35.70
32	42.12	36.20
33	42.74	36.72
34	43.35	37.23
35	43.95	37.76
36	44.55	38.29
37	45.15	38.82
38	45.74	39.36
39	46.32	39.90
40	46.91	40.45
41	47.48	41.01

42	48.05	41.57
43	48.62	42.14
44	49.18	42.71
45	49.73	43.28
46	50.28	43.87
47	50.83	44.45
48	51.36	45.04
49	51.90	45.64
50	52.43	46.24
51	52.95	46.85
52	53.47	47.46
53	53.98	48.07
54	54.48	48.69
55	54.98	49.32
56	55.48	49.95
57	55.97	50.58
58	56.45	51.22
59	56.93	51.86
60	57.40	52.51
61	57.86	53.16
62	58.32	53.81
63	58.78	54.47
64	59.22	55.13
65	59.66	55.80
66	60.10	56.47
67	60.53	57.15
68	60.95	57.83
69	61.37	58.51
70	61.78	59.20
71	61.81	59.25

Circle Center At X = -13.80 ; Y = 103.90 ; and Radius = 87.81

Factor of Safety

*** 1.064 ***

Individual data on the 77 slices

Slice No.	Width (m)	Weight (kN)	Water Force		Tie Force		Earthquake Force		Surcharge Load (kN)
			Top (kN)	Bot (kN)	Norm (kN)	Tan (kN)	Hor (kN)	Ver (kN)	
1	0.7	8.8	0.0	0.5	0.	0.	0.0	0.0	0.0
2	0.7	26.2	0.0	1.4	0.	0.	0.0	0.0	0.0
3	0.7	43.2	0.0	2.4	0.	0.	0.0	0.0	0.0
4	0.7	60.0	0.0	3.3	0.	0.	0.0	0.0	0.0
5	0.6	60.8	0.0	3.4	0.	0.	0.0	0.0	0.0
6	0.1	15.2	0.0	0.8	0.	0.	0.0	0.0	0.0
7	0.7	77.0	0.0	4.3	0.	0.	0.0	0.0	0.0
8	0.7	70.7	0.0	4.0	0.	0.	0.0	0.0	0.0
9	0.7	64.3	0.0	3.6	0.	0.	0.0	0.0	0.0
10	0.7	57.9	0.0	3.3	0.	0.	0.0	0.0	0.0
11	0.7	51.4	0.0	2.9	0.	0.	0.0	0.0	0.0
12	0.3	20.7	0.0	1.2	0.	0.	0.0	0.0	0.0
13	0.4	27.5	0.0	1.6	0.	0.	0.0	0.0	0.0
14	0.7	60.7	0.0	3.5	0.	0.	0.0	0.0	0.0
15	0.7	74.9	0.0	4.3	0.	0.	0.0	0.0	0.0
16	0.7	88.7	0.0	5.1	0.	0.	0.0	0.0	0.0
17	0.4	63.8	0.0	3.7	0.	0.	0.0	0.0	0.0
18	0.2	38.4	0.0	2.2	0.	0.	0.0	0.0	0.0
19	0.7	115.0	0.0	6.7	0.	0.	0.0	0.0	0.0
20	0.7	127.4	0.0	7.5	0.	0.	0.0	0.0	0.0
21	0.5	98.4	0.0	5.8	0.	0.	0.0	0.0	0.0
22	0.2	40.3	0.0	2.4	0.	0.	0.0	0.0	0.0
23	0.7	136.2	0.0	8.1	0.	0.	0.0	0.0	0.0
24	0.7	128.8	0.0	7.7	0.	0.	0.0	0.0	0.0
25	0.7	121.4	0.0	7.3	0.	0.	0.0	0.0	0.0
26	0.7	114.0	0.0	6.9	0.	0.	0.0	0.0	0.0
27	0.7	106.6	0.0	6.5	0.	0.	0.0	0.0	0.0
28	0.5	76.1	0.0	4.7	0.	0.	0.0	0.0	0.0
29	0.2	23.6	0.0	1.5	0.	0.	0.0	0.0	0.0
30	0.6	104.7	0.0	6.5	0.	0.	0.0	0.0	0.0
31	0.6	114.6	0.0	7.1	0.	0.	0.0	0.0	0.0
32	0.6	124.1	0.0	7.8	0.	0.	0.0	0.0	0.0
33	0.6	133.3	0.0	8.4	0.	0.	0.0	0.0	0.0
34	0.6	142.1	0.0	9.0	0.	0.	0.0	0.0	0.0
35	0.4	85.5	0.0	5.5	0.	0.	0.0	0.0	0.0
36	0.3	64.0	0.0	4.1	0.	0.	0.0	0.0	0.0
37	0.6	148.5	0.0	9.6	0.	0.	0.0	0.0	0.0

38	0.6	145.5	0.0	9.5	0.	0.	0.0	0.0	0.0
39	0.6	142.4	0.0	9.3	0.	0.	0.0	0.0	0.0
40	0.6	139.2	0.0	9.2	0.	0.	0.0	0.0	0.0
41	0.6	135.9	0.0	9.1	0.	0.	0.0	0.0	0.0
42	0.6	132.5	0.0	8.9	0.	0.	0.0	0.0	0.0
43	0.6	129.1	0.0	8.7	0.	0.	0.0	0.0	0.0
44	0.6	125.6	0.0	8.6	0.	0.	0.0	0.0	0.0
45	0.6	122.0	0.0	8.4	0.	0.	0.0	0.0	0.0
46	0.6	118.4	0.0	8.2	0.	0.	0.0	0.0	0.0
47	0.6	114.7	0.0	8.0	0.	0.	0.0	0.0	0.0
48	0.6	110.9	0.0	7.8	0.	0.	0.0	0.0	0.0
49	0.6	107.1	0.0	7.6	0.	0.	0.0	0.0	0.0
50	0.6	103.2	0.0	7.4	0.	0.	0.0	0.0	0.0
51	0.5	99.3	0.0	7.2	0.	0.	0.0	0.0	0.0
52	0.5	95.3	0.0	7.0	0.	0.	0.0	0.0	0.0
53	0.5	91.3	0.0	6.8	0.	0.	0.0	0.0	0.0
54	0.5	87.3	0.0	6.5	0.	0.	0.0	0.0	0.0
55	0.5	83.2	0.0	6.3	0.	0.	0.0	0.0	0.0
56	0.5	79.1	0.0	6.1	0.	0.	0.0	0.0	0.0
57	0.5	75.0	0.0	5.8	0.	0.	0.0	0.0	0.0
58	0.5	70.8	0.0	5.5	0.	0.	0.0	0.0	0.0
59	0.5	66.7	0.0	5.3	0.	0.	0.0	0.0	0.0
60	0.5	62.5	0.0	5.0	0.	0.	0.0	0.0	0.0
61	0.0	5.5	0.0	0.4	0.	0.	0.0	0.0	0.0
62	0.4	52.9	0.0	4.3	0.	0.	0.0	0.0	0.0
63	0.5	54.2	0.0	4.4	0.	0.	0.0	0.0	0.0
64	0.5	50.1	0.0	4.1	0.	0.	0.0	0.0	0.0
65	0.5	46.0	0.0	3.9	0.	0.	0.0	0.0	0.0
66	0.5	41.9	0.0	3.6	0.	0.	0.0	0.0	0.0
67	0.5	37.8	0.0	3.2	0.	0.	0.0	0.0	0.0
68	0.5	33.7	0.0	2.9	0.	0.	0.0	0.0	0.0
69	0.5	29.7	0.0	2.6	0.	0.	0.0	0.0	0.0
70	0.4	25.6	0.0	2.3	0.	0.	0.0	0.0	0.0
71	0.4	21.6	0.0	2.0	0.	0.	0.0	0.0	0.0
72	0.4	17.7	0.0	1.6	0.	0.	0.0	0.0	0.0
73	0.4	13.7	0.0	1.3	0.	0.	0.0	0.0	0.0
74	0.4	9.8	0.0	0.9	0.	0.	0.0	0.0	0.0
75	0.4	6.0	0.0	0.6	0.	0.	0.0	0.0	0.0
76	0.4	2.2	0.0	0.2	0.	0.	0.0	0.0	0.0
77	0.0	0.0	0.0	0.0	0.	0.	0.0	0.0	0.0

Failure Surface Specified By 64 Coordinate Points

Point No.	X-Surf (m)	Y-Surf (m)
1	21.04	23.30
2	21.78	23.60
3	22.52	23.91
4	23.25	24.23
5	23.98	24.56
6	24.71	24.89
7	25.43	25.24
8	26.15	25.59
9	26.86	25.95
10	27.57	26.32
11	28.28	26.69
12	28.98	27.08
13	29.68	27.47
14	30.37	27.88
15	31.06	28.29
16	31.74	28.70
17	32.42	29.13
18	33.09	29.56
19	33.75	30.01
20	34.42	30.45
21	35.07	30.91
22	35.72	31.38
23	36.37	31.85
24	37.01	32.33
25	37.64	32.82
26	38.27	33.31
27	38.90	33.81
28	39.51	34.32
29	40.12	34.84
30	40.73	35.36
31	41.33	35.89
32	41.92	36.43

33	42.51	36.98
34	43.09	37.53
35	43.66	38.08
36	44.22	38.65
37	44.78	39.22
38	45.34	39.80
39	45.88	40.38
40	46.42	40.97
41	46.96	41.57
42	47.48	42.17
43	48.00	42.78
44	48.51	43.40
45	49.02	44.02
46	49.51	44.65
47	50.00	45.28
48	50.48	45.92
49	50.96	46.56
50	51.43	47.21
51	51.88	47.87
52	52.34	48.53
53	52.78	49.19
54	53.22	49.86
55	53.64	50.54
56	54.06	51.22
57	54.48	51.91
58	54.88	52.60
59	55.28	53.29
60	55.66	53.99
61	56.04	54.70
62	56.41	55.40
63	56.78	56.12
64	56.90	56.36

Circle Center At X = -4.30 ; Y = 86.76 ; and Radius = 68.33

Factor of Safety

*** 1.066 ***

Failure Surface Specified By 60 Coordinate Points

Point No.	X-Surf (m)	Y-Surf (m)
1	21.04	23.30
2	21.79	23.59
3	22.53	23.89
4	23.27	24.20
5	24.00	24.51
6	24.73	24.84
7	25.46	25.18
8	26.18	25.53
9	26.89	25.88
10	27.60	26.25
11	28.31	26.63
12	29.01	27.01
13	29.71	27.41
14	30.40	27.81
15	31.08	28.23
16	31.76	28.65
17	32.43	29.08
18	33.10	29.52
19	33.76	29.97
20	34.42	30.43
21	35.07	30.90
22	35.71	31.38
23	36.35	31.86
24	36.97	32.35
25	37.60	32.86
26	38.21	33.37
27	38.82	33.89
28	39.43	34.41
29	40.02	34.95
30	40.61	35.49
31	41.19	36.04
32	41.76	36.60
33	42.33	37.16
34	42.88	37.74
35	43.43	38.32
36	43.98	38.91
37	44.51	39.50

38	45.04	40.11
39	45.55	40.72
40	46.06	41.33
41	46.56	41.96
42	47.06	42.59
43	47.54	43.22
44	48.02	43.87
45	48.48	44.52
46	48.94	45.17
47	49.39	45.83
48	49.83	46.50
49	50.26	47.18
50	50.68	47.86
51	51.10	48.54
52	51.50	49.23
53	51.90	49.93
54	52.28	50.63
55	52.66	51.33
56	53.02	52.05
57	53.38	52.76
58	53.72	53.48
59	54.06	54.21
60	54.36	54.87

Circle Center At X = 0.01 ; Y = 78.86 ; and Radius = 59.41

Factor of Safety

*** 1.072 ***

Failure Surface Specified By 73 Coordinate Points

Point No.	X-Surf (m)	Y-Surf (m)
1	21.04	23.30
2	21.77	23.64
3	22.49	23.98
4	23.21	24.33
5	23.93	24.68
6	24.64	25.04
7	25.35	25.40
8	26.06	25.77
9	26.77	26.15
10	27.47	26.53
11	28.17	26.92
12	28.87	27.31
13	29.56	27.71
14	30.25	28.11
15	30.94	28.52
16	31.63	28.94
17	32.31	29.36
18	32.98	29.78
19	33.66	30.21
20	34.33	30.65
21	35.00	31.09
22	35.66	31.54
23	36.32	31.99
24	36.98	32.45
25	37.63	32.91
26	38.28	33.38
27	38.92	33.85
28	39.57	34.33
29	40.20	34.81
30	40.84	35.30
31	41.47	35.79
32	42.09	36.29
33	42.72	36.79
34	43.33	37.30
35	43.95	37.81
36	44.56	38.33
37	45.16	38.85
38	45.77	39.38
39	46.36	39.91
40	46.96	40.45
41	47.55	40.99
42	48.13	41.53
43	48.71	42.09
44	49.29	42.64
45	49.86	43.20
46	50.43	43.76

47	50.99	44.33
48	51.55	44.91
49	52.10	45.48
50	52.65	46.07
51	53.19	46.65
52	53.73	47.24
53	54.27	47.84
54	54.80	48.44
55	55.32	49.04
56	55.85	49.65
57	56.36	50.26
58	56.87	50.87
59	57.38	51.49
60	57.88	52.12
61	58.38	52.74
62	58.87	53.38
63	59.35	54.01
64	59.83	54.65
65	60.31	55.29
66	60.78	55.94
67	61.25	56.59
68	61.71	57.24
69	62.16	57.90
70	62.61	58.56
71	63.06	59.23
72	63.50	59.90
73	63.85	60.45

Circle Center At X = -20.99 ; Y = 114.99 ; and Radius = 100.87

Factor of Safety
*** 1.073 ***

Failure Surface Specified By 71 Coordinate Points

Point No.	X-Surf (m)	Y-Surf (m)
1	21.97	25.16
2	22.74	25.38
3	23.51	25.60
4	24.27	25.84
5	25.03	26.09
6	25.79	26.35
7	26.55	26.61
8	27.30	26.89
9	28.04	27.17
10	28.79	27.47
11	29.53	27.77
12	30.26	28.08
13	31.00	28.40
14	31.72	28.74
15	32.45	29.08
16	33.17	29.43
17	33.88	29.78
18	34.59	30.15
19	35.30	30.53
20	36.00	30.91
21	36.70	31.31
22	37.39	31.71
23	38.08	32.12
24	38.76	32.54
25	39.43	32.97
26	40.10	33.41
27	40.77	33.85
28	41.43	34.30
29	42.08	34.77
30	42.73	35.24
31	43.37	35.71
32	44.00	36.20
33	44.63	36.70
34	45.25	37.20
35	45.87	37.71
36	46.48	38.22
37	47.08	38.75
38	47.68	39.28
39	48.27	39.82
40	48.86	40.37
41	49.43	40.92
42	50.00	41.49

43	50.56	42.06
44	51.12	42.63
45	51.67	43.22
46	52.21	43.80
47	52.74	44.40
48	53.26	45.00
49	53.78	45.61
50	54.29	46.23
51	54.79	46.85
52	55.29	47.48
53	55.78	48.12
54	56.25	48.76
55	56.72	49.41
56	57.19	50.06
57	57.64	50.72
58	58.09	51.38
59	58.52	52.05
60	58.95	52.73
61	59.37	53.41
62	59.78	54.09
63	60.19	54.79
64	60.58	55.48
65	60.97	56.18
66	61.34	56.89
67	61.71	57.60
68	62.07	58.31
69	62.42	59.03
70	62.76	59.76
71	62.79	59.82

Circle Center At X = 5.01 ; Y = 86.49 ; and Radius = 63.63

Factor of Safety

*** 1.081 ***

Failure Surface Specified By 74 Coordinate Points

Point No.	X-Surf (m)	Y-Surf (m)
1	20.73	22.68
2	21.46	23.02
3	22.18	23.36
4	22.90	23.70
5	23.62	24.06
6	24.33	24.42
7	25.05	24.78
8	25.76	25.15
9	26.46	25.53
10	27.17	25.91
11	27.87	26.30
12	28.56	26.69
13	29.26	27.09
14	29.95	27.49
15	30.63	27.90
16	31.32	28.31
17	32.00	28.73
18	32.68	29.16
19	33.35	29.59
20	34.02	30.03
21	34.69	30.47
22	35.35	30.92
23	36.01	31.37
24	36.66	31.83
25	37.32	32.29
26	37.97	32.76
27	38.61	33.24
28	39.25	33.71
29	39.89	34.20
30	40.52	34.69
31	41.15	35.18
32	41.77	35.68
33	42.40	36.19
34	43.01	36.70
35	43.62	37.21
36	44.23	37.73
37	44.84	38.25
38	45.44	38.78
39	46.03	39.32
40	46.63	39.85

41	47.21	40.40
42	47.80	40.95
43	48.37	41.50
44	48.95	42.06
45	49.52	42.62
46	50.08	43.18
47	50.64	43.75
48	51.20	44.33
49	51.75	44.91
50	52.30	45.49
51	52.84	46.08
52	53.37	46.68
53	53.91	47.27
54	54.43	47.88
55	54.96	48.48
56	55.47	49.09
57	55.99	49.71
58	56.49	50.32
59	57.00	50.95
60	57.49	51.57
61	57.99	52.20
62	58.47	52.84
63	58.96	53.48
64	59.43	54.12
65	59.91	54.76
66	60.37	55.41
67	60.83	56.07
68	61.29	56.72
69	61.74	57.38
70	62.19	58.05
71	62.63	58.72
72	63.06	59.39
73	63.49	60.06
74	63.66	60.34

Circle Center At X = -20.59 ; Y = 113.09 ; and Radius = 99.40

Factor of Safety

*** 1.088 ***

Failure Surface Specified By 74 Coordinate Points

Point No.	X-Surf (m)	Y-Surf (m)
1	20.73	22.68
2	21.46	23.02
3	22.18	23.36
4	22.90	23.71
5	23.62	24.06
6	24.33	24.42
7	25.04	24.79
8	25.75	25.16
9	26.46	25.54
10	27.16	25.92
11	27.86	26.31
12	28.55	26.70
13	29.25	27.10
14	29.94	27.51
15	30.62	27.92
16	31.31	28.33
17	31.99	28.75
18	32.67	29.18
19	33.34	29.61
20	34.01	30.05
21	34.68	30.49
22	35.34	30.94
23	36.00	31.39
24	36.66	31.85
25	37.31	32.31
26	37.96	32.78
27	38.60	33.25
28	39.24	33.73
29	39.88	34.21
30	40.51	34.70
31	41.14	35.19
32	41.77	35.69
33	42.39	36.20
34	43.01	36.70
35	43.62	37.22

36	44.23	37.73
37	44.84	38.26
38	45.44	38.78
39	46.04	39.32
40	46.63	39.85
41	47.22	40.39
42	47.81	40.94
43	48.39	41.49
44	48.96	42.05
45	49.53	42.61
46	50.10	43.17
47	50.66	43.74
48	51.22	44.31
49	51.78	44.89
50	52.32	45.47
51	52.87	46.06
52	53.41	46.65
53	53.94	47.24
54	54.47	47.84
55	55.00	48.44
56	55.52	49.05
57	56.04	49.66
58	56.55	50.28
59	57.05	50.90
60	57.56	51.52
61	58.05	52.15
62	58.54	52.78
63	59.03	53.41
64	59.51	54.05
65	59.99	54.70
66	60.46	55.34
67	60.93	55.99
68	61.39	56.65
69	61.84	57.30
70	62.29	57.96
71	62.74	58.63
72	63.18	59.30
73	63.61	59.97
74	63.96	60.51

Circle Center At X = -21.64 ; Y = 114.71 ; and Radius = 101.32

Factor of Safety

*** 1.089 ***

Failure Surface Specified By 64 Coordinate Points

Point No.	X-Surf (m)	Y-Surf (m)
1	21.97	25.16
2	22.74	25.39
3	23.50	25.63
4	24.26	25.88
5	25.02	26.14
6	25.77	26.42
7	26.52	26.70
8	27.26	26.99
9	28.00	27.30
10	28.74	27.61
11	29.47	27.94
12	30.19	28.27
13	30.91	28.62
14	31.63	28.97
15	32.34	29.34
16	33.05	29.71
17	33.75	30.10
18	34.45	30.49
19	35.14	30.90
20	35.82	31.32
21	36.50	31.74
22	37.17	32.17
23	37.84	32.62
24	38.49	33.07
25	39.15	33.53
26	39.79	34.00
27	40.43	34.48
28	41.07	34.97
29	41.69	35.47
30	42.31	35.98

31	42.92	36.50
32	43.53	37.02
33	44.12	37.55
34	44.71	38.09
35	45.29	38.64
36	45.87	39.20
37	46.43	39.77
38	46.99	40.34
39	47.54	40.92
40	48.08	41.51
41	48.61	42.11
42	49.14	42.71
43	49.65	43.32
44	50.16	43.94
45	50.66	44.57
46	51.15	45.20
47	51.63	45.84
48	52.10	46.49
49	52.56	47.14
50	53.02	47.80
51	53.46	48.46
52	53.89	49.14
53	54.32	49.81
54	54.73	50.50
55	55.14	51.19
56	55.54	51.88
57	55.92	52.58
58	56.30	53.29
59	56.66	54.00
60	57.02	54.72
61	57.36	55.44
62	57.70	56.17
63	58.02	56.90
64	58.10	57.07

Circle Center At X = 6.09 ; Y = 79.55 ; and Radius = 56.66
Factor of Safety
*** 1.094 ***

Failure Surface Specified By 69 Coordinate Points

Point No.	X-Surf (m)	Y-Surf (m)
1	21.66	24.54
2	22.43	24.77
3	23.19	25.02
4	23.95	25.27
5	24.70	25.54
6	25.45	25.81
7	26.20	26.09
8	26.95	26.38
9	27.69	26.68
10	28.43	26.99
11	29.16	27.31
12	29.89	27.64
13	30.62	27.98
14	31.34	28.32
15	32.05	28.68
16	32.77	29.04
17	33.47	29.41
18	34.18	29.80
19	34.88	30.19
20	35.57	30.58
21	36.26	30.99
22	36.94	31.41
23	37.62	31.83
24	38.29	32.27
25	38.96	32.71
26	39.62	33.16
27	40.28	33.61
28	40.93	34.08
29	41.57	34.55
30	42.21	35.04
31	42.84	35.53
32	43.47	36.02
33	44.09	36.53
34	44.70	37.04
35	45.31	37.56

36	45.91	38.09
37	46.50	38.63
38	47.09	39.17
39	47.67	39.72
40	48.25	40.28
41	48.81	40.84
42	49.37	41.42
43	49.92	41.99
44	50.47	42.58
45	51.01	43.17
46	51.54	43.77
47	52.06	44.38
48	52.58	44.99
49	53.08	45.61
50	53.58	46.23
51	54.08	46.86
52	54.56	47.50
53	55.04	48.14
54	55.51	48.79
55	55.97	49.44
56	56.42	50.10
57	56.86	50.77
58	57.30	51.44
59	57.72	52.12
60	58.14	52.80
61	58.55	53.49
62	58.95	54.18
63	59.35	54.87
64	59.73	55.58
65	60.11	56.28
66	60.47	56.99
67	60.83	57.71
68	61.18	58.43
69	61.47	59.05

Circle Center At X = 3.19 ; Y = 86.07 ; and Radius = 64.24

Factor of Safety
*** 1.095 ***

Failure Surface Specified By 69 Coordinate Points

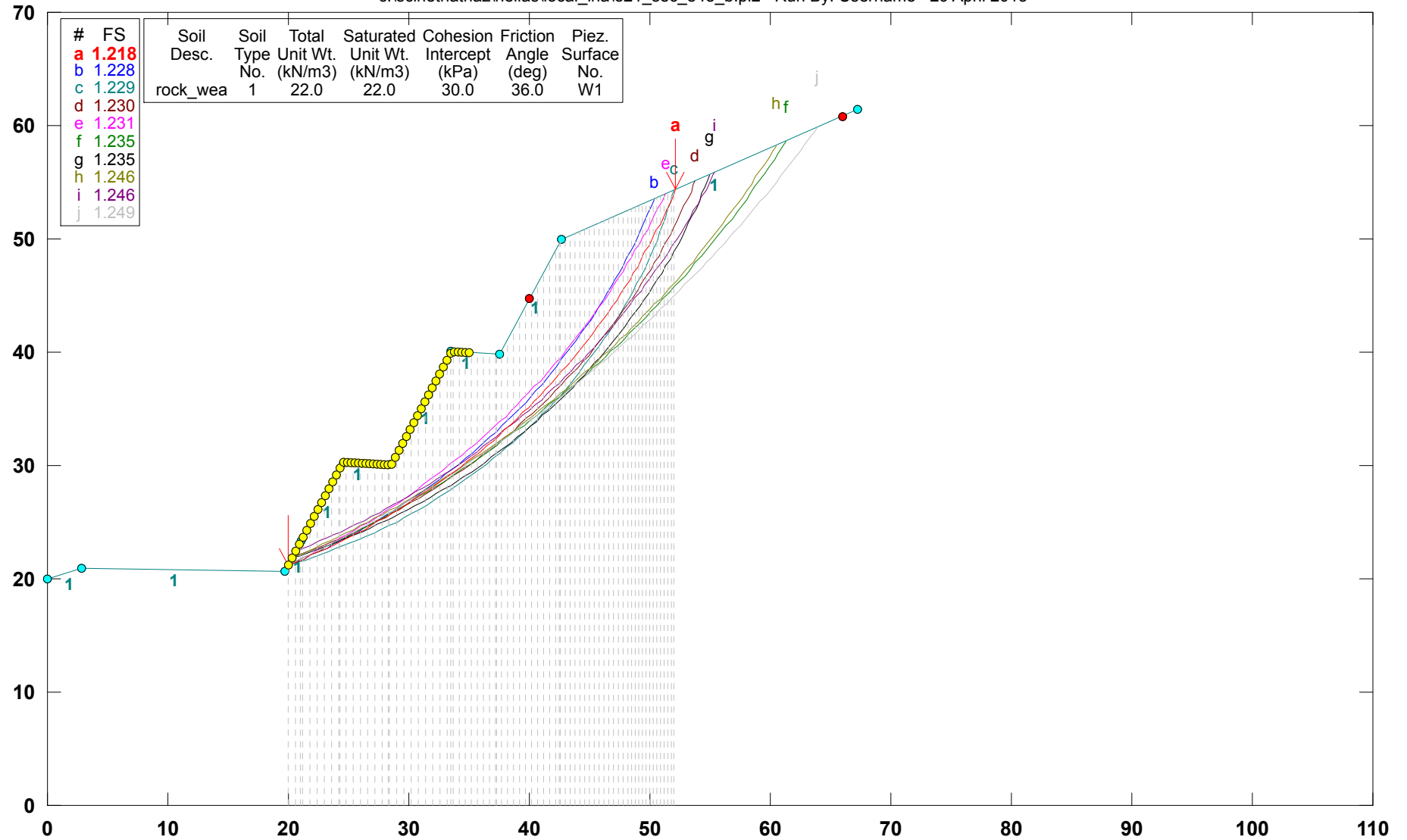
Point No.	X-Surf (m)	Y-Surf (m)
1	22.59	26.40
2	23.37	26.59
3	24.14	26.80
4	24.91	27.01
5	25.68	27.24
6	26.44	27.48
7	27.20	27.72
8	27.96	27.98
9	28.72	28.25
10	29.47	28.53
11	30.21	28.82
12	30.95	29.11
13	31.69	29.42
14	32.43	29.74
15	33.16	30.07
16	33.88	30.41
17	34.60	30.75
18	35.32	31.11
19	36.03	31.48
20	36.73	31.86
21	37.43	32.24
22	38.13	32.64
23	38.82	33.04
24	39.50	33.46
25	40.18	33.88
26	40.85	34.31
27	41.52	34.76
28	42.18	35.21
29	42.84	35.67
30	43.48	36.14
31	44.13	36.61
32	44.76	37.10
33	45.39	37.60
34	46.01	38.10
35	46.63	38.61

36	47.23	39.13
37	47.83	39.66
38	48.43	40.20
39	49.01	40.74
40	49.59	41.29
41	50.16	41.85
42	50.73	42.42
43	51.28	43.00
44	51.83	43.58
45	52.37	44.17
46	52.90	44.77
47	53.43	45.37
48	53.94	45.99
49	54.45	46.60
50	54.95	47.23
51	55.44	47.86
52	55.92	48.50
53	56.39	49.15
54	56.85	49.80
55	57.31	50.46
56	57.75	51.12
57	58.19	51.79
58	58.62	52.47
59	59.04	53.15
60	59.45	53.84
61	59.85	54.53
62	60.24	55.23
63	60.62	55.93
64	60.99	56.64
65	61.35	57.35
66	61.70	58.07
67	62.04	58.80
68	62.38	59.52
69	62.41	59.60

Circle Center At X = 8.64 ; Y = 83.61 ; and Radius = 58.89
Factor of Safety
*** 1.104 ***
**** END OF GSTABL7 OUTPUT ****

Hellas_Local_Landslide_Hazard Cut slope O21_sec_848_B

c:\scinetnathaz\hellas\local_lha\o21_sec_848_b.pl2 Run By: Username 29 April 2015



GSTABL7 v.2 FSmin=1.218

Safety Factors Are Calculated By The Modified Bishop Method



*** GSTABL7 ***

** GSTABL7 by Garry H. Gregory, P.E. **

** Original Version 1.0, January 1996; Current Version 2.003, June 2002 **

(All Rights Reserved-Unauthorized Use Prohibited)

SLOPE STABILITY ANALYSIS SYSTEM

Modified Bishop, Simplified Janbu, or GLE Method of Slices.

(Includes Spencer & Morgenstern-Price Type Analysis)

Including Pier/Pile, Reinforcement, Soil Nail, Tieback,

Nonlinear Undrained Shear Strength, Curved Phi Envelope,

Anisotropic Soil, Fiber-Reinforced Soil, Boundary Loads, Water

Surfaces, Pseudo-Static & Newmark Earthquake, and Applied Forces.

Analysis Run Date: 29 April 2015

Time of Run:

Run By: Username

Input Data Filename: C:\SciNetNatHaz\Hellas\Local_LHA\O21_sec_848_b.in

Output Filename: C:\SciNetNatHaz\Hellas\Local_LHA\O21_sec_848_b.OUT

Unit System: SI

Plotted Output Filename: C:\SciNetNatHaz\Hellas\Local_LHA_sec_848_b.PLT

PROBLEM DESCRIPTION: Hellas_Local_Landslide_Hazard

Cut slope O21_sec_848_B

BOUNDARY COORDINATES

9 Top Boundaries

9 Total Boundaries

Boundary No.	X-Left (m)	Y-Left (m)	X-Right (m)	Y-Right (m)	Soil Type Below Bnd
1	0.00	20.00	2.80	20.93	1
2	2.80	20.93	19.72	20.66	1
3	19.72	20.66	21.09	23.40	1
4	21.09	23.40	24.54	30.29	1
5	24.54	30.29	28.54	30.05	1
6	28.54	30.05	33.54	40.05	1
7	33.54	40.05	37.54	39.81	1

8	37.54	39.81	42.60	49.94	1
9	42.60	49.94	67.26	61.37	1

Default Y-Origin = 0.00(m)
 Default X-Plus Value = 0.00(m)
 Default Y-Plus Value = 0.00(m)

ISOTROPIC SOIL PARAMETERS

1 Type(s) of Soil

Soil Type No.	Total Unit Wt. (kN/m3)	Saturated Unit Wt. (kN/m3)	Cohesion Intercept (kPa)	Friction Angle (deg)	Pore Pressure Param.	Pressure Constant (kPa)	Piez. Surface No.
1	22.0	22.0	30.0	36.0	0.00	0.0	1

SOIL NAIL LOAD(S)

16 SOIL NAIL LOAD(S) SPECIFIED

Nail No.	X-Pos (m)	Y-Pos (m)	Nail Dia (mm)	Tendon Dia (mm)	Spacing (m)	Inclin. (deg)	Length (m)
1	20.68	22.58	89.0	22.0	2.00	15.00	12.00
2	21.59	24.40	89.0	22.0	2.00	15.00	12.00
3	22.50	26.22	89.0	22.0	2.00	15.00	12.00
4	23.42	28.05	89.0	22.0	2.00	15.00	12.00
5	24.33	29.87	89.0	22.0	2.00	15.00	12.00
6	28.88	30.73	89.0	22.0	2.00	15.00	12.00
7	29.79	32.55	89.0	22.0	2.00	15.00	12.00
8	30.70	34.37	89.0	22.0	2.00	15.00	12.00
9	31.62	36.21	89.0	22.0	2.00	15.00	12.00
10	32.53	38.03	89.0	22.0	2.00	15.00	12.00
11	33.44	39.85	89.0	22.0	2.00	15.00	12.00
12	37.99	40.71	89.0	22.0	2.00	15.00	12.00
13	38.90	42.53	89.0	22.0	2.00	15.00	12.00
14	39.81	44.35	89.0	22.0	2.00	15.00	12.00
15	40.72	46.18	89.0	22.0	2.00	15.00	12.00
16	41.64	48.02	89.0	22.0	2.00	15.00	12.00

SOIL NAIL LOAD DATA

Soil Nail No. 1 3 Load Points Apply to This Nail

Load Diagram Type = 2

POINT NO.	X-COORD.(m)	Y-COORD.(m)	FORCE(kN)
1	20.68	22.58	82.64
2	28.32	20.60	82.64
3	32.27	19.47	0.00

Allowable Pullout Stress = 200.0(kPa)

Allowable Tendon Stress = 434782.6

Allowable Nail Head Load = 210.0(kN)

Soil Nail No. 2 3 Load Points Apply to This Nail

Load Diagram Type = 2

POINT NO.	X-COORD.(m)	Y-COORD.(m)	FORCE(kN)
1	21.59	24.40	82.64
2	29.20	22.43	82.64
3	33.18	21.29	0.00

Allowable Pullout Stress = 200.0(kPa)

Allowable Tendon Stress = 434782.6

Allowable Nail Head Load = 210.0(kN)

Soil Nail No. 3 3 Load Points Apply to This Nail

Load Diagram Type = 2

POINT NO.	X-COORD.(m)	Y-COORD.(m)	FORCE(kN)
1	22.50	26.22	82.64
2	30.07	24.26	82.64
3	34.09	23.11	0.00

Allowable Pullout Stress = 200.0(kPa)

Allowable Tendon Stress = 434782.6

Allowable Nail Head Load = 210.0(kN)

Soil Nail No. 4 3 Load Points Apply to This Nail

Load Diagram Type = 2

POINT NO.	X-COORD.(m)	Y-COORD.(m)	FORCE(kN)
1	23.42	28.05	82.64
2	30.96	26.10	82.64
3	35.01	24.95	0.00

Allowable Pullout Stress = 200.0(kPa)

Allowable Tendon Stress = 434782.6

Allowable Nail Head Load = 210.0(kN)

Soil Nail No. 5 3 Load Points Apply to This Nail

Load Diagram Type = 2

POINT NO.	X-COORD.(m)	Y-COORD.(m)	FORCE(kN)
1	24.33	29.87	82.64
2	31.84	27.93	82.64
3	35.92	26.76	0.00

Allowable Pullout Stress = 200.0(kPa)

Allowable Tendon Stress = 434782.6
 Allowable Nail Head Load = 210.0(kN)
 Soil Nail No. 6 3 Load Points Apply to This Nail
 Load Diagram Type = 2

POINT NO.	X-COORD.(m)	Y-COORD.(m)	FORCE(kN)
1	28.88	30.73	82.64
2	36.24	28.83	82.64
3	40.47	27.62	0.00

 Allowable Pullout Stress = 200.0(kPa)
 Allowable Tendon Stress = 434782.6
 Allowable Nail Head Load = 210.0(kN)
 Soil Nail No. 7 3 Load Points Apply to This Nail
 Load Diagram Type = 2

POINT NO.	X-COORD.(m)	Y-COORD.(m)	FORCE(kN)
1	29.79	32.55	82.64
2	37.12	30.65	82.64
3	41.38	29.44	0.00

 Allowable Pullout Stress = 200.0(kPa)
 Allowable Tendon Stress = 434782.6
 Allowable Nail Head Load = 210.0(kN)
 Soil Nail No. 8 3 Load Points Apply to This Nail
 Load Diagram Type = 2

POINT NO.	X-COORD.(m)	Y-COORD.(m)	FORCE(kN)
1	30.70	34.37	82.64
2	38.00	32.48	82.64
3	42.29	31.26	0.00

 Allowable Pullout Stress = 200.0(kPa)
 Allowable Tendon Stress = 434782.6
 Allowable Nail Head Load = 210.0(kN)
 Soil Nail No. 9 3 Load Points Apply to This Nail
 Load Diagram Type = 2

POINT NO.	X-COORD.(m)	Y-COORD.(m)	FORCE(kN)
1	31.62	36.21	82.64
2	38.88	34.33	82.64
3	43.21	33.10	0.00

 Allowable Pullout Stress = 200.0(kPa)
 Allowable Tendon Stress = 434782.6
 Allowable Nail Head Load = 210.0(kN)
 Soil Nail No. 10 3 Load Points Apply to This Nail
 Load Diagram Type = 2

POINT NO.	X-COORD.(m)	Y-COORD.(m)	FORCE(kN)
1	32.53	38.03	82.64
2	39.76	36.16	82.64
3	44.12	34.92	0.00

 Allowable Pullout Stress = 200.0(kPa)
 Allowable Tendon Stress = 434782.6
 Allowable Nail Head Load = 210.0(kN)
 Soil Nail No. 11 3 Load Points Apply to This Nail
 Load Diagram Type = 2

POINT NO.	X-COORD.(m)	Y-COORD.(m)	FORCE(kN)
1	33.44	39.85	82.64
2	40.64	37.99	82.64
3	45.03	36.74	0.00

 Allowable Pullout Stress = 200.0(kPa)
 Allowable Tendon Stress = 434782.6
 Allowable Nail Head Load = 210.0(kN)
 Soil Nail No. 12 3 Load Points Apply to This Nail
 Load Diagram Type = 2

POINT NO.	X-COORD.(m)	Y-COORD.(m)	FORCE(kN)
1	37.99	40.71	82.64
2	45.04	38.89	82.64
3	49.58	37.61	0.00

 Allowable Pullout Stress = 200.0(kPa)
 Allowable Tendon Stress = 434782.6
 Allowable Nail Head Load = 210.0(kN)
 Soil Nail No. 13 3 Load Points Apply to This Nail
 Load Diagram Type = 2

POINT NO.	X-COORD.(m)	Y-COORD.(m)	FORCE(kN)
1	38.90	42.53	82.64
2	45.92	40.72	82.64
3	50.49	39.43	0.00

 Allowable Pullout Stress = 200.0(kPa)
 Allowable Tendon Stress = 434782.6
 Allowable Nail Head Load = 210.0(kN)
 Soil Nail No. 14 3 Load Points Apply to This Nail

Load Diagram Type = 2
 POINT NO. X-COORD.(m) Y-COORD.(m) FORCE(kN)
 1 39.81 44.35 82.64
 2 46.79 42.55 82.64
 3 51.40 41.25 0.00

Allowable Pullout Stress = 200.0(kPa)
 Allowable Tendon Stress = 434782.6
 Allowable Nail Head Load = 210.0(kN)
 Soil Nail No. 15 3 Load Points Apply to This Nail
 Load Diagram Type = 2

POINT NO. X-COORD.(m) Y-COORD.(m) FORCE(kN)
 1 40.72 46.18 82.64
 2 47.67 44.38 82.64
 3 52.31 43.07 0.00

Allowable Pullout Stress = 200.0(kPa)
 Allowable Tendon Stress = 434782.6
 Allowable Nail Head Load = 210.0(kN)
 Soil Nail No. 16 3 Load Points Apply to This Nail
 Load Diagram Type = 2

POINT NO. X-COORD.(m) Y-COORD.(m) FORCE(kN)
 1 41.64 48.02 82.64
 2 48.56 46.23 82.64
 3 53.23 44.91 0.00

Allowable Pullout Stress = 200.0(kPa)
 Allowable Tendon Stress = 434782.6
 Allowable Nail Head Load = 210.0(kN)

NOTE - An Equivalent Line Load Is Calculated For Each Row Of Soil Nails
 Assuming A Uniform Distribution Of Load Horizontally Between
 Individual Nails.

SOIL NAIL LOAD DATA HAS BEEN SUPPRESSED

A Critical Failure Surface Searching Method, Using A Random
 Technique For Generating Circular Surfaces, Has Been Specified.
 2500 Trial Surfaces Have Been Generated.

50 Surface(s) Initiate(s) From Each Of 50 Points Equally Spaced

Along The Ground Surface Between X = 20.00(m)
 and X = 35.00(m)

Each Surface Terminates Between X = 40.00(m)
 and X = 66.00(m)

Unless Further Limitations Were Imposed, The Minimum Elevation
 At Which A Surface Extends Is Y = 0.00(m)

0.70(m) Line Segments Define Each Trial Failure Surface.
 Following Are Displayed The Ten Most Critical Of The Trial

Failure Surfaces Evaluated. They Are
 Ordered - Most Critical First.

* * Safety Factors Are Calculated By The Modified Bishop Method * *

Total Number of Trial Surfaces Evaluated = 2500

Statistical Data On All Valid FS Values:

FS Max = 3.186 FS Min = 1.218 FS Ave = 1.751

Standard Deviation = 0.252 Coefficient of Variation = 14.38 %

Failure Surface Specified By 69 Coordinate Points

Point No.	X-Surf (m)	Y-Surf (m)
1	20.00	21.22
2	20.64	21.50
3	21.28	21.78
4	21.92	22.08
5	22.55	22.38
6	23.18	22.69
7	23.80	23.00
8	24.42	23.33
9	25.04	23.66
10	25.65	24.00
11	26.26	24.34
12	26.87	24.69
13	27.47	25.05
14	28.06	25.42
15	28.66	25.79
16	29.24	26.17
17	29.83	26.56
18	30.41	26.95
19	30.98	27.35
20	31.55	27.76
21	32.11	28.17
22	32.67	28.59
23	33.23	29.02

24	33.78	29.45
25	34.32	29.89
26	34.86	30.34
27	35.40	30.79
28	35.92	31.25
29	36.45	31.72
30	36.97	32.19
31	37.48	32.67
32	37.98	33.15
33	38.48	33.64
34	38.98	34.13
35	39.47	34.63
36	39.95	35.14
37	40.43	35.65
38	40.90	36.17
39	41.37	36.69
40	41.82	37.22
41	42.28	37.76
42	42.72	38.29
43	43.16	38.84
44	43.60	39.39
45	44.02	39.94
46	44.45	40.50
47	44.86	41.07
48	45.27	41.64
49	45.67	42.21
50	46.06	42.79
51	46.45	43.37
52	46.83	43.96
53	47.20	44.55
54	47.57	45.15
55	47.93	45.75
56	48.28	46.35
57	48.62	46.96
58	48.96	47.58
59	49.29	48.19
60	49.62	48.81
61	49.93	49.44
62	50.24	50.07
63	50.54	50.70
64	50.84	51.33
65	51.12	51.97
66	51.40	52.62
67	51.67	53.26
68	51.94	53.91
69	52.11	54.35

Circle Center At X = -3.42 ; Y = 76.04 ; and Radius = 59.61

Factor of Safety
*** 1.218 ***

Individual data on the 74 slices

Slice No.	Width (m)	Weight (kN)	Water Force		Tie Force Norm (kN)	Tie Force Tan (kN)	Earthquake Force		Surcharge Load (kN)
			Top (kN)	Bot (kN)			Hor (kN)	Ver (kN)	
1	0.6	7.1	0.0	0.0	0.	0.	0.0	0.0	0.0
2	0.4	13.3	0.0	0.0	0.	0.	0.0	0.0	0.0
3	0.2	7.8	0.0	0.0	0.	0.	0.0	0.0	0.0
4	0.6	34.7	0.0	0.0	0.	0.	0.0	0.0	0.0
5	0.6	48.0	0.0	0.0	0.	0.	0.0	0.0	0.0
6	0.6	60.9	0.0	0.0	0.	0.	0.0	0.0	0.0
7	0.6	73.4	0.0	0.0	0.	0.	0.0	0.0	0.0
8	0.6	85.6	0.0	0.0	0.	0.	0.0	0.0	0.0
9	0.1	17.7	0.0	0.0	0.	0.	0.0	0.0	0.0
10	0.5	74.1	0.0	0.0	0.	0.	0.0	0.0	0.0
11	0.6	86.5	0.0	0.0	0.	0.	0.0	0.0	0.0
12	0.6	80.9	0.0	0.0	0.	0.	0.0	0.0	0.0
13	0.6	75.2	0.0	0.0	0.	0.	0.0	0.0	0.0
14	0.6	69.5	0.0	0.0	0.	0.	0.0	0.0	0.0
15	0.6	63.8	0.0	0.0	0.	0.	0.0	0.0	0.0
16	0.5	47.1	0.0	0.0	0.	0.	0.0	0.0	0.0
17	0.1	11.3	0.0	0.0	0.	0.	0.0	0.0	0.0
18	0.6	63.2	0.0	0.0	0.	0.	0.0	0.0	0.0
19	0.6	72.8	0.0	0.0	0.	0.	0.0	0.0	0.0
20	0.6	82.1	0.0	0.0	0.	0.	0.0	0.0	0.0
21	0.6	91.0	0.0	0.0	0.	0.	0.0	0.0	0.0

22	0.6	99.5	0.0	0.0	0.	0.	0.0	0.0	0.0
23	0.6	107.6	0.0	0.0	0.	0.	0.0	0.0	0.0
24	0.6	115.4	0.0	0.0	0.	0.	0.0	0.0	0.0
25	0.6	122.8	0.0	0.0	0.	0.	0.0	0.0	0.0
26	0.3	72.6	0.0	0.0	0.	0.	0.0	0.0	0.0
27	0.2	55.9	0.0	0.0	0.	0.	0.0	0.0	0.0
28	0.5	123.9	0.0	0.0	0.	0.	0.0	0.0	0.0
29	0.5	117.1	0.0	0.0	0.	0.	0.0	0.0	0.0
30	0.5	110.3	0.0	0.0	0.	0.	0.0	0.0	0.0
31	0.5	103.5	0.0	0.0	0.	0.	0.0	0.0	0.0
32	0.5	96.8	0.0	0.0	0.	0.	0.0	0.0	0.0
33	0.5	90.1	0.0	0.0	0.	0.	0.0	0.0	0.0
34	0.5	83.4	0.0	0.0	0.	0.	0.0	0.0	0.0
35	0.1	9.8	0.0	0.0	0.	0.	0.0	0.0	0.0
36	0.4	71.4	0.0	0.0	0.	0.	0.0	0.0	0.0
37	0.5	86.0	0.0	0.0	0.	0.	0.0	0.0	0.0
38	0.5	90.5	0.0	0.0	0.	0.	0.0	0.0	0.0
39	0.5	94.7	0.0	0.0	0.	0.	0.0	0.0	0.0
40	0.5	98.5	0.0	0.0	0.	0.	0.0	0.0	0.0
41	0.5	102.1	0.0	0.0	0.	0.	0.0	0.0	0.0
42	0.5	105.3	0.0	0.0	0.	0.	0.0	0.0	0.0
43	0.5	108.2	0.0	0.0	0.	0.	0.0	0.0	0.0
44	0.5	110.8	0.0	0.0	0.	0.	0.0	0.0	0.0
45	0.5	113.1	0.0	0.0	0.	0.	0.0	0.0	0.0
46	0.3	82.8	0.0	0.0	0.	0.	0.0	0.0	0.0
47	0.1	32.0	0.0	0.0	0.	0.	0.0	0.0	0.0
48	0.4	111.6	0.0	0.0	0.	0.	0.0	0.0	0.0
49	0.4	106.7	0.0	0.0	0.	0.	0.0	0.0	0.0
50	0.4	101.8	0.0	0.0	0.	0.	0.0	0.0	0.0
51	0.4	96.9	0.0	0.0	0.	0.	0.0	0.0	0.0
52	0.4	92.1	0.0	0.0	0.	0.	0.0	0.0	0.0
53	0.4	87.2	0.0	0.0	0.	0.	0.0	0.0	0.0
54	0.4	82.4	0.0	0.0	0.	0.	0.0	0.0	0.0
55	0.4	77.6	0.0	0.0	0.	0.	0.0	0.0	0.0
56	0.4	72.8	0.0	0.0	0.	0.	0.0	0.0	0.0
57	0.4	68.1	0.0	0.0	0.	0.	0.0	0.0	0.0
58	0.4	63.5	0.0	0.0	0.	0.	0.0	0.0	0.0
59	0.4	58.9	0.0	0.0	0.	0.	0.0	0.0	0.0
60	0.4	54.3	0.0	0.0	0.	0.	0.0	0.0	0.0
61	0.4	49.9	0.0	0.0	0.	0.	0.0	0.0	0.0
62	0.3	45.5	0.0	0.0	0.	0.	0.0	0.0	0.0
63	0.3	41.2	0.0	0.0	0.	0.	0.0	0.0	0.0
64	0.3	37.0	0.0	0.0	0.	0.	0.0	0.0	0.0
65	0.3	32.8	0.0	0.0	0.	0.	0.0	0.0	0.0
66	0.3	28.8	0.0	0.0	0.	0.	0.0	0.0	0.0
67	0.3	24.8	0.0	0.0	0.	0.	0.0	0.0	0.0
68	0.3	21.0	0.0	0.0	0.	0.	0.0	0.0	0.0
69	0.3	17.3	0.0	0.0	0.	0.	0.0	0.0	0.0
70	0.3	13.7	0.0	0.0	0.	0.	0.0	0.0	0.0
71	0.3	10.2	0.0	0.0	0.	0.	0.0	0.0	0.0
72	0.3	6.8	0.0	0.0	0.	0.	0.0	0.0	0.0
73	0.3	3.6	0.0	0.0	0.	0.	0.0	0.0	0.0
74	0.2	0.7	0.0	0.0	0.	0.	0.0	0.0	0.0

Failure Surface Specified By 67 Coordinate Points

Point No.	X-Surf (m)	Y-Surf (m)
1	20.00	21.22
2	20.64	21.51
3	21.28	21.80
4	21.91	22.10
5	22.54	22.41
6	23.16	22.72
7	23.78	23.05
8	24.40	23.38
9	25.01	23.72
10	25.62	24.07
11	26.22	24.42
12	26.82	24.78
13	27.41	25.15
14	28.00	25.53
15	28.59	25.91
16	29.17	26.30
17	29.74	26.70
18	30.32	27.11
19	30.88	27.52

20	31.44	27.94
21	32.00	28.37
22	32.55	28.80
23	33.09	29.24
24	33.63	29.69
25	34.16	30.14
26	34.69	30.60
27	35.21	31.07
28	35.73	31.54
29	36.24	32.02
30	36.74	32.51
31	37.24	33.00
32	37.73	33.50
33	38.22	34.00
34	38.70	34.51
35	39.17	35.03
36	39.63	35.55
37	40.09	36.08
38	40.55	36.61
39	40.99	37.15
40	41.43	37.69
41	41.87	38.24
42	42.29	38.80
43	42.71	39.36
44	43.13	39.93
45	43.53	40.50
46	43.93	41.07
47	44.32	41.65
48	44.70	42.24
49	45.08	42.83
50	45.45	43.42
51	45.81	44.02
52	46.17	44.63
53	46.51	45.23
54	46.85	45.85
55	47.18	46.46
56	47.51	47.08
57	47.82	47.71
58	48.13	48.34
59	48.43	48.97
60	48.72	49.61
61	49.01	50.24
62	49.28	50.89
63	49.55	51.53
64	49.81	52.18
65	50.07	52.84
66	50.31	53.49
67	50.32	53.52

Circle Center At X = -2.64 ; Y = 72.85 ; and Radius = 56.37

Factor of Safety

*** 1.228 ***

Failure Surface Specified By 70 Coordinate Points

Point No.	X-Surf (m)	Y-Surf (m)
1	20.00	21.22
2	20.67	21.43
3	21.33	21.65
4	21.99	21.88
5	22.65	22.12
6	23.31	22.37
7	23.96	22.63
8	24.60	22.90
9	25.24	23.17
10	25.88	23.46
11	26.52	23.76
12	27.15	24.06
13	27.77	24.38
14	28.39	24.70
15	29.01	25.04
16	29.62	25.38
17	30.22	25.73
18	30.82	26.09
19	31.42	26.46
20	32.01	26.84
21	32.59	27.22

22	33.17	27.62
23	33.74	28.02
24	34.31	28.43
25	34.87	28.85
26	35.42	29.28
27	35.97	29.72
28	36.51	30.16
29	37.05	30.61
30	37.58	31.07
31	38.10	31.54
32	38.61	32.01
33	39.12	32.50
34	39.62	32.99
35	40.11	33.48
36	40.60	33.99
37	41.07	34.50
38	41.54	35.02
39	42.01	35.54
40	42.46	36.07
41	42.91	36.61
42	43.35	37.16
43	43.78	37.71
44	44.20	38.27
45	44.62	38.83
46	45.02	39.40
47	45.42	39.98
48	45.81	40.56
49	46.19	41.14
50	46.57	41.74
51	46.93	42.34
52	47.28	42.94
53	47.63	43.55
54	47.97	44.16
55	48.29	44.78
56	48.61	45.40
57	48.92	46.03
58	49.22	46.66
59	49.51	47.30
60	49.80	47.94
61	50.07	48.58
62	50.33	49.23
63	50.58	49.89
64	50.83	50.54
65	51.06	51.20
66	51.29	51.87
67	51.50	52.53
68	51.70	53.20
69	51.90	53.87
70	52.02	54.31

Circle Center At X = 6.00 ; Y = 66.80 ; and Radius = 47.69

Factor of Safety

*** 1.229 ***

Failure Surface Specified By 71 Coordinate Points

Point No.	X-Surf (m)	Y-Surf (m)
1	20.31	21.83
2	20.96	22.09
3	21.61	22.35
4	22.25	22.62
5	22.90	22.89
6	23.54	23.18
7	24.17	23.47
8	24.80	23.77
9	25.43	24.08
10	26.06	24.40
11	26.68	24.72
12	27.30	25.05
13	27.91	25.39
14	28.52	25.73
15	29.12	26.08
16	29.72	26.44
17	30.32	26.81
18	30.91	27.18
19	31.50	27.56
20	32.08	27.95

21	32.66	28.35
22	33.23	28.75
23	33.80	29.16
24	34.36	29.57
25	34.92	30.00
26	35.48	30.43
27	36.02	30.86
28	36.57	31.30
29	37.10	31.75
30	37.63	32.21
31	38.16	32.67
32	38.68	33.14
33	39.20	33.61
34	39.71	34.09
35	40.21	34.58
36	40.71	35.07
37	41.20	35.57
38	41.68	36.07
39	42.16	36.58
40	42.64	37.10
41	43.10	37.62
42	43.56	38.15
43	44.02	38.68
44	44.47	39.22
45	44.91	39.76
46	45.34	40.31
47	45.77	40.86
48	46.19	41.42
49	46.61	41.99
50	47.02	42.55
51	47.42	43.13
52	47.81	43.71
53	48.20	44.29
54	48.58	44.88
55	48.95	45.47
56	49.32	46.07
57	49.68	46.67
58	50.03	47.27
59	50.37	47.88
60	50.71	48.50
61	51.04	49.11
62	51.36	49.74
63	51.67	50.36
64	51.98	50.99
65	52.28	51.62
66	52.57	52.26
67	52.85	52.90
68	53.13	53.54
69	53.40	54.19
70	53.66	54.84
71	53.77	55.12

Circle Center At X = -0.46 ; Y = 76.17 ; and Radius = 58.16

Factor of Safety

*** 1.230 ***

Failure Surface Specified By 67 Coordinate Points

Point No.	X-Surf (m)	Y-Surf (m)
1	20.00	21.22
2	20.62	21.54
3	21.25	21.86
4	21.86	22.19
5	22.48	22.52
6	23.09	22.86
7	23.70	23.21
8	24.30	23.57
9	24.90	23.93
10	25.50	24.29
11	26.09	24.67
12	26.68	25.04
13	27.26	25.43
14	27.84	25.82
15	28.42	26.22
16	28.99	26.62
17	29.56	27.03
18	30.12	27.45

19	30.68	27.87
20	31.24	28.30
21	31.79	28.73
22	32.33	29.17
23	32.87	29.61
24	33.41	30.06
25	33.94	30.52
26	34.47	30.98
27	34.99	31.45
28	35.50	31.92
29	36.02	32.40
30	36.52	32.88
31	37.02	33.37
32	37.52	33.86
33	38.01	34.36
34	38.50	34.86
35	38.98	35.37
36	39.45	35.89
37	39.92	36.40
38	40.39	36.93
39	40.85	37.46
40	41.30	37.99
41	41.75	38.53
42	42.19	39.07
43	42.63	39.62
44	43.06	40.17
45	43.48	40.73
46	43.90	41.29
47	44.32	41.85
48	44.72	42.42
49	45.12	42.99
50	45.52	43.57
51	45.91	44.15
52	46.29	44.74
53	46.67	45.33
54	47.04	45.92
55	47.40	46.52
56	47.76	47.12
57	48.11	47.73
58	48.46	48.34
59	48.80	48.95
60	49.13	49.57
61	49.45	50.19
62	49.77	50.81
63	50.09	51.43
64	50.39	52.06
65	50.69	52.70
66	50.99	53.33
67	51.27	53.96

Circle Center At X = -9.78 ; Y = 80.96 ; and Radius = 66.75

Factor of Safety

*** 1.231 ***

Failure Surface Specified By 82 Coordinate Points

Point No.	X-Surf (m)	Y-Surf (m)
1	20.00	21.22
2	20.63	21.52
3	21.26	21.83
4	21.89	22.14
5	22.51	22.46
6	23.13	22.78
7	23.75	23.10
8	24.37	23.43
9	24.99	23.77
10	25.60	24.11
11	26.21	24.45
12	26.82	24.80
13	27.42	25.15
14	28.02	25.50
15	28.62	25.86
16	29.22	26.23
17	29.82	26.60
18	30.41	26.97
19	31.00	27.35
20	31.59	27.73

21	32.17	28.12
22	32.75	28.51
23	33.33	28.90
24	33.90	29.30
25	34.48	29.70
26	35.05	30.11
27	35.61	30.52
28	36.18	30.94
29	36.74	31.36
30	37.29	31.78
31	37.85	32.21
32	38.40	32.64
33	38.95	33.07
34	39.49	33.51
35	40.03	33.96
36	40.57	34.40
37	41.11	34.86
38	41.64	35.31
39	42.17	35.77
40	42.69	36.23
41	43.22	36.70
42	43.73	37.17
43	44.25	37.64
44	44.76	38.12
45	45.27	38.60
46	45.77	39.09
47	46.28	39.57
48	46.77	40.07
49	47.27	40.56
50	47.76	41.06
51	48.25	41.56
52	48.73	42.07
53	49.21	42.58
54	49.68	43.09
55	50.16	43.61
56	50.63	44.13
57	51.09	44.65
58	51.55	45.18
59	52.01	45.71
60	52.46	46.24
61	52.91	46.78
62	53.36	47.32
63	53.80	47.86
64	54.23	48.41
65	54.67	48.96
66	55.10	49.51
67	55.52	50.07
68	55.94	50.63
69	56.36	51.19
70	56.78	51.75
71	57.19	52.32
72	57.59	52.89
73	57.99	53.47
74	58.39	54.04
75	58.78	54.62
76	59.17	55.21
77	59.55	55.79
78	59.93	56.38
79	60.31	56.97
80	60.68	57.56
81	61.05	58.16
82	61.33	58.62

Circle Center At X = -21.48 ; Y = 108.59 ; and Radius = 96.72

Factor of Safety
*** 1.235 ***

Failure Surface Specified By 73 Coordinate Points

Point No.	X-Surf (m)	Y-Surf (m)
1	20.31	21.83
2	20.97	22.06
3	21.63	22.29
4	22.28	22.54
5	22.94	22.79
6	23.59	23.05
7	24.23	23.32

8	24.88	23.59
9	25.52	23.88
10	26.15	24.17
11	26.79	24.47
12	27.41	24.78
13	28.04	25.09
14	28.66	25.41
15	29.28	25.75
16	29.89	26.09
17	30.50	26.43
18	31.10	26.79
19	31.70	27.15
20	32.30	27.52
21	32.89	27.89
22	33.47	28.28
23	34.05	28.67
24	34.63	29.07
25	35.20	29.47
26	35.76	29.89
27	36.32	30.31
28	36.88	30.73
29	37.43	31.17
30	37.97	31.61
31	38.51	32.06
32	39.04	32.51
33	39.57	32.97
34	40.09	33.44
35	40.60	33.91
36	41.11	34.39
37	41.61	34.88
38	42.11	35.37
39	42.60	35.87
40	43.09	36.38
41	43.56	36.89
42	44.04	37.41
43	44.50	37.93
44	44.96	38.46
45	45.41	39.00
46	45.85	39.54
47	46.29	40.08
48	46.72	40.63
49	47.15	41.19
50	47.57	41.75
51	47.98	42.32
52	48.38	42.89
53	48.77	43.47
54	49.16	44.05
55	49.54	44.64
56	49.92	45.23
57	50.28	45.83
58	50.64	46.43
59	50.99	47.03
60	51.34	47.64
61	51.67	48.26
62	52.00	48.88
63	52.32	49.50
64	52.63	50.13
65	52.94	50.76
66	53.23	51.39
67	53.52	52.03
68	53.80	52.67
69	54.08	53.31
70	54.34	53.96
71	54.60	54.61
72	54.85	55.27
73	55.00	55.69

Circle Center At X = 2.58 ; Y = 74.70 ; and Radius = 55.77

Factor of Safety

*** 1.235 ***

Failure Surface Specified By 80 Coordinate Points

Point No.	X-Surf (m)	Y-Surf (m)
1	20.31	21.83
2	20.94	22.13
3	21.58	22.42

4	22.21	22.73
5	22.83	23.03
6	23.46	23.35
7	24.08	23.67
8	24.71	23.99
9	25.32	24.32
10	25.94	24.65
11	26.55	24.99
12	27.16	25.33
13	27.77	25.67
14	28.38	26.03
15	28.98	26.38
16	29.58	26.74
17	30.18	27.11
18	30.77	27.48
19	31.36	27.85
20	31.95	28.23
21	32.54	28.62
22	33.12	29.01
23	33.70	29.40
24	34.27	29.80
25	34.85	30.20
26	35.42	30.61
27	35.98	31.02
28	36.55	31.43
29	37.11	31.85
30	37.66	32.28
31	38.22	32.71
32	38.77	33.14
33	39.31	33.58
34	39.85	34.02
35	40.39	34.46
36	40.93	34.91
37	41.46	35.37
38	41.99	35.83
39	42.52	36.29
40	43.04	36.76
41	43.56	37.23
42	44.07	37.70
43	44.58	38.18
44	45.09	38.66
45	45.59	39.15
46	46.09	39.64
47	46.59	40.13
48	47.08	40.63
49	47.57	41.13
50	48.05	41.64
51	48.53	42.15
52	49.01	42.66
53	49.48	43.18
54	49.95	43.70
55	50.41	44.23
56	50.87	44.75
57	51.33	45.29
58	51.78	45.82
59	52.22	46.36
60	52.67	46.90
61	53.10	47.45
62	53.54	48.00
63	53.97	48.55
64	54.39	49.10
65	54.82	49.66
66	55.23	50.23
67	55.64	50.79
68	56.05	51.36
69	56.46	51.93
70	56.86	52.51
71	57.25	53.09
72	57.64	53.67
73	58.03	54.25
74	58.41	54.84
75	58.78	55.43
76	59.15	56.02
77	59.52	56.62
78	59.88	57.22

79 60.24 57.82
 80 60.48 58.23
 Circle Center At X = -16.85 ; Y = 103.22 ; and Radius = 89.47
 Factor of Safety
 *** 1.246 ***

Failure Surface Specified By 72 Coordinate Points

Point No.	X-Surf (m)	Y-Surf (m)
1	20.61	22.44
2	21.26	22.72
3	21.90	23.00
4	22.53	23.29
5	23.17	23.59
6	23.80	23.89
7	24.43	24.20
8	25.05	24.51
9	25.68	24.83
10	26.29	25.16
11	26.91	25.49
12	27.52	25.83
13	28.13	26.18
14	28.73	26.54
15	29.33	26.89
16	29.93	27.26
17	30.52	27.63
18	31.11	28.01
19	31.70	28.39
20	32.28	28.79
21	32.86	29.18
22	33.43	29.58
23	34.00	29.99
24	34.56	30.41
25	35.12	30.83
26	35.68	31.25
27	36.23	31.68
28	36.77	32.12
29	37.32	32.56
30	37.85	33.01
31	38.39	33.47
32	38.91	33.93
33	39.44	34.39
34	39.96	34.86
35	40.47	35.34
36	40.98	35.82
37	41.48	36.31
38	41.98	36.80
39	42.47	37.30
40	42.96	37.80
41	43.44	38.30
42	43.92	38.82
43	44.39	39.33
44	44.86	39.86
45	45.32	40.38
46	45.77	40.91
47	46.22	41.45
48	46.67	41.99
49	47.11	42.54
50	47.54	43.09
51	47.97	43.64
52	48.39	44.20
53	48.80	44.76
54	49.21	45.33
55	49.62	45.90
56	50.01	46.48
57	50.41	47.06
58	50.79	47.64
59	51.17	48.23
60	51.55	48.82
61	51.91	49.42
62	52.27	50.02
63	52.63	50.62
64	52.98	51.23
65	53.32	51.84
66	53.65	52.46
67	53.98	53.07

68 54.31 53.69
 69 54.62 54.32
 70 54.93 54.95
 71 55.24 55.58
 72 55.37 55.86
 Circle Center At X = -5.49 ; Y = 84.38 ; and Radius = 67.21
 Factor of Safety
 *** 1.246 ***

Failure Surface Specified By 86 Coordinate Points

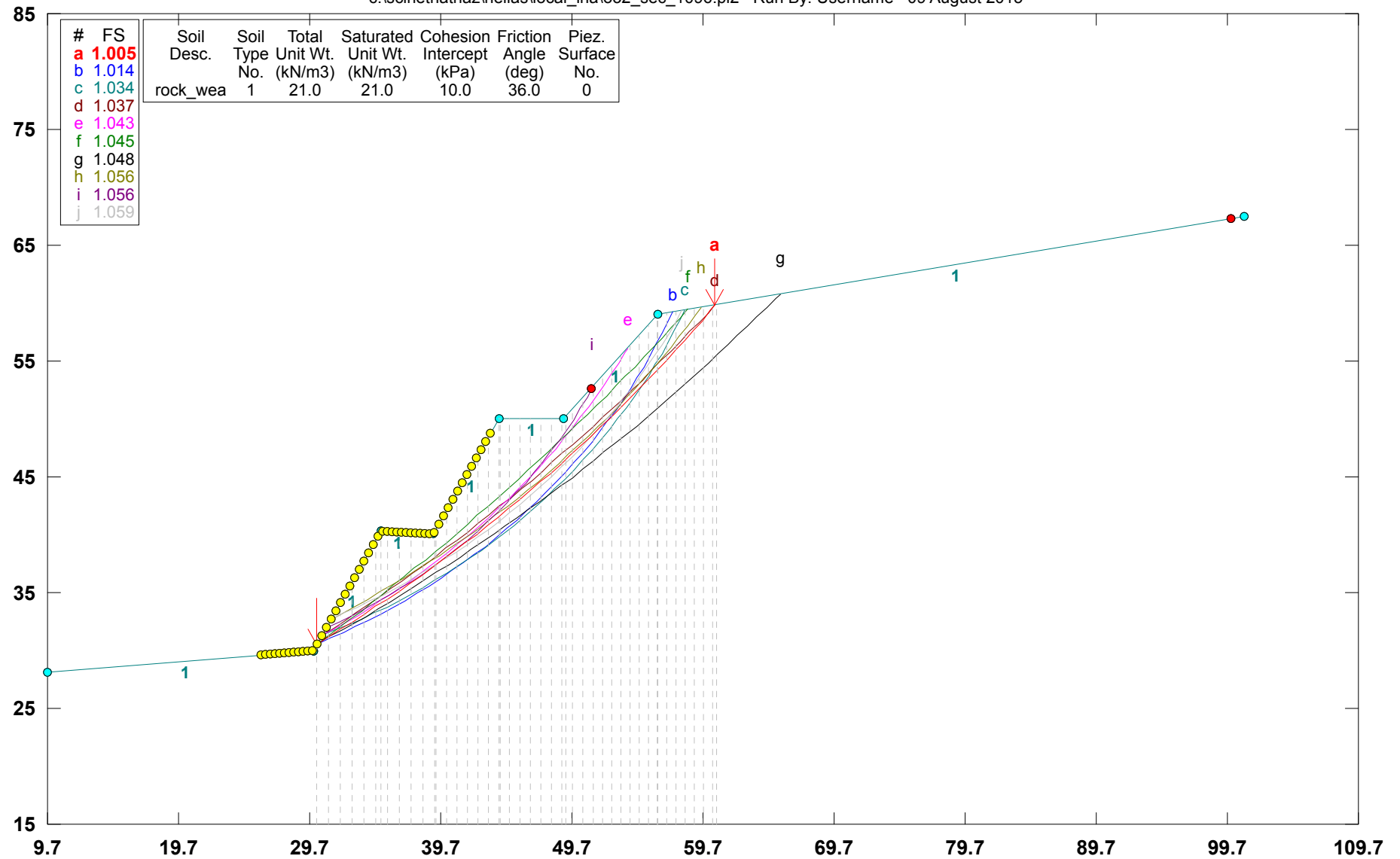
Point No.	X-Surf (m)	Y-Surf (m)
1	20.00	21.22
2	20.63	21.53
3	21.25	21.85
4	21.87	22.18
5	22.49	22.50
6	23.11	22.83
7	23.72	23.17
8	24.33	23.50
9	24.95	23.84
10	25.56	24.19
11	26.16	24.54
12	26.77	24.89
13	27.37	25.25
14	27.97	25.61
15	28.57	25.97
16	29.16	26.34
17	29.76	26.71
18	30.35	27.08
19	30.94	27.46
20	31.53	27.84
21	32.11	28.23
22	32.69	28.62
23	33.27	29.01
24	33.85	29.40
25	34.42	29.80
26	35.00	30.21
27	35.57	30.61
28	36.13	31.02
29	36.70	31.44
30	37.26	31.85
31	37.82	32.27
32	38.38	32.70
33	38.93	33.12
34	39.49	33.55
35	40.04	33.99
36	40.58	34.42
37	41.13	34.86
38	41.67	35.31
39	42.21	35.75
40	42.74	36.21
41	43.28	36.66
42	43.81	37.12
43	44.33	37.58
44	44.86	38.04
45	45.38	38.51
46	45.90	38.97
47	46.42	39.45
48	46.93	39.92
49	47.44	40.40
50	47.95	40.88
51	48.45	41.37
52	48.95	41.86
53	49.45	42.35
54	49.95	42.84
55	50.44	43.34
56	50.93	43.84
57	51.42	44.35
58	51.90	44.85
59	52.38	45.36
60	52.86	45.87
61	53.33	46.39
62	53.80	46.91
63	54.27	47.43
64	54.73	47.95

65	55.19	48.48
66	55.65	49.01
67	56.11	49.54
68	56.56	50.07
69	57.01	50.61
70	57.45	51.15
71	57.89	51.70
72	58.33	52.24
73	58.77	52.79
74	59.20	53.34
75	59.63	53.89
76	60.05	54.45
77	60.47	55.01
78	60.89	55.57
79	61.30	56.14
80	61.72	56.70
81	62.12	57.27
82	62.53	57.84
83	62.93	58.42
84	63.33	58.99
85	63.72	59.57
86	63.87	59.80

Circle Center At X = -31.21 ; Y = 123.69 ; and Radius = 114.55
Factor of Safety
*** 1.249 ***
**** END OF GSTABL7 OUTPUT ****

Hellas_Local_Landslide_Hazard Cut slope_O32_sec_1096

c:\scinetnathaz\hellas\local_lha\o32_sec_1096.pl2 Run By: Username 09 August 2015



GSTABL7 v.2 FSmin=1.005

Safety Factors Are Calculated By The Modified Bishop Method



```

*** GSTABL7 ***
** GSTABL7 by Garry H. Gregory, P.E. **
** Original Version 1.0, January 1996; Current Version 2.003, June 2002 **
  (All Rights Reserved-Unauthorized Use Prohibited)
*****
      SLOPE STABILITY ANALYSIS SYSTEM
      Modified Bishop, Simplified Janbu, or GLE Method of Slices.
      (Includes Spencer & Morgenstern-Price Type Analysis)
      Including Pier/Pile, Reinforcement, Soil Nail, Tieback,
      Nonlinear Undrained Shear Strength, Curved Phi Envelope,
      Anisotropic Soil, Fiber-Reinforced Soil, Boundary Loads, Water
      Surfaces, Pseudo-Static & Newmark Earthquake, and Applied Forces.
*****
Analysis Run Date:      09 August 2015
Time of Run:
Run By:      Username
Input Data Filename:   C:\SciNetNatHaz\Hellas\Local_LHA\032_sec_1096.in
Output Filename:      C:\SciNetNatHaz\Hellas\Local_LHA\032_sec_1096.OUT
Unit System:      SI
Plotted Output Filename: C:\SciNetNatHaz\Hellas\Local_LHA_sec_1096.PLT
PROBLEM DESCRIPTION:  Hellas_Local_Landslide_Hazard
                      Cut slope_032_sec_1096

BOUNDARY COORDINATES
  7 Top      Boundaries
  7 Total Boundaries

Boundary   X-Left   Y-Left   X-Right   Y-Right   Soil Type
  No.      (m)      (m)      (m)      (m)      Below Bnd
  1         9.72    28.15    30.00    30.00      1
  2        30.00    30.00    35.15    40.31      1
  3        35.15    40.31    39.15    40.07      1
  4        39.15    40.07    44.15    50.07      1
  5        44.15    50.07    49.13    50.00      1
  6        49.13    50.00    56.25    59.00      1

```


Slice No.	Width (m)	Individual data on the			44 slices		Earthquake			
		Weight (kN)	Water Force	Water Force	Tie Force	Tie Force	Force Hor (kN)	Ver (kN)	Surcharge Load (kN)	
			Top (kN)	Bot (kN)	Norm (kN)	Tan (kN)				
1	0.9	11.2	0.0	0.0	0.	0.	0.0	0.0	0.0	
2	0.9	33.3	0.0	0.0	0.	0.	0.0	0.0	0.0	
3	0.9	54.8	0.0	0.0	0.	0.	0.0	0.0	0.0	
4	0.9	75.6	0.0	0.0	0.	0.	0.0	0.0	0.0	
5	0.9	95.8	0.0	0.0	0.	0.	0.0	0.0	0.0	
6	0.4	50.1	0.0	0.0	0.	0.	0.0	0.0	0.0	
7	0.5	60.4	0.0	0.0	0.	0.	0.0	0.0	0.0	
8	0.9	100.0	0.0	0.0	0.	0.	0.0	0.0	0.0	
9	0.9	86.1	0.0	0.0	0.	0.	0.0	0.0	0.0	
10	0.9	72.3	0.0	0.0	0.	0.	0.0	0.0	0.0	
11	0.9	58.5	0.0	0.0	0.	0.	0.0	0.0	0.0	
12	0.1	4.5	0.0	0.0	0.	0.	0.0	0.0	0.0	
13	0.8	53.1	0.0	0.0	0.	0.	0.0	0.0	0.0	
14	0.8	74.5	0.0	0.0	0.	0.	0.0	0.0	0.0	
15	0.8	90.8	0.0	0.0	0.	0.	0.0	0.0	0.0	
16	0.8	106.5	0.0	0.0	0.	0.	0.0	0.0	0.0	
17	0.8	121.7	0.0	0.0	0.	0.	0.0	0.0	0.0	
18	0.8	136.3	0.0	0.0	0.	0.	0.0	0.0	0.0	
19	0.1	15.2	0.0	0.0	0.	0.	0.0	0.0	0.0	
20	0.7	123.9	0.0	0.0	0.	0.	0.0	0.0	0.0	
21	0.8	125.4	0.0	0.0	0.	0.	0.0	0.0	0.0	
22	0.8	111.6	0.0	0.0	0.	0.	0.0	0.0	0.0	
23	0.8	97.8	0.0	0.0	0.	0.	0.0	0.0	0.0	
24	0.8	84.2	0.0	0.0	0.	0.	0.0	0.0	0.0	
25	0.8	70.6	0.0	0.0	0.	0.	0.0	0.0	0.0	
26	0.3	24.2	0.0	0.0	0.	0.	0.0	0.0	0.0	
27	0.5	35.9	0.0	0.0	0.	0.	0.0	0.0	0.0	
28	0.8	61.2	0.0	0.0	0.	0.	0.0	0.0	0.0	
29	0.8	63.3	0.0	0.0	0.	0.	0.0	0.0	0.0	
30	0.7	65.1	0.0	0.0	0.	0.	0.0	0.0	0.0	
31	0.7	66.6	0.0	0.0	0.	0.	0.0	0.0	0.0	
32	0.7	67.9	0.0	0.0	0.	0.	0.0	0.0	0.0	
33	0.7	68.8	0.0	0.0	0.	0.	0.0	0.0	0.0	
34	0.7	69.5	0.0	0.0	0.	0.	0.0	0.0	0.0	
35	0.7	69.9	0.0	0.0	0.	0.	0.0	0.0	0.0	
36	0.7	70.1	0.0	0.0	0.	0.	0.0	0.0	0.0	
37	0.0	3.3	0.0	0.0	0.	0.	0.0	0.0	0.0	
38	0.7	61.8	0.0	0.0	0.	0.	0.0	0.0	0.0	
39	0.7	53.9	0.0	0.0	0.	0.	0.0	0.0	0.0	
40	0.7	42.9	0.0	0.0	0.	0.	0.0	0.0	0.0	
41	0.7	32.0	0.0	0.0	0.	0.	0.0	0.0	0.0	
42	0.7	21.2	0.0	0.0	0.	0.	0.0	0.0	0.0	
43	0.7	10.5	0.0	0.0	0.	0.	0.0	0.0	0.0	
44	0.3	1.3	0.0	0.0	0.	0.	0.0	0.0	0.0	

Failure Surface Specified By 38 Coordinate Points

Point No.	X-Surf (m)	Y-Surf (m)
1	30.29	30.57
2	31.28	31.05
3	32.26	31.55
4	33.23	32.07
5	34.19	32.61
6	35.13	33.16
7	36.07	33.74
8	37.00	34.34
9	37.91	34.95
10	38.81	35.58
11	39.69	36.23
12	40.57	36.90
13	41.43	37.59
14	42.27	38.29
15	43.10	39.01
16	43.92	39.75
17	44.72	40.50
18	45.51	41.27
19	46.28	42.06
20	47.03	42.86
21	47.77	43.68
22	48.49	44.51
23	49.19	45.35

24	49.88	46.21
25	50.55	47.09
26	51.20	47.98
27	51.83	48.88
28	52.44	49.79
29	53.04	50.71
30	53.62	51.65
31	54.17	52.60
32	54.71	53.56
33	55.23	54.53
34	55.73	55.51
35	56.21	56.50
36	56.66	57.50
37	57.10	58.51
38	57.39	59.22

Circle Center At X = 7.23 ; Y = 79.54 ; and Radius = 54.12

Factor of Safety
*** 1.014 ***

Failure Surface Specified By 38 Coordinate Points

Point No.	X-Surf (m)	Y-Surf (m)
1	30.64	31.29
2	31.65	31.73
3	32.64	32.20
4	33.63	32.69
5	34.60	33.20
6	35.57	33.73
7	36.52	34.28
8	37.46	34.85
9	38.39	35.44
10	39.30	36.05
11	40.21	36.68
12	41.10	37.33
13	41.97	37.99
14	42.83	38.68
15	43.68	39.38
16	44.51	40.10
17	45.33	40.83
18	46.13	41.59
19	46.92	42.36
20	47.69	43.14
21	48.44	43.94
22	49.18	44.76
23	49.90	45.59
24	50.60	46.44
25	51.28	47.30
26	51.94	48.18
27	52.59	49.07
28	53.22	49.97
29	53.83	50.89
30	54.42	51.82
31	54.99	52.76
32	55.53	53.71
33	56.06	54.68
34	56.57	55.65
35	57.06	56.64
36	57.53	57.63
37	57.98	58.64
38	58.29	59.39

Circle Center At X = 9.78 ; Y = 79.46 ; and Radius = 52.50

Factor of Safety
*** 1.034 ***

Failure Surface Specified By 39 Coordinate Points

Point No.	X-Surf (m)	Y-Surf (m)
1	30.64	31.29
2	31.53	31.94
3	32.41	32.60
4	33.28	33.27
5	34.15	33.94
6	35.02	34.62
7	35.88	35.31
8	36.73	36.00
9	37.58	36.69
10	38.43	37.40

11	39.27	38.10
12	40.11	38.82
13	40.95	39.53
14	41.77	40.26
15	42.60	40.99
16	43.41	41.72
17	44.23	42.46
18	45.04	43.21
19	45.84	43.96
20	46.64	44.72
21	47.43	45.48
22	48.22	46.25
23	49.00	47.02
24	49.78	47.80
25	50.56	48.58
26	51.32	49.37
27	52.09	50.16
28	52.84	50.96
29	53.59	51.76
30	54.34	52.57
31	55.08	53.38
32	55.82	54.20
33	56.55	55.02
34	57.27	55.85
35	57.99	56.68
36	58.70	57.52
37	59.41	58.36
38	60.11	59.21
39	60.63	59.83

Circle Center At X = -67.26 ; Y = 164.14 ; and Radius = 165.03

Factor of Safety

*** 1.037 ***

Failure Surface Specified By 33 Coordinate Points

Point No.	X-Surf (m)	Y-Surf (m)
1	30.64	31.29
2	31.58	31.87
3	32.50	32.47
4	33.41	33.08
5	34.31	33.71
6	35.21	34.35
7	36.09	35.01
8	36.96	35.69
9	37.81	36.38
10	38.66	37.08
11	39.49	37.80
12	40.31	38.53
13	41.12	39.28
14	41.92	40.04
15	42.70	40.81
16	43.47	41.60
17	44.22	42.40
18	44.96	43.21
19	45.69	44.04
20	46.40	44.87
21	47.10	45.72
22	47.79	46.58
23	48.46	47.46
24	49.11	48.34
25	49.75	49.23
26	50.38	50.14
27	50.98	51.06
28	51.58	51.98
29	52.15	52.92
30	52.71	53.87
31	53.26	54.82
32	53.79	55.79
33	53.94	56.09

Circle Center At X = -2.99 ; Y = 86.24 ; and Radius = 64.42

Factor of Safety

*** 1.043 ***

Failure Surface Specified By 38 Coordinate Points

Point No.	X-Surf (m)	Y-Surf (m)
1	30.29	30.57

2	31.13	31.28
3	31.97	31.99
4	32.80	32.71
5	33.63	33.43
6	34.46	34.15
7	35.28	34.88
8	36.10	35.62
9	36.92	36.35
10	37.73	37.10
11	38.54	37.84
12	39.34	38.60
13	40.14	39.35
14	40.93	40.11
15	41.73	40.88
16	42.51	41.64
17	43.30	42.42
18	44.07	43.20
19	44.85	43.98
20	45.62	44.76
21	46.38	45.55
22	47.14	46.35
23	47.90	47.14
24	48.65	47.95
25	49.40	48.75
26	50.15	49.56
27	50.89	50.38
28	51.62	51.20
29	52.35	52.02
30	53.08	52.84
31	53.80	53.67
32	54.52	54.51
33	55.23	55.35
34	55.94	56.19
35	56.64	57.03
36	57.34	57.88
37	58.03	58.74
38	58.61	59.45

Circle Center At X = -99.68 ; Y = 186.37 ; and Radius = 202.89

Factor of Safety

*** 1.045 ***

Failure Surface Specified By 44 Coordinate Points

Point No.	X-Surf (m)	Y-Surf (m)
1	30.29	30.57
2	31.22	31.16
3	32.14	31.75
4	33.06	32.36
5	33.98	32.96
6	34.89	33.58
7	35.80	34.20
8	36.71	34.82
9	37.61	35.45
10	38.50	36.09
11	39.39	36.74
12	40.28	37.39
13	41.16	38.05
14	42.04	38.71
15	42.91	39.38
16	43.78	40.05
17	44.64	40.74
18	45.50	41.42
19	46.36	42.12
20	47.21	42.82
21	48.05	43.52
22	48.89	44.23
23	49.72	44.95
24	50.55	45.67
25	51.38	46.40
26	52.20	47.13
27	53.01	47.87
28	53.82	48.62
29	54.63	49.37
30	55.42	50.12
31	56.22	50.88
32	57.01	51.65

33	57.79	52.42
34	58.57	53.20
35	59.34	53.99
36	60.11	54.77
37	60.87	55.57
38	61.62	56.37
39	62.37	57.17
40	63.12	57.98
41	63.86	58.80
42	64.59	59.62
43	65.32	60.44
44	65.61	60.78

Circle Center At X = -54.15 ; Y = 165.07 ; and Radius = 158.81

Factor of Safety
*** 1.048 ***

Failure Surface Specified By 37 Coordinate Points

Point No.	X-Surf (m)	Y-Surf (m)
1	31.36	32.72
2	32.30	33.28
3	33.24	33.85
4	34.17	34.44
5	35.10	35.03
6	36.01	35.64
7	36.92	36.27
8	37.82	36.90
9	38.71	37.54
10	39.59	38.20
11	40.47	38.87
12	41.33	39.55
13	42.19	40.24
14	43.04	40.94
15	43.88	41.65
16	44.71	42.37
17	45.53	43.10
18	46.34	43.85
19	47.14	44.60
20	47.93	45.37
21	48.71	46.14
22	49.48	46.93
23	50.24	47.72
24	50.99	48.53
25	51.73	49.34
26	52.46	50.16
27	53.18	51.00
28	53.88	51.84
29	54.58	52.69
30	55.27	53.55
31	55.94	54.42
32	56.60	55.30
33	57.25	56.19
34	57.89	57.08
35	58.52	57.98
36	59.14	58.89
37	59.63	59.64

Circle Center At X = -11.49 ; Y = 106.02 ; and Radius = 84.91

Factor of Safety
*** 1.056 ***

Failure Surface Specified By 28 Coordinate Points

Point No.	X-Surf (m)	Y-Surf (m)
1	31.00	32.00
2	31.98	32.51
3	32.94	33.04
4	33.89	33.59
5	34.83	34.17
6	35.75	34.77
7	36.65	35.39
8	37.55	36.04
9	38.42	36.71
10	39.28	37.39
11	40.12	38.10
12	40.94	38.83
13	41.75	39.58
14	42.54	40.35

15	43.30	41.14
16	44.05	41.94
17	44.78	42.77
18	45.49	43.61
19	46.18	44.47
20	46.84	45.35
21	47.48	46.24
22	48.11	47.14
23	48.71	48.07
24	49.28	49.00
25	49.83	49.95
26	50.36	50.92
27	50.87	51.90
28	51.26	52.69

Circle Center At X = 10.86 ; Y = 71.99 ; and Radius = 44.77

Factor of Safety

*** 1.056 ***

Failure Surface Specified By 36 Coordinate Points

Point No.	X-Surf (m)	Y-Surf (m)
1	31.36	32.72
2	32.34	33.21
3	33.32	33.71
4	34.28	34.24
5	35.24	34.78
6	36.19	35.35
7	37.12	35.93
8	38.04	36.52
9	38.96	37.14
10	39.86	37.77
11	40.74	38.42
12	41.62	39.09
13	42.48	39.77
14	43.33	40.47
15	44.17	41.18
16	44.99	41.91
17	45.80	42.66
18	46.59	43.42
19	47.37	44.19
20	48.14	44.98
21	48.89	45.79
22	49.62	46.61
23	50.34	47.44
24	51.05	48.29
25	51.73	49.15
26	52.40	50.02
27	53.06	50.90
28	53.69	51.80
29	54.31	52.71
30	54.92	53.63
31	55.50	54.56
32	56.07	55.50
33	56.62	56.45
34	57.15	57.42
35	57.66	58.39
36	58.15	59.36

Circle Center At X = 6.03 ; Y = 84.98 ; and Radius = 58.08

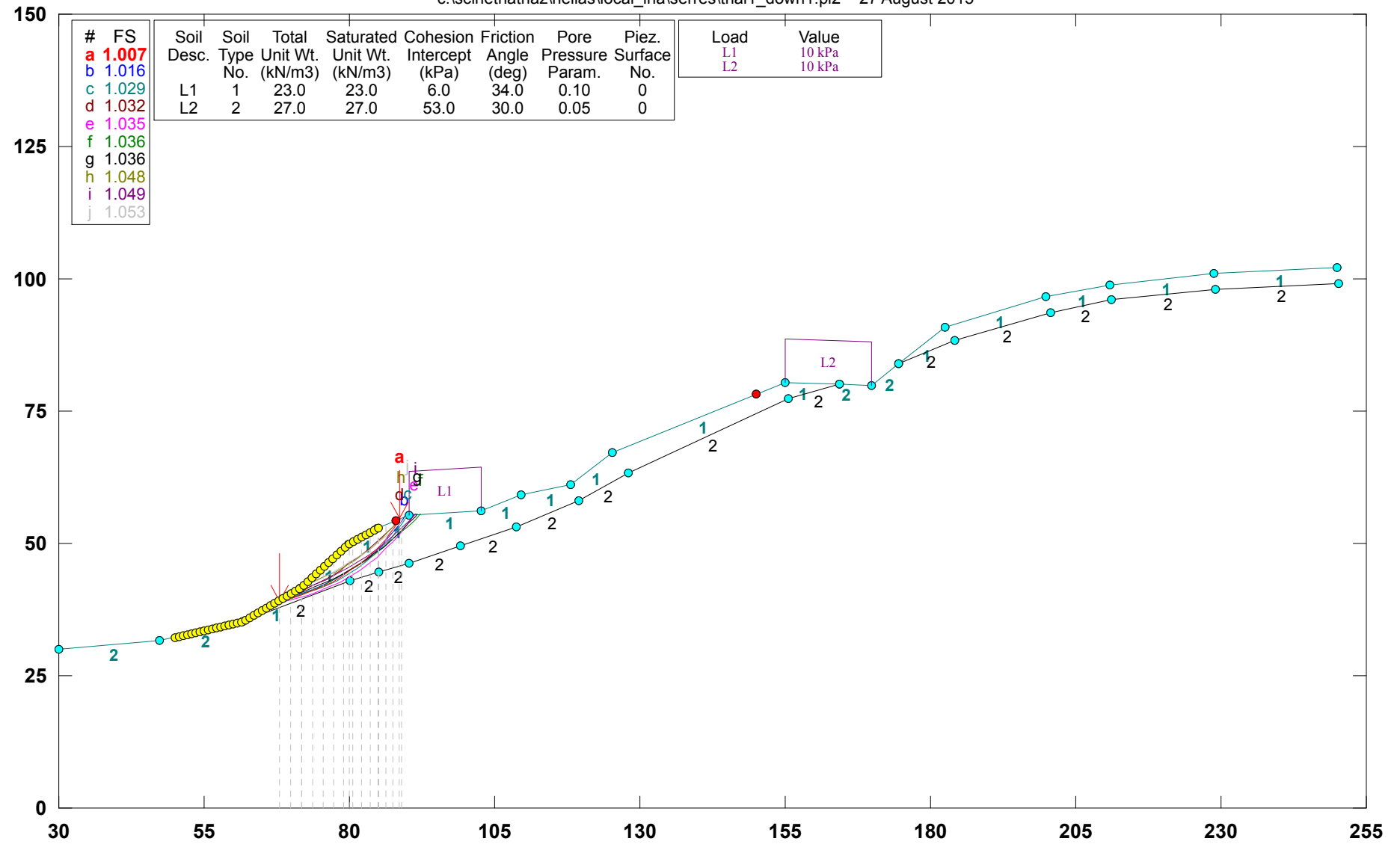
Factor of Safety

*** 1.059 ***

**** END OF GSTABL7 OUTPUT ****

Hellas_Local_Landslide_Hazard Slope Serres Down 1

c:\scinetnathaz\hellas\local_lha\serres\trial1_down1.pl2 27 August 2015



GSTABL7 v.2 FSmin=1.007

Safety Factors Are Calculated By The Modified Bishop Method



*** GSTABL7 ***

** GSTABL7 by Garry H. Gregory, P.E. **

** Original Version 1.0, January 1996; Current Version 2.003, June 2002 **

(All Rights Reserved-Unauthorized Use Prohibited)

SLOPE STABILITY ANALYSIS SYSTEM

Modified Bishop, Simplified Janbu, or GLE Method of Slices.

(Includes Spencer & Morgenstern-Price Type Analysis)

Including Pier/Pile, Reinforcement, Soil Nail, Tieback,

Nonlinear Undrained Shear Strength, Curved Phi Envelope,

Anisotropic Soil, Fiber-Reinforced Soil, Boundary Loads, Water

Surfaces, Pseudo-Static & Newmark Earthquake, and Applied Forces.

Analysis Run Date: 27 August 2015

Time of Run:

Run By:

Input Data Filename: C:\SciNetNatHaz\Hellas\Local_LHA\Serres\trial1_down1.in

Output Filename: C:\SciNetNatHaz\Hellas\Local_LHA\Serres\trial1_down1.OUT

Unit System: SI

Plotted Output Filename: C:\SciNetNatHaz\Hellas\Local_LHAres\trial1_down1.PLT

PROBLEM DESCRIPTION: Hellas_Local_Landslide_Hazard

Slope Serres Down 1

BOUNDARY COORDINATES

19 Top Boundaries

33 Total Boundaries

Boundary	X-Left	Y-Left	X-Right	Y-Right	Soil Type
No.	(m)	(m)	(m)	(m)	Below Bnd
1	30.00	30.00	47.43	31.53	2
2	47.43	31.53	61.70	35.20	2
3	61.70	35.20	71.69	41.61	1
4	71.69	41.61	79.83	49.81	1
5	79.83	49.81	84.83	52.81	1
6	84.83	52.81	90.42	55.46	1

7	90.42	55.46	102.68	56.25	1
8	102.68	56.25	109.49	59.12	1
9	109.49	59.12	118.12	60.99	1
10	118.12	60.99	125.38	67.13	1
11	125.38	67.13	154.89	80.44	1
12	154.89	80.44	164.24	80.11	1
13	164.24	80.11	169.87	79.91	2
14	169.87	79.91	174.52	83.95	2
15	174.52	83.95	182.58	90.94	1
16	182.58	90.94	199.83	96.52	1
17	199.83	96.52	210.75	98.96	1
18	210.75	98.96	228.81	101.09	1
19	228.81	101.09	250.09	102.15	1
20	61.70	35.20	80.18	42.99	2
21	80.18	42.99	85.02	44.58	2
22	85.02	44.58	90.19	46.19	2
23	90.19	46.19	99.06	49.43	2
24	99.06	49.43	108.77	53.19	2
25	108.77	53.19	119.48	58.22	2
26	119.48	58.22	127.97	63.36	2
27	127.97	63.36	155.48	77.42	2
28	155.48	77.42	164.24	80.11	2
29	174.52	83.95	184.08	88.28	2
30	184.08	88.28	200.62	93.62	2
31	200.62	93.62	211.25	96.00	2
32	211.25	96.00	229.06	98.10	2
33	229.06	98.10	250.24	99.15	2

Default Y-Origin = 0.00(m)

Default X-Plus Value = 0.00(m)

Default Y-Plus Value = 0.00(m)

ISOTROPIC SOIL PARAMETERS

2 Type(s) of Soil

Soil Type No.	Total Unit Wt. (kN/m ³)	Saturated Unit Wt. (kN/m ³)	Cohesion Intercept (kPa)	Friction Angle (deg)	Pore Pressure Param. (kPa)	Pressure Constant (kPa)	Piez. Surface No.
1	23.0	23.0	6.0	34.0	0.10	0.0	0
2	27.0	27.0	53.0	30.0	0.05	0.0	0

BOUNDARY LOAD(S)

2 Load(s) Specified

Load No.	X-Left (m)	X-Right (m)	Intensity (kPa)	Deflection (deg)
1	90.41	102.67	10.0	0.0
2	154.88	169.86	10.0	0.0

NOTE - Intensity Is Specified As A Uniformly Distributed Force Acting On A Horizontally Projected Surface.

A Critical Failure Surface Searching Method, Using A Random Technique For Generating Circular Surfaces, Has Been Specified.
2500 Trial Surfaces Have Been Generated.

50 Surface(s) Initiate(s) From Each Of 50 Points Equally Spaced Along The Ground Surface Between X = 50.00(m)

and X = 85.00(m)

Each Surface Terminates Between X = 88.00(m)

and X = 150.00(m)

Unless Further Limitations Were Imposed, The Minimum Elevation At Which A Surface Extends Is Y = 0.00(m)

2.00(m) Line Segments Define Each Trial Failure Surface.

Following Are Displayed The Ten Most Critical Of The Trial

Failure Surfaces Evaluated. They Are Ordered - Most Critical First.

* * Safety Factors Are Calculated By The Modified Bishop Method * *

Total Number of Trial Surfaces Evaluated = 2500

Statistical Data On All Valid FS Values:

FS Max = 7.483 FS Min = 1.007 FS Ave = 2.471

Standard Deviation = 0.803 Coefficient of Variation = 32.49 %

Failure Surface Specified By 15 Coordinate Points

Point No.	X-Surf (m)	Y-Surf (m)
1	67.86	39.15
2	69.80	39.64
3	71.70	40.26
4	73.56	40.99
5	75.37	41.84
6	77.13	42.80
7	78.82	43.87
8	80.44	45.04

9 81.98 46.31
 10 83.44 47.67
 11 84.82 49.13
 12 86.10 50.66
 13 87.28 52.28
 14 88.36 53.96
 15 88.74 54.67

Circle Center At X = 60.96 ; Y = 70.29 ; and Radius = 31.90

Factor of Safety

*** 1.007 ***

Individual data on the 17 slices

Slice No.	Width (m)	Weight (kN)	Water Force		Tie Force Norm (kN)	Tie Force Tan (kN)	Earthquake Force		Surcharge Load (kN)
			Top (kN)	Bot (kN)			Hor (kN)	Ver (kN)	
1	1.9	16.7	0.0	1.7	0.	0.	0.0	0.0	0.0
2	1.9	45.8	0.0	4.8	0.	0.	0.0	0.0	0.0
3	0.0	0.3	0.0	0.0	0.	0.	0.0	0.0	0.0
4	1.9	82.7	0.0	8.9	0.	0.	0.0	0.0	0.0
5	1.8	124.6	0.0	13.8	0.	0.	0.0	0.0	0.0
6	1.8	156.8	0.0	17.9	0.	0.	0.0	0.0	0.0
7	1.7	179.2	0.0	21.2	0.	0.	0.0	0.0	0.0
8	1.0	118.0	0.0	14.6	0.	0.	0.0	0.0	0.0
9	0.6	72.4	0.0	8.9	0.	0.	0.0	0.0	0.0
10	1.5	176.4	0.0	22.8	0.	0.	0.0	0.0	0.0
11	1.5	153.0	0.0	20.9	0.	0.	0.0	0.0	0.0
12	1.4	126.1	0.0	18.4	0.	0.	0.0	0.0	0.0
13	0.0	1.0	0.0	0.2	0.	0.	0.0	0.0	0.0
14	1.3	93.5	0.0	14.6	0.	0.	0.0	0.0	0.0
15	1.2	60.3	0.0	10.2	0.	0.	0.0	0.0	0.0
16	1.1	27.4	0.0	5.1	0.	0.	0.0	0.0	0.0
17	0.4	2.3	0.0	0.5	0.	0.	0.0	0.0	0.0

Failure Surface Specified By 15 Coordinate Points

Point No.	X-Surf (m)	Y-Surf (m)
1	68.57	39.61
2	70.50	40.15
3	72.39	40.81
4	74.24	41.57
5	76.04	42.44
6	77.79	43.41
7	79.47	44.48
8	81.10	45.65
9	82.65	46.91
10	84.13	48.25
11	85.53	49.68
12	86.84	51.19
13	88.06	52.78
14	89.19	54.43
15	89.57	55.06

Circle Center At X = 60.17 ; Y = 73.06 ; and Radius = 34.49

Factor of Safety

*** 1.016 ***

Failure Surface Specified By 15 Coordinate Points

Point No.	X-Surf (m)	Y-Surf (m)
1	68.57	39.61
2	70.52	40.05
3	72.44	40.61
4	74.32	41.30
5	76.15	42.11
6	77.92	43.03
7	79.63	44.07
8	81.27	45.21
9	82.83	46.46
10	84.31	47.81
11	85.70	49.25
12	86.99	50.78
13	88.18	52.38
14	89.27	54.06
15	89.91	55.22

Circle Center At X = 62.76 ; Y = 69.97 ; and Radius = 30.91

Factor of Safety

*** 1.029 ***

Failure Surface Specified By 15 Coordinate Points

Point No.	X-Surf (m)	Y-Surf (m)
1	67.86	39.15
2	69.69	39.95
3	71.49	40.83
4	73.26	41.76
5	74.99	42.77
6	76.68	43.83
7	78.33	44.96
8	79.93	46.16
9	81.49	47.41
10	83.01	48.71
11	84.47	50.08
12	85.88	51.49
13	87.24	52.96
14	88.54	54.48
15	88.65	54.62

Circle Center At X = 47.32 ; Y = 88.47 ; and Radius = 53.43
Factor of Safety
*** 1.032 ***

Failure Surface Specified By 17 Coordinate Points

Point No.	X-Surf (m)	Y-Surf (m)
1	67.14	38.69
2	69.10	39.09
3	71.04	39.60
4	72.94	40.22
5	74.80	40.96
6	76.61	41.79
7	78.38	42.73
8	80.09	43.78
9	81.73	44.91
10	83.31	46.15
11	84.81	47.47
12	86.23	48.87
13	87.57	50.36
14	88.82	51.92
15	89.98	53.55
16	91.04	55.24
17	91.19	55.51

Circle Center At X = 61.24 ; Y = 72.74 ; and Radius = 34.56
Factor of Safety
*** 1.035 ***

Failure Surface Specified By 17 Coordinate Points

Point No.	X-Surf (m)	Y-Surf (m)
1	66.43	38.23
2	68.31	38.91
3	70.17	39.64
4	72.01	40.44
5	73.81	41.30
6	75.59	42.22
7	77.33	43.20
8	79.04	44.24
9	80.71	45.33
10	82.35	46.48
11	83.95	47.69
12	85.50	48.95
13	87.01	50.26
14	88.47	51.62
15	89.89	53.03
16	91.26	54.49
17	92.21	55.58

Circle Center At X = 47.55 ; Y = 94.16 ; and Radius = 59.03
Factor of Safety
*** 1.036 ***

Failure Surface Specified By 16 Coordinate Points

Point No.	X-Surf (m)	Y-Surf (m)
1	68.57	39.61
2	70.46	40.25
3	72.33	40.98
4	74.16	41.78
5	75.96	42.65
6	77.72	43.60

7	79.44	44.62
8	81.12	45.72
9	82.74	46.88
10	84.32	48.10
11	85.85	49.40
12	87.32	50.75
13	88.73	52.17
14	90.09	53.64
15	91.38	55.17
16	91.67	55.54

Circle Center At X = 54.06 ; Y = 85.36 ; and Radius = 47.99

Factor of Safety

*** 1.036 ***

Failure Surface Specified By 12 Coordinate Points

Point No.	X-Surf (m)	Y-Surf (m)
1	72.14	42.07
2	73.98	42.85
3	75.78	43.72
4	77.53	44.69
5	79.23	45.74
6	80.88	46.88
7	82.46	48.11
8	83.98	49.41
9	85.43	50.79
10	86.80	52.24
11	88.11	53.75
12	88.85	54.71

Circle Center At X = 57.86 ; Y = 78.28 ; and Radius = 38.93

Factor of Safety

*** 1.048 ***

Failure Surface Specified By 14 Coordinate Points

Point No.	X-Surf (m)	Y-Surf (m)
1	70.71	40.98
2	72.58	41.69
3	74.42	42.48
4	76.22	43.35
5	77.99	44.29
6	79.71	45.31
7	81.39	46.39
8	83.02	47.55
9	84.60	48.78
10	86.13	50.07
11	87.60	51.43
12	89.01	52.85
13	90.36	54.32
14	91.36	55.52

Circle Center At X = 54.99 ; Y = 85.25 ; and Radius = 46.97

Factor of Safety

*** 1.049 ***

Failure Surface Specified By 13 Coordinate Points

Point No.	X-Surf (m)	Y-Surf (m)
1	71.43	41.44
2	73.23	42.31
3	75.00	43.25
4	76.73	44.24
5	78.43	45.30
6	80.09	46.41
7	81.71	47.59
8	83.29	48.82
9	84.82	50.10
10	86.30	51.44
11	87.74	52.83
12	89.13	54.27
13	90.03	55.27

Circle Center At X = 47.70 ; Y = 92.80 ; and Radius = 56.57

Factor of Safety

*** 1.053 ***

**** END OF GSTABL7 OUTPUT ****